The Biomicrofluidics of Microbiologically Induced Calcite Precipitation Mediated by *Sporosarcina pasteurii*

by

Swayamdipta Bhaduri

A thesis submitted in partial fulfillment of the requirements for the degree of

Doctor of Philosophy

Department of Mechanical Engineering

University of Alberta

© *Swayamdipta Bhaduri*, 2018

Abstract

I studied a particular bacterium *Sporosarcina pasteurii* (*S. Pasteurii*) which has a unique ability to cause chemical precipitation in an aqueous medium in the presence of certain molecules like urea. These precipitated chemicals can go deep inside a network of micro-scale pores and cause clogging. As a result, the porous matrix may gain significantly in terms of structural and mechanical strength.

The clogging of pores has wide-ranging implications in areas spanning from heritage structure remediation to carbon sequestration. These reasons have led to a significant increase in interest in *S. Pasteurii* and the mechanism behind the induction of precipitation, especially inside porous media with a characteristic pore size of the order of microns.

I prepared cultures of *S. Pasteurii* which were subsequently enriched through a recipe of external additives. These chemicals, through a complex chain of reactions, lead to the formation of calcium carbonate. The role of *S. Pasteurii* comes from the fact that it secretes large volumes of extracellular urease which acts as a catalyst, thus accelerating the reaction kinetics. This phenomenon, in its entirety, is often called Microbiologically Induced Calcite Precipitation (MICP).

For the present work, I have analyzed MICP from various physical, chemical and biological angles. Firstly, a new protocol of culturing the bacterium and enriching it suitably thereafter has been developed. This provides us with a reliable tool to accelerate in situ precipitation and study the temporal evolution of the system.

Secondly, a semi-solid platform to observe the movement of bacteria inside a micro-porous medium and measure their speeds has been developed. Based on experiments on this

platform, I have studied the spatial location of nucleation sites for crystals; the interplay between flagellar and diffusive motilities, as well as the role of cell membranes in inducing precipitation.

Finally, a mechanistic analysis has also been undertaken to quantify the enhancement in mechanical strength and structural properties, such as porosity and permeability of the representative porous medium. A full range of mechanical tests and chemical characterization have been performed to understand the effects of MICP on bulk and surface properties of the system.

Preface

The research presented in this thesis has been completed as part of my PhD. This thesis is presented in a paper-based format. Three journal articles have been presented as Chapters 2 to 5. I have been the responsible for literature review, laboratory experiments, data analysis and manuscript writing. Dr. Carlo Montemagno and Dr. Aloke Kumar have been supervisory co-authors. Chapter 2 is already published after peer review, Chapter 3 is under peer review, and Chapter 4 is to be communicated very shortly. The list of papers include:

1. Microbiologically Induced Calcite Precipitation mediated by *Sporosarcina pasteurii*. **Bhaduri, S.**, Debnath, N., Mitra, S. K., Liu, Y., Kumar, A. (2016). Journal of Visualized Experiments, e53253, doi:10.3791/53253 (published after peer review).

2. *Sporosarcina pasteurii* can form nanoscale crystals on cell surface. **Bhaduri, S.**, Ghosh, T., Montemagno, C., Kumar, A. (under peer review).

3. *Sporosarcina pasteurii* can clog and strengthen a porous medium mimic. **Bhaduri, S.**, Montemagno, C., Kumar, A. (to be submitted shortly).

Acknowledgements

It seems like a long time has passed since I first arrived here. Although it's just four years, I've had the opportunity to work with four different PhD advisers, work in at least six different labs and regularly attend at least three different group meetings! Consequently, my list of acknowledgements would run long and wide. In spite of my best efforts, it's quite possible to miss a name or two; and my apologies in advance if that happened. If you're somebody who has helped, guided, mentored, advised, or just shared a friendly conversation with me over the course of my doctoral journey, you're heartily acknowledged…even if your name doesn't appear here.

To begin with, I'm indebted to my three primary graduate supervisors for teaching me the art of science and the finer points of good research. For the endless sessions of critical analyses, thoughtful feedback, and timely suggestions; a big thank you to professors Sushanta Mitra (now the Executive Director at the Waterloo Institute of Nanotechnology), Aloke Kumar (now at IISc) and Carlo Montemagno (now the Chancellor at Southern Illinois University). Dr. Montemagno is the preeminent authority on nanotechnology and has been called the father of nanobiotechnology. I am fortunate to have worked with one of the most famous nanoscientists on planet earth today. Dr. John Doucette, who is my mentor, departmental advisor, and committee chair, deserves warm and heartfelt thanks for so many reasons, big and small. Finally, Dr. Reghan Hill (the external examiner form McGill University) is gratefully acknowledged for heavily enhancing the quality of this thesis by providing very detailed and insightful comments on many critical aspects of the research.

Special thanks to Dr. Thomas Thundat, Dr. Vinay Prasad, Dr. Hyo-Jick Choi, Dr. Mrinal Mandal, Dr. Janet Elliott, Dr. Amy Tsai and Dr. Don Raboud for helping with different aspects of my program at many different junctures. I made it a point to take the best courses from the best professors on campus. Both for their magical lectures and their inspiration outside the class; thanks to Dr. Xi Chen, Dr. Stephane Evoy, Dr. Morris Flynn, Dr. Sina Ghaemi, Dr. Rouslan Krechetnikov, Dr. Brendan Pass, Dr. Chong-Qing Ru, Dr. Peter Schiavone, Dr. Lorenz Sigurdson and Dr. Tiang Tang. Many other members of the faculty have helped with their pearls of wisdom on many occasions, including Dr. Siddhartha Das, Dr. Kajsa Duke, Dr. James Hogan, Dr. Chun il Kim, Dr. Yang Liu and Dr. Stefan Pukatzki.

Now to colleagues and friends. In chronological sequence, thanks first to the MNT Lab people: Aleksey, Amrit, Arnab, Dibyo, Hazel, Naga, Pankaj and Sourayon. Thanks next to the Kumar Biomicrofluidics Lab people: Ishita, Nandini, Tanushree and Rajorshi. Last but not the least, the huge Ingenuity Lab family has been my home for the last two years and special thanks go to: Advaita, Antonio, Dawson, Devon, Elizabeth, Jeanine, Jonathan, Morgan, Robin, Samira, Susan and Wendi.

Table of Contents

Chapter 1 : Introduction

Bacteria are simple unicellular organisms. Being prokaryotes, their genetic material is not enclosed within a nuclear membrane. They are the most ubiquitous life-form on earth and are found in a bewildering variety of habitats ranging from soil, frozen lakes, hot springs, radioactive minerals, all organic matter and inside living bodies of plants and animals. It is estimated that an average gram of soil contains 40 million bacterial cells whereas an average milliliter of fresh water contains a million. There are approximately 5×10^{30} bacteria on earth, forming much of the total biomass. Almost every step of the key biogeochemical nutrient cycles (O, C, N, S etc.) involves a multitude of bacterial species. Still, most bacteria have not yet been characterized as of today and less than half of the bacterial phyla have species that can be grown in the laboratory. The study of bacteria is known as bacteriology (Siddique & Chahal, 2011a).

Bacterial cells vary widely in sizes. A typical cell is about one-tenth of an eukaryotic cell and is of the order of a few microns. However, a few species can grow as large as a few tenths of a millimeter and are visible to the naked eye. On the other hand, some ultrasmall bacteria can be as small as a virus. They have a wide variety of shapes, ranging from rod-like (bacillus), spherical (coccus) and helical (spiral) forms. A few other species have special shapes like cuboidal and tetrahedral. Some recently discovered bacteria deep inside the earth's crust have long prismatic shapes with a star-like cross-section (Wanger, Onstott, & Southam, 2008). Several factors determine bacterial morphology and these include nutrient acquisition, surface attachment, motility and evasion from predators (Siddique & Chahal, 2011b).

In the laboratory, bacteria are grown using solid or liquid media. Solid media like Agar plates are used to grow isolated pure cultures. Liquid media are used for bulk cell volumes. In a continuously stirred liquid medium, a homogeneous suspension of cells can be cultured. The use of selective media with specifically added nutrients and antibiotics may be used to tailor particular cultures or strains (Siddique & Chahal, 2011b).

Although laboratory techniques utilize artificial growth conditions with highly controlled microenvironments and abundance of nutrients, natural growth conditions in the real world are far from perfect. To maximize their chances of growth and reproduction, several bacterial species have

evolved elaborate and complex survival strategies under conditions of nutrient depletion, stress and toxicity. Close-knit microbial colonies like biofilms are spectacular examples of this kind of an association and may be of particular importance in the process of Microbiologically Induced Calcite Precipitation (MICP) (Siddique & Chahal, 2011b).

1.1 Microbiologically Induced Calcite Precipitation

Many organisms have an ability to produce different kinds of minerals (Biomineralization). Some algae and diatoms produce silicates while some vertebrates can produce phosphates and carbonates. Prokaryotic biomineralization can be classified into two distinct categories: Biologically controlled and biologically induced (Heinz A Lowenstam, 1981; Heinz Adolf Lowenstam & Weiner, 1989). In the former mode, biominerals are formed directly at certain particular locations on or inside the cells. In the latter, biominerals are synthesized extracellularly as metabolic byproducts (Navdeep K. Dhami, Reddy, & Mukherjee, 2013).

Carbonates happen to be the most conspicuous of all minerals attributed to biomineralization. In addition, these quite often tend to be precipitated as carbonates of calcium (primarily calcites) which in turn lead to the label of Microbiologically Induced Calcite Precipitation (MICP). Hence, MICP tends to attract the most research attention from across diverse fields that include chemistry, microbiology, mineralogy, biotechnology and structural engineering. It is a promising research topic in several areas ranging from atmospheric carbon sequestration (Chafetz & Buczynski, 1992; Folk, 1993; Krumbein, 1979; Monger, Daugherty, Lindemann, & Liddell, 1991), solid-state treatment of inorganic waste (Warren, Maurice, Parmar, & Ferris, 2001), pathological mineral concretions in human patients (Keefe, 1976), extraterrestrial biological phenomena like carbonate precipitation by Martian bacteria etc. (McKay et al., 1996; Thomas-Keprta et al., 1998).

MICP is primarily governed by four key parameters: 1. Calcium concentration, 2. Concentration of dissolved inorganic carbon (DIC), 3. pH and 4. Availability of nucleation sites (Hammes et al., 2003). For MICP, calcium and carbonate ions must be present in quantities that are large enough to ensure that the magnitude of Ionic Activity Product (IAP) exceeds that of the solubility product (K_{So}). For $K_{So} > IAP$, the system is ionically supersaturated and is likely to precipitate (Morse, 1983).

MICP is believed to be a function of several parameters that might include the bacteria species, strain, cell concentration, concentration of other chemicals in the medium (like urea, calcium), pH etc. Certain characteristic features must be present in the microorganism responsible for MICP: alkalophilicity (optimum growth environment is believed to be around pH=9 with no growth around 6.5), high efficiency for ureolysis, non-pathogenicity, high negative zeta potential (De Muynck, Verbeken, De Belie, & Verstraete, 2013; Dick et al., 2006) that promotes adhesion and surface colonization, ability to produce high volumes of urease in presence of high ammonium concentration (Friedrich & Magasanik, 1977; Kaltwasser, Krämer, & Conger, 1972). These traits ensure high rates both of ureolysis and MICP (Nemati & Voordouw, 2003; Okwadha & Li, 2010a).

The set of reactions that leads to MICP is given below. Urea is a naturally occurring bio-organic compound which has a ubiquitous distribution. This urea reacts with water in the presence of urease (which acts as a catalyst and accelerates the reaction) to produce carbamic acid and ammonia gas. This urease has a microbial origin and comes from the extracellular activities of certain class of microorganisms. The carbamic acid further reacts with water to form more ammonia as well as carbonic acid. The ammonia molecules react with water to produce ammonium and hydroxyl ions. The carbonic acid in turn also hydrolyses to form protons and doubly charged carbonate ions. These carbonate ions ultimately react with positively charged metal ions (like calcium) to form solid precipitates of calcium carbonates or other metal carbonates (Navdeep Kaur Dhami, Reddy, & Mukherjee, 2013).

It is well known now that the process of MICP is much more complex than chemically induced precipitation. It is possible for a bacterial cell surface to induce non-specific mineral deposition by providing specific nucleation sites in the form of its many different embedded atoms (Ferris, Beveridge, & Fyfe, 1986). It has been conjectured that certain ions like Ca^{++}, which don't get utilized in the metabolic pathway, might accumulate external to the cell surface (Silver, Toth, & Scribner, 1975). It is also believed that individual cells produce ammonia at some point of the enzymatic ureolytic cycle which fosters an alkaline micro-environment in their immediate vicinity. Although there is no net increase in the medium pH, these localized pH hotspots act as precursor sites that trigger $CaCO_3$ precipitation. In a culture medium enriched by external additives like urea and $CaCl_2$, the biochemical reactions that lead to MICP are most likely as follows:

$CO(NH_2)_2 + H_2O \rightarrow NH_2COOH + NH_3$ (Ureolysis catalyzed by *urease*)

$NH_2COOH + H_2O \rightarrow NH_3 + H_2CO_3$

$2\ NH_3 + 2\ H_2O \rightarrow 2NH_4^+ + 2OH^-$

$H_2CO_3 \rightarrow HCO_3^- + H^+$

$HCO_3^- \rightarrow H^+ + CO_3^{2-}$

$Ca^{2+} + CO_3^{2-} \rightarrow CaCO_3 (s) \downarrow$ (Bacterial cells allegedly act as nucleating agents at this step)

$CO(NH_2)_2 + 2H_2O + Ca^{2+} \rightarrow 2NH_4^+ + CaCO_3 \downarrow$
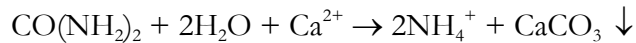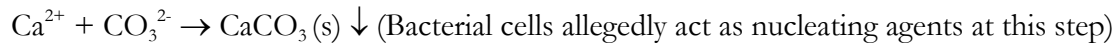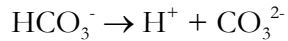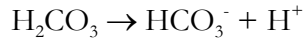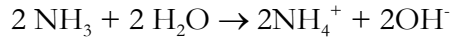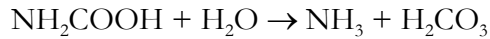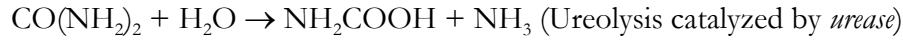
1.2 The hydrolysis of urea

Ureolysis or urea hydrolysis is the decomposition of urea into simpler substances like ammonium and carbonate ions in the presence of water molecules. At pH = 7, bicarbonate (HCO_3^-) ions are more abundant than carbonate (CO_3^{--}) ions. As they dissociate into carbonates, they release protons (H^+) into the chemical environment leading to an enhancement in pH from neutral to alkaline. This in turn induces the dissociation of ammonium (NH_4^+) ions into ammonia (NH_3). An equilibrium between the ratios of NH_4^+ / NH_3 and HCO_3^- / CO_3^{--} is reached at an optimum pH = 9.3. This is also the optimum pH for the most efficient urease activity. Urease is a very potent catalyst for ureolysis and can speed reactions upto 10^{14} times (Benini et al., 1999). Although it is a common enzyme secreted by many other bacteria, plants and yeasts; *S. pasteurii* is especially well-known for its high ureolytic activity.

As an ureolysis reaction proceeds in the forward direction, carbonate ions are continuously generated. The higher the reaction rate, the higher is the degree of supersaturation in solution, which implies a longer time lag between the termination of reaction due to urea exhaustion and the attainment of saturation or sub-saturation. Until this happens, the metastable forms (like vaterite) are more abundant in solution. As time elapses, with depleted supply of urea and drop in saturation levels, the stabler forms (like calcite) become the favored species in chemical equilibrium (Whiffin, 2004).

It has been argued elsewhere that a longer time lag, as described above, may also skew the distribution in favor of calcite over vaterite. A prolonged nucleation phase allows the formation of more smaller crystals, thus effectively enhancing the cross-sectional surface area. With more effective crystallization surfaces available, supersaturation drops quicker and recrystallization is hastened (van Paassen, 2009).

Another important parameter to consider is the migration of ions from the bulk outwards to the surface to attach to the crystal interface and cause its growth. At high ureolytic rates, more ions are produced at a given location than can be diffusively carried away. Due to this diffusive limitation, localized precipitation occurs. Amorphous $CaCO_3$ is the first to be precipitated, forming the innermost core of a nascent crystal. It is followed by metastable vaterite, which forms an intermediate layer. The outermost shell is the latest to form, and comprises of stable calcite (Söhnel and Garside, 1992). There are differences between stagnant and stirred cultures as well. A continuous movement of fluid prevents settling down or sedimentation of the crystal nuclei and delays crystallization. Nonetheless, when crystals reach a critical size of ~ 5μm, they do sediment down, often trapping bacteria cells within them, a phenomenon called 'entombment'. With the elimination of more and more viable enzyme-producing cells from solution through encapsulation and entombment, the rate of ureolysis falls. This further assists the stabilization of calcite as the more dominant form of polymorph (van Paassen, 2009).

1.3 Rate of Ureolysis

The rate of ureolysis is known to be a function of several factors like pH, temperature, cell concentration, degree of saturation etc. (Ferris, Phoenix, Fujita, & Smith, 2004). There exist multiple mathematical kinetic models to quantify ureolytic rates. Three main modeling strategies have been described in the literature. Under excess urea conditions, a simplified zeroth order model is sufficient:

$$r_{urea} = \frac{[urea]}{time} = -k_{urea}$$

where r and k denote ureolytic and kinetic rate constants, respectively. The brackets […] denote molar concentration. Clearly, the rate of ureolysis is a constant and independent of [urea].

More generally though, the rate of ureolysis would depend on [urea] and be given by a first order kinetics:

$$r_{urea} = -k_{urea}[urea]$$

Even more general rate laws have been proposed in the literature which incorporate the effects of competition from NH_4^+ ions. The resulting expression is essentially a modified Michaelis-Menten type rate law (Fidaleo & Lavecchia, 2003):

$$r_{urea} = \frac{v_{max}[urea]}{(k_m + [urea])\left(1 + \frac{[p]}{K_p}\right)}$$

Here

v_{max} = maximum rate of ureolysis,

K_m = half-saturation coefficient,

$[p]$ = concentration of ammonium, and

K_p = inhibition constant for NH_4^+ (Phillips, Gerlach, et al., 2013).

1.4 Other factors influencing MICP

It is now known that at least four different classes of microorganisms might be involved in MICP (Hammes et al., 2003; Stocks-Fischer, Galinat, & Bang, 1999a): (a) Photosynthetic microbes: algae, blue-green algae, (b) Sulfur-reducing bacteria, (c) Microorganisms utilizing organic acids and (d) Microorganisms involved in the nitrogen cycle.

Of the above four, MICP via ureolysis (a key reaction within the nitrogen-cycle involving organisms under (d)) has been most widely studied due to its simplicity. It also remains the most popular option in terms of applications of MICP to a broad spectrum of engineering problems. For bacteria falling under the last category as above, their ability to create a highly alkaline environment plays a key role in MICP. Their cell surfaces also have a vital role in ensuring precipitation. At near-neutral pH, the presence of several negatively charged groups underneath the cell membrane leads to an attraction of positive metal ions onto the surface. These metal ions sitting on the cell surface membrane mediate heterogeneous nucleation. Some examples of bacteria believed to be precipitating via this route are *Sporosarcina pasteurii*, *Pseudomonas* sp., *Variovorax* sp., *Micrococcus* sp., *Bacillus subtilis*, *Deleyahalophila*, *Halomonaseurihalina* and *Myxococcusxanthus* (Hammes et al., 2013; Stocks-Fischer, Galinat, & Bang, 1999b).

Bacterial MICP occurs via active and passive pathways. In the passive mode, metabolic processes change the bulk fluid environment and induce precipitation by shifting mineral ionic saturation. An example of this is the ureolytic pathway wherein an elevation in pH via ammonification leads the change and is relevant for *S. pasteurii* (a. B. Cunningham, Gerlach, Spangler, & Mitchell, 2009).

In the active mode, the cellular membranes act as nucleation sites. Cellular clusters attain a net electronegativity and attract positively charged metal ions like Ca^{++}, which in turn react with negative carbonate groups to precipitate into calcium carbonate (A. Kantzas et al., 1992; Wei, Liping, Long, & Longjiang, 2009). It is believed that for bacteria precipitating carbonates, the EPS of their biofilms might also be involved in MICP. The EPS matrix, being composed primarily of polysaccharides (with carboxyl, pyruvate, phosphate or sulfate side chains), exhibits gross electronegative attributes and possibly plays an important role in trapping positive ions (McConnaughey & Whelan, 1997; Siddique & Chahal, 2011b).

The individual cells of *S. pasteurii* can induce MICP by removing the kinetic barriers to $CaCO_3$ precipitation. This ability to increase the pH and $[CO_3^{2-}]$ depends on the buffering of the medium by dissolved inorganic carbon (DIC). Microbial activity in poorly buffered systems like underground aquifers is more likely to induce MICP than in well-buffered systems like freshwater lakes. When external $CaCO_3$ is sparse, nucleation of crystals is the most energetically demanding step in the process of precipitation. Organic matter like cell membranes or EPS can favor this process by lowering down the free energy barrier (Bosak, 2011). For this to happen, the interfacial energy between the cell and the crystal must be lower than the interfacial energy between the crystal and the solution. It is known that the cells are always encapsulated within a tiny water envelope. This zone creates a small chemical microenvironment in which chemical species can have concentrations very much different from that prevailing in bulk. EPS is also known to slow down ionic transport, thus creating sharper chemical potential gradients across the thin water films. This further helps in achieving higher localized concentrations and overcoming the activation energy barrier. It has also been argued that viscosity changes as a function of the EPS composition can modify advective and diffusive transport, thus leading to polymorphism (Hammes, 2002).

It has been found that rate of MICP is directly proportional to growth rate of bacteria and inversely proportional to concentration of ammonia. The rate kinetic data points of MICP have been found to fit well with a modified logistic curve of the form:

$$y = \left(\frac{a}{1 + e^{-b(x-c)}} \right) + d$$

where the rate constants were determined from a regression analysis and found to be independent of initial $[Ca^{++}]$. Here, $y=[Ca^{++}]$, a=range of variation in $[Ca^{++}]$, b=Rate constant, c=time corresponding to maximum (dy/dt) and $d=[Ca^{++}]_{t=0}$ (Parks, 2009).

		Initial Concentration of $[Ca^{++}]$ (mM)	
Rate Constant	12.6	25.2	50.4
$k_{Ammonia}$ (h^{-1})	0.76	0.77	0.72
$k_{Precipitate}$ (h^{-1})	0.1	0.1	0.13

Tab. 1.1: Rate constants for MICP by S. pasteurii at different initial concentration of CaCl$_2$
(Stocks-Fischer et al., 1999b)

Another reason which makes *S. pasteurii* especially relevant is the fact that it has a unique mechanism for the formation of ATP which couples this with production of urease. The generation of ATP is controlled by proton-motive force (Δp) which is the sum of transmembrane pH gradient (ΔpH) and the membrane potential (Δψ):

Δp = ΔpH + Δψ

This is a non-dimensional equation where the two potential terms have been normalized using a characteristic potential (Whiffin, 2004). A class of organisms pump out cellular electrons from the electron transport chain and create a chemiosmotic proton gradient. These are neutrophilic organisms and they generate ATP via this process. The effective proton concentration gradient leads to an influx of protons inside the cells and through ATP-synthesase generates ATP. Since an efflux of protons out of the cells is detrimental to ATP production, alkaliphiles like *S. pasteurii* have developed elaborate strategies to combat proton loss:

a) Alkalinisation of the cytoplasm, resulting in a reduction of ΔpH.

b) Efflux of cations other than protons, resulting in an enhancement of Δψ.

If Δψ is large enough, Δp is sufficient to drive protons into the cell in spite of low ΔpH. In *S. pasteurii*, the ions that are flushed out to increase Δψ depend upon the history of culture. In case of low urea concentrations; K^+, Na^+ and NH_4^+, all get flushed out. In case of higher concentrations, only NH_4^+ ions are involved. Interestingly, the optimum pH (9.25) for *S. pasteurii* is equal to half of the pK_a value for NH_3/NH_4^+. The schematic is shown in Fig. 1 (Whiffin, 2004).

CO(NH$_2$)$_2$

External pH 9.25
NH$_3$: NH$_4^+$
Ratio 50 : 50

①

Internal pH 8.4
NH$_3$: NH$_4^+$
Ratio 30 : 70

CO(NH$_2$)$_2$

2 H$_2$O

Urease

② = ↓ Δ pH

2 NH$_4^+$ + CO$_3^{2-}$

70% 30%

H$^+$ + NH$_3$

2 NH$_3$ + 2 H$^+$

50% 50%

NH$_4^+$

ATP

ADP + P$_i$

H$^+$

NH$_4^+$

③ = ↑ Δψ

④

H$^+$

NH$_4^+$

50% 50%

NH$_3$ + H$^+$
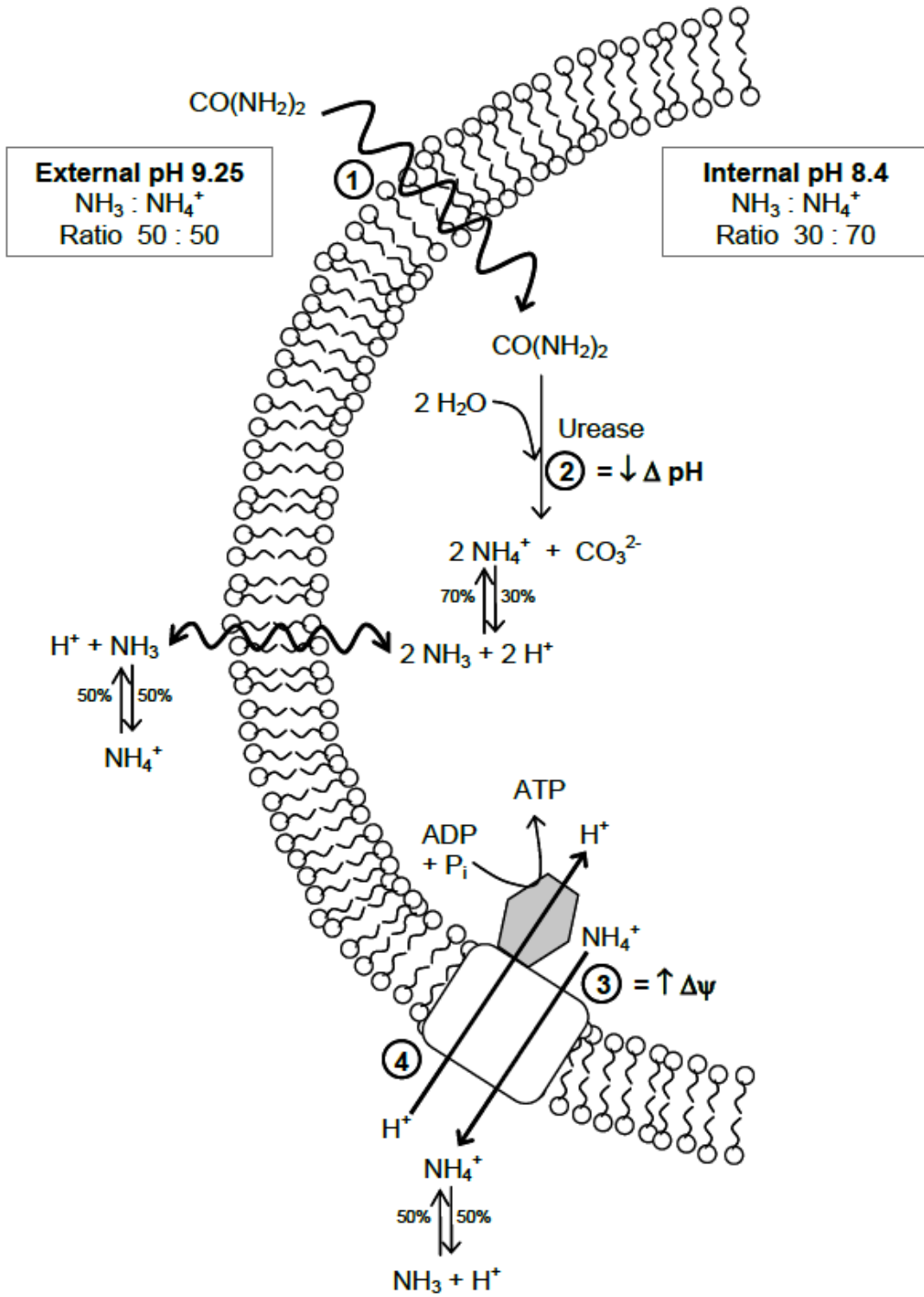
Fig. 1.1: Coupling of ATP synthesis and ureolysis in S. pasteurii (Whiffin, 2004) [*Reproduced with permission*]

10

1.5 Crystal Nucleation and Crystal Growth

The first step in a series of connected steps that lead to crystal formation is oversaturation. It's known from basic chemical equilibrium theory that precipitation occurs when the ionic product exceeds the solubility product in solution. However, insoluble precipitates don't appear until a certain degree of oversaturation or supersaturation is achieved. This is because any precipitate nuclei, if formed, are not stable until a threshold activation energy barrier has been surmounted. There is a transition process in which unstable nuclei which can re-dissolve back in solution move over the energy barrier to a point of no-return at which they are stabilized and cannot go back to the solution phase. The individual nuclei grow to form solid crystals. This process is called nucleation. Nucleation can be homogeneous and heterogeneous. As the names suggest, in homogeneous nucleation, critical nuclei are formed in solution via random atomic or ionic collisions in solution. In heterogeneous nucleation, on the other hand, there are surfaces involved which have preferential locations acting as nucleation sites. These sites have a bias to promote nucleation.

Once the nuclei attain a critical mass, they attract more and more ions form the solution. This process leads to a further reduction in free energy. This is the growth phase of the crystal, during which there is a significant gain in mass and size on the surface. It's common during this phase for various macromolecules, both organic and inorganic, to be embedded into the crystal lattice. The last step of the cycle is what's called ripening, when the small crystallites merge to form large crystals (Hammes, 2002).

1.6 The Crystalline Nature of $CaCO_3$

There are more than 60 different known carbonate minerals like magnesite ($MgCO_3$), siderite ($FeCO_3$) and dolomite ($CaMg(CO_3)_2$). Calcium carbonate or $CaCO_3$ is one of the commonest of carbonate minerals. There are 5 different polymorphous forms of $CaCO_3$: aragonite, vaterite, calcite I, calcite II and calcite III. Aragonite is the abundant precipitate in biological precipitation reactions. However, it is much more soluble than calcite I and thermodynamically less favorable. As a result, it often rearranges to calcite I. Vaterite does form under normal temperatures and pressures but is metastable. Calcites II and III, on the other hand, are synthetic forms that exist only under special artificial conditions and are not found in nature. This leaves Calcite I, very often simple called calcite, to be the predominant polymorph of $CaCO_3$. Calcite exists in many different crystal shapes as well. It can form different combinations of rhombohedrons, scalahedrons and prisms; giving rise

to more than 300 different crystal forms. These in turn permute in many different ways to give rise to thousands of variations (Hammes, 2002).

1.7 Selection basis for polymorphism

The exact mechanism of self-selection of a particular polymorphic form of $CaCO_3$ over another is unknown. However, there have been a few attempts to explain the phenomenon using the role of the organic macromolecules constituting the EPS and membrane proteins.

Hunter (1996) tried to correlate the dominant polymorph with the pattern of spacing between acid residues of surface proteins. They showed that the selective binding of proteins and polysaccharides to certain crystal faces promotes crystal growth along certain preferred axes while inhibiting it along other normal axes. Much earlier, Watabe and Wilbur (1960) had shown the formation of aragonite in mollusk shells to be a function of the protein matrix. Braissant, Verrecchia and Aragno (2002) have tried to explain the formation of vaterite over calcite in *X. autotrophicus* by introducing rheological arguments on tuning of viscosity via slime production. Kawaguchi and Decho (2002) have also reported on the relation between aragonite formation and EPS composition (Hammes, 2002).

There also exist literature which discuss the different mechanisms behind the genesis of the different forms of $CaCO_3$. The various proposed mechanisms (mono or polynuclear, linear or spiral growth etc.) are functions of many physical and chemical factors like temperature, saturation and nature of solution. In a series of papers, Kralj, Brečević and Nielsen (1990, 1994); Kralj, Brečević and Kontrec (1997) have reported that the precipitation of stable phases (like calcite) is energetically favorable at lower saturations whereas metastable forms like vaterite are more likely to be precipitated at higher supersaturation levels. It is known that aragonite is formed in the presence of Mg^{2+} ions (Berner, 1975). Also, Ikaite ($CaCO_3.6H_2O$) is found at low temperatures (Gal, Bollinger, Tolosa, & Gache, 1996).

When crystals grow beyond a threshold size, their further growth is diffusion limited. Also, since the ionic activity on the surface is lesser than what it is in the bulk liquid, the supersaturation at the surface is lower than the liquid. Once a crystal is formed, its lattice structure is not invariant. If it continues to remain in physical contact with the liquid molecules, it may dissolve back into solution and re-crystallize into a different form. Many crystals would cycle through the transitions between

metastable vaterite at high supersaturation, eventual dissolution and recrystallization as stable calcite at low saturations (van Paassen, 2009).

1.8 Biological implications of precipitation

It's not clear whether the phenomenon of MICP in itself has any biological utility or if it is an undesirable wasteful process. There exist a few hypotheses. Knorre and Krumbein (2000) reported that the phenomenon is lethal to cells. Southam (2000) provided further explanations by asserting that the mineral crystals reduce the available cross-sectional area necessary for nutrient absorption and lead to death by starvation. It is possible that some organisms use precipitation as a defense mechanism. Southam (2000) and Ferris and Beveridge (1985) have given examples of cases where localized precipitation is used to create a protective encapsulation for the continued survival of the organisms under adverse conditions (Whiffin, 2004).

1.9 Role of bacteria

It's possible that bacteria cells themselves act as nucleation sites for calcite precipitation. Stumm and Morgan (1981) conjectured that microbes catalyze crystal formation by lowering down the energy barrier. This is possible if the activation energy at the bacteria-crystal interface is lower than the activation energy at the crystal-solution interface. Being very tiny, bacteria cells have surface: volume ratios which further facilitate nucleation. The composition of the cell wall plays a huge role in dictating the interaction between a bacterium and the dissolved metal ions in an aqueous environment. Most bacteria act as if their cell walls have a net negative charge in aqueous environments. Warren *et al.* (2001) have proposed this observation using the pK_a values of the carboxyl and phosphoryl groups on the cell walls. Doubly charged metal ions (like Ca^{++}, Mg^{++}, Na^{++} etc.) have an affinity to stabilize the acidic polymeric groups on the cell membrane by binding onto the walls. This is a key initial step that triggers precipitation.

Schultze-Lam *et al.* (1996) have discussed the role of a thin water layer in precipitation. Since the Reynolds Numbers are typically very low for microbes, they are almost always enveloped within a very thin shell of water molecules, forming an aqueous microenvironment. This acts as a buffer zone which regulates the transport of ions across the layer from the external bulk chemical environment. The situation is further complicated in EPS-secreting bacteria like *S. pasteurii* where the EPS acts as an additional layer which might slow down ionic diffusion, creating localized concentration gradients

(Kawaguchi & Decho, 2002). This might modulate the saturation state of the solution and help surmount the free energy barrier (Whiffin, 2004).

There does exist an opposing point of view too regarding the role of EPS in nucleation. Stocks-Fischer, Johnna K Galinat and Bang (1999) indicated that EPS plays no role in the nucleation process and might even be detrimental to the process by restricting calcium transport. They reported that bacteria prefer to avoid precipitation because the process might be harmful to the cell health.

1.10 *Sporosarcina pasteurii*

Definitive evidence of the role of *S. pasteurii* in the process of MICP can be drawn from the XRD analyses as well as multiple electron micrographic studies undertaken by various researchers (Gollapudi, Knutson, Bang, & Islam, 1995; Zhong, Islam, & others, 1995). *S. pasteurii* cells provide nucleation sites for MICP in addition to creating an alkaline environment which further promotes precipitation.
Chemical kinetic studies have confirmed that the rate of MICP has a strong correlation with cell growth. In addition, urease also exhibits a higher efficiency in enzymatic activities as well as a better affinity for urea under high pH environment (Hammes et al., 2013).

Sporosarcina pasteurii biofilms and its associated MICP mechanism has been widely proposed as a possible tool for carbon sequestration and carbon storage inside high pressure reservoirs. There are several factors that make it impossible for other types or strains of microorganisms to facilitate similar objectives as *S. pasteurii* under drastic conditions. It is known that high pressure CO_2 dramatically reduces the number of living cells in a colony of planktonic microorganisms (Zhang et al., 2006). In particular, supercritical (SC) CO_2, due to its low viscosity and surface tension, is especially damaging to living cells because it can readily penetrate the complex protective layers. This is very much enhanced at high temperatures (due to increased membrane fluidity (Hong, Park, & Pyun, 1997)) and high pressures (due to increased solubility of CO_2 which leads to ease of access via the cell wall (Lin, Cao and Chen, 1994; Cunningham *et al.*, 2009).

On the other hand, gram-positive cells like *S. pasteurii* are much more suited to survive in extreme environments primarily because of a thick peptidoglycan cell wall that helps reduce intercellular transport and cope better with mechanical stresses. *S. pasteurii* also has the ability to sporulate and form hardy spores that can sustain long periods of impoverishment. On top, their secreted EPS

serves as an additional barrier to foreign bodies and antimicrobial agents (Costerton & Stewart, 2001; Lewandowski & Beyenal, 2013; Stewart, 2003). All the above factors make *S. pasteurii* the microbe of choice for these kinds of extreme applications (Mitchell et al., 2009a).

1.11 Advantages of using *Sporosarcina pasteurii*

S. *pasteurii* is one of the fewer urease-secreting organisms which doesn't use the enzyme solely for N_2-assimilation, its primary purpose. It is an alkaliphile and faces a challenge typical to all alkaliphiles during energy production via conversion of ADP to ATP through the attachment of protons. In neutraphiles, protons are effluxed out of the cell from the electron transport chain, creating a differential proton concentration gradient with high concentration outside the cell membrane. This gradient pumps protons inside through a specialized enzyme, ATP-synthase. However, this gradient is switched in the opposite direction under high pH, like what this bacterium thrives in. This must be overcompensated by creating an additional charge gradient realized through a mass exodus of cations from within. In S. *pasteurii*, these cations are primarily NH_4^+, which is an end-product of ureolysis. This is the primary advantage of using S. *pasteurii* (Jahns, 1996; Whiffin, 2004).

There many other good secondary reasons as well. E.g. S. *pasteurii* is one of few organisms where urease production is not downregulated in the presence of ammonium ions. It has a very high urease production capacity which is stable, consistent and is also non-toxic (bio-safety level BSL-1).

1.12 Mechanical behavior of a clogged porous medium

The extent and degree of mechanical enhancement in a porous medium after MICP is a function of many variables including the nature and distribution of precipitation inside the pore network. Ismail *et al.* (2002) have discussed the effects of reaction rates on strength. At very small reaction rates, the crystals are likely to be fewer, larger and non-uniformly distributed. At very large reaction rates, the precipitation is so fast that most crystals settle down near the inlets of the pores and cannot penetrate sufficiently deep enough, once again causing a non-uniform distribution. It's only at an optimal intermediate rate that continued nucleation and fast growth rates balance each other to create a uniform distribution of many small crystals that cause sufficient plugging of grain contact points and a significant enhancement in mechanical strength. Nonetheless, it remains impossible to quantify the mechanical enhancement in different media under different conditions because of the

existence of many additional uncontrolled variables like moisture content, mineral composition of the medium and even the mode of mechanical testing (van Paassen, 2009).

1.13 Applications of Biologically Precipitated Biominerals

1.13.1 Elimination of radioactive waste and heavy metals

Radioactive wastes and heavy metals are major sources of contamination of ground water reservoirs. The traditional techniques of using filters and biochemical treatment of the source water often fall short of the desired quality that is safe for human consumption. Recent approaches based on ureolytic bacteria capable of biomineralization have slowly gained popularity over the last decade. Broadly speaking, these bacteria trigger MICP and produce solid crystals of metal carbonates which themselves act as traps for the target undesirable waste molecules. Through competitive co-precipitation reactions, the radioactive and heavy metal waste molecules get entombed inside the resulting crystal lattice of carbonates and thus are eliminated from the bulk. This method is especially effective for removal of doubly charged heavy metal ions like Sr, which co-precipitate with Ca. An important application is the remediation of ground water.

These approaches essentially substitute Ca ions inside the carbonate crystals with their heavier counterparts, forming less soluble heavy metal carbonates that often succeed in eliminating as high as 95% of all contamination.

Contamination of soil by metal ions is an especially tricky problem for various reasons. Metal ions adsorb strongly onto soil and are hard to remove. There exist a few conventional technologies for removal of toxic metals from soil viz. in situ vitrification, excavation and confinement inside hazmat containments, chemical fixatives, asphalt treatment, chemical leaching, phytoremediation and bioremediation using highly metal-resistant bacteria. However, all these solutions suffer from serious drawbacks like high cost and destruction of soil fertility. MICP has recently been identified as a promising option that significantly eliminates most of the negatives. New research over the last decade has focused on the potential of MICP to eliminate various toxins like Arsenic (Varenyam Achal, Pan, Fu, & Zhang, 2012), Copper (Varenyam Achal et al., 2012), Lead, Cadmium, Zinc, Nickel and Chromium (Kurmaç, 2009) etc.

1.13.2. **Treatment for complex organics and lighter metals**

MICP has a bright future in the field of treatment of complex organic compounds like polychlorinated biphenyls (PCBs). While there are traditional options like hydro and sandblasting followed by epoxy encapsulation as well as washing with solvents, they remain ineffective in the long-term due to oil resurfacing. Okwadha and Li (2010b) have reported the possibility of using *S. pasteurii* to treat PCB-rich oils.

Another major problem widespread in domestic water supply systems is that of high calcium concentration. This causes issues like scaling of interior surfaces of pipelines and deposition of calcium precipitates like carbonates and gypsum. Hammes and Verstraete (2002) have investigated the application of MICP to treat Ca-rich industrial wastewater via addition of low concentrations of urea. An efficiency as high as 90% was reported.

1.13.3. CO$_2$ Sequestration

Massive natural mineral deposits of carbon have existed on our planet for millions of years. Inspired by these huge reserves of carbon both on land and in the sea, scientists have designed strategies to synthetically capture carbon from the atmosphere and help mitigate global warming. The central idea is to convert free atmospheric carbon into mineral forms like calcite, magnesite and dolomite. These forms are much more convenient to store inside containments and are also safer than gases stored under high pressures. Additionally, they are stable and benign. The proposed storage locations range from natural structures like underground geologic aquifers to abandoned mines with large void spaces underneath.

However, for this strategy to work properly, one must ensure a reliable sealing mechanism that prevents the escapement of the stored contents due to compromised integrity of the well-bore or rise in cap rock permeability. This is where MICP has a wide range of applications in what has been called underground carbon capture and sequestration (CCS). Essentially, enhanced carbon capture is realized by increasing the volume of dissolved CO$_2$ in the forms of carbonates and bicarbonates in water and also by the precipitation of carbonates in solid form.

Key applications of MICP in CCS technology range from protection of reservoir cement wall from supercritical CO$_2$ (A. B. Cunningham, Gerlach, Spangler, & Mitchell, 2009), plugging microscale fractures to prevent the rise of cap rock permeability (Phillips, Lauchnor, et al., 2013), fixation of

gaseous CO_2 by transforming it into solid forms via mineral trapping (Dupraz, Parmentier, Ménez, & Guyot, 2009), using the extracellular enzyme carbonic anhydrase (CA) to convert free carbon into $CaCO_3$ (Kupriyanova et al., 2007) and use of cyanobacteria for point-source CCS (Jansson & Northen, 2010).

1.13.4. **Biogrouting**

Quite often, the natural mechanical properties of soil in its native state are not good enough for the intended engineering application. Engineers in these cases resort to artificial enhancement of the requisite mechanical properties through injection of various chemicals via specially drilled wells. This is called chemical grouting and has many intrinsic disadvantages including high cost, inconvenience and adverse environmental effects. The new green alternative is called biogrouting.

Biogrouting is an on-demand in situ soil strengthening technique where the desired outcome is achieved by mimicking real biogeochemical processes in pinpointed geospatial locations. This is carried out by injecting relatively smaller volumes of biological reagents and catalysts (enzymes) that trigger a specific biochemical reaction that produces as end products certain target chemicals with properties of choice. Several strains of ureolytic bacteria and their associated MICP have attracted especial interest in recent years.

Some of the newer findings (Kantzas *et al.*, 1992) have reported a reduction in porosity by 50% and permeability by 90% post-treatment mediated by *S. pasteurii*. Other studies have discussed enhancement in strength of packed sand columns due to carbonate precipitation (Kantzas *et al.*, 1992; Whiffin, 2004; de Jong *et al.*, 2007). It is now known that the mechanism behind the increase in strength is primarily due to small calcite micro-bridges that form between grains of sand and arrest their relative movement by particle interlocking, thus increasing the net stiffness. This phenomenon doesn't lead to a change in permeability.

Some species of ureolytic bacteria isolated from sands found in tropical beaches are known to improve the shear strength of soils via MICP (Chu, 2005). Elsewhere, several bacilli bacteria have successfully been used to seal sand embankments (Stabnikov, Naeimi, Ivanov, & Chu, 2011). The researchers were able to achieve near-perfect impermeability to massively reduce seepage rate in a sand column by successive percolation treatment with high concentrations of calcium and urea.

Another application of MICP discussed recently is the suppression of dust using ureolytic bacteria (Bang, Galinat, & Ramakrishnan, 2001).

1.13.5. **Enhancement of compressive strength in cementitious materials**

There has been a multitude of research studies on the use of biomineralization for treating cementitious materials like cement, mortar and concrete with various different microbial agents. In one particular study, concrete was made resistant towards elements like free-thaw cycles, alkaline environments and thermal shrinkage using bacteria (Bang & Ramakrishnan, 2001). In another study, *B. sphaericus* cells were used to produce mortar that exhibits superior properties (De Muynck, De Belie, & Verstraete, 2010). In yet another study, the researchers were able to treat concrete cubes with *S. pasteurii* and reduce water penetration from surface to bulk (Varenyam Achal, Mukerjee, & Sudhakara Reddy, 2013).

1.13.6. **Management of marble structures**

MICP has been a popular option to modify various stone structures including those of limestone and increase their durability by tuning their permeation properties. *M. xanthus* has been used to induce carbonate, phosphate and sulfate precipitation inside a wide range of porous media (Rodriguez-Navarro, Rodriguez-Gallego, Chekroun, & Gonzalez-Munoz, 2003). *B. subtilis* and *Micrococcus sp.* have been used to consolidate Pietra di Lecce bioclastic limestones (Tiano, Biagiotti, & Mastromei, 1999). Cappitelli *et al.* (2006) have suggested using carbogels as a delivery agent for bacteria onto limestone masonry structures.

1.13.7. **Heritage structure conservation**

Environmental pollution has been taking its toll on several buildings of historic and archaeological importance. The various physical, chemical and biological components present in polluted air cause long-term damage to sculptures, paintings and frescos in important heritage sites. To exemplify, in Lascaux, France a widespread case of fungal infection by the mold *Fusarium* caused a continuous surface coverage on the art of the chamber decorations (Rosenbaum, 2006).

Other instances of art under threat from microbial precipitations include the famous Altamira cave system in Spain and the early Christian paintings on Russian catacomb walls. All these are being tackled by MICP-based approaches where the induced precipitate serves as an antidote to the causal

agent behind deterioration. Webster and May have successfully eliminated black sulfur crusts from decorative surfaces using *Desulfovibrio desulfuricans* and *D. vulgaris*. Garcia-Vallès *et al.* (1997) have managed to biologically induce an oxalate patina coating on the desired stone surface for protective purposes. *Shewanella oneidensis* has also been successfully used to suppress the rate of limestone dissolution in marble structures (Lüttge & Conrad, 2004).

1.13.8. Biobricks and Green Construction

There is a massive carbon footprint associated with the construction industry. Every step that goes into building a house demands a lot of energy and creates a lot of pollution. MICP can help mitigate this in two ways.

The first option is to replace conventional cement, mortar and concrete with low-energy alternatives, which are composed of greener ingredients. However, they are currently not as strong as their traditional counterparts in terms of mechanical properties like compressive strengths. MICP can be the key player here by acting as a strength-enhancing agent that works by targeted biodeposition of select chemicals (Reddy & Jagadish, 2003).

The other more ingenuous option is to completely get away with classical bricks as we know today and 'grow' biological bricks or biobricks from scratch. As opposed to firing bricks in conventional kilns, a biobrick can be grown in the lab-scale akin to a microbial culture in a Petri dish. Several start-ups have come up around this idea already, more notably bioMASON.

1.13.9. Renovation of sandstone structures

A smart and green solution to management of sandstone structures has emerged through MICP. Roughly, this suite of techniques works through a general strategy where a special mixture is sprayed onto the affected surface. This mixture usually consists of an ureolytic bacteria and a recipe for nutrients along with a source of Calcium. This sprayed layer is regularly provided with a 'nutrient shower' at periodic intervals until sufficient precipitation has been obtained which is enough to achieve the desired enhancement in strength. Upscaling trials of this technology have shown good promise and have led to several patents (Adolphe, Loubière, Paradas, & Soleilhavoup, 1990; Castanier, Le Métayer-Levrel, & Perthuisot, 1999; Le Metayer-Levrel, Castanier, Orial, Loubiere, & Perthuisot, 1999).

A related but different patented application concerns with a biological cement or a bio-mortar for managing larger fractures. The main difference lies with the fact that the mixture of bacteria and nutrients is a finely divided solid powder instead of a liquid. This solid powder is mixed with finely ground limestone, sand grains and additional external particles (chemical pigments) responsible for imparting aesthetic properties like color or gloss (Castanier et al., 1999; Le Metayer-Levrel et al., 1999; Heinz Adolf Lowenstam et al., 2011).

1.14 Open Questions

Understanding and simulating the fluid flow and transport processes behind MICP inside micro-scale porous media are highly challenging. This is due to the existence of a large number of physical and chemical variables.

Until now, a majority of research in MICP inside micro-scale porous media has been experimental. Plugging of pores as a result of accumulation of biomass and other complex colloid-like biological substances has been studied by various groups. A few other studies have been concerned with the interrelationships between such biophysical aspects as biofilm formation and surface chemistry, cell adhesion and surface topography, fluid properties and colonization etc. (Stoner et al., 2005).

In spite of all these advancements, several open questions regarding the biochemical and biophysical aspects of MICP still remain unanswered:

1) No quantitative relations exist in the literature between MICP and thermodynamic variables like temperature, pressure and chemical potential of a system. Even the effects of such variables as cell concentration of culture, extent of external enrichment and material substrate are not well-understood.

2) The reasons behind the occurrence or otherwise of a particular polymorph of the precipitated chemical is not yet known. It is still unknown how and why does a particular polymorphous form of the precipitate (carbonate) get chosen and whether there exists a thermodynamic basis to this self-selection. It is hypothesized that the morphology and phase of the carbonate molecules might depend on saturation index, pH, temperature as well as the ratio $[Ca^{2+}]/[CO_3^{2-}]$. The saturation index is defined as $SI=\log(IAP/K_s)$ and precipitation is believed to be triggered only at SI>1 (Mitchell & Ferris, 2005). Engineers are more interested in the precipitation of calcite which is durable and

coherent. However, often this is not possible to achieve due the associated formation of vaterite, which is metastable and more soluble (Rodriguez-Navarro et al., 2003). An ability to understand and manipulate the occurrence of the different polymorphs would have deep consequences for a multitude of engineering applications (Okwadha & Li, 2010a).

3) The role of an enzyme, carbonic anhydrase (CA) remains a mystery. Apart from urease, this enzyme is believed to be critical to the process of MICP. CA plays a key role in the process of interconversion between CO_2 and HCO_3. CAs have a wide distribution and play roles in almost all biochemical cycles involving carbon dioxide and carbonic acid. This includes regulation of cellular pH and acid-base transport. It is also central to several eukaryotic physiological processes like photosynthesis, ionic balance and respiration. The relationships between CA and the phenomena of biocalcification/biomineralization have been studied in connection with eukaryotic life forms like molluscs and certain marine invertebrates (Smith & Ferry, 2000). Only recently has its role in similar prokaryotic processes been recognized. For bacteria, CA is suspected to have important roles and might well be a key piece of puzzle in the biochemistry of MICP (Varenyam Achal & Pan, 2011).

4) The exact reasons behind the phenomenon of MICP are still unclear. The exact location where the process materializes also continues to be debated. It is believed that MICP might be a natural or an accidental unwanted by-product of metabolic processes (Rivadeneyra *et al.*, 1994; Douglas and Beveridge, 1998; Castanier, Le Métayer-Levrel and Perthuisot, 1999; Lian *et al.*, 2006; Montoya, 2012).

1.15 Organization of the thesis

This is a paper-based thesis with five chapters. The present chapter (Chapter 1) acts as the introduction and discusses the context, motivation and challenges associated with the general problem. The next three chapters are based on three journal papers that have been written based on the results of the research:

Chapter 2 describes the detailed protocol to culture the bacterium of interest, *Sporosarcina pasteurii*. Although there exist previously reported culture protocols in literature, we describe in detail the exact methodology to properly enrich a culture with external additives and accelerate controlled precipitation. This is a key step in the bigger scheme of the overall research and sets the stage for a

variety of experiments to follow. The protocol developed and reported is new for two reasons:

1. This is the first protocol that standardized the enrichment of a regular *S. Pasteurii* culture via the addition of external reagents.
2. This protocol significantly accelerates the formation of crystals. Most data reported in the thesis are newer than 5 days or less. This is important for the success of any large-scale bioremediation technology that depends on MICP as the source of calcite.

Lastly, this protocol is highly repeatable and less sensitive to thermodynamic variables like temperature and pressure than older protocols like the ones recommended by ATCC. One of the important features of this protocol is the guaranteed induction of calcite precipitation within a short period of time if all procedures are followed carefully. While most preexisting protocols for culture of *S. pasteurii* focus on the cell growth itself, this work instead ensures the generation of a significant mass of solid precipitation that can be potentially used to clog pores.

Chapter 3 addresses the question of MICP from several physical, chemical and biological perspectives. We investigate the formation of micro and nano-scale crystals inside a semi-solid culture platform that provides us with a powerful tool to study various aspects of the formation, transport and distribution of precipitated chemicals inside the porous matrix. We have drawn two important conclusions in this chapter that address the open question on the genesis of MICP and its location on the cell. Firstly, we have shown that *S. pasteurii* induces the formation of nanoscale $CaCO_3$ crystals on its cell membranes. This assertion has been supported with microscopy and characterization. Secondly, we have also provided evidence that the bacteria use powered flagellar mode of locomotion to move inside a porous medium and don't rely on diffusion alone. This claim has been backed up with electron micrographs that show flagella and also a mathematical analysis of cellular motility using the Stokes-Einstein equation.

Chapter 4 attempts to quantify the enhancement in mechanical properties of a model porous medium as a result of being treated with *S. pasteurii* and the subsequent MICP. A full suite of experiments including micro-CT scans, multi-mode microscopy and compression tests capture different aspects of the effects of MICP on the mechanical strength of the porous medium. We have tried answering three main questions in this chapter. Firstly, we have quantified the nature of distribution of crystal and pore sizes, respectively. Secondly, we have quantified the reduction in porosity resulting from MICP inside a representative porous medium and shown a decrement of 3

times. Lastly, we have also quantified the enhancement in mechanical strength post-MICP and measured the increment in compressive Young's moduli to be 5 times. These data have been supported by X-ray micro-computed tomography and quasi-static load test data.

The concluding Chapter 5 summarizes the results, findings and conclusions of each chapter as well as outlines directions for future research.

For this work, two different porous medium mimics have been used. They capture different sets of physics associated with MICP. For Chapter 3, it is a semi-solid agar medium. The semi-solid agar platform is a 'stabbed' culture where an inoculation loop is used to 'poke' the agar gel and transfer a small mass of bacteria along the central axis of the cylindrical volume. Due to their intrinsic motility and the availability of a connected pore network, the cells travel radially outwards and branch out to the form the *tree-like* pattern seen in the figure. As they move, they leave behind tiny calcite microcrystals which show up as white trails against the yellow background. This process continues for 2-4 days and can be seen in progress with a naked eye examination at regular intervals. This is very different from a standard agar culture which tends to be done inside petri dishes. The novelty lies with an enhanced mobility (by reducing the agar content) and a vertical orientation that allows visualization of cell penetration.

In Chapter 4, commercial sponge blocks have been used as porous media mimics. Commercial sponge blocks were selected on the basis of a few different reasons:

    (i)   Existence of multiple length scales (described in details in Chapter 3),

    (ii) Relative non-reactivity with the culture reagents,

    (iii) Ease of procurement due to commercial availability and

    (iv) Consistency of physical properties across individual samples.

Additionally, it has been clearly shown in Chapter 3, through EM images, that there exist a decade of length scales in a sponge block. Big pores lead to small pores in a continuous tiered hierarchy and the characteristic length scale away from the surface is of the order of microns. This value is very close to those of structural material like geologic rocks, sandstone and clay in ground-based systems. Another additional motivation lies with the fact that the present research ultimately aims at an underground carbon capture technology that could use MICP for storing greenhouse gases underneath the soil substratum inside natural reservoirs which are inherently porous. In this spirit,

the sponge block nicely mimic fluid transport inside real soil-based porous media like clay, sand and stones.

Last but not the least, the effect of chemistry in MICP would be complex and interesting. Nonetheless, its effect is quite mild at the short time scales under investigation here. Our operating philosophy is quite simple: given a porous media, generate enough solid powder that is sufficient to cause enough pore blockage that in turn leads to a sufficient gain in strength.

As long as the bacteria population thrives inside the pore network for the critical period of time (~ 5 days), we're guaranteed to have precipitation above the threshold value required to cause clogging. *S. pasteurii* being an extremophile can survive most adverse conditions for about a week and its activity inside a synthetic sponge network is not much different from its migration inside a rock fracture, for example.

References

Achal, V., Mukerjee, A., & Sudhakara Reddy, M. (2013). Biogenic treatment improves the durability and remediates the cracks of concrete structures. *Construction and Building Materials*, *48*, 1–5. https://doi.org/10.1016/j.conbuildmat.2013.06.061

Achal, V., Mukherjee, a, Basu, P. C., & Reddy, M. S. (2009). Strain improvement of Sporosarcina pasteurii for enhanced urease and calcite production. *Journal of Industrial Microbiology & Biotechnology*, *36*(7), 981–988. https://doi.org/10.1007/s10295-009-0578-z

Achal, V., & Pan, X. (2011). Characterization of urease and carbonic anhydrase producing bacteria and their role in calcite precipitation. *Current Microbiology*, *62*(3), 894–902. https://doi.org/10.1007/s00284-010-9801-4

Achal, V., Pan, X., Fu, Q., & Zhang, D. (2012). Biomineralization based remediation of As(III) contaminated soil by Sporosarcina ginsengisoli. *Journal of Hazardous Materials*, *201–202*, 178–184. https://doi.org/10.1016/j.jhazmat.2011.11.067

Adolphe, J. P., Loubière, J. F., Paradas, J., & Soleilhavoup, F. (1990). Procédé de traitement biologique d'une surface artificielle. *European Patent 90400G97. 0*, *1989*.

Al Qabany, A., Soga, K., & Santamarina, C. (2012). Factors Affecting Efficiency of Microbially

Induced Calcite Precipitation. *Journal of Geotechnical and Geoenvironmental Engineering, 138*(8), 992–1001. https://doi.org/10.1061/(ASCE)GT.1943-5606.0000666

Anbu, P., Kang, C.-H., Shin, Y.-J., & So, J.-S. (2016). Formations of calcium carbonate minerals by bacteria and its multiple applications. *Springerplus, 5*(1), 250.

Arias, J. L., & Fernández, M. S. (2008). Polysaccharides and proteoglycans in calcium carbonate-based biomineralization. *Chemical Reviews, 108*(11), 4475–4482.

Bang, S. S., Galinat, J. K., & Ramakrishnan, V. (2001). Calcite precipitation induced by polyurethane-immobilized Bacillus pasteurii. *Enzyme and Microbial Technology, 28*(4–5), 404–409.

Bang, S. S., & Ramakrishnan, V. (2001). Microbiologically-enhanced crack remediation (MECR). In *proceedings of the international symposium on industrial application of microbial genomes* (Vol. 20, pp. 3–13).

Benini, S., Rypniewski, W. R., Wilson, K. S., Miletti, S., Ciurli, S., & Mangani, S. (1999). A new proposal for urease mechanism based on the crystal structures of the native and inhibited enzyme from Bacillus pasteurii: why urea hydrolysis costs two nickels. *Structure, 7*(2), 205–216.

Berner, R. A. (1975). The role of magnesium in the crystal growth of calcite and aragonite from sea water. *Geochimica et Cosmochimica Acta, 39*(4), 489IN3495--494504.

Bhaduri, S., Debnath, N., Mitra, S., Liu, Y., & Kumar, A. (2016). Microbiologically induced calcite precipitation mediated by sporosarcina pasteurii. *Journal of Visualized Experiments, 2016*(110). https://doi.org/10.3791/53253

bioMASON. (2018). No Title. Retrieved January 2, 2018, from www.biomason.com

Bosak, T. (2011). Calcite precipitation, microbially induced. In *Encyclopedia of Geobiology* (pp. 223–227). Springer.

Braissant, O., Verrecchia, E. P., & Aragno, M. (2002). Is the contribution of bacteria to terrestrial carbon budget greatly underestimated? *Naturwissenschaften, 89*(8), 366–370.

Bray, J. M., Lauchnor, E. G., Redden, G. D., Gerlach, R., Fujita, Y., Codd, S. L., & Seymour, J. D. (2017). Impact of Mineral Precipitation on Flow and Mixing in Porous Media Determined by Microcomputed Tomography and MRI. *Environmental Science & Technology, 51*(3), 1562–1569.

https://doi.org/10.1021/acs.est.6b02999

Bundeleva, I. A., Shirokova, L. S., Bénézeth, P., Pokrovsky, O. S., Kompantseva, E. I., & Balor, S. (2012). Calcium carbonate precipitation by anoxygenic phototrophic bacteria. *Chemical Geology*, *291*, 116–131.

Camesano, T. A., & Logan, B. E. (1998). Influence of fluid velocity and cell concentration on the transport of motile and nonmotile bacteria in porous media. *Environmental Science and Technology*. https://doi.org/10.1021/es970996m

Cappitelli, F., Zanardini, E., Ranalli, G., Mello, E., Daffonchio, D., & Sorlini, C. (2006). Improved methodology for bioremoval of black crusts on historical stone artworks by use of sulfate-reducing bacteria. *Applied and Environmental Microbiology*, *72*(5), 3733–3737.

Castanier, S., Le Métayer-Levrel, G., & Perthuisot, J.-P. (1999). Ca-carbonates precipitation and limestone genesis—the microbiogeologist point of view. *Sedimentary Geology*, *126*(1–4), 9–23.

Chafetz, H. S. (1986). Marine peloids: a product of bacterially induced precipitation of calcite. *Journal of Sedimentary Research*, *56*(6).

Chafetz, H. S., & Buczynski, C. (1992). Bacterially induced lithification of microbial mats. *Palaios*, 277–293.

Chu, K. T. (2005). by.

Chunxiang, Q., Jianyun, W., Ruixing, W., & Liang, C. (2009). Corrosion protection of cement-based building materials by surface deposition of CaCO3 by Bacillus pasteurii. *Materials Science and Engineering: C*, *29*(4), 1273–1280.

Costerton, J. W., & Stewart, P. S. (2001). Battling biofilms. *Scientific American*, *285*(1), 74–81.

Cunningham, A. B., & Gerlach, R. (2010). Microbially Enhanced Carbon Capture and Storage by Mineral-Trapping and, *44*(13), 5270–5276.

Cunningham, A. B., Gerlach, R., Spangler, L., & Mitchell, A. C. (2009). Microbially enhanced geologic containment of sequestered supercritical CO2. *Energy Procedia*, *1*(1), 3245–3252.

Cunningham, a. B., Gerlach, R., Spangler, L., & Mitchell, a. C. (2009). Microbially enhanced

geologic containment of sequestered supercritical CO2. *Energy Procedia*, *1*(1), 3245–3252. https://doi.org/10.1016/j.egypro.2009.02.109

Cunningham, a. B., Gerlach, R., Spangler, L., Mitchell, a. C., Parks, S., & Phillips, a. (2011). Reducing the risk of well bore leakage of CO2 using engineered biomineralization barriers. *Energy Procedia*, *4*, 5178–5185. https://doi.org/10.1016/j.egypro.2011.02.495

Cuthbert, M. O., Riley, M. S., Handley-Sidhu, S., Renshaw, J. C., Tobler, D. J., Phoenix, V. R., & Mackay, R. (2012). Controls on the rate of ureolysis and the morphology of carbonate precipitated by S. Pasteurii biofilms and limits due to bacterial encapsulation. *Ecological Engineering*, *41*, 32–40. https://doi.org/10.1016/j.ecoleng.2012.01.008

De Muynck, W., De Belie, N., & Verstraete, W. (2010). Microbial carbonate precipitation in construction materials: A review. *Ecological Engineering*, *36*(2), 118–136. https://doi.org/10.1016/j.ecoleng.2009.02.006

De Muynck, W., Verbeken, K., De Belie, N., & Verstraete, W. (2013). Influence of temperature on the effectiveness of a biogenic carbonate surface treatment for limestone conservation. *Applied Microbiology and Biotechnology*, *97*(3), 1335–1347.

Demény, A., Németh, P., Czuppon, G., Leél-\HOssy, S., Szabó, M., Judik, K., … Stieber, J. (2016). Formation of amorphous calcium carbonate in caves and its implications for speleothem research. *Scientific Reports*, *6*, 39602.

der Heide, P. (2011). *X-ray photoelectron spectroscopy: an introduction to principles and practices*. John Wiley & Sons.

Dhami, N. K., Reddy, M. S., & Mukherjee, A. (2013). Bacillus megaterium mediated mineralization of calcium carbonate as biogenic surface treatment of green building materials. *World Journal of Microbiology and Biotechnology*, *29*(12), 2397–2406. https://doi.org/10.1007/s11274-013-1408-z

Dhami, N. K., Reddy, M. S., & Mukherjee, M. S. (2013). Biomineralization of calcium carbonates and their engineered applications: A review. *Frontiers in Microbiology*, *4*(OCT), 1–13. https://doi.org/10.3389/fmicb.2013.00314

Dick, J., De Windt, W., De Graef, B., Saveyn, H., der Meeren, P., De Belie, N., & Verstraete, W.

(2006). Bio-deposition of a calcium carbonate layer on degraded limestone by Bacillus species. *Biodegradation*, *17*(4), 357–367.

Douglas, S., & Beveridge, T. J. (1998). Mineral formation by bacteria in natural microbial communities. *FEMS Microbiology Ecology*, *26*(2), 79–88.

Duffy, K. J., Cummings, P. T., & Ford, R. M. (1995). Random walk calculations for bacterial migration in porous media. *Biophysical Journal*, *68*(3), 800–806. https://doi.org/10.1016/S0006-3495(95)80256-0

Dupraz, S., Parmentier, M., Ménez, B., & Guyot, F. (2009). Experimental and numerical modeling of bacterially induced pH increase and calcite precipitation in saline aquifers. *Chemical Geology*, *265*(1–2), 44–53. https://doi.org/10.1016/j.chemgeo.2009.05.003

Ehrlich, H. L. (1996). How microbes influence mineral growth and dissolution. *Chemical Geology*, *132*(1–4), 5–9.

Ehrlich, H. L. (1998). Geomicrobiology: its significance for geology. *Earth-Science Reviews*, *45*(1–2), 45–60.

Ferris, F. G., & Beveridge, T. J. (1985). Functions of bacterial cell surface structures. *BioScience*, *35*(3), 172–177.

Ferris, F. G., Beveridge, T. J., & Fyfe, W. S. (1986). Iron-silica crystallite nucleation by bacteria in a geothermal sediment. *Nature*, *320*(6063), 609–611.

Ferris, F. G., Phoenix, V., Fujita, Y., & Smith, R. W. (2004). Kinetics of calcite precipitation induced by ureolytic bacteria at 10 to 20 C in artificial groundwater. *Geochimica et Cosmochimica Acta*, *68*(8), 1701–1710.

Fidaleo, M., & Lavecchia, R. (2003). Kinetic study of enzymatic urea hydrolysis in the pH range 4-9. *Chemical and Biochemical Engineering Quarterly*, *17*(4), 311–318.

Folk, R. L. (1993). SEM imaging of bacteria and nannobacteria in carbonate sediments and rocks. *Journal of Sedimentary Research*, *63*(5).

Fontes, D. E., Mills, A. L., Hornberger, G. M., & Herman, J. S. (1991). Physical and Chemical

Factors Influencing Transport of Microorganisms through Porous Media. *APPLIED AND ENVIRONMENTAL MICROBIOLOGY*, *57*(9), 2473–2481.

Friedrich, B., & Magasanik, B. (1977). Urease of Klebsiella aerogenes: control of its synthesis by glutamine synthetase. *Journal of Bacteriology*, *131*(2), 446–452.

Gal, J.-Y., Bollinger, J.-C., Tolosa, H., & Gache, N. (1996). Calcium carbonate solubility: a reappraisal of scale formation and inhibition. *Talanta*, *43*(9), 1497–1509.

Ganendra, G., De Muynck, W., Ho, A., Arvaniti, E. C., Hosseinkhani, B., Ramos, J. A., … Boon, N. (2014). Formate oxidation-driven calcium carbonate precipitation by Methylocystis parvus OBBP. *Applied and Environmental Microbiology*, *80*(15), 4659–4667.

Garcia-Vallès, M., Vendrell-Saz, M., Krumbein, W. E., & Urz\`\i, C. (1997). Coloured mineral coatings on monument surfaces as a result of biomineralization: the case of the Tarragona cathedral (Catalonia). *Applied Geochemistry*, *12*(3), 255–266.

Ghashghaei, S., & Emtiazi, G. (2013). Production of calcite nanocrystal by a urease-positive strain of enterobacter ludwigii and study of its structure by SEM. *Current Microbiology*, *67*(4), 406–413. https://doi.org/10.1007/s00284-013-0379-5

Gibson, T. (1934). An Investigation of the Bacillus Pasteuri Group: II. Special Physiology of the Organisms. *Journal of Bacteriology*, *28*(3), 313.

Gollapudi, U. K., Knutson, C. L., Bang, S. S., & Islam, M. R. (1995). A new method for controlling leaching through permeable channels. *Chemosphere*, *30*(4), 695–705.

Gorospe, C. M., Han, S.-H., Kim, S.-G., Park, J.-Y., Kang, C.-H., Jeong, J.-H., & So, J.-S. (2013). Effects of different calcium salts on calcium carbonate crystal formation by Sporosarcina pasteurii KCTC 3558. *Biotechnology and Bioprocess Engineering*, *18*(5), 903–908.

Greenfield, L. J. (1963). Metabolism and concentration of calcium and magnesium and precipitation of calcium carbonate by a marine bacterium. *Annals of the New York Academy of Sciences*, *109*(1), 23–45.

Hammes, F. (2002). *Ureolytic microbial calcium carbonate precipitation*. Ph. D. Thesis, Ghent University, Ghent.

Hammes, F. (2003). UREOLYTIC MICROBIAL CALCIUM CARBONATE PRECIPITATION UREOLYTISCHE MICROBIELE CALCIUMCARBONAAT- door. *Scanning Electron Microscopy*.

Hammes, F., Arnold, J., Krupka, K. M., Cantrell, K. J., McGrail, B. P., Tagliaferri, F., … Gerlach, R. (2013). Calcium carbonate precipitation by different bacterial strains. *Ecological Engineering*, *36*(3), 172. https://doi.org/http://researchrepository.murdoch.edu.au/399/2/02Whole.pdf

Hammes, F., Boon, N., De Villiers, J., Verstraete, W., Siciliano, S. D., & Villiers, J. De. (2003). Strain-Specific Ureolytic Microbial Calcium Carbonate Precipitation Strain-Specific Ureolytic Microbial Calcium Carbonate Precipitation. *Applied and Environmental Microbiology*, *69*(8), 4901–4909. https://doi.org/10.1128/AEM.69.8.4901

Hammes, F., & Verstraete, W. (2002). Key roles of pH and calcium metabolism in microbial carbonate precipitation. *Reviews in Environmental Science and Biotechnology*, *1*(1), 3–7.

Hong, S.-I., Park, W.-S., & Pyun, Y.-R. (1997). Inactivation ofLactobacillussp. fromKimchiby High Pressure Carbon Dioxide. *LWT-Food Science and Technology*, *30*(7), 681–685.

Hunter, G. K. (1996). Interfacial aspects of biomineralization. *Current Opinion in Solid State and Materials Science*, *1*(3), 430–435.

Ismail, M. A., Joer, H. A., Randolph, M. F., & Meritt, A. (2002). Cementation of porous materials using calcite. *Geotechnique*, *52*(5), 313–324.

Jahns, T. (1996). Ammonium/urea-dependent generation of a proton electrochemical potential and synthesis of ATP in Bacillus pasteurii. *Journal of Bacteriology*, *178*(2), 403–409.

Jansson, C., & Northen, T. (2010). Calcifying cyanobacteria—the potential of biomineralization for carbon capture and storage. *Current Opinion in Biotechnology*, *21*(3), 365–371.

Jonkers, H. M., Thijssen, A., Muyzer, G., Copuroglu, O., & Schlangen, E. (2010). Application of bacteria as self-healing agent for the development of sustainable concrete. *Ecological Engineering*, *36*(2), 230–235. https://doi.org/10.1016/j.ecoleng.2008.12.036

Kaltwasser, H., Krämer, J., & Conger, W. R. (1972). Control of urease formation in certain aerobic bacteria. *Archiv Für Mikrobiologie*, *81*(2), 178–196.

Kantzas, A., Stehmeier, L., Marentette, D. F., Ferris, F. G., Jha, K. N., Maurits, F. M., & others. (1992). A novel method of sand consolidation through bacteriogenic mineral plugging. In *Annual Technical Meeting.*

Kantzas, a, Stehmeier, L., Marentette, D. F., Ferris, F. G., Jha, K. N., & Mourits, F. M. (1992). A Novel Method of Sand Consolidation Through Bacteriogenic Mineral Plugging. *43rd Annual Technical Meeting, Petroleum Society of CIM, CIM 92-46*(Cim), 1–15. https://doi.org/10.2118/92-46

Kawaguchi, T., & Decho, A. W. (2002). A laboratory investigation of cyanobacterial extracellular polymeric secretions (EPS) in influencing CaCO 3 polymorphism. *Journal of Crystal Growth*, *240*(1), 230–235.

Keefe, W. E. (1976). Formation of crystalline deposits by several genera of the family Enterobacteriaceae. *Infection and Immunity*, *14*(2), 590–592.

Knorre, H. v, & Krumbein, W. E. (2000). Bacterial calcification. In *Microbial sediments* (pp. 25–31). Springer.

Konishi, Y., Tsukiyama, T., Ohno, K., Saitoh, N., Nomura, T., & Nagamine, S. (2006). Intracellular recovery of gold by microbial reduction of AuCl4- ions using the anaerobic bacterium Shewanella algae. *Hydrometallurgy*, *81*(1), 24–29.

Kralj, D., Brečević, L., & Kontrec, J. (1997). Vaterite growth and dissolution in aqueous solution III. Kinetics of transformation. *Journal of Crystal Growth*, *177*(3–4), 248–257.

Kralj, D., Brečević, L., & Nielsen, A. E. (1990). Vaterite growth and dissolution in aqueous solution I. Kinetics of crystal growth. *Journal of Crystal Growth*, *104*(4), 793–800.

Kralj, D., Brečević, L., & Nielsen, A. E. (1994). Vaterite growth and dissolution in aqueous solution II. Kinetics of dissolution. *Journal of Crystal Growth*, *143*(3–4), 269–276.

Krumbein, W. E. (1979). Photolithotropic and chemoorganotrophic activity of bacteria and algae as related to beachrock formation and degradation (Gulf of Aqaba, Sinai). *Geomicrobiology Journal*, *1*(2), 139–203.

Kumar, A., Karig, D., Acharya, R., Neethirajan, S., Mukherjee, P. P., Retterer, S., & Doktycz, M. J. (2013). Microscale confinement features can affect biofilm formation. *Microfluidics and*

Nanofluidics, *14*(5), 895–902.

Kupriyanova, E., Villarejo, A., Markelova, A., Gerasimenko, L., Zavarzin, G., Samuelsson, G., … Pronina, N. (2007). Extracellular carbonic anhydrases of the stromatolite-forming cyanobacterium Microcoleus chthonoplastes. *Microbiology*, *153*(4), 1149–1156.

Kurmaç, Y. (2009). The impact of toxicity of metals on the activity of ureolytic mixed culture during the precipitation of calcium. *Journal of Hazardous Materials*, *163*(2–3), 1063–1067.

Lauchnor, E. G., Topp, D. M., Parker, A. E., & Gerlach, R. (2015). Whole cell kinetics of ureolysis by Sporosarcina pasteurii. *Journal of Applied Microbiology*, *118*(6), 1321–1332. https://doi.org/10.1111/jam.12804

Le Metayer-Levrel, G., Castanier, S., Orial, G., Loubiere, J.-F., & Perthuisot, J.-P. (1999). Applications of bacterial carbonatogenesis to the protection and regeneration of limestones in buildings and historic patrimony. *Sedimentary Geology*, *126*(1–4), 25–34.

Lewandowski, Z., & Beyenal, H. (2013). *Fundamentals of biofilm research*. CRC press.

Li, M., Fu, Q.-L., Zhang, Q., Achal, V., & Kawasaki, S. (2015). Bio-grout based on microbially induced sand solidification by means of asparaginase activity. *Scientific Reports*, *5*, 16128.

Lian, B., Hu, Q., Chen, J., Ji, J., & Teng, H. H. (2006). Carbonate biomineralization induced by soil bacterium Bacillus megaterium. *Geochimica et Cosmochimica Acta*, *70*(22), 5522–5535.

Life Technologies. (2004). No Title. Retrieved January 2, 2018, from https://tools.lifetechnologies.com/content/sfs/manuals/mp07007.pdf

LIN, H.-M., Cao, N., & CHEN, L.-F. (1994). Antimicrobial effect of pressurized carbon dioxide on Listeria monocytogenes. *Journal of Food Science*, *59*(3), 657–659.

Lowenstam, H. A. (1981). Minerals formed by organisms. *Science*, *211*(4487), 1126–1131.

Lowenstam, H. A., & Weiner, S. (1989). *On biomineralization*. Oxford University Press on Demand.

Lowenstam, H. A., Weiner, S., bioMASON, Robbins, R., Technologies, L., Lowenstam, H. A., … Whitesides, G. M. M. (2011). No Title. *Annual Review of Fluid Mechanics*, *1*(1), 1–5. https://doi.org/http://researchrepository.murdoch.edu.au/399/2/02Whole.pdf

Lüttge, A., & Conrad, P. G. (2004). Direct observation of microbial inhibition of calcite dissolution. *Applied and Environmental Microbiology*, *70*(3), 1627–1632.

McConnaughey, T. A., & Whelan, J. F. (1997). Calcification generates protons for nutrient and bicarbonate uptake. *Earth-Science Reviews*, *42*(1–2), 95–117.

McKay, D. S., Gibson, E. K., Thomas-Keprta, K. L., Vali, H., Romanek, C. S., Clemett, S. J., … Zare, R. N. (1996). Search for past life on Mars: possible relic biogenic activity in Martian meteorite ALH84001. *Science*, *273*(5277), 924–930.

Minto, J. M., MacLachlan, E., El Mountassir, G., & Lunn, R. J. (2016). Rock fracture grouting with microbially induced carbonate precipitation. *Water Resources Research*. https://doi.org/10.1002/2016WR018884

Mitchell, A. C., & Ferris, F. G. (2005). The coprecipitation of Sr into calcite precipitates induced by bacterial ureolysis in artificial groundwater: temperature and kinetic dependence. *Geochimica et Cosmochimica Acta*, *69*(17), 4199–4210.

Mitchell, A. C., & Ferris, F. G. (2006). The influence of Bacillus pasteurii on the nucleation and growth of calcium carbonate. *Geomicrobiology Journal*, *23*(3–4), 213–226.

Mitchell, A. C., Phillips, A. J., Hiebert, R., Gerlach, R., Spangler, L. H., & Cunningham, A. B. (2009a). Biofilm enhanced geologic sequestration of supercritical CO2. *International Journal of Greenhouse Gas Control*, *3*(1), 90–99.

Mitchell, A. C., Phillips, A. J., Hiebert, R., Gerlach, R., Spangler, L. H., & Cunningham, A. B. (2009b). Biofilm enhanced geologic sequestration of supercritical CO2. *International Journal of Greenhouse Gas Control*, *3*(1), 90–99. https://doi.org/10.1016/j.ijggc.2008.05.002

Monger, H. C., Daugherty, L. A., Lindemann, W. C., & Liddell, C. M. (1991). Microbial precipitation of pedogenic calcite. *Geology*, *19*(10), 997–1000.

Montemagno, C., & Pyrak-Nolte, L. (1995). Porosity of natural fracture networks. *Geophysical Research Letters*, *22*(11), 1397–1400.

Montemagno, C., & Pyrak-Nolte, L. (1999). Fracture Netwok versus Single Structures: Measurement of Fracture Geometry with X-ray Tomography. *Phys. Chem. Earth (A)*, *24*(7), 575–579.

Montoya, B. M. (2012). *Bio-mediated soil improvement and the effect of cementation on the behavior, improvement, and performance of sand.* University of California, Davis.

Morita, R. Y. (1980). Calcite precipitation by marine bacteria. *Geomicrobiology Journal*, *2*(1), 63–82.

Morse, J. W. (1983). The kinetics of calcium carbonate dissolution and precipitation. *Reviews in Mineralogy and Geochemistry*, *11*(1), 227–264.

Mortensen, B. M., Haber, M. J., Dejong, J. T., Caslake, L. F., & Nelson, D. C. (2011). Effects of environmental factors on microbial induced calcium carbonate precipitation. *Journal of Applied Microbiology*, *111*(2), 338–349. https://doi.org/10.1111/j.1365-2672.2011.05065.x

Nemati, M., & Voordouw, G. (2003). Modification of porous media permeability, using calcium carbonate produced enzymatically in situ. *Enzyme and Microbial Technology*, *33*(5), 635–642. https://doi.org/10.1016/S0141-0229(03)00191-1

Okwadha, G. D. O., & Li, J. (2010a). Optimum conditions for microbial carbonate precipitation. *Chemosphere*, *81*(9), 1143–1148.

Okwadha, G. D. O., & Li, J. (2010b). Optimum conditions for microbial carbonate precipitation. *Chemosphere*, *81*(9), 1143–1148. https://doi.org/10.1016/j.chemosphere.2010.09.066

Parks, S. L. (2009). Kinetics of Calcite Precipitation By Ureolytic Bacteria Under Aerobic and Anaerobic Conditions. *Chemical and Biological Engineering*, (April), 93.

Phillips, A. J., Gerlach, R., Lauchnor, E., Mitchell, A. C., Cunningham, A. B., & Spangler, L. (2013). Engineered applications of ureolytic biomineralization: a review. *Biofouling*, *29*(6), 715–733. https://doi.org/10.1080/08927014.2013.796550

Phillips, A. J., Lauchnor, E., Eldring, J. J., Esposito, R., Mitchell, A. C., Gerlach, R., … Spangler, L. H. (2013). Potential CO2 leakage reduction through biofilm-induced calcium carbonate precipitation. *Environmental Science & Technology*, *47*(1), 142–149. https://doi.org/10.1021/es301294q

Pyrak-Nolte, L. J., Montemagno, C. D., Yang, G., Cook, N. G. W., & Myer, L. R. (1995). Three-dimensional tomographic visuallzatlon of natural fracture networks and graph theory analysis of the transport properties. In *8th ISRM Congress* (pp. 855–859). Tokyo, Japan: International

Society for Rock Mechanics. Retrieved from https://www.onepetro.org/conference-paper/ISRM-8CONGRESS-1995-174

Pyrak-Nolte, L., Montemagno, C., & Nolte, D. (1997). Volumetric imaging of aperture distributions in connected fracture networks. *Geophysical Research Letters*, *24*(18), 2343–2346.

R. Robbins. (2010). No Title. Retrieved January 2, 2018, from http://www.utdallas.edu/~rar011300/SEM/Scanning Electron Microscope Operation.pdf

Reddy, B. V. V., & Jagadish, K. S. (2003). Embodied energy of common and alternative building materials and technologies. *Energy and Buildings*, *35*(2), 129–137.

Rivadeneyra, M. A., Delgado, R., del Moral, A., Ferrer, M. R., & Ramos-Cormenzana, A. (1994). Precipatation of calcium carbonate by Vibrio spp. from an inland saltern. *FEMS Microbiology Ecology*, *13*(3), 197–204.

Rodriguez-Navarro, C., Rodriguez-Gallego, M., Chekroun, K. Ben, & Gonzalez-Munoz, M. T. (2003). Conservation of ornamental stone by Myxococcus xanthus-induced carbonate biomineralization. *Applied and Environmental Microbiology*, *69*(4), 2182–2193.

Rosenbaum, L. (2006). Prehistoric artistry, real and recreated. *The Wall Street Journal*, *13*.

Sarikaya, M. (1999). Biomimetics: materials fabrication through biology. *Proceedings of the National Academy of Sciences*, *96*(25), 14183–14185.

Schultze-Lam, S., Fortin, D., Davis, B. S., & Beveridge, T. J. (1996). Mineralization of bacterial surfaces. *Chemical Geology*, *132*(1–4), 171–181.

Sham, E., Mantle, M. D., Mitchell, J., Tobler, D. J., Phoenix, V. R., & Johns, M. L. (2013). Monitoring bacterially induced calcite precipitation in porous media using magnetic resonance imaging and flow measurements. *Journal of Contaminant Hydrology*, *152*, 35–43. https://doi.org/10.1016/j.jconhyd.2013.06.003

Sherwood, J. L., Sung, J. C., Maneval, J. E., & Smith, J. A. (2003). Analysis of Bacterial Random Motility in a Porous Medium Using Magnetic Resonance Imaging and Immunomagnetic Labeling, *37*(4), 781–785.

Siddique, R., & Chahal, N. K. (2011a). Effect of ureolytic bacteria on concrete properties. *Construction and Building Materials*, *25*(10), 3791–3801.

Siddique, R., & Chahal, N. K. (2011b). Effect of ureolytic bacteria on concrete properties. *Construction and Building Materials*, *25*(10), 3791–3801. https://doi.org/10.1016/j.conbuildmat.2011.04.010

Silver, S., Toth, K., & Scribner, H. (1975). Facilitated transport of calcium by cells and subcellular membranes of Bacillus subtilis and Escherichia coli. *Journal of Bacteriology*, *122*(3), 880–885.

Smith, K. S., & Ferry, J. G. (2000). Prokaryotic carbonic anhydrases. *FEMS Microbiology Reviews*, *24*(4), 335–366.

Söhnel, O., & Garside, J. (n.d.). Precipitation: Basic principles and industrial applications. 1992. Oxford: Butterworth-Heinemann.

Southam, G. (2000). Bacterial surface-mediated mineral formation. In *Environmental microbe-metal interactions* (pp. 257–276). American Society of Microbiology.

Stabnikov, V., Naeimi, M., Ivanov, V., & Chu, J. (2011). Formation of water-impermeable crust on sand surface using biocement. *Cement and Concrete Research*, *41*(11), 1143–1149.

Stewart, P. S. (2003). Diffusion in biofilms. *Journal of Bacteriology*, *185*(5), 1485–1491.

Stocks-Fischer, S., Galinat, J. K., & Bang, S. S. (1999a). Microbiological precipitation of CaCO3. *Soil Biology and Biochemistry*, *31*(11), 1563–1571.

Stocks-Fischer, S., Galinat, J. K., & Bang, S. S. (1999b). Microbiological precipitation of CaCO3. *Soil Biology and Biochemistry*, *31*(11), 1563–1571. https://doi.org/10.1016/S0038-0717(99)00082-6

Stoner, D. L., Watson, S. M., Stedtfeld, R. D., Meakin, P., Tyler, T. L., Pegram, L. M., … Griffel, L. K. (2005). Application of Stereolithographic Custom Models for Studying the Impact of Biofilms and Mineral Precipitation on Fluid Flow Application of Stereolithographic Custom Models for Studying the Impact of Biofilms and Mineral Precipitation on Fluid Flow. https://doi.org/10.1128/AEM.71.12.8721

Stumm, W., & Morgan, J. J. (1981). Aquatic Chemistry, 780 pp. *J. Wi L Ey & Sons.*

Tagliaferri, F., Waller, J., And??, E., Hall, S. A., Viggiani, G., B??suelle, P., & DeJong, J. T. (2011). Observing strain localisation processes in bio-cemented sand using x-ray imaging. *Granular Matter*, *13*(3), 247–250. https://doi.org/10.1007/s10035-011-0257-4

Thomas-Keprta, K. L., McKay, D. S., Wentworth, S. J., Stevens, T. O., Taunton, A. E., Allen, C. C., … Romanek, C. S. (1998). Bacterial mineralization patterns in basaltic aquifers: Implications for possible life in martian meteorite ALH84001. *Geology*, *26*(11), 1031–1034.

Thompson, J. B., & Ferris, F. G. (1990). Cyanobacterial precipitation of gypsum, calcite, and magnesite from natural alkaline lake water. *Geology*, *18*(10), 995–998.

Tiano, P., Biagiotti, L., & Mastromei, G. (1999). Bacterial bio-mediated calcite precipitation for monumental stones conservation: methods of evaluation. *Journal of Microbiological Methods*, *36*(1–2), 139–145.

Tobler, D. J., Cuthbert, M. O., & Phoenix, V. R. (2014). Transport of Sporosarcina pasteurii in sandstone and its significance for subsurface engineering technologies. *Applied Geochemistry*, *42*, 38–44. https://doi.org/10.1016/j.apgeochem.2014.01.004

Valiei, A., Kumar, A., Mukherjee, P. P., Liu, Y., & Thundat, T. (2012). A web of streamers: biofilm formation in a porous microfluidic device. *Lab on a Chip*, *12*(24), 5133–5137. https://doi.org/10.1039/c2lc40815e

van Paassen, L. (2009). *Biogrout: Ground Improvement by Microbially Induced Carbonate Precipitation*. *Technology*.

Von Der Schulenburg, D. A. G., Paterson-Beedle, M., MacAskie, L. E., Gladden, L. F., & Johns, M. L. (2007). Flow through an evolving porous media-compressed foam. *Journal of Materials Science*, *42*(16), 6541–6548. https://doi.org/10.1007/s10853-007-1523-z

Wanger, G., Onstott, T. C., & Southam, G. (2008). Stars of the terrestrial deep subsurface: A novel "star-shaped" bacterial morphotype from a South African platinum mine. *Geobiology*. https://doi.org/10.1111/j.1472-4669.2008.00163.x

Warren, L. A., Maurice, P. A., Parmar, N., & Ferris, F. G. (2001). Microbially mediated calcium carbonate precipitation: implications for interpreting calcite precipitation and for solid-phase

capture of inorganic contaminants. *Geomicrobiology Journal*, *18*(1), 93–115.

Warthmann, R., Van Lith, Y., Vasconcelos, C., McKenzie, J. A., & Karpoff, A. M. (2000). Bacterially induced dolomite precipitation in anoxic culture experiments. *Geology*, *28*(12), 1091–1094.

Watabe, N., & Wilbur, K. M. (1960). Influence of the organic matrix on crystal type in molluscs. *Nature*, *188*(4747), 334.

Wei, L., Liping, L., Long, C., & Longjiang, Y. (2009). Research status and prospect of biological precipitation of carbonate. *Advances in Earth Science*, *24*(6), 597–605.

Whiffin, V. S. (2004). Microbial CaCO3 Precipitation for the Production of Biocement. *Phd Thesis*, (September), 1–162. https://doi.org/http://researchrepository.murdoch.edu.au/399/2/02Whole.pdf

Wiley, W. R., & Stokes, J. L. (1962). Requirement of an alkaline pH and ammonia for substrate oxidation by Bacillus pasteurii. *Journal of Bacteriology*, *84*(4), 730–734.

Zhang, J., Davis, T. A., Matthews, M. A., Drews, M. J., LaBerge, M., & An, Y. H. (2006). Sterilization using high-pressure carbon dioxide. *The Journal of Supercritical Fluids*, *38*(3), 354–372.

Zhong, L., Islam, M. R., & others. (1995). A new microbial plugging process and its impact on fracture remediation. In *SPE Annual Technical Conference and Exhibition*.

Chapter 2

Microbiologically induced calcite precipitation mediated by *Sporosarcina pasteurii* [1]

Abstract

The particular bacterium under investigation here (*S. pasteurii*) is unique in its ability, under the right conditions, to induce the hydrolysis of urea (ureolysis) in naturally occurring environments through secretion of an enzyme urease. This process of ureolysis, through a chain of chemical reactions, leads to the formation of calcium carbonate precipitates. This is known as Microbiologically Induced Calcite Precipitation (MICP). The proper culture protocols for MICP are detailed here. Finally, visualization experiments under different modes of microscopy were performed to understand various aspects of the precipitation process. Techniques like optical microscopy, Scanning Electron Microscopy (SEM) and X-Ray Photo-electron Spectroscopy (XPS) were employed to chemically characterize the end-product. Further, the ability of these precipitates to clog pores inside a natural porous medium was demonstrated through a qualitative experiment where sponge bars were used to mimic a pore network with a range of length scales. A sponge bar dipped in the culture medium containing the bacterial cells hardens due to the clogging of its pores resulting from the continuous process of chemical precipitation. This hardened sponge bar exhibits superior strength when compared to a control sponge bar which becomes compressed and squeezed under the action of an applied external load, while the hardened bar is able to support the same weight with little deformation.

Video Link

The video component of this article can be found at https://www.jove.com/video/53253/

---

[1]A version of this chapter has been published as:
Microbiologically Induced Calcite Precipitation mediated by *Sporosarcina pasteurii*. Bhaduri, S., Debnath, N., Mitra, S. K., Liu, Y., Kumar, A. (2016). Journal of Visualized Experiments, e53253, doi:10.3791/53253.

2.1 Introduction

Sporosarcina pasteurii is a gram-positive bacterium able to survive in highly alkaline environments (pH~10) (Gibson, 1934) and is one of the bacterial species that can become a causative agent of a phenomenon called Microbiologically Induced Calcite Precipitation (MICP) (Navdeep K. Dhami et al., 2013; Greenfield, 1963; Phillips, Gerlach, et al., 2013). MICP is a process wherein precipitation of calcium carbonate is induced by certain microbes under suitable environmental conditions. *S. pasteurii* has assumed importance in recent years due to its identification as a possible agent for inducing significant volumes of MICP under certain conditions. This possibility stems from the fact that *S. pasteurii* has the unique ability to secrete copious amounts of the enzyme urease. This enzyme acts as a catalyst, promoting an accelerated lysis of urea (a naturally occurring biochemical compound with widespread and abundant supply) in the presence of water molecules. Through a cascade of reactions, this process ultimately leads to the generation of negatively charged carbonate ions. These ions, in turn, react with positive metal ions like calcium to finally form precipitates of calcium carbonate (calcite); hence the label MICP (Okwadha and Li, 2010; Cuthbert *et al.*, 2012; Stocks-Fischer, Galinat and Bang, 1999; Al Qabany, Soga and Santamarina, 2012; Lauchnor *et al.*, 2015).

The process of MICP has been known and studied for several decades (Chafetz, 1986; Morita, 1980). Over the past few years, MICP has been investigated for a wide range of engineering and environmental applications [2] including bottom-up green construction (bioMASON, 2018), enhancement of large-scale structures (van Paassen, 2009; Whiffin, 2004) and carbon sequestration and storage (a. B. Cunningham et al., 2011; Mitchell et al., 2009b).

For example, Cunnigham (a. B. Cunningham et al., 2011) et. al designed a high pressure moderate temperature flow reactor containing a Berea sandstone core. The reactor was inoculated with the bacteria *S. fridgidimarina* and under conditions of high-pressure supercritical carbon dioxide injection, a massive accumulation of biomass inside the pore volumes was observed, which led to more than 95% reduction in permeability. Jonkers and Schlangen (Jonkers, Thijssen, Muyzer, Copuroglu, & Schlangen, 2010) studied the effect of certain special strains of bacteria on the self-healing process in concrete. External water transported into the pore network entering through the surface pores is

expected to activate the dormant bacteria which in turn help structural strength via MICP. Tobler (Tobler, Cuthbert, & Phoenix, 2014) et al. have compared the ureolytic activity of *S. pasteurii* with an indigenous groundwater ureolytic microcosm under conditions favoring large-scale MCIP and found that *S. pasteurii* has a consistent capability to improve calcite precipitation even when the indigenous communities lacked prior urease activity. Mortensen (Mortensen, Haber, Dejong, Caslake, & Nelson, 2011) et.al have studied the effects of external factors like soil type, concentration of ammonium chloride, salinity, oxygen concentration and lysis of cells on MICP. Their demonstration that the biological treatment process is very robust with respect to a wide variation in parameter space substantiates the fitness of this process for various large-scale remediation applications provided a proper enrichment process to reinforce the bacteria is undertaken. Phillips (Phillips, Gerlach, et al., 2013) et. al designed experiments to study the changes in permeability and strength of a sand column and a sandstone core after being injected with *S. pasteurii* cultures. They found that while the permeability decreased 2 - 4 times while the fracture strength increased three times.

S. pasteurii and its role in MICP are topics of active research and several issues relating to the mechanism of chemical precipitation are still not fully understood. In light of this, it is very important to have a set of consistent standardized protocols to accurately culture a suitably enriched stock of *S. pasteurii* to achieve MICP. Here, we outline a rigorous protocol that will ensure repeatability and reproducibility. One of the important features of this protocol is the guaranteed induction of calcite precipitation within a short period of time if all procedures are followed carefully. While most preexisting protocols for culture of *S. pasteurii* focus on the cell growth itself, this work instead ensures the generation of a significant mass of solid precipitation that can be potentially used to clog pores. This manuscript describes the detailed protocols for culturing *S. pasteurii* and suitably enriching the culture medium to induce precipitation. The process is investigated through various microscopic techniques such as optical and Scanning Electron Microscopy (SEM) and X-Ray Photo-electron Spectroscopy (XPS). The focus of the manuscript is on the process of MICP. Procedures like SEM and SIMS, being well-established standard protocols, are not described separately.

2.2 Protocol

NOTE: Perform the experimental protocols in the order described below. The bacterial culture protocol is discussed in Section 1 (Also see Figure 2. 1). Section 2 describes the protocol for enriching the culture medium using external additives. Section 3 describes the protocols for multimode microscopy. Weights of all the individual components may be measured using an analytical balance. Volume of each solution may be measured using a volumetric cylinder.

NOTE: Proper biosafety protocols must be followed for Sections 1 - 2. Consult the institutional safety office for details.

2.2.1   Bacterial Culture

2.2.1.1 Culture Bacteria - Agar Plate Medium Preparation

1. Assemble equipment and ingredients viz. Petri dishes, flask, Tris-base, HCl, agar, Millipore water, and pH-meter ~~etc~~. Sterilize all containers by autoclaving at 121 °C before use.

2. Prepare 1 L of 0.13 M aqueous solution of Tris-buffer by mixing 15.75 g Tris-base with 1 L of Millipore water. To lower the pH level of the original solution (pH 10.4) add 2,800 μl of HCl (50% concentration). Check continuously using a pH-meter to set pH = 9.

3. Divide the 1 L buffer solution into two parts as follows:

1. Take 800 ml of this solution. Divide it equally into two parts of 400 ml each. Dissolve 8 g $(NH4)_2SO_4$ to one solution and 16 g yeast extract to the other solution.

2. Take the remaining (200 ml of) solution and divide it again into two parts of 100 ml each. Mix 2 g $(NH4)_2SO_4$ to one. Add 4 g yeast extract and 4 g agar to the other.

4. Autoclave the 4 solutions separately after wrapping the respective flasks in Al foil and sticking autoclave tapes.

NOTE: If a benchtop autoclave unit is used, the volume should be set to 500 ml (temperature and pressure automatically specified as a function of volume).

5. After taking them out from the autoclave, set the two 400 ml solutions aside for step 1.3.1 (below). Mix the two 100 ml solutions to have a 200 ml solution. Pour the mixture into 10 - 12 Petri dishes.

2.2.1.2 Culture Bacteria - Agar Plate Sample Preparation

1. Remove the bacterial stock from freezer (-80 °C) and allow it to thaw. After thawing properly, place the bacterial stock and the agar plate inside a biosafety hood.

2. Select the micropipette of smallest available dimension (0.5 - 10 µl is a good choice) to infest the tip with the *Sporosarcina pasteurii* stock. Streak an agar plate with the micropipette tip. Place the streaked agar plate inside a non-shaking incubator at 31 °C for 48 hr.

3. After 48 hr, remove the plate from the incubator and visually examine for the existence of single colonies. If there are no single colonies, then place it in the incubator for another 24 hr.

4. Repeat the process until single colonies are detected. Do not exceed 7 days of trial.

NOTE: If single colonies do not appear even after a week, then it is concluded that the steps have not been followed properly and the entire process must be repeated from step 1.

2.2.1.3 Culture Bacteria - Final Sample Preparation

1. Mix the two 400 ml solutions (Tris buffer + (NH4)2SO4 and Tris buffer + yeast extract (1.5.1) together to obtain an 800 ml solution. Transfer 125 ml of this solution into a flask.

2. Perform a visual examination of the surface of the agar plate to identify regions with high concentration of single colonies. Gently nudge and break one of the colonies with a micropipette tip.

3. Dip the same micropipette tip into the 125 ml flask and stir it thoroughly to ensure that sufficient number of cells for robust multiplication get transferred. Place the flask in a shaking incubator at 150 rpm, 30 °C for 2 - 3 days. After 2 - 3 days, remove the flask from the incubator.

2.2.1.4 Culture Bacteria - Final Cell Count

1. Perform serial dilution of the non-diluted culture solution using PBS to attain a dilution of at least ten million (10-7) to ensure countable single colonies appear. Draw seven parallel equidistant lines on one of the agar-plates.

    1. Do this by drawing bold lines on the bottom surface of the Petri dish, prominent enough to be visible from top. Drop 3 little drops of non-diluted solution into one segment. Add 1 ml of non-diluted solution to 9 ml of Phosphate Buffered Saline (PBS) to obtain a 1:10 dilution.

2. Take a small aliquot (~ 0.1 ml) of this newly diluted solution with a pipette and drop 3 more small drops on the next segment. Transfer the newly diluted solution to a new flask and further diluted ten times (10x) by adding PBS. This brings down the dilution to 10-2 or 1:100.

    1. Use this 1:100 solution in the next segment. Repeat this he process with small volumes of the freshly diluted solutions by successively transferring them to new flasks and continuously diluting ten-fold (10x) in tandem with PBS to obtain more and more dilute samples from 10-3 or 1:1,000 all the way down to 10-7 or 1:10 million into the last segment.

1. Perform Colony-Forming Unit (CFU) plate count to count the number of cells present in the agar plate after incubating the plate for 1 – 2 days at 31 °C. This gives a quantitative measure of the bacterial count in the undiluted sample.

NOTE: The CFU value is measured based on the ability of the system to give rise to colonies under the specific conditions of nutrient medium, temperature and time assuming that every colony is separate and founded by a single viable microbial cell.

2. Seal the Petri dishes with self-sealing film and store remaining items in a refrigerator for future use.

2.2.2 Protocol for Enrichment of Nutrient to Accelerate Precipitation

1. Transfer 9 ml of the prepared culture liquid (cells + medium) into several sterilized centrifuge tubes, each of 10 ml volume.

2. Prepare a 100 ml stock solution of the external enrichment consisting of four components in the following concentrations in fresh medium:

Urea: 2 g/L, Ammonium chloride: 1 g/L, Sodium bicarbonate: 212 mg/L, Calcium chloride: 280 mg/L. Carefully measure all the ingredients using an analytical balance and mix all but urea with fresh medium in a beaker and place in the autoclave (121 °C, 15 psi, 15 min).

1. Following autoclave, mix the requisite amount of urea (2 mg) with 1 ml of fresh medium and pass through a syringe fitted with 0.22 μm syringe filter to complete the process of enrichment.

2. Add 1 ml of this enrichment medium with additives to the sterilized centrifuge tubes containing 9 ml of the prepared culture liquid (cells + medium) (see step 2.1).

NOTE: Of all these components, urea being degradable at elevated temperatures, cannot be sterilized in an autoclave. Hence, after the other components have been autoclaved (121 °C, 15 psi, 15 min), urea is added last through a 0.22 μm syringe filter.

3. Vortex each tube thoroughly using a mechanical vortexer. Place the enriched liquids (cells + medium + additives) in a non-shaking incubator at 30 °C. Monitor all the units regularly for initiation of precipitation. Using a light microscope, begin microscopic observations once onset of precipitation is detected with the naked eye. This is usually between 30 - 36 hr after start of experiments.

2.2.3   Protocol for Multi-mode Microscopy

1. Transfer a small volume (~ 1 ml) of fluid to a high-magnification microscopy-chambered coverglass system to perform initial observations with bright field mode. To begin with, start all observations with the lowest magnification (4X). which provides a wide area of coverage and hence global information about the distribution of precipitates.

2. Select particular areas with significant volumes of precipitations and zoom in (20X, 40X, 60X) by progressively increasing the magnification.

NOTE: Since it's impossible to properly resolve the cells from the Extracellular Polymeric Substance (EPS) under bright-field (due to very close refractive indices), switch on phase-contrast

mode whenever necessary. In this mode, just the outlines of the cell membranes (being a different phase than the bulk cell) are visible, thus enabling visual differentiation.

3. Finally, stain some chambers with Live/ Dead stain that selectively dyes the live components as green while coloring the dead components in red. Refer to standard protocols (Life Technologies, 2004).

4. Switch on fluorescent mode to properly distinguish between the red and green regions. Red (Red filter cube with Excitation wavelength of 540 - 580 nm, Dichroic mirror of 595 nm and Barrier filter of 600 - 660 nm) and Green (GFP Long-pass Green filter cube with Excitation wavelength of 440 - 480 nm, Dichroic mirror of 505 nm and Barrier filter of 510 nm) filter cubes are used to facilitate fluorescent micrographs.

5. Once all multi-mode data have been gathered, select the best images and manually overlay (individual brightfield, phase-contrast and fluorescent images) to obtain the best possible contrast and clarity.

6. Perform SEM on the dried solid samples to understand crystal structures. This is a well-established and standard procedure (R. Robbins, 2010). Perform XPS to identify chemical signatures of functional groups (carbonates). This is a well-established and standard procedure as well (der Heide, 2011).

2.3 Representative Results

S. pasteurii being an alkaliphile (Wiley & Stokes, 1962) can survive relatively harsh conditions. When the above mentioned culture protocol is followed, and *S. pasteurii* is grown inside a chamber, the bacteria leads to the precipitation of calcium carbonate over time (Figure 2.2A). Figure 2.2B shows a phase contrast optical microscopic image of the bacterial cell population within the culture medium. Individual cells can be clearly distinguished, with rod-like shapes characteristic of the bacillus class of bacteria quite evident. Small brown arrows have been used to specifically highlight two individual cells. The precipitation of calcium carbonate occurs over a period of several days. Figure 2.2A shows how the precipitates settle down at the bottom of a centrifuge tube. This can be vividly seen with the naked eye as a whitish powder sitting below the liquid medium with a sharp contrast in color as opposed to the yellowish liquid. The yellowish liquid contains bacteria suspended in their culture medium. The white precipitates were collected and dried and later imaged using SEM (Figure 2.2C).

In Figure 2.3A, the well-defined cleavage lines, a hallmark of crystallinity, can be easily identified. Figure 2.3B shows the XPS graph for the same sample for characterization. Peaks corresponding to carbonate groups pin-point the existence of calcium carbonate. Thus, Figure 2.3A and B together conclusively prove the generation of calcite as the precipitated chemical.

A qualitative experiment was performed in order to assess the ability of MICP to change the properties of porous media. To this end, we performed an experiment involving sponges which are expected to mimic a porous medium with a range of length scales of the pore structures, as is found in a typical natural structure. A sponge bar (Mr. Clean, P&G) was immersed in a solution of *S. pasteurii* for a period of 7 days and then dried. The sponge after long exposure to the MICP process hardened and displayed enhanced compressive strength. This is depicted in Figure 2.4. The sponge, before immersion (control case), showed significant compression when subjected to a 1 kg weight (Figure 2.4A - B). On the other hand, after being subjected to immersion in the *S. pasteurii* solution, it suffered pore clogging due to the resulting calcite precipitation. This led to a massive increase in strength resulting from a bridging of the pore spaces and subsequently enabled the bar to support the 1 kg load without allowing significant compression (Figure 2.4C - D).

A semi-quantitative idea regarding the hardening process can be gained through measurements of deflection height of the loaded bar. The original sponge sample is a rectangular bar with a height of 4.5 cm. The deflection of the control specimen, very near the point of application of load, is approximately 1.6 cm. In the case of the treated specimen, the deflection reduces to 0.6 cm. Further rigorous quantification of the hardening process is also possible. For example, a mechanistic explanation of this process in terms of increase in shear strength, peak deviatoric stress and dilatancy angles has been proposed by Tagliaferri *et al.* (2011) through X-ray imaging and digital image correlation.
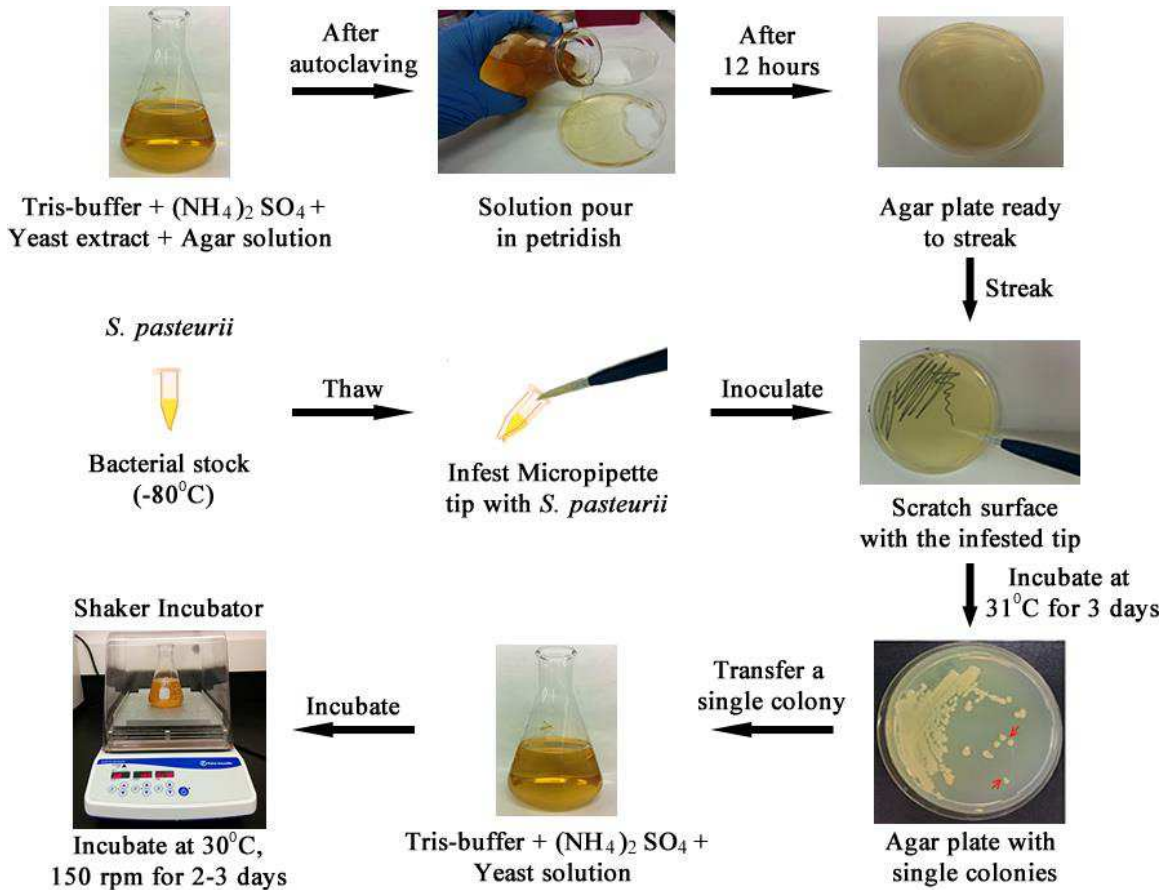
Figure 2.1. The Outline of the Entire Culture Protocol Represented as an Algorithmic Schematic. To start with, Tris-buffer and agar solution is poured in a Petri dish. Once agar plate is ready, it is streaked with a tip infested with the bacteria. The streaked plate is incubated to grow single colonies. One of the single colonies is transferred to a media flask and incubated again.
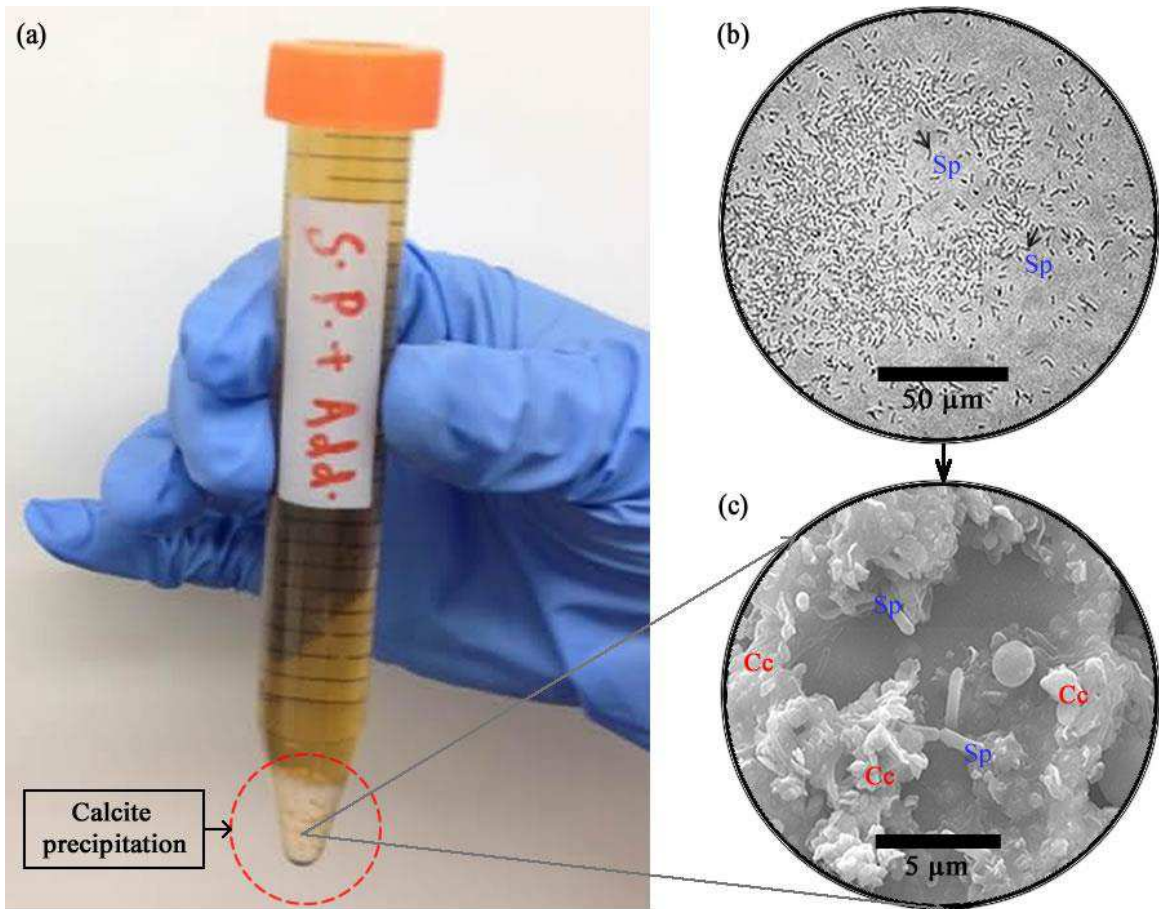
Figure 2.2. The Cells and the Precipitates. (**A**) The cells in the culture medium confined inside a centrifuge tube lead to clear observable chemical precipitation (after 5 - 7 days) that settles down at the bottom and is visible to the naked eye. (**B**) Population of bacteria immobilized on a surface seen under phase-contrast. Individual rod-shaped cells (bacilli, labeled Sp) may be seen clearly (a couple of them highlighted by arrows). (**C**) SEM image of the white precipitate showing both cells (Sp) and crystals (Cc).
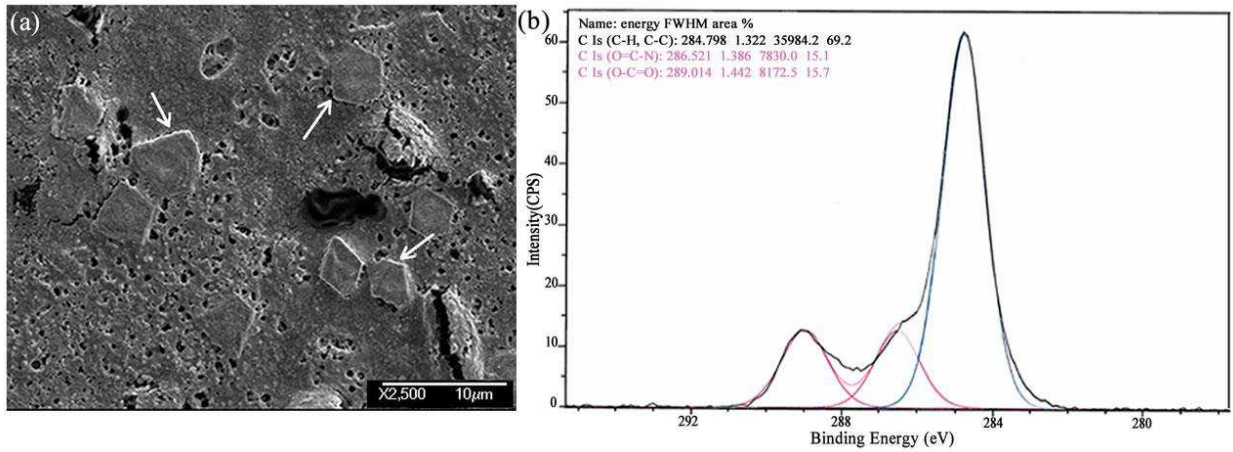
Figure 2.3. The Crystals and Their Characterization. (**A**) Scanning electron microscope image of the dried precipitate. Individual crystals and associated cleavage lines are clearly visible. (**B**) X-Ray Photo-electron Spectroscopy (XPS) graph of the chemical precipitate; mass spectrometry peaks corresponding to carbonate functional group reinforce the possibility of the existence of calcite.
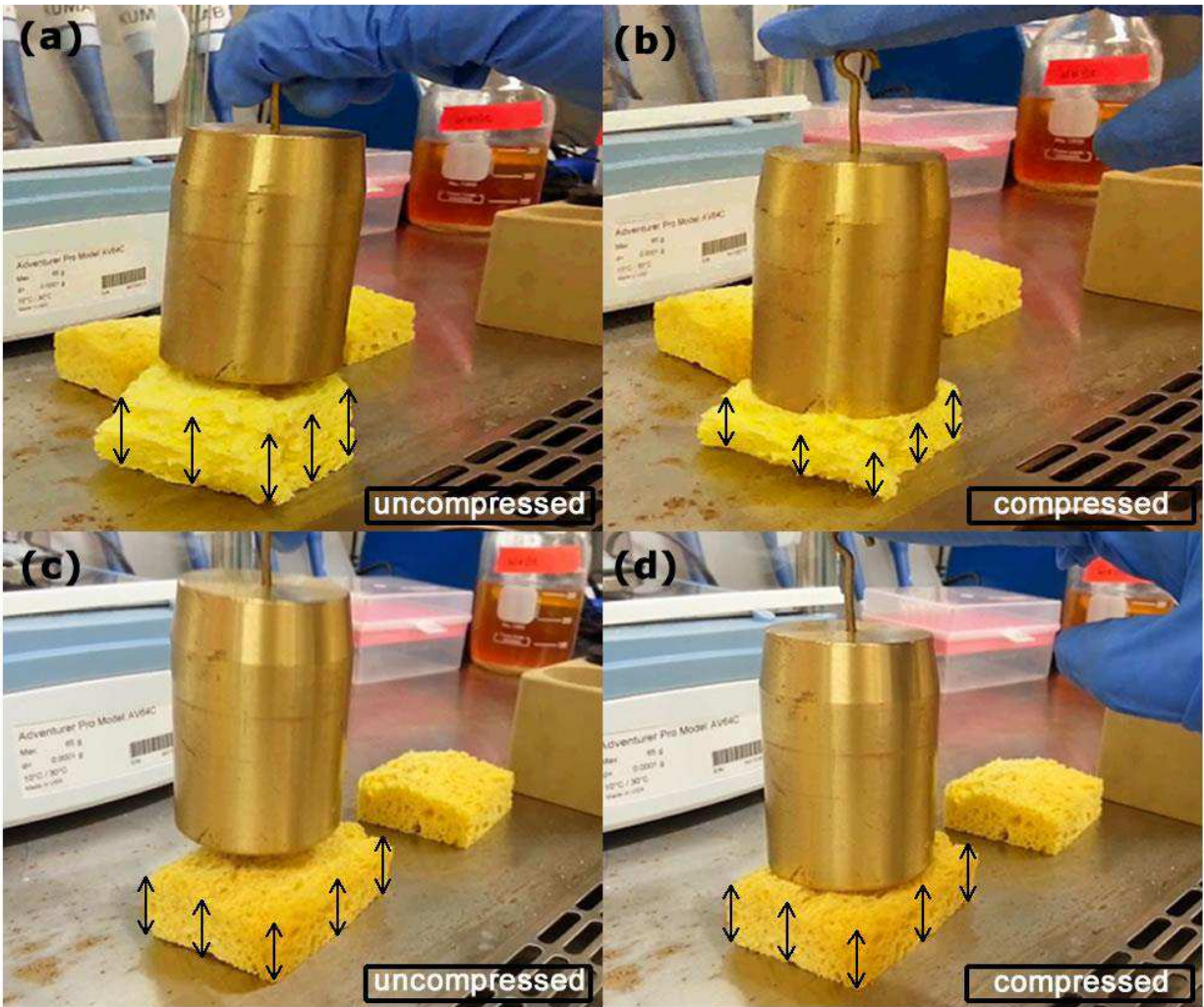
Figure 2.4. A Semi-quantitative Experiment with Sponge Bars Serving as Prototype Porous Media. (**A**) and (**B**) are fresh dry samples not dipped. (**C**) and (**D**) are wet samples drenched in a solution of medium and cells; they exhibit a significant increase in material resistance due to pore clogging resulting from calcite precipitation as seen here from reduced compression under the action of a constant weight. Untreated samples are naturally porous and suffer massive reduction in volume when subjected to an 1 kg weight. The pores squeeze out the air and contract, leading to an overall reduction in size. On the other hand, the treated sample has artificially gained a significant amount of stiffness by virtue of pore clogging. It demonstrates a marked enhancement in strength when it comfortably supports the same load without any compression.

2.4 Discussion

2.4.1 Critical Steps: This manuscript describes in detail the protocols for culturing a viable sample of *S. pasteurii*. Once the culture has been readied, it must be suitably enriched. This is a key step vital to the success of the experiment because a failure to provide the proper chemical environment leads to either very long time scales of precipitation or a complete lack thereof. *S. pasteurii* is quite sensitive to several external agencies and must be cultured with a high degree of care and precision to ensure biochemical robustness and repeatability. The extent and dosage of enrichment is now known to dictate the chemical nature of precipitation and hence must be controlled accurately as well.

2.4.2 Modifications/Troubleshooting: Several aspects may be modified with little variance in end-results. The plate count need not be performed per the technique described above (Serial Dilution per the Miles Misra Method). Here, the serial dilution has been performed on a single agar plate by dividing it into seven regions by chords drawn on its bottom surface. This is not mandatory. It's also a common practice to use an entire agar plate for a particular dilution by preparing a spread plate. Serial dilution is performed on a series of successive spread plates and the one with a countable number of single colonies (20 - 200) is chosen for the final calculation. Any of the various other cell counting techniques may be applied here as well. Microscopy may well be performed with simple cover slips or slides. A chamber unit is not at all mandatory.

Sometimes, the bacteria may fail to form precipitates. It is useful to transfer a small amount of the frozen culture into a liquid medium first. Streaking may be performed after growth has occurred in the liquid first.

2.4.3 Limitations: This is a slow technique with a number of steps, one leading to another. There are significant chances of contamination, cross-contamination and other cultural defects at all steps. Intense care must be maintained at all times. Around 180 mg of precipitate is formed per ml of culture solution.
There are two main bottlenecks to the success of this protocol:

  a) Probability of cross-contamination: *S. pasteurii* is a feeble bacterium in its initial stages of

growth and doesn't survive any contamination from competing species sharing the same nutrient pool. Intense care must be exercised while inoculating the plate and also while transferring the cultures between hoods and incubators. In my personal experience, I had to discard an otherwise perfect plate many a times simply because it shared a few hours of incubation with another species in a different plate.

b) The enrichment step where external additives are added is equally critical. Under-enrichment leads to long time-scales of precipitation, over-enrichment wipes the population out.

2.4.4 Significance: The present protocol outlines in detail all the steps necessary to ensure that a culture of the bacterium *S. pasteurii* faithfully precipitates calcite under the influence of externally added enrichments. Although the culture of this bacterium itself is a well-established protocol, the entire process of enrichment and quantification is not. This issue has been addressed here.

2.4.5 Future Applications: It might be possible to suitably modulate this bacterium to precipitate in different manners that in turn can be engineered to various applications depending on the nature of precipitates. It was previously mentioned that there exist several unknowns with respect to MICP involving *S. pasteurii*. Some of these unknowns include role of aggregative dynamics of *S. pasteurii* in the MICP process, role of the microscale environment (Kumar et al., 2013; Valiei, Kumar, Mukherjee, Liu, & Thundat, 2012) such as effect of porous media and fluid flow. A standardized protocol can be developed that ensures fast precipitation with a clear opportunity for performing proper multi-mode microscopy.

2.5 Disclosures

The authors have nothing to disclose.

2.6 Acknowledgements

References

Achal, V., Mukerjee, A., & Sudhakara Reddy, M. (2013). Biogenic treatment improves the durability and remediates the cracks of concrete structures. *Construction and Building Materials*, *48*, 1–5. https://doi.org/10.1016/j.conbuildmat.2013.06.061

Achal, V., Mukherjee, a, Basu, P. C., & Reddy, M. S. (2009). Strain improvement of Sporosarcina pasteurii for enhanced urease and calcite production. *Journal of Industrial Microbiology & Biotechnology*, *36*(7), 981–988. https://doi.org/10.1007/s10295-009-0578-z

Achal, V., & Pan, X. (2011). Characterization of urease and carbonic anhydrase producing bacteria and their role in calcite precipitation. *Current Microbiology*, *62*(3), 894–902. https://doi.org/10.1007/s00284-010-9801-4

Achal, V., Pan, X., Fu, Q., & Zhang, D. (2012). Biomineralization based remediation of As(III) contaminated soil by Sporosarcina ginsengisoli. *Journal of Hazardous Materials*, *201–202*, 178–184. https://doi.org/10.1016/j.jhazmat.2011.11.067

Adolphe, J. P., Loubière, J. F., Paradas, J., & Soleilhavoup, F. (1990). Procédé de traitement biologique d'une surface artificielle. *European Patent 90400G97. 0*, *1989*.

Al Qabany, A., Soga, K., & Santamarina, C. (2012). Factors Affecting Efficiency of Microbially Induced Calcite Precipitation. *Journal of Geotechnical and Geoenvironmental Engineering*, *138*(8), 992–1001. https://doi.org/10.1061/(ASCE)GT.1943-5606.0000666

Anbu, P., Kang, C.-H., Shin, Y.-J., & So, J.-S. (2016). Formations of calcium carbonate minerals by bacteria and its multiple applications. *Springerplus*, *5*(1), 250.

Arias, J. L., & Fernández, M. S. (2008). Polysaccharides and proteoglycans in calcium carbonate-based biomineralization. *Chemical Reviews*, *108*(11), 4475–4482.

Bang, S. S., Galinat, J. K., & Ramakrishnan, V. (2001). Calcite precipitation induced by polyurethane-immobilized Bacillus pasteurii. *Enzyme and Microbial Technology*, *28*(4–5), 404–409.

Bang, S. S., & Ramakrishnan, V. (2001). Microbiologically-enhanced crack remediation (MECR). In *proceedings of the international symposium on industrial application of microbial genomes* (Vol. 20, pp. 3–13).

Benini, S., Rypniewski, W. R., Wilson, K. S., Miletti, S., Ciurli, S., & Mangani, S. (1999). A new proposal for urease mechanism based on the crystal structures of the native and inhibited

enzyme from Bacillus pasteurii: why urea hydrolysis costs two nickels. *Structure*, *7*(2), 205–216.

Berner, R. A. (1975). The role of magnesium in the crystal growth of calcite and aragonite from sea water. *Geochimica et Cosmochimica Acta*, *39*(4), 489IN3495--494504.

Bhaduri, S., Debnath, N., Mitra, S., Liu, Y., & Kumar, A. (2016). Microbiologically induced calcite precipitation mediated by sporosarcina pasteurii. *Journal of Visualized Experiments*, *2016*(110). https://doi.org/10.3791/53253

bioMASON. (2018). No Title. Retrieved January 2, 2018, from www.biomason.com

Bosak, T. (2011). Calcite precipitation, microbially induced. In *Encyclopedia of Geobiology* (pp. 223–227). Springer.

Braissant, O., Verrecchia, E. P., & Aragno, M. (2002). Is the contribution of bacteria to terrestrial carbon budget greatly underestimated? *Naturwissenschaften*, *89*(8), 366–370.

Bray, J. M., Lauchnor, E. G., Redden, G. D., Gerlach, R., Fujita, Y., Codd, S. L., & Seymour, J. D. (2017). Impact of Mineral Precipitation on Flow and Mixing in Porous Media Determined by Microcomputed Tomography and MRI. *Environmental Science & Technology*, *51*(3), 1562–1569. https://doi.org/10.1021/acs.est.6b02999

Bundeleva, I. A., Shirokova, L. S., Bénézeth, P., Pokrovsky, O. S., Kompantseva, E. I., & Balor, S. (2012). Calcium carbonate precipitation by anoxygenic phototrophic bacteria. *Chemical Geology*, *291*, 116–131.

Camesano, T. A., & Logan, B. E. (1998). Influence of fluid velocity and cell concentration on the transport of motile and nonmotile bacteria in porous media. *Environmental Science and Technology*. https://doi.org/10.1021/es970996m

Cappitelli, F., Zanardini, E., Ranalli, G., Mello, E., Daffonchio, D., & Sorlini, C. (2006). Improved methodology for bioremoval of black crusts on historical stone artworks by use of sulfate-reducing bacteria. *Applied and Environmental Microbiology*, *72*(5), 3733–3737.

Castanier, S., Le Métayer-Levrel, G., & Perthuisot, J.-P. (1999). Ca-carbonates precipitation and limestone genesis—the microbiogeologist point of view. *Sedimentary Geology*, *126*(1–4), 9–23.

Chafetz, H. S. (1986). Marine peloids: a product of bacterially induced precipitation of calcite. *Journal of Sedimentary Research*, *56*(6).

Chafetz, H. S., & Buczynski, C. (1992). Bacterially induced lithification of microbial mats. *Palaios*, 277–293.

Chu, K. T. (2005). by.

Chunxiang, Q., Jianyun, W., Ruixing, W., & Liang, C. (2009). Corrosion protection of cement-based

building materials by surface deposition of CaCO3 by Bacillus pasteurii. *Materials Science and Engineering: C*, *29*(4), 1273–1280.

Costerton, J. W., & Stewart, P. S. (2001). Battling biofilms. *Scientific American*, *285*(1), 74–81.

Cunningham, A. B., & Gerlach, R. (2010). Microbially Enhanced Carbon Capture and Storage by Mineral-Trapping and, *44*(13), 5270–5276.

Cunningham, A. B., Gerlach, R., Spangler, L., & Mitchell, A. C. (2009). Microbially enhanced geologic containment of sequestered supercritical CO2. *Energy Procedia*, *1*(1), 3245–3252.

Cunningham, a. B., Gerlach, R., Spangler, L., & Mitchell, a. C. (2009). Microbially enhanced geologic containment of sequestered supercritical CO2. *Energy Procedia*, *1*(1), 3245–3252. https://doi.org/10.1016/j.egypro.2009.02.109

Cunningham, a. B., Gerlach, R., Spangler, L., Mitchell, a. C., Parks, S., & Phillips, a. (2011). Reducing the risk of well bore leakage of CO2 using engineered biomineralization barriers. *Energy Procedia*, *4*, 5178–5185. https://doi.org/10.1016/j.egypro.2011.02.495

Cuthbert, M. O., Riley, M. S., Handley-Sidhu, S., Renshaw, J. C., Tobler, D. J., Phoenix, V. R., & Mackay, R. (2012). Controls on the rate of ureolysis and the morphology of carbonate precipitated by S. Pasteurii biofilms and limits due to bacterial encapsulation. *Ecological Engineering*, *41*, 32–40. https://doi.org/10.1016/j.ecoleng.2012.01.008

De Muynck, W., De Belie, N., & Verstraete, W. (2010). Microbial carbonate precipitation in construction materials: A review. *Ecological Engineering*, *36*(2), 118–136. https://doi.org/10.1016/j.ecoleng.2009.02.006

De Muynck, W., Verbeken, K., De Belie, N., & Verstraete, W. (2013). Influence of temperature on the effectiveness of a biogenic carbonate surface treatment for limestone conservation. *Applied Microbiology and Biotechnology*, *97*(3), 1335–1347.

Demény, A., Németh, P., Czuppon, G., Leél-\HOssy, S., Szabó, M., Judik, K., … Stieber, J. (2016). Formation of amorphous calcium carbonate in caves and its implications for speleothem research. *Scientific Reports*, *6*, 39602.

der Heide, P. (2011). *X-ray photoelectron spectroscopy: an introduction to principles and practices*. John Wiley & Sons.

Dhami, N. K., Reddy, M. S., & Mukherjee, A. (2013). Bacillus megaterium mediated mineralization of calcium carbonate as biogenic surface treatment of green building materials. *World Journal of Microbiology and Biotechnology*, *29*(12), 2397–2406. https://doi.org/10.1007/s11274-013-1408-z

Dhami, N. K., Reddy, M. S., & Mukherjee, M. S. (2013). Biomineralization of calcium carbonates

and their engineered applications: A review. *Frontiers in Microbiology*, *4*(OCT), 1–13. https://doi.org/10.3389/fmicb.2013.00314

Dick, J., De Windt, W., De Graef, B., Saveyn, H., der Meeren, P., De Belie, N., & Verstraete, W. (2006). Bio-deposition of a calcium carbonate layer on degraded limestone by Bacillus species. *Biodegradation*, *17*(4), 357–367.

Douglas, S., & Beveridge, T. J. (1998). Mineral formation by bacteria in natural microbial communities. *FEMS Microbiology Ecology*, *26*(2), 79–88.

Duffy, K. J., Cummings, P. T., & Ford, R. M. (1995). Random walk calculations for bacterial migration in porous media. *Biophysical Journal*, *68*(3), 800–806. https://doi.org/10.1016/S0006-3495(95)80256-0

Dupraz, S., Parmentier, M., Ménez, B., & Guyot, F. (2009). Experimental and numerical modeling of bacterially induced pH increase and calcite precipitation in saline aquifers. *Chemical Geology*, *265*(1–2), 44–53. https://doi.org/10.1016/j.chemgeo.2009.05.003

Ehrlich, H. L. (1996). How microbes influence mineral growth and dissolution. *Chemical Geology*, *132*(1–4), 5–9.

Ehrlich, H. L. (1998). Geomicrobiology: its significance for geology. *Earth-Science Reviews*, *45*(1–2), 45–60.

Ferris, F. G., & Beveridge, T. J. (1985). Functions of bacterial cell surface structures. *BioScience*, *35*(3), 172–177.

Ferris, F. G., Beveridge, T. J., & Fyfe, W. S. (1986). Iron-silica crystallite nucleation by bacteria in a geothermal sediment. *Nature*, *320*(6063), 609–611.

Ferris, F. G., Phoenix, V., Fujita, Y., & Smith, R. W. (2004). Kinetics of calcite precipitation induced by ureolytic bacteria at 10 to 20 C in artificial groundwater. *Geochimica et Cosmochimica Acta*, *68*(8), 1701–1710.

Fidaleo, M., & Lavecchia, R. (2003). Kinetic study of enzymatic urea hydrolysis in the pH range 4-9. *Chemical and Biochemical Engineering Quarterly*, *17*(4), 311–318.

Folk, R. L. (1993). SEM imaging of bacteria and nannobacteria in carbonate sediments and rocks. *Journal of Sedimentary Research*, *63*(5).

Fontes, D. E., Mills, A. L., Hornberger, G. M., & Herman, J. S. (1991). Physical and Chemical Factors Influencing Transport of Microorganisms through Porous Media. *APPLIED AND ENVIRONMENTAL MICROBIOLOGY*, *57*(9), 2473–2481.

Friedrich, B., & Magasanik, B. (1977). Urease of Klebsiella aerogenes: control of its synthesis by

glutamine synthetase. *Journal of Bacteriology*, *131*(2), 446–452.

Gal, J.-Y., Bollinger, J.-C., Tolosa, H., & Gache, N. (1996). Calcium carbonate solubility: a reappraisal of scale formation and inhibition. *Talanta*, *43*(9), 1497–1509.

Ganendra, G., De Muynck, W., Ho, A., Arvaniti, E. C., Hosseinkhani, B., Ramos, J. A., … Boon, N. (2014). Formate oxidation-driven calcium carbonate precipitation by Methylocystis parvus OBBP. *Applied and Environmental Microbiology*, *80*(15), 4659–4667.

Garcia-Vallès, M., Vendrell-Saz, M., Krumbein, W. E., & Urz\`\i, C. (1997). Coloured mineral coatings on monument surfaces as a result of biomineralization: the case of the Tarragona cathedral (Catalonia). *Applied Geochemistry*, *12*(3), 255–266.

Ghashghaei, S., & Emtiazi, G. (2013). Production of calcite nanocrystal by a urease-positive strain of enterobacter ludwigii and study of its structure by SEM. *Current Microbiology*, *67*(4), 406–413. https://doi.org/10.1007/s00284-013-0379-5

Gibson, T. (1934). An Investigation of the Bacillus Pasteuri Group: II. Special Physiology of the Organisms. *Journal of Bacteriology*, *28*(3), 313.

Gollapudi, U. K., Knutson, C. L., Bang, S. S., & Islam, M. R. (1995). A new method for controlling leaching through permeable channels. *Chemosphere*, *30*(4), 695–705.

Gorospe, C. M., Han, S.-H., Kim, S.-G., Park, J.-Y., Kang, C.-H., Jeong, J.-H., & So, J.-S. (2013). Effects of different calcium salts on calcium carbonate crystal formation by Sporosarcina pasteurii KCTC 3558. *Biotechnology and Bioprocess Engineering*, *18*(5), 903–908.

Greenfield, L. J. (1963). Metabolism and concentration of calcium and magnesium and precipitation of calcium carbonate by a marine bacterium. *Annals of the New York Academy of Sciences*, *109*(1), 23–45.

Hammes, F. (2002). *Ureolytic microbial calcium carbonate precipitation*. Ph. D. Thesis, Ghent University, Ghent.

Hammes, F. (2003). UREOLYTIC MICROBIAL CALCIUM CARBONATE PRECIPITATION UREOLYTISCHE MICROBIELE CALCIUMCARBONAAT- door. *Scanning Electron Microscopy*.

Hammes, F., Arnold, J., Krupka, K. M., Cantrell, K. J., McGrail, B. P., Tagliaferri, F., … Gerlach, R. (2013). Calcium carbonate precipitation by different bacterial strains. *Ecological Engineering*, *36*(3), 172. https://doi.org/http://researchrepository.murdoch.edu.au/399/2/02Whole.pdf

Hammes, F., Boon, N., De Villiers, J., Verstraete, W., Siciliano, S. D., & Villiers, J. De. (2003). Strain-Specific Ureolytic Microbial Calcium Carbonate Precipitation Strain-Specific Ureolytic

Microbial Calcium Carbonate Precipitation. *Applied and Environmental Microbiology*, *69*(8), 4901–4909. https://doi.org/10.1128/AEM.69.8.4901

Hammes, F., & Verstraete, W. (2002). Key roles of pH and calcium metabolism in microbial carbonate precipitation. *Reviews in Environmental Science and Biotechnology*, *1*(1), 3–7.

Hong, S.-I., Park, W.-S., & Pyun, Y.-R. (1997). Inactivation ofLactobacillussp. fromKimchiby High Pressure Carbon Dioxide. *LWT-Food Science and Technology*, *30*(7), 681–685.

Hunter, G. K. (1996). Interfacial aspects of biomineralization. *Current Opinion in Solid State and Materials Science*, *1*(3), 430–435.

Ismail, M. A., Joer, H. A., Randolph, M. F., & Meritt, A. (2002). Cementation of porous materials using calcite. *Geotechnique*, *52*(5), 313–324.

Jahns, T. (1996). Ammonium/urea-dependent generation of a proton electrochemical potential and synthesis of ATP in Bacillus pasteurii. *Journal of Bacteriology*, *178*(2), 403–409.

Jansson, C., & Northen, T. (2010). Calcifying cyanobacteria—the potential of biomineralization for carbon capture and storage. *Current Opinion in Biotechnology*, *21*(3), 365–371.

Jonkers, H. M., Thijssen, A., Muyzer, G., Copuroglu, O., & Schlangen, E. (2010). Application of bacteria as self-healing agent for the development of sustainable concrete. *Ecological Engineering*, *36*(2), 230–235. https://doi.org/10.1016/j.ecoleng.2008.12.036

Kaltwasser, H., Krämer, J., & Conger, W. R. (1972). Control of urease formation in certain aerobic bacteria. *Archiv Für Mikrobiologie*, *81*(2), 178–196.

Kantzas, A., Stehmeier, L., Marentette, D. F., Ferris, F. G., Jha, K. N., Maurits, F. M., & others. (1992). A novel method of sand consolidation through bacteriogenic mineral plugging. In *Annual Technical Meeting*.

Kantzas, a, Stehmeier, L., Marentette, D. F., Ferris, F. G., Jha, K. N., & Mourits, F. M. (1992). A Novel Method of Sand Consolidation Through Bacteriogenic Mineral Plugging. *43rd Annual Technical Meeting, Petroleum Society of CIM*, *CIM 92-46*(Cim), 1–15. https://doi.org/10.2118/92-46

Kawaguchi, T., & Decho, A. W. (2002). A laboratory investigation of cyanobacterial extracellular polymeric secretions (EPS) in influencing CaCO 3 polymorphism. *Journal of Crystal Growth*, *240*(1), 230–235.

Keefe, W. E. (1976). Formation of crystalline deposits by several genera of the family Enterobacteriaceae. *Infection and Immunity*, *14*(2), 590–592.

Knorre, H. v, & Krumbein, W. E. (2000). Bacterial calcification. In *Microbial sediments* (pp. 25–31). Springer.

Konishi, Y., Tsukiyama, T., Ohno, K., Saitoh, N., Nomura, T., & Nagamine, S. (2006). Intracellular recovery of gold by microbial reduction of AuCl4- ions using the anaerobic bacterium Shewanella algae. *Hydrometallurgy*, *81*(1), 24–29.

Kralj, D., Brečević, L., & Kontrec, J. (1997). Vaterite growth and dissolution in aqueous solution III. Kinetics of transformation. *Journal of Crystal Growth*, *177*(3–4), 248–257.

Kralj, D., Brečević, L., & Nielsen, A. E. (1990). Vaterite growth and dissolution in aqueous solution I. Kinetics of crystal growth. *Journal of Crystal Growth*, *104*(4), 793–800.

Kralj, D., Brečević, L., & Nielsen, A. E. (1994). Vaterite growth and dissolution in aqueous solution II. Kinetics of dissolution. *Journal of Crystal Growth*, *143*(3–4), 269–276.

Krumbein, W. E. (1979). Photolithotropic and chemoorganotrophic activity of bacteria and algae as related to beachrock formation and degradation (Gulf of Aqaba, Sinai). *Geomicrobiology Journal*, *1*(2), 139–203.

Kumar, A., Karig, D., Acharya, R., Neethirajan, S., Mukherjee, P. P., Retterer, S., & Doktycz, M. J. (2013). Microscale confinement features can affect biofilm formation. *Microfluidics and Nanofluidics*, *14*(5), 895–902.

Kupriyanova, E., Villarejo, A., Markelova, A., Gerasimenko, L., Zavarzin, G., Samuelsson, G., … Pronina, N. (2007). Extracellular carbonic anhydrases of the stromatolite-forming cyanobacterium Microcoleus chthonoplastes. *Microbiology*, *153*(4), 1149–1156.

Kurmaç, Y. (2009). The impact of toxicity of metals on the activity of ureolytic mixed culture during the precipitation of calcium. *Journal of Hazardous Materials*, *163*(2–3), 1063–1067.

Lauchnor, E. G., Topp, D. M., Parker, A. E., & Gerlach, R. (2015). Whole cell kinetics of ureolysis by Sporosarcina pasteurii. *Journal of Applied Microbiology*, *118*(6), 1321–1332. https://doi.org/10.1111/jam.12804

Le Metayer-Levrel, G., Castanier, S., Orial, G., Loubiere, J.-F., & Perthuisot, J.-P. (1999). Applications of bacterial carbonatogenesis to the protection and regeneration of limestones in buildings and historic patrimony. *Sedimentary Geology*, *126*(1–4), 25–34.

Lewandowski, Z., & Beyenal, H. (2013). *Fundamentals of biofilm research*. CRC press.

Li, M., Fu, Q.-L., Zhang, Q., Achal, V., & Kawasaki, S. (2015). Bio-grout based on microbially induced sand solidification by means of asparaginase activity. *Scientific Reports*, *5*, 16128.

Lian, B., Hu, Q., Chen, J., Ji, J., & Teng, H. H. (2006). Carbonate biomineralization induced by soil bacterium Bacillus megaterium. *Geochimica et Cosmochimica Acta*, *70*(22), 5522–5535.

Life Technologies. (2004). No Title. Retrieved January 2, 2018, from

https://tools.lifetechnologies.com/content/sfs/manuals/mp07007.pdf

LIN, H.-M., Cao, N., & CHEN, L.-F. (1994). Antimicrobial effect of pressurized carbon dioxide on Listeria monocytogenes. *Journal of Food Science*, *59*(3), 657–659.

Lowenstam, H. A. (1981). Minerals formed by organisms. *Science*, *211*(4487), 1126–1131.

Lowenstam, H. A., & Weiner, S. (1989). *On biomineralization*. Oxford University Press on Demand.

Lowenstam, H. A., Weiner, S., bioMASON, Robbins, R., Technologies, L., Lowenstam, H. A., … Whitesides, G. M. M. (2011). No Title. *Annual Review of Fluid Mechanics*, *1*(1), 1–5. https://doi.org/http://researchrepository.murdoch.edu.au/399/2/02Whole.pdf

Lüttge, A., & Conrad, P. G. (2004). Direct observation of microbial inhibition of calcite dissolution. *Applied and Environmental Microbiology*, *70*(3), 1627–1632.

McConnaughey, T. A., & Whelan, J. F. (1997). Calcification generates protons for nutrient and bicarbonate uptake. *Earth-Science Reviews*, *42*(1–2), 95–117.

McKay, D. S., Gibson, E. K., Thomas-Keprta, K. L., Vali, H., Romanek, C. S., Clemett, S. J., … Zare, R. N. (1996). Search for past life on Mars: possible relic biogenic activity in Martian meteorite ALH84001. *Science*, *273*(5277), 924–930.

Minto, J. M., MacLachlan, E., El Mountassir, G., & Lunn, R. J. (2016). Rock fracture grouting with microbially induced carbonate precipitation. *Water Resources Research*. https://doi.org/10.1002/2016WR018884

Mitchell, A. C., & Ferris, F. G. (2005). The coprecipitation of Sr into calcite precipitates induced by bacterial ureolysis in artificial groundwater: temperature and kinetic dependence. *Geochimica et Cosmochimica Acta*, *69*(17), 4199–4210.

Mitchell, A. C., & Ferris, F. G. (2006). The influence of Bacillus pasteurii on the nucleation and growth of calcium carbonate. *Geomicrobiology Journal*, *23*(3–4), 213–226.

Mitchell, A. C., Phillips, A. J., Hiebert, R., Gerlach, R., Spangler, L. H., & Cunningham, A. B. (2009a). Biofilm enhanced geologic sequestration of supercritical CO2. *International Journal of Greenhouse Gas Control*, *3*(1), 90–99.

Mitchell, A. C., Phillips, A. J., Hiebert, R., Gerlach, R., Spangler, L. H., & Cunningham, A. B. (2009b). Biofilm enhanced geologic sequestration of supercritical CO2. *International Journal of Greenhouse Gas Control*, *3*(1), 90–99. https://doi.org/10.1016/j.ijggc.2008.05.002

Monger, H. C., Daugherty, L. A., Lindemann, W. C., & Liddell, C. M. (1991). Microbial precipitation of pedogenic calcite. *Geology*, *19*(10), 997–1000.

Montemagno, C., & Pyrak-Nolte, L. (1995). Porosity of natural fracture networks. *Geophysical Research*

Letters, *22*(11), 1397–1400.

Montemagno, C., & Pyrak-Nolte, L. (1999). Fracture Netwok versus Single Structures: Measurement of Fracture Geometry with X-ray Tomography. *Phys. Chem. Earth (A)*, *24*(7), 575–579.

Montoya, B. M. (2012). *Bio-mediated soil improvement and the effect of cementation on the behavior, improvement, and performance of sand*. University of California, Davis.

Morita, R. Y. (1980). Calcite precipitation by marine bacteria. *Geomicrobiology Journal*, *2*(1), 63–82.

Morse, J. W. (1983). The kinetics of calcium carbonate dissolution and precipitation. *Reviews in Mineralogy and Geochemistry*, *11*(1), 227–264.

Mortensen, B. M., Haber, M. J., Dejong, J. T., Caslake, L. F., & Nelson, D. C. (2011). Effects of environmental factors on microbial induced calcium carbonate precipitation. *Journal of Applied Microbiology*, *111*(2), 338–349. https://doi.org/10.1111/j.1365-2672.2011.05065.x

Nemati, M., & Voordouw, G. (2003). Modification of porous media permeability, using calcium carbonate produced enzymatically in situ. *Enzyme and Microbial Technology*, *33*(5), 635–642. https://doi.org/10.1016/S0141-0229(03)00191-1

Okwadha, G. D. O., & Li, J. (2010a). Optimum conditions for microbial carbonate precipitation. *Chemosphere*, *81*(9), 1143–1148.

Okwadha, G. D. O., & Li, J. (2010b). Optimum conditions for microbial carbonate precipitation. *Chemosphere*, *81*(9), 1143–1148. https://doi.org/10.1016/j.chemosphere.2010.09.066

Parks, S. L. (2009). Kinetics of Calcite Precipitation By Ureolytic Bacteria Under Aerobic and Anaerobic Conditions. *Chemical and Biological Engineering*, (April), 93.

Phillips, A. J., Gerlach, R., Lauchnor, E., Mitchell, A. C., Cunningham, A. B., & Spangler, L. (2013). Engineered applications of ureolytic biomineralization: a review. *Biofouling*, *29*(6), 715–733. https://doi.org/10.1080/08927014.2013.796550

Phillips, A. J., Lauchnor, E., Eldring, J. J., Esposito, R., Mitchell, A. C., Gerlach, R., … Spangler, L. H. (2013). Potential CO2 leakage reduction through biofilm-induced calcium carbonate precipitation. *Environmental Science & Technology*, *47*(1), 142–149. https://doi.org/10.1021/es301294q

Pyrak-Nolte, L. J., Montemagno, C. D., Yang, G., Cook, N. G. W., & Myer, L. R. (1995). Three-dimensional tomographic visuallzatlon of natural fracture networks and graph theory analysis of the transport properties. In *8th ISRM Congress* (pp. 855–859). Tokyo, Japan: International Society for Rock Mechanics. Retrieved from https://www.onepetro.org/conference-paper/ISRM-8CONGRESS-1995-174

Pyrak-Nolte, L., Montemagno, C., & Nolte, D. (1997). Volumetric imaging of aperture distributions in connected fracture networks. *Geophysical Research Letters*, *24*(18), 2343–2346.

R. Robbins. (2010). No Title. Retrieved January 2, 2018, from http://www.utdallas.edu/~rar011300/SEM/Scanning Electron Microscope Operation.pdf

Reddy, B. V. V., & Jagadish, K. S. (2003). Embodied energy of common and alternative building materials and technologies. *Energy and Buildings*, *35*(2), 129–137.

Rivadeneyra, M. A., Delgado, R., del Moral, A., Ferrer, M. R., & Ramos-Cormenzana, A. (1994). Precipatation of calcium carbonate by Vibrio spp. from an inland saltern. *FEMS Microbiology Ecology*, *13*(3), 197–204.

Rodriguez-Navarro, C., Rodriguez-Gallego, M., Chekroun, K. Ben, & Gonzalez-Munoz, M. T. (2003). Conservation of ornamental stone by Myxococcus xanthus-induced carbonate biomineralization. *Applied and Environmental Microbiology*, *69*(4), 2182–2193.

Rosenbaum, L. (2006). Prehistoric artistry, real and recreated. *The Wall Street Journal*, *13*.

Sarikaya, M. (1999). Biomimetics: materials fabrication through biology. *Proceedings of the National Academy of Sciences*, *96*(25), 14183–14185.

Schultze-Lam, S., Fortin, D., Davis, B. S., & Beveridge, T. J. (1996). Mineralization of bacterial surfaces. *Chemical Geology*, *132*(1–4), 171–181.

Sham, E., Mantle, M. D., Mitchell, J., Tobler, D. J., Phoenix, V. R., & Johns, M. L. (2013). Monitoring bacterially induced calcite precipitation in porous media using magnetic resonance imaging and flow measurements. *Journal of Contaminant Hydrology*, *152*, 35–43. https://doi.org/10.1016/j.jconhyd.2013.06.003

Sherwood, J. L., Sung, J. C., Maneval, J. E., & Smith, J. A. (2003). Analysis of Bacterial Random Motility in a Porous Medium Using Magnetic Resonance Imaging and Immunomagnetic Labeling, *37*(4), 781–785.

Siddique, R., & Chahal, N. K. (2011a). Effect of ureolytic bacteria on concrete properties. *Construction and Building Materials*, *25*(10), 3791–3801.

Siddique, R., & Chahal, N. K. (2011b). Effect of ureolytic bacteria on concrete properties. *Construction and Building Materials*, *25*(10), 3791–3801. https://doi.org/10.1016/j.conbuildmat.2011.04.010

Silver, S., Toth, K., & Scribner, H. (1975). Facilitated transport of calcium by cells and subcellular membranes of Bacillus subtilis and Escherichia coli. *Journal of Bacteriology*, *122*(3), 880–885.

Smith, K. S., & Ferry, J. G. (2000). Prokaryotic carbonic anhydrases. *FEMS Microbiology Reviews*,

24(4), 335–366.

Söhnel, O., & Garside, J. (n.d.). Precipitation: Basic principles and industrial applications. 1992. Oxford: Butterworth-Heinemann.

Southam, G. (2000). Bacterial surface-mediated mineral formation. In *Environmental microbe-metal interactions* (pp. 257–276). American Society of Microbiology.

Stabnikov, V., Naeimi, M., Ivanov, V., & Chu, J. (2011). Formation of water-impermeable crust on sand surface using biocement. *Cement and Concrete Research*, *41*(11), 1143–1149.

Stewart, P. S. (2003). Diffusion in biofilms. *Journal of Bacteriology*, *185*(5), 1485–1491.

Stocks-Fischer, S., Galinat, J. K., & Bang, S. S. (1999a). Microbiological precipitation of CaCO3. *Soil Biology and Biochemistry*, *31*(11), 1563–1571.

Stocks-Fischer, S., Galinat, J. K., & Bang, S. S. (1999b). Microbiological precipitation of CaCO3. *Soil Biology and Biochemistry*, *31*(11), 1563–1571. https://doi.org/10.1016/S0038-0717(99)00082-6

Stoner, D. L., Watson, S. M., Stedtfeld, R. D., Meakin, P., Tyler, T. L., Pegram, L. M., … Griffel, L. K. (2005). Application of Stereolithographic Custom Models for Studying the Impact of Biofilms and Mineral Precipitation on Fluid Flow Application of Stereolithographic Custom Models for Studying the Impact of Biofilms and Mineral Precipitation on Fluid Flow. https://doi.org/10.1128/AEM.71.12.8721

Stumm, W., & Morgan, J. J. (1981). Aquatic Chemistry, 780 pp. *J. Wi L Ey & Sons*.

Tagliaferri, F., Waller, J., And??, E., Hall, S. A., Viggiani, G., B??suelle, P., & DeJong, J. T. (2011). Observing strain localisation processes in bio-cemented sand using x-ray imaging. *Granular Matter*, *13*(3), 247–250. https://doi.org/10.1007/s10035-011-0257-4

Thomas-Keprta, K. L., McKay, D. S., Wentworth, S. J., Stevens, T. O., Taunton, A. E., Allen, C. C., … Romanek, C. S. (1998). Bacterial mineralization patterns in basaltic aquifers: Implications for possible life in martian meteorite ALH84001. *Geology*, *26*(11), 1031–1034.

Thompson, J. B., & Ferris, F. G. (1990). Cyanobacterial precipitation of gypsum, calcite, and magnesite from natural alkaline lake water. *Geology*, *18*(10), 995–998.

Tiano, P., Biagiotti, L., & Mastromei, G. (1999). Bacterial bio-mediated calcite precipitation for monumental stones conservation: methods of evaluation. *Journal of Microbiological Methods*, *36*(1–2), 139–145.

Tobler, D. J., Cuthbert, M. O., & Phoenix, V. R. (2014). Transport of Sporosarcina pasteurii in sandstone and its significance for subsurface engineering technologies. *Applied Geochemistry*, *42*, 38–44. https://doi.org/10.1016/j.apgeochem.2014.01.004

Valiei, A., Kumar, A., Mukherjee, P. P., Liu, Y., & Thundat, T. (2012). A web of streamers: biofilm formation in a porous microfluidic device. *Lab on a Chip*, *12*(24), 5133–5137. https://doi.org/10.1039/c2lc40815e

van Paassen, L. (2009). *Biogrout: Ground Improvement by Microbially Induced Carbonate Precipitation*. *Technology*.

Von Der Schulenburg, D. A. G., Paterson-Beedle, M., MacAskie, L. E., Gladden, L. F., & Johns, M. L. (2007). Flow through an evolving porous media-compressed foam. *Journal of Materials Science*, *42*(16), 6541–6548. https://doi.org/10.1007/s10853-007-1523-z

Wanger, G., Onstott, T. C., & Southam, G. (2008). Stars of the terrestrial deep subsurface: A novel "star-shaped" bacterial morphotype from a South African platinum mine. *Geobiology*. https://doi.org/10.1111/j.1472-4669.2008.00163.x

Warren, L. A., Maurice, P. A., Parmar, N., & Ferris, F. G. (2001). Microbially mediated calcium carbonate precipitation: implications for interpreting calcite precipitation and for solid-phase capture of inorganic contaminants. *Geomicrobiology Journal*, *18*(1), 93–115.

Warthmann, R., Van Lith, Y., Vasconcelos, C., McKenzie, J. A., & Karpoff, A. M. (2000). Bacterially induced dolomite precipitation in anoxic culture experiments. *Geology*, *28*(12), 1091–1094.

Watabe, N., & Wilbur, K. M. (1960). Influence of the organic matrix on crystal type in molluscs. *Nature*, *188*(4747), 334.

Wei, L., Liping, L., Long, C., & Longjiang, Y. (2009). Research status and prospect of biological precipitation of carbonate. *Advances in Earth Science*, *24*(6), 597–605.

Whiffin, V. S. (2004). Microbial CaCO3 Precipitation for the Production of Biocement. *Phd Thesis*, (September), 1–162. https://doi.org/http://researchrepository.murdoch.edu.au/399/2/02Whole.pdf

Wiley, W. R., & Stokes, J. L. (1962). Requirement of an alkaline pH and ammonia for substrate oxidation by Bacillus pasteurii. *Journal of Bacteriology*, *84*(4), 730–734.

Zhang, J., Davis, T. A., Matthews, M. A., Drews, M. J., LaBerge, M., & An, Y. H. (2006). Sterilization using high-pressure carbon dioxide. *The Journal of Supercritical Fluids*, *38*(3), 354–372.

Zhong, L., Islam, M. R., & others. (1995). A new microbial plugging process and its impact on fracture remediation. In *SPE Annual Technical Conference and Exhibition*.

Chapter 3

Sporosarcina pasteurii can form nanoscale crystals on cell surface

** A version of this chapter is under review for publication as a journal article

Abstract

Using a semi-solid 0.5% agar column, we study the phenomenon of microbially induced mineral (calcium carbonate) by the bacterium *Sporosarcina pasteurii*. Our platform allows for in-situ visualization of the phenomena, and we found clear evidence of bacterial cell surface facilitating formation of nanoscale crystals. Moreover, in the bulk agar we found the presence of microspheres, which seem to arise from an aggregation of nanoscale crystals with needle like morphology. A range of chemical characterization studies (e.g. EDX, XRD, XPS/SIMS) confirmed that the crystals to be calcium carbonate, and two different polymorphs (calcite and vaterite) were identified.

3.1 Introduction

Biomineralization refers to the process of mineral precipitation due to chemical alteration of the environment induced by the microbial activity (De Muynck et al., 2010; Sarikaya, 1999; Stocks-Fischer et al., 1999a; Warren et al., 2001). For unicellular organisms such as bacteria (Sarikaya, 1999), the biomineralization process can be either extracellular (Navdeep Kaur Dhami et al., 2013) or intracellular (Konishi et al., 2006). Microbially induced calcite precipitation (MICP) is an excellent example of an extracellular mineral deposition. Several microbial species take part in MICP by means of various mechanisms such as photosynthesis (McConnaughey & Whelan, 1997; Thompson & Ferris, 1990), urea hydrolysis (Navdeep K. Dhami et al., 2013; Stocks-Fischer et al., 1999a), sulfate reduction (Castanier et al., 1999; Hammes & Verstraete, 2002), anaerobic sulfide oxidation (Warthmann, Van Lith, Vasconcelos, McKenzie, & Karpoff, 2000), biofilm and extracellular polymeric substances (Arias & Fernández, 2008; Kawaguchi & Decho, 2002). There has been significant interest in microorganisms that can produce urease (urea amidohydrolase; EC 3.5.1.5) and hence are able to hydrolyze urea to induce calcite precipitation (Hammes & Verstraete, 2002). *Sporosarcina pasteurii* (formerly *Bacillus pasteurii*) is a non-pathogenic, endospore producing soil bacteria that also produces urease and can tolerate highly basic environments. *Sporosarcina pasteurii* has attracted significant attention from researchers for its unique feature of calcium carbonate

precipitation, which can be easily controlled (V Achal, Mukherjee, Basu, & Reddy, 2009; Bang et al., 2001; Gorospe et al., 2013; Hammes, 2003; Mitchell & Ferris, 2005; Okwadha & Li, 2010b). *S. pasteurii* is being investigated for the possibility of its utilization towards a multitude of applications including underground storage of carbon, healing masonry structures of archaeological importance and long-term sealing of geologic cracks in large-scale structures (Anbu, Kang, Shin, & So, 2016; Navdeep Kaur Dhami et al., 2013; Ganendra et al., 2014; Li, Fu, Zhang, Achal, & Kawasaki, 2015; Phillips, Lauchnor, et al., 2013). Hammes and Verstraete (2002) reported the four very important parameters for MICP as pH, dissolved inorganic carbon, calcium concentration and available nucleation site. The saturation rate of carbonate ions concentration (CO_3^{2-}) is controlled by the first three parameters and it is believed that bacterial cell wall as the nucleation site facilitate the stable and continuous calcium carbonate deposition (Phillips, Lauchnor, et al., 2013). However the bacteria-free solution loaded with urease enzyme can also induce calcium carbonate precipitation. Mitchell and Ferris (2006) studied the influence of bacteria (*Bacillus pasturii*) on the nucleation of MICP. The bacteria-free enzyme solution was compared to the bacteria induced environment. Authors reported significant positive effect of bacterial presence (referred as "bacteria-inclusive") on the increase of size and growth rate of the precipitated crystal though the idea of bacterial control of MICP was rejected. The bacteria-free urease solution showed similarities with the bulk chemical precipitation whereas differences were observed for aqueous microenvironment of bacteria (Mitchell & Ferris, 2006).

It has been suggested that the bacterial cell walls can serve as nucleation sites (Anbu et al., 2016; Ganendra et al., 2014; Hammes, 2003; Morita, 1980) as bacterial cell surfaces carry negatively charged groups at neutral pH (Douglas & Beveridge, 1998; Ehrlich, 1996, 1998). These negative charges can influence the binding of cations (e.g. Ca^{2+}) on the cell surface and eventually acting as nucleation sites when reacting with carbonate anions from the solution to form insoluble calcium carbonate (Chunxiang, Jianyun, Ruixing, & Liang, 2009; Douglas & Beveridge, 1998; a Kantzas et al., 1992). Definitive proofs of involvement of bacterial cell walls in complex environments on the nucleation process are rare. Ghashghaei and Emtiazi reported the presence of nanocrystals of calcium carbonate on cell walls of the bacteria *E. ludwigii* for experiments performed with a liquid culture (Ghashghaei & Emtiazi, 2013). While the data is suggestive of the role of cell wall, a more definite proof is desirable. In a contrasting study, Bundeleva et al. reported on MICP by the anoxygenic *Rhodovulum* sp. Their TEM analyses failed to show the existence of $CaCO_3$ on or near live cells. The authors claim the existence of certain cell protection mechanisms against mineral

incrustation at the vicinity of live bacteria and they invoke the idea of mineral precipitation at a certain distance from the cell surface (Bundeleva et al., 2012; Ganendra et al., 2014). Thus, we see that the issue of role of cell wall on mineral precipitation in MICP remains controversial and detailed studies delineating the exact mechanism leading to the nucleation of crystals in *in-situ* conditions are desirable.

To the best of our knowledge, no conclusive reports of the role of cell wall in MICP in complex environments have been reported. Applications of *S. pasteurii*'s MICP often include their activity in porous media such as concrete and rocks (Demény et al., 2016; Dick et al., 2006; Phillips, Lauchnor, et al., 2013), where *in-situ* visualization is often challenging. In order to the address the fundamental mechanism of MICP by *S. pasteurii* in complex environments, we designed an agar column setup, which allows us to investigate mineral precipitation by direct observation. Our setup consists of a 0.5% agar-column that is stab-inoculated and MICP proceeds in the setup as downward travelling conspicuous mineral trails. We investigate the morphology of precipitated crystals and conclusively demonstrate ~~that~~ the presence of nano-crystals of calcite on the bacterial cell wall. While this can be considered as definitive evidence that the cell wall does serve as a nucleation site, other mechanisms of nucleation are not ruled out.

3.2 Results and Discussion:
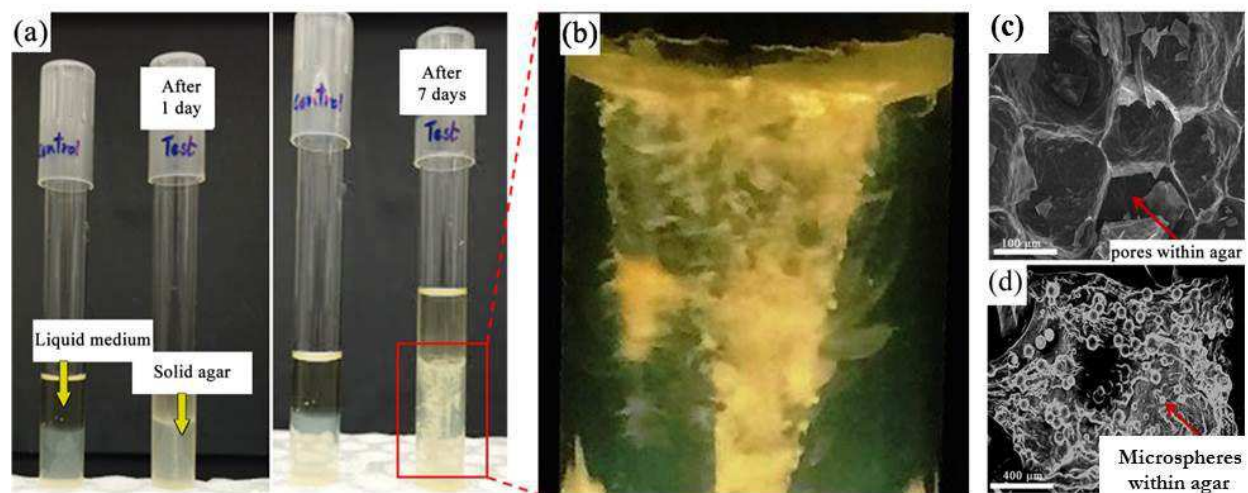
Fig. 3.1 (a) Two samples containing the semi-solid 0.5% agar medium in two identical 20 mL test tubes. The one to the left is the control sample which is devoid of any bacterial cells. To the right is

the *S. pasteurii* inoculated sample where the resulting mineral precipitation has left a conspicuous trail. Images were taken after 1 day and 7 days of the inoculation. (b) Blown out magnified image of the mineral deposition. (c-d) SEM image of agar showing pores in control set (c) and numerous mineral microspheres after 7 days (d) of incubation.

3.2.1 Agar Column: To understand growth of *S. pasteurii* is a porous environment, an agar column with stab culture was observed for a period of one week. Figure 3.1(a) shows the original culture tubes containg growth spans after day-1 and day-7. Extensive calcite deposition can be prominently seen in Fig 3.1(b) after 7 days of incubation. The agar media acted as soft, porous and transperant nutrient riched environment to monitor the bacterial motility and calcite precipitation. Figure 3.1(c) depicts a scanning electron microscopy image of the agar column, where porous structures can clearly be seen. *S. pasteurii* bacterium possesses flagellum (see Fig. 3.S1(b)) which likely allows it to navigate the porous structure of the agar column. The agar column was sectioned at a height of 1.25 cm after 4 days, and the bacterial motion observed through optical microscopy. Figure 3.S2 a,b show a motile bacteria within the agar column and the corresponding velocity historgram. The histogram indicates within the agar matrix the bacterium can travel at velocities $\sim 10^{-7}$ m/s and hence it can be expected that bacterial cells can travel approximately 1 cm of agar column per day. This 'seeping speed' is also corroborated through macroscale observations (Fig. 3.1b). Figure 3.1(d) also shows the presence of deposits in the agar column after 7 days of bacterial activity.
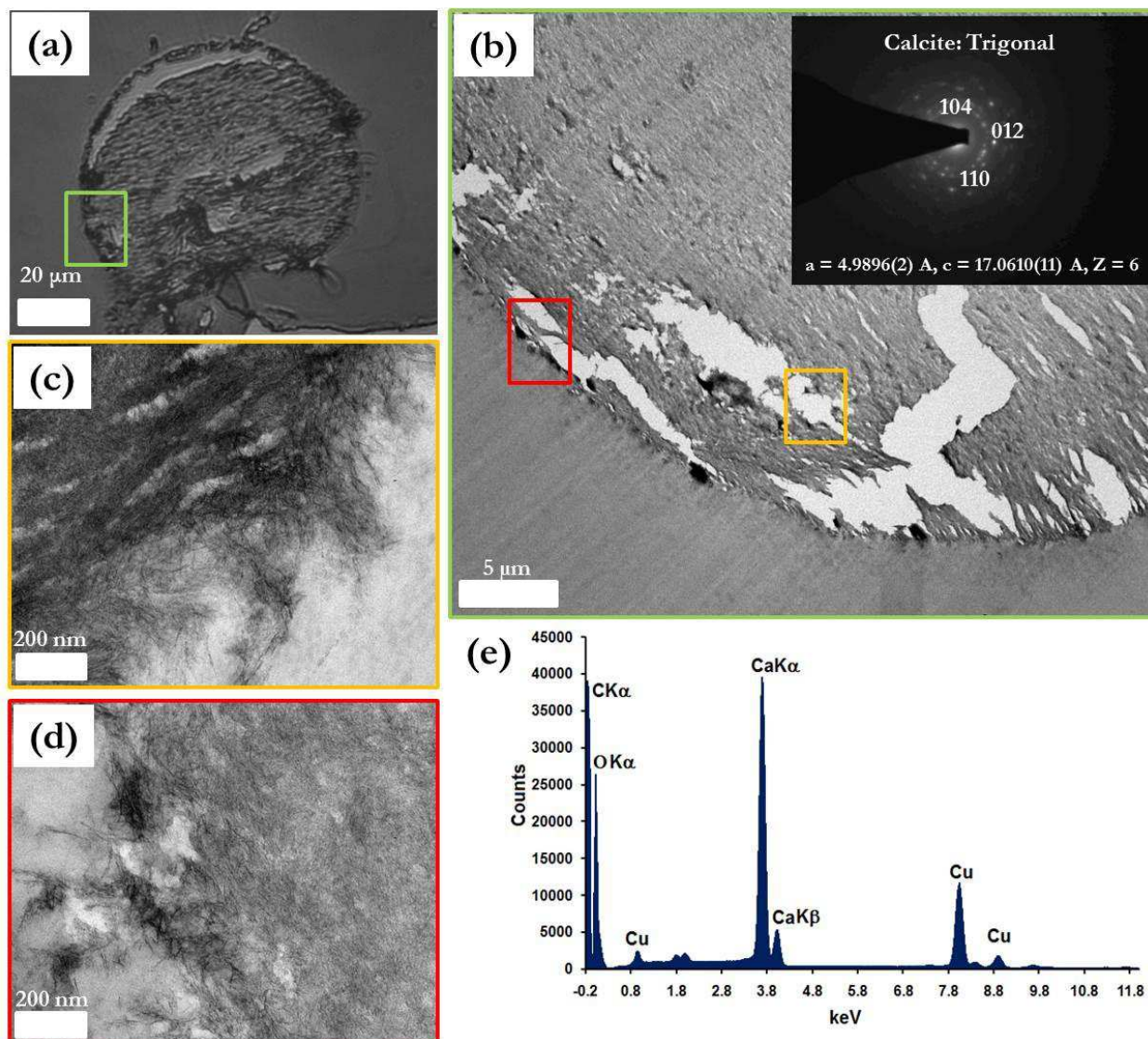
Fig. 3.2 (a) An optical microscopy image of an ultrathin (80 nm) section of agar column with crystal, which was stained with crystal violet. (b) TEM image of a portion of the same crystal. (Inset) The SAED pattern of the crystalline structure. (c)-(d) Higher magnification TEM images of the crystal shown in (b). Corresponding locations are boxed and color coded (e) The EDX analysis indicates the presence of C, Ca and O. The Cu-signals in (e) originate from the copper-grids used for holding the samples.

3.2.2 Calcite micro-spheres: The primary advantage of the agar-column experimental setup is *in-situ* visualization and easy access for supporting characterizations. The agar column was section at a height of 2.5 cm after a period of 7 days and crystalline depositions were characterized by other forms of microscopy. Specifically, the agar colunm was characterized using optical micrsopy,

71

transmission electron microscopy (TEM), selected area diffraction pattern (SAED) and elemental characteization was determined by powder XRD and energy-dispersive X-ray spectroscopy (EDS). Optical microscopy of ultrathin (~80 nm) sections of the agar medium revealed depositions of crystalline mircrospheres profusely within the agar column. Optical and TEM imaging revealed that the visible white deposits within the column were mostly crystalline micropheres of about 10-50 μm in diameter. Figure 3.2(a) shows a crystal violet stained cross-section of microsphere (diameter ~10 μm) and Figure 3.2(b) shows the TEM image of the same with a SAED pattern (Inset of Figure 3.2(b)) proves the crystalline nature of the precipitates and also consistent with the Miller indices of calcium carbonate observed in XRD. The detailed magnified observation of the microspheres in Figure 3.2 (c and d) revealed the spatial arrangement of calcite nano-needles at the interface of agar-calcite microsphere. Elemental confirmation was performed with EDS on selected microsperes at the agar-crystal interface (Figure 3.2c) and within the microcrystal (Figure 3.2d). EDS (Figure 3.2e) spectral results indicated the presence of Ca, C and O.
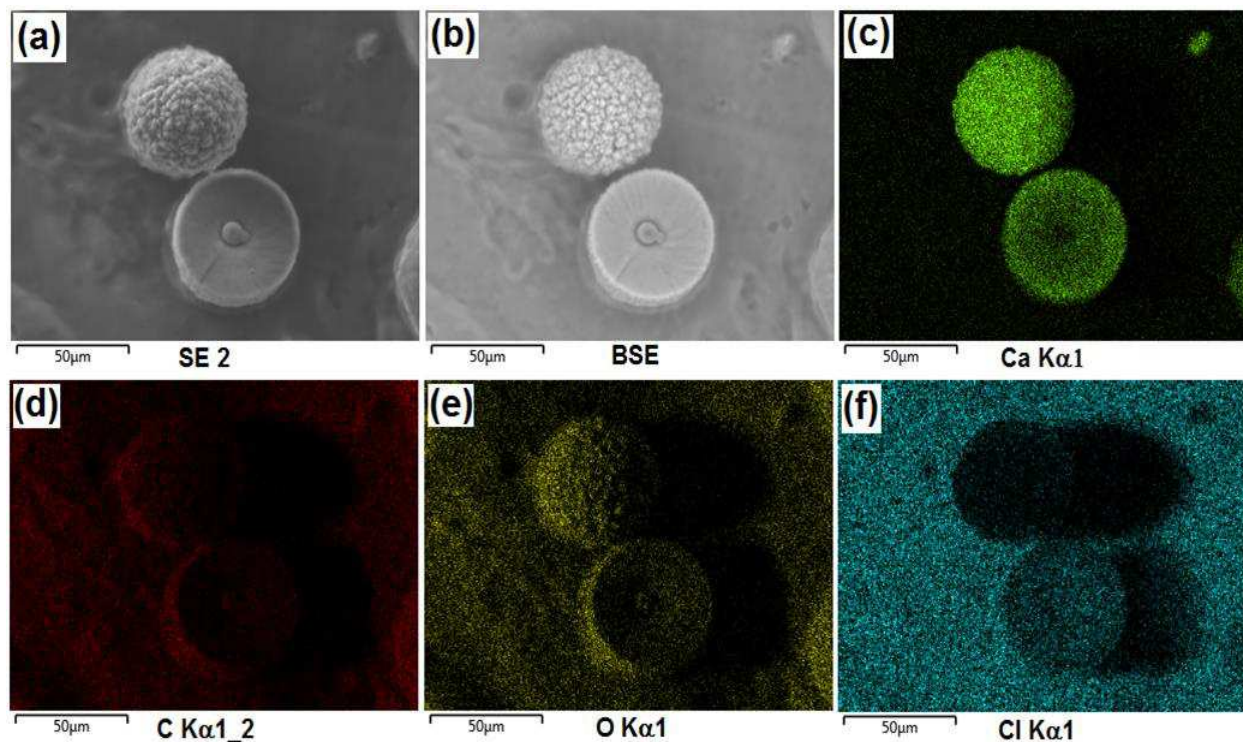
Fig. 3.3 SEM and EDX mapping of elemental distribution analysis for calcite microspheres. (a) Secondary electron microscopy (SE 2) (b) backscattered electron microscopy (BSE) images. (c-f) EDS mapping of elemental distribution showing Ca (c), C (d) and O (e) as the main ingredient of

microspheres. Appearance of Cl (f) within microspheres and surrounding agar possibly originates from added NaCl salt in the bacterial growth medium.

The direct *in-situ* visualization on the MICP provides a new window to explore the arrangement of calcium carbonate nano-needles, which give rise microspheres within the semi-solid porous agar media.

To further confirm the elemental distribution, the dissected calcium carbonate microspheres (diameter ~50 μm) were identified within the freeze-dried agar column and subjected to secondary electron SEM (Figure 3.3(a)) and backscattered SEM (BSE) (Figure 3.3(b)). Back-scattered electrons are high energy particles which are reflected back from the sample after multiple elastic scattering interactions with the component atoms inside the crystal. The heavier elements tend to scatter electrons more strongly than their lighter counterparts. Hence, they appear brighter in the final image. In general, BSE images are brighter and have a better contrast. Here, the increased intensity in BSE image (Figure 3.3(b)) confirmed the presence of highly dense elements with higher atomic number e.g. Ca. EDS elemental mapping (with false colors to different elements) also supported the compositional presence of Ca (Figure 3.3(c)) along with other pertinent elemental compositions of the microspheres to be C (Figure 3.3(d)) and O (Figure 3.3(e)) were once again verified. The Cl mapping (Figure 3.3(f)) showed negligible signal on the surface whereas prominent signal from the dissection. This signal is likely due to the added NaCl in the bacterial growth media. The transparent agar column therefore provided a real time monitoring platform to study *S. pasteurii* induced calcium carbonate precipitation. The optical and elemental confirmation of the precipitate provides an experimental support to the mineral deposition phenomenon induced by bacteria.

3.2.3 *S. pasteurii* micro-environment. TEM imaging of the micro-environment of bacterial cell surface shed light on the likely nucleation route for the calcite microspheres. The 80 nm ultra-thin sections of agar column containing embedded bacteria shows in Figure 3.4(a, b and c) clearly depict the micro-environment of the bacterium (Fig. 3.4). Oval shaped bacterial cells can be seen along with formation of spores. Nano-needles that were previously encountered (Fig 3.2(c)) can also be seen in the vicinity of the cells (Fig 3.4(a)). Magnified images indicate nanoscale spherical depositions on cell surface (Figure 3.4(b)) and needle-like depositions in the surrounding agar media (Figure 3.4(c)). The elemental confirmation was performed with EDS on bacterial cell surface deposition. EDS results (Figure 3.4(d)) indicated the presence of Ca, C and O. The powder XRD

73

results of the whole colunm used to identify the crystalline phases of the inorganic compounds. The identified signature peaks of calcite (Figure 3.4(e)) at 2θ valus of 26.83°, 34.26° and 42.01° respectively correlated with lattice (hkl) indiced of (012), (104) and (110). Low intensity vaterite peaks (Figure 3.4(e): Inset) were also identified at 2θ valus of 28.98°, 31.52° and 38.22° correlated with lattice (hkl) indices of (100), (101) and (102), respectively. Calcite forms a trigonal system of crystals which belong to the hexagonal scalenohedral class. Vaterite forms a hexagonal system of crystals which belong to the dihexagonal dipyramidal class.
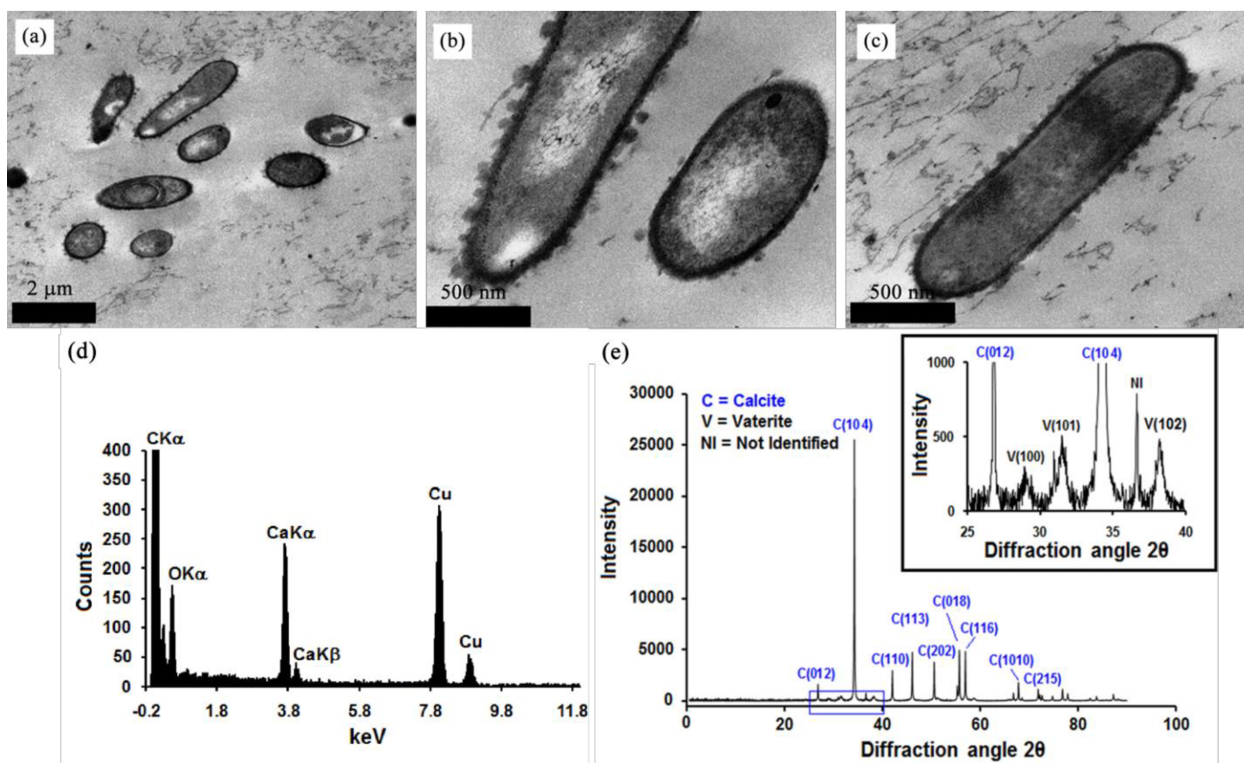
Fig. 3.4 (a)-(c) TEM images of ultrathin sections of the agar medium depicting the presence of cells and spores. They also show the presence of bacterial cell surface depositions. (d) EDX pattern of cell surface deposition shows existence of Ca, C and O. (e) XRD plot of the same location indicates the presence of calcite and vaterite polymorphs. (inset) Blown-up sub-section of (e) clearly demonstrates presence of vaterite. The Cu-signals in (d) originate from the copper-grids used for holding the samples.

3.3 Conclusion

In this work, we develop a simple, yet effective experimental platform for *in-situ* imaging of the MICP process by *Sporosarcina pasteurii*. Agar (0.5%) was used to create a porous column, which was inncoluated with a stab culture. As *S. pasteurii* cells migrated down the agar column they left conspicuous trail of crystals. Samples of the agar column at different locations were taken and subjected to microscopy and we found that the crystal train consisted of calcite microspheres, which on closer inspection were found to be an aggregate of needle-like nanoscale crystals. Moreover, cells whose surface contained calcite nanocrystals were also observed confirming the hypothesis that cell surface plays a role in nucleation.

3.4 Materials and Methods (Supplementary Information)
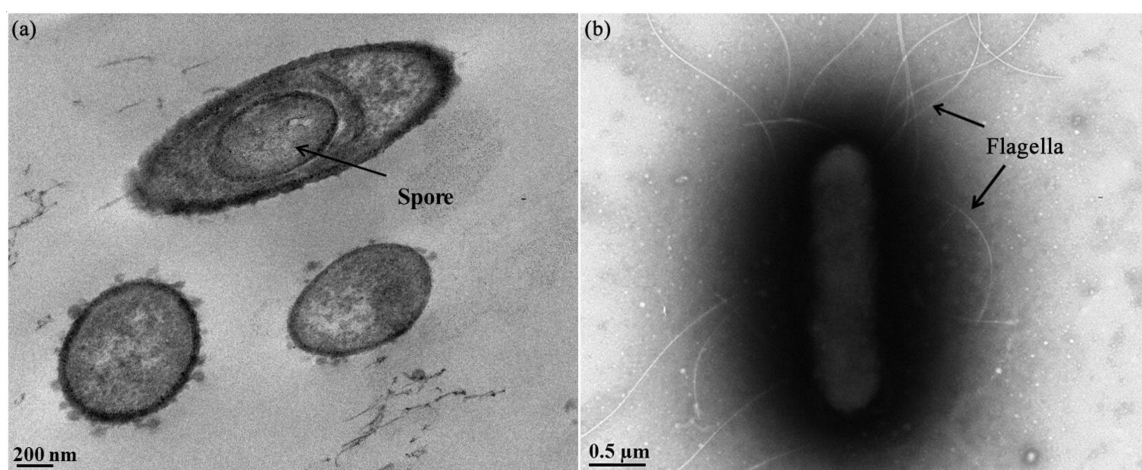
Fig. 3.S1 TEM images showing the presence of spores (a) and flagella (b) with *S. pasteurii*.

3.4.1 Bacteria culture: The bacterial strain *Sporosarcina pasteurii* (Miquel) Yoon et al. ATCC® 11859™ was obtained from American Type Culture Collection (ATCC) in freeze-dried condition. The strain was first cultured in ATCC recommended medium. *S. pasteurii* cultures were prepared in nutrient media. Nutrient Broth (NB) was prepared, which contained 5 g peptone; 3 g beef extract and 2 g sodium chloride per 1L of distilled water. The pH of this medium was adjusted to 7.0 using HCl and NaOH. Nutrient agar medium was prepared by utilizing the same ingredients as NB with an additional supplement of 1.5% bacteriological agar. Solution mixtures were sterilized by autoclave wet sterilization method (121 °C, 15 psi) for 15 min. NB and NB-agar were subsequently used for

suspension culture and sub-culturing of S. pasteurii before the experiments. All the cultures were incubated in aerobic conditions at 30 °C. Peptone, beef extract, urea, NaCl, HCl, NaOH and bacteriological agar were purchased from Fischer scientific (Thermo-Fisher Scientific, Waltham, Massachusetts, USA). $CaCl_2$. 2H2O (ACS reagent ≥ 99%) was purchased from Sigma-Aldrich (Sigma-Aldrich, St. Louis, Missouri, USA). All the chemicals were used as purchased and solutions were prepared in Milli Q (18.2 MΩ) water.

3.4.2 Preparation of semi-solid Agar column: Semisolid-agar columns were prepared by following Bang's urea-$CaCl_2$ liquid media with modification. The modified media contain peptone 0.5 %; beef extract 0.3 %, sodium chloride 0.2 % and $CaCl_2$, 0.25 %. The pH of the medium was adjusted to 7.0 and then 0.5 % agar was added prior to autoclaving. Urea (2%) was added separately after autoclaving when media temperature cooled down to approximately 50-60° C. To create the agar columns, 10 ml of liquid agar was poured into upright test tubes and allowed to cool inside a biosafety cabinet, which finally resulted in columns of approximately 5 cm in length. Subsequently, these agar columns were inoculated by stabbing the free surface of the agar column with pre-cultured *S. pasteurii* using a stabbing needle. Fresh liquid media were poured on to the agar column to prevent drying out from the agar surface. The bacteria inoculated columns along with a control were incubated at 30 °C for a maximum duration of 7 days.

3.4.3 Microscopy: For microscopy, sample volumes were cut from the agar-column approximately at mid-height (~ 2.5 cm). Agar slices were cut into small cubes and fixed in solution containing 2.5% glutaraldehyde, 2% paraformaldehyde in 0.1 M phosphate buffer (pH=7.5) for 30 min. The fixation process was followed by buffer wash (0.1M phosphate buffer). Post-fixation treatment of 1% Osmium tetroxide in 0.1 phosphate buffer was performed for 1 h. Standard protocols for buffer washing and dehydration through graded alcohol were followed 4. Samples were infiltrated with Spurr™ resin (1:1 of Ethanol: Spurr mixture) for 3h and then kept in 100% spur for 24h embedding. Samples were embedded in flat molds with fresh Spurr and cured at 70°C for overnight. Cured embedded resin capsules were sectioned in 70-90 nm thin sections using ultramicrotome (Reichert-Jung UltraCut E, Vienna, Austria) and mounted on copper grid for transmission electron microscopy (TEM, Philip-FEI, Morgangni 268, Oregon, USA) operated at 80kV.

Bacterial cultures grown in urea-$CaCl_2$ liquid and solid media were observed for calcium carbonate deposition using scanning electron microscopy (SEM, Zeiss EVO M10, Oberkochen, Germany) and

optical microscopy (Nikon Eclipse Ti, Nikon Instruments Inc., Melville, USA). The SEM samples were prepared by fixing and dehydration in graded alcohol similar to TEM. Dehydrated sample were kept in 100% ethanol and mounted up on carbon tape. The cross-sections of the agar-column were freeze dried (SuperModulyo Freeze Dryer, Savant Instruments Inc., New York, USA) after fixation and directly used for SEM imaging. Every sample was gold sputtered (Denton Vacuum, Desk II, Moorestown, New Jersey) before SEM imaging.

For cell motility experiments, two parallel setups were used – liquid and semi-solid agar media. The liquid media experiment was set up in a Lab Tek II Chambered Coverglass Slide (Thermo Fisher Scientific, Waltham, MA) and agar media experiment was conducted by taking a slice from the agar column at approximately mid-height. Images were obtained using the Nikon Ti inverted microscope using the bright field mode. The camera used was Nikon DS-Qi1Mc, which was operated at 10 fps. Image analysis was performed using ImageJ.
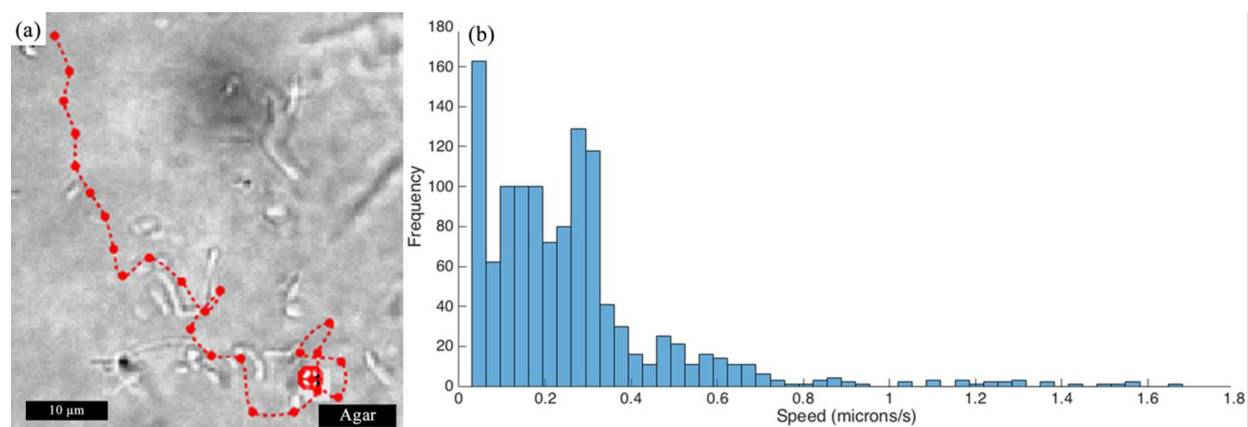
Fig. 3.S2 Analysis of cellular motion (a) Sample bacterial track in agar (b) Corresponding velocity magnitude histogram for bacterial motion in agar.

In addition to Fig. 3.S2, we have computed the mean squared displacement values for single cells in both liquid and semi-solid media. These values are at least one order of magnitude higher than the corresponding Brownian diffusion values. This provides an evidence of the existence of additional mechanisms of locomotion being used by the bacteria. As shown above, these bacteria are equipped with flagella which explain the much larger values of the means squared displacements computed from image analysis.

Here, $\bar{x}^2$ = Mean Squared Displacement (m²),

t = time-lag (~100 s in our experiments),

K = Boltzmann's constant,

T = Temperature (~300 K),

η = Viscosity of the medium (Pa s), and

r = Radius of a cell (~1 μm).

The computed values (from image analysis) of $\bar{x}^2$ and $\bar{y}^2$ for semi-solid medium are 8.15 μm² and 8.69 μm², respectively [O ~ 10^{-11}]. The corresponding Brownian value (calculated from Einstein's relation above) is O ~ 10^{-13}.

The computed values (from image analysis) of $\bar{x}^2$ and $\bar{y}^2$ for liquid medium are 264.0 μm² and 273.6 μm², respectively [O ~ 10^{-10}]. The corresponding Brownian value (calculated from Einstein's relation above) is O ~ 10^{-12}.

Clearly, flagellar locomotion contributes significantly to the transport capacity of the cells.

3.4.4 Zeta Potential Measurements

The surface zeta potential on a concentrated culture was measured using a Malvern *Zetasizer nano* (Malvern, UK) DLS-multiplexer. The results are summarized in the table below. The cells are seen to have a negative charge:

Run	Mobility	Zeta Potential (mV)	Rel. Residual
1	0.91	-20.0	0.0045
2	0.99	-20.1	0.0034
3	1.00	-19.2	0.005

| 4 | 0.82 | -20.1 | 0.0043 |
| 5 | 1.03 | -19.3 | 0.0032 |

Table 3.1: Surface Zeta Potential values measured in a liquid culture of *S. pasteurii*.

The zeta potential values are quite negative. This provides a strong evidence of the existence of negative charge on the cell surface. Although the zeta potential is measured at the Stern Layer of the electric double layer and not exactly on the wall (the cell membrane in this case), it cannot be highly negative as seen here unless the cell surface itself is negative. This is especially true for an ionic solution of ions in a polar liquid like water which would have very poor dielectric screening. These measurements provide additional indirect support to the earlier claim on the existence of negative charge centers acting as nucleation sites for MICP.

This, coupled with the fact that cells move far and wide using flagella, essentially makes *S. pasteurii* good candidate organisms for realizing MICP-based engineering solutions inside an extend porous medium.

3.4.5 Characterization

3.4.5.1 Energy-dispersive X-ray spectroscopy: EDX (or EDS) is a powerful technique used to analyze a sample for its elemental composition. The specimen is illuminated by a focused beam of high-energy electrons. The x-rays excite the electrons within the atoms. As a result, some electrons get knocked off of the sample, leaving behind vacancies or holes. These holes in turn are filled up electrons originally occupying a different energy level. As a result of this transition, a characteristic x-ray is emitted by the atom. The energy of the emitted photon equals the energy difference between the two electronic levels. All the individual photons emitted are detected by an energy-dispersive spectrometer which statistically correlates the distribution with the atomic structure of the sample. For our experiments, the Aztec Synergy system with a resolution of 133 eV at the nanoFAB was used.

3.4.5.2 Selected Area Diffraction: SAED is a popular tool used in conjugation with a TEM for chemical characterization. A TEM sample is illuminated by a beam of parallel high energy electrons. The electrons behave as waves and have wavelengths of the order of picometres. On the other hand, a typical crystal lattice would have an average atomic spacing of the order of nanometers. This

effectively leads to the sample behaving as a diffraction grating for the incident electron beam. The incoming electrons would be diffracted along various directions based on the orientation of the crystal planes and the resulting image appears as a pattern of bright dots. This pattern is a characteristic signature of a particular crystal system and can be matched with a library through proper indexing. This helps in establishing the chemical identity of the crystal. The user can exercise good control on the area of interest by inserting a perforated metal disc in the electron path. This disc selectively allows electrons to strike a selected region while blocking off the others. For our experiments, we used the Phillips/FEI (Morgagni) TEM at the Biological Sciences Advanced Microscopy Facility.

3.4.5.3 X-ray Diffraction: XRD is philosophically similar to EDX with a few differences in operating principle. The incident radiation is a high-energy monochromatic x-ray beam. The sample is placed on a rotating holder and allowed to produce its typical diffraction pattern via elastic scattering. The pattern is recorded in three dimensions for all possible orientations of the sample. All gathered data is analyzed computationally and matched with a database of crystal structures to perform the chemical identification. In this work, the Rigaku Ultimate IV unit at the nanoFAB was used for experiments and the JADE program was used for analysis.

Author contributions

AK conceived part of the work and analyzed data. AK and CM supervised the overall research and participated in manuscript writing. TG and **SB** performed experiments, analyzed data, prepared results and wrote the manuscript. TG and **SB** shared equal contributions.

For the data shown in Fig. 3.1, **SB** performed the microscopy and TG set up the experiment.

For the data shown in Fig. 3.2, both **SB** and TG set up the experiment together. **SB** performed the microscopy and carried out the EDX analysis. TG performed the SAED.

For the data shown in Fig. 3.3, both **SB** and TG set up the experiment together. TG performed the microscopy.

For the data shown in Fig. 3.4, both **SB** and TG set up the experiment together. The microscopy was performed by the TEM-technician (Arlene Oatway) at the Biological Sciences Advance Microscopy Facility.

For the data shown in Fig. 3.S1, both **SB** and TG set up the experiment together. The microscopy was performed by the SEM-specialist (Dr. Anqiang He) at the nanoFAB.

For the data shown in Fig. 3.S2, everything was performed by **SB**.

Conflict of interest

The authors declare no competing interests.

References

Achal, V., Mukerjee, A., & Sudhakara Reddy, M. (2013). Biogenic treatment improves the durability and remediates the cracks of concrete structures. *Construction and Building Materials*, *48*, 1–5. https://doi.org/10.1016/j.conbuildmat.2013.06.061

Achal, V., Mukherjee, a, Basu, P. C., & Reddy, M. S. (2009). Strain improvement of Sporosarcina pasteurii for enhanced urease and calcite production. *Journal of Industrial Microbiology & Biotechnology*, *36*(7), 981–988. https://doi.org/10.1007/s10295-009-0578-z

Achal, V., & Pan, X. (2011). Characterization of urease and carbonic anhydrase producing bacteria and their role in calcite precipitation. *Current Microbiology*, *62*(3), 894–902. https://doi.org/10.1007/s00284-010-9801-4

Achal, V., Pan, X., Fu, Q., & Zhang, D. (2012). Biomineralization based remediation of As(III) contaminated soil by Sporosarcina ginsengisoli. *Journal of Hazardous Materials*, *201–202*, 178–184. https://doi.org/10.1016/j.jhazmat.2011.11.067

Adolphe, J. P., Loubière, J. F., Paradas, J., & Soleilhavoup, F. (1990). Procédé de traitement biologique d'une surface artificielle. *European Patent 90400G97*. *0*, *1989*.

Al Qabany, A., Soga, K., & Santamarina, C. (2012). Factors Affecting Efficiency of Microbially

Induced Calcite Precipitation. *Journal of Geotechnical and Geoenvironmental Engineering*, *138*(8), 992–1001. https://doi.org/10.1061/(ASCE)GT.1943-5606.0000666

Anbu, P., Kang, C.-H., Shin, Y.-J., & So, J.-S. (2016). Formations of calcium carbonate minerals by bacteria and its multiple applications. *Springerplus*, *5*(1), 250.

Arias, J. L., & Fernández, M. S. (2008). Polysaccharides and proteoglycans in calcium carbonate-based biomineralization. *Chemical Reviews*, *108*(11), 4475–4482.

Bang, S. S., Galinat, J. K., & Ramakrishnan, V. (2001). Calcite precipitation induced by polyurethane-immobilized Bacillus pasteurii. *Enzyme and Microbial Technology*, *28*(4–5), 404–409.

Bang, S. S., & Ramakrishnan, V. (2001). Microbiologically-enhanced crack remediation (MECR). In *proceedings of the international symposium on industrial application of microbial genomes* (Vol. 20, pp. 3–13).

Benini, S., Rypniewski, W. R., Wilson, K. S., Miletti, S., Ciurli, S., & Mangani, S. (1999). A new proposal for urease mechanism based on the crystal structures of the native and inhibited enzyme from Bacillus pasteurii: why urea hydrolysis costs two nickels. *Structure*, *7*(2), 205–216.

Berner, R. A. (1975). The role of magnesium in the crystal growth of calcite and aragonite from sea water. *Geochimica et Cosmochimica Acta*, *39*(4), 489IN3495--494504.

Bhaduri, S., Debnath, N., Mitra, S., Liu, Y., & Kumar, A. (2016). Microbiologically induced calcite precipitation mediated by sporosarcina pasteurii. *Journal of Visualized Experiments*, *2016*(110). https://doi.org/10.3791/53253

bioMASON. (2018). No Title. Retrieved January 2, 2018, from www.biomason.com

Bosak, T. (2011). Calcite precipitation, microbially induced. In *Encyclopedia of Geobiology* (pp. 223–227). Springer.

Braissant, O., Verrecchia, E. P., & Aragno, M. (2002). Is the contribution of bacteria to terrestrial carbon budget greatly underestimated? *Naturwissenschaften*, *89*(8), 366–370.

Bray, J. M., Lauchnor, E. G., Redden, G. D., Gerlach, R., Fujita, Y., Codd, S. L., & Seymour, J. D. (2017). Impact of Mineral Precipitation on Flow and Mixing in Porous Media Determined by Microcomputed Tomography and MRI. *Environmental Science & Technology*, *51*(3), 1562–1569.

https://doi.org/10.1021/acs.est.6b02999

Bundeleva, I. A., Shirokova, L. S., Bénézeth, P., Pokrovsky, O. S., Kompantseva, E. I., & Balor, S. (2012). Calcium carbonate precipitation by anoxygenic phototrophic bacteria. *Chemical Geology*, *291*, 116–131.

Camesano, T. A., & Logan, B. E. (1998). Influence of fluid velocity and cell concentration on the transport of motile and nonmotile bacteria in porous media. *Environmental Science and Technology*. https://doi.org/10.1021/es970996m

Cappitelli, F., Zanardini, E., Ranalli, G., Mello, E., Daffonchio, D., & Sorlini, C. (2006). Improved methodology for bioremoval of black crusts on historical stone artworks by use of sulfate-reducing bacteria. *Applied and Environmental Microbiology*, *72*(5), 3733–3737.

Castanier, S., Le Métayer-Levrel, G., & Perthuisot, J.-P. (1999). Ca-carbonates precipitation and limestone genesis—the microbiogeologist point of view. *Sedimentary Geology*, *126*(1–4), 9–23.

Chafetz, H. S. (1986). Marine peloids: a product of bacterially induced precipitation of calcite. *Journal of Sedimentary Research*, *56*(6).

Chafetz, H. S., & Buczynski, C. (1992). Bacterially induced lithification of microbial mats. *Palaios*, 277–293.

Chu, K. T. (2005). by.

Chunxiang, Q., Jianyun, W., Ruixing, W., & Liang, C. (2009). Corrosion protection of cement-based building materials by surface deposition of CaCO3 by Bacillus pasteurii. *Materials Science and Engineering: C*, *29*(4), 1273–1280.

Costerton, J. W., & Stewart, P. S. (2001). Battling biofilms. *Scientific American*, *285*(1), 74–81.

Cunningham, A. B., & Gerlach, R. (2010). Microbially Enhanced Carbon Capture and Storage by Mineral-Trapping and, *44*(13), 5270–5276.

Cunningham, A. B., Gerlach, R., Spangler, L., & Mitchell, A. C. (2009). Microbially enhanced geologic containment of sequestered supercritical CO2. *Energy Procedia*, *1*(1), 3245–3252.

Cunningham, a. B., Gerlach, R., Spangler, L., & Mitchell, a. C. (2009). Microbially enhanced

geologic containment of sequestered supercritical CO2. *Energy Procedia*, *1*(1), 3245–3252. https://doi.org/10.1016/j.egypro.2009.02.109

Cunningham, a. B., Gerlach, R., Spangler, L., Mitchell, a. C., Parks, S., & Phillips, a. (2011). Reducing the risk of well bore leakage of CO2 using engineered biomineralization barriers. *Energy Procedia*, *4*, 5178–5185. https://doi.org/10.1016/j.egypro.2011.02.495

Cuthbert, M. O., Riley, M. S., Handley-Sidhu, S., Renshaw, J. C., Tobler, D. J., Phoenix, V. R., & Mackay, R. (2012). Controls on the rate of ureolysis and the morphology of carbonate precipitated by S. Pasteurii biofilms and limits due to bacterial encapsulation. *Ecological Engineering*, *41*, 32–40. https://doi.org/10.1016/j.ecoleng.2012.01.008

De Muynck, W., De Belie, N., & Verstraete, W. (2010). Microbial carbonate precipitation in construction materials: A review. *Ecological Engineering*, *36*(2), 118–136. https://doi.org/10.1016/j.ecoleng.2009.02.006

De Muynck, W., Verbeken, K., De Belie, N., & Verstraete, W. (2013). Influence of temperature on the effectiveness of a biogenic carbonate surface treatment for limestone conservation. *Applied Microbiology and Biotechnology*, *97*(3), 1335–1347.

Demény, A., Németh, P., Czuppon, G., Leél-\HOssy, S., Szabó, M., Judik, K., … Stieber, J. (2016). Formation of amorphous calcium carbonate in caves and its implications for speleothem research. *Scientific Reports*, *6*, 39602.

der Heide, P. (2011). *X-ray photoelectron spectroscopy: an introduction to principles and practices*. John Wiley & Sons.

Dhami, N. K., Reddy, M. S., & Mukherjee, A. (2013). Bacillus megaterium mediated mineralization of calcium carbonate as biogenic surface treatment of green building materials. *World Journal of Microbiology and Biotechnology*, *29*(12), 2397–2406. https://doi.org/10.1007/s11274-013-1408-z

Dhami, N. K., Reddy, M. S., & Mukherjee, M. S. (2013). Biomineralization of calcium carbonates and their engineered applications: A review. *Frontiers in Microbiology*, *4*(OCT), 1–13. https://doi.org/10.3389/fmicb.2013.00314

Dick, J., De Windt, W., De Graef, B., Saveyn, H., der Meeren, P., De Belie, N., & Verstraete, W.

(2006). Bio-deposition of a calcium carbonate layer on degraded limestone by Bacillus species. *Biodegradation*, *17*(4), 357–367.

Douglas, S., & Beveridge, T. J. (1998). Mineral formation by bacteria in natural microbial communities. *FEMS Microbiology Ecology*, *26*(2), 79–88.

Duffy, K. J., Cummings, P. T., & Ford, R. M. (1995). Random walk calculations for bacterial migration in porous media. *Biophysical Journal*, *68*(3), 800–806. https://doi.org/10.1016/S0006-3495(95)80256-0

Dupraz, S., Parmentier, M., Ménez, B., & Guyot, F. (2009). Experimental and numerical modeling of bacterially induced pH increase and calcite precipitation in saline aquifers. *Chemical Geology*, *265*(1–2), 44–53. https://doi.org/10.1016/j.chemgeo.2009.05.003

Ehrlich, H. L. (1996). How microbes influence mineral growth and dissolution. *Chemical Geology*, *132*(1–4), 5–9.

Ehrlich, H. L. (1998). Geomicrobiology: its significance for geology. *Earth-Science Reviews*, *45*(1–2), 45–60.

Ferris, F. G., & Beveridge, T. J. (1985). Functions of bacterial cell surface structures. *BioScience*, *35*(3), 172–177.

Ferris, F. G., Beveridge, T. J., & Fyfe, W. S. (1986). Iron-silica crystallite nucleation by bacteria in a geothermal sediment. *Nature*, *320*(6063), 609–611.

Ferris, F. G., Phoenix, V., Fujita, Y., & Smith, R. W. (2004). Kinetics of calcite precipitation induced by ureolytic bacteria at 10 to 20 C in artificial groundwater. *Geochimica et Cosmochimica Acta*, *68*(8), 1701–1710.

Fidaleo, M., & Lavecchia, R. (2003). Kinetic study of enzymatic urea hydrolysis in the pH range 4-9. *Chemical and Biochemical Engineering Quarterly*, *17*(4), 311–318.

Folk, R. L. (1993). SEM imaging of bacteria and nannobacteria in carbonate sediments and rocks. *Journal of Sedimentary Research*, *63*(5).

Fontes, D. E., Mills, A. L., Hornberger, G. M., & Herman, J. S. (1991). Physical and Chemical

Factors Influencing Transport of Microorganisms through Porous Media. *APPLIED AND ENVIRONMENTAL MICROBIOLOGY*, *57*(9), 2473–2481.

Friedrich, B., & Magasanik, B. (1977). Urease of Klebsiella aerogenes: control of its synthesis by glutamine synthetase. *Journal of Bacteriology*, *131*(2), 446–452.

Gal, J.-Y., Bollinger, J.-C., Tolosa, H., & Gache, N. (1996). Calcium carbonate solubility: a reappraisal of scale formation and inhibition. *Talanta*, *43*(9), 1497–1509.

Ganendra, G., De Muynck, W., Ho, A., Arvaniti, E. C., Hosseinkhani, B., Ramos, J. A., … Boon, N. (2014). Formate oxidation-driven calcium carbonate precipitation by Methylocystis parvus OBBP. *Applied and Environmental Microbiology*, *80*(15), 4659–4667.

Garcia-Vallès, M., Vendrell-Saz, M., Krumbein, W. E., & Urz\`\i, C. (1997). Coloured mineral coatings on monument surfaces as a result of biomineralization: the case of the Tarragona cathedral (Catalonia). *Applied Geochemistry*, *12*(3), 255–266.

Ghashghaei, S., & Emtiazi, G. (2013). Production of calcite nanocrystal by a urease-positive strain of enterobacter ludwigii and study of its structure by SEM. *Current Microbiology*, *67*(4), 406–413. https://doi.org/10.1007/s00284-013-0379-5

Gibson, T. (1934). An Investigation of the Bacillus Pasteuri Group: II. Special Physiology of the Organisms. *Journal of Bacteriology*, *28*(3), 313.

Gollapudi, U. K., Knutson, C. L., Bang, S. S., & Islam, M. R. (1995). A new method for controlling leaching through permeable channels. *Chemosphere*, *30*(4), 695–705.

Gorospe, C. M., Han, S.-H., Kim, S.-G., Park, J.-Y., Kang, C.-H., Jeong, J.-H., & So, J.-S. (2013). Effects of different calcium salts on calcium carbonate crystal formation by Sporosarcina pasteurii KCTC 3558. *Biotechnology and Bioprocess Engineering*, *18*(5), 903–908.

Greenfield, L. J. (1963). Metabolism and concentration of calcium and magnesium and precipitation of calcium carbonate by a marine bacterium. *Annals of the New York Academy of Sciences*, *109*(1), 23–45.

Hammes, F. (2002). *Ureolytic microbial calcium carbonate precipitation*. Ph. D. Thesis, Ghent University, Ghent.

Hammes, F. (2003). UREOLYTIC MICROBIAL CALCIUM CARBONATE PRECIPITATION UREOLYTISCHE MICROBIELE CALCIUMCARBONAAT- door. *Scanning Electron Microscopy*.

Hammes, F., Arnold, J., Krupka, K. M., Cantrell, K. J., McGrail, B. P., Tagliaferri, F., … Gerlach, R. (2013). Calcium carbonate precipitation by different bacterial strains. *Ecological Engineering*, *36*(3), 172. https://doi.org/http://researchrepository.murdoch.edu.au/399/2/02Whole.pdf

Hammes, F., Boon, N., De Villiers, J., Verstraete, W., Siciliano, S. D., & Villiers, J. De. (2003). Strain-Specific Ureolytic Microbial Calcium Carbonate Precipitation Strain-Specific Ureolytic Microbial Calcium Carbonate Precipitation. *Applied and Environmental Microbiology*, *69*(8), 4901–4909. https://doi.org/10.1128/AEM.69.8.4901

Hammes, F., & Verstraete, W. (2002). Key roles of pH and calcium metabolism in microbial carbonate precipitation. *Reviews in Environmental Science and Biotechnology*, *1*(1), 3–7.

Hong, S.-I., Park, W.-S., & Pyun, Y.-R. (1997). Inactivation ofLactobacillussp. fromKimchiby High Pressure Carbon Dioxide. *LWT-Food Science and Technology*, *30*(7), 681–685.

Hunter, G. K. (1996). Interfacial aspects of biomineralization. *Current Opinion in Solid State and Materials Science*, *1*(3), 430–435.

Ismail, M. A., Joer, H. A., Randolph, M. F., & Meritt, A. (2002). Cementation of porous materials using calcite. *Geotechnique*, *52*(5), 313–324.

Jahns, T. (1996). Ammonium/urea-dependent generation of a proton electrochemical potential and synthesis of ATP in Bacillus pasteurii. *Journal of Bacteriology*, *178*(2), 403–409.

Jansson, C., & Northen, T. (2010). Calcifying cyanobacteria—the potential of biomineralization for carbon capture and storage. *Current Opinion in Biotechnology*, *21*(3), 365–371.

Jonkers, H. M., Thijssen, A., Muyzer, G., Copuroglu, O., & Schlangen, E. (2010). Application of bacteria as self-healing agent for the development of sustainable concrete. *Ecological Engineering*, *36*(2), 230–235. https://doi.org/10.1016/j.ecoleng.2008.12.036

Kaltwasser, H., Krämer, J., & Conger, W. R. (1972). Control of urease formation in certain aerobic bacteria. *Archiv Für Mikrobiologie*, *81*(2), 178–196.

Kantzas, A., Stehmeier, L., Marentette, D. F., Ferris, F. G., Jha, K. N., Maurits, F. M., & others. (1992). A novel method of sand consolidation through bacteriogenic mineral plugging. In *Annual Technical Meeting*.

Kantzas, a, Stehmeier, L., Marentette, D. F., Ferris, F. G., Jha, K. N., & Mourits, F. M. (1992). A Novel Method of Sand Consolidation Through Bacteriogenic Mineral Plugging. *43rd Annual Technical Meeting, Petroleum Society of CIM*, *CIM 92-46*(Cim), 1–15. https://doi.org/10.2118/92-46

Kawaguchi, T., & Decho, A. W. (2002). A laboratory investigation of cyanobacterial extracellular polymeric secretions (EPS) in influencing CaCO 3 polymorphism. *Journal of Crystal Growth*, *240*(1), 230–235.

Keefe, W. E. (1976). Formation of crystalline deposits by several genera of the family Enterobacteriaceae. *Infection and Immunity*, *14*(2), 590–592.

Knorre, H. v, & Krumbein, W. E. (2000). Bacterial calcification. In *Microbial sediments* (pp. 25–31). Springer.

Konishi, Y., Tsukiyama, T., Ohno, K., Saitoh, N., Nomura, T., & Nagamine, S. (2006). Intracellular recovery of gold by microbial reduction of AuCl4- ions using the anaerobic bacterium Shewanella algae. *Hydrometallurgy*, *81*(1), 24–29.

Kralj, D., Brečević, L., & Kontrec, J. (1997). Vaterite growth and dissolution in aqueous solution III. Kinetics of transformation. *Journal of Crystal Growth*, *177*(3–4), 248–257.

Kralj, D., Brečević, L., & Nielsen, A. E. (1990). Vaterite growth and dissolution in aqueous solution I. Kinetics of crystal growth. *Journal of Crystal Growth*, *104*(4), 793–800.

Kralj, D., Brečević, L., & Nielsen, A. E. (1994). Vaterite growth and dissolution in aqueous solution II. Kinetics of dissolution. *Journal of Crystal Growth*, *143*(3–4), 269–276.

Krumbein, W. E. (1979). Photolithotropic and chemoorganotrophic activity of bacteria and algae as related to beachrock formation and degradation (Gulf of Aqaba, Sinai). *Geomicrobiology Journal*, *1*(2), 139–203.

Kumar, A., Karig, D., Acharya, R., Neethirajan, S., Mukherjee, P. P., Retterer, S., & Doktycz, M. J. (2013). Microscale confinement features can affect biofilm formation. *Microfluidics and*

Nanofluidics, *14*(5), 895–902.

Kupriyanova, E., Villarejo, A., Markelova, A., Gerasimenko, L., Zavarzin, G., Samuelsson, G., … Pronina, N. (2007). Extracellular carbonic anhydrases of the stromatolite-forming cyanobacterium Microcoleus chthonoplastes. *Microbiology*, *153*(4), 1149–1156.

Kurmaç, Y. (2009). The impact of toxicity of metals on the activity of ureolytic mixed culture during the precipitation of calcium. *Journal of Hazardous Materials*, *163*(2–3), 1063–1067.

Lauchnor, E. G., Topp, D. M., Parker, A. E., & Gerlach, R. (2015). Whole cell kinetics of ureolysis by Sporosarcina pasteurii. *Journal of Applied Microbiology*, *118*(6), 1321–1332. https://doi.org/10.1111/jam.12804

Le Metayer-Levrel, G., Castanier, S., Orial, G., Loubiere, J.-F., & Perthuisot, J.-P. (1999). Applications of bacterial carbonatogenesis to the protection and regeneration of limestones in buildings and historic patrimony. *Sedimentary Geology*, *126*(1–4), 25–34.

Lewandowski, Z., & Beyenal, H. (2013). *Fundamentals of biofilm research*. CRC press.

Li, M., Fu, Q.-L., Zhang, Q., Achal, V., & Kawasaki, S. (2015). Bio-grout based on microbially induced sand solidification by means of asparaginase activity. *Scientific Reports*, *5*, 16128.

Lian, B., Hu, Q., Chen, J., Ji, J., & Teng, H. H. (2006). Carbonate biomineralization induced by soil bacterium Bacillus megaterium. *Geochimica et Cosmochimica Acta*, *70*(22), 5522–5535.

Life Technologies. (2004). No Title. Retrieved January 2, 2018, from https://tools.lifetechnologies.com/content/sfs/manuals/mp07007.pdf

LIN, H.-M., Cao, N., & CHEN, L.-F. (1994). Antimicrobial effect of pressurized carbon dioxide on Listeria monocytogenes. *Journal of Food Science*, *59*(3), 657–659.

Lowenstam, H. A. (1981). Minerals formed by organisms. *Science*, *211*(4487), 1126–1131.

Lowenstam, H. A., & Weiner, S. (1989). *On biomineralization*. Oxford University Press on Demand.

Lowenstam, H. A., Weiner, S., bioMASON, Robbins, R., Technologies, L., Lowenstam, H. A., … Whitesides, G. M. M. (2011). No Title. *Annual Review of Fluid Mechanics*, *1*(1), 1–5. https://doi.org/http://researchrepository.murdoch.edu.au/399/2/02Whole.pdf

Lüttge, A., & Conrad, P. G. (2004). Direct observation of microbial inhibition of calcite dissolution. *Applied and Environmental Microbiology*, *70*(3), 1627–1632.

McConnaughey, T. A., & Whelan, J. F. (1997). Calcification generates protons for nutrient and bicarbonate uptake. *Earth-Science Reviews*, *42*(1–2), 95–117.

McKay, D. S., Gibson, E. K., Thomas-Keprta, K. L., Vali, H., Romanek, C. S., Clemett, S. J., … Zare, R. N. (1996). Search for past life on Mars: possible relic biogenic activity in Martian meteorite ALH84001. *Science*, *273*(5277), 924–930.

Minto, J. M., MacLachlan, E., El Mountassir, G., & Lunn, R. J. (2016). Rock fracture grouting with microbially induced carbonate precipitation. *Water Resources Research*. https://doi.org/10.1002/2016WR018884

Mitchell, A. C., & Ferris, F. G. (2005). The coprecipitation of Sr into calcite precipitates induced by bacterial ureolysis in artificial groundwater: temperature and kinetic dependence. *Geochimica et Cosmochimica Acta*, *69*(17), 4199–4210.

Mitchell, A. C., & Ferris, F. G. (2006). The influence of Bacillus pasteurii on the nucleation and growth of calcium carbonate. *Geomicrobiology Journal*, *23*(3–4), 213–226.

Mitchell, A. C., Phillips, A. J., Hiebert, R., Gerlach, R., Spangler, L. H., & Cunningham, A. B. (2009a). Biofilm enhanced geologic sequestration of supercritical CO2. *International Journal of Greenhouse Gas Control*, *3*(1), 90–99.

Mitchell, A. C., Phillips, A. J., Hiebert, R., Gerlach, R., Spangler, L. H., & Cunningham, A. B. (2009b). Biofilm enhanced geologic sequestration of supercritical CO2. *International Journal of Greenhouse Gas Control*, *3*(1), 90–99. https://doi.org/10.1016/j.ijggc.2008.05.002

Monger, H. C., Daugherty, L. A., Lindemann, W. C., & Liddell, C. M. (1991). Microbial precipitation of pedogenic calcite. *Geology*, *19*(10), 997–1000.

Montemagno, C., & Pyrak-Nolte, L. (1995). Porosity of natural fracture networks. *Geophysical Research Letters*, *22*(11), 1397–1400.

Montemagno, C., & Pyrak-Nolte, L. (1999). Fracture Netwok versus Single Structures: Measurement of Fracture Geometry with X-ray Tomography. *Phys. Chem. Earth (A)*, *24*(7), 575–579.

Montoya, B. M. (2012). *Bio-mediated soil improvement and the effect of cementation on the behavior, improvement, and performance of sand*. University of California, Davis.

Morita, R. Y. (1980). Calcite precipitation by marine bacteria. *Geomicrobiology Journal*, *2*(1), 63–82.

Morse, J. W. (1983). The kinetics of calcium carbonate dissolution and precipitation. *Reviews in Mineralogy and Geochemistry*, *11*(1), 227–264.

Mortensen, B. M., Haber, M. J., Dejong, J. T., Caslake, L. F., & Nelson, D. C. (2011). Effects of environmental factors on microbial induced calcium carbonate precipitation. *Journal of Applied Microbiology*, *111*(2), 338–349. https://doi.org/10.1111/j.1365-2672.2011.05065.x

Nemati, M., & Voordouw, G. (2003). Modification of porous media permeability, using calcium carbonate produced enzymatically in situ. *Enzyme and Microbial Technology*, *33*(5), 635–642. https://doi.org/10.1016/S0141-0229(03)00191-1

Okwadha, G. D. O., & Li, J. (2010a). Optimum conditions for microbial carbonate precipitation. *Chemosphere*, *81*(9), 1143–1148.

Okwadha, G. D. O., & Li, J. (2010b). Optimum conditions for microbial carbonate precipitation. *Chemosphere*, *81*(9), 1143–1148. https://doi.org/10.1016/j.chemosphere.2010.09.066

Parks, S. L. (2009). Kinetics of Calcite Precipitation By Ureolytic Bacteria Under Aerobic and Anaerobic Conditions. *Chemical and Biological Engineering*, (April), 93.

Phillips, A. J., Gerlach, R., Lauchnor, E., Mitchell, A. C., Cunningham, A. B., & Spangler, L. (2013). Engineered applications of ureolytic biomineralization: a review. *Biofouling*, *29*(6), 715–733. https://doi.org/10.1080/08927014.2013.796550

Phillips, A. J., Lauchnor, E., Eldring, J. J., Esposito, R., Mitchell, A. C., Gerlach, R., … Spangler, L. H. (2013). Potential CO2 leakage reduction through biofilm-induced calcium carbonate precipitation. *Environmental Science & Technology*, *47*(1), 142–149. https://doi.org/10.1021/es301294q

Pyrak-Nolte, L. J., Montemagno, C. D., Yang, G., Cook, N. G. W., & Myer, L. R. (1995). Three-dimensional tomographic visuallzatlon of natural fracture networks and graph theory analysis of the transport properties. In *8th ISRM Congress* (pp. 855–859). Tokyo, Japan: International

Society for Rock Mechanics. Retrieved from https://www.onepetro.org/conference-paper/ISRM-8CONGRESS-1995-174

Pyrak-Nolte, L., Montemagno, C., & Nolte, D. (1997). Volumetric imaging of aperture distributions in connected fracture networks. *Geophysical Research Letters*, *24*(18), 2343–2346.

R. Robbins. (2010). No Title. Retrieved January 2, 2018, from http://www.utdallas.edu/~rar011300/SEM/Scanning Electron Microscope Operation.pdf

Reddy, B. V. V., & Jagadish, K. S. (2003). Embodied energy of common and alternative building materials and technologies. *Energy and Buildings*, *35*(2), 129–137.

Rivadeneyra, M. A., Delgado, R., del Moral, A., Ferrer, M. R., & Ramos-Cormenzana, A. (1994). Precipatation of calcium carbonate by Vibrio spp. from an inland saltern. *FEMS Microbiology Ecology*, *13*(3), 197–204.

Rodriguez-Navarro, C., Rodriguez-Gallego, M., Chekroun, K. Ben, & Gonzalez-Munoz, M. T. (2003). Conservation of ornamental stone by Myxococcus xanthus-induced carbonate biomineralization. *Applied and Environmental Microbiology*, *69*(4), 2182–2193.

Rosenbaum, L. (2006). Prehistoric artistry, real and recreated. *The Wall Street Journal*, *13*.

Sarikaya, M. (1999). Biomimetics: materials fabrication through biology. *Proceedings of the National Academy of Sciences*, *96*(25), 14183–14185.

Schultze-Lam, S., Fortin, D., Davis, B. S., & Beveridge, T. J. (1996). Mineralization of bacterial surfaces. *Chemical Geology*, *132*(1–4), 171–181.

Sham, E., Mantle, M. D., Mitchell, J., Tobler, D. J., Phoenix, V. R., & Johns, M. L. (2013). Monitoring bacterially induced calcite precipitation in porous media using magnetic resonance imaging and flow measurements. *Journal of Contaminant Hydrology*, *152*, 35–43. https://doi.org/10.1016/j.jconhyd.2013.06.003

Sherwood, J. L., Sung, J. C., Maneval, J. E., & Smith, J. A. (2003). Analysis of Bacterial Random Motility in a Porous Medium Using Magnetic Resonance Imaging and Immunomagnetic Labeling, *37*(4), 781–785.

Siddique, R., & Chahal, N. K. (2011a). Effect of ureolytic bacteria on concrete properties. *Construction and Building Materials*, *25*(10), 3791–3801.

Siddique, R., & Chahal, N. K. (2011b). Effect of ureolytic bacteria on concrete properties. *Construction and Building Materials*, *25*(10), 3791–3801. https://doi.org/10.1016/j.conbuildmat.2011.04.010

Silver, S., Toth, K., & Scribner, H. (1975). Facilitated transport of calcium by cells and subcellular membranes of Bacillus subtilis and Escherichia coli. *Journal of Bacteriology*, *122*(3), 880–885.

Smith, K. S., & Ferry, J. G. (2000). Prokaryotic carbonic anhydrases. *FEMS Microbiology Reviews*, *24*(4), 335–366.

Söhnel, O., & Garside, J. (n.d.). Precipitation: Basic principles and industrial applications. 1992. Oxford: Butterworth-Heinemann.

Southam, G. (2000). Bacterial surface-mediated mineral formation. In *Environmental microbe-metal interactions* (pp. 257–276). American Society of Microbiology.

Stabnikov, V., Naeimi, M., Ivanov, V., & Chu, J. (2011). Formation of water-impermeable crust on sand surface using biocement. *Cement and Concrete Research*, *41*(11), 1143–1149.

Stewart, P. S. (2003). Diffusion in biofilms. *Journal of Bacteriology*, *185*(5), 1485–1491.

Stocks-Fischer, S., Galinat, J. K., & Bang, S. S. (1999a). Microbiological precipitation of CaCO3. *Soil Biology and Biochemistry*, *31*(11), 1563–1571.

Stocks-Fischer, S., Galinat, J. K., & Bang, S. S. (1999b). Microbiological precipitation of CaCO3. *Soil Biology and Biochemistry*, *31*(11), 1563–1571. https://doi.org/10.1016/S0038-0717(99)00082-6

Stoner, D. L., Watson, S. M., Stedtfeld, R. D., Meakin, P., Tyler, T. L., Pegram, L. M., … Griffel, L. K. (2005). Application of Stereolithographic Custom Models for Studying the Impact of Biofilms and Mineral Precipitation on Fluid Flow Application of Stereolithographic Custom Models for Studying the Impact of Biofilms and Mineral Precipitation on Fluid Flow. https://doi.org/10.1128/AEM.71.12.8721

Stumm, W., & Morgan, J. J. (1981). Aquatic Chemistry, 780 pp. *J. Wi L Ey & Sons*.

Tagliaferri, F., Waller, J., And??, E., Hall, S. A., Viggiani, G., B??suelle, P., & DeJong, J. T. (2011). Observing strain localisation processes in bio-cemented sand using x-ray imaging. *Granular Matter*, *13*(3), 247–250. https://doi.org/10.1007/s10035-011-0257-4

Thomas-Keprta, K. L., McKay, D. S., Wentworth, S. J., Stevens, T. O., Taunton, A. E., Allen, C. C., … Romanek, C. S. (1998). Bacterial mineralization patterns in basaltic aquifers: Implications for possible life in martian meteorite ALH84001. *Geology*, *26*(11), 1031–1034.

Thompson, J. B., & Ferris, F. G. (1990). Cyanobacterial precipitation of gypsum, calcite, and magnesite from natural alkaline lake water. *Geology*, *18*(10), 995–998.

Tiano, P., Biagiotti, L., & Mastromei, G. (1999). Bacterial bio-mediated calcite precipitation for monumental stones conservation: methods of evaluation. *Journal of Microbiological Methods*, *36*(1–2), 139–145.

Tobler, D. J., Cuthbert, M. O., & Phoenix, V. R. (2014). Transport of Sporosarcina pasteurii in sandstone and its significance for subsurface engineering technologies. *Applied Geochemistry*, *42*, 38–44. https://doi.org/10.1016/j.apgeochem.2014.01.004

Valiei, A., Kumar, A., Mukherjee, P. P., Liu, Y., & Thundat, T. (2012). A web of streamers: biofilm formation in a porous microfluidic device. *Lab on a Chip*, *12*(24), 5133–5137. https://doi.org/10.1039/c2lc40815e

van Paassen, L. (2009). *Biogrout: Ground Improvement by Microbially Induced Carbonate Precipitation*. *Technology*.

Von Der Schulenburg, D. A. G., Paterson-Beedle, M., MacAskie, L. E., Gladden, L. F., & Johns, M. L. (2007). Flow through an evolving porous media-compressed foam. *Journal of Materials Science*, *42*(16), 6541–6548. https://doi.org/10.1007/s10853-007-1523-z

Wanger, G., Onstott, T. C., & Southam, G. (2008). Stars of the terrestrial deep subsurface: A novel "star-shaped" bacterial morphotype from a South African platinum mine. *Geobiology*. https://doi.org/10.1111/j.1472-4669.2008.00163.x

Warren, L. A., Maurice, P. A., Parmar, N., & Ferris, F. G. (2001). Microbially mediated calcium carbonate precipitation: implications for interpreting calcite precipitation and for solid-phase

capture of inorganic contaminants. *Geomicrobiology Journal*, *18*(1), 93–115.

Warthmann, R., Van Lith, Y., Vasconcelos, C., McKenzie, J. A., & Karpoff, A. M. (2000). Bacterially induced dolomite precipitation in anoxic culture experiments. *Geology*, *28*(12), 1091–1094.

Watabe, N., & Wilbur, K. M. (1960). Influence of the organic matrix on crystal type in molluscs. *Nature*, *188*(4747), 334.

Wei, L., Liping, L., Long, C., & Longjiang, Y. (2009). Research status and prospect of biological precipitation of carbonate. *Advances in Earth Science*, *24*(6), 597–605.

Whiffin, V. S. (2004). Microbial CaCO3 Precipitation for the Production of Biocement. *Phd Thesis*, (September), 1–162. https://doi.org/http://researchrepository.murdoch.edu.au/399/2/02Whole.pdf

Wiley, W. R., & Stokes, J. L. (1962). Requirement of an alkaline pH and ammonia for substrate oxidation by Bacillus pasteurii. *Journal of Bacteriology*, *84*(4), 730–734.

Zhang, J., Davis, T. A., Matthews, M. A., Drews, M. J., LaBerge, M., & An, Y. H. (2006). Sterilization using high-pressure carbon dioxide. *The Journal of Supercritical Fluids*, *38*(3), 354–372.

Zhong, L., Islam, M. R., & others. (1995). A new microbial plugging process and its impact on fracture remediation. In *SPE Annual Technical Conference and Exhibition*.

Chapter 4

Sporosarcina pasteurii can clog and strengthen a porous medium mimic

Abstract

The bacterium *Sporosarcina pasteurii* can produce significant volumes of solid precipitation in the presence of specific chemical environments. These solid precipitate particles can enter a network of microscale pores and cause long-range clogging. As a result, the medium gains ~~in~~ strength and exhibits superior mechanical properties. This concept is also known as Microbiologically Induced Calcite Precipitation (MICP). In this study, we have used sponge blocks as surrogate porous media mimics and analyzed several aspects of MICP. A synergistic approach involving electron microscopy (SEM), computerized X-Ray tomography (μCT), quasi-static compressive load testing and chemical characterization (EDX) has been used to understand several physical and chemical aspects of MICP.

Keywords: *Sporosarcina pasteurii*, Microbiologically Induced Calcite Precipitation (MICP), Porous medium, Pore network, Clogging, Compressive Strength, Micro-scale Computerized Tomography (μCT).

4.1 Introduction

Using microorganisms like bacteria to seal cracks and plug fractures is a relatively new idea. Some bacteria like *Sporosarcina pasteurii* have the unique capability to secrete large volumes of urease, an enzyme that catalyzes the hydrolysis of urea into simpler organic molecules(a Kantzas et al., 1992). Through a series of linked chemical reactions, these bacteria can ultimately lead to the formation of calcium carbonates in aqueous media. This phenomenon is often called Microbiologically Induced Calcite Precipitation (MICP) and has the potential of causing both short and long-range clogging in porous media. MICP has attracted attention in recent years in applications as varied as underground carbon storage and sequestration(A. B. Cunningham & Gerlach, 2010) (Mitchell et al., 2009b), heritage structure conservation(De Muynck et al., 2010) (a. B. Cunningham et al., 2011), reservoir engineering (Jonkers et al., 2010), high-pressure bore-wells(De Muynck et al., 2010) (a. B. Cunningham et al., 2009)and many others.

The existing body of literature in this area focusses primarily on macro-scale systems and the enhancement in their mechanical properties resulting from MICP. These studies do not report on the microscale bacteria-level analysis of the complex interplay between fluid mechanics, solid mechanics and chemical thermodynamics of the precipitation process. Furthermore, a majority of the previous literature on bacterial transport inside porous media deal with packed column experiments, which do not attempt to capture the heterogeneous nature of the bio-hydrodynamics (w.r.t. permeability and porosity) inside real pore networks. It has also been argued (Tobler et al., 2014) that the hydraulic regime inside granular matrices is intrinsically dissimilar to those inside structural fractures and hence, a transfer of transport parameters from one system to another is complicated.

It is now well established that enhancement in strength is possible in porous structural material via microbiological means. Examples of microbes (bacteria) which have recently been popular within the structural engineering community include *S. pasteurii*, *B. megaterium* and *Shewenella sp.*

Achal et al. designed experiments with specimens of cement mortar paste containing various ratios of fly ash and *B. megaterium* cells. The specimens were subjected to a post-treatment with a mixture of nutrient broth urea (NBU) enriched with $CaCl_2$. Compared to control samples, these exhibited superior compressive strength. Although there was no significant improvement after a week, the strength increased by more than 20% in four weeks.

There have also been instances of results that question the effectiveness of MICP-based strengthening techniques. Jonkers et al. compared the 3-point compressive and bending strengths of concrete slabs containing four different bacterial strains (*S. pasteurii, B. pseudofirmus, B. halodurnas* and *B. cohnii*) with control samples and failed to measure any improvements.

At least one piece of literature casts a doubt on the capability of *S. pasteurii* to enhance mechanical strength via MICP. This study investigated the effects of five calcite-forming bacteria (CFB) species including *S. pasteurii* on mortar strength (Park et al.). For the experiments, a fresh inoculum was cultured to be mixed with the mortar, which was subsequently cured in a solution of urea and $CaCl_2$. The other four species under investigation were: *S. soli, B. massiliensis, A. crystallopoietes* and *L. fusiformis*. Only two out of the five species (*B. massiliensis, L. fusiformis*) could produce measurable difference in compressive strengths.

Another study involving *Shewenella sp.* extracted from river waters and mixed with mortar paste showed definitive increase in strength at concentrations higher than 10^5 CFU/mL. This measurement was further complemented with imaging studies showing the existence of fibrous structures inside the porous network that reduce the effective porosity (Ghosh et al.).

A notable work on the effect of buffers in the culture media needs to be mentioned here. In this study, the researchers used saline and phosphate buffer solutions to grow *S. pasteurii* and *P. aeuruginosa*. Both live and dead cells were used for comparison. It was found that saline buffers are detrimental to increase of strength. This observation was explained using ionic equilibrium arguments resulting form addition of Cl^- ions (Ramachandran et al.).

A clever study was undertaken by Bang et al. who encapsulated *S. pasteurii* cells inside Siran^{TM} glass beads. They used concrete bars with artificially indented cracks of uniform dimensions on them. The control samples had their cracks filled with empty beads, nutrient solution and $CaCl_2$. The other set had, in addition to the above, live cells of *S. pasteurii* injected onto the cracks. This set showed better strength for all concentrations ($10^7 - 10^9$ cells/cm^3) after a week and a month. It may be noted that the glass beads immobilized with bacteria provided additional surface area for the formation of a calcite layer that served as a protective coating on the cement, this increasing durability.

Another new idea that has been explored is that of autogeneous healing via MICP. In contrast to the usual approach where the bacterial agent is supplied externally, this technique involves integrating active cells in the construction material (cement, mortar, concrete) under application. It is proposed that self-integrated microbial populations are more efficient than external populations in achieving MICP-based bioremediation (sealing cracks and plugging holes) under a wider range of conditions. The study involving *B. cohnii* cells integrated onto coarse concrete is worth referencing (Wiktor et al.).

In the present work, we have used commercial sponge blocks as porous media mimics. We have attempted a holistic understanding of the process from its physical, chemical and biological perspectives by performing comprehensive examinations of several mechanistic aspects such as compressive strength, pore-scale geometry (via μ-CT scanning technology) as well as electron microscopy visualizations at the length scale of the pore-network. A critical challenge surrounding all MICP-based technologies is the prevention of enhanced cementation in the immediate neighborhood of the inlet, an artifact of the inherent non-uniform distribution of bacteria inside a

micro-scale network. In this respect too, our study complements the pre-existing breakthrough-curve based analyses in the literature.

Although it's possible to construct relatively simple network geometries via machining, glass etching or lithography; fabrication of complex 3-D pore systems that resemble a natural fracture is extremely difficult (Stoner et al., 2005). Here we have used off-the-shelf commercial sponge blocks as experimental specimens. The typical sponge block has a range of characteristic length scales in the form of variable pore-size and geometry that is similar to a real inhomogeneous porous medium like a geologic structure, rock, sandstone etc. The objective of the present work is to characterize the sponge samples used as test samples and to examine the extent of enhancement in mechanical properties post-treatment by pore blockage from the bacteria-induced chemical precipitation. We have analyzed the samples before and after treatment with respect to multiple factors.

There have been a few previous studies on *S. pasteurii* or other bacteria and their roles in enzyme-mediated ureolysis/calcite precipitation inside porous media. Most of these studies have focused on large-scale systems and modifications in bulk properties. These studies have not concentrated on the smaller length scales of the order of microns and none have applied a combination of tools like x-ray imaging and scanning technology to quantify systemic parameters.

Phillips *et al.* (2013) investigated the possibility of using *S. pasteurii* to mitigate potential CO_2-leakage from underground storage reservoirs. They have argued that low-viscosity fluids like biofilms are advantageous in this context given they reduce the required injection pressures and increase the radius of influence around the point of injection. They designed a strategy to uniformly distribute biofilm-induced calcite precipitation inside a sand-filled column and also to seal a Boyles sandstone core which had been hydraulically fractured. They reported a 2-4 orders of magnitude reduction in permeability and a tripling of tolerance for bore pressure.

Minto *et al.* (2016) have investigated the efficiency of *S. pasteurii* - induced MICP inside small and large-scale artificial fractures consisting of a rough rock lower surface and a smooth plastic upper surface. Tracer imaging and time-lapse photographs were used to determine the spatio-temporal distribution of calcite crystals. A modified injection strategy was designed to accelerate the process as compared to the continuous flow arrangement. They were also able to control the extent of precipitation by regulating the injection fluid velocity.

One main novelty of the present work is the application of high-resolution x-ray imaging and computerized tomography tools to visualize the pore network and understand the three-dimensional nature of the pore geometry. There exist some examples of similar studies in non-biological contexts.

Montemagno and Pyrak-Nolte (1999) have previously compared the geometric aspects of an entire pore network with individual fractures in the network. In a natural coal sample, they combined Wood's metal injection technique with X-ray Computerized Tomography (CT) to analyze the aperture distribution. The distribution was found to be anisotropic and a function of individual pore geometry. A 3-D autocorrelation analysis and a 2-D planar analysis were performed respectively at the network and individual fracture levels.

Montemagno and Pyrak-Nolte (1995) also developed an integrated system to measure and analyze a fracture network. It can correlate network geometry with physical properties of the system. They used a hybrid approach involving X-ray tomography and 3-D image processing to visualize the fracture geometry in a coal core sample. They quantified the variation in porosity as a function of displacement along the core axes as well.

Pyrak-Nolte, Montemagno and Nolte (1997) obtained spatial quantifications on the distribution of pore sizes and connectivity inside an opaque bituminous coal sample. Using a high-density high-contrast metal injection technique combined with gravimetric analysis and tomographic imaging under lithostatic conditions, they obtained a superb resolution of one micron while reconstructing the fracture topology.

In yet another study, Pyrak-Nolte *et al.* (1995) have analyzed the distribution of network porosity in core rock samples containing natural fractures. They combined medical imaging algorithms with Wood's metal injection technique to compute the mean network aperture over the length scale of the core and to analyze the associated 3-D geometry. They applied graph theory to the reconstructed network to determine transport parameters like the capillary pressure-saturation relationships.

Tagliaferri *et al.* (2011) have used x-ray imaging on bio-cemented Ottawa 50-70 sand samples before and after triaxial compression tests. They observed an abrupt change in the mechanism of deformation from homogeneous to dilatant shearing at peak stress.

A different paradigm in scanning technology, the magnetic resonance imaging (MRI) has also been used to study bacterial systems. Sherwood *et al.* (2003) used a combination of MRI and immuno-magnetic labeling to non-invasively visualize the changes in spatial distribution of a bacteria population inside a saturated porous medium. They attached magnetite particles on the cell surface of *E. coli* to track the movements of individual cells and compared the observations with existing transport models for motile and non-motile biological cells.

Bray *et al.* (2017) have very recently combined MRI and μ-CT as complementary techniques to quantify the advective and dispersive aspects of chemical precipitation inside a porous medium. Although they did not use bacteria, their technique can well be extended to any reactive transport system such as MICP.

Sham *et al.* (2013) used MRI in conjugation with Nuclear Magnetic Resonance (NMR) imaging to study the process of MICP inside a model glass bead pack and a real sandstone core. Precipitation was seen to occur mostly near the inlet for the model bead system whereas it was more uniform for the natural system. A study by Von Der Schulenburg *et al.* (2007) discusses the problem of fluid transport inside a polyurethane foam and the effects of compression on the velocity field using MRI.

Camesano and Logan (1998) used *P. fluorescens* and *P. cepacia* cells labeled with radionuclides to understand the effect of fluid velocity on motile and non-motile bacterial transport inside saturated porous media. They applied the colloid filtration theory to examine the effects of fluid flow on cell retention rates and observed some deviations from theoretical predictions. An effort to introduce additional parameters to account for the discrepancy and identify an optimum was also made.

Fontes *et al.* (1991) have studied general physical and chemical variables influencing microbial transport inside porous media. They added resting-cell suspensions of bacteria on top of packed clean quartz sand columns and pumped artificial groundwater all the way through. Effects of several variables like ionic strength, cell size, grain size and heterogeneity of the media on cellular transport were quantified.

Nemati and Voordouw (2003) studied the change in permeability of a porous medium resulting from in situ enzymatic production of calcium carbonate. They didn't use any bacteria for their experiments. Effects of enzyme concentration, temperature and amount of reactants (urea and

calcium chloride) were studied on a batch system of Berea sandstone cores and unconsolidated porous media. They also studied how multiple injections affect the efficiency of plugging.

Duffy, Cummings and Ford (1995) extended random walk calculations originally developed for abiotic disordered continuum systems to the problem of bacterial motility in porous media. They generated model porous media using molecular dynamic simulations and applied the Einstein relation to compute the effective bacterial diffusion coefficient.

4.2 Materials and methods

4.2.1 Compression tests

All compression tests were performed on carefully prepared cuboidal sponge blocks. Each specimen was cut out from a larger sponge block procured directly from commercial vendors (LeadingSponge, Guangdong, China). ASTM standards for open foam cellular material was followed as precisely as possible. A 100-teeth per inch (tpi) industrial saw was used in conjugation with a 3-D printed cutting jig to ensure the planarity of faces. The individual block size was maintained at 100 x 25 x 100 mm^3.

The untreated control specimens were not subjected to any modification and were tested in their pristine state. We immersed a second set of specimens in the culture medium liquid which was not inoculated. A third set of specimens was immersed in an inoculated medium and left for 120 hours before being withdrawn from the liquid and air dried inside a biosafety hood for 48 hours. We followed the existing protocol for enrichment and accelerating precipitation as described in Bhaduri *et al.* (2016).

For our experiments, we used an Instron 5960-series Dual Column mechanical test unit with compression loading cells (10kN) to load the samples. A load cell is a device used to measure weight or force under compressive, tensile, bending or shear loadings. It is essentially a transducer unit which has a membrane stressed to a predetermined magnitude. The membrane is usually connected to metal foil strain gauges that produce an electrical output when subjected to external stress. The electrical signal is amplified and read as a calibrated result and displayed with units of mechanical stress/strain.

A very small loading rate of 1mm/min was selected to approximate quasi-static conditions. We selected a test termination criterion of 9kN compressive load before the beginning of compression.

Computations of compressive stresses, strains, stretch ratios and Young's Moduli were performed in MATLAB from the load-displacement raw data generated by the machine.

4.2.2 Micro-computed tomography (μCT)

For the second aspect of our experiments, we performed extensive μ-CT scans on the specimens. This helped us numerically compute parameters such as porosity and pore connectedness. A comparison of unclogged and clogged samples demonstrated the reduction of porosity post-treatment. The 3-D reconstruction of the clogged samples also gave a clear visual representation of the network topology of pores and the nature of connectedness.

CT stands for computerized tomography. It uses an X-ray source to image a solid volume from many different angles in space and combines all the virtual slices of the specific areas to produce a complete tomography or a cross-sectional image of the body. It thus allows one to see inside an otherwise opaque object without cutting through it physically. Comprehensive reconstruction and volume rendering algorithms are available for generating a 3-dimensional image of the interior of the target specimen being scanned using a large stack of plane 2-dimensional images acquired about a predetermined axis of rotation.

We used the high-performance Bruker SkyScan 1172 High Resolution Desktop μCT for our experiments. The system has a full distortion correction 10 megapixel X-ray camera which can acquire up to 8000 x 8000 pixels in each single slice while going down to as low as 0.5μm in isotropic detail detectability. It also has a dynamically variable acquisition geometry for the shortest scan at any magnification. All analyses were performed using the in-house surface and volume rendering packages (CTAn and CTVol).

4.2.3 Microscopy and chemical analyses

Finely sliced segments of the control and non-control sponge specimens were subjected to SEM imaging and characterization via Electron Dispersive X-ray spectroscopy (EDX). The sample set under examination contained both Au (metallic) and C (non-metallic) sputtered-specimens. Carbon-coated samples allow the advantage of using much higher accelerating voltages (25-30 kV) that lead to better penetration depths, thus facilitating the imaging of deeply buried precipitate fragments. The microscopy unit was a Zeiss EVO equipped with EDX. Most chemical analyses were performed within the *Aztec* commercial package.

4.3 Results and Discussions
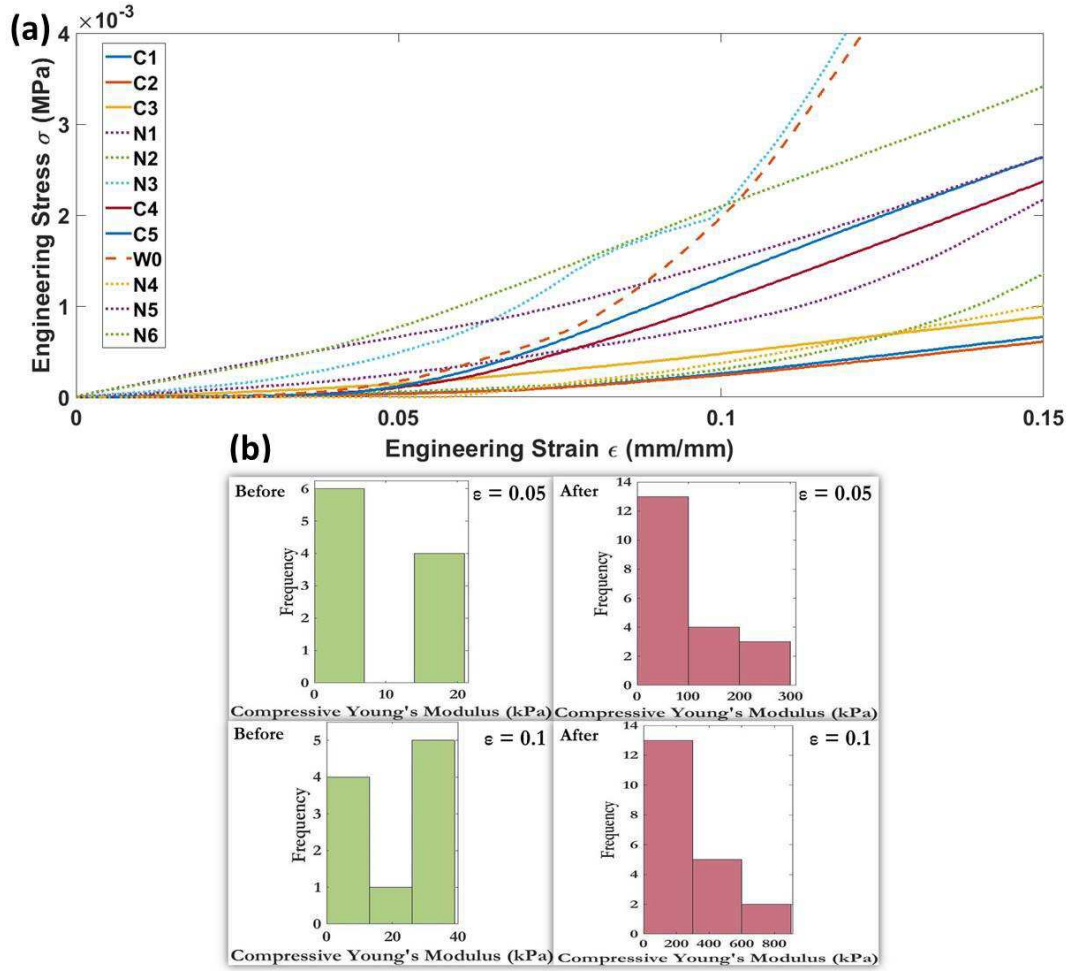
Fig. 4.1: Stress-strain curves and Young's Moduli for the test specimens: (a) Engineering stress as a function of engineering strain for low deformation ($\varepsilon=0.1$) limit, (b): Young's Modulus variation at two strain values (0.05, 0.1). C denotes a control sample which is dry and not treated, N denotes a non-control sample which has been immersed in the bacterial culture and dried before measurements. W is a sample immersed in a non-inoculated culture medium.

We have plotted the load-displacement data showing the variation of engineering stress as a function of the compression strain (Fig. 4.1). It can be seen that there has been a significant enhancement in mechanical strength post-treatment.

We have restricted all experiments to the small deformation ($\varepsilon = 10\%$) limit. No comparative conclusions have been drawn beyond this limit to ensure the reliability of engineering stress and

engineering strain measurements. All stress and strain values reported in this work are pure scalars and simply use the definitions given below:

$$\varepsilon_{Engg.} = \frac{\text{Change in linear dimension (mm)}}{\text{Initial linear dimension (mm)}},$$

$$\sigma_{Engg.} = \frac{\text{Normal Compressive Force (N)}}{\text{Area of Cross-section (mm}^2)}.$$

For all loading tests, we have used specimens of uniform dimensions. The loading force has been applied along an axis of length 25 mm and normal to a square plane of size 100 x 100 mm^2. Thus, the initial dimension before the application of loading has always been 25 mm (denominator of ε). Similarly, the area of cross-section normal to the loading axis has always been 100 x 100 mm^2 (denominator of σ). The numerators have been obtained from force-displacement experiments.

Fig. 4.1(a) shows the stress-strain curve for twelve different samples. The ones denoted with a **'C'** are control samples which are dry, never subjected to any treatment and are soft. The ones denoted with an **'N'** are non-control samples which have been immersed in an inoculum and subsequently dried prior to measurements and have experienced significant hardening. It can be clearly seen that **N**-samples demonstrate much higher stress values than **C**-samples at any given strain point.

Fig. 4.1(b) plots the Young's Moduli (E) under compression at two representative strain values of 5% and 10% for both samples. The maximum E-values at 5% are about 20kPa and 300kPa before and after treatment, respectively. Similarly, the numbers at 10% are ~ 40kPa and 800kPa, respectively. In terms of arithmetic mean values, there is an enhancement by more than a factor of 5.
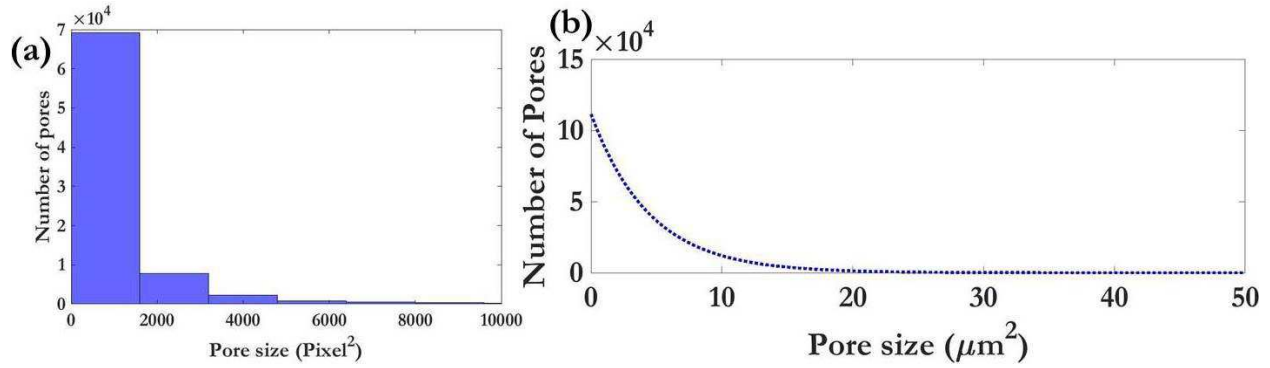
Fig. 4.2: Analysis of pore network via µ-CT scans: (a) Histogram of pore sizes in an untreated specimen (b): Probability distribution function of pore sizes in an untreated specimen.

We started with the determination of the right representative volume element (RVE) for the 3-D mesh and checked for convergence of porosity, the key parameter under investigation. Once convergence had been ensured, a statistical analysis of the pore size distribution was also performed (Fig. 4.2).

Fig. 4.2 shows the distribution of pore sizes in the sponge blocks. This is a cumulative distribution of individual pore size quantification performed on twelve different samples. Not surprisingly, the pore network has an exponential-type trend where a majority of pores are of the order of 10 µm^2 or larger. This type of a trend also hints at the presence of an intrinsic randomness inherent in the porous medium. This reinforces the selection of the particular sponge as the porous media mimic of choice because it's able to partially capture the random nature of a real engineering porous medium like sand or concrete.

We compared it with the distribution of crystal sizes in a liquid culture, extracted form a micrograph via image processing on *ImageJ*. We see that most crystals can enter most pores which entail a faithful and reliable long-range clogging (Fig. 4.3). Fig. 4.3(a) is a phase-contrast image taken on a stagnant liquid culture prepared on a *Lab Tek*^{TM} II Chambered Coverglass system. The distribution of crystals may be seen as white speckles against the darker background. Fig. 4.3(b) is a histogram of the crystal size distribution which shows that most crystals are about 10µm in size or smaller. When this is compared with the range of pores in a typical porous medium used for our studies, one can clearly see that most crystals would be able to enter most pores. As a result, there would be a penetration that is sufficiently deep to cause sufficient strengthening.

The tomographical slices were individually color rendered and a full 360° sweep was performed to calculate porosities of unclogged and clogged samples. It was found that there has been a significant reduction in porosity from ~ 90% to about 30%, which correspond to a 3x enhancement in mechanical strength (Fig. 4.4). Fig. 4.4(a) shows the sequence of steps that have been used to extract quantitative information form the raw scan data files. The raw data in the native proprietary format must be suitably enhanced and successively filtered before it is subjected to voxel thresholding for resolving the three different phases in three dimensions: the void pores which were not accessible to the precipitated particles, the precipitate particles themselves and the material of the porous medium (sponge) itself. This can be computed only when a suitable definition of pore boundaries has been incorporated into the image processing routine and a numerical distinction between pore space and pore connections (throats and necks) been made. This definition was included *ab initio* through externally developed codes in MATLAB^{TM}, used in conjugation with the commercial program available with the hardware. The last step is to do the calculations of the parameters of interest like porosity (Fig. 4.4(b)).
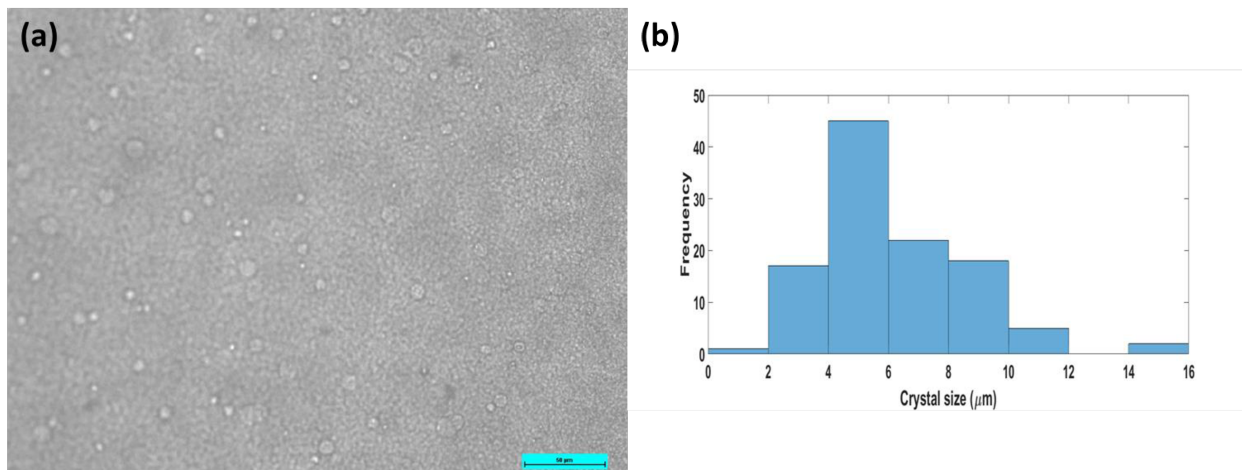
Fig. 4.3 Analysis of crystal size distribution from a phase-contrast image: (a) Field of view under analysis. (b) Frequency distribution of crystal size distribution in a liquid medium.

Total area of pore space	Po.Ar(tot)	747139.37500
Open porosity (percent)	Po(op)	90.30135
Total porosity (percent)	Po(tot)	90.41630
Centroid (x)	Crd.X	104.99723

Before

Total area of pore space	Po.Ar(tot)	30985.37500
Open porosity (percent)	Po(op)	35.31179
Total porosity (percent)	Po(tot)	53.14724
Centroid (x)	Crd.X	455.71578

After
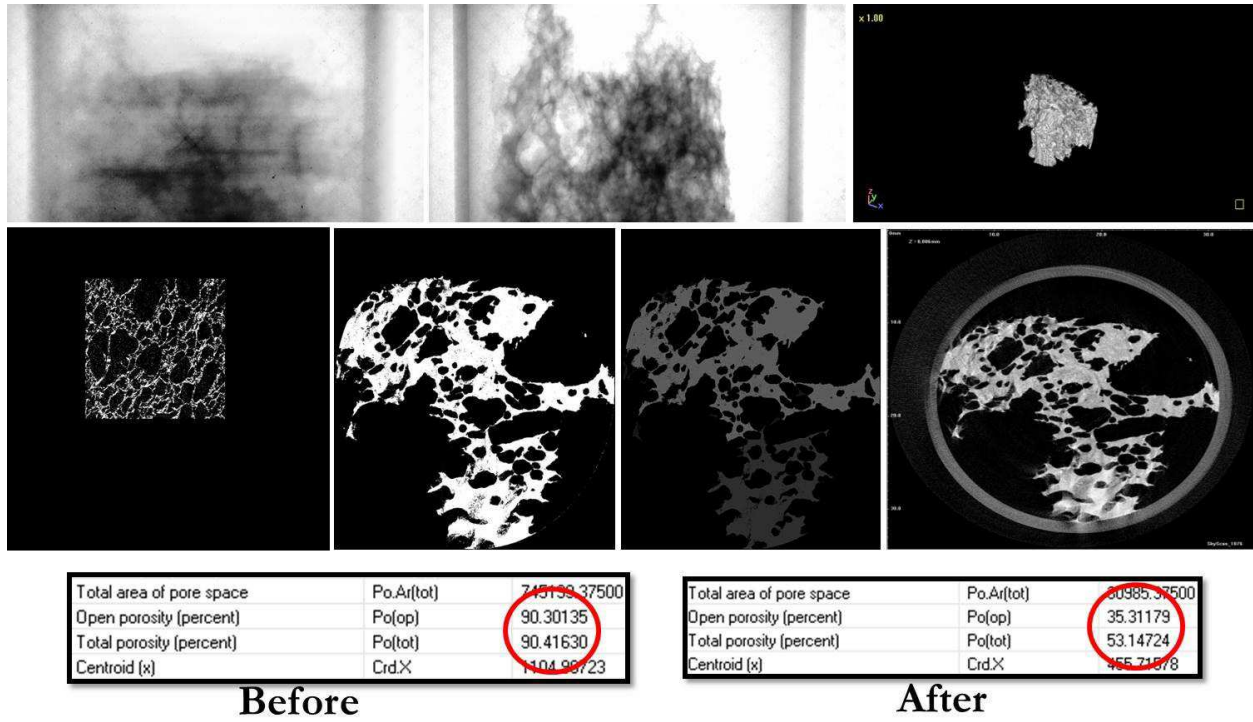
Fig. 4.4: µ-CT investigations of the pore network: Sequence of operations (segmentation, filtration and thresholding) to resolve the different phases in the clogged and unclogged samples. A 3x reduction in porosity has been highlighted.
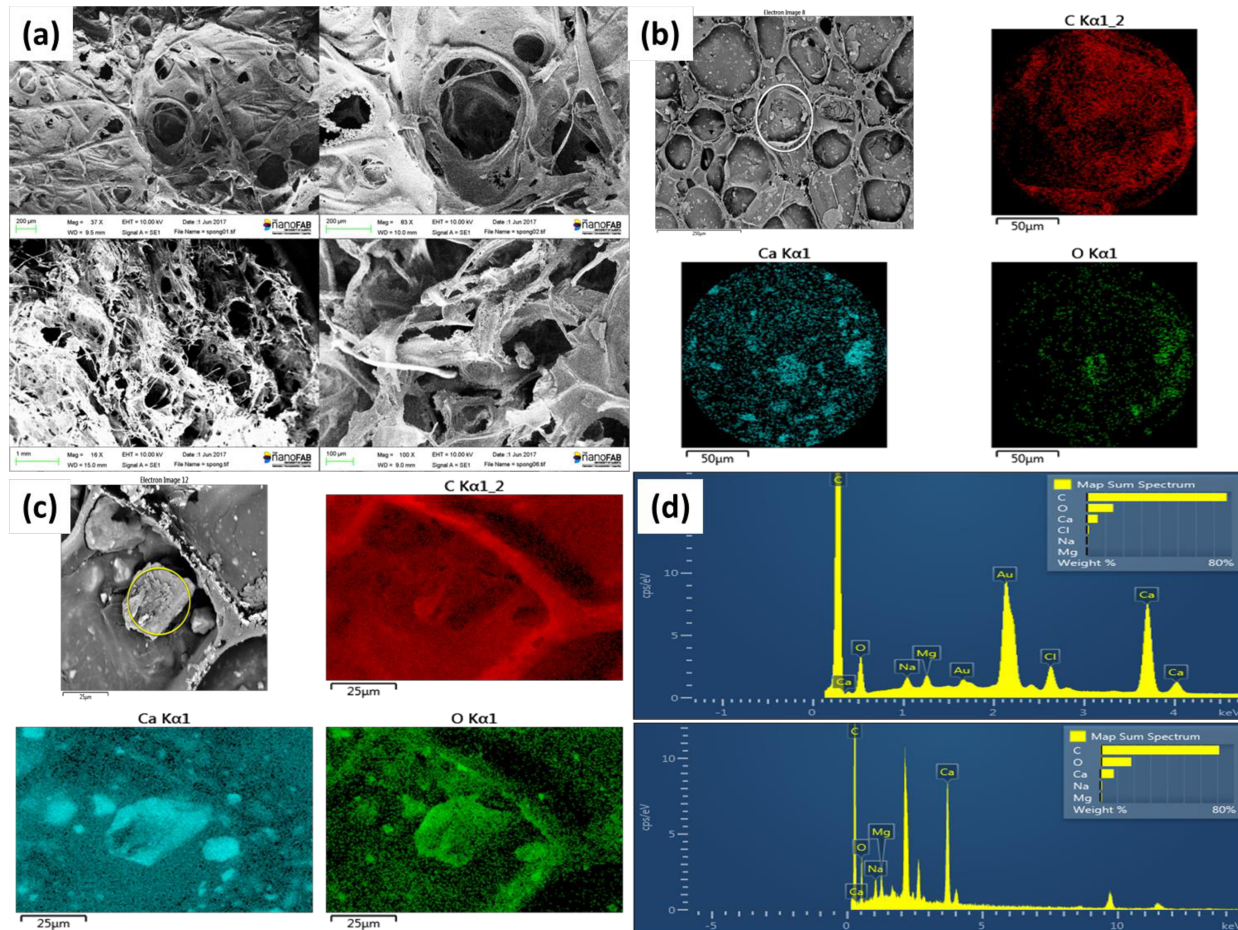
Fig. 4.5: SEM and EDX of the porous medium matrix and the precipitated crystals: (a) Structure of the pore network as imaged under SEM. (b)-(c): Targeted chemical characterization on two pin-pointed locations via EDX. (d) Elemental maps corresponding to (b) and (c) confirming the presence of the signature elements in calcite. The Cl-signals in (d) originate from the NaCl in the culture medium. The Au-signals originate from the sputtered gold layer on the sample.

We observed the pore network surface architecture under SEM. For samples treated with the inoculated bacteria culture, we see conspicuous precipitation. We performed targeted chemical signature ID on the precipitated solids with an EDX probe and constructed elemental maps which show the presence and distribution of the chemicals expected from MICP viz. Calcium, Carbon and Oxygen (Fig. 4.5). Gold (Au) was present by virtue of the thin conductive coating deposited by sputtering.

This characterization data provides a conclusive evidence of the actual chemical nature of the precipitates.

4.4 Conclusion

The present work has utilized sponge blocks as surrogate porous medium mimics to study the phenomenon of MICP. This approach has several advantages in terms of the ease of experimentation and the analysis of the various physical, chemical and biological aspects associated with the process. Through techniques such as μ-CT scanning and SEM, we have tried to understand the nature and extent of precipitation inside the real pore network and also correlated precipitation with enhancement in mechanical strength. This is the first study that quantifies the phenomenon of MICP inside micro-scale pores with compressive strength and porosity data.

4.5 Supplementary Information

We present here additional supporting information that complements the main data presented in the paper.

4.5.1. Chemical characterization of the precipitates inside the porous media

The sponge specimens were subjected to detailed chemical analyses post-precipitation. Thin sections were cut out from the standard sponge blocks used for compression tests and imaged under SEM. The images clearly show the existence of solid precipitated particles entrapped within the pore matrix. This imaging was coupled with targeted EDX scans to pinpoint the signatures of individual elements expected as the end-products of MICP.

Electron Image 1

250μm
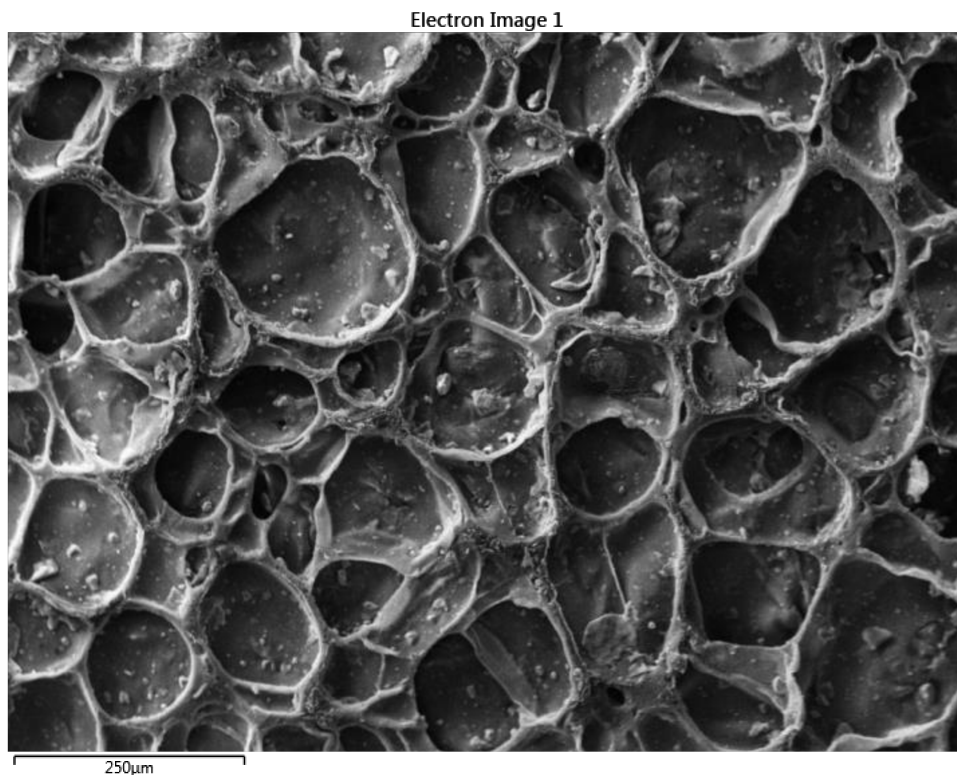
Fig. 4.A: SEM image performed on the surface of a specimen. Deposits of white precipitate particles can clearly be seen within the pore wall boundaries.

Fig. 4.A above shows the surface pore network architecture. Big pores lead to small pores and small pores lead to even smaller pores, thus creating a hierarchy of various sizes within the pore system. This network can be accessed through the tiny openings visible on the surface. Coexisting are white

crystals of solid precipitates. Some small crystals may even be seen being trapped inside some of the smaller pores located at slightly deeper depths.
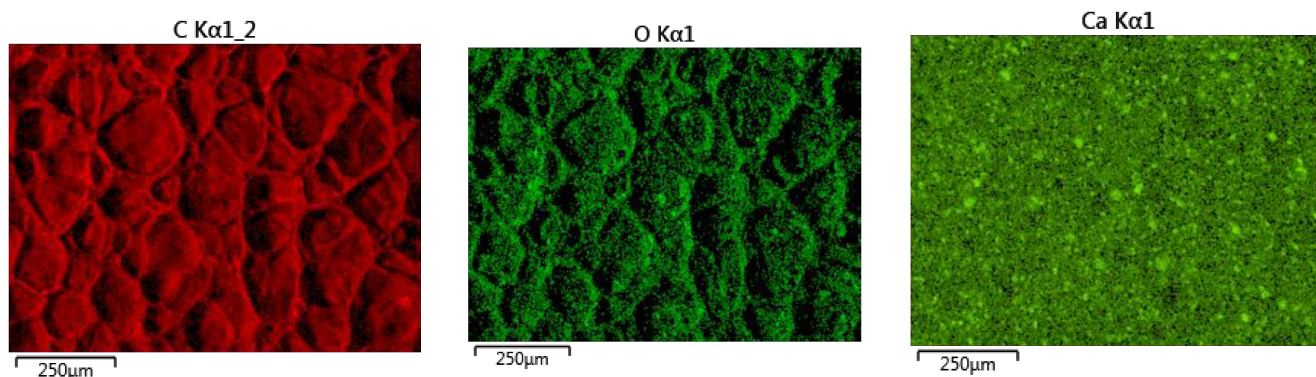
Fig. 4.B: Targeted EDX performed on the same sample as shown in Fig. 4.A above. Individual chemical IDs corresponding to Ca, C and O confirm the existence of the three elements produced via MICP.

In Fig. 4.B above, three different panels correspond to three different chemical signatures of Ca, C and O. On the image that corresponds to Ca, the bright speckles closely correlate to the actual distribution of the solid crystals. The other two (C and O) show a more uniform illumination pattern. This provides us with a strong positive evidence about the nature of the chemical precipitation.

Element	Line Type	Apparent Concentration	k Ratio	Wt%	Wt% Sigma	Standard Label	Factory Standard
C	K series	32.79	0.32793	77.28	0.14	C Vit	Yes
Ca	K series	7.57	0.06764	5.98	0.03	Wollastonite	Yes
O	K series	4.16	0.01399	14.59	0.14	SiO_2	Yes
Cl	K series	1.36	0.01191	1.13	0.01	NaCl	Yes
Na	K series	0.61	0.00258	0.55	0.02	Albite	Yes
Mg	K series	0.49	0.00324	0.48	0.01	MgO	Yes
Total:				100.00			

Tab. 4.1: Various elements identified within the solid precipitates as imaged in Fig. 4.A.

Table 4.1 shows all the individual elements found in the sample. Ca, C and O are the usual suspects. Na and Mg are present in very low concentrations that are very likely contaminations in Ca. Chlorine shows up as a fixation artifact due to the sample preparation process.

Element	Line Type	Quant	Area	Sigma	Fit Index
C	K series	Yes	403731.58	1112.40	1514.22
Ca	K series	Yes	170552.70	742.07	4.22
Ca	L series	No	-3352.91	793.01	1162.57
O	K series	Yes	35502.21	388.82	326.82
Au	L series	No	55714.13	596.02	5.53
Au	M series	No	262554.66	1624.96	18.72
	Noise 1	No	148417.51	3065.60	56.27
	Noise 2	No	-173997.32	5509.53	54.28
	Noise 3	No	98041.61	2861.82	53.97

Tab. 4.2: Dispersive spectroscopic information for the characterization corresponding to Tab. 4.1 above

Table 4.2 provides detailed spectroscopic information on the key elements identified by the characterization process. Ca, C and O are expected elements. Au is an artifact present due to the gold-sputtering process that must be completed prior to the SEM.
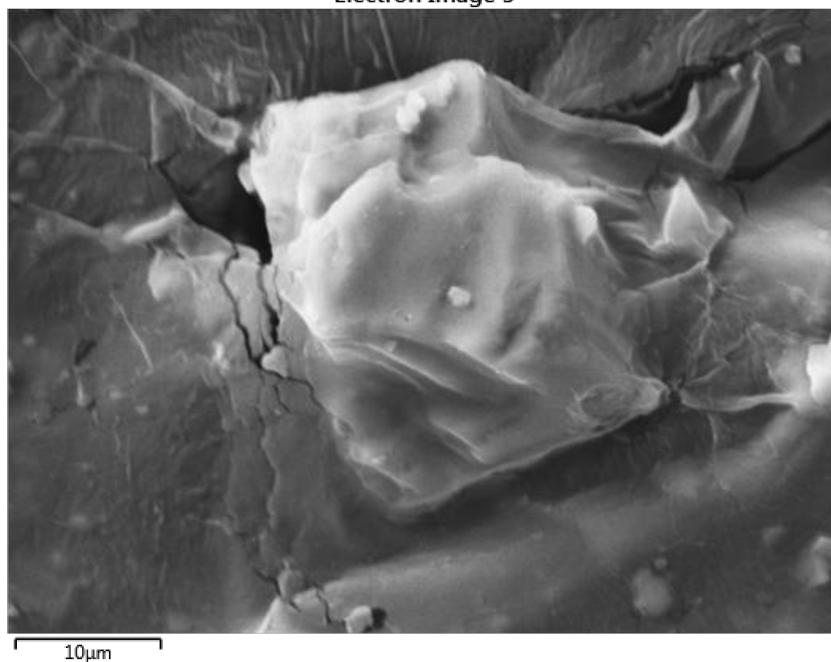
Fig. 4.C: High magnification image of precipitated crystals.

Fig. 4.C shows a big chunk of solid precipitate. Also visible are smaller grains near the periphery.
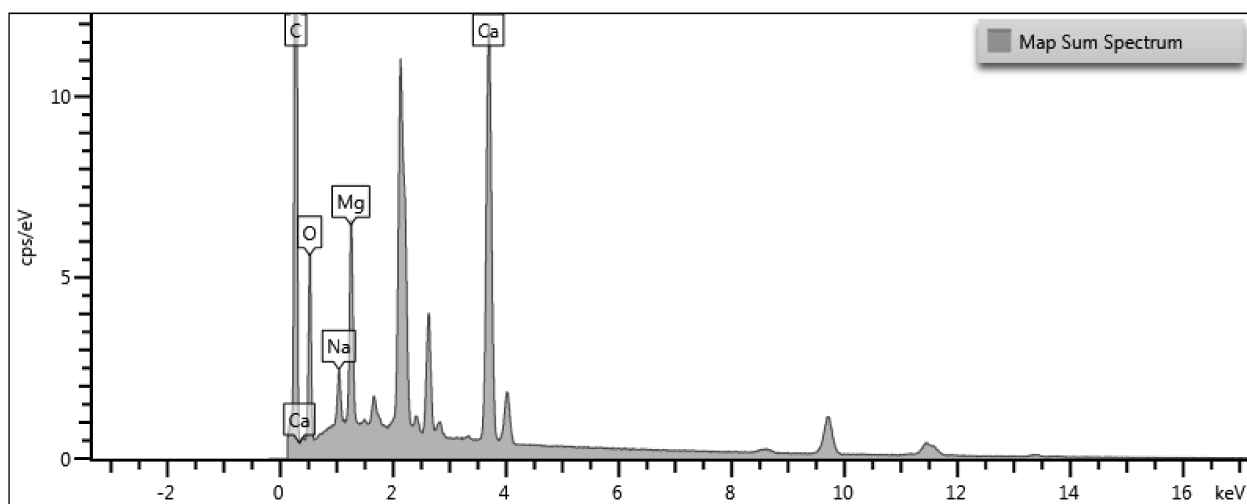
Fig. 4.D: EDX spectrum corresponding to Fig. 4.C above

Fig. 4.D shows the spectrum corresponding to a targeted ID performed on Fig. 4.C. Ca, C and O are clearly present. Trace amounts of Mg and Na have also been detected and these are attributed to impurities.

Element	Line Type	Apparent Concentration	k Ratio	Wt%	Wt% Sigma	Standard Label	Factory Standard	Standard Calibration Date
C	K series	18.66	0.18661	58.76	0.15	C Vit	Yes	
O	K series	7.35	0.02475	25.56	0.16	SiO_2	Yes	
Ca	K series	12.30	0.10994	11.00	0.05	Wollastonite	Yes	
Total:				100.00				

Tab. 4.3: Various elements identified within the solid precipitates as imaged in Fig. 4.C.

Element	Line Type	Quant	Area	Sigma	Fit Index
C	K series	Yes	229747.62	890.59	860.58
O	K series	Yes	62790.98	493.07	187.96
Ca	K series	Yes	277210.51	911.27	6.67
Ca	L series	No	-5613.27	801.36	679.87
Au	L series	No	61632.84	630.37	4.70
Au	M series	No	308486.58	1724.68	908.16
	Noise 1	No	130271.46	2863.93	14.44
	Noise 2	No	-147771.86	5150.02	13.92
	Noise 3	No	84389.92	2674.28	12.95

Tab. 4.4: Dispersive spectroscopic information for the characterization corresponding to Tab. 4.3 above

Tables 4.3 and 4.4 provide the pertinent information related to the characterization performed on the larger chunk of solid shown in Fig. 4.C. As earlier, gold atoms are present as a thin layer of coating on the SEM stubs and hence get picked up as Au peak signals in the spectrograph.
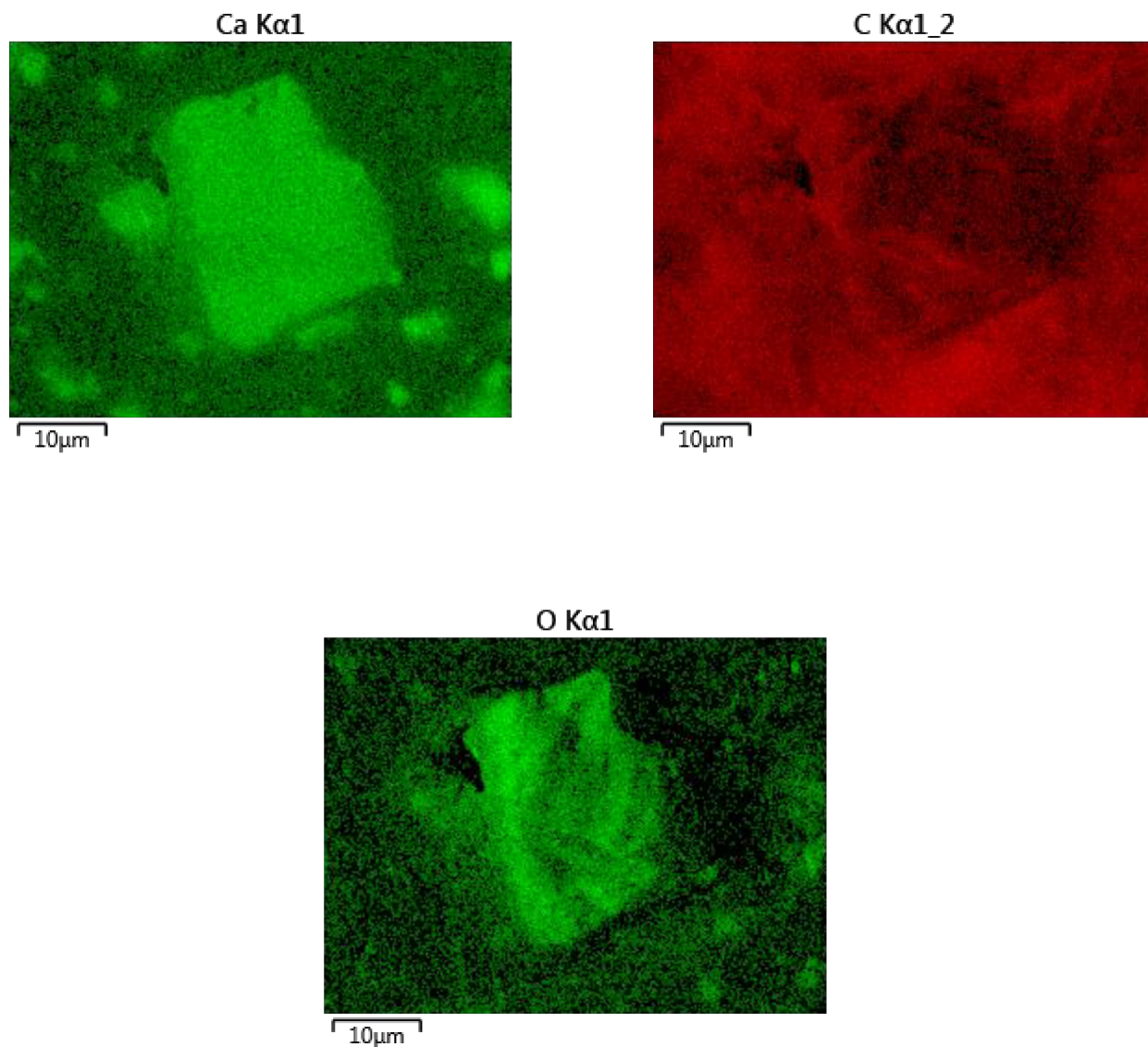
Fig. 4.E: Targeted EDX performed on the same sample as shown in Fig. 4.C above. Individual chemical IDs corresponding to Ca, C and O confirm the existence of the three elements produced via MICP.

Fig. 4.E shows the three individual EDX channels corresponding to the elemental signals for Ca, C and O. The C channel shows homogeneous carpet coverage unlike the two others due to the existence of carbon pigments in the sponge sample.

116

Label:	Map Sum Spectrum
Source:	Acquired
Created:	5/19/2017 11:26:23 AM
Livetime:	195.0s
Process Time:	5
Accelerating Voltage:	20.00kV
Magnification:	2052 x
Working Distance:	8.4mm
Specimen Tilt (degrees):	0.0
Elevation (degrees):	35.0
Azimuth (degrees):	0.0
Number Of Channels:	2048
Energy Range (keV):	20 keV
Energy per Channel (eV):	10.0eV
Detector Type Id:	28
Detector Type:	X-Max
Window Type:	SATW
Pulse Pile Up Correction:	Succeeded
Primary Detector:	EDS 1
Primary Detector Serial Number:	37456

Tab. 4.5: EDX detector system parameters corresponding to Fig. 4.D

Table 4.5 gives all the relevant information related to the EDX detector used in conjugation with the SEM system. All imaging was performed under an accelerating voltage of 20 kV. This is a relatively low value adjusted so to prevent burn damage on the sample. The gold coating enhances conductivity and facilitates high-contrast imaging under these operating voltages.

Label:	Electron Image 5
Collected:	5/19/2017 11:50:29 AM
Input Signal:	BSE
Resolution (Width):	1024 pixels
Resolution (Height):	768 pixels
Image Width:	770μm
Image Height:	577μm
Stage Tilt Degrees:	0.00°
Specimen Tilt Degrees:	0.00°
Software Tilt Correction:	Not applied
Magnification:	153 x
Number of Averaged Frames:	1
Dwell Time:	20μs

Tab. 4.6: Back-scattered electron spectroscopy data acquisition parameters corresponding to Fig. 4.C

Table 4.6 provides information on the key operational variables related to the image acquisition for Fig. 4.C. The image obtained is a high-resolution (1024 x 768) BSE image acquired for 20 μs

Fig. 4.F: Single crystals trapped within the walls of a pore

Fig. 4.F shows a big calcite crystal trapped inside a pore hole. The pore boundaries, which are essentially walled discontinuities between the voids in the sponge, may clearly be seen. There also are smaller grains, which are scattered throughout the area under investigation. Deposits of smaller calcite pigments can be seen everywhere: on the edges, near the boundaries and around the central region.
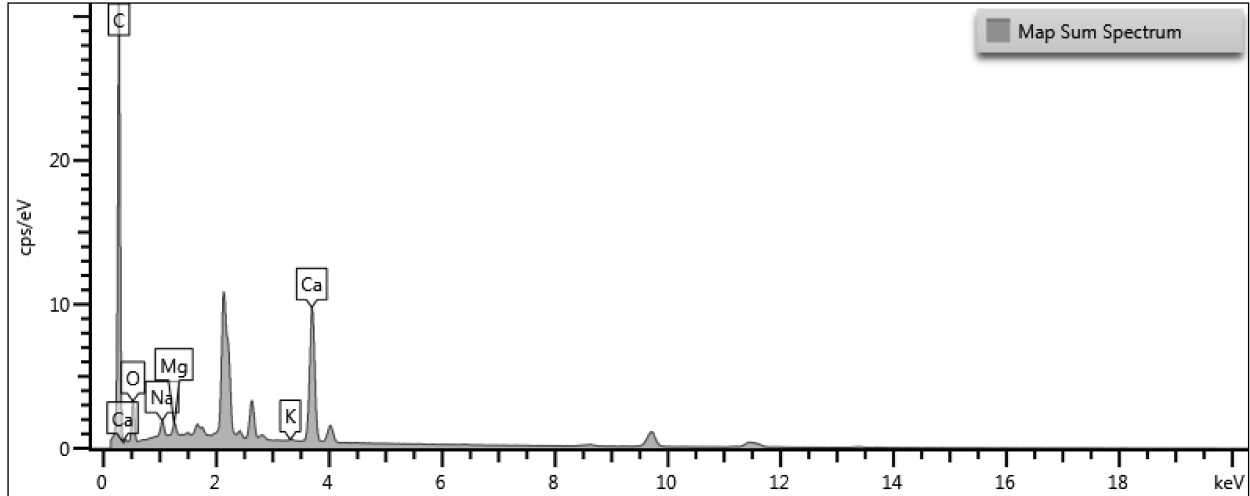
Fig. 4.G: EDX spectrum corresponding to Fig. 4.F above

Fig. 4.G shows the EDX graph resulting form the analysis carried out on the sample shown in Fig. 6. Apart from trace amounts of Mg, Na and K present through impurities; Ca, C and O are strongly detected.

Element	Line Type	Apparent Concentration	k Ratio	Wt%	Wt% Sigma	Standard Label	Factory Standard	Standard Calibration Date
C	K series	31.83	0.31831	73.43	0.15	C Vit	Yes	
O	K series	4.26	0.01434	16.48	0.16	SiO_2	Yes	
Ca	K series	10.06	0.08987	8.73	0.04	Wollastonite	Yes	
Na	K series	0.80	0.00336	0.82	0.02	Albite	Yes	
Mg	K series	0.42	0.00276	0.46	0.01	MgO	Yes	
K	K series	0.08	0.00072	0.07	0.01	KBr	Yes	
Total:				100.00				

Tab. 4.7: Various elements identified within the solid precipitates as imaged in Fig. 4.F.

Element	Line Type	Quant	Area	Sigma	Fit Index
C	K series	Yes	391885.65	1338.71	122.26
Ca	K series	Yes	226608.71	835.51	2.64
Ca	L series	No	-10508.96	819.43	103.98
O	K series	Yes	36373.86	399.74	52.83
Na	K series	Yes	14154.09	379.22	6.60
Mg	K series	Yes	11979.85	380.20	24.13
K	K series	Yes	2025.35	333.15	519.03
K	L series	No	-100407.25	1194.67	126.80
	Noise 1	No	213634.89	3507.52	41.34
	Noise 2	No	-262569.61	6328.08	40.04
	Noise 3	No	142784.37	3300.50	40.46

Tab. 4.8: Dispersive spectroscopic information for the characterization corresponding to Tab. 4.7 above

Label:	Map Sum Spectrum
Source:	Acquired
Created:	5/19/2017 12:13:52 PM
Livetime:	195.0s
Process Time:	5
Accelerating Voltage:	20.00kV
Magnification:	1026 x
Working Distance:	8.3mm
Specimen Tilt (degrees):	0.0
Elevation (degrees):	35.0

Azimuth (degrees):	0.0
Number Of Channels:	2048
Energy Range (keV):	20 keV
Energy per Channel (eV):	10.0eV
Detector Type Id:	28
Detector Type:	X-Max
Window Type:	SATW
Pulse Pile Up Correction:	Succeeded
Primary Detector:	EDS 1
Primary Detector Serial Number:	37456

Tab. 4.9: EDX detector system parameters corresponding to Fig. 4.G

Tables 4.7 and 4.8 show all the important systemic variables present in the analysis of the sample shown in Fig. 6. All the three compositional elements of calcite ($CaCO_3$) namely Ca, C and O remain the major elements detected along with small quantities of Na, Mg and K which enter as impurities of Calcium. Table 4.9 accordingly presents the key detector information used in the experiments.
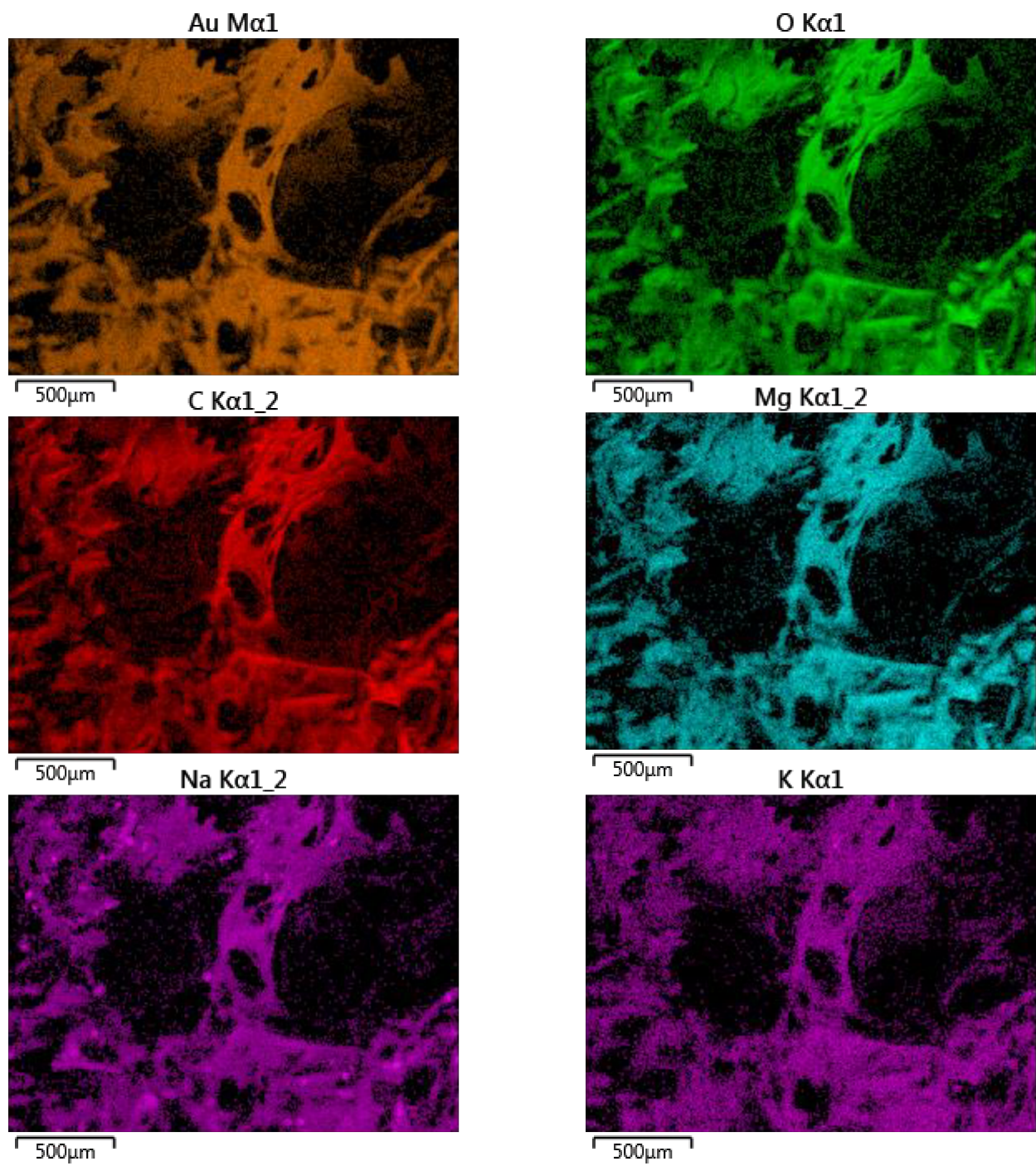
Fig. 4.H: Targeted EDX performed on yet another sponge specimen. Individual chemical IDs corresponding to Ca, C and O confirm the existence of the three elements produced via MICP.

Fig. 4.H shows individual channels for one more sample. Au is clearly an artifact of sputtering. The rest are expected results and once again confirm the existence of $CaCO_3$.
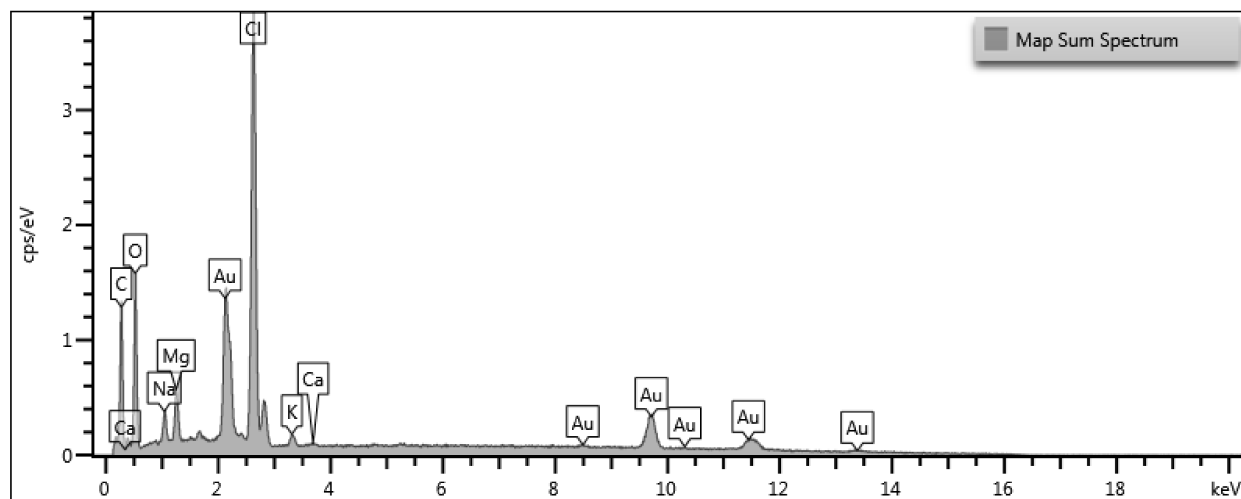
Fig. 4.I: EDX spectrum corresponding to Fig. 4.H above

Fig. 4.I shows the spectrogram corresponding to the sample shown above. Apart from Ca, C and O; three extraneous signals have been picked up. Cl is found due to NaCl being used as a fixative. Au originates from the conductive gold plating. Na-Mg-K are impurities present in Ca.

Element	Line Type	Apparent Concentration	k Ratio	Wt%	Wt% Sigma	Standard Label	Factory Standard	Standard Calibration Date
C	K series	1.29	0.01289	54.24	0.54	C Vit	Yes	
O	K series	2.19	0.00736	30.81	0.44	SiO_2	Yes	
Na	K series	0.20	0.00086	1.08	0.05	Albite	Yes	
Mg	K series	0.24	0.00159	1.35	0.04	MgO	Yes	
Cl	K series	2.63	0.02295	11.98	0.15	NaCl	Yes	
K	K series	0.10	0.00081	0.43	0.03	KBr	Yes	
Ca	K series	0.02	0.00022	0.11	0.03	Wollastonite	Yes	

			100.00			
Total:						

Tab. 4.10: Various elements identified within the solid precipitates as imaged in Fig. 4.H

Element	Line Type	Quant	Area	Sigma	Fit Index
C	K series	Yes	15874.32	314.16	6.37
O	K series	Yes	18664.31	246.15	10.46
Na	K series	Yes	3632.18	155.76	0.93
Mg	K series	Yes	6868.93	186.75	1.68
Cl	K series	Yes	78655.39	488.79	6.17
Cl	L series	No	700.80	121.25	18.87
K	K series	Yes	2287.68	151.51	2.37
K	L series	No	-4559.48	317.07	7.73
Ca	K series	Yes	545.70	134.69	0.64
Ca	L series	No	-3016.30	290.96	10.17
Au	L series	No	17641.58	371.40	1.16
Au	M series	No	38259.29	646.97	5.42
	Noise 1	No	137930.29	2566.83	24.11
	Noise 2	No	-158509.91	4671.28	23.23
	Noise 3	No	90043.67	2448.35	24.06

Tab. 4.11: Dispersive spectroscopic information for the characterization corresponding to Tab. 4.10 above

Tables 4.10 and 4.11 above provide all the remaining information to complete the characterization picture presented in Figs. 4.H and 4.I. This data complements the EDX curves with parametric statistics on spectroscopic and data acquisition aspects of the chemical analysis.

4.5.2 Compression tests along the two orthogonal axes

As described in the main text, we used a 100 x 100 x 25 mm³ sponge bar for all our experiments. All data reported were obtained while compressing the sample along the 25 mm (**Z**) axis i.e. the face being compressed was the 100 x 100 mm² (**XY**) plane.

We also performed some tests with the 25 x 100 mm² (**ZX**) plane parallel to the compression platens i.e. loading along the 100 mm (**Y**) axis as well as with the 100 x 25 mm² (**YZ**) face parallel to the platens i.e. compressing along the other 100 mm (**X**) axis.
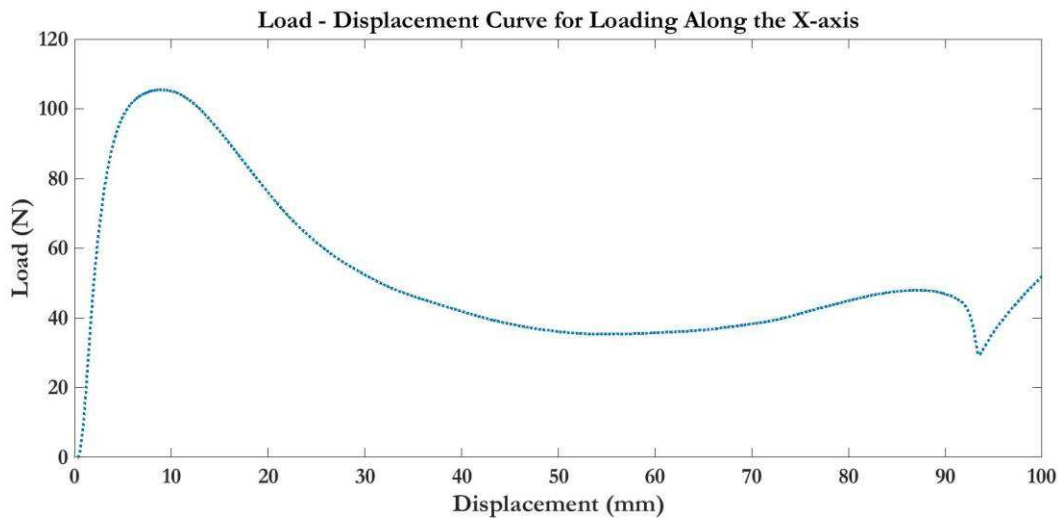
Fig. 4.J1: Load-displacement curve for loading along the x-axis.
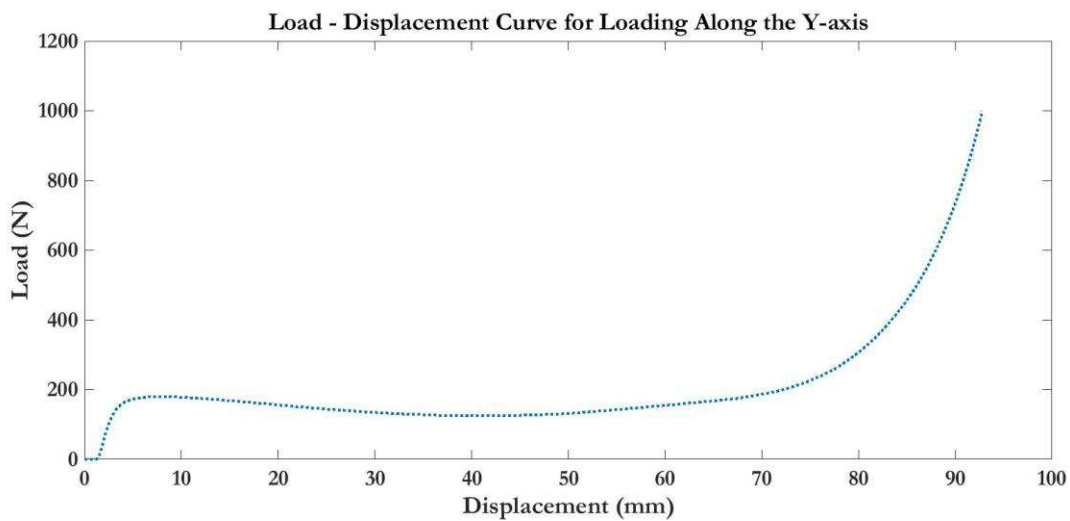
Fig. 4.J2: Load-displacement curve for loading along the y-axis.

4.5.3 Measuring the growth of *S. pasteurii* with time

We performed standard spectrophotometry on liquid cultures of *S. pasteurii* and compared growth rates with three different media compositions. This helped us select the right temporal point of immersion of the test samples.
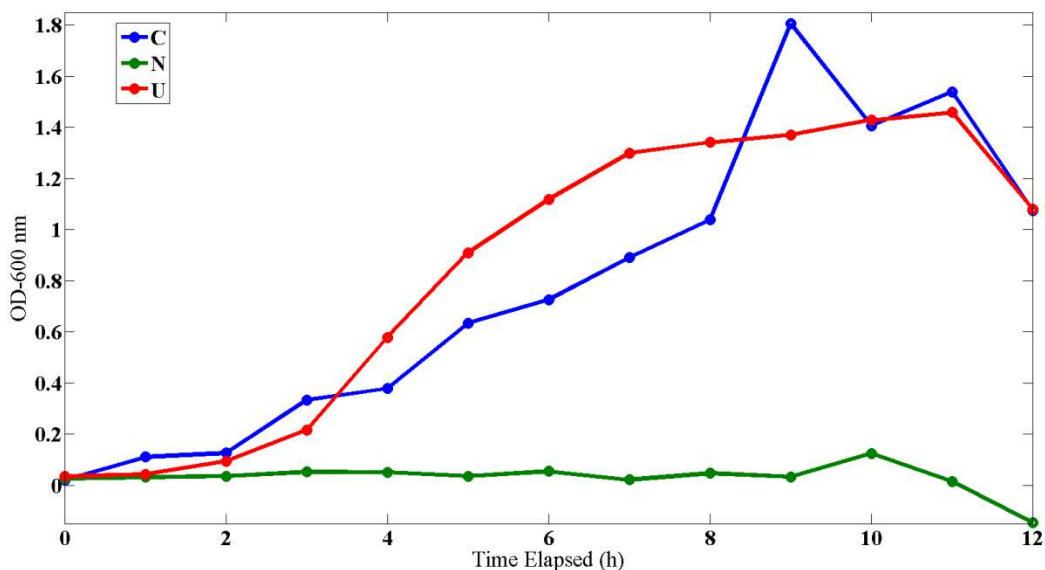
Fig. 4.K: Growth curves of *S. pasteurii* under different media compositions (*C* – Medium prepared as described in [*Bhaduri* (2016)], *N* – NB medium, *U* – NB medium with pre-enrichment of Urea). All results reported here correspond to *C* above).

Fig. 4.K shows the growth curves for three different media. These graphs are for single batches monitored over 12 hours. 'N' denotes a normal NB medium, 'U' denotes an NB medium enriched with urea and 'C' denotes the new protocol described in Chapter 2. C is seen to reach a higher peak than both N and U. However, the primary merit of C lies with its applicability under a wide range of conditions and the guaranteed induction of precipitation if all steps are properly followed.

4.5.4 Pore continuity verification

View from left **View from top** **View from right**
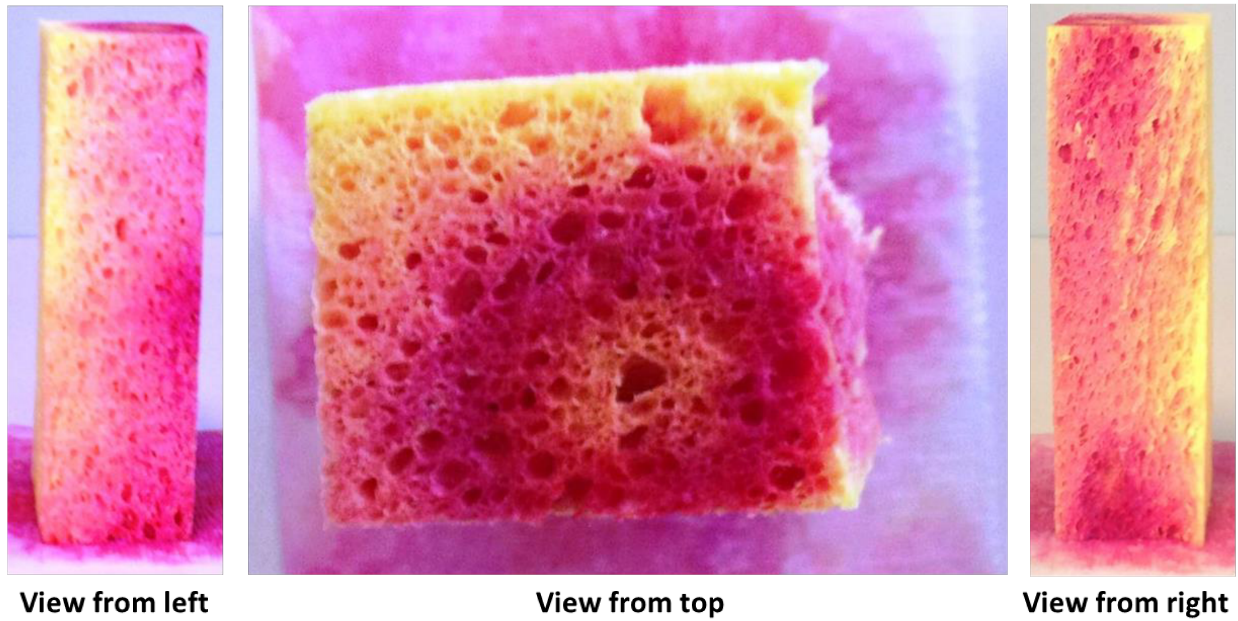
Fig. 4.L: Pore continuity check via capillary ascent of red dye.

Some experiments to confirm the continuity of pores inside the sponge bars were also performed. Smaller cut-pieces of the block were immersed in a shallow pool of red-dyed water and kept standing up with a small volume of the bottom portion physically touching the liquid. It was expected that a continuous pore connection would facilitate ascent of the red liquid via capillary action which could then be visualized. Pore continuity could be established along all three axes: *x, y* and *z.*

4.5.5 The Compression-test rig

1 – Load cell
2 – Top compression platen
3 – Bottom compression platen
4 – Compressed sponge sample
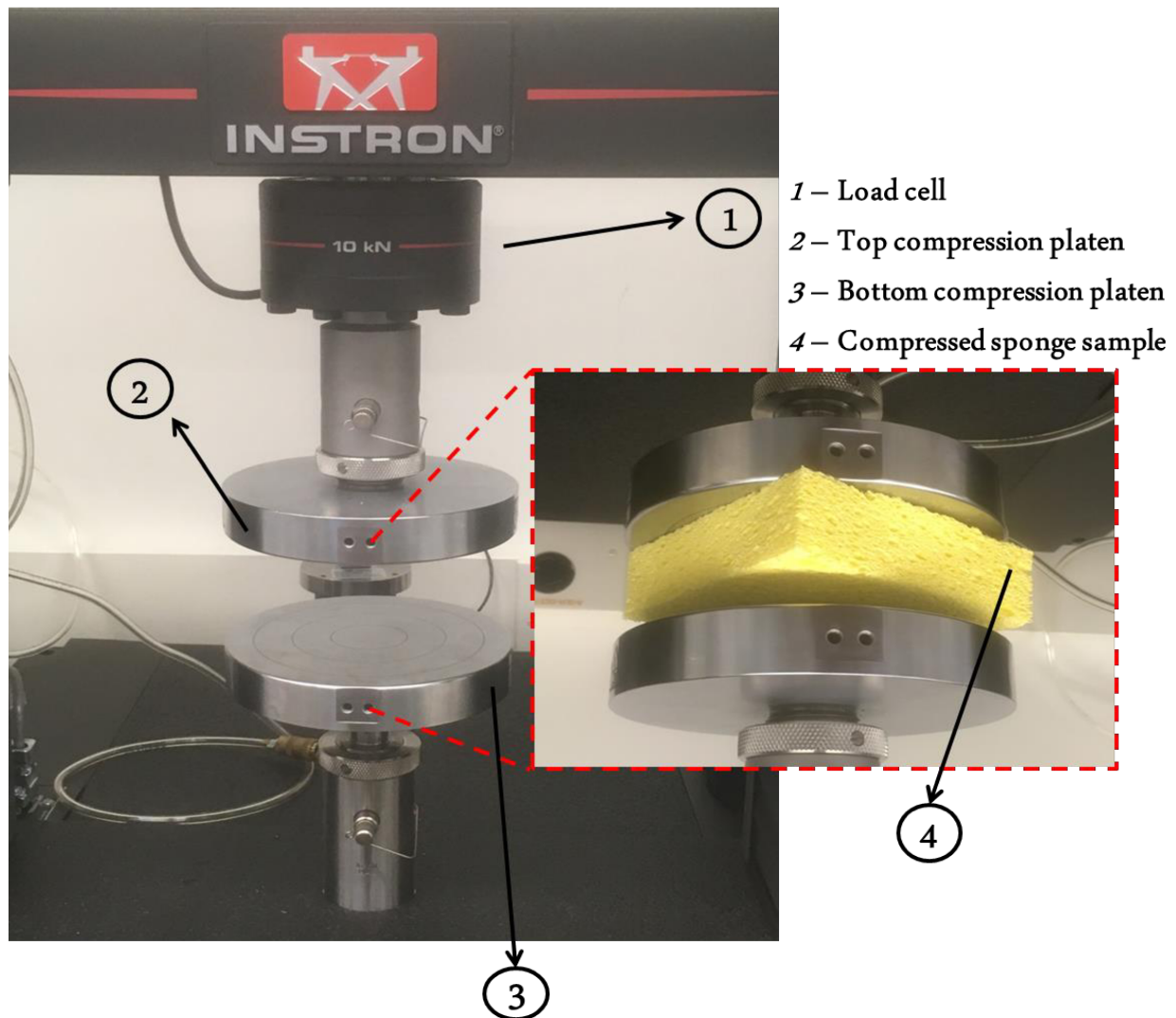
Fig. 4.M: The compression test-rig.

Fig. 4.M shows the actual Instron™ universal testing machine. We have used a 10 kN load cell and flat circular compression platens mad of stainless steel. The yellow sponge specimen may be seen being squeezed between the platens. The top platen moves downwards while the bottom platen is stationary. The speed of downward movement of the top platen is regulated to ensure the correctness of the quasi-static approximation.

References

Achal, V., Mukerjee, A., & Sudhakara Reddy, M. (2013). Biogenic treatment improves the durability and remediates the cracks of concrete structures. *Construction and Building Materials*, *48*, 1–5. https://doi.org/10.1016/j.conbuildmat.2013.06.061

Achal, V., Mukherjee, a, Basu, P. C., & Reddy, M. S. (2009). Strain improvement of Sporosarcina pasteurii for enhanced urease and calcite production. *Journal of Industrial Microbiology & Biotechnology*, *36*(7), 981–988. https://doi.org/10.1007/s10295-009-0578-z

Achal, V., & Pan, X. (2011). Characterization of urease and carbonic anhydrase producing bacteria and their role in calcite precipitation. *Current Microbiology*, *62*(3), 894–902. https://doi.org/10.1007/s00284-010-9801-4

Achal, V., Pan, X., Fu, Q., & Zhang, D. (2012). Biomineralization based remediation of As(III) contaminated soil by Sporosarcina ginsengisoli. *Journal of Hazardous Materials*, *201–202*, 178–184. https://doi.org/10.1016/j.jhazmat.2011.11.067

Adolphe, J. P., Loubière, J. F., Paradas, J., & Soleilhavoup, F. (1990). Procédé de traitement biologique d'une surface artificielle. *European Patent 90400G97. 0*, *1989*.

Al Qabany, A., Soga, K., & Santamarina, C. (2012). Factors Affecting Efficiency of Microbially Induced Calcite Precipitation. *Journal of Geotechnical and Geoenvironmental Engineering*, *138*(8), 992–1001. https://doi.org/10.1061/(ASCE)GT.1943-5606.0000666

Anbu, P., Kang, C.-H., Shin, Y.-J., & So, J.-S. (2016). Formations of calcium carbonate minerals by bacteria and its multiple applications. *Springerplus*, *5*(1), 250.

Arias, J. L., & Fernández, M. S. (2008). Polysaccharides and proteoglycans in calcium carbonate-based biomineralization. *Chemical Reviews*, *108*(11), 4475–4482.

Bang, S. S., Galinat, J. K., & Ramakrishnan, V. (2001). Calcite precipitation induced by polyurethane-immobilized Bacillus pasteurii. *Enzyme and Microbial Technology*, *28*(4–5), 404–409.

Bang, S. S., & Ramakrishnan, V. (2001). Microbiologically-enhanced crack remediation (MECR). In *proceedings of the international symposium on industrial application of microbial genomes* (Vol. 20, pp. 3–13).

Benini, S., Rypniewski, W. R., Wilson, K. S., Miletti, S., Ciurli, S., & Mangani, S. (1999). A new proposal for urease mechanism based on the crystal structures of the native and inhibited enzyme from Bacillus pasteurii: why urea hydrolysis costs two nickels. *Structure*, *7*(2), 205–216.

Berner, R. A. (1975). The role of magnesium in the crystal growth of calcite and aragonite from sea water. *Geochimica et Cosmochimica Acta*, *39*(4), 489IN3495--494504.

Bhaduri, S., Debnath, N., Mitra, S., Liu, Y., & Kumar, A. (2016). Microbiologically induced calcite precipitation mediated by sporosarcina pasteurii. *Journal of Visualized Experiments*, *2016*(110). https://doi.org/10.3791/53253

bioMASON. (2018). No Title. Retrieved January 2, 2018, from www.biomason.com

Bosak, T. (2011). Calcite precipitation, microbially induced. In *Encyclopedia of Geobiology* (pp. 223–227). Springer.

Braissant, O., Verrecchia, E. P., & Aragno, M. (2002). Is the contribution of bacteria to terrestrial carbon budget greatly underestimated? *Naturwissenschaften*, *89*(8), 366–370.

Bray, J. M., Lauchnor, E. G., Redden, G. D., Gerlach, R., Fujita, Y., Codd, S. L., & Seymour, J. D. (2017). Impact of Mineral Precipitation on Flow and Mixing in Porous Media Determined by Microcomputed Tomography and MRI. *Environmental Science & Technology*, *51*(3), 1562–1569. https://doi.org/10.1021/acs.est.6b02999

Bundeleva, I. A., Shirokova, L. S., Bénézeth, P., Pokrovsky, O. S., Kompantseva, E. I., & Balor, S. (2012). Calcium carbonate precipitation by anoxygenic phototrophic bacteria. *Chemical Geology*, *291*, 116–131.

Camesano, T. A., & Logan, B. E. (1998). Influence of fluid velocity and cell concentration on the transport of motile and nonmotile bacteria in porous media. *Environmental Science and Technology*. https://doi.org/10.1021/es970996m

Cappitelli, F., Zanardini, E., Ranalli, G., Mello, E., Daffonchio, D., & Sorlini, C. (2006). Improved methodology for bioremoval of black crusts on historical stone artworks by use of sulfate-reducing bacteria. *Applied and Environmental Microbiology*, *72*(5), 3733–3737.

Castanier, S., Le Métayer-Levrel, G., & Perthuisot, J.-P. (1999). Ca-carbonates precipitation and

limestone genesis—the microbiogeologist point of view. *Sedimentary Geology*, *126*(1–4), 9–23.

Chafetz, H. S. (1986). Marine peloids: a product of bacterially induced precipitation of calcite. *Journal of Sedimentary Research*, *56*(6).

Chafetz, H. S., & Buczynski, C. (1992). Bacterially induced lithification of microbial mats. *Palaios*, 277–293.

Chu, K. T. (2005). by.

Chunxiang, Q., Jianyun, W., Ruixing, W., & Liang, C. (2009). Corrosion protection of cement-based building materials by surface deposition of CaCO3 by Bacillus pasteurii. *Materials Science and Engineering: C*, *29*(4), 1273–1280.

Costerton, J. W., & Stewart, P. S. (2001). Battling biofilms. *Scientific American*, *285*(1), 74–81.

Cunningham, A. B., & Gerlach, R. (2010). Microbially Enhanced Carbon Capture and Storage by Mineral-Trapping and, *44*(13), 5270–5276.

Cunningham, A. B., Gerlach, R., Spangler, L., & Mitchell, A. C. (2009). Microbially enhanced geologic containment of sequestered supercritical CO2. *Energy Procedia*, *1*(1), 3245–3252.

Cunningham, a. B., Gerlach, R., Spangler, L., & Mitchell, a. C. (2009). Microbially enhanced geologic containment of sequestered supercritical CO2. *Energy Procedia*, *1*(1), 3245–3252. https://doi.org/10.1016/j.egypro.2009.02.109

Cunningham, a. B., Gerlach, R., Spangler, L., Mitchell, a. C., Parks, S., & Phillips, a. (2011). Reducing the risk of well bore leakage of CO2 using engineered biomineralization barriers. *Energy Procedia*, *4*, 5178–5185. https://doi.org/10.1016/j.egypro.2011.02.495

Cuthbert, M. O., Riley, M. S., Handley-Sidhu, S., Renshaw, J. C., Tobler, D. J., Phoenix, V. R., & Mackay, R. (2012). Controls on the rate of ureolysis and the morphology of carbonate precipitated by S. Pasteurii biofilms and limits due to bacterial encapsulation. *Ecological Engineering*, *41*, 32–40. https://doi.org/10.1016/j.ecoleng.2012.01.008

De Muynck, W., De Belie, N., & Verstraete, W. (2010). Microbial carbonate precipitation in construction materials: A review. *Ecological Engineering*, *36*(2), 118–136.

https://doi.org/10.1016/j.ecoleng.2009.02.006

De Muynck, W., Verbeken, K., De Belie, N., & Verstraete, W. (2013). Influence of temperature on the effectiveness of a biogenic carbonate surface treatment for limestone conservation. *Applied Microbiology and Biotechnology*, *97*(3), 1335–1347.

Demény, A., Németh, P., Czuppon, G., Leél-\HOssy, S., Szabó, M., Judik, K., … Stieber, J. (2016). Formation of amorphous calcium carbonate in caves and its implications for speleothem research. *Scientific Reports*, *6*, 39602.

der Heide, P. (2011). *X-ray photoelectron spectroscopy: an introduction to principles and practices*. John Wiley & Sons.

Dhami, N. K., Reddy, M. S., & Mukherjee, A. (2013). Bacillus megaterium mediated mineralization of calcium carbonate as biogenic surface treatment of green building materials. *World Journal of Microbiology and Biotechnology*, *29*(12), 2397–2406. https://doi.org/10.1007/s11274-013-1408-z

Dhami, N. K., Reddy, M. S., & Mukherjee, M. S. (2013). Biomineralization of calcium carbonates and their engineered applications: A review. *Frontiers in Microbiology*, *4*(OCT), 1–13. https://doi.org/10.3389/fmicb.2013.00314

Dick, J., De Windt, W., De Graef, B., Saveyn, H., der Meeren, P., De Belie, N., & Verstraete, W. (2006). Bio-deposition of a calcium carbonate layer on degraded limestone by Bacillus species. *Biodegradation*, *17*(4), 357–367.

Douglas, S., & Beveridge, T. J. (1998). Mineral formation by bacteria in natural microbial communities. *FEMS Microbiology Ecology*, *26*(2), 79–88.

Duffy, K. J., Cummings, P. T., & Ford, R. M. (1995). Random walk calculations for bacterial migration in porous media. *Biophysical Journal*, *68*(3), 800–806. https://doi.org/10.1016/S0006-3495(95)80256-0

Dupraz, S., Parmentier, M., Ménez, B., & Guyot, F. (2009). Experimental and numerical modeling of bacterially induced pH increase and calcite precipitation in saline aquifers. *Chemical Geology*, *265*(1–2), 44–53. https://doi.org/10.1016/j.chemgeo.2009.05.003

Ehrlich, H. L. (1996). How microbes influence mineral growth and dissolution. *Chemical Geology*,

132(1–4), 5–9.

Ehrlich, H. L. (1998). Geomicrobiology: its significance for geology. *Earth-Science Reviews*, *45*(1–2), 45–60.

Ferris, F. G., & Beveridge, T. J. (1985). Functions of bacterial cell surface structures. *BioScience*, *35*(3), 172–177.

Ferris, F. G., Beveridge, T. J., & Fyfe, W. S. (1986). Iron-silica crystallite nucleation by bacteria in a geothermal sediment. *Nature*, *320*(6063), 609–611.

Ferris, F. G., Phoenix, V., Fujita, Y., & Smith, R. W. (2004). Kinetics of calcite precipitation induced by ureolytic bacteria at 10 to 20 C in artificial groundwater. *Geochimica et Cosmochimica Acta*, *68*(8), 1701–1710.

Fidaleo, M., & Lavecchia, R. (2003). Kinetic study of enzymatic urea hydrolysis in the pH range 4-9. *Chemical and Biochemical Engineering Quarterly*, *17*(4), 311–318.

Folk, R. L. (1993). SEM imaging of bacteria and nannobacteria in carbonate sediments and rocks. *Journal of Sedimentary Research*, *63*(5).

Fontes, D. E., Mills, A. L., Hornberger, G. M., & Herman, J. S. (1991). Physical and Chemical Factors Influencing Transport of Microorganisms through Porous Media. *APPLIED AND ENVIRONMENTAL MICROBIOLOGY*, *57*(9), 2473–2481.

Friedrich, B., & Magasanik, B. (1977). Urease of Klebsiella aerogenes: control of its synthesis by glutamine synthetase. *Journal of Bacteriology*, *131*(2), 446–452.

Gal, J.-Y., Bollinger, J.-C., Tolosa, H., & Gache, N. (1996). Calcium carbonate solubility: a reappraisal of scale formation and inhibition. *Talanta*, *43*(9), 1497–1509.

Ganendra, G., De Muynck, W., Ho, A., Arvaniti, E. C., Hosseinkhani, B., Ramos, J. A., … Boon, N. (2014). Formate oxidation-driven calcium carbonate precipitation by Methylocystis parvus OBBP. *Applied and Environmental Microbiology*, *80*(15), 4659–4667.

Garcia-Vallès, M., Vendrell-Saz, M., Krumbein, W. E., & Urz\`\i, C. (1997). Coloured mineral coatings on monument surfaces as a result of biomineralization: the case of the Tarragona

cathedral (Catalonia). *Applied Geochemistry*, *12*(3), 255–266.

Ghashghaei, S., & Emtiazi, G. (2013). Production of calcite nanocrystal by a urease-positive strain of enterobacter ludwigii and study of its structure by SEM. *Current Microbiology*, *67*(4), 406–413. https://doi.org/10.1007/s00284-013-0379-5

Gibson, T. (1934). An Investigation of the Bacillus Pasteuri Group: II. Special Physiology of the Organisms. *Journal of Bacteriology*, *28*(3), 313.

Gollapudi, U. K., Knutson, C. L., Bang, S. S., & Islam, M. R. (1995). A new method for controlling leaching through permeable channels. *Chemosphere*, *30*(4), 695–705.

Gorospe, C. M., Han, S.-H., Kim, S.-G., Park, J.-Y., Kang, C.-H., Jeong, J.-H., & So, J.-S. (2013). Effects of different calcium salts on calcium carbonate crystal formation by Sporosarcina pasteurii KCTC 3558. *Biotechnology and Bioprocess Engineering*, *18*(5), 903–908.

Greenfield, L. J. (1963). Metabolism and concentration of calcium and magnesium and precipitation of calcium carbonate by a marine bacterium. *Annals of the New York Academy of Sciences*, *109*(1), 23–45.

Hammes, F. (2002). *Ureolytic microbial calcium carbonate precipitation*. Ph. D. Thesis, Ghent University, Ghent.

Hammes, F. (2003). UREOLYTIC MICROBIAL CALCIUM CARBONATE PRECIPITATION UREOLYTISCHE MICROBIELE CALCIUMCARBONAAT- door. *Scanning Electron Microscopy*.

Hammes, F., Arnold, J., Krupka, K. M., Cantrell, K. J., McGrail, B. P., Tagliaferri, F., … Gerlach, R. (2013). Calcium carbonate precipitation by different bacterial strains. *Ecological Engineering*, *36*(3), 172. https://doi.org/http://researchrepository.murdoch.edu.au/399/2/02Whole.pdf

Hammes, F., Boon, N., De Villiers, J., Verstraete, W., Siciliano, S. D., & Villiers, J. De. (2003). Strain-Specific Ureolytic Microbial Calcium Carbonate Precipitation Strain-Specific Ureolytic Microbial Calcium Carbonate Precipitation. *Applied and Environmental Microbiology*, *69*(8), 4901–4909. https://doi.org/10.1128/AEM.69.8.4901

Hammes, F., & Verstraete, W. (2002). Key roles of pH and calcium metabolism in microbial

carbonate precipitation. *Reviews in Environmental Science and Biotechnology*, *1*(1), 3–7.

Hong, S.-I., Park, W.-S., & Pyun, Y.-R. (1997). Inactivation ofLactobacillussp. fromKimchiby High Pressure Carbon Dioxide. *LWT-Food Science and Technology*, *30*(7), 681–685.

Hunter, G. K. (1996). Interfacial aspects of biomineralization. *Current Opinion in Solid State and Materials Science*, *1*(3), 430–435.

Ismail, M. A., Joer, H. A., Randolph, M. F., & Meritt, A. (2002). Cementation of porous materials using calcite. *Geotechnique*, *52*(5), 313–324.

Jahns, T. (1996). Ammonium/urea-dependent generation of a proton electrochemical potential and synthesis of ATP in Bacillus pasteurii. *Journal of Bacteriology*, *178*(2), 403–409.

Jansson, C., & Northen, T. (2010). Calcifying cyanobacteria—the potential of biomineralization for carbon capture and storage. *Current Opinion in Biotechnology*, *21*(3), 365–371.

Jonkers, H. M., Thijssen, A., Muyzer, G., Copuroglu, O., & Schlangen, E. (2010). Application of bacteria as self-healing agent for the development of sustainable concrete. *Ecological Engineering*, *36*(2), 230–235. https://doi.org/10.1016/j.ecoleng.2008.12.036

Kaltwasser, H., Krämer, J., & Conger, W. R. (1972). Control of urease formation in certain aerobic bacteria. *Archiv Für Mikrobiologie*, *81*(2), 178–196.

Kantzas, A., Stehmeier, L., Marentette, D. F., Ferris, F. G., Jha, K. N., Maurits, F. M., & others. (1992). A novel method of sand consolidation through bacteriogenic mineral plugging. In *Annual Technical Meeting*.

Kantzas, a, Stehmeier, L., Marentette, D. F., Ferris, F. G., Jha, K. N., & Mourits, F. M. (1992). A Novel Method of Sand Consolidation Through Bacteriogenic Mineral Plugging. *43rd Annual Technical Meeting, Petroleum Society of CIM*, *CIM 92-46*(Cim), 1–15. https://doi.org/10.2118/92-46

Kawaguchi, T., & Decho, A. W. (2002). A laboratory investigation of cyanobacterial extracellular polymeric secretions (EPS) in influencing CaCO 3 polymorphism. *Journal of Crystal Growth*, *240*(1), 230–235.

Keefe, W. E. (1976). Formation of crystalline deposits by several genera of the family

Enterobacteriaceae. *Infection and Immunity*, *14*(2), 590–592.

Knorre, H. v, & Krumbein, W. E. (2000). Bacterial calcification. In *Microbial sediments* (pp. 25–31). Springer.

Konishi, Y., Tsukiyama, T., Ohno, K., Saitoh, N., Nomura, T., & Nagamine, S. (2006). Intracellular recovery of gold by microbial reduction of AuCl4- ions using the anaerobic bacterium Shewanella algae. *Hydrometallurgy*, *81*(1), 24–29.

Kralj, D., Brečević, L., & Kontrec, J. (1997). Vaterite growth and dissolution in aqueous solution III. Kinetics of transformation. *Journal of Crystal Growth*, *177*(3–4), 248–257.

Kralj, D., Brečević, L., & Nielsen, A. E. (1990). Vaterite growth and dissolution in aqueous solution I. Kinetics of crystal growth. *Journal of Crystal Growth*, *104*(4), 793–800.

Kralj, D., Brečević, L., & Nielsen, A. E. (1994). Vaterite growth and dissolution in aqueous solution II. Kinetics of dissolution. *Journal of Crystal Growth*, *143*(3–4), 269–276.

Krumbein, W. E. (1979). Photolithotropic and chemoorganotrophic activity of bacteria and algae as related to beachrock formation and degradation (Gulf of Aqaba, Sinai). *Geomicrobiology Journal*, *1*(2), 139–203.

Kumar, A., Karig, D., Acharya, R., Neethirajan, S., Mukherjee, P. P., Retterer, S., & Doktycz, M. J. (2013). Microscale confinement features can affect biofilm formation. *Microfluidics and Nanofluidics*, *14*(5), 895–902.

Kupriyanova, E., Villarejo, A., Markelova, A., Gerasimenko, L., Zavarzin, G., Samuelsson, G., … Pronina, N. (2007). Extracellular carbonic anhydrases of the stromatolite-forming cyanobacterium Microcoleus chthonoplastes. *Microbiology*, *153*(4), 1149–1156.

Kurmaç, Y. (2009). The impact of toxicity of metals on the activity of ureolytic mixed culture during the precipitation of calcium. *Journal of Hazardous Materials*, *163*(2–3), 1063–1067.

Lauchnor, E. G., Topp, D. M., Parker, A. E., & Gerlach, R. (2015). Whole cell kinetics of ureolysis by Sporosarcina pasteurii. *Journal of Applied Microbiology*, *118*(6), 1321–1332. https://doi.org/10.1111/jam.12804

Le Metayer-Levrel, G., Castanier, S., Orial, G., Loubiere, J.-F., & Perthuisot, J.-P. (1999). Applications of bacterial carbonatogenesis to the protection and regeneration of limestones in buildings and historic patrimony. *Sedimentary Geology*, *126*(1–4), 25–34.

Lewandowski, Z., & Beyenal, H. (2013). *Fundamentals of biofilm research*. CRC press.

Li, M., Fu, Q.-L., Zhang, Q., Achal, V., & Kawasaki, S. (2015). Bio-grout based on microbially induced sand solidification by means of asparaginase activity. *Scientific Reports*, *5*, 16128.

Lian, B., Hu, Q., Chen, J., Ji, J., & Teng, H. H. (2006). Carbonate biomineralization induced by soil bacterium Bacillus megaterium. *Geochimica et Cosmochimica Acta*, *70*(22), 5522–5535.

Life Technologies. (2004). No Title. Retrieved January 2, 2018, from https://tools.lifetechnologies.com/content/sfs/manuals/mp07007.pdf

LIN, H.-M., Cao, N., & CHEN, L.-F. (1994). Antimicrobial effect of pressurized carbon dioxide on Listeria monocytogenes. *Journal of Food Science*, *59*(3), 657–659.

Lowenstam, H. A. (1981). Minerals formed by organisms. *Science*, *211*(4487), 1126–1131.

Lowenstam, H. A., & Weiner, S. (1989). *On biomineralization*. Oxford University Press on Demand.

Lowenstam, H. A., Weiner, S., bioMASON, Robbins, R., Technologies, L., Lowenstam, H. A., … Whitesides, G. M. M. (2011). No Title. *Annual Review of Fluid Mechanics*, *1*(1), 1–5. https://doi.org/http://researchrepository.murdoch.edu.au/399/2/02Whole.pdf

Lüttge, A., & Conrad, P. G. (2004). Direct observation of microbial inhibition of calcite dissolution. *Applied and Environmental Microbiology*, *70*(3), 1627–1632.

McConnaughey, T. A., & Whelan, J. F. (1997). Calcification generates protons for nutrient and bicarbonate uptake. *Earth-Science Reviews*, *42*(1–2), 95–117.

McKay, D. S., Gibson, E. K., Thomas-Keprta, K. L., Vali, H., Romanek, C. S., Clemett, S. J., … Zare, R. N. (1996). Search for past life on Mars: possible relic biogenic activity in Martian meteorite ALH84001. *Science*, *273*(5277), 924–930.

Minto, J. M., MacLachlan, E., El Mountassir, G., & Lunn, R. J. (2016). Rock fracture grouting with microbially induced carbonate precipitation. *Water Resources Research*.

https://doi.org/10.1002/2016WR018884

Mitchell, A. C., & Ferris, F. G. (2005). The coprecipitation of Sr into calcite precipitates induced by bacterial ureolysis in artificial groundwater: temperature and kinetic dependence. *Geochimica et Cosmochimica Acta*, *69*(17), 4199–4210.

Mitchell, A. C., & Ferris, F. G. (2006). The influence of Bacillus pasteurii on the nucleation and growth of calcium carbonate. *Geomicrobiology Journal*, *23*(3–4), 213–226.

Mitchell, A. C., Phillips, A. J., Hiebert, R., Gerlach, R., Spangler, L. H., & Cunningham, A. B. (2009a). Biofilm enhanced geologic sequestration of supercritical CO2. *International Journal of Greenhouse Gas Control*, *3*(1), 90–99.

Mitchell, A. C., Phillips, A. J., Hiebert, R., Gerlach, R., Spangler, L. H., & Cunningham, A. B. (2009b). Biofilm enhanced geologic sequestration of supercritical CO2. *International Journal of Greenhouse Gas Control*, *3*(1), 90–99. https://doi.org/10.1016/j.ijggc.2008.05.002

Monger, H. C., Daugherty, L. A., Lindemann, W. C., & Liddell, C. M. (1991). Microbial precipitation of pedogenic calcite. *Geology*, *19*(10), 997–1000.

Montemagno, C., & Pyrak-Nolte, L. (1995). Porosity of natural fracture networks. *Geophysical Research Letters*, *22*(11), 1397–1400.

Montemagno, C., & Pyrak-Nolte, L. (1999). Fracture Netwok versus Single Structures: Measurement of Fracture Geometry with X-ray Tomography. *Phys. Chem. Earth (A)*, *24*(7), 575–579.

Montoya, B. M. (2012). *Bio-mediated soil improvement and the effect of cementation on the behavior, improvement, and performance of sand*. University of California, Davis.

Morita, R. Y. (1980). Calcite precipitation by marine bacteria. *Geomicrobiology Journal*, *2*(1), 63–82.

Morse, J. W. (1983). The kinetics of calcium carbonate dissolution and precipitation. *Reviews in Mineralogy and Geochemistry*, *11*(1), 227–264.

Mortensen, B. M., Haber, M. J., Dejong, J. T., Caslake, L. F., & Nelson, D. C. (2011). Effects of environmental factors on microbial induced calcium carbonate precipitation. *Journal of Applied Microbiology*, *111*(2), 338–349. https://doi.org/10.1111/j.1365-2672.2011.05065.x

Nemati, M., & Voordouw, G. (2003). Modification of porous media permeability, using calcium carbonate produced enzymatically in situ. *Enzyme and Microbial Technology*, *33*(5), 635–642. https://doi.org/10.1016/S0141-0229(03)00191-1

Okwadha, G. D. O., & Li, J. (2010a). Optimum conditions for microbial carbonate precipitation. *Chemosphere*, *81*(9), 1143–1148.

Okwadha, G. D. O., & Li, J. (2010b). Optimum conditions for microbial carbonate precipitation. *Chemosphere*, *81*(9), 1143–1148. https://doi.org/10.1016/j.chemosphere.2010.09.066

Parks, S. L. (2009). Kinetics of Calcite Precipitation By Ureolytic Bacteria Under Aerobic and Anaerobic Conditions. *Chemical and Biological Engineering*, (April), 93.

Phillips, A. J., Gerlach, R., Lauchnor, E., Mitchell, A. C., Cunningham, A. B., & Spangler, L. (2013). Engineered applications of ureolytic biomineralization: a review. *Biofouling*, *29*(6), 715–733. https://doi.org/10.1080/08927014.2013.796550

Phillips, A. J., Lauchnor, E., Eldring, J. J., Esposito, R., Mitchell, A. C., Gerlach, R., … Spangler, L. H. (2013). Potential CO2 leakage reduction through biofilm-induced calcium carbonate precipitation. *Environmental Science & Technology*, *47*(1), 142–149. https://doi.org/10.1021/es301294q

Pyrak-Nolte, L. J., Montemagno, C. D., Yang, G., Cook, N. G. W., & Myer, L. R. (1995). Three-dimensional tomographic visuallzatlon of natural fracture networks and graph theory analysis of the transport properties. In *8th ISRM Congress* (pp. 855–859). Tokyo, Japan: International Society for Rock Mechanics. Retrieved from https://www.onepetro.org/conference-paper/ISRM-8CONGRESS-1995-174

Pyrak-Nolte, L., Montemagno, C., & Nolte, D. (1997). Volumetric imaging of aperture distributions in connected fracture networks. *Geophysical Research Letters*, *24*(18), 2343–2346.

R. Robbins. (2010). No Title. Retrieved January 2, 2018, from http://www.utdallas.edu/~rar011300/SEM/Scanning Electron Microscope Operation.pdf

Reddy, B. V. V., & Jagadish, K. S. (2003). Embodied energy of common and alternative building materials and technologies. *Energy and Buildings*, *35*(2), 129–137.

Rivadeneyra, M. A., Delgado, R., del Moral, A., Ferrer, M. R., & Ramos-Cormenzana, A. (1994). Precipatation of calcium carbonate by Vibrio spp. from an inland saltern. *FEMS Microbiology Ecology*, *13*(3), 197–204.

Rodriguez-Navarro, C., Rodriguez-Gallego, M., Chekroun, K. Ben, & Gonzalez-Munoz, M. T. (2003). Conservation of ornamental stone by Myxococcus xanthus-induced carbonate biomineralization. *Applied and Environmental Microbiology*, *69*(4), 2182–2193.

Rosenbaum, L. (2006). Prehistoric artistry, real and recreated. *The Wall Street Journal, 13*.

Sarikaya, M. (1999). Biomimetics: materials fabrication through biology. *Proceedings of the National Academy of Sciences*, *96*(25), 14183–14185.

Schultze-Lam, S., Fortin, D., Davis, B. S., & Beveridge, T. J. (1996). Mineralization of bacterial surfaces. *Chemical Geology*, *132*(1–4), 171–181.

Sham, E., Mantle, M. D., Mitchell, J., Tobler, D. J., Phoenix, V. R., & Johns, M. L. (2013). Monitoring bacterially induced calcite precipitation in porous media using magnetic resonance imaging and flow measurements. *Journal of Contaminant Hydrology*, *152*, 35–43. https://doi.org/10.1016/j.jconhyd.2013.06.003

Sherwood, J. L., Sung, J. C., Maneval, J. E., & Smith, J. A. (2003). Analysis of Bacterial Random Motility in a Porous Medium Using Magnetic Resonance Imaging and Immunomagnetic Labeling, *37*(4), 781–785.

Siddique, R., & Chahal, N. K. (2011a). Effect of ureolytic bacteria on concrete properties. *Construction and Building Materials*, *25*(10), 3791–3801.

Siddique, R., & Chahal, N. K. (2011b). Effect of ureolytic bacteria on concrete properties. *Construction and Building Materials*, *25*(10), 3791–3801. https://doi.org/10.1016/j.conbuildmat.2011.04.010

Silver, S., Toth, K., & Scribner, H. (1975). Facilitated transport of calcium by cells and subcellular membranes of Bacillus subtilis and Escherichia coli. *Journal of Bacteriology*, *122*(3), 880–885.

Smith, K. S., & Ferry, J. G. (2000). Prokaryotic carbonic anhydrases. *FEMS Microbiology Reviews*, *24*(4), 335–366.

Söhnel, O., & Garside, J. (n.d.). Precipitation: Basic principles and industrial applications. 1992. Oxford: Butterworth-Heinemann.

Southam, G. (2000). Bacterial surface-mediated mineral formation. In *Environmental microbe-metal interactions* (pp. 257–276). American Society of Microbiology.

Stabnikov, V., Naeimi, M., Ivanov, V., & Chu, J. (2011). Formation of water-impermeable crust on sand surface using biocement. *Cement and Concrete Research*, *41*(11), 1143–1149.

Stewart, P. S. (2003). Diffusion in biofilms. *Journal of Bacteriology*, *185*(5), 1485–1491.

Stocks-Fischer, S., Galinat, J. K., & Bang, S. S. (1999a). Microbiological precipitation of CaCO3. *Soil Biology and Biochemistry*, *31*(11), 1563–1571.

Stocks-Fischer, S., Galinat, J. K., & Bang, S. S. (1999b). Microbiological precipitation of CaCO3. *Soil Biology and Biochemistry*, *31*(11), 1563–1571. https://doi.org/10.1016/S0038-0717(99)00082-6

Stoner, D. L., Watson, S. M., Stedtfeld, R. D., Meakin, P., Tyler, T. L., Pegram, L. M., … Griffel, L. K. (2005). Application of Stereolithographic Custom Models for Studying the Impact of Biofilms and Mineral Precipitation on Fluid Flow Application of Stereolithographic Custom Models for Studying the Impact of Biofilms and Mineral Precipitation on Fluid Flow. https://doi.org/10.1128/AEM.71.12.8721

Stumm, W., & Morgan, J. J. (1981). Aquatic Chemistry, 780 pp. *J. Wi L Ey & Sons*.

Tagliaferri, F., Waller, J., And??, E., Hall, S. A., Viggiani, G., B??suelle, P., & DeJong, J. T. (2011). Observing strain localisation processes in bio-cemented sand using x-ray imaging. *Granular Matter*, *13*(3), 247–250. https://doi.org/10.1007/s10035-011-0257-4

Thomas-Keprta, K. L., McKay, D. S., Wentworth, S. J., Stevens, T. O., Taunton, A. E., Allen, C. C., … Romanek, C. S. (1998). Bacterial mineralization patterns in basaltic aquifers: Implications for possible life in martian meteorite ALH84001. *Geology*, *26*(11), 1031–1034.

Thompson, J. B., & Ferris, F. G. (1990). Cyanobacterial precipitation of gypsum, calcite, and magnesite from natural alkaline lake water. *Geology*, *18*(10), 995–998.

Tiano, P., Biagiotti, L., & Mastromei, G. (1999). Bacterial bio-mediated calcite precipitation for

monumental stones conservation: methods of evaluation. *Journal of Microbiological Methods*, *36*(1–2), 139–145.

Tobler, D. J., Cuthbert, M. O., & Phoenix, V. R. (2014). Transport of Sporosarcina pasteurii in sandstone and its significance for subsurface engineering technologies. *Applied Geochemistry*, *42*, 38–44. https://doi.org/10.1016/j.apgeochem.2014.01.004

Valiei, A., Kumar, A., Mukherjee, P. P., Liu, Y., & Thundat, T. (2012). A web of streamers: biofilm formation in a porous microfluidic device. *Lab on a Chip*, *12*(24), 5133–5137. https://doi.org/10.1039/c2lc40815e

van Paassen, L. (2009). *Biogrout: Ground Improvement by Microbially Induced Carbonate Precipitation*. *Technology*.

Von Der Schulenburg, D. A. G., Paterson-Beedle, M., MacAskie, L. E., Gladden, L. F., & Johns, M. L. (2007). Flow through an evolving porous media-compressed foam. *Journal of Materials Science*, *42*(16), 6541–6548. https://doi.org/10.1007/s10853-007-1523-z

Wanger, G., Onstott, T. C., & Southam, G. (2008). Stars of the terrestrial deep subsurface: A novel "star-shaped" bacterial morphotype from a South African platinum mine. *Geobiology*. https://doi.org/10.1111/j.1472-4669.2008.00163.x

Warren, L. A., Maurice, P. A., Parmar, N., & Ferris, F. G. (2001). Microbially mediated calcium carbonate precipitation: implications for interpreting calcite precipitation and for solid-phase capture of inorganic contaminants. *Geomicrobiology Journal*, *18*(1), 93–115.

Warthmann, R., Van Lith, Y., Vasconcelos, C., McKenzie, J. A., & Karpoff, A. M. (2000). Bacterially induced dolomite precipitation in anoxic culture experiments. *Geology*, *28*(12), 1091–1094.

Watabe, N., & Wilbur, K. M. (1960). Influence of the organic matrix on crystal type in molluscs. *Nature*, *188*(4747), 334.

Wei, L., Liping, L., Long, C., & Longjiang, Y. (2009). Research status and prospect of biological precipitation of carbonate. *Advances in Earth Science*, *24*(6), 597–605.

Whiffin, V. S. (2004). Microbial CaCO3 Precipitation for the Production of Biocement. *Phd Thesis*, (September), 1–162.

https://doi.org/http://researchrepository.murdoch.edu.au/399/2/02Whole.pdf

Wiley, W. R., & Stokes, J. L. (1962). Requirement of an alkaline pH and ammonia for substrate oxidation by Bacillus pasteurii. *Journal of Bacteriology*, *84*(4), 730–734.

Zhang, J., Davis, T. A., Matthews, M. A., Drews, M. J., LaBerge, M., & An, Y. H. (2006). Sterilization using high-pressure carbon dioxide. *The Journal of Supercritical Fluids*, *38*(3), 354–372.

Zhong, L., Islam, M. R., & others. (1995). A new microbial plugging process and its impact on fracture remediation. In *SPE Annual Technical Conference and Exhibition*.

Chapter 5 : Summary and Conclusions

5.1 Summary

The objectives of the present research have primarily been a understanding of the various mechanistic aspects associated with the process of MICP mediated by *S. pasteurii*. An interdisciplinary study was undertaken to tackle the biomicrofluidic, solid mechanical and materials aspects of the phenomenon occurring inside a porous medium.

Chapter 2 outlines a detailed culture protocol and enrichment recipe via external additives for accomplishing an accelerated precipitation within a system of choice. This chapter also discusses microscopy and characterization experiments to analyze the chemical nature of precipitates and visualize MICP. The major contribution outlined in this chapter is the development of a rigorous protocol for culturing *S. pasteurii* that guarantees the induction of calcite precipitates under a wide range of operating conditions inside a structural porous medium. This is a new extension of pre-existing protocols which focus exclusively on the culture component but not on MICP induced via external enrichment.

Chapter 3 revolves around a cleverly designed semi-solid agar-based platform that closely mimics several fluid dynamic and transport aspects of a real porous medium (like a geologic structure, soil, sand, clay, concrete or rock). This platform facilitates a variety of experiments to observe and measure some key parameters of MICP. The power of this design lies with an enhanced mobility (by reducing the agar content) and a vertical orientation that allows visualization of cell penetration. The semi-solid agar platform shown in Fig. 3.1(a) is a "stabbed" culture where an inoculation loop is used to "poke" the agar gel and transfer a small mass of bacteria along the central axis of the cylindrical volume. Due to their intrinsic motility and the availability of a connected pore network, the cells travel radially outwards and branch out to the form the *tree-like* pattern seen in the figure. As they move, they leave behind tiny calcite microcrystals which show up as white trails against the yellow background. This process continues for 2-4 days and can be seen in progress with a naked eye examination at regular intervals.

We report the existence of micro and nanoscale needle like calcite crystals on the cell surface of *S. pasteurii*. Several related aspects like cell surface charge, zeta potential and kinematic mobility of the cells under diffusive and powered flagellar modes of locomotion are also discussed. We attempt to answer three important questions in this chapter. To begin with, we provide supporting evidence of the existence of negative surface charge centers on the cell membrane through zeta potential measurements. We extend this

finding to claim that the charge centers indeed act as nucleation sites for MICP by facilitating the neutralization of positively charged metal ions like Ca^{++}. This addresses the question of the spatial origin of MICP asked initially at the beginning of the thesis. Finally, we show the existence of powered flagellar mode of locomotion in this bacterium that is many orders of magnitude more efficient than a reliance on pure diffusion. All hypotheses have been backed up with kinematic data from analyses with the Stokes-Einstein equation, image processing of bacterial motility and single-cell tracking, electron microscopy (SEM & TEM) as well as chemical characterization.

Chapter 4 deals with comparative quantifications of the modifications in bulk and surface properties of a porous medium mimic before and after treatment. Extensive compression tests were performed to study the effects of MICP in terms of change in elastic moduli and mechanical strength.

Electron microscopy visualization and 3-dimensional micro-CT scans were performed to observe the pore network connectivity and compute parameters such as porosity and pore connectedness. A range of chemical analyses supplemented the visual data to complete the picture and provide a better understanding of induced-MICP inside the target porous medium. This chapter primarily attempted to address a few engineering questions on MICP. To begin with, a quantification of the distribution of pore and crystal sizes was undertaken. Next, clogged and unclogged porous specimens were imaged under x-ray micro-computed tomography (μ-CT scans) to compute relevant network parameters like porosity before and after MICP. It was shown that a clogged sample experiences about three times reduction in open pore porosity. Lastly, mechanical compression load tests were performed to quantify the enhancement in mechanical strength due to MICP. It was found that a clogged specimen demonstrates more than five times improvement in compressive strength at a ten per cent strain point. These results provide new quantitative comparisons between representative porous media before and after pore blockage induced by MICP.

5.2 Conclusions

Key conclusions from the present research are:

- *S. pasteurii* has the capacity to produce significant volumes of chemical precipitation via MICP. This process can be reliably accelerated via the addition of suitable external enrichment. An understanding of MICP is important to the success of such translational technologies as underground carbon storage and sequestration, heritage structure conservation and bioremediation/ biocementation. We have developed a simple and efficient protocol that ensures MICP if all steps are suitable followed.

- There exists at least a weak correlation between the external enrichment added to the native culture and the chemical nature of the solid precipitates. This idea may be exploited to regulate and control selective precipitation mediated by MICP. Since different polymorphs of the same chemical have different mechanical properties, this would have wide-ranging consequences in large-scale structural applications.

- The growth process is complex, and this makes it difficult to draw definitive conclusions on how precipitation depends on experimental parameters. There is a complicated interdependence and interplay of physical, chemical and biological factors in the background. A proper identification of the interrelationships and control thereof would lead to cleaner, faster and more efficient sealing/ clogging/ plugging strategies in management of pore blockage in an arbitrary porous medium matrix.

- *S. pasteurii* cells are capable of acting as nucleation sites for calcium carbonate precipitation in aqueous and semi-solid media. The precipitated solid powder contains in it nanoscale nanocrystals which may or may not grow into micro-scale or even larger aggregates. A large fraction of these crystals can be made to enter the pores of a microscale porous medium and cause clogging. We have provided clear evidence of the origin of nanoscale crystals on the cell membrane.

- We have designed a semi-transparent semi-solid platform to culture, grow and study *S. pasteurii* transport as it navigates a porous medium in real time. This platform helps one gain quantitative insights into the kinematic natures of the bacterial propagation as well as origin and progress of MICP with time. We have shown that *S. pasteurii* navigates using a powered flagellar mode of locomotion as opposed to purely diffusive movement. We have quantified the mean-squared displacement and drawn comparisons between experimentally observed magnitudes and those calculated using the classical Stokes-Einstein equation for Brownian motion.

- We have studied several mechanistic aspects of a real structural porous medium in a small, lab-scale surrogate system that fairly accurately captures the physics of MICP and bacteria transport. Experiments on this mimic medium can provide valuable quantitative ideas on change in mechanical properties of the target system caused due to MICP.

- Synergistic visualization/ reconstruction of the pore network using tools like electron microscopy and μ-CT scan reveals the nature, extend and distribution of deposited chemicals that enter the pore interior post-precipitation. This coupled with compression testing under the small deformation regime can provide numerical data to calculate performance metrics on the effectiveness and suitability of different sealing strategies in the context of macroscopic fracture engineering for mitigating cracks in an extended system. We have provided quantification on the enhancement in strength of a porous media after induction of MICP as well as computed the reduction in porosity as a result. We have shown a 3x reduction in porosity and 5x enhancements in compressive strength by virtue of MICP-related pore plugging.

5.3 Further study

The phenomenon of MICP is complex with various length and time scales involved. The fluid dynamics itself is very complicated as *S. pasteurii* and its associated biofilm acts as a complex colloid at the length scale of the pores inside the network. Although the present research manages to shed some light on the mysteries behind MICP, a lot of biophysical and biochemical questions nonetheless remain unresolved:

- *S. pasteurii* has been found to form biofilm streamers under flow conditions inside a microfluidic chip. It's not clear if this is a global phenomenon that can be extended to an arbitrary porous medium and whether the formation of streamers can be optimized. This is a key question to ask especially with respect to applications that leverage the pore closure property of MICP as entanglement of intertwined streamers can create a flow ratchet that traps the nascent nanocrystalline calcite particles and facilitate quick, long-range clogging *in situ*. Experiments involving microfluidic chips with in-built micropillars (MCIPs) that act as porous medium clones would be a very interesting, rich and fertile research direction to probe the physics of fluids at the pore-scale.

- Evidently, there are multiple thermodynamic variables in operation underneath MICP. The understanding of the effects of parameters like temperature, pressure, concentration, pH etc. on the efficiency of MICP remains a big grey area that needs to be suitably addressed using both analytical modeling and numerical simulations.

- The role of biofilm secreted by *S. pasteurii* remains an interesting problem to address. The biofilm behaves as a complex colloid with viscoelastic properties and exhibits highly non-linear response when subjected to shear and other dynamic forces inside a confined flow field. Several interesting mechanical engineering questions like creep, impact and hysteresis of the biofilm inside a microfluidic configuration would lead to important answers related to the nature, extent and time evolution of MICP.

List of References

Achal, V., Mukerjee, A., & Sudhakara Reddy, M. (2013). Biogenic treatment improves the durability and remediates the cracks of concrete structures. *Construction and Building Materials*, *48*, 1–5. https://doi.org/10.1016/j.conbuildmat.2013.06.061

Achal, V., Mukherjee, a, Basu, P. C., & Reddy, M. S. (2009). Strain improvement of Sporosarcina pasteurii for enhanced urease and calcite production. *Journal of Industrial Microbiology & Biotechnology*, *36*(7), 981–988. https://doi.org/10.1007/s10295-009-0578-z

Achal, V., & Pan, X. (2011). Characterization of urease and carbonic anhydrase producing bacteria and their role in calcite precipitation. *Current Microbiology*, *62*(3), 894–902. https://doi.org/10.1007/s00284-010-9801-4

Achal, V., Pan, X., Fu, Q., & Zhang, D. (2012). Biomineralization based remediation of As(III) contaminated soil by Sporosarcina ginsengisoli. *Journal of Hazardous Materials*, *201–202*, 178–184. https://doi.org/10.1016/j.jhazmat.2011.11.067

Adolphe, J. P., Loubière, J. F., Paradas, J., & Soleilhavoup, F. (1990). Procédé de traitement biologique d'une surface artificielle. *European Patent 90400G97. 0, 1989*.

Al Qabany, A., Soga, K., & Santamarina, C. (2012). Factors Affecting Efficiency of Microbially Induced Calcite Precipitation. *Journal of Geotechnical and Geoenvironmental Engineering*, *138*(8), 992–1001. https://doi.org/10.1061/(ASCE)GT.1943-5606.0000666

Anbu, P., Kang, C.-H., Shin, Y.-J., & So, J.-S. (2016). Formations of calcium carbonate minerals by bacteria and its multiple applications. *Springerplus*, *5*(1), 250.

Arias, J. L., & Fernández, M. S. (2008). Polysaccharides and proteoglycans in calcium carbonate-based biomineralization. *Chemical Reviews*, *108*(11), 4475–4482.

Bang, S. S., Galinat, J. K., & Ramakrishnan, V. (2001). Calcite precipitation induced by polyurethane-immobilized Bacillus pasteurii. *Enzyme and Microbial Technology*, *28*(4–5), 404–409.

Bang, S. S., & Ramakrishnan, V. (2001). Microbiologically-enhanced crack remediation (MECR). In *proceedings of the international symposium on industrial application of microbial genomes* (Vol. 20, pp. 3–13).

Benini, S., Rypniewski, W. R., Wilson, K. S., Miletti, S., Ciurli, S., & Mangani, S. (1999). A new proposal for urease mechanism based on the crystal structures of the native and inhibited enzyme from Bacillus pasteurii: why urea hydrolysis costs two nickels. *Structure*, *7*(2), 205–216.

Berner, R. A. (1975). The role of magnesium in the crystal growth of calcite and aragonite from sea

water. *Geochimica et Cosmochimica Acta*, *39*(4), 489IN3495--494504.

Bhaduri, S., Debnath, N., Mitra, S., Liu, Y., & Kumar, A. (2016). Microbiologically induced calcite precipitation mediated by sporosarcina pasteurii. *Journal of Visualized Experiments*, *2016*(110). https://doi.org/10.3791/53253

bioMASON. (2018). No Title. Retrieved January 2, 2018, from www.biomason.com

Bosak, T. (2011). Calcite precipitation, microbially induced. In *Encyclopedia of Geobiology* (pp. 223–227). Springer.

Braissant, O., Verrecchia, E. P., & Aragno, M. (2002). Is the contribution of bacteria to terrestrial carbon budget greatly underestimated? *Naturwissenschaften*, *89*(8), 366–370.

Bray, J. M., Lauchnor, E. G., Redden, G. D., Gerlach, R., Fujita, Y., Codd, S. L., & Seymour, J. D. (2017). Impact of Mineral Precipitation on Flow and Mixing in Porous Media Determined by Microcomputed Tomography and MRI. *Environmental Science & Technology*, *51*(3), 1562–1569. https://doi.org/10.1021/acs.est.6b02999

Bundeleva, I. A., Shirokova, L. S., Bénézeth, P., Pokrovsky, O. S., Kompantseva, E. I., & Balor, S. (2012). Calcium carbonate precipitation by anoxygenic phototrophic bacteria. *Chemical Geology*, *291*, 116–131.

Camesano, T. A., & Logan, B. E. (1998). Influence of fluid velocity and cell concentration on the transport of motile and nonmotile bacteria in porous media. *Environmental Science and Technology*. https://doi.org/10.1021/es970996m

Cappitelli, F., Zanardini, E., Ranalli, G., Mello, E., Daffonchio, D., & Sorlini, C. (2006). Improved methodology for bioremoval of black crusts on historical stone artworks by use of sulfate-reducing bacteria. *Applied and Environmental Microbiology*, *72*(5), 3733–3737.

Castanier, S., Le Métayer-Levrel, G., & Perthuisot, J.-P. (1999). Ca-carbonates precipitation and limestone genesis—the microbiogeologist point of view. *Sedimentary Geology*, *126*(1–4), 9–23.

Chafetz, H. S. (1986). Marine peloids: a product of bacterially induced precipitation of calcite. *Journal of Sedimentary Research*, *56*(6).

Chafetz, H. S., & Buczynski, C. (1992). Bacterially induced lithification of microbial mats. *Palaios*, 277–293.

Chu, K. T. (2005). by.

Chunxiang, Q., Jianyun, W., Ruixing, W., & Liang, C. (2009). Corrosion protection of cement-based building materials by surface deposition of CaCO3 by Bacillus pasteurii. *Materials Science and Engineering: C*, *29*(4), 1273–1280.

Costerton, J. W., & Stewart, P. S. (2001). Battling biofilms. *Scientific American*, *285*(1), 74–81.

Cunningham, A. B., & Gerlach, R. (2010). Microbially Enhanced Carbon Capture and Storage by Mineral-Trapping and, *44*(13), 5270–5276.

Cunningham, A. B., Gerlach, R., Spangler, L., & Mitchell, A. C. (2009). Microbially enhanced geologic containment of sequestered supercritical CO2. *Energy Procedia*, *1*(1), 3245–3252.

Cunningham, a. B., Gerlach, R., Spangler, L., & Mitchell, a. C. (2009). Microbially enhanced geologic containment of sequestered supercritical CO2. *Energy Procedia*, *1*(1), 3245–3252. https://doi.org/10.1016/j.egypro.2009.02.109

Cunningham, a. B., Gerlach, R., Spangler, L., Mitchell, a. C., Parks, S., & Phillips, a. (2011). Reducing the risk of well bore leakage of CO2 using engineered biomineralization barriers. *Energy Procedia*, *4*, 5178–5185. https://doi.org/10.1016/j.egypro.2011.02.495

Cuthbert, M. O., Riley, M. S., Handley-Sidhu, S., Renshaw, J. C., Tobler, D. J., Phoenix, V. R., & Mackay, R. (2012). Controls on the rate of ureolysis and the morphology of carbonate precipitated by S. Pasteurii biofilms and limits due to bacterial encapsulation. *Ecological Engineering*, *41*, 32–40. https://doi.org/10.1016/j.ecoleng.2012.01.008

De Muynck, W., De Belie, N., & Verstraete, W. (2010). Microbial carbonate precipitation in construction materials: A review. *Ecological Engineering*, *36*(2), 118–136. https://doi.org/10.1016/j.ecoleng.2009.02.006

De Muynck, W., Verbeken, K., De Belie, N., & Verstraete, W. (2013). Influence of temperature on the effectiveness of a biogenic carbonate surface treatment for limestone conservation. *Applied Microbiology and Biotechnology*, *97*(3), 1335–1347.

Demény, A., Németh, P., Czuppon, G., Leél-\HOssy, S., Szabó, M., Judik, K., … Stieber, J. (2016). Formation of amorphous calcium carbonate in caves and its implications for speleothem research. *Scientific Reports*, *6*, 39602.

der Heide, P. (2011). *X-ray photoelectron spectroscopy: an introduction to principles and practices*. John Wiley & Sons.

Dhami, N. K., Reddy, M. S., & Mukherjee, A. (2013). Bacillus megaterium mediated mineralization of calcium carbonate as biogenic surface treatment of green building materials. *World Journal of Microbiology and Biotechnology*, *29*(12), 2397–2406. https://doi.org/10.1007/s11274-013-1408-z

Dhami, N. K., Reddy, M. S., & Mukherjee, M. S. (2013). Biomineralization of calcium carbonates and their engineered applications: A review. *Frontiers in Microbiology*, *4*(OCT), 1–13. https://doi.org/10.3389/fmicb.2013.00314

Dick, J., De Windt, W., De Graef, B., Saveyn, H., der Meeren, P., De Belie, N., & Verstraete, W. (2006). Bio-deposition of a calcium carbonate layer on degraded limestone by Bacillus species. *Biodegradation*, *17*(4), 357–367.

Douglas, S., & Beveridge, T. J. (1998). Mineral formation by bacteria in natural microbial communities. *FEMS Microbiology Ecology*, *26*(2), 79–88.

Duffy, K. J., Cummings, P. T., & Ford, R. M. (1995). Random walk calculations for bacterial migration in porous media. *Biophysical Journal*, *68*(3), 800–806. https://doi.org/10.1016/S0006-3495(95)80256-0

Dupraz, S., Parmentier, M., Ménez, B., & Guyot, F. (2009). Experimental and numerical modeling of bacterially induced pH increase and calcite precipitation in saline aquifers. *Chemical Geology*, *265*(1–2), 44–53. https://doi.org/10.1016/j.chemgeo.2009.05.003

Ehrlich, H. L. (1996). How microbes influence mineral growth and dissolution. *Chemical Geology*, *132*(1–4), 5–9.

Ehrlich, H. L. (1998). Geomicrobiology: its significance for geology. *Earth-Science Reviews*, *45*(1–2), 45–60.

Ferris, F. G., & Beveridge, T. J. (1985). Functions of bacterial cell surface structures. *BioScience*, *35*(3), 172–177.

Ferris, F. G., Beveridge, T. J., & Fyfe, W. S. (1986). Iron-silica crystallite nucleation by bacteria in a geothermal sediment. *Nature*, *320*(6063), 609–611.

Ferris, F. G., Phoenix, V., Fujita, Y., & Smith, R. W. (2004). Kinetics of calcite precipitation induced by ureolytic bacteria at 10 to 20 C in artificial groundwater. *Geochimica et Cosmochimica Acta*, *68*(8), 1701–1710.

Fidaleo, M., & Lavecchia, R. (2003). Kinetic study of enzymatic urea hydrolysis in the pH range 4-9. *Chemical and Biochemical Engineering Quarterly*, *17*(4), 311–318.

Folk, R. L. (1993). SEM imaging of bacteria and nannobacteria in carbonate sediments and rocks. *Journal of Sedimentary Research*, *63*(5).

Fontes, D. E., Mills, A. L., Hornberger, G. M., & Herman, J. S. (1991). Physical and Chemical Factors Influencing Transport of Microorganisms through Porous Media. *APPLIED AND ENVIRONMENTAL MICROBIOLOGY*, *57*(9), 2473–2481.

Friedrich, B., & Magasanik, B. (1977). Urease of Klebsiella aerogenes: control of its synthesis by glutamine synthetase. *Journal of Bacteriology*, *131*(2), 446–452.

Gal, J.-Y., Bollinger, J.-C., Tolosa, H., & Gache, N. (1996). Calcium carbonate solubility: a

reappraisal of scale formation and inhibition. *Talanta*, *43*(9), 1497–1509.

Ganendra, G., De Muynck, W., Ho, A., Arvaniti, E. C., Hosseinkhani, B., Ramos, J. A., … Boon, N. (2014). Formate oxidation-driven calcium carbonate precipitation by Methylocystis parvus OBBP. *Applied and Environmental Microbiology*, *80*(15), 4659–4667.

Garcia-Vallès, M., Vendrell-Saz, M., Krumbein, W. E., & Urz\`\i, C. (1997). Coloured mineral coatings on monument surfaces as a result of biomineralization: the case of the Tarragona cathedral (Catalonia). *Applied Geochemistry*, *12*(3), 255–266.

Ghashghaei, S., & Emtiazi, G. (2013). Production of calcite nanocrystal by a urease-positive strain of enterobacter ludwigii and study of its structure by SEM. *Current Microbiology*, *67*(4), 406–413. https://doi.org/10.1007/s00284-013-0379-5

Gibson, T. (1934). An Investigation of the Bacillus Pasteuri Group: II. Special Physiology of the Organisms. *Journal of Bacteriology*, *28*(3), 313.

Gollapudi, U. K., Knutson, C. L., Bang, S. S., & Islam, M. R. (1995). A new method for controlling leaching through permeable channels. *Chemosphere*, *30*(4), 695–705.

Gorospe, C. M., Han, S.-H., Kim, S.-G., Park, J.-Y., Kang, C.-H., Jeong, J.-H., & So, J.-S. (2013). Effects of different calcium salts on calcium carbonate crystal formation by Sporosarcina pasteurii KCTC 3558. *Biotechnology and Bioprocess Engineering*, *18*(5), 903–908.

Greenfield, L. J. (1963). Metabolism and concentration of calcium and magnesium and precipitation of calcium carbonate by a marine bacterium. *Annals of the New York Academy of Sciences*, *109*(1), 23–45.

Hammes, F. (2002). *Ureolytic microbial calcium carbonate precipitation*. Ph. D. Thesis, Ghent University, Ghent.

Hammes, F. (2003). UREOLYTIC MICROBIAL CALCIUM CARBONATE PRECIPITATION UREOLYTISCHE MICROBIELE CALCIUMCARBONAAT- door. *Scanning Electron Microscopy*.

Hammes, F., Arnold, J., Krupka, K. M., Cantrell, K. J., McGrail, B. P., Tagliaferri, F., … Gerlach, R. (2013). Calcium carbonate precipitation by different bacterial strains. *Ecological Engineering*, *36*(3), 172. https://doi.org/http://researchrepository.murdoch.edu.au/399/2/02Whole.pdf

Hammes, F., Boon, N., De Villiers, J., Verstraete, W., Siciliano, S. D., & Villiers, J. De. (2003). Strain-Specific Ureolytic Microbial Calcium Carbonate Precipitation Strain-Specific Ureolytic Microbial Calcium Carbonate Precipitation. *Applied and Environmental Microbiology*, *69*(8), 4901–4909. https://doi.org/10.1128/AEM.69.8.4901

Hammes, F., & Verstraete, W. (2002). Key roles of pH and calcium metabolism in microbial carbonate precipitation. *Reviews in Environmental Science and Biotechnology*, *1*(1), 3–7.

Hong, S.-I., Park, W.-S., & Pyun, Y.-R. (1997). Inactivation ofLactobacillussp. fromKimchiby High Pressure Carbon Dioxide. *LWT-Food Science and Technology*, *30*(7), 681–685.

Hunter, G. K. (1996). Interfacial aspects of biomineralization. *Current Opinion in Solid State and Materials Science*, *1*(3), 430–435.

Ismail, M. A., Joer, H. A., Randolph, M. F., & Meritt, A. (2002). Cementation of porous materials using calcite. *Geotechnique*, *52*(5), 313–324.

Jahns, T. (1996). Ammonium/urea-dependent generation of a proton electrochemical potential and synthesis of ATP in Bacillus pasteurii. *Journal of Bacteriology*, *178*(2), 403–409.

Jansson, C., & Northen, T. (2010). Calcifying cyanobacteria—the potential of biomineralization for carbon capture and storage. *Current Opinion in Biotechnology*, *21*(3), 365–371.

Jonkers, H. M., Thijssen, A., Muyzer, G., Copuroglu, O., & Schlangen, E. (2010). Application of bacteria as self-healing agent for the development of sustainable concrete. *Ecological Engineering*, *36*(2), 230–235. https://doi.org/10.1016/j.ecoleng.2008.12.036

Kaltwasser, H., Krämer, J., & Conger, W. R. (1972). Control of urease formation in certain aerobic bacteria. *Archiv Für Mikrobiologie*, *81*(2), 178–196.

Kantzas, A., Stehmeier, L., Marentette, D. F., Ferris, F. G., Jha, K. N., Maurits, F. M., & others. (1992). A novel method of sand consolidation through bacteriogenic mineral plugging. In *Annual Technical Meeting*.

Kantzas, a, Stehmeier, L., Marentette, D. F., Ferris, F. G., Jha, K. N., & Mourits, F. M. (1992). A Novel Method of Sand Consolidation Through Bacteriogenic Mineral Plugging. *43rd Annual Technical Meeting, Petroleum Society of CIM*, *CIM 92-46*(Cim), 1–15. https://doi.org/10.2118/92-46

Kawaguchi, T., & Decho, A. W. (2002). A laboratory investigation of cyanobacterial extracellular polymeric secretions (EPS) in influencing CaCO 3 polymorphism. *Journal of Crystal Growth*, *240*(1), 230–235.

Keefe, W. E. (1976). Formation of crystalline deposits by several genera of the family Enterobacteriaceae. *Infection and Immunity*, *14*(2), 590–592.

Knorre, H. v, & Krumbein, W. E. (2000). Bacterial calcification. In *Microbial sediments* (pp. 25–31). Springer.

Konishi, Y., Tsukiyama, T., Ohno, K., Saitoh, N., Nomura, T., & Nagamine, S. (2006). Intracellular recovery of gold by microbial reduction of AuCl4- ions using the anaerobic bacterium

Shewanella algae. *Hydrometallurgy*, *81*(1), 24–29.

Kralj, D., Brečević, L., & Kontrec, J. (1997). Vaterite growth and dissolution in aqueous solution III. Kinetics of transformation. *Journal of Crystal Growth*, *177*(3–4), 248–257.

Kralj, D., Brečević, L., & Nielsen, A. E. (1990). Vaterite growth and dissolution in aqueous solution I. Kinetics of crystal growth. *Journal of Crystal Growth*, *104*(4), 793–800.

Kralj, D., Brečević, L., & Nielsen, A. E. (1994). Vaterite growth and dissolution in aqueous solution II. Kinetics of dissolution. *Journal of Crystal Growth*, *143*(3–4), 269–276.

Krumbein, W. E. (1979). Photolithotropic and chemoorganotrophic activity of bacteria and algae as related to beachrock formation and degradation (Gulf of Aqaba, Sinai). *Geomicrobiology Journal*, *1*(2), 139–203.

Kumar, A., Karig, D., Acharya, R., Neethirajan, S., Mukherjee, P. P., Retterer, S., & Doktycz, M. J. (2013). Microscale confinement features can affect biofilm formation. *Microfluidics and Nanofluidics*, *14*(5), 895–902.

Kupriyanova, E., Villarejo, A., Markelova, A., Gerasimenko, L., Zavarzin, G., Samuelsson, G., … Pronina, N. (2007). Extracellular carbonic anhydrases of the stromatolite-forming cyanobacterium Microcoleus chthonoplastes. *Microbiology*, *153*(4), 1149–1156.

Kurmaç, Y. (2009). The impact of toxicity of metals on the activity of ureolytic mixed culture during the precipitation of calcium. *Journal of Hazardous Materials*, *163*(2–3), 1063–1067.

Lauchnor, E. G., Topp, D. M., Parker, A. E., & Gerlach, R. (2015). Whole cell kinetics of ureolysis by Sporosarcina pasteurii. *Journal of Applied Microbiology*, *118*(6), 1321–1332. https://doi.org/10.1111/jam.12804

Le Metayer-Levrel, G., Castanier, S., Orial, G., Loubiere, J.-F., & Perthuisot, J.-P. (1999). Applications of bacterial carbonatogenesis to the protection and regeneration of limestones in buildings and historic patrimony. *Sedimentary Geology*, *126*(1–4), 25–34.

Lewandowski, Z., & Beyenal, H. (2013). *Fundamentals of biofilm research*. CRC press.

Li, M., Fu, Q.-L., Zhang, Q., Achal, V., & Kawasaki, S. (2015). Bio-grout based on microbially induced sand solidification by means of asparaginase activity. *Scientific Reports*, *5*, 16128.

Lian, B., Hu, Q., Chen, J., Ji, J., & Teng, H. H. (2006). Carbonate biomineralization induced by soil bacterium Bacillus megaterium. *Geochimica et Cosmochimica Acta*, *70*(22), 5522–5535.

Life Technologies. (2004). No Title. Retrieved January 2, 2018, from https://tools.lifetechnologies.com/content/sfs/manuals/mp07007.pdf

LIN, H.-M., Cao, N., & CHEN, L.-F. (1994). Antimicrobial effect of pressurized carbon dioxide on

Listeria monocytogenes. *Journal of Food Science*, *59*(3), 657–659.

Lowenstam, H. A. (1981). Minerals formed by organisms. *Science*, *211*(4487), 1126–1131.

Lowenstam, H. A., & Weiner, S. (1989). *On biomineralization*. Oxford University Press on Demand.

Lowenstam, H. A., Weiner, S., bioMASON, Robbins, R., Technologies, L., Lowenstam, H. A., … Whitesides, G. M. M. (2011). No Title. *Annual Review of Fluid Mechanics*, *1*(1), 1–5. https://doi.org/http://researchrepository.murdoch.edu.au/399/2/02Whole.pdf

Lüttge, A., & Conrad, P. G. (2004). Direct observation of microbial inhibition of calcite dissolution. *Applied and Environmental Microbiology*, *70*(3), 1627–1632.

McConnaughey, T. A., & Whelan, J. F. (1997). Calcification generates protons for nutrient and bicarbonate uptake. *Earth-Science Reviews*, *42*(1–2), 95–117.

McKay, D. S., Gibson, E. K., Thomas-Keprta, K. L., Vali, H., Romanek, C. S., Clemett, S. J., … Zare, R. N. (1996). Search for past life on Mars: possible relic biogenic activity in Martian meteorite ALH84001. *Science*, *273*(5277), 924–930.

Minto, J. M., MacLachlan, E., El Mountassir, G., & Lunn, R. J. (2016). Rock fracture grouting with microbially induced carbonate precipitation. *Water Resources Research*. https://doi.org/10.1002/2016WR018884

Mitchell, A. C., & Ferris, F. G. (2005). The coprecipitation of Sr into calcite precipitates induced by bacterial ureolysis in artificial groundwater: temperature and kinetic dependence. *Geochimica et Cosmochimica Acta*, *69*(17), 4199–4210.

Mitchell, A. C., & Ferris, F. G. (2006). The influence of Bacillus pasteurii on the nucleation and growth of calcium carbonate. *Geomicrobiology Journal*, *23*(3–4), 213–226.

Mitchell, A. C., Phillips, A. J., Hiebert, R., Gerlach, R., Spangler, L. H., & Cunningham, A. B. (2009a). Biofilm enhanced geologic sequestration of supercritical CO2. *International Journal of Greenhouse Gas Control*, *3*(1), 90–99.

Mitchell, A. C., Phillips, A. J., Hiebert, R., Gerlach, R., Spangler, L. H., & Cunningham, A. B. (2009b). Biofilm enhanced geologic sequestration of supercritical CO2. *International Journal of Greenhouse Gas Control*, *3*(1), 90–99. https://doi.org/10.1016/j.ijggc.2008.05.002

Monger, H. C., Daugherty, L. A., Lindemann, W. C., & Liddell, C. M. (1991). Microbial precipitation of pedogenic calcite. *Geology*, *19*(10), 997–1000.

Montemagno, C., & Pyrak-Nolte, L. (1995). Porosity of natural fracture networks. *Geophysical Research Letters*, *22*(11), 1397–1400.

Montemagno, C., & Pyrak-Nolte, L. (1999). Fracture Netwok versus Single Structures: Measurement

of Fracture Geometry with X-ray Tomography. *Phys. Chem. Earth (A)*, *24*(7), 575–579.

Montoya, B. M. (2012). *Bio-mediated soil improvement and the effect of cementation on the behavior, improvement, and performance of sand.* University of California, Davis.

Morita, R. Y. (1980). Calcite precipitation by marine bacteria. *Geomicrobiology Journal*, *2*(1), 63–82.

Morse, J. W. (1983). The kinetics of calcium carbonate dissolution and precipitation. *Reviews in Mineralogy and Geochemistry*, *11*(1), 227–264.

Mortensen, B. M., Haber, M. J., Dejong, J. T., Caslake, L. F., & Nelson, D. C. (2011). Effects of environmental factors on microbial induced calcium carbonate precipitation. *Journal of Applied Microbiology*, *111*(2), 338–349. https://doi.org/10.1111/j.1365-2672.2011.05065.x

Nemati, M., & Voordouw, G. (2003). Modification of porous media permeability, using calcium carbonate produced enzymatically in situ. *Enzyme and Microbial Technology*, *33*(5), 635–642. https://doi.org/10.1016/S0141-0229(03)00191-1

Okwadha, G. D. O., & Li, J. (2010a). Optimum conditions for microbial carbonate precipitation. *Chemosphere*, *81*(9), 1143–1148.

Okwadha, G. D. O., & Li, J. (2010b). Optimum conditions for microbial carbonate precipitation. *Chemosphere*, *81*(9), 1143–1148. https://doi.org/10.1016/j.chemosphere.2010.09.066

Parks, S. L. (2009). Kinetics of Calcite Precipitation By Ureolytic Bacteria Under Aerobic and Anaerobic Conditions. *Chemical and Biological Engineering*, (April), 93.

Phillips, A. J., Gerlach, R., Lauchnor, E., Mitchell, A. C., Cunningham, A. B., & Spangler, L. (2013). Engineered applications of ureolytic biomineralization: a review. *Biofouling*, *29*(6), 715–733. https://doi.org/10.1080/08927014.2013.796550

Phillips, A. J., Lauchnor, E., Eldring, J. J., Esposito, R., Mitchell, A. C., Gerlach, R., … Spangler, L. H. (2013). Potential CO2 leakage reduction through biofilm-induced calcium carbonate precipitation. *Environmental Science & Technology*, *47*(1), 142–149. https://doi.org/10.1021/es301294q

Pyrak-Nolte, L. J., Montemagno, C. D., Yang, G., Cook, N. G. W., & Myer, L. R. (1995). Three-dimensional tomographic visuallzatlon of natural fracture networks and graph theory analysis of the transport properties. In *8th ISRM Congress* (pp. 855–859). Tokyo, Japan: International Society for Rock Mechanics. Retrieved from https://www.onepetro.org/conference-paper/ISRM-8CONGRESS-1995-174

Pyrak-Nolte, L., Montemagno, C., & Nolte, D. (1997). Volumetric imaging of aperture distributions in connected fracture networks. *Geophysical Research Letters*, *24*(18), 2343–2346.

R. Robbins. (2010). No Title. Retrieved January 2, 2018, from
http://www.utdallas.edu/~rar011300/SEM/Scanning Electron Microscope Operation.pdf

Reddy, B. V. V., & Jagadish, K. S. (2003). Embodied energy of common and alternative building materials and technologies. *Energy and Buildings*, *35*(2), 129–137.

Rivadeneyra, M. A., Delgado, R., del Moral, A., Ferrer, M. R., & Ramos-Cormenzana, A. (1994). Precipatation of calcium carbonate by Vibrio spp. from an inland saltern. *FEMS Microbiology Ecology*, *13*(3), 197–204.

Rodriguez-Navarro, C., Rodriguez-Gallego, M., Chekroun, K. Ben, & Gonzalez-Munoz, M. T. (2003). Conservation of ornamental stone by Myxococcus xanthus-induced carbonate biomineralization. *Applied and Environmental Microbiology*, *69*(4), 2182–2193.

Rosenbaum, L. (2006). Prehistoric artistry, real and recreated. *The Wall Street Journal*, *13*.

Sarikaya, M. (1999). Biomimetics: materials fabrication through biology. *Proceedings of the National Academy of Sciences*, *96*(25), 14183–14185.

Schultze-Lam, S., Fortin, D., Davis, B. S., & Beveridge, T. J. (1996). Mineralization of bacterial surfaces. *Chemical Geology*, *132*(1–4), 171–181.

Sham, E., Mantle, M. D., Mitchell, J., Tobler, D. J., Phoenix, V. R., & Johns, M. L. (2013). Monitoring bacterially induced calcite precipitation in porous media using magnetic resonance imaging and flow measurements. *Journal of Contaminant Hydrology*, *152*, 35–43. https://doi.org/10.1016/j.jconhyd.2013.06.003

Sherwood, J. L., Sung, J. C., Maneval, J. E., & Smith, J. A. (2003). Analysis of Bacterial Random Motility in a Porous Medium Using Magnetic Resonance Imaging and Immunomagnetic Labeling, *37*(4), 781–785.

Siddique, R., & Chahal, N. K. (2011a). Effect of ureolytic bacteria on concrete properties. *Construction and Building Materials*, *25*(10), 3791–3801.

Siddique, R., & Chahal, N. K. (2011b). Effect of ureolytic bacteria on concrete properties. *Construction and Building Materials*, *25*(10), 3791–3801. https://doi.org/10.1016/j.conbuildmat.2011.04.010

Silver, S., Toth, K., & Scribner, H. (1975). Facilitated transport of calcium by cells and subcellular membranes of Bacillus subtilis and Escherichia coli. *Journal of Bacteriology*, *122*(3), 880–885.

Smith, K. S., & Ferry, J. G. (2000). Prokaryotic carbonic anhydrases. *FEMS Microbiology Reviews*, *24*(4), 335–366.

Söhnel, O., & Garside, J. (n.d.). Precipitation: Basic principles and industrial applications. 1992.

Oxford: Butterworth-Heinemann.

Southam, G. (2000). Bacterial surface-mediated mineral formation. In *Environmental microbe-metal interactions* (pp. 257–276). American Society of Microbiology.

Stabnikov, V., Naeimi, M., Ivanov, V., & Chu, J. (2011). Formation of water-impermeable crust on sand surface using biocement. *Cement and Concrete Research*, *41*(11), 1143–1149.

Stewart, P. S. (2003). Diffusion in biofilms. *Journal of Bacteriology*, *185*(5), 1485–1491.

Stocks-Fischer, S., Galinat, J. K., & Bang, S. S. (1999a). Microbiological precipitation of CaCO3. *Soil Biology and Biochemistry*, *31*(11), 1563–1571.

Stocks-Fischer, S., Galinat, J. K., & Bang, S. S. (1999b). Microbiological precipitation of CaCO3. *Soil Biology and Biochemistry*, *31*(11), 1563–1571. https://doi.org/10.1016/S0038-0717(99)00082-6

Stoner, D. L., Watson, S. M., Stedtfeld, R. D., Meakin, P., Tyler, T. L., Pegram, L. M., … Griffel, L. K. (2005). Application of Stereolithographic Custom Models for Studying the Impact of Biofilms and Mineral Precipitation on Fluid Flow Application of Stereolithographic Custom Models for Studying the Impact of Biofilms and Mineral Precipitation on Fluid Flow. https://doi.org/10.1128/AEM.71.12.8721

Stumm, W., & Morgan, J. J. (1981). Aquatic Chemistry, 780 pp. *J. Wi L Ey & Sons*.

Tagliaferri, F., Waller, J., And??, E., Hall, S. A., Viggiani, G., B??suelle, P., & DeJong, J. T. (2011). Observing strain localisation processes in bio-cemented sand using x-ray imaging. *Granular Matter*, *13*(3), 247–250. https://doi.org/10.1007/s10035-011-0257-4

Thomas-Keprta, K. L., McKay, D. S., Wentworth, S. J., Stevens, T. O., Taunton, A. E., Allen, C. C., … Romanek, C. S. (1998). Bacterial mineralization patterns in basaltic aquifers: Implications for possible life in martian meteorite ALH84001. *Geology*, *26*(11), 1031–1034.

Thompson, J. B., & Ferris, F. G. (1990). Cyanobacterial precipitation of gypsum, calcite, and magnesite from natural alkaline lake water. *Geology*, *18*(10), 995–998.

Tiano, P., Biagiotti, L., & Mastromei, G. (1999). Bacterial bio-mediated calcite precipitation for monumental stones conservation: methods of evaluation. *Journal of Microbiological Methods*, *36*(1–2), 139–145.

Tobler, D. J., Cuthbert, M. O., & Phoenix, V. R. (2014). Transport of Sporosarcina pasteurii in sandstone and its significance for subsurface engineering technologies. *Applied Geochemistry*, *42*, 38–44. https://doi.org/10.1016/j.apgeochem.2014.01.004

Valiei, A., Kumar, A., Mukherjee, P. P., Liu, Y., & Thundat, T. (2012). A web of streamers: biofilm formation in a porous microfluidic device. *Lab on a Chip*, *12*(24), 5133–5137.

https://doi.org/10.1039/c2lc40815e

van Paassen, L. (2009). *Biogrout: Ground Improvement by Microbially Induced Carbonate Precipitation*. *Technology*.

Von Der Schulenburg, D. A. G., Paterson-Beedle, M., MacAskie, L. E., Gladden, L. F., & Johns, M. L. (2007). Flow through an evolving porous media-compressed foam. *Journal of Materials Science*, *42*(16), 6541–6548. https://doi.org/10.1007/s10853-007-1523-z

Wanger, G., Onstott, T. C., & Southam, G. (2008). Stars of the terrestrial deep subsurface: A novel "star-shaped" bacterial morphotype from a South African platinum mine. *Geobiology*. https://doi.org/10.1111/j.1472-4669.2008.00163.x

Warren, L. A., Maurice, P. A., Parmar, N., & Ferris, F. G. (2001). Microbially mediated calcium carbonate precipitation: implications for interpreting calcite precipitation and for solid-phase capture of inorganic contaminants. *Geomicrobiology Journal*, *18*(1), 93–115.

Warthmann, R., Van Lith, Y., Vasconcelos, C., McKenzie, J. A., & Karpoff, A. M. (2000). Bacterially induced dolomite precipitation in anoxic culture experiments. *Geology*, *28*(12), 1091–1094.

Watabe, N., & Wilbur, K. M. (1960). Influence of the organic matrix on crystal type in molluscs. *Nature*, *188*(4747), 334.

Wei, L., Liping, L., Long, C., & Longjiang, Y. (2009). Research status and prospect of biological precipitation of carbonate. *Advances in Earth Science*, *24*(6), 597–605.

Whiffin, V. S. (2004). Microbial CaCO3 Precipitation for the Production of Biocement. *Phd Thesis*, (September), 1–162. https://doi.org/http://researchrepository.murdoch.edu.au/399/2/02Whole.pdf

Wiley, W. R., & Stokes, J. L. (1962). Requirement of an alkaline pH and ammonia for substrate oxidation by Bacillus pasteurii. *Journal of Bacteriology*, *84*(4), 730–734.

Zhang, J., Davis, T. A., Matthews, M. A., Drews, M. J., LaBerge, M., & An, Y. H. (2006). Sterilization using high-pressure carbon dioxide. *The Journal of Supercritical Fluids*, *38*(3), 354–372.

Zhong, L., Islam, M. R., & others. (1995). A new microbial plugging process and its impact on fracture remediation. In *SPE Annual Technical Conference and Exhibition*.

Appendix A

Complete Load – Displacement data for the Compression Tests performed on the set of sponge samples

<u>Sample C1</u>

All data has been reported as Load (N) and Displacement (mm)

N	mm										
0.0	0.0	0.0	0.2	0.0	0.4	0.1	0.5	0.1	0.7	0.2	0.9
0.0	0.0	0.0	0.2	0.0	0.4	0.1	0.5	0.1	0.7	0.2	0.9
0.0	0.0	0.0	0.2	0.0	0.4	0.0	0.5	0.1	0.7	0.2	0.9
0.0	0.0	0.0	0.2	0.0	0.4	0.1	0.5	0.1	0.7	0.2	0.9
0.0	0.0	0.0	0.2	0.0	0.4	0.1	0.5	0.1	0.7	0.2	0.9
0.0	0.0	0.0	0.2	0.0	0.4	0.1	0.6	0.1	0.7	0.2	0.9
0.0	0.0	0.0	0.2	0.0	0.4	0.1	0.6	0.1	0.7	0.2	0.9
0.0	0.0	0.0	0.2	0.0	0.4	0.1	0.6	0.2	0.7	0.2	0.9
0.0	0.0	0.0	0.2	0.0	0.4	0.0	0.6	0.2	0.8	0.2	0.9
0.0	0.0	0.0	0.2	0.0	0.4	0.1	0.6	0.1	0.8	0.2	0.9
0.0	0.0	0.0	0.2	0.0	0.4	0.1	0.6	0.2	0.8	0.2	0.9
0.0	0.0	0.1	0.2	0.1	0.4	0.1	0.6	0.1	0.8	0.3	0.9
0.0	0.0	0.0	0.2	0.0	0.4	0.1	0.6	0.1	0.8	0.2	1.0
0.0	0.1	0.0	0.2	0.0	0.4	0.1	0.6	0.1	0.8	0.2	1.0
0.1	0.1	0.0	0.2	0.0	0.4	0.1	0.6	0.2	0.8	0.2	1.0
0.1	0.1	0.0	0.2	0.1	0.4	0.1	0.6	0.1	0.8	0.2	1.0
0.0	0.1	0.0	0.2	0.1	0.4	0.1	0.6	0.2	0.8	0.2	1.0
0.0	0.1	0.0	0.3	0.0	0.4	0.1	0.6	0.1	0.8	0.2	1.0
0.0	0.1	0.0	0.3	0.1	0.4	0.1	0.6	0.2	0.8	0.2	1.0
0.0	0.1	0.0	0.3	0.0	0.4	0.1	0.6	0.2	0.8	0.2	1.0
0.0	0.1	0.0	0.3	0.1	0.5	0.1	0.6	0.1	0.8	0.2	1.0
0.0	0.1	0.0	0.3	0.1	0.5	0.1	0.6	0.2	0.8	0.3	1.0
0.1	0.1	0.0	0.3	0.0	0.5	0.1	0.6	0.2	0.8	0.3	1.0
0.0	0.1	0.0	0.3	0.0	0.5	0.1	0.6	0.2	0.8	0.3	1.0
0.0	0.1	0.0	0.3	0.0	0.5	0.1	0.6	0.1	0.8	0.3	1.0
0.0	0.1	0.1	0.3	0.1	0.5	0.1	0.7	0.2	0.8	0.3	1.0
0.0	0.1	0.0	0.3	0.1	0.5	0.1	0.7	0.2	0.8	0.2	1.0
0.0	0.1	0.0	0.3	0.0	0.5	0.1	0.7	0.2	0.8	0.3	1.0
0.0	0.1	0.0	0.3	0.1	0.5	0.1	0.7	0.2	0.9	0.3	1.0
0.0	0.1	0.0	0.3	0.1	0.5	0.1	0.7	0.2	0.9	0.3	1.0
0.0	0.1	0.0	0.3	0.0	0.5	0.1	0.7	0.2	0.9	0.3	1.0
0.0	0.1	0.0	0.3	0.1	0.5	0.1	0.7	0.2	0.9	0.3	1.0
0.0	0.2	0.0	0.3	0.1	0.5	0.1	0.7	0.2	0.9	0.3	1.1
0.0	0.2	0.0	0.3	0.0	0.5	0.1	0.7	0.2	0.9	0.3	1.1
0.0	0.2	0.0	0.3	0.1	0.5	0.1	0.7	0.2	0.9	0.3	1.1
0.0	0.2	0.0	0.3	0.0	0.5	0.1	0.7	0.2	0.9	0.3	1.1

0.3	1.1	0.5	1.3	0.6	1.5	0.9	1.7	1.2	2.0	1.8	2.2
0.3	1.1	0.4	1.3	0.6	1.5	0.8	1.8	1.3	2.0	1.8	2.2
0.3	1.1	0.5	1.3	0.6	1.5	0.9	1.8	1.3	2.0	1.8	2.2
0.3	1.1	0.5	1.3	0.6	1.5	0.9	1.8	1.3	2.0	1.8	2.2
0.3	1.1	0.5	1.3	0.7	1.5	0.9	1.8	1.3	2.0	1.9	2.2
0.3	1.1	0.5	1.3	0.6	1.5	0.9	1.8	1.3	2.0	1.9	2.2
0.3	1.1	0.4	1.3	0.7	1.5	0.9	1.8	1.3	2.0	1.9	2.2
0.3	1.1	0.5	1.3	0.7	1.6	0.9	1.8	1.3	2.0	1.9	2.2
0.3	1.1	0.5	1.3	0.6	1.6	0.9	1.8	1.4	2.0	1.9	2.2
0.3	1.1	0.5	1.3	0.7	1.6	1.0	1.8	1.3	2.0	1.9	2.2
0.4	1.1	0.5	1.3	0.6	1.6	0.9	1.8	1.4	2.0	1.9	2.2
0.4	1.1	0.5	1.3	0.7	1.6	1.0	1.8	1.4	2.0	1.9	2.3
0.3	1.1	0.5	1.4	0.7	1.6	1.0	1.8	1.4	2.0	1.9	2.3
0.4	1.1	0.5	1.4	0.7	1.6	1.0	1.8	1.4	2.0	2.0	2.3
0.3	1.1	0.5	1.4	0.7	1.6	1.0	1.8	1.4	2.0	2.0	2.3
0.3	1.1	0.5	1.4	0.7	1.6	1.0	1.8	1.4	2.0	2.0	2.3
0.4	1.2	0.5	1.4	0.7	1.6	1.0	1.8	1.4	2.1	2.0	2.3
0.4	1.2	0.5	1.4	0.7	1.6	1.0	1.8	1.5	2.1	2.0	2.3
0.4	1.2	0.5	1.4	0.7	1.6	1.0	1.8	1.5	2.1	2.0	2.3
0.4	1.2	0.6	1.4	0.7	1.6	1.0	1.8	1.5	2.1	2.0	2.3
0.4	1.2	0.5	1.4	0.7	1.6	1.0	1.8	1.5	2.1	2.1	2.3
0.4	1.2	0.5	1.4	0.7	1.6	1.0	1.9	1.5	2.1	2.1	2.3
0.4	1.2	0.5	1.4	0.7	1.6	1.0	1.9	1.5	2.1	2.1	2.3
0.4	1.2	0.5	1.4	0.7	1.6	1.1	1.9	1.5	2.1	2.1	2.3
0.4	1.2	0.5	1.4	0.7	1.6	1.1	1.9	1.6	2.1	2.1	2.3
0.4	1.2	0.5	1.4	0.7	1.6	1.1	1.9	1.6	2.1	2.1	2.3
0.4	1.2	0.5	1.4	0.7	1.7	1.1	1.9	1.6	2.1	2.1	2.3
0.4	1.2	0.6	1.4	0.7	1.7	1.1	1.9	1.6	2.1	2.1	2.3
0.4	1.2	0.6	1.4	0.7	1.7	1.1	1.9	1.6	2.1	2.2	2.3
0.4	1.2	0.6	1.4	0.7	1.7	1.1	1.9	1.6	2.1	2.2	2.3
0.4	1.2	0.5	1.4	0.7	1.7	1.1	1.9	1.6	2.1	2.2	2.3
0.4	1.2	0.5	1.5	0.8	1.7	1.1	1.9	1.6	2.1	2.2	2.4
0.4	1.2	0.5	1.5	0.7	1.7	1.1	1.9	1.6	2.1	2.2	2.4
0.4	1.2	0.6	1.5	0.7	1.7	1.1	1.9	1.7	2.1	2.2	2.4
0.4	1.2	0.5	1.5	0.7	1.7	1.1	1.9	1.7	2.1	2.2	2.4
0.4	1.2	0.6	1.5	0.8	1.7	1.2	1.9	1.7	2.1	2.2	2.4
0.4	1.2	0.6	1.5	0.8	1.7	1.2	1.9	1.7	2.2	2.2	2.4
0.4	1.3	0.6	1.5	0.8	1.7	1.2	1.9	1.7	2.2	2.3	2.4
0.4	1.3	0.6	1.5	0.8	1.7	1.2	1.9	1.7	2.2	2.3	2.4
0.4	1.3	0.6	1.5	0.8	1.7	1.2	1.9	1.7	2.2	2.3	2.4
0.5	1.3	0.6	1.5	0.8	1.7	1.2	1.9	1.8	2.2	2.3	2.4
0.4	1.3	0.6	1.5	0.8	1.7	1.2	1.9	1.7	2.2	2.3	2.4
0.5	1.3	0.6	1.5	0.8	1.7	1.2	2.0	1.8	2.2	2.4	2.4
0.4	1.3	0.6	1.5	0.8	1.7	1.3	2.0	1.8	2.2	2.3	2.4
0.4	1.3	0.6	1.5	0.9	1.7	1.2	2.0	1.8	2.2	2.4	2.4

2.4	2.4	3.0	2.6	3.7	2.9	4.5	3.1	5.2	3.3	6.0	3.5
2.4	2.4	3.0	2.6	3.7	2.9	4.5	3.1	5.3	3.3	6.0	3.6
2.4	2.4	3.1	2.7	3.8	2.9	4.5	3.1	5.2	3.3	6.0	3.6
2.4	2.4	3.1	2.7	3.8	2.9	4.5	3.1	5.2	3.3	6.0	3.6
2.4	2.4	3.1	2.7	3.8	2.9	4.6	3.1	5.3	3.3	6.0	3.6
2.4	2.4	3.1	2.7	3.8	2.9	4.6	3.1	5.3	3.3	6.0	3.6
2.5	2.5	3.1	2.7	3.9	2.9	4.6	3.1	5.3	3.3	6.0	3.6
2.5	2.5	3.1	2.7	3.9	2.9	4.6	3.1	5.4	3.4	6.1	3.6
2.5	2.5	3.1	2.7	3.9	2.9	4.6	3.1	5.4	3.4	6.1	3.6
2.5	2.5	3.2	2.7	3.9	2.9	4.6	3.1	5.4	3.4	6.1	3.6
2.5	2.5	3.2	2.7	3.9	2.9	4.6	3.1	5.4	3.4	6.1	3.6
2.6	2.5	3.2	2.7	3.9	2.9	4.7	3.2	5.4	3.4	6.1	3.6
2.5	2.5	3.2	2.7	3.9	2.9	4.7	3.2	5.4	3.4	6.2	3.6
2.6	2.5	3.2	2.7	4.0	2.9	4.7	3.2	5.4	3.4	6.2	3.6
2.6	2.5	3.2	2.7	3.9	2.9	4.7	3.2	5.5	3.4	6.2	3.6
2.6	2.5	3.3	2.7	4.0	2.9	4.7	3.2	5.5	3.4	6.2	3.6
2.6	2.5	3.3	2.7	4.0	3.0	4.8	3.2	5.5	3.4	6.2	3.6
2.6	2.5	3.3	2.7	4.0	3.0	4.8	3.2	5.5	3.4	6.2	3.6
2.6	2.5	3.3	2.7	4.1	3.0	4.8	3.2	5.5	3.4	6.3	3.6
2.6	2.5	3.3	2.7	4.1	3.0	4.8	3.2	5.5	3.4	6.3	3.6
2.7	2.5	3.3	2.7	4.1	3.0	4.8	3.2	5.5	3.4	6.3	3.6
2.7	2.5	3.4	2.8	4.1	3.0	4.9	3.2	5.5	3.4	6.3	3.7
2.7	2.5	3.4	2.8	4.1	3.0	4.8	3.2	5.6	3.4	6.3	3.7
2.7	2.5	3.4	2.8	4.1	3.0	4.8	3.2	5.6	3.4	6.4	3.7
2.7	2.5	3.4	2.8	4.1	3.0	4.9	3.2	5.6	3.4	6.4	3.7
2.7	2.5	3.4	2.8	4.2	3.0	4.9	3.2	5.6	3.4	6.4	3.7
2.8	2.5	3.4	2.8	4.2	3.0	4.9	3.2	5.7	3.5	6.4	3.7
2.8	2.6	3.4	2.8	4.2	3.0	4.9	3.2	5.6	3.5	6.4	3.7
2.8	2.6	3.5	2.8	4.2	3.0	4.9	3.2	5.7	3.5	6.4	3.7
2.8	2.6	3.5	2.8	4.2	3.0	5.0	3.2	5.7	3.5	6.4	3.7
2.8	2.6	3.5	2.8	4.2	3.0	5.0	3.2	5.7	3.5	6.5	3.7
2.8	2.6	3.5	2.8	4.3	3.0	5.0	3.2	5.7	3.5	6.5	3.7
2.8	2.6	3.5	2.8	4.2	3.0	5.0	3.3	5.7	3.5	6.5	3.7
2.9	2.6	3.5	2.8	4.3	3.0	5.0	3.3	5.8	3.5	6.6	3.7
2.8	2.6	3.6	2.8	4.3	3.0	5.0	3.3	5.8	3.5	6.5	3.7
2.9	2.6	3.6	2.8	4.3	3.0	5.1	3.3	5.8	3.5	6.6	3.7
2.9	2.6	3.6	2.8	4.3	3.1	5.1	3.3	5.8	3.5	6.6	3.7
2.9	2.6	3.6	2.8	4.4	3.1	5.1	3.3	5.8	3.5	6.6	3.7
2.9	2.6	3.6	2.8	4.4	3.1	5.1	3.3	5.9	3.5	6.6	3.7
3.0	2.6	3.6	2.8	4.4	3.1	5.1	3.3	5.9	3.5	6.6	3.7
3.0	2.6	3.6	2.8	4.4	3.1	5.1	3.3	5.9	3.5	6.6	3.7
3.0	2.6	3.7	2.9	4.4	3.1	5.1	3.3	5.9	3.5	6.6	3.8
3.0	2.6	3.7	2.9	4.4	3.1	5.2	3.3	5.9	3.5	6.7	3.8
3.0	2.6	3.7	2.9	4.4	3.1	5.2	3.3	5.9	3.5	6.7	3.8
3.0	2.6	3.7	2.9	4.5	3.1	5.2	3.3	5.9	3.5	6.7	3.8

6.7	3.8	7.6	4.0	8.5	4.2	9.4	4.4	10.4	4.7	11.3	4.9
6.7	3.8	7.6	4.0	8.5	4.2	9.4	4.5	10.4	4.7	11.3	4.9
6.8	3.8	7.6	4.0	8.5	4.2	9.4	4.5	10.4	4.7	11.3	4.9
6.8	3.8	7.6	4.0	8.5	4.2	9.4	4.5	10.4	4.7	11.4	4.9
6.8	3.8	7.6	4.0	8.5	4.2	9.5	4.5	10.5	4.7	11.4	4.9
6.8	3.8	7.6	4.0	8.6	4.2	9.5	4.5	10.5	4.7	11.4	4.9
6.8	3.8	7.7	4.0	8.6	4.3	9.5	4.5	10.5	4.7	11.4	4.9
6.8	3.8	7.7	4.0	8.6	4.3	9.5	4.5	10.5	4.7	11.5	4.9
6.8	3.8	7.7	4.0	8.6	4.3	9.5	4.5	10.5	4.7	11.5	4.9
6.9	3.8	7.7	4.0	8.6	4.3	9.6	4.5	10.5	4.7	11.5	4.9
6.9	3.8	7.7	4.0	8.6	4.3	9.6	4.5	10.6	4.7	11.5	4.9
6.9	3.8	7.8	4.0	8.7	4.3	9.6	4.5	10.6	4.7	11.5	5.0
6.9	3.8	7.8	4.1	8.7	4.3	9.6	4.5	10.6	4.7	11.6	5.0
7.0	3.8	7.8	4.1	8.7	4.3	9.6	4.5	10.6	4.7	11.6	5.0
7.0	3.8	7.8	4.1	8.7	4.3	9.7	4.5	10.6	4.7	11.6	5.0
7.0	3.8	7.9	4.1	8.8	4.3	9.7	4.5	10.7	4.7	11.6	5.0
7.0	3.9	7.8	4.1	8.8	4.3	9.8	4.5	10.7	4.8	11.7	5.0
7.0	3.9	7.8	4.1	8.8	4.3	9.8	4.5	10.7	4.8	11.7	5.0
7.0	3.9	7.9	4.1	8.8	4.3	9.8	4.5	10.7	4.8	11.7	5.0
7.1	3.9	7.9	4.1	8.8	4.3	9.8	4.5	10.8	4.8	11.7	5.0
7.1	3.9	7.9	4.1	8.8	4.3	9.8	4.5	10.8	4.8		
7.1	3.9	8.0	4.1	8.9	4.3	9.8	4.6	10.8	4.8		
7.1	3.9	8.0	4.1	8.9	4.3	9.9	4.6	10.8	4.8		
7.1	3.9	8.0	4.1	8.9	4.3	9.9	4.6	10.9	4.8		
7.1	3.9	8.0	4.1	8.9	4.3	9.9	4.6	10.9	4.8		
7.2	3.9	8.0	4.1	9.0	4.3	9.9	4.6	10.9	4.8		
7.2	3.9	8.0	4.1	9.0	4.4	9.9	4.6	10.9	4.8		
7.2	3.9	8.0	4.1	9.0	4.4	10.0	4.6	11.0	4.8		
7.2	3.9	8.1	4.1	9.0	4.4	10.0	4.6	10.9	4.8		
7.2	3.9	8.1	4.1	9.0	4.4	10.0	4.6	11.0	4.8		
7.3	3.9	8.1	4.1	9.1	4.4	10.0	4.6	11.0	4.8		
7.2	3.9	8.2	4.2	9.1	4.4	10.0	4.6	11.0	4.8		
7.3	3.9	8.1	4.2	9.1	4.4	10.1	4.6	11.1	4.8		
7.3	3.9	8.2	4.2	9.1	4.4	10.1	4.6	11.0	4.8		
7.4	3.9	8.2	4.2	9.2	4.4	10.1	4.6	11.1	4.8		
7.4	3.9	8.3	4.2	9.2	4.4	10.1	4.6	11.1	4.8		
7.4	3.9	8.3	4.2	9.2	4.4	10.2	4.6	11.1	4.9		
7.4	4.0	8.3	4.2	9.2	4.4	10.2	4.6	11.1	4.9		
7.4	4.0	8.3	4.2	9.2	4.4	10.2	4.6	11.1	4.9		
7.4	4.0	8.3	4.2	9.3	4.4	10.2	4.6	11.2	4.9		
7.5	4.0	8.3	4.2	9.3	4.4	10.2	4.6	11.2	4.9		
7.5	4.0	8.3	4.2	9.3	4.4	10.3	4.6	11.2	4.9		
7.5	4.0	8.4	4.2	9.3	4.4	10.3	4.7	11.3	4.9		
7.5	4.0	8.4	4.2	9.3	4.4	10.3	4.7	11.3	4.9		
7.6	4.0	8.4	4.2	9.4	4.4	10.3	4.7	11.3	4.9		

Sample C2

N	mm	0.0	0.2	0.0	0.4	0.0	0.6	0.1	0.8	0.2	1.1
		0.0	0.2	0.0	0.4	0.0	0.6	0.1	0.8	0.2	1.1
		0.0	0.2	0.0	0.4	0.1	0.6	0.1	0.8	0.2	1.1
0	0.0	0.0	0.2	0.0	0.4	0.0	0.6	0.1	0.9	0.2	1.1
0.0	0.0	0.0	0.2	0.0	0.4	0.0	0.6	0.1	0.9	0.2	1.1
0.0	0.0	0.0	0.2	0.0	0.4	0.0	0.6	0.1	0.9	0.2	1.1
0.0	0.0	0.0	0.2	0.0	0.4	0.1	0.7	0.1	0.9	0.2	1.1
0.0	0.0	0.0	0.2	0.0	0.4	0.1	0.7	0.1	0.9	0.2	1.1
0.0	0.0	0.0	0.2	0.0	0.4	0.0	0.7	0.1	0.9	0.2	1.1
0.0	0.0	0.0	0.2	0.0	0.5	0.1	0.7	0.1	0.9	0.2	1.1
0.0	0.0	0.0	0.2	0.0	0.5	0.1	0.7	0.1	0.9	0.3	1.1
0.0	0.0	0.0	0.2	0.0	0.5	0.0	0.7	0.1	0.9	0.2	1.1
0.0	0.0	0.0	0.3	0.0	0.5	0.1	0.7	0.1	0.9	0.3	1.1
0.0	0.0	0.0	0.3	0.0	0.5	0.0	0.7	0.2	0.9	0.3	1.1
0.0	0.0	0.0	0.3	0.0	0.5	0.1	0.7	0.1	0.9	0.2	1.1
0.0	0.1	0.0	0.3	0.0	0.5	0.1	0.7	0.1	0.9	0.3	1.1
0.0	0.1	0.0	0.3	0.0	0.5	0.1	0.7	0.1	0.9	0.2	1.1
0.0	0.1	0.0	0.3	0.0	0.5	0.1	0.7	0.2	0.9	0.2	1.1
0.0	0.1	0.0	0.3	0.0	0.5	0.1	0.7	0.1	0.9	0.3	1.1
0.0	0.1	0.0	0.3	0.0	0.5	0.1	0.7	0.2	0.9	0.3	1.2
0.0	0.1	0.0	0.3	0.0	0.5	0.1	0.7	0.2	0.9	0.3	1.2
0.0	0.1	0.0	0.3	0.0	0.5	0.1	0.7	0.1	0.9	0.3	1.2
0.0	0.1	0.0	0.3	0.0	0.5	0.0	0.7	0.2	0.9	0.3	1.2
0.0	0.1	0.0	0.3	0.0	0.5	0.1	0.7	0.2	1.0	0.3	1.2
0.0	0.1	0.0	0.3	0.0	0.5	0.1	0.7	0.2	1.0	0.3	1.2
0.0	0.1	0.0	0.3	0.0	0.5	0.1	0.8	0.2	1.0	0.3	1.2
0.0	0.1	0.0	0.3	0.0	0.5	0.1	0.8	0.2	1.0	0.3	1.2
0.0	0.1	0.0	0.3	0.0	0.5	0.1	0.8	0.2	1.0	0.3	1.2
0.0	0.1	0.0	0.3	0.0	0.5	0.1	0.8	0.2	1.0	0.3	1.2
0.0	0.1	0.0	0.3	0.0	0.6	0.1	0.8	0.2	1.0	0.3	1.2
0.0	0.1	0.0	0.3	0.1	0.6	0.1	0.8	0.2	1.0	0.3	1.2
0.0	0.1	0.0	0.3	0.0	0.6	0.1	0.8	0.2	1.0	0.3	1.2
0.0	0.1	0.0	0.4	0.0	0.6	0.1	0.8	0.2	1.0	0.3	1.2
0.0	0.1	0.0	0.4	0.0	0.6	0.1	0.8	0.2	1.0	0.3	1.2
0.0	0.1	0.0	0.4	0.1	0.6	0.1	0.8	0.2	1.0	0.4	1.2
0.0	0.2	0.0	0.4	0.0	0.6	0.1	0.8	0.2	1.0	0.3	1.2
0.0	0.2	0.0	0.4	0.1	0.6	0.1	0.8	0.2	1.0	0.3	1.2
0.0	0.2	0.0	0.4	0.0	0.6	0.1	0.8	0.2	1.0	0.4	1.2
0.0	0.2	0.0	0.4	0.0	0.6	0.1	0.8	0.2	1.0	0.4	1.2
0.0	0.2	0.0	0.4	0.0	0.6	0.1	0.8	0.2	1.0	0.3	1.2
0.0	0.2	0.0	0.4	0.0	0.6	0.1	0.8	0.2	1.0	0.4	1.3
0.0	0.2	0.0	0.4	0.1	0.6	0.1	0.8	0.2	1.0	0.3	1.3
0.0	0.2	0.0	0.4	0.0	0.6	0.1	0.8	0.2	1.1	0.4	1.3
0.0	0.2	0.0	0.4	0.0	0.6	0.1	0.8	0.2	1.1	0.3	1.3

0.4	1.3	0.5	1.5	0.8	1.7	1.2	1.9	1.7	2.2	2.2	2.4
0.4	1.3	0.6	1.5	0.8	1.7	1.2	2.0	1.7	2.2	2.2	2.4
0.4	1.3	0.6	1.5	0.8	1.7	1.2	2.0	1.7	2.2	2.2	2.4
0.4	1.3	0.6	1.5	0.8	1.7	1.2	2.0	1.7	2.2	2.2	2.4
0.4	1.3	0.6	1.5	0.8	1.7	1.2	2.0	1.7	2.2	2.2	2.4
0.4	1.3	0.6	1.5	0.8	1.7	1.3	2.0	1.7	2.2	2.2	2.4
0.4	1.3	0.6	1.5	0.8	1.8	1.2	2.0	1.8	2.2	2.2	2.4
0.4	1.3	0.6	1.5	0.9	1.8	1.3	2.0	1.8	2.2	2.3	2.4
0.4	1.3	0.6	1.5	0.9	1.8	1.3	2.0	1.8	2.2	2.3	2.4
0.4	1.3	0.6	1.5	0.9	1.8	1.3	2.0	1.8	2.2	2.3	2.4
0.4	1.3	0.6	1.5	0.9	1.8	1.3	2.0	1.8	2.2	2.3	2.5
0.4	1.3	0.6	1.6	0.9	1.8	1.3	2.0	1.8	2.2	2.3	2.5
0.4	1.3	0.6	1.6	0.9	1.8	1.3	2.0	1.8	2.2	2.3	2.5
0.4	1.3	0.6	1.6	0.9	1.8	1.3	2.0	1.8	2.2	2.3	2.5
0.4	1.3	0.6	1.6	0.9	1.8	1.3	2.0	1.8	2.2	2.3	2.5
0.4	1.4	0.6	1.6	0.9	1.8	1.3	2.0	1.8	2.3	2.4	2.5
0.4	1.4	0.6	1.6	1.0	1.8	1.4	2.0	1.8	2.3	2.4	2.5
0.5	1.4	0.7	1.6	0.9	1.8	1.4	2.0	1.9	2.3	2.4	2.5
0.5	1.4	0.6	1.6	1.0	1.8	1.4	2.0	1.9	2.3	2.4	2.5
0.4	1.4	0.6	1.6	1.0	1.8	1.4	2.1	1.9	2.3	2.4	2.5
0.5	1.4	0.6	1.6	1.0	1.8	1.4	2.1	1.9	2.3	2.4	2.5
0.5	1.4	0.7	1.6	1.0	1.8	1.4	2.1	1.9	2.3	2.4	2.5
0.5	1.4	0.7	1.6	1.0	1.8	1.4	2.1	1.9	2.3	2.4	2.5
0.5	1.4	0.7	1.6	1.0	1.8	1.5	2.1	1.9	2.3	2.4	2.5
0.5	1.4	0.7	1.6	1.0	1.8	1.4	2.1	1.9	2.3	2.4	2.5
0.5	1.4	0.7	1.6	1.0	1.9	1.5	2.1	2.0	2.3	2.4	2.5
0.5	1.4	0.7	1.6	1.0	1.9	1.4	2.1	2.0	2.3	2.5	2.5
0.5	1.4	0.7	1.6	1.0	1.9	1.5	2.1	2.0	2.3	2.5	2.5
0.5	1.4	0.7	1.6	1.0	1.9	1.5	2.1	2.0	2.3	2.5	2.5
0.5	1.4	0.7	1.7	1.0	1.9	1.5	2.1	2.0	2.3	2.6	2.6
0.5	1.4	0.7	1.7	1.0	1.9	1.5	2.1	2.0	2.3	2.5	2.6
0.5	1.4	0.7	1.7	1.1	1.9	1.5	2.1	2.0	2.3	2.6	2.6
0.5	1.4	0.7	1.7	1.1	1.9	1.5	2.1	2.0	2.3	2.6	2.6
0.5	1.4	0.7	1.7	1.1	1.9	1.5	2.1	2.1	2.3	2.6	2.6
0.5	1.5	0.7	1.7	1.1	1.9	1.5	2.1	2.1	2.4	2.6	2.6
0.5	1.5	0.8	1.7	1.1	1.9	1.5	2.1	2.1	2.4	2.6	2.6
0.5	1.5	0.8	1.7	1.1	1.9	1.6	2.1	2.1	2.4	2.6	2.6
0.5	1.5	0.8	1.7	1.2	1.9	1.6	2.1	2.1	2.4	2.7	2.6
0.5	1.5	0.8	1.7	1.2	1.9	1.6	2.1	2.1	2.4	2.7	2.6
0.6	1.5	0.8	1.7	1.1	1.9	1.6	2.2	2.1	2.4	2.7	2.6
0.6	1.5	0.8	1.7	1.2	1.9	1.6	2.2	2.2	2.4	2.7	2.6
0.5	1.5	0.8	1.7	1.2	1.9	1.6	2.2	2.1	2.4	2.7	2.6
0.6	1.5	0.8	1.7	1.2	1.9	1.6	2.2	2.2	2.4	2.7	2.6

2.7	2.6	3.4	2.8	4.0	3.1	4.7	3.3	5.4	3.5	6.1	3.8
2.7	2.6	3.4	2.9	4.0	3.1	4.7	3.3	5.4	3.5	6.2	3.8
2.7	2.6	3.4	2.9	4.0	3.1	4.7	3.3	5.4	3.5	6.1	3.8
2.7	2.6	3.4	2.9	4.1	3.1	4.7	3.3	5.4	3.5	6.2	3.8
2.8	2.6	3.4	2.9	4.1	3.1	4.7	3.3	5.5	3.5	6.2	3.8
2.8	2.6	3.4	2.9	4.1	3.1	4.7	3.3	5.5	3.5	6.2	3.8
2.8	2.7	3.4	2.9	4.1	3.1	4.8	3.3	5.5	3.6	6.2	3.8
2.8	2.7	3.5	2.9	4.1	3.1	4.8	3.3	5.5	3.6	6.2	3.8
2.8	2.7	3.5	2.9	4.1	3.1	4.8	3.3	5.5	3.6	6.2	3.8
2.9	2.7	3.4	2.9	4.1	3.1	4.8	3.3	5.5	3.6	6.2	3.8
2.8	2.7	3.5	2.9	4.2	3.1	4.8	3.3	5.6	3.6	6.3	3.8
2.9	2.7	3.5	2.9	4.2	3.1	4.9	3.4	5.6	3.6	6.3	3.8
2.9	2.7	3.5	2.9	4.2	3.1	4.9	3.4	5.6	3.6	6.3	3.8
2.9	2.7	3.5	2.9	4.2	3.1	4.9	3.4	5.6	3.6	6.3	3.8
2.9	2.7	3.5	2.9	4.2	3.1	4.9	3.4	5.6	3.6	6.3	3.8
2.9	2.7	3.6	2.9	4.2	3.1	4.9	3.4	5.6	3.6	6.4	3.8
2.9	2.7	3.6	2.9	4.2	3.2	4.9	3.4	5.6	3.6	6.3	3.8
2.9	2.7	3.6	2.9	4.3	3.2	5.0	3.4	5.6	3.6	6.4	3.8
3.0	2.7	3.6	2.9	4.3	3.2	5.0	3.4	5.7	3.6	6.4	3.8
3.0	2.7	3.6	2.9	4.3	3.2	5.0	3.4	5.7	3.6	6.4	3.8
3.0	2.7	3.6	2.9	4.3	3.2	5.0	3.4	5.7	3.6	6.4	3.9
3.0	2.7	3.7	3.0	4.3	3.2	5.0	3.4	5.7	3.6	6.4	3.9
3.0	2.7	3.7	3.0	4.3	3.2	5.0	3.4	5.8	3.6	6.5	3.9
3.0	2.7	3.7	3.0	4.3	3.2	5.0	3.4	5.7	3.6	6.5	3.9
3.1	2.7	3.7	3.0	4.4	3.2	5.1	3.4	5.8	3.6	6.5	3.9
3.1	2.7	3.7	3.0	4.4	3.2	5.1	3.4	5.8	3.6	6.5	3.9
3.1	2.8	3.7	3.0	4.4	3.2	5.1	3.4	5.8	3.7	6.5	3.9
3.1	2.8	3.8	3.0	4.4	3.2	5.1	3.4	5.8	3.7	6.5	3.9
3.1	2.8	3.8	3.0	4.4	3.2	5.2	3.4	5.8	3.7	6.6	3.9
3.1	2.8	3.8	3.0	4.5	3.2	5.1	3.4	5.8	3.7	6.6	3.9
3.1	2.8	3.7	3.0	4.4	3.2	5.2	3.5	5.9	3.7	6.6	3.9
3.1	2.8	3.8	3.0	4.4	3.2	5.2	3.5	5.9	3.7	6.6	3.9
3.2	2.8	3.8	3.0	4.5	3.2	5.2	3.5	5.9	3.7	6.6	3.9
3.2	2.8	3.9	3.0	4.5	3.2	5.2	3.5	5.9	3.7	6.7	3.9
3.2	2.8	3.9	3.0	4.5	3.2	5.2	3.5	5.9	3.7	6.6	3.9
3.2	2.8	3.9	3.0	4.5	3.2	5.2	3.5	5.9	3.7	6.7	3.9
3.2	2.8	3.9	3.0	4.5	3.3	5.3	3.5	6.0	3.7	6.7	3.9
3.2	2.8	3.9	3.0	4.6	3.3	5.3	3.5	6.0	3.7	6.7	3.9
3.2	2.8	3.9	3.0	4.6	3.3	5.3	3.5	6.0	3.7	6.7	3.9
3.2	2.8	3.9	3.0	4.6	3.3	5.3	3.5	6.0	3.7	6.7	3.9
3.3	2.8	3.9	3.0	4.6	3.3	5.3	3.5	6.1	3.7	6.7	3.9
3.3	2.8	4.0	3.1	4.6	3.3	5.4	3.5	6.1	3.7	6.8	4.0
3.3	2.8	4.0	3.1	4.6	3.3	5.3	3.5	6.1	3.7	6.8	4.0
3.3	2.8	4.0	3.1	4.7	3.3	5.4	3.5	6.1	3.7	6.8	4.0
3.4	2.8	4.0	3.1	4.7	3.3	5.4	3.5	6.1	3.7	6.8	4.0

6.8	4.0	7.4	4.2	8.2	4.4	8.8	4.6	9.5	4.8	10.2	5.0
6.9	4.0	7.5	4.2	8.1	4.4	8.9	4.6	9.5	4.8	10.2	5.0
6.8	4.0	7.5	4.2	8.1	4.4	8.8	4.6	9.6	4.8	10.3	5.0
6.9	4.0	7.5	4.2	8.2	4.4	8.9	4.6	9.6	4.8	10.3	5.0
6.9	4.0	7.5	4.2	8.1	4.4	8.9	4.6	9.6	4.8		
6.9	4.0	7.5	4.2	8.2	4.4	8.9	4.6	9.6	4.8		
6.9	4.0	7.6	4.2	8.2	4.4	8.9	4.6	9.6	4.8		
6.9	4.0	7.6	4.2	8.2	4.4	8.9	4.6	9.6	4.8		
6.9	4.0	7.6	4.2	8.2	4.4	9.0	4.6	9.7	4.8		
7.0	4.0	7.6	4.2	8.2	4.4	9.0	4.6	9.7	4.8		
7.0	4.0	7.6	4.2	8.3	4.4	9.0	4.6	9.7	4.8		
7.0	4.0	7.7	4.2	8.3	4.4	9.0	4.6	9.7	4.8		
7.0	4.0	7.7	4.2	8.3	4.4	9.0	4.6	9.7	4.8		
7.1	4.0	7.7	4.2	8.3	4.4	9.0	4.6	9.8	4.8		
7.0	4.0	7.7	4.2	8.4	4.4	9.1	4.6	9.8	4.8		
7.1	4.0	7.7	4.2	8.4	4.4	9.1	4.6	9.8	4.8		
7.1	4.1	7.7	4.3	8.4	4.5	9.1	4.7	9.8	4.9		
7.1	4.1	7.7	4.3	8.4	4.5	9.1	4.7	9.8	4.9		
7.1	4.1	7.8	4.3	8.5	4.5	9.2	4.7	9.8	4.9		
7.1	4.1	7.8	4.3	8.4	4.5	9.1	4.7	9.9	4.9		
7.2	4.1	7.8	4.3	8.5	4.5	9.2	4.7	9.9	4.9		
7.2	4.1	7.7	4.3	8.5	4.5	9.2	4.7	9.9	4.9		
7.2	4.1	7.8	4.3	8.5	4.5	9.2	4.7	9.9	4.9		
7.2	4.1	7.8	4.3	8.5	4.5	9.2	4.7	9.9	4.9		
7.2	4.1	7.9	4.3	8.5	4.5	9.3	4.7	10.0	4.9		
7.2	4.1	7.9	4.3	8.6	4.5	9.3	4.7	10.0	4.9		
7.3	4.1	7.9	4.3	8.6	4.5	9.3	4.7	10.0	4.9		
7.3	4.1	7.9	4.3	8.6	4.5	9.3	4.7	10.0	4.9		
7.3	4.1	7.9	4.3	8.6	4.5	9.3	4.7	10.0	4.9		
7.3	4.1	7.9	4.3	8.6	4.5	9.3	4.7	10.1	4.9		
7.3	4.1	8.0	4.3	8.6	4.5	9.3	4.7	10.0	4.9		
7.3	4.1	8.0	4.3	8.7	4.5	9.4	4.7	10.1	4.9		
7.3	4.1	8.0	4.3	8.6	4.5	9.4	4.7	10.1	4.9		
7.4	4.1	8.0	4.3	8.7	4.5	9.4	4.7	10.1	4.9		
7.4	4.1	8.0	4.3	8.7	4.5	9.4	4.7	10.1	4.9		
7.4	4.1	8.0	4.3	8.7	4.5	9.4	4.8	10.2	4.9		
7.4	4.2	8.0	4.4	8.7	4.6	9.5	4.8	10.2	5.0		
7.4	4.2	8.1	4.4	8.8	4.6	9.5	4.8	10.2	5.0		
7.4	4.2	8.1	4.4	8.8	4.6	9.5	4.8	10.2	5.0		
7.4	4.2	8.1	4.4	8.8	4.6	9.5	4.8	10.2	5.0		

Sample C3

N	mm	0.2	0.2	0.3	0.4	0.5	0.6	0.8	0.9	1.2	1.1
0.0	0.0	0.1	0.2	0.3	0.4	0.6	0.6	0.8	0.9	1.2	1.1
0.0	0.0	0.1	0.2	0.3	0.4	0.6	0.6	0.8	0.9	1.2	1.1
0.0	0.0	0.2	0.2	0.3	0.4	0.6	0.7	0.9	0.9	1.2	1.1
0.0	0.0	0.1	0.2	0.3	0.4	0.6	0.7	0.8	0.9	1.2	1.1
0.0	0.0	0.2	0.2	0.3	0.4	0.6	0.7	0.8	0.9	1.2	1.1
0.0	0.0	0.2	0.2	0.3	0.5	0.6	0.7	0.8	0.9	1.2	1.1
0.0	0.0	0.2	0.2	0.3	0.5	0.6	0.7	0.9	0.9	1.2	1.1
0.0	0.0	0.2	0.2	0.4	0.5	0.6	0.7	0.9	0.9	1.2	1.1
0.0	0.0	0.2	0.3	0.4	0.5	0.6	0.7	0.9	0.9	1.3	1.1
0.0	0.0	0.2	0.3	0.4	0.5	0.6	0.7	0.9	0.9	1.2	1.1
0.0	0.0	0.2	0.3	0.4	0.5	0.6	0.7	0.9	0.9	1.3	1.1
0.0	0.1	0.2	0.3	0.4	0.5	0.6	0.7	0.9	0.9	1.2	1.1
0.0	0.1	0.2	0.3	0.4	0.5	0.6	0.7	0.9	0.9	1.2	1.1
0.0	0.1	0.2	0.3	0.4	0.5	0.6	0.7	0.9	0.9	1.2	1.1
0.0	0.1	0.2	0.3	0.4	0.5	0.6	0.7	0.9	0.9	1.3	1.1
0.1	0.1	0.2	0.3	0.4	0.5	0.6	0.7	0.9	0.9	1.3	1.1
0.0	0.1	0.2	0.3	0.4	0.5	0.7	0.7	1.0	0.9	1.3	1.2
0.0	0.1	0.2	0.3	0.4	0.5	0.7	0.7	0.9	0.9	1.3	1.2
0.1	0.1	0.2	0.3	0.4	0.5	0.7	0.7	1.0	0.9	1.3	1.2
0.0	0.1	0.2	0.3	0.4	0.5	0.6	0.7	1.0	1.0	1.3	1.2
0.1	0.1	0.2	0.3	0.4	0.5	0.7	0.7	1.0	1.0	1.3	1.2
0.1	0.1	0.2	0.3	0.4	0.5	0.6	0.7	1.0	1.0	1.3	1.2
0.0	0.1	0.2	0.3	0.4	0.5	0.7	0.8	1.0	1.0	1.3	1.2
0.1	0.1	0.2	0.3	0.5	0.5	0.7	0.8	1.0	1.0	1.3	1.2
0.1	0.1	0.2	0.3	0.4	0.5	0.7	0.8	1.0	1.0	1.4	1.2
0.1	0.1	0.2	0.3	0.4	0.6	0.7	0.8	1.0	1.0	1.4	1.2
0.1	0.1	0.2	0.3	0.4	0.6	0.7	0.8	1.0	1.0	1.4	1.2
0.1	0.1	0.3	0.3	0.5	0.6	0.7	0.8	1.0	1.0	1.4	1.2
0.1	0.1	0.3	0.4	0.5	0.6	0.7	0.8	1.0	1.0	1.4	1.2
0.1	0.1	0.3	0.4	0.5	0.6	0.7	0.8	1.0	1.0	1.4	1.2
0.1	0.1	0.3	0.4	0.4	0.6	0.8	0.8	1.1	1.0	1.4	1.2
0.1	0.2	0.3	0.4	0.5	0.6	0.8	0.8	1.1	1.0	1.4	1.2
0.1	0.2	0.3	0.4	0.5	0.6	0.8	0.8	1.1	1.0	1.4	1.2
0.1	0.2	0.3	0.4	0.5	0.6	0.8	0.8	1.1	1.0	1.4	1.2
0.1	0.2	0.3	0.4	0.5	0.6	0.8	0.8	1.1	1.0	1.5	1.2
0.2	0.2	0.3	0.4	0.5	0.6	0.8	0.8	1.1	1.0	1.5	1.2
0.1	0.2	0.3	0.4	0.5	0.6	0.8	0.8	1.1	1.0	1.5	1.3
0.1	0.2	0.3	0.4	0.5	0.6	0.8	0.8	1.1	1.0	1.5	1.3
0.1	0.2	0.3	0.4	0.5	0.6	0.8	0.8	1.1	1.0	1.5	1.3
0.2	0.2	0.3	0.4	0.5	0.6	0.8	0.8	1.1	1.1	1.5	1.3
0.1	0.2	0.3	0.4	0.6	0.6	0.8	0.8	1.2	1.1	1.5	1.3
0.2	0.2	0.3	0.4	0.5	0.6	0.8	0.8	1.1	1.1	1.5	1.3

1.6	1.3	2.0	1.5	2.6	1.7	3.2	2.0	3.8	2.2	4.5	2.4
1.5	1.3	2.0	1.5	2.6	1.7	3.2	2.0	3.8	2.2	4.5	2.4
1.6	1.3	2.0	1.5	2.6	1.7	3.2	2.0	3.8	2.2	4.5	2.4
1.5	1.3	2.1	1.5	2.6	1.7	3.2	2.0	3.8	2.2	4.5	2.4
1.6	1.3	2.0	1.5	2.6	1.8	3.3	2.0	3.8	2.2	4.5	2.4
1.6	1.3	2.0	1.5	2.6	1.8	3.2	2.0	3.9	2.2	4.5	2.4
1.6	1.3	2.1	1.5	2.6	1.8	3.3	2.0	3.9	2.2	4.6	2.4
1.6	1.3	2.1	1.5	2.7	1.8	3.3	2.0	3.9	2.2	4.5	2.4
1.6	1.3	2.1	1.5	2.7	1.8	3.3	2.0	3.9	2.2	4.6	2.4
1.6	1.3	2.1	1.6	2.7	1.8	3.3	2.0	3.9	2.2	4.6	2.5
1.6	1.3	2.1	1.6	2.7	1.8	3.3	2.0	3.9	2.2	4.6	2.5
1.6	1.3	2.2	1.6	2.7	1.8	3.3	2.0	4.0	2.2	4.6	2.5
1.6	1.3	2.1	1.6	2.7	1.8	3.3	2.0	4.0	2.2	4.7	2.5
1.6	1.3	2.2	1.6	2.8	1.8	3.3	2.0	4.0	2.2	4.7	2.5
1.7	1.4	2.2	1.6	2.8	1.8	3.4	2.0	4.0	2.3	4.7	2.5
1.7	1.4	2.2	1.6	2.7	1.8	3.4	2.0	4.0	2.3	4.7	2.5
1.7	1.4	2.2	1.6	2.8	1.8	3.4	2.0	4.0	2.3	4.7	2.5
1.7	1.4	2.2	1.6	2.8	1.8	3.4	2.0	4.0	2.3	4.7	2.5
1.7	1.4	2.2	1.6	2.8	1.8	3.4	2.0	4.0	2.3	4.8	2.5
1.7	1.4	2.3	1.6	2.8	1.8	3.4	2.1	4.1	2.3	4.7	2.5
1.7	1.4	2.2	1.6	2.8	1.8	3.4	2.1	4.1	2.3	4.8	2.5
1.7	1.4	2.3	1.6	2.8	1.8	3.4	2.1	4.1	2.3	4.8	2.5
1.8	1.4	2.3	1.6	2.8	1.8	3.5	2.1	4.1	2.3	4.8	2.5
1.7	1.4	2.3	1.6	2.9	1.8	3.5	2.1	4.1	2.3	4.8	2.5
1.8	1.4	2.3	1.6	2.9	1.9	3.5	2.1	4.1	2.3	4.9	2.5
1.8	1.4	2.3	1.6	2.9	1.9	3.5	2.1	4.1	2.3	4.9	2.5
1.8	1.4	2.3	1.6	2.9	1.9	3.5	2.1	4.2	2.3	4.9	2.5
1.8	1.4	2.3	1.6	2.9	1.9	3.5	2.1	4.2	2.3	4.9	2.5
1.8	1.4	2.3	1.6	2.9	1.9	3.6	2.1	4.2	2.3	4.9	2.5
1.8	1.4	2.4	1.7	2.9	1.9	3.6	2.1	4.2	2.3	4.9	2.6
1.8	1.4	2.3	1.7	3.0	1.9	3.6	2.1	4.2	2.3	4.9	2.6
1.8	1.4	2.4	1.7	3.0	1.9	3.6	2.1	4.2	2.3	5.0	2.6
1.9	1.4	2.4	1.7	3.0	1.9	3.6	2.1	4.3	2.3	5.0	2.6
1.9	1.4	2.5	1.7	3.0	1.9	3.6	2.1	4.3	2.3	5.0	2.6
1.9	1.5	2.4	1.7	3.0	1.9	3.7	2.1	4.3	2.4	5.0	2.6
1.9	1.5	2.5	1.7	3.0	1.9	3.6	2.1	4.3	2.4	5.0	2.6
1.9	1.5	2.5	1.7	3.1	1.9	3.7	2.1	4.3	2.4	5.1	2.6
1.9	1.5	2.5	1.7	3.1	1.9	3.7	2.1	4.3	2.4	5.1	2.6
2.0	1.5	2.5	1.7	3.1	1.9	3.7	2.1	4.3	2.4	5.1	2.6
1.9	1.5	2.5	1.7	3.1	1.9	3.7	2.2	4.4	2.4	5.1	2.6
1.9	1.5	2.5	1.7	3.1	1.9	3.7	2.2	4.4	2.4	5.1	2.6
1.9	1.5	2.5	1.7	3.1	1.9	3.7	2.2	4.4	2.4	5.1	2.6
2.0	1.5	2.5	1.7	3.1	1.9	3.7	2.2	4.4	2.4	5.2	2.6
2.0	1.5	2.6	1.7	3.1	1.9	3.7	2.2	4.5	2.4	5.1	2.6
2.0	1.5	2.6	1.7	3.2	2.0	3.8	2.2	4.5	2.4	5.2	2.6

5.2	2.6	5.9	2.9	6.7	3.1	7.4	3.3	8.1	3.5	8.8	3.8
5.2	2.6	5.9	2.9	6.7	3.1	7.4	3.3	8.1	3.5	8.8	3.8
5.2	2.6	6.0	2.9	6.7	3.1	7.4	3.3	8.2	3.5	8.9	3.8
5.2	2.6	6.0	2.9	6.7	3.1	7.4	3.3	8.1	3.5	8.9	3.8
5.3	2.7	6.0	2.9	6.7	3.1	7.5	3.3	8.2	3.6	8.9	3.8
5.3	2.7	6.0	2.9	6.7	3.1	7.5	3.3	8.2	3.6	8.9	3.8
5.3	2.7	6.0	2.9	6.8	3.1	7.5	3.3	8.2	3.6	8.9	3.8
5.3	2.7	6.0	2.9	6.8	3.1	7.5	3.3	8.2	3.6	8.9	3.8
5.3	2.7	6.0	2.9	6.8	3.1	7.5	3.3	8.2	3.6	9.0	3.8
5.4	2.7	6.1	2.9	6.8	3.1	7.5	3.4	8.2	3.6	9.0	3.8
5.3	2.7	6.1	2.9	6.8	3.1	7.6	3.4	8.3	3.6	9.0	3.8
5.4	2.7	6.1	2.9	6.9	3.1	7.6	3.4	8.3	3.6	9.0	3.8
5.4	2.7	6.1	2.9	6.9	3.1	7.6	3.4	8.3	3.6	9.1	3.8
5.4	2.7	6.2	2.9	6.9	3.1	7.6	3.4	8.3	3.6	9.0	3.8
5.4	2.7	6.2	2.9	6.9	3.2	7.6	3.4	8.3	3.6	9.1	3.8
5.4	2.7	6.2	2.9	6.9	3.2	7.6	3.4	8.4	3.6	9.1	3.8
5.4	2.7	6.2	2.9	6.9	3.2	7.6	3.4	8.4	3.6	9.1	3.8
5.5	2.7	6.2	2.9	6.9	3.2	7.6	3.4	8.4	3.6	9.1	3.8
5.5	2.7	6.2	2.9	7.0	3.2	7.7	3.4	8.4	3.6	9.1	3.8
5.5	2.7	6.3	3.0	7.0	3.2	7.7	3.4	8.4	3.6	9.1	3.9
5.5	2.7	6.3	3.0	7.0	3.2	7.7	3.4	8.4	3.6	9.1	3.9
5.5	2.7	6.3	3.0	7.0	3.2	7.7	3.4	8.4	3.6	9.2	3.9
5.5	2.7	6.2	3.0	7.0	3.2	7.8	3.4	8.5	3.6	9.2	3.9
5.6	2.7	6.3	3.0	7.0	3.2	7.8	3.4	8.5	3.6	9.2	3.9
5.6	2.8	6.3	3.0	7.1	3.2	7.8	3.4	8.5	3.7	9.2	3.9
5.6	2.8	6.3	3.0	7.1	3.2	7.8	3.4	8.5	3.7	9.2	3.9
5.6	2.8	6.4	3.0	7.1	3.2	7.8	3.4	8.5	3.7	9.3	3.9
5.6	2.8	6.4	3.0	7.1	3.2	7.8	3.4	8.6	3.7	9.3	3.9
5.6	2.8	6.4	3.0	7.1	3.2	7.8	3.4	8.6	3.7	9.3	3.9
5.7	2.8	6.4	3.0	7.1	3.2	7.9	3.5	8.6	3.7	9.3	3.9
5.7	2.8	6.4	3.0	7.2	3.2	7.9	3.5	8.6	3.7	9.3	3.9
5.7	2.8	6.5	3.0	7.2	3.2	7.9	3.5	8.6	3.7	9.3	3.9
5.7	2.8	6.5	3.0	7.2	3.2	7.9	3.5	8.6	3.7	9.4	3.9
5.7	2.8	6.5	3.0	7.2	3.2	7.9	3.5	8.6	3.7	9.3	3.9
5.7	2.8	6.5	3.0	7.2	3.3	7.9	3.5	8.7	3.7	9.4	3.9
5.7	2.8	6.5	3.0	7.2	3.3	8.0	3.5	8.6	3.7	9.4	3.9
5.8	2.8	6.5	3.0	7.3	3.3	7.9	3.5	8.7	3.7	9.4	3.9
5.8	2.8	6.6	3.0	7.3	3.3	8.0	3.5	8.7	3.7	9.4	3.9
5.8	2.8	6.5	3.0	7.3	3.3	8.0	3.5	8.7	3.7	9.4	3.9
5.8	2.8	6.6	3.1	7.3	3.3	8.1	3.5	8.7	3.7	9.4	4.0
5.8	2.8	6.5	3.1	7.3	3.3	8.0	3.5	8.8	3.7	9.5	4.0
5.9	2.8	6.6	3.1	7.3	3.3	8.1	3.5	8.8	3.7	9.5	4.0
5.9	2.8	6.6	3.1	7.4	3.3	8.1	3.5	8.8	3.7	9.5	4.0
5.9	2.8	6.7	3.1	7.4	3.3	8.1	3.5	8.8	3.7	9.5	4.0
5.9	2.9	6.6	3.1	7.4	3.3	8.1	3.5	8.8	3.8	9.5	4.0

9.5	4.0	10.2	4.2	10.8	4.4	11.4	4.6	12.0	4.8	12.7	5.0
9.6	4.0	10.2	4.2	10.8	4.4	11.4	4.6	12.0	4.8	12.7	5.0
9.6	4.0	10.2	4.2	10.8	4.4	11.4	4.6	12.1	4.8	12.7	5.0
9.6	4.0	10.2	4.2	10.8	4.4	11.4	4.6	12.0	4.8		
9.6	4.0	10.2	4.2	10.8	4.4	11.4	4.6	12.1	4.8		
9.6	4.0	10.3	4.2	10.9	4.4	11.4	4.6	12.1	4.8		
9.6	4.0	10.2	4.2	10.8	4.4	11.4	4.6	12.1	4.8		
9.7	4.0	10.3	4.2	10.9	4.4	11.5	4.6	12.1	4.8		
9.7	4.0	10.3	4.2	10.9	4.4	11.5	4.6	12.1	4.8		
9.7	4.0	10.3	4.2	10.9	4.4	11.5	4.6	12.1	4.8		
9.7	4.0	10.3	4.2	10.9	4.4	11.5	4.6	12.2	4.8		
9.7	4.0	10.4	4.2	11.0	4.4	11.6	4.6	12.2	4.8		
9.7	4.0	10.4	4.2	11.0	4.4	11.6	4.6	12.2	4.8		
9.8	4.0	10.4	4.2	11.0	4.4	11.6	4.6	12.2	4.8		
9.7	4.1	10.4	4.3	11.0	4.5	11.6	4.7	12.2	4.9		
9.8	4.1	10.4	4.3	11.0	4.5	11.6	4.7	12.2	4.9		
9.8	4.1	10.4	4.3	11.0	4.5	11.6	4.7	12.3	4.9		
9.8	4.1	10.4	4.3	11.1	4.5	11.6	4.7	12.3	4.9		
9.8	4.1	10.5	4.3	11.0	4.5	11.6	4.7	12.3	4.9		
9.8	4.1	10.5	4.3	11.1	4.5	11.7	4.7	12.3	4.9		
9.9	4.1	10.5	4.3	11.1	4.5	11.7	4.7	12.3	4.9		
9.9	4.1	10.5	4.3	11.1	4.5	11.7	4.7	12.3	4.9		
9.9	4.1	10.5	4.3	11.1	4.5	11.7	4.7	12.4	4.9		
9.9	4.1	10.5	4.3	11.1	4.5	11.7	4.7	12.4	4.9		
9.9	4.1	10.5	4.3	11.1	4.5	11.8	4.7	12.4	4.9		
9.9	4.1	10.6	4.3	11.2	4.5	11.8	4.7	12.4	4.9		
10.0	4.1	10.6	4.3	11.2	4.5	11.8	4.7	12.4	4.9		
10.0	4.1	10.6	4.3	11.2	4.5	11.8	4.7	12.5	4.9		
10.0	4.1	10.6	4.3	11.2	4.5	11.8	4.7	12.5	4.9		
10.0	4.1	10.6	4.3	11.2	4.5	11.8	4.7	12.5	4.9		
10.0	4.1	10.6	4.3	11.2	4.5	11.8	4.7	12.5	4.9		
10.1	4.1	10.6	4.3	11.2	4.5	11.9	4.7	12.5	4.9		
10.1	4.1	10.6	4.3	11.2	4.5	11.9	4.7	12.6	4.9		
10.1	4.1	10.7	4.3	11.3	4.5	11.9	4.7	12.5	4.9		
10.1	4.2	10.7	4.4	11.3	4.6	11.9	4.8	12.6	5.0		
10.1	4.2	10.7	4.4	11.3	4.6	11.9	4.8	12.5	5.0		
10.1	4.2	10.7	4.4	11.3	4.6	12.0	4.8	12.6	5.0		
10.1	4.2	10.7	4.4	11.3	4.6	12.0	4.8	12.6	5.0		
10.1	4.2	10.7	4.4	11.3	4.6	12.0	4.8	12.6	5.0		
10.2	4.2	10.7	4.4	11.4	4.6	12.0	4.8	12.6	5.0		

Sample C4

N	mm	0.0	0.4	0.2	0.8	1.2	1.3	3.5	1.7	7.0	2.1
0.0	0.0	0.0	0.4	0.2	0.9	1.2	1.3	3.6	1.7	7.1	2.1
0.1	0.0	0.0	0.4	0.2	0.9	1.2	1.3	3.7	1.7	7.2	2.2
0.0	0.0	0.0	0.4	0.2	0.9	1.3	1.3	3.7	1.7	7.3	2.2
0.0	0.0	0.0	0.5	0.3	0.9	1.3	1.3	3.9	1.7	7.4	2.2
0.0	0.0	0.0	0.5	0.3	0.9	1.3	1.3	4.0	1.8	7.5	2.2
0.0	0.0	0.0	0.5	0.3	0.9	1.3	1.3	3.9	1.8	7.6	2.2
0.0	0.1	0.0	0.5	0.3	0.9	1.4	1.3	4.1	1.8	7.7	2.2
0.0	0.1	0.0	0.5	0.3	0.9	1.4	1.4	4.2	1.8	7.7	2.2
0.0	0.1	0.0	0.5	0.3	0.9	1.5	1.4	4.2	1.8	7.9	2.2
0.0	0.1	0.0	0.5	0.3	0.9	1.5	1.4	4.3	1.8	7.9	2.2
0.0	0.1	0.0	0.5	0.4	1.0	1.6	1.4	4.4	1.8	8.0	2.2
0.0	0.1	0.0	0.5	0.4	1.0	1.6	1.4	4.5	1.8	8.1	2.3
0.0	0.1	0.0	0.5	0.4	1.0	1.6	1.4	4.5	1.8	8.3	2.3
0.0	0.1	0.0	0.6	0.4	1.0	1.7	1.4	4.6	1.8	8.3	2.3
0.0	0.1	0.0	0.6	0.4	1.0	1.8	1.4	4.7	1.9	8.4	2.3
0.0	0.1	0.0	0.6	0.5	1.0	1.8	1.4	4.8	1.9	8.5	2.3
0.0	0.2	0.0	0.6	0.4	1.0	1.8	1.4	4.8	1.9	8.6	2.3
0.0	0.2	0.0	0.6	0.5	1.0	1.9	1.5	5.0	1.9	8.7	2.3
0.0	0.2	0.0	0.6	0.5	1.0	1.9	1.5	5.0	1.9	8.8	2.3
0.0	0.2	0.0	0.6	0.5	1.0	2.0	1.5	5.1	1.9	8.9	2.3
0.0	0.2	0.0	0.6	0.5	1.1	2.1	1.5	5.2	1.9	9.0	2.3
0.0	0.2	0.0	0.6	0.6	1.1	2.1	1.5	5.3	1.9	9.1	2.4
0.0	0.2	0.0	0.6	0.6	1.1	2.2	1.5	5.3	1.9	9.2	2.4
0.0	0.2	0.0	0.7	0.6	1.1	2.2	1.5	5.4	1.9	9.3	2.4
0.0	0.2	0.0	0.7	0.6	1.1	2.3	1.5	5.5	2.0	9.4	2.4
0.0	0.2	0.0	0.7	0.7	1.1	2.3	1.5	5.6	2.0	9.5	2.4
0.0	0.3	0.0	0.7	0.7	1.1	2.4	1.5	5.6	2.0	9.6	2.4
0.0	0.3	0.1	0.7	0.7	1.1	2.5	1.6	5.7	2.0	9.7	2.4
0.0	0.3	0.0	0.7	0.8	1.1	2.5	1.6	5.8	2.0	9.7	2.4
0.0	0.3	0.0	0.7	0.8	1.1	2.6	1.6	5.9	2.0	9.9	2.4
0.0	0.3	0.1	0.7	0.8	1.2	2.7	1.6	6.0	2.0	10.0	2.4
0.0	0.3	0.1	0.7	0.8	1.2	2.7	1.6	6.1	2.0	10.0	2.5
0.0	0.3	0.1	0.7	0.8	1.2	2.8	1.6	6.1	2.0	10.1	2.5
0.0	0.3	0.1	0.8	0.8	1.2	2.9	1.6	6.2	2.0	10.3	2.5
0.0	0.3	0.1	0.8	0.9	1.2	3.0	1.6	6.4	2.1	10.4	2.5
0.0	0.3	0.1	0.8	1.0	1.2	3.0	1.6	6.4	2.1	10.4	2.5
0.1	0.4	0.1	0.8	1.0	1.2	3.1	1.6	6.5	2.1	10.6	2.5
0.0	0.4	0.2	0.8	0.9	1.2	3.2	1.7	6.6	2.1	10.7	2.5
0.0	0.4	0.1	0.8	1.0	1.2	3.2	1.7	6.7	2.1	10.7	2.5
0.0	0.4	0.1	0.8	1.1	1.2	3.3	1.7	6.8	2.1	10.9	2.5
0.0	0.4	0.2	0.8	1.1	1.3	3.4	1.7	6.8	2.1	11.0	2.5
0.0	0.4	0.2	0.8	1.1	1.3	3.5	1.7	6.9	2.1	11.0	2.6

11.2	2.6	15.8	3.0	20.6	3.5	25.5	3.9	30.6	4.4	35.7	4.8
11.3	2.6	16.0	3.0	20.7	3.5	25.6	3.9	30.7	4.4	35.9	4.8
11.4	2.6	16.1	3.0	20.8	3.5	25.7	3.9	30.8	4.4	35.9	4.8
11.4	2.6	16.1	3.0	21.0	3.5	25.9	3.9	30.9	4.4	36.0	4.8
11.6	2.6	16.3	3.1	21.1	3.5	25.9	4.0	31.0	4.4	36.2	4.9
11.7	2.6	16.4	3.1	21.2	3.5	26.1	4.0	31.1	4.4	36.3	4.9
11.8	2.6	16.4	3.1	21.3	3.5	26.2	4.0	31.2	4.4	36.4	4.9
11.8	2.6	16.6	3.1	21.4	3.5	26.3	4.0	31.4	4.4	36.5	4.9
12.0	2.6	16.7	3.1	21.5	3.5	26.4	4.0	31.5	4.4	36.6	4.9
12.1	2.7	16.8	3.1	21.6	3.6	26.5	4.0	31.6	4.5	36.7	4.9
12.2	2.7	16.9	3.1	21.7	3.6	26.7	4.0	31.8	4.5	36.8	4.9
12.3	2.7	17.0	3.1	21.8	3.6	26.7	4.0	31.8	4.5	37.0	4.9
12.4	2.7	17.1	3.1	21.9	3.6	26.9	4.0	31.9	4.5	37.1	4.9
12.4	2.7	17.2	3.1	22.0	3.6	27.0	4.0	32.0	4.5	37.2	4.9
12.6	2.7	17.3	3.2	22.1	3.6	27.1	4.1	32.2	4.5	37.3	5.0
12.7	2.7	17.4	3.2	22.2	3.6	27.2	4.1	32.3	4.5	37.4	5.0
12.8	2.7	17.5	3.2	22.4	3.6	27.3	4.1	32.4	4.5	37.6	5.0
12.9	2.7	17.6	3.2	22.4	3.6	27.4	4.1	32.5	4.5	37.6	5.0
13.0	2.7	17.8	3.2	22.6	3.6	27.5	4.1	32.6	4.5	37.7	5.0
13.1	2.8	17.8	3.2	22.8	3.7	27.6	4.1	32.7	4.6	37.8	5.0
13.2	2.8	18.0	3.2	22.8	3.7	27.7	4.1	32.9	4.6	38.0	5.0
13.4	2.8	18.1	3.2	22.9	3.7	27.8	4.1	32.9	4.6	38.1	5.0
13.4	2.8	18.2	3.2	23.0	3.7	27.9	4.1	33.0	4.6	38.2	5.0
13.5	2.8	18.3	3.2	23.1	3.7	28.1	4.1	33.2	4.6	38.3	5.0
13.6	2.8	18.4	3.3	23.2	3.7	28.2	4.2	33.3	4.6	38.4	5.1
13.8	2.8	18.5	3.3	23.3	3.7	28.3	4.2	33.4	4.6	38.5	5.1
13.9	2.8	18.6	3.3	23.4	3.7	28.4	4.2	33.5	4.6	38.7	5.1
13.9	2.8	18.7	3.3	23.5	3.7	28.5	4.2	33.6	4.6	38.8	5.1
14.0	2.8	18.8	3.3	23.7	3.7	28.6	4.2	33.8	4.6	38.8	5.1
14.2	2.9	18.9	3.3	23.8	3.8	28.7	4.2	33.8	4.7	39.0	5.1
14.3	2.9	19.0	3.3	23.9	3.8	28.8	4.2	34.0	4.7	39.2	5.1
14.4	2.9	19.1	3.3	24.0	3.8	29.0	4.2	34.1	4.7	39.2	5.1
14.5	2.9	19.3	3.3	24.1	3.8	29.1	4.2	34.2	4.7	39.3	5.1
14.6	2.9	19.3	3.3	24.2	3.8	29.2	4.2	34.3	4.7	39.5	5.1
14.7	2.9	19.4	3.4	24.3	3.8	29.3	4.3	34.4	4.7	39.6	5.2
14.8	2.9	19.6	3.4	24.5	3.8	29.4	4.3	34.6	4.7	39.7	5.2
14.9	2.9	19.7	3.4	24.5	3.8	29.5	4.3	34.7	4.7	39.8	5.2
15.0	2.9	19.8	3.4	24.6	3.8	29.6	4.3	34.8	4.7	39.9	5.2
15.1	2.9	19.9	3.4	24.7	3.8	29.8	4.3	34.9	4.7	40.0	5.2
15.2	3.0	20.0	3.4	24.9	3.9	29.9	4.3	35.0	4.8	40.1	5.2
15.3	3.0	20.1	3.4	25.0	3.9	29.9	4.3	35.1	4.8	40.3	5.2
15.4	3.0	20.2	3.4	25.1	3.9	30.1	4.3	35.3	4.8	40.3	5.2
15.5	3.0	20.3	3.4	25.2	3.9	30.3	4.3	35.4	4.8	40.4	5.2
15.6	3.0	20.4	3.4	25.3	3.9	30.3	4.3	35.5	4.8	40.6	5.2
15.8	3.0	20.5	3.5	25.4	3.9	30.5	4.4	35.6	4.8	40.6	5.3

40.8	5.3	45.7	5.7	50.3	6.2	55.0	6.6	59.3	7.1	63.5	7.5
40.9	5.3	45.8	5.7	50.5	6.2	55.0	6.6	59.4	7.1	63.6	7.5
41.0	5.3	46.0	5.7	50.6	6.2	55.1	6.6	59.5	7.1	63.6	7.5
41.1	5.3	46.0	5.7	50.7	6.2	55.2	6.6	59.6	7.1	63.8	7.5
41.2	5.3	46.1	5.8	50.8	6.2	55.3	6.7	59.7	7.1	63.9	7.6
41.4	5.3	46.2	5.8	50.9	6.2	55.4	6.7	59.8	7.1	63.9	7.6
41.5	5.3	46.3	5.8	51.0	6.2	55.5	6.7	59.9	7.1	64.0	7.6
41.6	5.3	46.4	5.8	51.0	6.2	55.6	6.7	60.0	7.1	64.2	7.6
41.7	5.3	46.6	5.8	51.2	6.2	55.7	6.7	60.0	7.1	64.2	7.6
41.8	5.4	46.7	5.8	51.3	6.3	55.8	6.7	60.1	7.2	64.3	7.6
41.9	5.4	46.8	5.8	51.4	6.3	55.9	6.7	60.3	7.2	64.4	7.6
42.0	5.4	46.8	5.8	51.5	6.3	56.0	6.7	60.3	7.2	64.5	7.6
42.1	5.4	47.0	5.8	51.6	6.3	56.1	6.7	60.4	7.2	64.5	7.6
42.2	5.4	47.0	5.8	51.7	6.3	56.2	6.7	60.5	7.2	64.7	7.6
42.3	5.4	47.2	5.9	51.8	6.3	56.3	6.8	60.6	7.2	64.7	7.7
42.4	5.4	47.3	5.9	51.9	6.3	56.4	6.8	60.7	7.2	64.8	7.7
42.6	5.4	47.4	5.9	52.0	6.3	56.5	6.8	60.8	7.2	64.9	7.7
42.7	5.4	47.5	5.9	52.1	6.3	56.6	6.8	60.9	7.2	65.1	7.7
42.8	5.4	47.6	5.9	52.2	6.3	56.7	6.8	61.0	7.2	65.1	7.7
42.9	5.5	47.7	5.9	52.4	6.4	56.8	6.8	61.1	7.3	65.2	7.7
43.0	5.5	47.8	5.9	52.4	6.4	56.9	6.8	61.2	7.3	65.3	7.7
43.1	5.5	47.9	5.9	52.5	6.4	57.0	6.8	61.2	7.3	65.3	7.7
43.2	5.5	48.1	5.9	52.7	6.4	57.1	6.8	61.4	7.3	65.4	7.7
43.3	5.5	48.1	5.9	52.7	6.4	57.2	6.8	61.5	7.3	65.5	7.7
43.4	5.5	48.2	6.0	52.8	6.4	57.3	6.9	61.5	7.3	65.6	7.8
43.5	5.5	48.3	6.0	53.0	6.4	57.4	6.9	61.6	7.3	65.7	7.8
43.6	5.5	48.4	6.0	53.0	6.4	57.5	6.9	61.7	7.3	65.8	7.8
43.8	5.5	48.6	6.0	53.1	6.4	57.5	6.9	61.8	7.3	66.0	7.8
43.9	5.5	48.6	6.0	53.3	6.4	57.7	6.9	61.9	7.3	66.0	7.8
44.0	5.6	48.7	6.0	53.3	6.5	57.8	6.9	62.0	7.4	66.1	7.8
44.1	5.6	48.8	6.0	53.4	6.5	57.8	6.9	62.1	7.4	66.2	7.8
44.2	5.6	49.0	6.0	53.5	6.5	57.9	6.9	62.2	7.4	66.2	7.8
44.3	5.6	49.1	6.0	53.6	6.5	58.0	6.9	62.3	7.4	66.3	7.8
44.4	5.6	49.2	6.0	53.7	6.5	58.1	6.9	62.4	7.4	66.4	7.8
44.5	5.6	49.2	6.1	53.9	6.5	58.3	7.0	62.4	7.4	66.5	7.9
44.6	5.6	49.3	6.1	54.0	6.5	58.4	7.0	62.6	7.4	66.6	7.9
44.7	5.6	49.5	6.1	54.0	6.5	58.5	7.0	62.7	7.4	66.7	7.9
44.9	5.6	49.6	6.1	54.2	6.5	58.5	7.0	62.7	7.4	66.8	7.9
44.9	5.6	49.7	6.1	54.2	6.5	58.6	7.0	62.8	7.4	66.9	7.9
45.0	5.7	49.8	6.1	54.3	6.6	58.8	7.0	62.9	7.5	66.9	7.9
45.2	5.7	49.9	6.1	54.4	6.6	58.8	7.0	63.0	7.5	67.0	7.9
45.3	5.7	50.0	6.1	54.5	6.6	58.9	7.0	63.1	7.5	67.1	7.9
45.4	5.7	50.0	6.1	54.7	6.6	59.1	7.0	63.2	7.5	67.2	7.9
45.4	5.7	50.2	6.1	54.8	6.6	59.1	7.0	63.3	7.5	67.3	7.9
45.6	5.7	50.3	6.2	54.8	6.6	59.2	7.1	63.3	7.5	67.4	8.0

67.4	8.0	70.8	8.4	74.0	8.8	77.2	9.2	80.2	9.6	83.3	10.0
67.5	8.0	70.9	8.4	74.1	8.8	77.3	9.2	80.3	9.6	83.3	10.0
67.6	8.0	71.0	8.4	74.2	8.8	77.4	9.2	80.4	9.6	83.4	10.0
67.7	8.0	71.1	8.4	74.3	8.8	77.4	9.2	80.5	9.6		
67.7	8.0	71.2	8.4	74.4	8.8	77.5	9.2	80.6	9.6		
67.9	8.0	71.2	8.4	74.5	8.8	77.6	9.2	80.6	9.6		
67.9	8.0	71.3	8.4	74.6	8.8	77.7	9.2	80.7	9.6		
68.0	8.0	71.4	8.4	74.6	8.8	77.8	9.2	80.8	9.6		
68.2	8.0	71.4	8.4	74.7	8.8	77.8	9.2	80.8	9.6		
68.2	8.1	71.6	8.5	74.8	8.9	77.9	9.3	80.9	9.7		
68.3	8.1	71.7	8.5	74.8	8.9	78.0	9.3	81.0	9.7		
68.4	8.1	71.7	8.5	74.9	8.9	78.0	9.3	81.1	9.7		
68.4	8.1	71.8	8.5	75.0	8.9	78.1	9.3	81.1	9.7		
68.6	8.1	71.9	8.5	75.1	8.9	78.2	9.3	81.2	9.7		
68.6	8.1	72.0	8.5	75.2	8.9	78.3	9.3	81.4	9.7		
68.7	8.1	72.1	8.5	75.2	8.9	78.4	9.3	81.3	9.7		
68.8	8.1	72.1	8.5	75.4	8.9	78.4	9.3	81.4	9.7		
68.9	8.1	72.2	8.5	75.4	8.9	78.5	9.3	81.6	9.7		
69.0	8.1	72.3	8.5	75.5	8.9	78.6	9.3	81.6	9.7		
69.1	8.2	72.4	8.6	75.6	9.0	78.6	9.4	81.7	9.8		
69.2	8.2	72.5	8.6	75.6	9.0	78.7	9.4	81.7	9.8		
69.3	8.2	72.5	8.6	75.7	9.0	78.8	9.4	81.8	9.8		
69.3	8.2	72.6	8.6	75.8	9.0	78.8	9.4	81.9	9.8		
69.5	8.2	72.7	8.6	75.8	9.0	79.0	9.4	82.0	9.8		
69.5	8.2	72.8	8.6	75.9	9.0	79.1	9.4	82.1	9.8		
69.5	8.2	72.9	8.6	76.0	9.0	79.1	9.4	82.1	9.8		
69.7	8.2	72.9	8.6	76.1	9.0	79.1	9.4	82.1	9.8		
69.8	8.2	73.0	8.6	76.1	9.0	79.3	9.4	82.3	9.8		
69.8	8.2	73.1	8.6	76.3	9.0	79.3	9.4	82.3	9.8		
69.9	8.3	73.2	8.7	76.4	9.1	79.4	9.5	82.4	9.9		
70.0	8.3	73.3	8.7	76.4	9.1	79.5	9.5	82.5	9.9		
70.1	8.3	73.3	8.7	76.5	9.1	79.6	9.5	82.5	9.9		
70.1	8.3	73.4	8.7	76.6	9.1	79.6	9.5	82.6	9.9		
70.2	8.3	73.5	8.7	76.6	9.1	79.7	9.5	82.7	9.9		
70.4	8.3	73.5	8.7	76.7	9.1	79.8	9.5	82.8	9.9		
70.4	8.3	73.7	8.7	76.8	9.1	79.8	9.5	82.9	9.9		
70.5	8.3	73.8	8.7	76.9	9.1	79.9	9.5	82.9	9.9		
70.6	8.3	73.8	8.7	76.9	9.1	80.0	9.5	83.0	9.9		
70.6	8.3	73.9	8.7	77.0	9.1	80.1	9.5	83.1	9.9		
70.7	8.4	74.0	8.8	77.1	9.2	80.1	9.6	83.1	10.0		

Sample C5

N	mm	0.1	0.4	0.2	0.8	1.3	1.3	4.5	1.7	9.0	2.1
0.0	0.0	0.1	0.4	0.2	0.9	1.4	1.3	4.6	1.7	9.1	2.1
0.0	0.0	0.1	0.4	0.2	0.9	1.5	1.3	4.6	1.7	9.2	2.2
0.0	0.0	0.1	0.4	0.2	0.9	1.4	1.3	4.8	1.7	9.3	2.2
0.0	0.0	0.1	0.5	0.3	0.9	1.5	1.3	4.9	1.7	9.4	2.2
0.0	0.0	0.1	0.5	0.2	0.9	1.6	1.3	4.9	1.8	9.5	2.2
0.0	0.0	0.1	0.5	0.2	0.9	1.6	1.3	5.1	1.8	9.7	2.2
0.0	0.1	0.1	0.5	0.3	0.9	1.7	1.3	5.2	1.8	9.7	2.2
0.0	0.1	0.0	0.5	0.3	0.9	1.8	1.4	5.3	1.8	9.8	2.2
0.0	0.1	0.1	0.5	0.3	0.9	1.8	1.4	5.3	1.8	10.0	2.2
0.0	0.1	0.1	0.5	0.3	0.9	1.9	1.4	5.5	1.8	10.1	2.2
0.0	0.1	0.1	0.5	0.3	1.0	2.0	1.4	5.5	1.8	10.2	2.2
0.0	0.1	0.1	0.5	0.3	1.0	2.0	1.4	5.6	1.8	10.3	2.3
0.0	0.1	0.1	0.5	0.3	1.0	2.0	1.4	5.7	1.8	10.4	2.3
0.0	0.1	0.1	0.6	0.3	1.0	2.1	1.4	5.9	1.8	10.5	2.3
0.0	0.1	0.1	0.6	0.3	1.0	2.2	1.4	5.9	1.9	10.6	2.3
0.0	0.1	0.1	0.6	0.4	1.0	2.3	1.4	6.0	1.9	10.8	2.3
0.0	0.2	0.2	0.6	0.4	1.0	2.4	1.4	6.2	1.9	10.9	2.3
0.0	0.2	0.1	0.6	0.4	1.0	2.4	1.5	6.3	1.9	10.9	2.3
0.0	0.2	0.1	0.6	0.4	1.0	2.5	1.5	6.3	1.9	11.1	2.3
0.0	0.2	0.1	0.6	0.4	1.0	2.6	1.5	6.5	1.9	11.2	2.3
0.1	0.2	0.1	0.6	0.5	1.1	2.6	1.5	6.6	1.9	11.3	2.3
0.0	0.2	0.2	0.6	0.5	1.1	2.7	1.5	6.6	1.9	11.4	2.4
0.0	0.2	0.2	0.6	0.5	1.1	2.8	1.5	6.7	1.9	11.5	2.4
0.1	0.2	0.1	0.7	0.6	1.1	2.8	1.5	6.9	1.9	11.6	2.4
0.1	0.2	0.1	0.7	0.6	1.1	2.9	1.5	7.0	2.0	11.8	2.4
0.0	0.2	0.1	0.7	0.6	1.1	3.0	1.5	7.1	2.0	11.9	2.4
0.0	0.3	0.2	0.7	0.6	1.1	3.1	1.5	7.2	2.0	12.0	2.4
0.1	0.3	0.2	0.7	0.7	1.1	3.2	1.6	7.3	2.0	12.1	2.4
0.0	0.3	0.1	0.7	0.7	1.1	3.2	1.6	7.4	2.0	12.2	2.4
0.1	0.3	0.1	0.7	0.7	1.1	3.3	1.6	7.5	2.0	12.3	2.4
0.1	0.3	0.1	0.7	0.8	1.2	3.4	1.6	7.6	2.0	12.4	2.4
0.1	0.3	0.2	0.7	0.8	1.2	3.5	1.6	7.7	2.0	12.6	2.5
0.1	0.3	0.2	0.7	0.8	1.2	3.6	1.6	7.8	2.0	12.7	2.5
0.0	0.3	0.1	0.8	0.9	1.2	3.7	1.6	8.0	2.0	12.7	2.5
0.0	0.3	0.2	0.8	1.0	1.2	3.7	1.6	8.1	2.1	12.9	2.5
0.1	0.3	0.2	0.8	1.0	1.2	3.9	1.6	8.2	2.1	13.1	2.5
0.1	0.4	0.2	0.8	1.0	1.2	3.9	1.6	8.3	2.1	13.1	2.5
0.0	0.4	0.2	0.8	1.1	1.2	4.0	1.7	8.4	2.1	13.2	2.5
0.1	0.4	0.2	0.8	1.1	1.2	4.1	1.7	8.5	2.1	13.3	2.5
0.1	0.4	0.2	0.8	1.1	1.2	4.2	1.7	8.6	2.1	13.4	2.5
0.1	0.4	0.2	0.8	1.2	1.3	4.3	1.7	8.8	2.1	13.5	2.5
0.1	0.4	0.2	0.8	1.3	1.3	4.3	1.7	8.8	2.1	13.7	2.6

13.8	2.6	18.7	3.0	23.5	3.5	28.0	3.9	32.4	4.4	36.6	4.8
13.9	2.6	18.8	3.0	23.6	3.5	28.1	3.9	32.5	4.4	36.8	4.8
14.0	2.6	18.9	3.0	23.6	3.5	28.2	3.9	32.6	4.4	36.8	4.8
14.1	2.6	19.0	3.0	23.8	3.5	28.3	3.9	32.7	4.4	36.9	4.8
14.2	2.6	19.1	3.1	23.9	3.5	28.4	4.0	32.8	4.4	37.0	4.9
14.3	2.6	19.2	3.1	24.0	3.5	28.5	4.0	32.9	4.4	37.1	4.9
14.5	2.6	19.3	3.1	24.1	3.5	28.6	4.0	33.0	4.4	37.2	4.9
14.5	2.6	19.4	3.1	24.2	3.5	28.7	4.0	33.1	4.4	37.3	4.9
14.6	2.6	19.5	3.1	24.3	3.5	28.8	4.0	33.2	4.4	37.4	4.9
14.8	2.7	19.7	3.1	24.4	3.6	28.9	4.0	33.2	4.5	37.6	4.9
14.9	2.7	19.8	3.1	24.5	3.6	29.0	4.0	33.3	4.5	37.6	4.9
15.0	2.7	19.9	3.1	24.6	3.6	29.1	4.0	33.4	4.5	37.7	4.9
15.1	2.7	20.0	3.1	24.7	3.6	29.2	4.0	33.5	4.5	37.8	4.9
15.3	2.7	20.1	3.1	24.8	3.6	29.3	4.0	33.6	4.5	37.9	4.9
15.4	2.7	20.2	3.2	24.9	3.6	29.4	4.1	33.7	4.5	37.9	5.0
15.4	2.7	20.3	3.2	25.0	3.6	29.5	4.1	33.8	4.5	38.1	5.0
15.5	2.7	20.4	3.2	25.1	3.6	29.6	4.1	33.9	4.5	38.1	5.0
15.7	2.7	20.5	3.2	25.2	3.6	29.7	4.1	34.0	4.5	38.2	5.0
15.8	2.7	20.6	3.2	25.3	3.6	29.8	4.1	34.1	4.5	38.4	5.0
15.8	2.8	20.7	3.2	25.4	3.7	29.9	4.1	34.2	4.6	38.4	5.0
16.0	2.8	20.9	3.2	25.5	3.7	30.0	4.1	34.3	4.6	38.5	5.0
16.1	2.8	21.0	3.2	25.6	3.7	30.1	4.1	34.4	4.6	38.6	5.0
16.2	2.8	21.1	3.2	25.7	3.7	30.1	4.1	34.5	4.6	38.7	5.0
16.3	2.8	21.2	3.2	25.8	3.7	30.3	4.1	34.5	4.6	38.8	5.0
16.4	2.8	21.3	3.3	25.9	3.7	30.4	4.2	34.7	4.6	38.9	5.1
16.5	2.8	21.4	3.3	26.0	3.7	30.4	4.2	34.8	4.6	39.0	5.1
16.7	2.8	21.5	3.3	26.1	3.7	30.6	4.2	34.8	4.6	39.1	5.1
16.8	2.8	21.6	3.3	26.2	3.7	30.6	4.2	35.0	4.6	39.2	5.1
16.9	2.8	21.7	3.3	26.3	3.7	30.8	4.2	35.0	4.6	39.3	5.1
17.0	2.9	21.8	3.3	26.4	3.8	30.9	4.2	35.1	4.7	39.4	5.1
17.1	2.9	21.9	3.3	26.6	3.8	31.0	4.2	35.2	4.7	39.4	5.1
17.2	2.9	22.0	3.3	26.6	3.8	31.0	4.2	35.3	4.7	39.5	5.1
17.3	2.9	22.1	3.3	26.7	3.8	31.1	4.2	35.4	4.7	39.7	5.1
17.4	2.9	22.3	3.3	26.8	3.8	31.3	4.2	35.5	4.7	39.7	5.1
17.5	2.9	22.3	3.4	26.9	3.8	31.3	4.3	35.6	4.7	39.8	5.2
17.6	2.9	22.4	3.4	27.0	3.8	31.4	4.3	35.7	4.7	39.9	5.2
17.7	2.9	22.5	3.4	27.1	3.8	31.5	4.3	35.8	4.7	40.0	5.2
17.8	2.9	22.7	3.4	27.3	3.8	31.6	4.3	35.9	4.7	40.1	5.2
18.0	2.9	22.8	3.4	27.3	3.8	31.7	4.3	36.0	4.7	40.2	5.2
18.1	3.0	22.8	3.4	27.4	3.9	31.8	4.3	36.1	4.8	40.3	5.2
18.2	3.0	23.0	3.4	27.5	3.9	31.9	4.3	36.2	4.8	40.4	5.2
18.3	3.0	23.0	3.4	27.6	3.9	32.0	4.3	36.3	4.8	40.5	5.2
18.4	3.0	23.1	3.4	27.7	3.9	32.1	4.3	36.4	4.8	40.6	5.2
18.5	3.0	23.3	3.4	27.8	3.9	32.2	4.3	36.5	4.8	40.6	5.2
18.6	3.0	23.4	3.5	27.9	3.9	32.3	4.4	36.6	4.8	40.7	5.3

179

40.8	5.3	45.0	5.7	49.2	6.2	53.4	6.6	57.7	7.1	62.2	7.5
40.9	5.3	45.1	5.7	49.3	6.2	53.5	6.6	57.8	7.1	62.4	7.5
41.0	5.3	45.2	5.7	49.3	6.2	53.6	6.6	57.9	7.1	62.5	7.5
41.1	5.3	45.3	5.7	49.4	6.2	53.6	6.6	58.0	7.1	62.6	7.5
41.2	5.3	45.4	5.8	49.6	6.2	53.7	6.7	58.1	7.1	62.6	7.6
41.3	5.3	45.4	5.8	49.6	6.2	53.8	6.7	58.2	7.1	62.8	7.6
41.4	5.3	45.6	5.8	49.7	6.2	54.0	6.7	58.3	7.1	62.9	7.6
41.5	5.3	45.7	5.8	49.8	6.2	54.0	6.7	58.5	7.1	63.0	7.6
41.6	5.3	45.8	5.8	49.9	6.2	54.2	6.7	58.5	7.1	63.1	7.6
41.7	5.4	45.8	5.8	50.0	6.3	54.3	6.7	58.6	7.2	63.2	7.6
41.8	5.4	46.0	5.8	50.1	6.3	54.4	6.7	58.7	7.2	63.3	7.6
41.9	5.4	46.0	5.8	50.2	6.3	54.5	6.7	58.8	7.2	63.4	7.6
42.0	5.4	46.1	5.8	50.3	6.3	54.5	6.7	58.9	7.2	63.5	7.6
42.1	5.4	46.2	5.8	50.4	6.3	54.6	6.7	59.0	7.2	63.6	7.6
42.1	5.4	46.3	5.9	50.5	6.3	54.8	6.8	59.1	7.2	63.7	7.7
42.3	5.4	46.4	5.9	50.5	6.3	54.8	6.8	59.2	7.2	63.8	7.7
42.3	5.4	46.5	5.9	50.7	6.3	54.9	6.8	59.3	7.2	63.9	7.7
42.4	5.4	46.6	5.9	50.8	6.3	55.0	6.8	59.4	7.2	64.0	7.7
42.5	5.4	46.7	5.9	50.8	6.3	55.1	6.8	59.5	7.2	64.1	7.7
42.6	5.5	46.8	5.9	51.0	6.4	55.1	6.8	59.6	7.3	64.2	7.7
42.7	5.5	46.9	5.9	51.1	6.4	55.3	6.8	59.7	7.3	64.3	7.7
42.8	5.5	46.9	5.9	51.1	6.4	55.4	6.8	59.8	7.3	64.4	7.7
42.9	5.5	47.0	5.9	51.2	6.4	55.5	6.8	59.9	7.3	64.6	7.7
43.0	5.5	47.1	5.9	51.3	6.4	55.6	6.8	60.0	7.3	64.6	7.7
43.1	5.5	47.2	6.0	51.4	6.4	55.7	6.9	60.1	7.3	64.7	7.8
43.2	5.5	47.3	6.0	51.5	6.4	55.8	6.9	60.2	7.3	64.9	7.8
43.2	5.5	47.4	6.0	51.6	6.4	55.9	6.9	60.3	7.3	64.9	7.8
43.3	5.5	47.5	6.0	51.7	6.4	56.0	6.9	60.5	7.3	65.1	7.8
43.4	5.5	47.6	6.0	51.8	6.4	56.1	6.9	60.5	7.3	65.2	7.8
43.5	5.6	47.7	6.0	51.9	6.5	56.1	6.9	60.6	7.4	65.3	7.8
43.6	5.6	47.8	6.0	52.0	6.5	56.3	6.9	60.7	7.4	65.4	7.8
43.8	5.6	47.9	6.0	52.0	6.5	56.4	6.9	60.8	7.4	65.5	7.8
43.9	5.6	48.0	6.0	52.2	6.5	56.4	6.9	60.9	7.4	65.6	7.8
43.9	5.6	48.1	6.0	52.3	6.5	56.6	6.9	61.0	7.4	65.7	7.8
44.0	5.6	48.1	6.1	52.3	6.5	56.7	7.0	61.1	7.4	65.8	7.9
44.1	5.6	48.3	6.1	52.4	6.5	56.7	7.0	61.2	7.4	65.9	7.9
44.2	5.6	48.4	6.1	52.5	6.5	56.9	7.0	61.3	7.4	66.0	7.9
44.2	5.6	48.4	6.1	52.6	6.5	57.0	7.0	61.4	7.4	66.2	7.9
44.4	5.6	48.5	6.1	52.7	6.5	57.0	7.0	61.5	7.4	66.3	7.9
44.4	5.7	48.6	6.1	52.8	6.6	57.1	7.0	61.6	7.5	66.3	7.9
44.5	5.7	48.7	6.1	52.9	6.6	57.3	7.0	61.7	7.5	66.5	7.9
44.6	5.7	48.8	6.1	53.0	6.6	57.3	7.0	61.9	7.5	66.5	7.9
44.7	5.7	48.9	6.1	53.2	6.6	57.4	7.0	61.9	7.5	66.7	7.9
44.8	5.7	49.0	6.1	53.2	6.6	57.5	7.0	62.1	7.5	66.8	7.9
44.9	5.7	49.1	6.2	53.2	6.6	57.7	7.1	62.2	7.5	66.9	8.0

67.0	8.0	71.5	8.4	76.3	8.8	81.4	9.2	87.0	9.6	93.0	10.0
67.1	8.0	71.6	8.4	76.4	8.8	81.5	9.2	87.1	9.6	93.2	10.0
67.2	8.0	71.7	8.4	76.4	8.8	81.7	9.2	87.3	9.6	93.3	10.0
67.3	8.0	71.7	8.4	76.6	8.8	81.9	9.2	87.4	9.6		
67.4	8.0	71.9	8.4	76.8	8.8	82.0	9.2	87.5	9.6		
67.6	8.0	72.1	8.4	76.9	8.8	82.1	9.2	87.7	9.6		
67.7	8.0	72.1	8.4	77.0	8.8	82.2	9.2	87.9	9.6		
67.7	8.0	72.2	8.4	77.1	8.8	82.3	9.2	88.0	9.6		
67.9	8.0	72.4	8.4	77.3	8.8	82.5	9.2	88.1	9.6		
68.0	8.1	72.5	8.5	77.3	8.9	82.6	9.3	88.3	9.7		
68.0	8.1	72.7	8.5	77.5	8.9	82.8	9.3	88.4	9.7		
68.2	8.1	72.7	8.5	77.7	8.9	82.9	9.3	88.6	9.7		
68.3	8.1	72.9	8.5	77.7	8.9	83.0	9.3	88.8	9.7		
68.4	8.1	73.0	8.5	77.9	8.9	83.2	9.3	88.9	9.7		
68.5	8.1	73.1	8.5	78.1	8.9	83.3	9.3	89.0	9.7		
68.6	8.1	73.3	8.5	78.1	8.9	83.5	9.3	89.2	9.7		
68.8	8.1	73.3	8.5	78.2	8.9	83.6	9.3	89.3	9.7		
68.8	8.1	73.5	8.5	78.4	8.9	83.7	9.3	89.4	9.7		
69.0	8.1	73.6	8.5	78.5	8.9	83.8	9.3	89.6	9.7		
69.1	8.2	73.7	8.6	78.6	9.0	83.9	9.4	89.8	9.8		
69.2	8.2	73.8	8.6	78.8	9.0	84.1	9.4	89.9	9.8		
69.3	8.2	74.0	8.6	79.0	9.0	84.2	9.4	90.1	9.8		
69.4	8.2	74.0	8.6	79.0	9.0	84.4	9.4	90.3	9.8		
69.5	8.2	74.2	8.6	79.2	9.0	84.6	9.4	90.4	9.8		
69.6	8.2	74.3	8.6	79.4	9.0	84.7	9.4	90.6	9.8		
69.7	8.2	74.4	8.6	79.4	9.0	84.9	9.4	90.8	9.8		
69.9	8.2	74.5	8.6	79.5	9.0	85.0	9.4	90.8	9.8		
69.9	8.2	74.7	8.6	79.7	9.0	85.1	9.4	91.0	9.8		
70.1	8.2	74.8	8.6	79.8	9.0	85.3	9.4	91.2	9.8		
70.3	8.3	74.9	8.7	80.0	9.1	85.5	9.5	91.3	9.9		
70.3	8.3	75.1	8.7	80.1	9.1	85.5	9.5	91.5	9.9		
70.4	8.3	75.2	8.7	80.2	9.1	85.7	9.5	91.6	9.9		
70.6	8.3	75.2	8.7	80.3	9.1	85.8	9.5	91.8	9.9		
70.7	8.3	75.4	8.7	80.5	9.1	86.0	9.5	91.9	9.9		
70.7	8.3	75.5	8.7	80.6	9.1	86.1	9.5	92.1	9.9		
70.9	8.3	75.6	8.7	80.7	9.1	86.2	9.5	92.3	9.9		
71.0	8.3	75.8	8.7	80.9	9.1	86.4	9.5	92.3	9.9		
71.1	8.3	75.9	8.7	81.0	9.1	86.5	9.5	92.6	9.9		
71.2	8.3	76.0	8.7	81.1	9.1	86.7	9.5	92.8	9.9		
71.4	8.4	76.1	8.8	81.3	9.2	86.9	9.6	92.8	10.0		

Sample W0

N	mm	0.0	0.4	0.4	0.8	1.9	1.3	5.2	1.7	11.1	2.1
0.0	0.0	0.0	0.4	0.4	0.9	1.9	1.3	5.3	1.7	11.3	2.1
0.0	0.0	0.0	0.4	0.4	0.9	2.0	1.3	5.4	1.7	11.5	2.2
0.0	0.0	0.1	0.4	0.4	0.9	2.0	1.3	5.5	1.7	11.6	2.2
0.0	0.0	0.0	0.5	0.5	0.9	2.1	1.3	5.6	1.7	11.9	2.2
0.0	0.0	0.0	0.5	0.5	0.9	2.2	1.3	5.6	1.8	12.0	2.2
0.0	0.0	0.0	0.5	0.5	0.9	2.2	1.3	5.7	1.8	12.3	2.2
0.0	0.1	0.0	0.5	0.5	0.9	2.3	1.3	5.8	1.8	12.5	2.2
-0.1	0.1	0.0	0.5	0.6	0.9	2.4	1.4	6.0	1.8	12.7	2.2
0.0	0.1	0.0	0.5	0.6	0.9	2.5	1.4	6.1	1.8	12.9	2.2
0.0	0.1	0.0	0.5	0.6	0.9	2.5	1.4	6.2	1.8	13.2	2.2
-0.1	0.1	0.0	0.5	0.6	1.0	2.6	1.4	6.3	1.8	13.4	2.2
0.0	0.1	0.0	0.5	0.6	1.0	2.6	1.4	6.4	1.8	13.6	2.3
0.0	0.1	0.0	0.5	0.6	1.0	2.7	1.4	6.5	1.8	13.8	2.3
0.0	0.1	0.0	0.6	0.7	1.0	2.8	1.4	6.6	1.8	14.0	2.3
0.0	0.1	0.0	0.6	0.7	1.0	2.9	1.4	6.7	1.9	14.3	2.3
0.0	0.1	0.1	0.6	0.7	1.0	2.9	1.4	6.8	1.9	14.5	2.3
0.0	0.2	0.1	0.6	0.7	1.0	3.0	1.4	7.0	1.9	14.8	2.3
0.0	0.2	0.1	0.6	0.8	1.0	3.1	1.5	7.1	1.9	15.0	2.3
0.0	0.2	0.1	0.6	0.8	1.0	3.2	1.5	7.1	1.9	15.2	2.3
0.0	0.2	0.1	0.6	0.8	1.0	3.3	1.5	7.3	1.9	15.5	2.3
0.0	0.2	0.1	0.6	0.9	1.1	3.4	1.5	7.5	1.9	15.7	2.3
0.0	0.2	0.1	0.6	0.9	1.1	3.4	1.5	7.6	1.9	16.0	2.4
0.0	0.2	0.1	0.6	0.9	1.1	3.5	1.5	7.7	1.9	16.2	2.4
0.0	0.2	0.1	0.7	1.0	1.1	3.6	1.5	7.8	1.9	16.5	2.4
0.0	0.2	0.2	0.7	1.0	1.1	3.7	1.5	8.0	2.0	16.7	2.4
0.0	0.2	0.2	0.7	1.0	1.1	3.8	1.5	8.1	2.0	16.9	2.4
0.0	0.3	0.2	0.7	1.1	1.1	3.9	1.5	8.3	2.0	17.2	2.4
0.0	0.3	0.2	0.7	1.1	1.1	4.0	1.6	8.5	2.0	17.5	2.4
0.0	0.3	0.2	0.7	1.1	1.1	4.0	1.6	8.6	2.0	17.7	2.4
0.0	0.3	0.2	0.7	1.2	1.1	4.1	1.6	8.7	2.0	18.0	2.4
0.0	0.3	0.2	0.7	1.3	1.2	4.2	1.6	8.9	2.0	18.2	2.4
0.0	0.3	0.2	0.7	1.3	1.2	4.3	1.6	9.1	2.0	18.4	2.5
0.0	0.3	0.2	0.7	1.3	1.2	4.4	1.6	9.2	2.0	18.7	2.5
0.0	0.3	0.2	0.8	1.4	1.2	4.4	1.6	9.4	2.0	19.0	2.5
0.0	0.3	0.3	0.8	1.5	1.2	4.5	1.6	9.6	2.1	19.2	2.5
0.0	0.3	0.3	0.8	1.5	1.2	4.6	1.6	9.7	2.1	19.5	2.5
0.0	0.4	0.3	0.8	1.5	1.2	4.7	1.6	10.0	2.1	19.8	2.5
0.0	0.4	0.3	0.8	1.6	1.2	4.8	1.7	10.2	2.1	20.1	2.5
0.0	0.4	0.3	0.8	1.7	1.2	4.9	1.7	10.3	2.1	20.4	2.5
0.0	0.4	0.4	0.8	1.7	1.2	4.9	1.7	10.5	2.1	20.7	2.5
0.0	0.4	0.3	0.8	1.8	1.3	5.0	1.7	10.7	2.1	20.9	2.5
0.0	0.4	0.3	0.8	1.8	1.3	5.1	1.7	10.9	2.1	21.2	2.6

21.5	2.6	38.4	3.0	58.8	3.5	84.0	3.9	115.2	4.4	150.5	4.8
21.8	2.6	38.8	3.0	59.4	3.5	84.6	3.9	115.8	4.4	151.4	4.8
22.1	2.6	39.3	3.0	59.9	3.5	85.2	3.9	116.7	4.4	152.2	4.8
22.4	2.6	39.6	3.0	60.3	3.5	86.0	3.9	117.6	4.4	153.1	4.8
22.7	2.6	40.1	3.1	60.9	3.5	86.5	4.0	118.2	4.4	154.0	4.9
23.0	2.6	40.5	3.1	61.4	3.5	87.2	4.0	118.9	4.4	154.7	4.9
23.4	2.6	40.8	3.1	61.9	3.5	87.9	4.0	119.7	4.4	155.6	4.9
23.7	2.6	41.3	3.1	62.4	3.5	88.4	4.0	120.5	4.4	156.6	4.9
24.1	2.6	41.8	3.1	62.9	3.5	89.1	4.0	121.2	4.4	157.2	4.9
24.4	2.7	42.1	3.1	63.5	3.6	89.7	4.0	122.1	4.5	158.2	4.9
24.8	2.7	42.6	3.1	64.0	3.6	90.3	4.0	122.9	4.5	159.2	4.9
25.1	2.7	43.0	3.1	64.5	3.6	90.9	4.0	123.5	4.5	159.9	4.9
25.5	2.7	43.4	3.1	65.1	3.6	91.6	4.0	124.4	4.5	160.7	4.9
25.8	2.7	43.8	3.1	65.4	3.6	92.3	4.0	125.2	4.5	161.6	4.9
26.2	2.7	44.3	3.2	66.1	3.6	92.9	4.1	125.8	4.5	162.6	5.0
26.6	2.7	44.8	3.2	66.7	3.6	93.6	4.1	126.7	4.5	163.4	5.0
26.9	2.7	45.2	3.2	67.1	3.6	94.3	4.1	127.5	4.5	164.4	5.0
27.3	2.7	45.6	3.2	67.7	3.6	94.9	4.1	128.2	4.5	165.3	5.0
27.7	2.7	46.1	3.2	68.2	3.6	95.7	4.1	129.0	4.5	166.0	5.0
28.1	2.8	46.5	3.2	68.8	3.7	96.3	4.1	129.7	4.6	167.0	5.0
28.4	2.8	47.0	3.2	69.3	3.7	96.9	4.1	130.6	4.6	168.1	5.0
28.8	2.8	47.4	3.2	69.9	3.7	97.7	4.1	131.3	4.6	168.7	5.0
29.2	2.8	47.8	3.2	70.5	3.7	98.4	4.1	132.1	4.6	169.8	5.0
29.6	2.8	48.3	3.2	71.0	3.7	99.0	4.1	132.9	4.6	170.7	5.0
30.0	2.8	48.8	3.3	71.6	3.7	99.7	4.2	133.6	4.6	171.6	5.1
30.4	2.8	49.2	3.3	72.2	3.7	100.4	4.2	134.5	4.6	172.3	5.1
30.8	2.8	49.7	3.3	72.7	3.7	101.1	4.2	135.3	4.6	173.3	5.1
31.2	2.8	50.2	3.3	73.3	3.7	101.8	4.2	135.9	4.6	174.3	5.1
31.5	2.8	50.7	3.3	73.9	3.7	102.5	4.2	136.8	4.6	175.1	5.1
32.0	2.9	51.1	3.3	74.4	3.8	103.3	4.2	137.7	4.7	176.2	5.1
32.4	2.9	51.6	3.3	74.9	3.8	103.9	4.2	138.3	4.7	177.1	5.1
32.8	2.9	52.1	3.3	75.6	3.8	104.7	4.2	139.1	4.7	177.8	5.1
33.2	2.9	52.5	3.3	76.2	3.8	105.5	4.2	139.9	4.7	178.9	5.1
33.6	2.9	53.1	3.3	76.6	3.8	106.1	4.2	140.8	4.7	179.9	5.1
34.0	2.9	53.5	3.4	77.3	3.8	106.9	4.3	141.5	4.7	180.6	5.2
34.3	2.9	53.9	3.4	78.0	3.8	107.7	4.3	142.3	4.7	181.6	5.2
34.8	2.9	54.5	3.4	78.4	3.8	108.3	4.3	143.3	4.7	182.6	5.2
35.2	2.9	54.9	3.4	79.1	3.8	109.0	4.3	143.9	4.7	183.5	5.2
35.5	2.9	55.4	3.4	79.8	3.8	109.9	4.3	144.8	4.7	184.3	5.2
36.0	3.0	55.8	3.4	80.2	3.9	110.6	4.3	145.7	4.8	185.3	5.2
36.4	3.0	56.4	3.4	80.9	3.9	111.3	4.3	146.3	4.8	186.3	5.2
36.8	3.0	57.0	3.4	81.6	3.9	112.1	4.3	147.3	4.8	187.1	5.2
37.2	3.0	57.3	3.4	82.1	3.9	112.9	4.3	148.1	4.8	188.2	5.2
37.6	3.0	57.9	3.4	82.7	3.9	113.5	4.3	148.9	4.8	189.3	5.2
38.0	3.0	58.4	3.5	83.4	3.9	114.5	4.4	149.7	4.8	190.0	5.3

191.1	5.3	234.9	5.7	279.3	6.2	321.7	6.6	359.4	7.1	390.6	7.5
192.1	5.3	235.9	5.7	280.5	6.2	322.4	6.6	359.7	7.1	391.3	7.5
192.8	5.3	237.1	5.7	281.5	6.2	323.3	6.6	360.8	7.1	391.9	7.5
193.9	5.3	237.9	5.7	282.3	6.2	324.4	6.6	361.6	7.1	392.4	7.5
194.9	5.3	239.0	5.8	283.3	6.2	325.1	6.7	362.2	7.1	393.2	7.6
195.8	5.3	240.1	5.8	284.4	6.2	326.1	6.7	362.8	7.1	393.6	7.6
196.7	5.3	240.9	5.8	285.3	6.2	327.1	6.7	363.7	7.1	394.5	7.6
197.7	5.3	242.0	5.8	286.2	6.2	327.7	6.7	364.5	7.1	395.2	7.6
198.8	5.3	243.1	5.8	287.2	6.2	328.7	6.7	365.1	7.1	395.5	7.6
199.7	5.4	243.8	5.8	288.3	6.3	329.7	6.7	365.9	7.2	396.2	7.6
200.7	5.4	244.9	5.8	289.0	6.3	330.4	6.7	366.8	7.2	396.9	7.6
201.8	5.4	246.0	5.8	290.2	6.3	331.3	6.7	367.3	7.2	397.4	7.6
202.4	5.4	247.0	5.8	291.2	6.3	332.1	6.7	368.2	7.2	397.9	7.6
203.7	5.4	247.8	5.8	291.9	6.3	333.1	6.7	369.1	7.2	398.6	7.6
204.7	5.4	248.8	5.9	293.1	6.3	333.8	6.8	369.5	7.2	399.2	7.7
205.4	5.4	249.9	5.9	294.1	6.3	334.7	6.8	370.4	7.2	399.8	7.7
206.5	5.4	250.8	5.9	294.8	6.3	335.7	6.8	371.1	7.2	400.4	7.7
207.5	5.4	251.9	5.9	295.8	6.3	336.4	6.8	371.8	7.2	401.1	7.7
208.4	5.4	253.0	5.9	296.9	6.3	337.4	6.8	372.4	7.2	401.4	7.7
209.4	5.5	253.7	5.9	297.8	6.4	338.4	6.8	373.2	7.3	402.3	7.7
210.4	5.5	254.8	5.9	298.6	6.4	338.8	6.8	373.9	7.3	402.9	7.7
211.4	5.5	256.0	5.9	299.6	6.4	339.9	6.8	374.5	7.3	403.2	7.7
212.3	5.5	256.7	5.9	300.7	6.4	340.9	6.8	375.2	7.3	403.9	7.7
213.3	5.5	257.7	5.9	301.4	6.4	341.5	6.8	376.2	7.3	404.6	7.7
214.4	5.5	258.8	6.0	302.5	6.4	342.4	6.9	376.6	7.3	405.0	7.8
215.2	5.5	259.8	6.0	303.6	6.4	343.1	6.9	377.4	7.3	405.5	7.8
216.4	5.5	260.7	6.0	304.3	6.4	344.1	6.9	378.2	7.3	406.1	7.8
217.4	5.5	261.6	6.0	305.3	6.4	344.8	6.9	378.6	7.3	406.8	7.8
218.2	5.5	262.8	6.0	306.4	6.4	345.7	6.9	379.5	7.3	407.2	7.8
219.2	5.6	263.6	6.0	307.0	6.5	346.6	6.9	380.2	7.4	407.8	7.8
220.3	5.6	264.8	6.0	308.0	6.5	347.3	6.9	380.8	7.4	408.5	7.8
221.2	5.6	265.8	6.0	309.0	6.5	348.2	6.9	381.4	7.4	408.7	7.8
222.1	5.6	266.6	6.0	310.0	6.5	349.1	6.9	382.1	7.4	409.5	7.8
223.2	5.6	267.7	6.0	310.7	6.5	349.6	6.9	382.9	7.4	410.2	7.8
224.2	5.6	268.7	6.1	311.6	6.5	350.6	7.0	383.5	7.4	410.5	7.9
225.0	5.6	269.5	6.1	312.7	6.5	351.5	7.0	384.1	7.4	411.0	7.9
226.1	5.6	270.6	6.1	313.4	6.5	352.1	7.0	385.0	7.4	411.7	7.9
227.2	5.6	271.6	6.1	314.5	6.5	352.8	7.0	385.4	7.4	412.1	7.9
227.9	5.6	272.6	6.1	315.5	6.5	353.7	7.0	386.2	7.4	412.6	7.9
229.2	5.7	273.5	6.1	316.1	6.6	354.5	7.0	386.9	7.5	413.1	7.9
230.2	5.7	274.4	6.1	317.1	6.6	355.1	7.0	387.3	7.5	413.8	7.9
231.0	5.7	275.6	6.1	318.2	6.6	356.1	7.0	388.1	7.5	414.1	7.9
232.0	5.7	276.4	6.1	318.8	6.6	356.9	7.0	388.8	7.5	414.7	7.9
233.1	5.7	277.5	6.1	319.8	6.6	357.5	7.0	389.3	7.5	415.4	7.9
234.0	5.7	278.6	6.2	320.7	6.6	358.4	7.1	389.9	7.5	415.7	8.0

416.4	8.0	435.3	8.4	451.2	8.8	465.8	9.2	479.2	9.6	492.1	10.0
417.0	8.0	435.5	8.4	451.8	8.8	466.3	9.2	479.6	9.6	492.2	10.0
417.2	8.0	436.1	8.4	452.1	8.8	466.6	9.2	479.8	9.6	492.6	10.0
417.8	8.0	436.6	8.4	452.5	8.8	466.8	9.2	480.1	9.6		
418.4	8.0	436.9	8.4	452.8	8.8	467.2	9.2	480.6	9.6		
418.8	8.0	437.2	8.4	453.1	8.8	467.7	9.2	480.8	9.6		
419.3	8.0	437.7	8.4	453.7	8.8	467.8	9.2	481.3	9.6		
419.7	8.0	438.3	8.4	453.9	8.8	468.3	9.2	481.6	9.6		
420.5	8.0	438.4	8.4	454.4	8.8	468.8	9.2	481.7	9.6		
420.8	8.1	439.0	8.5	454.9	8.9	468.8	9.3	482.2	9.7		
421.3	8.1	439.6	8.5	455.0	8.9	469.4	9.3	482.6	9.7		
421.9	8.1	439.8	8.5	455.6	8.9	469.8	9.3	482.7	9.7		
422.3	8.1	440.3	8.5	456.0	8.9	470.0	9.3	483.1	9.7		
422.9	8.1	440.8	8.5	456.1	8.9	470.3	9.3	483.4	9.7		
423.5	8.1	441.0	8.5	456.7	8.9	470.7	9.3	483.8	9.7		
423.7	8.1	441.5	8.5	456.9	8.9	471.0	9.3	484.0	9.7		
424.3	8.1	442.0	8.5	457.3	8.9	471.3	9.3	484.3	9.7		
424.8	8.1	442.4	8.5	457.6	8.9	471.6	9.3	484.8	9.7		
425.2	8.1	442.6	8.5	458.0	8.9	472.2	9.3	484.9	9.7		
425.6	8.2	443.1	8.6	458.5	9.0	472.3	9.4	485.4	9.8		
426.0	8.2	443.6	8.6	458.8	9.0	472.7	9.4	485.8	9.8		
426.7	8.2	443.8	8.6	459.2	9.0	473.2	9.4	485.9	9.8		
427.0	8.2	444.4	8.6	459.7	9.0	473.1	9.4	486.4	9.8		
427.5	8.2	444.9	8.6	459.8	9.0	473.7	9.4	486.8	9.8		
428.1	8.2	445.0	8.6	460.4	9.0	474.1	9.4	486.8	9.8		
428.3	8.2	445.6	8.6	460.7	9.0	474.2	9.4	487.2	9.8		
429.0	8.2	446.1	8.6	460.9	9.0	474.6	9.4	487.6	9.8		
429.6	8.2	446.2	8.6	461.3	9.0	475.0	9.4	487.9	9.8		
429.7	8.2	446.8	8.6	461.7	9.0	475.2	9.4	488.1	9.8		
430.3	8.3	447.1	8.7	462.0	9.1	475.7	9.5	488.5	9.9		
430.8	8.3	447.6	8.7	462.2	9.1	475.9	9.5	489.0	9.9		
431.1	8.3	447.8	8.7	462.7	9.1	476.5	9.5	489.0	9.9		
431.6	8.3	448.2	8.7	463.1	9.1	476.5	9.5	489.5	9.9		
432.0	8.3	448.7	8.7	463.4	9.1	477.0	9.5	489.9	9.9		
432.6	8.3	449.0	8.7	463.8	9.1	477.4	9.5	489.9	9.9		
432.9	8.3	449.4	8.7	464.4	9.1	477.5	9.5	490.4	9.9		
433.5	8.3	450.0	8.7	464.3	9.1	478.0	9.5	490.9	9.9		
434.0	8.3	450.1	8.7	464.9	9.1	478.4	9.5	490.9	9.9		
434.2	8.3	450.6	8.7	465.3	9.1	478.5	9.5	491.3	9.9		
434.8	8.4	451.1	8.8	465.5	9.2	478.9	9.6	491.6	10.0		

Sample N1

N	mm	0.3	0.2	0.6	0.4	1.0	0.6	1.4	0.8	2.0	1.1
0.0	0.0	0.4	0.2	0.7	0.4	1.0	0.6	1.5	0.9	2.0	1.1
0.0	0.0	0.4	0.2	0.6	0.4	1.0	0.6	1.4	0.9	2.0	1.1
0.0	0.0	0.3	0.2	0.7	0.4	1.0	0.6	1.5	0.9	2.0	1.1
0.0	0.0	0.4	0.2	0.6	0.4	1.0	0.7	1.5	0.9	2.0	1.1
0.0	0.0	0.4	0.2	0.7	0.4	1.1	0.7	1.5	0.9	2.1	1.1
0.0	0.0	0.4	0.2	0.7	0.4	1.0	0.7	1.5	0.9	2.0	1.1
0.1	0.0	0.4	0.2	0.7	0.5	1.1	0.7	1.5	0.9	2.1	1.1
0.1	0.0	0.4	0.2	0.7	0.5	1.1	0.7	1.5	0.9	2.1	1.1
0.0	0.0	0.4	0.2	0.7	0.5	1.1	0.7	1.5	0.9	2.1	1.1
0.1	0.0	0.4	0.3	0.7	0.5	1.1	0.7	1.6	0.9	2.1	1.1
0.1	0.0	0.4	0.3	0.7	0.5	1.1	0.7	1.6	0.9	2.1	1.1
0.1	0.0	0.4	0.3	0.7	0.5	1.1	0.7	1.6	0.9	2.1	1.1
0.1	0.1	0.4	0.3	0.7	0.5	1.1	0.7	1.6	0.9	2.1	1.1
0.1	0.1	0.4	0.3	0.8	0.5	1.1	0.7	1.6	0.9	2.2	1.1
0.1	0.1	0.5	0.3	0.7	0.5	1.1	0.7	1.6	0.9	2.2	1.1
0.1	0.1	0.4	0.3	0.8	0.5	1.2	0.7	1.6	0.9	2.2	1.1
0.2	0.1	0.3	0.3	0.8	0.5	1.2	0.7	1.6	0.9	2.2	1.1
0.2	0.1	0.5	0.3	0.8	0.5	1.2	0.7	1.6	0.9	2.2	1.2
0.1	0.1	0.3	0.3	0.8	0.5	1.2	0.7	1.6	0.9	2.3	1.2
0.2	0.1	0.5	0.3	0.8	0.5	1.2	0.7	1.7	0.9	2.3	1.2
0.2	0.1	0.4	0.3	0.8	0.5	1.2	0.7	1.7	1.0	2.3	1.2
0.2	0.1	0.5	0.3	0.8	0.5	1.2	0.7	1.7	1.0	2.3	1.2
0.2	0.1	0.4	0.3	0.8	0.5	1.2	0.7	1.7	1.0	2.3	1.2
0.2	0.1	0.5	0.3	0.8	0.5	1.2	0.8	1.7	1.0	2.3	1.2
0.2	0.1	0.5	0.3	0.8	0.5	1.3	0.8	1.7	1.0	2.3	1.2
0.2	0.1	0.5	0.3	0.8	0.5	1.2	0.8	1.8	1.0	2.4	1.2
0.2	0.1	0.5	0.3	0.9	0.6	1.3	0.8	1.8	1.0	2.4	1.2
0.2	0.1	0.5	0.3	0.9	0.6	1.3	0.8	1.8	1.0	2.4	1.2
0.2	0.1	0.5	0.3	0.9	0.6	1.3	0.8	1.8	1.0	2.5	1.2
0.2	0.1	0.5	0.4	0.9	0.6	1.3	0.8	1.8	1.0	2.4	1.2
0.2	0.1	0.6	0.4	0.9	0.6	1.3	0.8	1.8	1.0	2.5	1.2
0.2	0.1	0.4	0.4	0.9	0.6	1.3	0.8	1.9	1.0	2.5	1.2
0.3	0.2	0.6	0.4	0.9	0.6	1.3	0.8	1.9	1.0	2.5	1.2
0.3	0.2	0.5	0.4	1.0	0.6	1.3	0.8	1.9	1.0	2.5	1.2
0.3	0.2	0.6	0.4	1.0	0.6	1.4	0.8	1.9	1.0	2.5	1.2
0.3	0.2	0.5	0.4	1.0	0.6	1.4	0.8	1.9	1.0	2.6	1.2
0.3	0.2	0.6	0.4	0.9	0.6	1.4	0.8	1.9	1.0	2.6	1.2
0.3	0.2	0.6	0.4	1.0	0.6	1.4	0.8	1.9	1.0	2.6	1.3
0.3	0.2	0.6	0.4	1.0	0.6	1.4	0.8	1.9	1.0	2.6	1.3
0.3	0.2	0.6	0.4	1.0	0.6	1.4	0.8	1.9	1.0	2.6	1.3
0.3	0.2	0.6	0.4	1.0	0.6	1.4	0.8	1.9	1.1	2.6	1.3
0.3	0.2	0.6	0.4	1.0	0.6	1.4	0.8	2.0	1.1	2.7	1.3

2.7	1.3	3.5	1.5	4.4	1.7	5.4	2.0	6.4	2.2	7.5	2.4
2.7	1.3	3.4	1.5	4.4	1.7	5.4	2.0	6.4	2.2	7.5	2.4
2.7	1.3	3.5	1.5	4.5	1.7	5.4	2.0	6.4	2.2	7.5	2.4
2.7	1.3	3.5	1.5	4.4	1.7	5.4	2.0	6.4	2.2	7.6	2.4
2.7	1.3	3.5	1.5	4.5	1.8	5.5	2.0	6.5	2.2	7.6	2.4
2.7	1.3	3.6	1.5	4.5	1.8	5.5	2.0	6.5	2.2	7.6	2.4
2.8	1.3	3.5	1.5	4.6	1.8	5.6	2.0	6.5	2.2	7.6	2.4
2.8	1.3	3.6	1.5	4.6	1.8	5.5	2.0	6.5	2.2	7.6	2.4
2.8	1.3	3.6	1.5	4.6	1.8	5.6	2.0	6.6	2.2	7.7	2.4
2.8	1.3	3.7	1.5	4.6	1.8	5.5	2.0	6.6	2.2	7.7	2.4
2.8	1.3	3.7	1.6	4.6	1.8	5.6	2.0	6.6	2.2	7.8	2.5
2.8	1.3	3.7	1.6	4.6	1.8	5.6	2.0	6.6	2.2	7.7	2.5
2.9	1.3	3.7	1.6	4.7	1.8	5.6	2.0	6.6	2.2	7.8	2.5
2.9	1.3	3.7	1.6	4.7	1.8	5.7	2.0	6.6	2.2	7.8	2.5
2.9	1.3	3.8	1.6	4.7	1.8	5.7	2.0	6.7	2.2	7.8	2.5
2.9	1.4	3.8	1.6	4.8	1.8	5.7	2.0	6.7	2.3	7.9	2.5
2.9	1.4	3.8	1.6	4.8	1.8	5.7	2.0	6.8	2.3	7.9	2.5
3.0	1.4	3.8	1.6	4.8	1.8	5.7	2.0	6.8	2.3	8.0	2.5
2.9	1.4	3.8	1.6	4.8	1.8	5.8	2.0	6.8	2.3	8.0	2.5
3.0	1.4	3.9	1.6	4.9	1.8	5.8	2.0	6.8	2.3	8.0	2.5
3.0	1.4	3.9	1.6	4.9	1.8	5.8	2.1	6.8	2.3	8.0	2.5
3.0	1.4	3.9	1.6	4.9	1.8	5.8	2.1	6.9	2.3	8.1	2.5
3.1	1.4	3.9	1.6	4.9	1.8	5.8	2.1	6.9	2.3	8.1	2.5
3.0	1.4	3.9	1.6	4.9	1.8	5.9	2.1	6.9	2.3	8.1	2.5
3.1	1.4	4.0	1.6	5.0	1.8	5.9	2.1	6.9	2.3	8.1	2.5
3.1	1.4	4.0	1.6	5.0	1.9	5.9	2.1	7.0	2.3	8.2	2.5
3.1	1.4	4.0	1.6	4.9	1.9	5.9	2.1	7.0	2.3	8.2	2.5
3.1	1.4	4.0	1.6	5.0	1.9	6.0	2.1	7.0	2.3	8.2	2.5
3.2	1.4	4.1	1.6	5.0	1.9	6.0	2.1	7.0	2.3	8.3	2.5
3.1	1.4	4.1	1.6	5.1	1.9	6.0	2.1	7.1	2.3	8.3	2.5
3.2	1.4	4.1	1.7	5.1	1.9	6.0	2.1	7.1	2.3	8.3	2.6
3.2	1.4	4.1	1.7	5.1	1.9	6.0	2.1	7.1	2.3	8.4	2.6
3.2	1.4	4.2	1.7	5.1	1.9	6.0	2.1	7.2	2.3	8.4	2.6
3.3	1.4	4.2	1.7	5.1	1.9	6.1	2.1	7.1	2.3	8.4	2.6
3.2	1.4	4.2	1.7	5.2	1.9	6.1	2.1	7.2	2.3	8.4	2.6
3.3	1.5	4.2	1.7	5.2	1.9	6.1	2.1	7.2	2.4	8.5	2.6
3.3	1.5	4.2	1.7	5.2	1.9	6.1	2.1	7.3	2.4	8.5	2.6
3.3	1.5	4.3	1.7	5.2	1.9	6.1	2.1	7.3	2.4	8.5	2.6
3.3	1.5	4.3	1.7	5.3	1.9	6.2	2.1	7.3	2.4	8.6	2.6
3.3	1.5	4.3	1.7	5.3	1.9	6.2	2.1	7.3	2.4	8.6	2.6
3.4	1.5	4.3	1.7	5.3	1.9	6.2	2.2	7.3	2.4	8.6	2.6
3.4	1.5	4.3	1.7	5.3	1.9	6.2	2.2	7.4	2.4	8.7	2.6
3.4	1.5	4.4	1.7	5.3	1.9	6.3	2.2	7.4	2.4	8.7	2.6
3.4	1.5	4.4	1.7	5.4	1.9	6.3	2.2	7.4	2.4	8.7	2.6
3.4	1.5	4.4	1.7	5.4	1.9	6.3	2.2	7.4	2.4	8.8	2.6

8.8	2.6	10.4	2.9	12.6	3.1	15.2	3.3	18.5	3.5	21.8	3.8
8.8	2.6	10.4	2.9	12.6	3.1	15.3	3.3	18.5	3.5	21.9	3.8
8.8	2.6	10.5	2.9	12.7	3.1	15.2	3.3	18.6	3.5	22.0	3.8
8.8	2.6	10.5	2.9	12.7	3.1	15.4	3.3	18.7	3.5	22.0	3.8
8.9	2.6	10.5	2.9	12.8	3.1	15.4	3.3	18.7	3.5	22.1	3.8
8.9	2.7	10.6	2.9	12.8	3.1	15.5	3.3	18.8	3.6	22.2	3.8
9.0	2.7	10.6	2.9	12.9	3.1	15.6	3.3	18.9	3.6	22.3	3.8
9.0	2.7	10.7	2.9	13.0	3.1	15.6	3.3	19.0	3.6	22.3	3.8
9.0	2.7	10.7	2.9	13.0	3.1	15.7	3.3	19.1	3.6	22.4	3.8
9.1	2.7	10.8	2.9	13.1	3.1	15.8	3.3	19.1	3.6	22.5	3.8
9.1	2.7	10.8	2.9	13.1	3.1	15.8	3.4	19.1	3.6	22.5	3.8
9.1	2.7	10.9	2.9	13.2	3.1	15.9	3.4	19.2	3.6	22.6	3.8
9.2	2.7	10.9	2.9	13.2	3.1	16.0	3.4	19.3	3.6	22.7	3.8
9.2	2.7	11.0	2.9	13.3	3.1	16.0	3.4	19.4	3.6	22.8	3.8
9.2	2.7	11.0	2.9	13.4	3.1	16.2	3.4	19.4	3.6	22.8	3.8
9.2	2.7	11.0	2.9	13.4	3.2	16.1	3.4	19.6	3.6	22.9	3.8
9.3	2.7	11.1	2.9	13.4	3.2	16.2	3.4	19.6	3.6	23.0	3.8
9.3	2.7	11.1	2.9	13.5	3.2	16.3	3.4	19.7	3.6	23.0	3.8
9.3	2.7	11.2	2.9	13.6	3.2	16.4	3.4	19.8	3.6	23.1	3.8
9.4	2.7	11.2	2.9	13.6	3.2	16.5	3.4	19.9	3.6	23.1	3.8
9.4	2.7	11.3	3.0	13.7	3.2	16.5	3.4	19.9	3.6	23.1	3.9
9.5	2.7	11.3	3.0	13.7	3.2	16.6	3.4	20.0	3.6	23.2	3.9
9.5	2.7	11.3	3.0	13.8	3.2	16.7	3.4	20.0	3.6	23.1	3.9
9.5	2.7	11.4	3.0	13.9	3.2	16.8	3.4	20.1	3.6	23.1	3.9
9.5	2.7	11.5	3.0	14.0	3.2	16.9	3.4	20.2	3.6	23.1	3.9
9.6	2.8	11.5	3.0	14.0	3.2	16.9	3.4	20.3	3.7	23.2	3.9
9.6	2.8	11.6	3.0	14.0	3.2	17.0	3.4	20.4	3.7	23.2	3.9
9.7	2.8	11.6	3.0	14.1	3.2	17.1	3.4	20.4	3.7	23.1	3.9
9.7	2.8	11.6	3.0	14.2	3.2	17.1	3.4	20.5	3.7	23.3	3.9
9.7	2.8	11.7	3.0	14.2	3.2	17.2	3.4	20.6	3.7	23.2	3.9
9.8	2.8	11.8	3.0	14.3	3.2	17.3	3.5	20.6	3.7	23.3	3.9
9.8	2.8	11.8	3.0	14.3	3.2	17.4	3.5	20.7	3.7	23.3	3.9
9.9	2.8	11.9	3.0	14.4	3.2	17.5	3.5	20.8	3.7	23.4	3.9
9.9	2.8	11.9	3.0	14.5	3.2	17.5	3.5	20.9	3.7	23.5	3.9
9.9	2.8	12.0	3.0	14.5	3.2	17.6	3.5	21.0	3.7	23.5	3.9
10.0	2.8	12.0	3.0	14.6	3.3	17.7	3.5	21.1	3.7	23.6	3.9
10.0	2.8	12.1	3.0	14.6	3.3	17.7	3.5	21.1	3.7	23.6	3.9
10.1	2.8	12.2	3.0	14.7	3.3	17.8	3.5	21.2	3.7	23.6	3.9
10.1	2.8	12.2	3.0	14.7	3.3	17.9	3.5	21.3	3.7	23.7	3.9
10.1	2.8	12.3	3.1	14.8	3.3	18.0	3.5	21.4	3.7	23.8	3.9
10.2	2.8	12.3	3.1	14.9	3.3	18.1	3.5	21.4	3.7	23.8	4.0
10.2	2.8	12.4	3.1	14.9	3.3	18.1	3.5	21.5	3.7	23.9	4.0
10.3	2.8	12.4	3.1	15.0	3.3	18.2	3.5	21.6	3.7	24.0	4.0
10.3	2.8	12.5	3.1	15.1	3.3	18.3	3.5	21.6	3.7	24.1	4.0
10.3	2.8	12.5	3.1	15.1	3.3	18.3	3.5	21.7	3.7	24.1	4.0

24.2	4.0	26.3	4.2	27.5	4.4	29.8	4.6	34.8	4.8	39.7	5.0
24.3	4.0	26.3	4.2	27.6	4.4	29.8	4.6	34.8	4.8	39.9	5.0
24.3	4.0	26.4	4.2	27.6	4.4	29.8	4.6	35.0	4.8	40.0	5.0
24.4	4.0	26.4	4.2	27.7	4.4	30.0	4.6	35.2	4.8		
24.4	4.0	26.4	4.2	27.8	4.4	30.2	4.6	35.3	4.8		
24.5	4.0	26.5	4.2	27.9	4.4	30.3	4.6	35.4	4.8		
24.5	4.0	26.5	4.2	28.0	4.4	30.5	4.6	35.6	4.8		
24.5	4.0	26.5	4.2	28.1	4.4	30.5	4.6	35.7	4.8		
24.5	4.0	26.5	4.2	28.1	4.4	30.7	4.6	35.8	4.8		
24.6	4.0	26.6	4.2	28.0	4.4	30.8	4.6	36.0	4.8		
24.7	4.0	26.7	4.2	28.0	4.4	30.9	4.6	36.1	4.8		
24.9	4.0	26.8	4.2	27.9	4.4	31.1	4.6	36.1	4.8		
24.9	4.0	27.0	4.2	27.9	4.4	31.2	4.6	36.3	4.8		
25.0	4.0	27.1	4.2	27.8	4.4	31.4	4.6	36.4	4.8		
25.2	4.0	27.2	4.2	27.8	4.4	31.5	4.6	36.5	4.8		
25.3	4.1	27.3	4.3	27.9	4.5	31.5	4.7	36.7	4.9		
25.4	4.1	27.4	4.3	28.0	4.5	31.7	4.7	36.8	4.9		
25.4	4.1	27.5	4.3	28.1	4.5	31.9	4.7	36.9	4.9		
25.4	4.1	27.6	4.3	28.2	4.5	32.1	4.7	37.1	4.9		
25.5	4.1	27.7	4.3	28.3	4.5	32.2	4.7	37.2	4.9		
25.5	4.1	27.7	4.3	28.4	4.5	32.4	4.7	37.3	4.9		
25.5	4.1	27.7	4.3	28.5	4.5	32.5	4.7	37.4	4.9		
25.7	4.1	27.5	4.3	28.6	4.5	32.6	4.7	37.6	4.9		
25.7	4.1	27.4	4.3	28.7	4.5	32.7	4.7	37.7	4.9		
25.7	4.1	27.3	4.3	28.7	4.5	32.9	4.7	37.7	4.9		
25.7	4.1	27.3	4.3	28.7	4.5	32.9	4.7	37.9	4.9		
25.7	4.1	27.2	4.3	28.5	4.5	33.1	4.7	38.0	4.9		
25.8	4.1	27.0	4.3	28.6	4.5	33.2	4.7	38.0	4.9		
25.8	4.1	26.9	4.3	28.7	4.5	33.3	4.7	38.2	4.9		
25.9	4.1	26.8	4.3	28.8	4.5	33.5	4.7	38.3	4.9		
26.0	4.1	26.8	4.3	28.9	4.5	33.6	4.7	38.5	4.9		
25.9	4.1	27.0	4.3	29.1	4.5	33.7	4.7	38.6	4.9		
26.0	4.1	27.0	4.3	29.2	4.5	33.9	4.7	38.8	4.9		
26.0	4.1	27.1	4.3	29.4	4.5	34.0	4.7	38.9	4.9		
26.0	4.1	27.2	4.3	29.5	4.5	34.2	4.7	39.0	4.9		
26.0	4.2	27.3	4.4	29.6	4.6	34.2	4.8	39.1	5.0		
26.0	4.2	27.4	4.4	29.6	4.6	34.4	4.8	39.3	5.0		
26.0	4.2	27.4	4.4	29.7	4.6	34.5	4.8	39.3	5.0		
26.1	4.2	27.5	4.4	29.8	4.6	34.6	4.8	39.5	5.0		
26.2	4.2	27.5	4.4	29.8	4.6	34.7	4.8	39.6	5.0		

Sample N2

N	mm	0.0	0.2	0.0	0.4	0.1	0.6	0.3	0.9	0.4	1.1
0.0	0.0	0.0	0.2	0.1	0.4	0.1	0.6	0.3	0.9	0.4	1.1
0.0	0.0	0.0	0.2	0.0	0.4	0.1	0.6	0.3	0.9	0.4	1.1
0.0	0.0	0.0	0.2	0.0	0.4	0.1	0.7	0.3	0.9	0.5	1.1
0.0	0.0	0.0	0.2	0.0	0.4	0.1	0.7	0.3	0.9	0.5	1.1
0.0	0.0	0.0	0.2	0.1	0.4	0.1	0.7	0.2	0.9	0.4	1.1
0.0	0.0	0.0	0.2	0.0	0.5	0.1	0.7	0.3	0.9	0.5	1.1
0.0	0.0	0.0	0.2	0.1	0.5	0.1	0.7	0.3	0.9	0.5	1.1
0.0	0.0	0.0	0.2	0.0	0.5	0.1	0.7	0.3	0.9	0.5	1.1
0.0	0.0	0.0	0.3	0.0	0.5	0.1	0.7	0.3	0.9	0.5	1.1
0.0	0.0	0.0	0.3	0.1	0.5	0.1	0.7	0.3	0.9	0.4	1.1
0.0	0.0	0.0	0.3	0.0	0.5	0.1	0.7	0.3	0.9	0.5	1.1
0.0	0.1	0.0	0.3	0.1	0.5	0.2	0.7	0.3	0.9	0.5	1.1
0.0	0.1	0.0	0.3	0.0	0.5	0.1	0.7	0.3	0.9	0.5	1.1
0.0	0.1	0.0	0.3	0.0	0.5	0.2	0.7	0.3	0.9	0.5	1.1
0.0	0.1	0.0	0.3	0.1	0.5	0.2	0.7	0.3	0.9	0.5	1.1
0.0	0.1	0.0	0.3	0.0	0.5	0.2	0.7	0.3	0.9	0.5	1.1
0.0	0.1	0.0	0.3	0.1	0.5	0.1	0.7	0.3	0.9	0.5	1.2
0.0	0.1	0.0	0.3	0.1	0.5	0.2	0.7	0.3	0.9	0.5	1.2
0.0	0.1	0.0	0.3	0.1	0.5	0.2	0.7	0.3	0.9	0.5	1.2
0.0	0.1	0.0	0.3	0.0	0.5	0.2	0.7	0.4	1.0	0.5	1.2
0.0	0.1	0.0	0.3	0.1	0.5	0.2	0.7	0.4	1.0	0.5	1.2
0.0	0.1	0.0	0.3	0.1	0.5	0.2	0.7	0.3	1.0	0.5	1.2
0.0	0.1	0.0	0.3	0.1	0.5	0.2	0.8	0.4	1.0	0.5	1.2
0.0	0.1	0.0	0.3	0.1	0.5	0.2	0.8	0.4	1.0	0.6	1.2
0.0	0.1	0.0	0.3	0.1	0.5	0.2	0.8	0.3	1.0	0.5	1.2
0.0	0.1	0.0	0.3	0.1	0.6	0.2	0.8	0.4	1.0	0.5	1.2
0.0	0.1	0.0	0.3	0.1	0.6	0.2	0.8	0.4	1.0	0.6	1.2
0.0	0.1	0.0	0.3	0.1	0.6	0.2	0.8	0.4	1.0	0.5	1.2
0.0	0.1	0.0	0.4	0.1	0.6	0.2	0.8	0.4	1.0	0.6	1.2
0.0	0.1	0.1	0.4	0.1	0.6	0.2	0.8	0.4	1.0	0.6	1.2
0.0	0.1	0.0	0.4	0.1	0.6	0.2	0.8	0.4	1.0	0.6	1.2
0.0	0.2	0.0	0.4	0.1	0.6	0.2	0.8	0.4	1.0	0.6	1.2
0.0	0.2	0.0	0.4	0.1	0.6	0.2	0.8	0.4	1.0	0.6	1.2
0.0	0.2	0.0	0.4	0.1	0.6	0.2	0.8	0.4	1.0	0.6	1.2
0.0	0.2	0.0	0.4	0.1	0.6	0.2	0.8	0.4	1.0	0.6	1.2
0.0	0.2	0.0	0.4	0.1	0.6	0.2	0.8	0.4	1.0	0.6	1.2
0.0	0.2	0.0	0.4	0.1	0.6	0.2	0.8	0.4	1.0	0.6	1.3
0.0	0.2	0.1	0.4	0.0	0.6	0.3	0.8	0.4	1.0	0.6	1.3
0.0	0.2	0.0	0.4	0.1	0.6	0.3	0.8	0.4	1.0	0.6	1.3
0.0	0.2	0.0	0.4	0.1	0.6	0.3	0.8	0.4	1.1	0.6	1.3
0.0	0.2	0.0	0.4	0.1	0.6	0.3	0.8	0.4	1.1	0.6	1.3
0.0	0.2	0.1	0.4	0.1	0.6	0.3	0.8	0.4	1.1	0.6	1.3

0.6	1.3	0.9	1.5	1.2	1.7	1.5	2.0	2.1	2.2	2.7	2.4
0.7	1.3	0.9	1.5	1.1	1.7	1.6	2.0	2.1	2.2	2.7	2.4
0.7	1.3	0.8	1.5	1.2	1.7	1.6	2.0	2.1	2.2	2.8	2.4
0.6	1.3	0.9	1.5	1.2	1.7	1.6	2.0	2.1	2.2	2.8	2.4
0.6	1.3	0.9	1.5	1.2	1.8	1.6	2.0	2.1	2.2	2.8	2.4
0.6	1.3	0.9	1.5	1.2	1.8	1.6	2.0	2.1	2.2	2.8	2.4
0.6	1.3	0.9	1.5	1.2	1.8	1.6	2.0	2.1	2.2	2.8	2.4
0.7	1.3	0.9	1.5	1.2	1.8	1.6	2.0	2.1	2.2	2.9	2.4
0.6	1.3	0.9	1.5	1.2	1.8	1.7	2.0	2.2	2.2	2.9	2.4
0.7	1.3	0.9	1.6	1.2	1.8	1.7	2.0	2.2	2.2	2.9	2.5
0.7	1.3	0.9	1.6	1.2	1.8	1.7	2.0	2.2	2.2	2.9	2.5
0.7	1.3	0.9	1.6	1.3	1.8	1.7	2.0	2.2	2.2	2.9	2.5
0.7	1.3	0.9	1.6	1.2	1.8	1.7	2.0	2.2	2.2	2.9	2.5
0.7	1.3	0.9	1.6	1.2	1.8	1.7	2.0	2.2	2.2	2.9	2.5
0.7	1.4	0.9	1.6	1.3	1.8	1.7	2.0	2.2	2.3	3.0	2.5
0.7	1.4	1.0	1.6	1.2	1.8	1.7	2.0	2.2	2.3	3.0	2.5
0.7	1.4	1.0	1.6	1.2	1.8	1.7	2.0	2.3	2.3	3.0	2.5
0.7	1.4	1.0	1.6	1.3	1.8	1.7	2.0	2.3	2.3	3.0	2.5
0.7	1.4	1.0	1.6	1.3	1.8	1.8	2.0	2.3	2.3	3.0	2.5
0.7	1.4	1.0	1.6	1.3	1.8	1.8	2.1	2.3	2.3	3.1	2.5
0.7	1.4	1.0	1.6	1.3	1.8	1.8	2.1	2.3	2.3	3.1	2.5
0.7	1.4	1.0	1.6	1.3	1.8	1.8	2.1	2.4	2.3	3.1	2.5
0.7	1.4	1.0	1.6	1.3	1.8	1.8	2.1	2.3	2.3	3.1	2.5
0.7	1.4	1.0	1.6	1.3	1.8	1.8	2.1	2.4	2.3	3.1	2.5
0.7	1.4	1.0	1.6	1.3	1.9	1.8	2.1	2.4	2.3	3.1	2.5
0.7	1.4	1.0	1.6	1.4	1.9	1.8	2.1	2.4	2.3	3.2	2.5
0.7	1.4	1.0	1.6	1.4	1.9	1.8	2.1	2.4	2.3	3.2	2.5
0.8	1.4	1.0	1.6	1.4	1.9	1.9	2.1	2.4	2.3	3.2	2.5
0.8	1.4	1.0	1.6	1.4	1.9	1.9	2.1	2.5	2.3	3.3	2.5
0.8	1.4	1.0	1.7	1.4	1.9	1.9	2.1	2.5	2.3	3.3	2.6
0.8	1.4	1.0	1.7	1.4	1.9	1.9	2.1	2.5	2.3	3.3	2.6
0.8	1.4	1.0	1.7	1.4	1.9	1.9	2.1	2.5	2.3	3.3	2.6
0.8	1.4	1.0	1.7	1.4	1.9	1.9	2.1	2.5	2.3	3.3	2.6
0.8	1.4	1.0	1.7	1.4	1.9	1.9	2.1	2.5	2.3	3.4	2.6
0.8	1.5	1.1	1.7	1.4	1.9	1.9	2.1	2.5	2.4	3.4	2.6
0.8	1.5	1.1	1.7	1.4	1.9	1.9	2.1	2.5	2.4	3.4	2.6
0.8	1.5	1.1	1.7	1.4	1.9	2.0	2.1	2.6	2.4	3.4	2.6
0.8	1.5	1.1	1.7	1.5	1.9	2.0	2.1	2.6	2.4	3.5	2.6
0.8	1.5	1.1	1.7	1.5	1.9	2.0	2.1	2.6	2.4	3.5	2.6
0.8	1.5	1.1	1.7	1.5	1.9	2.0	2.2	2.6	2.4	3.5	2.6
0.8	1.5	1.2	1.7	1.5	1.9	2.0	2.2	2.6	2.4	3.5	2.6
0.8	1.5	1.1	1.7	1.5	1.9	2.0	2.2	2.7	2.4	3.5	2.6
0.8	1.5	1.1	1.7	1.5	1.9	2.0	2.2	2.6	2.4	3.5	2.6
0.8	1.5	1.1	1.7	1.6	1.9	2.1	2.2	2.7	2.4	3.6	2.6
0.8	1.5	1.2	1.7	1.5	2.0	2.0	2.2	2.7	2.4	3.6	2.6

3.6	2.6	4.8	2.9	6.3	3.1	8.2	3.3	10.5	3.5	13.7	3.8
3.6	2.6	4.8	2.9	6.4	3.1	8.2	3.3	10.6	3.5	13.8	3.8
3.7	2.6	4.9	2.9	6.4	3.1	8.3	3.3	10.7	3.5	13.9	3.8
3.7	2.6	4.9	2.9	6.4	3.1	8.3	3.3	10.7	3.5	13.9	3.8
3.7	2.7	5.0	2.9	6.5	3.1	8.4	3.3	10.8	3.6	14.0	3.8
3.7	2.7	4.9	2.9	6.5	3.1	8.4	3.3	10.9	3.6	14.1	3.8
3.8	2.7	5.0	2.9	6.6	3.1	8.5	3.3	10.9	3.6	14.1	3.8
3.8	2.7	5.0	2.9	6.6	3.1	8.5	3.3	11.0	3.6	14.3	3.8
3.8	2.7	5.1	2.9	6.6	3.1	8.6	3.3	11.1	3.6	14.3	3.8
3.9	2.7	5.1	2.9	6.7	3.1	8.6	3.4	11.1	3.6	14.4	3.8
3.9	2.7	5.1	2.9	6.7	3.1	8.7	3.4	11.2	3.6	14.5	3.8
3.9	2.7	5.1	2.9	6.7	3.1	8.7	3.4	11.2	3.6	14.6	3.8
3.9	2.7	5.2	2.9	6.8	3.1	8.8	3.4	11.3	3.6	14.7	3.8
4.0	2.7	5.2	2.9	6.8	3.1	8.8	3.4	11.4	3.6	14.7	3.8
4.0	2.7	5.2	2.9	6.8	3.2	8.9	3.4	11.4	3.6	14.8	3.8
4.0	2.7	5.3	2.9	6.9	3.2	8.9	3.4	11.5	3.6	14.9	3.8
4.0	2.7	5.3	2.9	6.9	3.2	9.0	3.4	11.6	3.6	15.0	3.8
4.0	2.7	5.3	2.9	7.0	3.2	9.0	3.4	11.7	3.6	15.1	3.8
4.1	2.7	5.4	2.9	7.1	3.2	9.1	3.4	11.7	3.6	15.2	3.8
4.1	2.7	5.4	3.0	7.1	3.2	9.1	3.4	11.8	3.6	15.3	3.9
4.1	2.7	5.4	3.0	7.1	3.2	9.2	3.4	11.9	3.6	15.4	3.9
4.2	2.7	5.5	3.0	7.2	3.2	9.2	3.4	11.9	3.6	15.4	3.9
4.2	2.7	5.5	3.0	7.2	3.2	9.3	3.4	12.0	3.6	15.5	3.9
4.2	2.7	5.5	3.0	7.2	3.2	9.3	3.4	12.1	3.6	15.6	3.9
4.2	2.8	5.5	3.0	7.3	3.2	9.4	3.4	12.2	3.7	15.7	3.9
4.3	2.8	5.6	3.0	7.3	3.2	9.4	3.4	12.2	3.7	15.8	3.9
4.3	2.8	5.6	3.0	7.3	3.2	9.5	3.4	12.3	3.7	15.8	3.9
4.3	2.8	5.7	3.0	7.4	3.2	9.5	3.4	12.4	3.7	15.8	3.9
4.3	2.8	5.7	3.0	7.5	3.2	9.6	3.4	12.5	3.7	15.9	3.9
4.4	2.8	5.7	3.0	7.5	3.2	9.6	3.5	12.5	3.7	15.9	3.9
4.4	2.8	5.8	3.0	7.5	3.2	9.7	3.5	12.6	3.7	16.0	3.9
4.4	2.8	5.8	3.0	7.6	3.2	9.7	3.5	12.7	3.7	16.1	3.9
4.4	2.8	5.8	3.0	7.6	3.2	9.8	3.5	12.8	3.7	16.1	3.9
4.5	2.8	5.9	3.0	7.7	3.2	9.9	3.5	12.8	3.7	16.1	3.9
4.5	2.8	5.9	3.0	7.7	3.3	9.9	3.5	12.9	3.7	16.2	3.9
4.5	2.8	6.0	3.0	7.7	3.3	10.0	3.5	13.0	3.7	16.3	3.9
4.5	2.8	6.0	3.0	7.8	3.3	10.0	3.5	13.0	3.7	16.3	3.9
4.6	2.8	6.0	3.0	7.8	3.3	10.1	3.5	13.1	3.7	16.4	3.9
4.6	2.8	6.0	3.0	7.9	3.3	10.1	3.5	13.2	3.7	16.5	3.9
4.7	2.8	6.1	3.1	7.9	3.3	10.2	3.5	13.2	3.7	16.5	4.0
4.7	2.8	6.1	3.1	7.9	3.3	10.2	3.5	13.3	3.7	16.5	4.0
4.7	2.8	6.2	3.1	8.0	3.3	10.3	3.5	13.4	3.7	16.6	4.0
4.7	2.8	6.2	3.1	8.0	3.3	10.4	3.5	13.5	3.7	16.6	4.0
4.8	2.8	6.2	3.1	8.1	3.3	10.4	3.5	13.5	3.7	16.7	4.0
4.8	2.9	6.3	3.1	8.1	3.3	10.5	3.5	13.6	3.8	16.8	4.0

16.8	4.0	18.8	4.2	20.3	4.4	25.8	4.6	33.2	4.8	42.0	5.0
16.9	4.0	18.9	4.2	20.3	4.4	26.0	4.6	33.3	4.8	42.4	5.0
16.9	4.0	18.8	4.2	20.4	4.4	26.1	4.6	33.6	4.8	42.6	5.0
17.0	4.0	18.9	4.2	20.4	4.4	26.3	4.6	33.8	4.8		
17.1	4.0	18.9	4.2	20.5	4.4	26.4	4.6	34.0	4.8		
17.2	4.0	18.9	4.2	20.4	4.4	26.6	4.6	34.2	4.8		
17.2	4.0	19.0	4.2	20.5	4.4	26.8	4.6	34.4	4.8		
17.2	4.0	19.0	4.2	20.5	4.4	27.0	4.6	34.7	4.8		
17.3	4.0	19.1	4.2	20.6	4.4	27.2	4.6	34.8	4.8		
17.3	4.0	19.1	4.2	20.6	4.4	27.3	4.6	35.1	4.8		
17.3	4.0	19.2	4.2	20.8	4.4	27.5	4.6	35.2	4.8		
17.4	4.0	19.2	4.2	21.0	4.4	27.7	4.6	35.4	4.8		
17.5	4.0	19.3	4.2	21.1	4.4	27.9	4.6	35.7	4.8		
17.6	4.0	19.3	4.2	21.3	4.4	28.0	4.6	35.9	4.8		
17.6	4.1	19.3	4.3	21.5	4.5	28.2	4.7	36.1	4.9		
17.6	4.1	19.3	4.3	21.6	4.5	28.4	4.7	36.4	4.9		
17.6	4.1	19.4	4.3	21.7	4.5	28.6	4.7	36.6	4.9		
17.8	4.1	19.4	4.3	21.9	4.5	28.8	4.7	36.8	4.9		
17.8	4.1	19.5	4.3	22.0	4.5	28.9	4.7	37.0	4.9		
17.9	4.1	19.5	4.3	22.2	4.5	29.1	4.7	37.2	4.9		
17.9	4.1	19.6	4.3	22.3	4.5	29.3	4.7	37.5	4.9		
18.0	4.1	19.6	4.3	22.5	4.5	29.5	4.7	37.7	4.9		
18.0	4.1	19.7	4.3	22.7	4.5	29.7	4.7	38.0	4.9		
18.0	4.1	19.6	4.3	22.9	4.5	29.9	4.7	38.1	4.9		
18.0	4.1	19.7	4.3	23.0	4.5	30.1	4.7	38.3	4.9		
18.1	4.1	19.7	4.3	23.2	4.5	30.2	4.7	38.6	4.9		
18.1	4.1	19.7	4.3	23.3	4.5	30.4	4.7	38.8	4.9		
18.2	4.1	19.8	4.3	23.5	4.5	30.7	4.7	39.0	4.9		
18.3	4.1	19.8	4.3	23.7	4.5	30.8	4.7	39.3	4.9		
18.3	4.1	19.8	4.3	23.9	4.5	31.1	4.7	39.5	4.9		
18.4	4.1	19.9	4.3	24.1	4.5	31.2	4.7	39.7	4.9		
18.4	4.1	19.9	4.3	24.2	4.5	31.4	4.7	39.9	4.9		
18.4	4.1	19.9	4.3	24.4	4.5	31.6	4.7	40.2	4.9		
18.5	4.1	20.0	4.3	24.6	4.5	31.7	4.7	40.4	4.9		
18.5	4.2	20.0	4.4	24.7	4.6	32.0	4.8	40.6	5.0		
18.6	4.2	20.0	4.4	24.9	4.6	32.2	4.8	40.9	5.0		
18.6	4.2	20.1	4.4	25.1	4.6	32.4	4.8	41.2	5.0		
18.7	4.2	20.1	4.4	25.3	4.6	32.6	4.8	41.4	5.0		
18.7	4.2	20.2	4.4	25.4	4.6	32.8	4.8	41.6	5.0		
18.8	4.2	20.2	4.4	25.6	4.6	33.0	4.8	41.8	5.0		

Sample N3

N	mm										
0.0	0.0	0.5	0.2	0.9	0.4	1.5	0.6	2.4	0.8	3.6	1.1
0.0	0.0	0.5	0.2	0.9	0.4	1.5	0.6	2.4	0.9	3.6	1.1
0.0	0.0	0.5	0.2	1.0	0.4	1.6	0.6	2.4	0.9	3.7	1.1
0.0	0.0	0.5	0.2	1.0	0.4	1.6	0.6	2.5	0.9	3.7	1.1
0.0	0.0	0.5	0.2	1.0	0.4	1.6	0.7	2.5	0.9	3.7	1.1
0.0	0.0	0.5	0.2	1.0	0.4	1.6	0.7	2.5	0.9	3.8	1.1
0.1	0.0	0.5	0.2	1.0	0.4	1.7	0.7	2.6	0.9	3.8	1.1
0.1	0.0	0.5	0.2	1.0	0.5	1.6	0.7	2.6	0.9	3.8	1.1
0.1	0.0	0.5	0.2	1.1	0.5	1.7	0.7	2.6	0.9	3.8	1.1
0.1	0.0	0.6	0.2	1.1	0.5	1.7	0.7	2.6	0.9	3.9	1.1
0.1	0.0	0.6	0.3	1.0	0.5	1.7	0.7	2.7	0.9	3.9	1.1
0.1	0.0	0.6	0.3	1.1	0.5	1.7	0.7	2.7	0.9	4.0	1.1
0.2	0.0	0.6	0.3	1.1	0.5	1.7	0.7	2.7	0.9	4.0	1.1
0.2	0.1	0.6	0.3	1.1	0.5	1.8	0.7	2.7	0.9	4.0	1.1
0.2	0.1	0.6	0.3	1.1	0.5	1.8	0.7	2.7	0.9	4.0	1.1
0.2	0.1	0.6	0.3	1.2	0.5	1.8	0.7	2.8	0.9	4.1	1.1
0.2	0.1	0.6	0.3	1.1	0.5	1.8	0.7	2.8	0.9	4.1	1.1
0.2	0.1	0.6	0.3	1.2	0.5	1.8	0.7	2.8	0.9	4.2	1.1
0.2	0.1	0.6	0.3	1.2	0.5	1.8	0.7	2.8	0.9	4.2	1.2
0.2	0.1	0.6	0.3	1.2	0.5	1.9	0.7	2.8	0.9	4.2	1.2
0.2	0.1	0.6	0.3	1.2	0.5	1.9	0.7	2.9	0.9	4.3	1.2
0.2	0.1	0.7	0.3	1.2	0.5	1.9	0.7	2.9	1.0	4.3	1.2
0.2	0.1	0.7	0.3	1.2	0.5	1.9	0.7	2.9	1.0	4.3	1.2
0.2	0.1	0.7	0.3	1.3	0.5	1.9	0.7	3.0	1.0	4.4	1.2
0.2	0.1	0.7	0.3	1.3	0.5	2.0	0.8	3.0	1.0	4.4	1.2
0.3	0.1	0.7	0.3	1.3	0.5	2.0	0.8	3.0	1.0	4.4	1.2
0.2	0.1	0.7	0.3	1.3	0.5	2.0	0.8	3.1	1.0	4.5	1.2
0.3	0.1	0.7	0.3	1.3	0.6	2.0	0.8	3.1	1.0	4.5	1.2
0.3	0.1	0.7	0.3	1.3	0.6	2.0	0.8	3.1	1.0	4.5	1.2
0.3	0.1	0.7	0.3	1.3	0.6	2.1	0.8	3.2	1.0	4.6	1.2
0.3	0.1	0.8	0.4	1.3	0.6	2.1	0.8	3.2	1.0	4.6	1.2
0.3	0.1	0.7	0.4	1.4	0.6	2.1	0.8	3.3	1.0	4.7	1.2
0.4	0.1	0.8	0.4	1.4	0.6	2.1	0.8	3.3	1.0	4.7	1.2
0.3	0.2	0.8	0.4	1.4	0.6	2.1	0.8	3.3	1.0	4.7	1.2
0.4	0.2	0.8	0.4	1.4	0.6	2.2	0.8	3.3	1.0	4.8	1.2
0.4	0.2	0.8	0.4	1.4	0.6	2.2	0.8	3.3	1.0	4.8	1.2
0.4	0.2	0.9	0.4	1.4	0.6	2.3	0.8	3.4	1.0	4.9	1.2
0.4	0.2	0.8	0.4	1.4	0.6	2.3	0.8	3.4	1.0	4.9	1.2
0.4	0.2	0.9	0.4	1.4	0.6	2.3	0.8	3.4	1.0	4.9	1.3
0.4	0.2	0.9	0.4	1.5	0.6	2.3	0.8	3.5	1.0	5.0	1.3
0.4	0.2	0.9	0.4	1.5	0.6	2.3	0.8	3.5	1.0	5.0	1.3
0.4	0.2	0.9	0.4	1.5	0.6	2.4	0.8	3.5	1.1	5.1	1.3
0.5	0.2	0.9	0.4	1.5	0.6	2.4	0.8	3.6	1.1	5.1	1.3

5.1	1.3	7.2	1.5	10.3	1.7	14.2	2.0	17.1	2.2	19.1	2.4
5.2	1.3	7.3	1.5	10.3	1.7	14.3	2.0	17.2	2.2	19.2	2.4
5.2	1.3	7.3	1.5	10.4	1.7	14.4	2.0	17.2	2.2	19.3	2.4
5.3	1.3	7.4	1.5	10.5	1.7	14.5	2.0	17.3	2.2	19.3	2.4
5.3	1.3	7.5	1.5	10.6	1.7	14.5	2.0	17.4	2.2	19.3	2.4
5.4	1.3	7.5	1.5	10.6	1.8	14.6	2.0	17.4	2.2	19.3	2.4
5.4	1.3	7.6	1.5	10.7	1.8	14.7	2.0	17.4	2.2	19.4	2.4
5.4	1.3	7.6	1.5	10.8	1.8	14.8	2.0	17.5	2.2	19.5	2.4
5.5	1.3	7.7	1.5	10.9	1.8	14.9	2.0	17.6	2.2	19.5	2.4
5.5	1.3	7.8	1.5	11.0	1.8	14.9	2.0	17.6	2.2	19.5	2.4
5.6	1.3	7.8	1.6	11.1	1.8	15.1	2.0	17.7	2.2	19.6	2.5
5.6	1.3	7.9	1.6	11.1	1.8	15.1	2.0	17.7	2.2	19.6	2.5
5.6	1.3	8.0	1.6	11.2	1.8	15.2	2.0	17.8	2.2	19.8	2.5
5.7	1.3	8.0	1.6	11.3	1.8	15.3	2.0	17.8	2.2	19.9	2.5
5.8	1.3	8.1	1.6	11.4	1.8	15.3	2.0	17.8	2.2	20.1	2.5
5.8	1.4	8.1	1.6	11.5	1.8	15.5	2.0	17.9	2.3	20.1	2.5
5.8	1.4	8.2	1.6	11.6	1.8	15.5	2.0	18.0	2.3	20.3	2.5
5.9	1.4	8.3	1.6	11.7	1.8	15.5	2.0	18.0	2.3	20.4	2.5
5.9	1.4	8.3	1.6	11.7	1.8	15.6	2.0	18.1	2.3	20.6	2.5
5.9	1.4	8.4	1.6	11.8	1.8	15.6	2.0	18.1	2.3	20.7	2.5
6.0	1.4	8.5	1.6	11.9	1.8	15.6	2.1	18.2	2.3	20.8	2.5
6.1	1.4	8.5	1.6	12.0	1.8	15.8	2.1	18.2	2.3	21.0	2.5
6.1	1.4	8.6	1.6	12.1	1.8	15.8	2.1	18.2	2.3	21.1	2.5
6.1	1.4	8.7	1.6	12.2	1.8	16.0	2.1	18.3	2.3	21.2	2.5
6.1	1.4	8.7	1.6	12.3	1.8	16.0	2.1	18.3	2.3	21.4	2.5
6.1	1.4	8.8	1.6	12.4	1.9	16.1	2.1	18.3	2.3	21.5	2.5
6.2	1.4	8.8	1.6	12.5	1.9	16.2	2.1	18.4	2.3	21.7	2.5
6.2	1.4	8.9	1.6	12.6	1.9	16.2	2.1	18.4	2.3	21.8	2.5
6.3	1.4	9.0	1.6	12.7	1.9	16.3	2.1	18.5	2.3	22.0	2.5
6.3	1.4	9.1	1.6	12.8	1.9	16.3	2.1	18.5	2.3	22.2	2.5
6.4	1.4	9.1	1.7	12.8	1.9	16.4	2.1	18.6	2.3	22.3	2.6
6.4	1.4	9.2	1.7	13.0	1.9	16.5	2.1	18.6	2.3	22.5	2.6
6.5	1.4	9.3	1.7	13.0	1.9	16.5	2.1	18.6	2.3	22.7	2.6
6.6	1.4	9.3	1.7	13.1	1.9	16.6	2.1	18.7	2.3	22.8	2.6
6.6	1.4	9.4	1.7	13.3	1.9	16.6	2.1	18.7	2.3	23.0	2.6
6.7	1.5	9.5	1.7	13.3	1.9	16.6	2.1	18.7	2.4	23.2	2.6
6.7	1.5	9.6	1.7	13.4	1.9	16.7	2.1	18.8	2.4	23.4	2.6
6.8	1.5	9.6	1.7	13.6	1.9	16.7	2.1	18.8	2.4	23.6	2.6
6.8	1.5	9.7	1.7	13.6	1.9	16.8	2.1	18.8	2.4	23.8	2.6
6.9	1.5	9.8	1.7	13.7	1.9	16.8	2.1	18.9	2.4	23.9	2.6
6.9	1.5	9.9	1.7	13.8	1.9	16.9	2.2	18.9	2.4	24.1	2.6
7.0	1.5	9.9	1.7	13.9	1.9	16.9	2.2	19.0	2.4	24.3	2.6
7.1	1.5	10.0	1.7	14.0	1.9	16.9	2.2	19.0	2.4	24.5	2.6
7.1	1.5	10.1	1.7	14.1	1.9	17.0	2.2	19.1	2.4	24.7	2.6
7.1	1.5	10.2	1.7	14.2	1.9	17.1	2.2	19.1	2.4	24.9	2.6

25.1	2.6	34.0	2.9	44.4	3.1	51.5	3.3	56.8	3.5	71.1	3.8
25.2	2.6	34.2	2.9	44.6	3.1	51.6	3.3	57.2	3.5	71.4	3.8
25.4	2.6	34.4	2.9	44.7	3.1	49.2	3.3	57.5	3.5	71.8	3.8
25.6	2.6	34.6	2.9	45.0	3.1	45.2	3.3	57.7	3.5	72.1	3.8
25.7	2.6	34.9	2.9	45.2	3.1	45.8	3.3	58.1	3.5	72.4	3.8
26.0	2.7	35.1	2.9	45.4	3.1	46.0	3.3	58.3	3.6	72.7	3.8
26.1	2.7	35.4	2.9	45.6	3.1	45.6	3.3	58.7	3.6	73.1	3.8
26.3	2.7	35.5	2.9	45.8	3.1	45.9	3.3	59.0	3.6	73.3	3.8
26.4	2.7	35.7	2.9	46.0	3.1	46.1	3.3	59.3	3.6	73.7	3.8
26.6	2.7	36.0	2.9	46.2	3.1	46.5	3.3	59.6	3.6	74.0	3.8
26.8	2.7	36.3	2.9	46.4	3.1	47.0	3.4	59.9	3.6	74.3	3.8
26.9	2.7	36.4	2.9	46.6	3.1	47.3	3.4	60.2	3.6	74.6	3.8
27.1	2.7	36.7	2.9	46.7	3.1	47.7	3.4	60.6	3.6	75.0	3.8
27.3	2.7	36.9	2.9	46.9	3.1	48.0	3.4	60.8	3.6	75.3	3.8
27.5	2.7	37.2	2.9	46.9	3.1	48.4	3.4	61.2	3.6	75.7	3.8
27.7	2.7	37.4	2.9	46.9	3.2	48.7	3.4	61.4	3.6	76.0	3.8
27.9	2.7	37.6	2.9	46.2	3.2	49.0	3.4	61.8	3.6	76.3	3.8
28.1	2.7	37.9	2.9	45.1	3.2	49.4	3.4	62.1	3.6	76.5	3.8
28.3	2.7	38.1	2.9	45.3	3.2	49.7	3.4	62.4	3.6	76.9	3.8
28.5	2.7	38.4	3.0	45.6	3.2	50.0	3.4	62.8	3.6	77.3	3.8
28.6	2.7	38.6	3.0	45.8	3.2	50.4	3.4	63.1	3.6	77.5	3.9
28.9	2.7	38.8	3.0	46.1	3.2	50.6	3.4	63.4	3.6	77.9	3.9
29.1	2.7	39.1	3.0	46.3	3.2	50.9	3.4	63.7	3.6	78.1	3.9
29.3	2.7	39.3	3.0	46.5	3.2	51.3	3.4	64.0	3.6	78.4	3.9
29.4	2.7	39.5	3.0	46.8	3.2	51.5	3.4	64.3	3.6	78.8	3.9
29.7	2.8	39.8	3.0	47.0	3.2	51.8	3.4	64.7	3.7	79.1	3.9
29.9	2.8	40.0	3.0	47.4	3.2	52.1	3.4	64.9	3.7	79.4	3.9
30.1	2.8	40.2	3.0	47.6	3.2	52.3	3.4	65.3	3.7	79.8	3.9
30.3	2.8	40.5	3.0	47.8	3.2	52.6	3.4	65.6	3.7	80.1	3.9
30.5	2.8	40.7	3.0	48.1	3.2	52.8	3.4	65.9	3.7	80.4	3.9
30.7	2.8	41.0	3.0	48.3	3.2	52.6	3.5	66.2	3.7	80.7	3.9
31.0	2.8	41.2	3.0	48.5	3.2	53.1	3.5	66.5	3.7	81.1	3.9
31.2	2.8	41.5	3.0	48.8	3.2	53.2	3.5	66.9	3.7	81.4	3.9
31.4	2.8	41.7	3.0	49.1	3.2	53.6	3.5	67.2	3.7	81.6	3.9
31.5	2.8	41.9	3.0	49.3	3.2	53.8	3.5	67.6	3.7	82.1	3.9
31.7	2.8	42.2	3.0	49.5	3.3	54.0	3.5	67.9	3.7	82.3	3.9
32.0	2.8	42.4	3.0	49.8	3.3	54.3	3.5	68.1	3.7	82.6	3.9
32.2	2.8	42.6	3.0	50.1	3.3	54.6	3.5	68.5	3.7	83.0	3.9
32.5	2.8	42.9	3.0	50.2	3.3	54.9	3.5	68.9	3.7	83.3	3.9
32.7	2.8	43.1	3.0	50.6	3.3	55.1	3.5	69.1	3.7	83.6	3.9
32.8	2.8	43.3	3.1	50.7	3.3	55.4	3.5	69.6	3.7	83.9	4.0
33.1	2.8	43.5	3.1	50.9	3.3	55.7	3.5	69.8	3.7	84.2	4.0
33.3	2.8	43.7	3.1	51.1	3.3	56.0	3.5	70.1	3.7	84.6	4.0
33.5	2.8	44.0	3.1	51.3	3.3	56.3	3.5	70.4	3.7	84.8	4.0
33.7	2.8	44.2	3.1	51.4	3.3	56.6	3.5	70.7	3.7	85.2	4.0

85.5	4.0	97.1	4.2	106.0	4.4	120.1	4.6	133.6	4.8	147.3	5.0
85.7	4.0	97.2	4.2	106.3	4.4	120.4	4.6	134.0	4.8	147.6	5.0
86.1	4.0	94.2	4.2	106.6	4.4	120.8	4.6	134.3	4.8	148.0	5.0
86.4	4.0	89.8	4.2	107.0	4.4	121.1	4.6	134.8	4.8		
86.7	4.0	90.7	4.2	107.4	4.4	121.5	4.6	135.0	4.8		
87.0	4.0	91.4	4.2	107.8	4.4	121.8	4.6	135.5	4.8		
87.3	4.0	92.0	4.2	108.1	4.4	122.2	4.6	135.7	4.8		
87.6	4.0	92.5	4.2	108.5	4.4	122.5	4.6	136.1	4.8		
87.9	4.0	93.0	4.2	108.9	4.4	122.7	4.6	136.4	4.8		
88.3	4.0	93.5	4.2	109.1	4.4	123.2	4.6	136.8	4.8		
88.5	4.0	94.0	4.2	109.5	4.4	123.6	4.6	137.0	4.8		
88.8	4.0	94.5	4.2	110.0	4.4	123.8	4.6	137.5	4.8		
89.1	4.0	95.0	4.2	110.2	4.4	124.2	4.6	137.7	4.8		
89.6	4.0	95.3	4.2	110.7	4.4	124.5	4.6	138.1	4.8		
89.8	4.0	95.9	4.3	111.0	4.4	124.8	4.6	138.4	4.8		
90.2	4.1	96.2	4.3	111.3	4.5	125.2	4.7	138.7	4.9		
90.4	4.1	96.7	4.3	111.7	4.5	125.5	4.7	139.2	4.9		
90.7	4.1	97.1	4.3	112.1	4.5	125.9	4.7	139.4	4.9		
91.1	4.1	97.5	4.3	112.4	4.5	126.2	4.7	139.8	4.9		
91.4	4.1	98.0	4.3	112.7	4.5	126.6	4.7	140.1	4.9		
91.7	4.1	98.4	4.3	113.2	4.5	126.9	4.7	140.4	4.9		
92.0	4.1	98.8	4.3	113.5	4.5	127.2	4.7	140.8	4.9		
92.3	4.1	99.2	4.3	113.8	4.5	127.6	4.7	141.2	4.9		
92.6	4.1	99.5	4.3	114.2	4.5	128.0	4.7	141.5	4.9		
92.8	4.1	99.9	4.3	114.6	4.5	128.2	4.7	141.9	4.9		
93.3	4.1	100.4	4.3	114.8	4.5	128.7	4.7	142.2	4.9		
93.6	4.1	100.7	4.3	115.3	4.5	129.0	4.7	142.5	4.9		
93.8	4.1	101.2	4.3	115.6	4.5	129.3	4.7	142.8	4.9		
94.2	4.1	101.5	4.3	115.9	4.5	129.6	4.7	143.1	4.9		
94.5	4.1	101.8	4.3	116.3	4.5	130.0	4.7	143.6	4.9		
94.7	4.1	102.3	4.3	116.6	4.5	130.4	4.7	143.8	4.9		
95.0	4.1	102.6	4.3	117.0	4.5	130.6	4.7	144.3	4.9		
95.3	4.1	103.0	4.3	117.3	4.5	131.0	4.7	144.6	4.9		
95.7	4.1	103.3	4.3	117.7	4.5	131.3	4.7	144.8	4.9		
95.9	4.1	103.8	4.3	118.0	4.5	131.6	4.7	145.2	4.9		
96.2	4.2	104.1	4.4	118.3	4.6	132.0	4.8	145.6	5.0		
96.5	4.2	104.4	4.4	118.7	4.6	132.3	4.8	145.9	5.0		
96.7	4.2	104.8	4.4	119.1	4.6	132.6	4.8	146.3	5.0		
96.9	4.2	105.3	4.4	119.4	4.6	133.1	4.8	146.6	5.0		
97.2	4.2	105.5	4.4	119.8	4.6	133.3	4.8	146.9	5.0		

Sample N4

N	mm	0.0	0.4	0.0	0.8	0.0	1.3	0.8	1.7	2.3	2.1
0.0	0.0	0.0	0.4	0.0	0.9	0.0	1.3	0.9	1.7	2.3	2.1
0.0	0.0	0.0	0.4	0.0	0.9	0.0	1.3	0.9	1.7	2.4	2.2
0.0	0.0	0.0	0.4	0.0	0.9	0.0	1.3	0.9	1.7	2.4	2.2
0.0	0.0	0.0	0.5	0.0	0.9	0.0	1.3	0.9	1.7	2.5	2.2
0.0	0.0	0.0	0.5	0.0	0.9	0.0	1.3	1.0	1.8	2.5	2.2
0.0	0.0	0.0	0.5	0.0	0.9	0.0	1.3	1.0	1.8	2.5	2.2
0.0	0.1	0.0	0.5	0.0	0.9	0.0	1.3	1.1	1.8	2.5	2.2
0.0	0.1	0.0	0.5	0.0	0.9	0.0	1.4	1.1	1.8	2.6	2.2
0.0	0.1	0.0	0.5	0.0	0.9	0.0	1.4	1.1	1.8	2.6	2.2
0.0	0.1	0.0	0.5	0.0	0.9	0.0	1.4	1.2	1.8	2.6	2.2
0.0	0.1	0.0	0.5	0.0	1.0	0.0	1.4	1.2	1.8	2.7	2.2
0.0	0.1	0.0	0.5	0.0	1.0	0.1	1.4	1.2	1.8	2.7	2.3
0.0	0.1	0.0	0.5	0.0	1.0	0.1	1.4	1.3	1.8	2.7	2.3
0.0	0.1	0.0	0.6	0.0	1.0	0.0	1.4	1.3	1.8	2.8	2.3
0.0	0.1	0.0	0.6	0.0	1.0	0.0	1.4	1.3	1.9	2.8	2.3
0.0	0.1	0.0	0.6	0.0	1.0	0.0	1.4	1.4	1.9	2.8	2.3
0.0	0.2	0.0	0.6	0.0	1.0	0.0	1.4	1.4	1.9	2.9	2.3
0.0	0.2	0.0	0.6	0.0	1.0	0.1	1.5	1.4	1.9	2.9	2.3
0.0	0.2	0.0	0.6	0.0	1.0	0.1	1.5	1.5	1.9	3.0	2.3
0.0	0.2	0.0	0.6	0.0	1.0	0.2	1.5	1.5	1.9	3.0	2.3
0.0	0.2	0.0	0.6	0.0	1.1	0.1	1.5	1.6	1.9	3.1	2.3
0.0	0.2	0.0	0.6	0.0	1.1	0.2	1.5	1.6	1.9	3.1	2.4
0.0	0.2	0.0	0.6	0.0	1.1	0.2	1.5	1.6	1.9	3.1	2.4
0.0	0.2	0.0	0.7	0.0	1.1	0.2	1.5	1.7	1.9	3.2	2.4
0.0	0.2	0.0	0.7	0.0	1.1	0.3	1.5	1.7	2.0	3.2	2.4
0.0	0.2	0.0	0.7	0.0	1.1	0.3	1.5	1.7	2.0	3.3	2.4
0.0	0.3	0.0	0.7	0.0	1.1	0.3	1.5	1.8	2.0	3.3	2.4
0.0	0.3	0.0	0.7	0.0	1.1	0.3	1.6	1.8	2.0	3.4	2.4
0.0	0.3	0.0	0.7	0.0	1.1	0.4	1.6	1.8	2.0	3.4	2.4
0.0	0.3	0.1	0.7	0.0	1.1	0.4	1.6	1.9	2.0	3.4	2.4
0.0	0.3	0.0	0.7	0.0	1.2	0.4	1.6	1.9	2.0	3.5	2.4
0.0	0.3	0.0	0.7	0.0	1.2	0.5	1.6	1.9	2.0	3.6	2.5
0.0	0.3	0.0	0.7	0.0	1.2	0.5	1.6	1.9	2.0	3.6	2.5
0.0	0.3	0.0	0.8	0.1	1.2	0.6	1.6	2.0	2.0	3.7	2.5
0.0	0.3	0.0	0.8	0.0	1.2	0.6	1.6	2.1	2.1	3.7	2.5
0.0	0.3	0.0	0.8	0.0	1.2	0.6	1.6	2.1	2.1	3.7	2.5
0.0	0.4	0.0	0.8	0.0	1.2	0.6	1.6	2.1	2.1	3.8	2.5
0.0	0.4	0.0	0.8	0.0	1.2	0.7	1.7	2.1	2.1	3.8	2.5
0.0	0.4	0.0	0.8	0.0	1.2	0.7	1.7	2.1	2.1	3.9	2.5
0.0	0.4	0.0	0.8	0.0	1.2	0.7	1.7	2.2	2.1	3.9	2.5
0.0	0.4	0.0	0.8	0.0	1.3	0.8	1.7	2.2	2.1	4.0	2.5
0.0	0.4	0.0	0.8	0.1	1.3	0.8	1.7	2.3	2.1	4.0	2.6

4.1	2.6	6.3	3.0	8.5	3.5	10.9	3.9	13.4	4.4	16.2	4.8
4.1	2.6	6.3	3.0	8.6	3.5	11.0	3.9	13.4	4.4	16.3	4.8
4.1	2.6	6.4	3.0	8.7	3.5	11.0	3.9	13.5	4.4	16.4	4.8
4.2	2.6	6.4	3.0	8.7	3.5	11.1	3.9	13.6	4.4	16.5	4.8
4.3	2.6	6.5	3.1	8.8	3.5	11.1	4.0	13.6	4.4	16.5	4.9
4.3	2.6	6.5	3.1	8.9	3.5	11.2	4.0	13.7	4.4	16.6	4.9
4.3	2.6	6.6	3.1	8.9	3.5	11.2	4.0	13.8	4.4	16.7	4.9
4.4	2.6	6.6	3.1	9.0	3.5	11.2	4.0	13.8	4.4	16.8	4.9
4.5	2.6	6.7	3.1	9.0	3.5	11.3	4.0	13.9	4.4	16.8	4.9
4.5	2.7	6.7	3.1	9.0	3.6	11.4	4.0	14.0	4.5	16.9	4.9
4.5	2.7	6.8	3.1	9.0	3.6	11.4	4.0	14.0	4.5	16.9	4.9
4.6	2.7	6.9	3.1	9.1	3.6	11.5	4.0	14.1	4.5	17.0	4.9
4.6	2.7	6.9	3.1	9.2	3.6	11.5	4.0	14.2	4.5	17.1	4.9
4.7	2.7	7.0	3.1	9.2	3.6	11.6	4.0	14.2	4.5	17.2	4.9
4.7	2.7	7.0	3.2	9.3	3.6	11.7	4.1	14.3	4.5	17.2	5.0
4.8	2.7	7.0	3.2	9.4	3.6	11.7	4.1	14.3	4.5	17.3	5.0
4.8	2.7	7.1	3.2	9.4	3.6	11.8	4.1	14.4	4.5	17.4	5.0
4.9	2.7	7.2	3.2	9.5	3.6	11.8	4.1	14.5	4.5	17.5	5.0
4.9	2.7	7.2	3.2	9.5	3.6	11.9	4.1	14.5	4.5	17.5	5.0
5.0	2.8	7.2	3.2	9.6	3.7	11.9	4.1	14.6	4.6	17.6	5.0
5.0	2.8	7.3	3.2	9.6	3.7	12.0	4.1	14.6	4.6	17.7	5.0
5.1	2.8	7.4	3.2	9.7	3.7	12.1	4.1	14.7	4.6	17.7	5.0
5.2	2.8	7.4	3.2	9.7	3.7	12.1	4.1	14.8	4.6	17.8	5.0
5.2	2.8	7.5	3.2	9.8	3.7	12.1	4.1	14.8	4.6	17.9	5.0
5.2	2.8	7.5	3.3	9.8	3.7	12.2	4.2	14.9	4.6	17.9	5.1
5.3	2.8	7.6	3.3	9.9	3.7	12.3	4.2	14.9	4.6	18.0	5.1
5.4	2.8	7.7	3.3	9.9	3.7	12.3	4.2	15.0	4.6	18.1	5.1
5.4	2.8	7.6	3.3	10.0	3.7	12.4	4.2	15.1	4.6	18.2	5.1
5.4	2.8	7.7	3.3	10.0	3.7	12.5	4.2	15.1	4.6	18.3	5.1
5.5	2.9	7.8	3.3	10.1	3.8	12.5	4.2	15.2	4.7	18.3	5.1
5.5	2.9	7.8	3.3	10.2	3.8	12.5	4.2	15.2	4.7	18.4	5.1
5.6	2.9	7.9	3.3	10.2	3.8	12.6	4.2	15.3	4.7	18.5	5.1
5.6	2.9	7.9	3.3	10.2	3.8	12.6	4.2	15.4	4.7	18.6	5.1
5.7	2.9	7.9	3.3	10.3	3.8	12.7	4.2	15.4	4.7	18.7	5.1
5.7	2.9	8.0	3.4	10.3	3.8	12.8	4.3	15.5	4.7	18.7	5.2
5.8	2.9	8.0	3.4	10.4	3.8	12.9	4.3	15.5	4.7	18.8	5.2
5.9	2.9	8.1	3.4	10.4	3.8	12.8	4.3	15.6	4.7	19.0	5.2
5.9	2.9	8.1	3.4	10.5	3.8	12.9	4.3	15.7	4.7	19.0	5.2
5.9	2.9	8.2	3.4	10.5	3.8	13.0	4.3	15.7	4.7	19.0	5.2
6.0	3.0	8.3	3.4	10.6	3.9	13.1	4.3	15.8	4.8	19.1	5.2
6.0	3.0	8.3	3.4	10.6	3.9	13.1	4.3	15.8	4.8	19.2	5.2
6.1	3.0	8.4	3.4	10.7	3.9	13.2	4.3	16.0	4.8	19.2	5.2
6.1	3.0	8.4	3.4	10.7	3.9	13.2	4.3	16.0	4.8	19.3	5.2
6.2	3.0	8.5	3.4	10.8	3.9	13.3	4.3	16.1	4.8	19.4	5.2
6.2	3.0	8.5	3.5	10.8	3.9	13.3	4.4	16.1	4.8	19.5	5.3

19.5	5.3	23.4	5.7	27.8	6.2	32.4	6.6	37.8	7.1	43.6	7.5
19.6	5.3	23.5	5.7	27.9	6.2	32.5	6.6	37.9	7.1	43.7	7.5
19.6	5.3	23.6	5.7	28.0	6.2	32.6	6.6	38.0	7.1	43.9	7.5
19.7	5.3	23.7	5.7	28.1	6.2	32.7	6.6	38.2	7.1	44.0	7.5
19.8	5.3	23.8	5.8	28.3	6.2	32.8	6.7	38.3	7.1	44.1	7.6
19.8	5.3	23.9	5.8	28.3	6.2	32.9	6.7	38.4	7.1	44.2	7.6
19.9	5.3	23.9	5.8	28.4	6.2	33.0	6.7	38.6	7.1	44.4	7.6
20.0	5.3	24.1	5.8	28.5	6.2	33.1	6.7	38.7	7.1	44.5	7.6
20.1	5.3	24.2	5.8	28.6	6.2	33.3	6.7	38.8	7.1	44.6	7.6
20.2	5.4	24.2	5.8	28.7	6.3	33.4	6.7	39.0	7.2	44.8	7.6
20.2	5.4	24.4	5.8	28.8	6.3	33.5	6.7	39.1	7.2	44.9	7.6
20.3	5.4	24.4	5.8	28.9	6.3	33.6	6.7	39.2	7.2	45.0	7.6
20.4	5.4	24.5	5.8	29.1	6.3	33.7	6.7	39.3	7.2	45.2	7.6
20.5	5.4	24.7	5.8	29.1	6.3	33.8	6.7	39.5	7.2	45.3	7.6
20.6	5.4	24.8	5.9	29.2	6.3	33.9	6.8	39.6	7.2	45.4	7.7
20.6	5.4	24.8	5.9	29.3	6.3	34.0	6.8	39.8	7.2	45.6	7.7
20.7	5.4	24.9	5.9	29.4	6.3	34.1	6.8	39.9	7.2	45.7	7.7
20.9	5.4	25.0	5.9	29.6	6.3	34.2	6.8	40.0	7.2	45.9	7.7
20.9	5.4	25.1	5.9	29.7	6.3	34.4	6.8	40.2	7.2	45.9	7.7
21.1	5.5	25.2	5.9	29.7	6.4	34.5	6.8	40.3	7.3	46.0	7.7
21.1	5.5	25.3	5.9	29.8	6.4	34.6	6.8	40.4	7.3	46.2	7.7
21.2	5.5	25.4	5.9	29.9	6.4	34.7	6.8	40.6	7.3	46.4	7.7
21.3	5.5	25.5	5.9	30.0	6.4	34.8	6.8	40.7	7.3	46.5	7.7
21.4	5.5	25.7	5.9	30.1	6.4	35.0	6.8	40.8	7.3	46.6	7.7
21.5	5.5	25.8	6.0	30.2	6.4	35.1	6.9	40.9	7.3	46.7	7.8
21.5	5.5	25.8	6.0	30.3	6.4	35.2	6.9	41.0	7.3	46.9	7.8
21.7	5.5	26.0	6.0	30.4	6.4	35.3	6.9	41.1	7.3	47.1	7.8
21.8	5.5	26.1	6.0	30.6	6.4	35.5	6.9	41.3	7.3	47.2	7.8
21.9	5.5	26.1	6.0	30.7	6.4	35.6	6.9	41.5	7.3	47.3	7.8
22.0	5.6	26.2	6.0	30.7	6.5	35.7	6.9	41.6	7.4	47.4	7.8
22.1	5.6	26.3	6.0	30.8	6.5	35.8	6.9	41.7	7.4	47.5	7.8
22.1	5.6	26.4	6.0	31.0	6.5	36.0	6.9	41.8	7.4	47.7	7.8
22.2	5.6	26.6	6.0	31.0	6.5	36.1	6.9	42.0	7.4	47.8	7.8
22.3	5.6	26.6	6.0	31.1	6.5	36.2	6.9	42.1	7.4	48.0	7.8
22.4	5.6	26.7	6.1	31.2	6.5	36.4	7.0	42.2	7.4	48.0	7.9
22.4	5.6	26.8	6.1	31.3	6.5	36.5	7.0	42.3	7.4	48.2	7.9
22.6	5.6	26.9	6.1	31.4	6.5	36.6	7.0	42.4	7.4	48.4	7.9
22.6	5.6	27.1	6.1	31.5	6.5	36.8	7.0	42.6	7.4	48.5	7.9
22.8	5.6	27.1	6.1	31.6	6.5	36.9	7.0	42.7	7.4	48.6	7.9
22.8	5.7	27.2	6.1	31.8	6.6	37.0	7.0	42.8	7.5	48.8	7.9
22.9	5.7	27.3	6.1	31.8	6.6	37.1	7.0	43.0	7.5	48.9	7.9
23.0	5.7	27.4	6.1	32.0	6.6	37.3	7.0	43.1	7.5	49.0	7.9
23.1	5.7	27.5	6.1	32.0	6.6	37.4	7.0	43.3	7.5	49.2	7.9
23.2	5.7	27.6	6.1	32.2	6.6	37.5	7.0	43.3	7.5	49.3	7.9
23.3	5.7	27.7	6.2	32.3	6.6	37.7	7.1	43.5	7.5	49.4	8.0

49.5	8.0	54.8	8.4	60.3	8.8	65.4	9.2	70.4	9.6	78.8	10.0
49.7	8.0	54.9	8.4	60.4	8.8	65.6	9.2	70.5	9.6	79.2	10.0
49.8	8.0	55.0	8.4	60.6	8.8	65.6	9.2	70.6	9.6	79.5	10.0
49.9	8.0	55.2	8.4	60.7	8.8	65.8	9.2	70.8	9.6		
50.1	8.0	55.3	8.4	60.8	8.8	65.9	9.2	70.9	9.6		
50.1	8.0	55.5	8.4	61.0	8.8	66.0	9.2	71.0	9.6		
50.3	8.0	55.7	8.4	61.1	8.8	66.1	9.2	71.2	9.6		
50.5	8.0	55.8	8.4	61.2	8.8	66.2	9.2	71.4	9.6		
50.5	8.0	55.9	8.4	61.3	8.8	66.4	9.2	71.5	9.6		
50.7	8.1	56.1	8.5	61.4	8.9	66.5	9.3	71.6	9.7		
50.8	8.1	56.3	8.5	61.6	8.9	66.6	9.3	71.8	9.7		
50.9	8.1	56.4	8.5	61.7	8.9	66.8	9.3	71.9	9.7		
51.1	8.1	56.5	8.5	61.9	8.9	66.8	9.3	72.1	9.7		
51.2	8.1	56.7	8.5	61.9	8.9	66.9	9.3	72.2	9.7		
51.3	8.1	56.8	8.5	62.1	8.9	67.1	9.3	72.3	9.7		
51.5	8.1	57.0	8.5	62.3	8.9	67.2	9.3	72.4	9.7		
51.6	8.1	57.1	8.5	62.3	8.9	67.3	9.3	72.6	9.7		
51.8	8.1	57.2	8.5	62.5	8.9	67.4	9.3	72.7	9.7		
51.9	8.1	57.4	8.5	62.6	8.9	67.6	9.3	72.9	9.7		
52.0	8.2	57.6	8.6	62.7	9.0	67.7	9.4	73.1	9.8		
52.1	8.2	57.6	8.6	62.8	9.0	67.8	9.4	73.3	9.8		
52.2	8.2	57.8	8.6	62.9	9.0	68.0	9.4	73.4	9.8		
52.4	8.2	57.9	8.6	63.1	9.0	68.1	9.4	73.7	9.8		
52.5	8.2	58.1	8.6	63.2	9.0	68.2	9.4	73.9	9.8		
52.6	8.2	58.2	8.6	63.3	9.0	68.4	9.4	74.1	9.8		
52.7	8.2	58.3	8.6	63.5	9.0	68.4	9.4	74.4	9.8		
52.9	8.2	58.5	8.6	63.6	9.0	68.7	9.4	74.6	9.8		
53.0	8.2	58.6	8.6	63.7	9.0	68.8	9.4	74.8	9.8		
53.1	8.2	58.7	8.6	63.8	9.0	68.8	9.4	75.1	9.8		
53.3	8.3	58.9	8.7	63.9	9.1	69.0	9.5	75.4	9.9		
53.5	8.3	59.0	8.7	64.1	9.1	69.2	9.5	75.7	9.9		
53.5	8.3	59.1	8.7	64.2	9.1	69.3	9.5	76.0	9.9		
53.7	8.3	59.3	8.7	64.3	9.1	69.4	9.5	76.3	9.9		
53.9	8.3	59.4	8.7	64.5	9.1	69.5	9.5	76.7	9.9		
53.9	8.3	59.6	8.7	64.6	9.1	69.6	9.5	76.9	9.9		
54.1	8.3	59.7	8.7	64.7	9.1	69.7	9.5	77.3	9.9		
54.2	8.3	59.8	8.7	64.8	9.1	69.9	9.5	77.6	9.9		
54.4	8.3	59.9	8.7	65.0	9.1	70.1	9.5	77.8	9.9		
54.5	8.3	60.1	8.7	65.1	9.1	70.1	9.5	78.2	9.9		
54.6	8.4	60.2	8.8	65.2	9.2	70.3	9.6	78.6	10.0		

N	mm	2.3	0.4	4.6	0.8	6.8	1.3	8.9	1.7	11.9	2.1
0.0	0.0	2.4	0.4	4.7	0.9	6.8	1.3	9.0	1.7	12.0	2.1
0.0	0.0	2.5	0.4	4.7	0.9	6.9	1.3	9.1	1.7	12.1	2.2
0.1	0.0	2.5	0.4	4.8	0.9	6.9	1.3	9.1	1.7	12.2	2.2
0.2	0.0	2.5	0.5	4.9	0.9	7.0	1.3	9.2	1.7	12.2	2.2
0.3	0.0	2.6	0.5	4.9	0.9	7.0	1.3	9.2	1.8	12.3	2.2
0.3	0.0	2.7	0.5	4.9	0.9	7.0	1.3	9.3	1.8	12.4	2.2
0.4	0.1	2.7	0.5	5.0	0.9	7.0	1.3	9.4	1.8	12.5	2.2
0.5	0.1	2.8	0.5	5.0	0.9	7.1	1.4	9.5	1.8	12.6	2.2
0.5	0.1	2.8	0.5	5.1	0.9	7.2	1.4	9.5	1.8	12.7	2.2
0.6	0.1	2.9	0.5	5.2	0.9	7.2	1.4	9.6	1.8	12.7	2.2
0.6	0.1	2.9	0.5	5.2	1.0	7.3	1.4	9.6	1.8	12.8	2.2
0.7	0.1	3.0	0.5	5.2	1.0	7.3	1.4	9.7	1.8	12.8	2.3
0.7	0.1	3.1	0.5	5.3	1.0	7.4	1.4	9.8	1.8	12.9	2.3
0.8	0.1	3.1	0.6	5.4	1.0	7.4	1.4	9.9	1.8	13.0	2.3
0.8	0.1	3.1	0.6	5.4	1.0	7.5	1.4	9.9	1.9	13.1	2.3
0.9	0.1	3.2	0.6	5.4	1.0	7.6	1.4	10.0	1.9	13.2	2.3
1.0	0.2	3.3	0.6	5.5	1.0	7.6	1.4	10.0	1.9	13.2	2.3
1.0	0.2	3.3	0.6	5.6	1.0	7.6	1.5	10.1	1.9	13.3	2.3
1.1	0.2	3.4	0.6	5.6	1.0	7.7	1.5	10.2	1.9	13.5	2.3
1.1	0.2	3.4	0.6	5.6	1.0	7.7	1.5	10.2	1.9	13.5	2.3
1.2	0.2	3.5	0.6	5.7	1.1	7.8	1.5	10.3	1.9	13.6	2.3
1.2	0.2	3.5	0.6	5.8	1.1	7.8	1.5	10.4	1.9	13.7	2.4
1.2	0.2	3.6	0.6	5.8	1.1	7.9	1.5	10.4	1.9	13.7	2.4
1.3	0.2	3.6	0.7	5.9	1.1	7.9	1.5	10.5	1.9	13.8	2.4
1.4	0.2	3.7	0.7	5.9	1.1	8.0	1.5	10.6	2.0	13.9	2.4
1.4	0.2	3.7	0.7	5.9	1.1	8.1	1.5	10.6	2.0	14.0	2.4
1.5	0.3	3.8	0.7	6.0	1.1	8.1	1.5	10.8	2.0	14.0	2.4
1.6	0.3	3.8	0.7	6.0	1.1	8.1	1.6	10.8	2.0	14.1	2.4
1.6	0.3	3.9	0.7	6.1	1.1	8.2	1.6	10.9	2.0	14.3	2.4
1.6	0.3	4.0	0.7	6.1	1.1	8.3	1.6	10.9	2.0	14.3	2.4
1.7	0.3	4.0	0.7	6.2	1.2	8.3	1.6	11.0	2.0	14.4	2.4
1.8	0.3	4.1	0.7	6.2	1.2	8.3	1.6	11.1	2.0	14.5	2.5
1.8	0.3	4.1	0.7	6.2	1.2	8.4	1.6	11.2	2.0	14.5	2.5
1.8	0.3	4.2	0.8	6.3	1.2	8.5	1.6	11.3	2.0	14.6	2.5
1.9	0.3	4.2	0.8	6.4	1.2	8.5	1.6	11.4	2.1	14.7	2.5
1.9	0.3	4.3	0.8	6.4	1.2	8.6	1.6	11.4	2.1	14.8	2.5
2.0	0.4	4.3	0.8	6.4	1.2	8.6	1.6	11.5	2.1	14.9	2.5
2.1	0.4	4.4	0.8	6.5	1.2	8.6	1.7	11.6	2.1	14.9	2.5
2.1	0.4	4.4	0.8	6.5	1.2	8.7	1.7	11.6	2.1	15.1	2.5
2.2	0.4	4.5	0.8	6.6	1.2	8.8	1.7	11.7	2.1	15.1	2.5
2.2	0.4	4.5	0.8	6.6	1.3	8.8	1.7	11.8	2.1	15.2	2.5
2.3	0.4	4.6	0.8	6.7	1.3	8.9	1.7	11.9	2.1	15.3	2.6

15.4	2.6	19.3	3.0	23.7	3.5	28.0	3.9	32.6	4.4	37.4	4.8
15.5	2.6	19.4	3.0	23.7	3.5	28.1	3.9	32.7	4.4	37.6	4.8
15.6	2.6	19.5	3.0	23.8	3.5	28.2	3.9	32.7	4.4	37.7	4.8
15.6	2.6	19.6	3.0	23.9	3.5	28.3	3.9	32.9	4.4	37.7	4.8
15.7	2.6	19.6	3.1	24.0	3.5	28.4	4.0	33.0	4.4	37.9	4.9
15.8	2.6	19.8	3.1	24.1	3.5	28.5	4.0	33.1	4.4	38.0	4.9
15.9	2.6	19.9	3.1	24.2	3.5	28.6	4.0	33.2	4.4	38.0	4.9
15.9	2.6	19.9	3.1	24.3	3.5	28.7	4.0	33.3	4.4	38.2	4.9
16.0	2.6	20.0	3.1	24.4	3.5	28.8	4.0	33.5	4.4	38.4	4.9
16.1	2.7	20.1	3.1	24.6	3.6	28.9	4.0	33.5	4.5	38.4	4.9
16.2	2.7	20.2	3.1	24.6	3.6	29.0	4.0	33.6	4.5	38.5	4.9
16.3	2.7	20.3	3.1	24.7	3.6	29.1	4.0	33.8	4.5	38.6	4.9
16.4	2.7	20.4	3.1	24.8	3.6	29.2	4.0	33.8	4.5	38.7	4.9
16.4	2.7	20.5	3.1	24.9	3.6	29.3	4.0	33.9	4.5	38.8	4.9
16.5	2.7	20.6	3.2	25.0	3.6	29.4	4.1	34.0	4.5	39.0	5.0
16.6	2.7	20.7	3.2	25.1	3.6	29.5	4.1	34.2	4.5	39.1	5.0
16.7	2.7	20.8	3.2	25.2	3.6	29.6	4.1	34.2	4.5	39.2	5.0
16.8	2.7	20.9	3.2	25.3	3.6	29.7	4.1	34.3	4.5	39.3	5.0
16.9	2.7	21.0	3.2	25.4	3.6	29.8	4.1	34.5	4.5	39.5	5.0
17.0	2.8	21.1	3.2	25.5	3.7	29.9	4.1	34.6	4.6	39.5	5.0
17.0	2.8	21.2	3.2	25.6	3.7	30.0	4.1	34.6	4.6	39.6	5.0
17.1	2.8	21.3	3.2	25.7	3.7	30.1	4.1	34.8	4.6	39.8	5.0
17.3	2.8	21.4	3.2	25.8	3.7	30.3	4.1	34.9	4.6	39.9	5.0
17.3	2.8	21.5	3.2	25.9	3.7	30.3	4.1	35.0	4.6	40.0	5.0
17.4	2.8	21.6	3.3	26.0	3.7	30.4	4.2	35.1	4.6	40.1	5.1
17.5	2.8	21.6	3.3	26.1	3.7	30.5	4.2	35.2	4.6	40.2	5.1
17.6	2.8	21.8	3.3	26.2	3.7	30.7	4.2	35.4	4.6	40.2	5.1
17.7	2.8	21.9	3.3	26.3	3.7	30.7	4.2	35.5	4.6	40.4	5.1
17.8	2.8	22.0	3.3	26.4	3.7	30.8	4.2	35.5	4.6	40.6	5.1
17.8	2.9	22.1	3.3	26.5	3.8	30.9	4.2	35.7	4.7	40.6	5.1
17.9	2.9	22.2	3.3	26.6	3.8	31.0	4.2	35.7	4.7	40.7	5.1
18.0	2.9	22.3	3.3	26.6	3.8	31.1	4.2	35.9	4.7	40.9	5.1
18.1	2.9	22.4	3.3	26.7	3.8	31.3	4.2	36.0	4.7	41.0	5.1
18.2	2.9	22.5	3.3	26.9	3.8	31.3	4.2	36.1	4.7	41.1	5.1
18.3	2.9	22.6	3.4	27.0	3.8	31.4	4.3	36.2	4.7	41.2	5.2
18.4	2.9	22.6	3.4	27.0	3.8	31.5	4.3	36.3	4.7	41.3	5.2
18.5	2.9	22.8	3.4	27.2	3.8	31.7	4.3	36.4	4.7	41.4	5.2
18.6	2.9	22.9	3.4	27.3	3.8	31.7	4.3	36.6	4.7	41.5	5.2
18.7	2.9	23.0	3.4	27.3	3.8	31.8	4.3	36.6	4.7	41.7	5.2
18.7	3.0	23.1	3.4	27.4	3.9	32.0	4.3	36.8	4.8	41.7	5.2
18.8	3.0	23.1	3.4	27.5	3.9	32.1	4.3	36.9	4.8	41.8	5.2
19.0	3.0	23.2	3.4	27.6	3.9	32.1	4.3	37.0	4.8	42.0	5.2
19.0	3.0	23.4	3.4	27.7	3.9	32.3	4.3	37.1	4.8	42.1	5.2
19.1	3.0	23.4	3.4	27.8	3.9	32.4	4.3	37.2	4.8	42.2	5.2
19.2	3.0	23.6	3.5	27.9	3.9	32.4	4.4	37.3	4.8	42.3	5.3

42.4	5.3	47.6	5.7	54.2	6.2	62.1	6.6	72.6	7.1	86.5	7.5
42.5	5.3	47.7	5.7	54.3	6.2	62.3	6.6	72.9	7.1	86.8	7.5
42.7	5.3	47.8	5.7	54.5	6.2	62.5	6.6	73.1	7.1	87.2	7.5
42.7	5.3	47.9	5.7	54.7	6.2	62.8	6.6	73.5	7.1	87.5	7.5
42.9	5.3	48.1	5.8	54.9	6.2	63.0	6.7	73.7	7.1	87.9	7.6
42.9	5.3	48.2	5.8	55.0	6.2	63.1	6.7	74.0	7.1	88.3	7.6
43.0	5.3	48.4	5.8	55.2	6.2	63.4	6.7	74.3	7.1	88.5	7.6
43.2	5.3	48.4	5.8	55.4	6.2	63.6	6.7	74.5	7.1	88.9	7.6
43.3	5.3	48.6	5.8	55.5	6.2	63.7	6.7	74.9	7.1	89.4	7.6
43.4	5.4	48.8	5.8	55.7	6.3	64.0	6.7	75.1	7.2	89.6	7.6
43.5	5.4	48.9	5.8	55.9	6.3	64.3	6.7	75.4	7.2	89.9	7.6
43.6	5.4	49.0	5.8	56.0	6.3	64.5	6.7	75.7	7.2	90.3	7.6
43.7	5.4	49.2	5.8	56.2	6.3	64.8	6.7	76.0	7.2	90.7	7.6
43.8	5.4	49.3	5.8	56.4	6.3	65.0	6.7	76.4	7.2	91.1	7.6
43.9	5.4	49.5	5.9	56.6	6.3	65.3	6.8	76.6	7.2	91.4	7.7
44.1	5.4	49.6	5.9	56.8	6.3	65.4	6.8	76.9	7.2	91.8	7.7
44.1	5.4	49.8	5.9	56.9	6.3	65.7	6.8	77.2	7.2	92.1	7.7
44.3	5.4	49.9	5.9	57.1	6.3	66.0	6.8	77.5	7.2	92.5	7.7
44.4	5.4	50.0	5.9	57.2	6.3	66.1	6.8	77.8	7.2	93.0	7.7
44.5	5.5	50.2	5.9	57.4	6.4	66.5	6.8	78.1	7.3	93.2	7.7
44.6	5.5	50.3	5.9	57.6	6.4	66.7	6.8	78.4	7.3	93.6	7.7
44.8	5.5	50.4	5.9	57.7	6.4	66.8	6.8	78.7	7.3	94.1	7.7
44.9	5.5	50.6	5.9	57.9	6.4	67.1	6.8	79.0	7.3	94.4	7.7
44.9	5.5	50.7	5.9	58.1	6.4	67.4	6.8	79.4	7.3	94.8	7.7
45.1	5.5	50.8	6.0	58.2	6.4	67.6	6.9	79.8	7.3	95.1	7.8
45.2	5.5	51.0	6.0	58.4	6.4	67.8	6.9	79.9	7.3	95.6	7.8
45.2	5.5	51.1	6.0	58.6	6.4	68.0	6.9	80.3	7.3	95.9	7.8
45.4	5.5	51.3	6.0	58.8	6.4	68.3	6.9	80.7	7.3	96.3	7.8
45.5	5.5	51.4	6.0	58.9	6.4	68.5	6.9	80.9	7.3	96.7	7.8
45.6	5.6	51.6	6.0	59.2	6.5	68.8	6.9	81.3	7.4	97.1	7.8
45.7	5.6	51.7	6.0	59.3	6.5	69.0	6.9	81.6	7.4	97.5	7.8
45.8	5.6	51.9	6.0	59.5	6.5	69.2	6.9	81.9	7.4	97.9	7.8
45.9	5.6	52.1	6.0	59.6	6.5	69.5	6.9	82.2	7.4	98.2	7.8
46.0	5.6	52.2	6.0	59.8	6.5	69.7	6.9	82.6	7.4	98.7	7.8
46.2	5.6	52.4	6.1	60.1	6.5	69.9	7.0	82.9	7.4	99.1	7.9
46.3	5.6	52.5	6.1	60.2	6.5	70.1	7.0	83.2	7.4	99.4	7.9
46.4	5.6	52.7	6.1	60.4	6.5	70.4	7.0	83.6	7.4	99.8	7.9
46.5	5.6	52.8	6.1	60.6	6.5	70.5	7.0	84.0	7.4	100.3	7.9
46.7	5.6	53.0	6.1	60.8	6.5	70.8	7.0	84.1	7.4	100.6	7.9
46.7	5.7	53.2	6.1	61.0	6.6	71.0	7.0	84.6	7.5	101.0	7.9
46.9	5.7	53.3	6.1	61.2	6.6	71.4	7.0	84.9	7.5	101.4	7.9
47.1	5.7	53.5	6.1	61.3	6.6	71.5	7.0	85.1	7.5	101.9	7.9
47.2	5.7	53.7	6.1	61.6	6.6	71.8	7.0	85.5	7.5	102.2	7.9
47.3	5.7	53.8	6.1	61.7	6.6	72.2	7.0	85.9	7.5	102.7	7.9
47.4	5.7	54.0	6.2	61.9	6.6	72.3	7.1	86.2	7.5	103.2	8.0

103.4	8.0	121.9	8.4	145.3	8.8	172.9	9.2	206.4	9.6	245.7	10.0
103.9	8.0	122.5	8.4	145.7	8.8	173.5	9.2	207.2	9.6	246.9	10.0
104.4	8.0	122.9	8.4	146.4	8.8	174.4	9.2	208.3	9.6	247.7	10.0
104.7	8.0	123.5	8.4	147.0	8.8	175.2	9.2	209.2	9.6		
105.1	8.0	124.0	8.4	147.8	8.8	175.9	9.2	210.1	9.6		
105.6	8.0	124.5	8.4	148.3	8.8	176.7	9.2	211.2	9.6		
106.0	8.0	125.1	8.4	149.0	8.8	177.5	9.2	212.0	9.6		
106.4	8.0	125.6	8.4	149.8	8.8	178.1	9.2	213.1	9.6		
106.8	8.0	126.3	8.4	150.3	8.8	179.2	9.2	214.1	9.6		
107.3	8.1	126.7	8.5	151.0	8.9	180.0	9.3	214.8	9.7		
107.7	8.1	127.4	8.5	151.7	8.9	180.5	9.3	215.9	9.7		
108.2	8.1	128.0	8.5	152.2	8.9	181.5	9.3	216.9	9.7		
108.7	8.1	128.4	8.5	153.0	8.9	182.3	9.3	217.8	9.7		
108.9	8.1	129.0	8.5	153.6	8.9	183.1	9.3	218.8	9.7		
109.5	8.1	129.7	8.5	154.3	8.9	183.8	9.3	219.8	9.7		
110.0	8.1	130.2	8.5	155.0	8.9	184.7	9.3	220.8	9.7		
110.3	8.1	130.7	8.5	155.6	8.9	185.6	9.3	221.7	9.7		
110.8	8.1	131.3	8.5	156.3	8.9	186.3	9.3	222.8	9.7		
111.2	8.1	131.9	8.5	157.0	8.9	187.1	9.3	223.8	9.7		
111.7	8.2	132.5	8.6	157.8	9.0	188.2	9.4	224.6	9.8		
112.1	8.2	133.1	8.6	158.5	9.0	188.7	9.4	225.9	9.8		
112.6	8.2	133.8	8.6	159.1	9.0	189.8	9.4	226.9	9.8		
113.2	8.2	134.2	8.6	159.9	9.0	190.7	9.4	227.5	9.8		
113.5	8.2	135.0	8.6	160.6	9.0	191.2	9.4	228.7	9.8		
114.1	8.2	135.6	8.6	161.2	9.0	192.2	9.4	229.7	9.8		
114.6	8.2	136.0	8.6	162.0	9.0	193.1	9.4	230.6	9.8		
114.9	8.2	136.7	8.6	162.7	9.0	193.9	9.4	231.6	9.8		
115.5	8.2	137.4	8.6	163.4	9.0	194.7	9.4	232.6	9.8		
115.9	8.2	137.8	8.6	164.1	9.0	195.6	9.4	233.7	9.8		
116.3	8.3	138.4	8.7	164.7	9.1	196.6	9.5	234.5	9.9		
116.8	8.3	139.0	8.7	165.5	9.1	197.4	9.5	235.7	9.9		
117.4	8.3	139.7	8.7	166.2	9.1	198.3	9.5	236.8	9.9		
117.8	8.3	140.2	8.7	167.0	9.1	199.3	9.5	237.5	9.9		
118.3	8.3	140.9	8.7	167.8	9.1	199.9	9.5	238.7	9.9		
118.8	8.3	141.5	8.7	168.4	9.1	201.0	9.5	239.8	9.9		
119.3	8.3	142.0	8.7	169.2	9.1	202.0	9.5	240.5	9.9		
119.7	8.3	142.7	8.7	170.1	9.1	202.6	9.5	241.6	9.9		
120.4	8.3	143.4	8.7	170.5	9.1	203.7	9.5	242.7	9.9		
120.9	8.3	143.8	8.7	171.4	9.1	204.5	9.5	243.7	9.9		
121.3	8.4	144.6	8.8	172.2	9.2	205.4	9.6	244.6	10.0		

Sample N6

N	mm										
		2.2	0.4	4.5	0.8	7.9	1.3	12.2	1.7	17.0	2.1
0.0	0.0	2.3	0.4	4.5	0.9	8.0	1.3	12.4	1.7	17.1	2.1
0.0	0.0	2.2	0.4	4.7	0.9	8.0	1.3	12.5	1.7	17.1	2.2
0.1	0.0	2.3	0.4	4.7	0.9	8.1	1.3	12.5	1.7	17.3	2.2
0.2	0.0	2.4	0.5	4.8	0.9	8.3	1.3	12.6	1.7	17.4	2.2
0.3	0.0	2.4	0.5	4.8	0.9	8.4	1.3	12.8	1.8	17.5	2.2
0.3	0.0	2.5	0.5	4.9	0.9	8.4	1.3	12.9	1.8	17.6	2.2
0.4	0.1	2.5	0.5	4.9	0.9	8.5	1.3	13.0	1.8	17.7	2.2
0.5	0.1	2.6	0.5	5.0	0.9	8.7	1.4	13.1	1.8	17.9	2.2
0.6	0.1	2.6	0.5	5.2	0.9	8.7	1.4	13.2	1.8	17.9	2.2
0.6	0.1	2.7	0.5	5.2	0.9	8.8	1.4	13.3	1.8	18.1	2.2
0.7	0.1	2.7	0.5	5.2	1.0	8.9	1.4	13.4	1.8	18.2	2.2
0.7	0.1	2.8	0.5	5.3	1.0	9.0	1.4	13.6	1.8	18.2	2.3
0.7	0.1	2.8	0.5	5.4	1.0	9.1	1.4	13.6	1.8	18.3	2.3
0.8	0.1	2.9	0.6	5.4	1.0	9.2	1.4	13.7	1.8	18.5	2.3
0.8	0.1	2.9	0.6	5.5	1.0	9.3	1.4	13.8	1.9	18.6	2.3
0.9	0.1	3.0	0.6	5.6	1.0	9.4	1.4	14.0	1.9	18.7	2.3
1.0	0.2	3.0	0.6	5.7	1.0	9.5	1.4	14.1	1.9	18.8	2.3
0.9	0.2	3.1	0.6	5.7	1.0	9.7	1.5	14.2	1.9	18.9	2.3
1.0	0.2	3.1	0.6	5.8	1.0	9.8	1.5	14.3	1.9	19.0	2.3
1.1	0.2	3.2	0.6	6.0	1.0	9.8	1.5	14.4	1.9	19.1	2.3
1.1	0.2	3.3	0.6	6.0	1.1	9.9	1.5	14.5	1.9	19.3	2.3
1.2	0.2	3.3	0.6	6.1	1.1	10.1	1.5	14.6	1.9	19.4	2.4
1.3	0.2	3.3	0.6	6.2	1.1	10.1	1.5	14.7	1.9	19.5	2.4
1.3	0.2	3.4	0.7	6.2	1.1	10.2	1.5	14.9	1.9	19.6	2.4
1.3	0.2	3.4	0.7	6.3	1.1	10.4	1.5	14.9	2.0	19.7	2.4
1.4	0.2	3.5	0.7	6.4	1.1	10.4	1.5	15.0	2.0	19.8	2.4
1.4	0.3	3.6	0.7	6.5	1.1	10.6	1.5	15.2	2.0	20.0	2.4
1.4	0.3	3.6	0.7	6.6	1.1	10.7	1.6	15.3	2.0	20.0	2.4
1.5	0.3	3.6	0.7	6.7	1.1	10.8	1.6	15.4	2.0	20.1	2.4
1.5	0.3	3.7	0.7	6.8	1.1	10.9	1.6	15.5	2.0	20.3	2.4
1.6	0.3	3.7	0.7	6.8	1.2	11.0	1.6	15.6	2.0	20.4	2.4
1.6	0.3	3.8	0.7	6.9	1.2	11.1	1.6	15.7	2.0	20.5	2.5
1.7	0.3	3.9	0.7	7.0	1.2	11.2	1.6	15.9	2.0	20.6	2.5
1.7	0.3	3.9	0.8	7.1	1.2	11.3	1.6	16.0	2.0	20.7	2.5
1.7	0.3	4.0	0.8	7.2	1.2	11.4	1.6	16.1	2.1	20.8	2.5
1.8	0.3	4.1	0.8	7.3	1.2	11.5	1.6	16.2	2.1	20.9	2.5
1.8	0.4	4.1	0.8	7.4	1.2	11.6	1.6	16.3	2.1	21.0	2.5
1.9	0.4	4.2	0.8	7.4	1.2	11.7	1.7	16.4	2.1	21.1	2.5
1.9	0.4	4.3	0.8	7.5	1.2	11.9	1.7	16.5	2.1	21.2	2.5
2.0	0.4	4.3	0.8	7.7	1.2	11.9	1.7	16.6	2.1	21.3	2.5
2.1	0.4	4.4	0.8	7.7	1.3	12.0	1.7	16.7	2.1	21.4	2.5
2.1	0.4	4.5	0.8	7.8	1.3	12.1	1.7	16.8	2.1	21.5	2.6

21.6	2.6	26.3	3.0	30.9	3.5	35.9	3.9	41.1	4.4	47.0	4.8
21.7	2.6	26.4	3.0	31.1	3.5	36.1	3.9	41.2	4.4	47.0	4.8
21.8	2.6	26.5	3.0	31.2	3.5	36.2	3.9	41.4	4.4	47.2	4.8
21.9	2.6	26.6	3.0	31.3	3.5	36.3	3.9	41.5	4.4	47.4	4.8
22.0	2.6	26.7	3.1	31.4	3.5	36.4	4.0	41.6	4.4	47.5	4.9
22.1	2.6	26.8	3.1	31.5	3.5	36.5	4.0	41.7	4.4	47.6	4.9
22.3	2.6	26.9	3.1	31.6	3.5	36.6	4.0	41.9	4.4	47.8	4.9
22.4	2.6	27.0	3.1	31.7	3.5	36.8	4.0	42.0	4.4	47.9	4.9
22.5	2.6	27.1	3.1	31.9	3.5	36.9	4.0	42.1	4.4	48.0	4.9
22.5	2.7	27.2	3.1	31.9	3.6	37.0	4.0	42.2	4.5	48.2	4.9
22.7	2.7	27.3	3.1	32.0	3.6	37.1	4.0	42.3	4.5	48.4	4.9
22.8	2.7	27.5	3.1	32.2	3.6	37.2	4.0	42.4	4.5	48.4	4.9
22.9	2.7	27.5	3.1	32.3	3.6	37.4	4.0	42.5	4.5	48.6	4.9
23.0	2.7	27.6	3.1	32.3	3.6	37.5	4.0	42.7	4.5	48.8	4.9
23.1	2.7	27.7	3.2	32.5	3.6	37.6	4.1	42.8	4.5	48.9	5.0
23.2	2.7	27.8	3.2	32.6	3.6	37.8	4.1	42.9	4.5	49.1	5.0
23.3	2.7	27.9	3.2	32.6	3.6	37.8	4.1	43.0	4.5	49.2	5.0
23.4	2.7	28.1	3.2	32.8	3.6	37.9	4.1	43.1	4.5	49.3	5.0
23.4	2.7	28.1	3.2	33.0	3.6	38.1	4.1	43.2	4.5	49.4	5.0
23.6	2.8	28.2	3.2	33.0	3.7	38.1	4.1	43.4	4.6	49.6	5.0
23.7	2.8	28.3	3.2	33.1	3.7	38.2	4.1	43.5	4.6	49.8	5.0
23.7	2.8	28.4	3.2	33.3	3.7	38.4	4.1	43.6	4.6	49.9	5.0
23.9	2.8	28.5	3.2	33.4	3.7	38.5	4.1	43.8	4.6	50.0	5.0
24.0	2.8	28.7	3.2	33.5	3.7	38.6	4.1	43.8	4.6	50.2	5.0
24.1	2.8	28.8	3.3	33.6	3.7	38.7	4.2	44.0	4.6	50.3	5.1
24.2	2.8	28.8	3.3	33.7	3.7	38.8	4.2	44.2	4.6	50.5	5.1
24.3	2.8	29.0	3.3	33.8	3.7	38.9	4.2	44.3	4.6	50.7	5.1
24.4	2.8	29.0	3.3	33.9	3.7	39.1	4.2	44.4	4.6	50.8	5.1
24.5	2.8	29.1	3.3	34.1	3.7	39.2	4.2	44.5	4.6	51.0	5.1
24.6	2.9	29.3	3.3	34.2	3.8	39.3	4.2	44.7	4.7	51.1	5.1
24.8	2.9	29.4	3.3	34.3	3.8	39.4	4.2	44.8	4.7	51.2	5.1
24.8	2.9	29.5	3.3	34.4	3.8	39.5	4.2	45.0	4.7	51.4	5.1
24.9	2.9	29.6	3.3	34.5	3.8	39.6	4.2	45.2	4.7	51.6	5.1
25.1	2.9	29.7	3.3	34.6	3.8	39.7	4.2	45.2	4.7	51.7	5.1
25.1	2.9	29.8	3.4	34.8	3.8	39.8	4.3	45.4	4.7	51.9	5.2
25.2	2.9	29.9	3.4	34.8	3.8	40.0	4.3	45.5	4.7	52.1	5.2
25.3	2.9	30.0	3.4	34.9	3.8	40.1	4.3	45.7	4.7	52.2	5.2
25.4	2.9	30.1	3.4	35.1	3.8	40.3	4.3	45.8	4.7	52.4	5.2
25.5	2.9	30.2	3.4	35.2	3.8	40.4	4.3	46.0	4.7	52.6	5.2
25.7	3.0	30.3	3.4	35.3	3.9	40.4	4.3	46.1	4.8	52.7	5.2
25.7	3.0	30.5	3.4	35.4	3.9	40.6	4.3	46.2	4.8	52.8	5.2
25.8	3.0	30.5	3.4	35.5	3.9	40.8	4.3	46.4	4.8	53.1	5.2
26.0	3.0	30.6	3.4	35.6	3.9	40.8	4.3	46.5	4.8	53.2	5.2
26.1	3.0	30.8	3.4	35.7	3.9	40.9	4.3	46.6	4.8	53.3	5.2
26.1	3.0	30.8	3.5	35.8	3.9	41.0	4.4	46.8	4.8	53.5	5.3

53.7	5.3	61.6	5.7	69.9	6.2	78.9	6.6	89.1	7.1	103.5	7.5
53.9	5.3	61.8	5.7	70.1	6.2	79.3	6.6	89.4	7.1	103.7	7.5
54.0	5.3	61.9	5.7	70.3	6.2	79.5	6.6	89.6	7.1	104.2	7.5
54.2	5.3	62.1	5.7	70.4	6.2	79.5	6.6	89.9	7.1	104.6	7.5
54.4	5.3	62.3	5.8	70.6	6.2	79.8	6.7	90.1	7.1	104.9	7.6
54.5	5.3	62.4	5.8	70.9	6.2	80.1	6.7	90.5	7.1	105.4	7.6
54.8	5.3	62.7	5.8	71.0	6.2	80.2	6.7	90.7	7.1	105.8	7.6
54.9	5.3	62.8	5.8	71.2	6.2	80.5	6.7	90.9	7.1	106.2	7.6
55.0	5.3	63.0	5.8	71.5	6.2	80.7	6.7	91.2	7.1	106.6	7.6
55.2	5.4	63.2	5.8	71.6	6.3	80.9	6.7	91.5	7.2	107.0	7.6
55.5	5.4	63.4	5.8	71.8	6.3	81.0	6.7	91.7	7.2	107.5	7.6
55.5	5.4	63.6	5.8	72.0	6.3	81.3	6.7	92.0	7.2	107.9	7.6
55.7	5.4	63.8	5.8	72.2	6.3	81.6	6.7	92.3	7.2	108.3	7.6
55.9	5.4	64.0	5.8	72.4	6.3	81.7	6.7	92.5	7.2	108.8	7.6
56.1	5.4	64.1	5.9	72.6	6.3	82.0	6.8	92.8	7.2	109.1	7.7
56.2	5.4	64.2	5.9	72.8	6.3	82.3	6.8	93.0	7.2	109.7	7.7
56.4	5.4	64.5	5.9	73.0	6.3	82.4	6.8	93.4	7.2	110.2	7.7
56.7	5.4	64.7	5.9	73.2	6.3	82.6	6.8	93.6	7.2	110.6	7.7
56.7	5.4	64.8	5.9	73.5	6.3	82.9	6.8	94.0	7.2	111.1	7.7
57.0	5.5	65.0	5.9	73.6	6.4	83.1	6.8	94.3	7.3	111.5	7.7
57.2	5.5	65.2	5.9	73.8	6.4	83.3	6.8	94.5	7.3	112.1	7.7
57.2	5.5	65.4	5.9	74.0	6.4	83.5	6.8	94.9	7.3	112.5	7.7
57.5	5.5	65.6	5.9	74.1	6.4	83.8	6.8	95.3	7.3	113.0	7.7
57.8	5.5	65.8	5.9	74.4	6.4	83.9	6.8	95.4	7.3	113.5	7.7
57.8	5.5	66.0	6.0	74.6	6.4	84.2	6.9	95.8	7.3	114.0	7.8
58.0	5.5	66.1	6.0	74.8	6.4	84.5	6.9	96.1	7.3	114.6	7.8
58.1	5.5	66.4	6.0	75.1	6.4	84.6	6.9	96.4	7.3	115.2	7.8
58.4	5.5	66.6	6.0	75.2	6.4	84.9	6.9	96.7	7.3	115.5	7.8
58.5	5.5	66.6	6.0	75.4	6.4	85.2	6.9	97.0	7.3	116.2	7.8
58.7	5.6	66.9	6.0	75.6	6.5	85.3	6.9	97.5	7.4	116.7	7.8
58.9	5.6	67.1	6.0	75.8	6.5	85.5	6.9	97.7	7.4	117.1	7.8
59.1	5.6	67.3	6.0	76.1	6.5	85.8	6.9	98.2	7.4	117.7	7.8
59.2	5.6	67.4	6.0	76.2	6.5	86.0	6.9	98.6	7.4	118.3	7.8
59.5	5.6	67.6	6.0	76.5	6.5	86.3	6.9	98.7	7.4	118.8	7.8
59.6	5.6	67.8	6.1	76.7	6.5	86.4	7.0	99.2	7.4	119.3	7.9
59.8	5.6	68.0	6.1	76.8	6.5	86.8	7.0	99.7	7.4	120.0	7.9
60.0	5.6	68.2	6.1	77.1	6.5	86.9	7.0	99.9	7.4	120.6	7.9
60.1	5.6	68.4	6.1	77.3	6.5	87.2	7.0	100.2	7.4	121.1	7.9
60.3	5.6	68.5	6.1	77.5	6.5	87.5	7.0	100.6	7.4	121.8	7.9
60.4	5.7	68.7	6.1	77.7	6.6	87.7	7.0	101.1	7.5	122.4	7.9
60.7	5.7	69.0	6.1	77.9	6.6	88.0	7.0	101.3	7.5	122.7	7.9
60.8	5.7	69.1	6.1	78.1	6.6	88.3	7.0	101.7	7.5	123.6	7.9
61.0	5.7	69.3	6.1	78.3	6.6	88.4	7.0	102.2	7.5	124.2	7.9
61.3	5.7	69.5	6.1	78.5	6.6	88.7	7.0	102.5	7.5	124.6	7.9
61.4	5.7	69.7	6.2	78.8	6.6	88.9	7.1	103.0	7.5	125.3	8.0

125.9	8.0	154.4	8.4	191.9	8.8	238.8	9.2	295.1	9.6	359.2	10.0
126.6	8.0	155.3	8.4	193.1	8.8	240.1	9.2	296.2	9.6	361.3	10.0
127.1	8.0	156.0	8.4	194.4	8.8	241.2	9.2	298.0	9.6	363.2	10.0
127.8	8.0	157.0	8.4	195.1	8.8	242.8	9.2	299.6	9.6		
128.5	8.0	157.6	8.4	196.5	8.8	244.2	9.2	300.6	9.6		
129.0	8.0	158.6	8.4	197.6	8.8	245.0	9.2	302.5	9.6		
129.8	8.0	159.5	8.4	198.5	8.8	246.6	9.2	304.0	9.6		
130.5	8.0	160.2	8.4	199.7	8.8	248.0	9.2	305.6	9.6		
130.9	8.0	161.3	8.4	200.9	8.8	249.2	9.2	307.1	9.6		
131.7	8.1	162.1	8.5	201.8	8.9	250.4	9.3	308.6	9.7		
132.5	8.1	162.8	8.5	203.0	8.9	251.8	9.3	310.3	9.7		
133.0	8.1	163.7	8.5	204.0	8.9	253.2	9.3	311.8	9.7		
133.6	8.1	164.7	8.5	205.4	8.9	254.4	9.3	313.4	9.7		
134.4	8.1	165.6	8.5	206.3	8.9	256.0	9.3	315.2	9.7		
135.1	8.1	166.4	8.5	207.5	8.9	257.5	9.3	316.4	9.7		
135.7	8.1	167.3	8.5	208.8	8.9	258.5	9.3	318.3	9.7		
136.4	8.1	168.4	8.5	209.7	8.9	260.1	9.3	320.0	9.7		
137.3	8.1	169.1	8.5	211.0	8.9	261.8	9.3	321.2	9.7		
137.7	8.1	170.3	8.5	212.3	8.9	262.6	9.3	323.0	9.7		
138.5	8.2	171.2	8.6	213.1	9.0	264.2	9.4	324.5	9.8		
139.4	8.2	171.9	8.6	214.4	9.0	265.7	9.4	326.2	9.8		
139.8	8.2	173.1	8.6	215.7	9.0	267.0	9.4	327.7	9.8		
140.7	8.2	174.0	8.6	216.7	9.0	268.2	9.4	329.3	9.8		
141.5	8.2	174.8	8.6	218.0	9.0	269.8	9.4	331.2	9.8		
142.1	8.2	175.7	8.6	219.0	9.0	271.4	9.4	332.6	9.8		
142.8	8.2	176.7	8.6	220.4	9.0	272.6	9.4	334.4	9.8		
143.5	8.2	177.7	8.6	221.4	9.0	274.1	9.4	336.3	9.8		
144.3	8.2	178.6	8.6	222.7	9.0	275.8	9.4	337.5	9.8		
145.1	8.2	179.6	8.6	223.9	9.0	276.9	9.4	339.5	9.8		
145.7	8.3	180.8	8.7	225.0	9.1	278.5	9.5	341.3	9.9		
146.7	8.3	181.5	8.7	226.4	9.1	280.2	9.5	342.5	9.9		
147.2	8.3	182.8	8.7	227.7	9.1	281.2	9.5	344.3	9.9		
148.1	8.3	183.9	8.7	228.5	9.1	282.8	9.5	346.1	9.9		
149.0	8.3	184.6	8.7	229.9	9.1	284.4	9.5	347.6	9.9		
149.5	8.3	185.7	8.7	231.2	9.1	285.9	9.5	349.2	9.9		
150.5	8.3	186.9	8.7	232.4	9.1	287.1	9.5	351.0	9.9		
151.2	8.3	187.8	8.7	233.7	9.1	288.7	9.5	352.8	9.9		
152.0	8.3	188.8	8.7	234.8	9.1	290.4	9.5	354.2	9.9		
152.7	8.3	189.9	8.7	236.3	9.1	291.6	9.5	356.1	9.9		
153.6	8.4	191.1	8.8	237.3	9.2	293.2	9.6	358.1	10.0		

Appendix B

This section provides all the key information related to the micro-CT system, the experimental variables and the operational parameters.

1 The System
Scanner=Skyscan1076
Instrument SN=13874
Hardware=B
Secure mode=OFF
Software=Version 2. 6 (build 5)
Tube=Hamamatsu 100/250
Camera=Hamamatsu Orca-HRF
Camera Pixel Size (μm)=   11.44
Camera X/Y Ratio=0.9820
2 Data Acquisition
Source Voltage (kV)= 100
Source Current (μA)= 100
Filter=Al 1.0 mm
Object to Source (mm)=121.000
Camera to Source (mm)=161.000
Number Of Rows= 1048
Number Of Columns= 2000
Optical Axis (line)= 400
Image Pixel Size (μm)= 17.2000
Image Format=TIFF
Depth (bits)=16
Data Offset (bytes)= 264
Horizontal overlap (pixel)=0
Camera horizontal position=Center
Visual Camera=OFF
Screen LUT=0
Exposure (ms)=   2360
Rotation Step (deg)=0.500
Frame Averaging=On (3)
Scanning position=88.800 mm
Suggested beam-hardening correction=10
Suggested HU-Calibration=7778
Number of connected scans=1
Use 360 Rotation=NO
Rotation Direction=CC
Scanning Trajectory=ROUND
Type Of Motion=STEP AND SHOOT
Camera Offset=OFF
Scanning Start Angle=196.500
Scan duration=01:01:55

3 Reconstruction statistics
Reconstruction Program=NRecon
Program Version=Version: 1.6.9.18
Reconstruction engine=NReconServer
Engine version=Version: 1.6.9
Reconstruction from batch=No
Postalignment=-2.00
Reconstruction mode=Standard
Dataset Origin=Skyscan1076
First Section=5
Last Section=850
Reconstruction duration per slice (seconds)=1.511820
Total reconstruction time (846 slices) in seconds=1279.000000
Section to Section Step=1
Sections Count=846
Result File Type=BMP
Result File Header Length (bytes)=1134
Result Image Width (pixels)=2000
Result Image Height (pixels)=2000
Pixel Size (µm)=17.20874
Reconstruction Angular Range (deg)=197.00
Use 180+=OFF
Angular Step (deg)=0.5000
Smoothing=0
Ring Artifact Correction=10
Draw Scales=ON
Object Bigger than FOV=OFF
Reconstruction from ROI=OFF
Filter cutoff relative to Nyquisit frequency=100
Filter type=0
Filter type meaning (1)
1: Hann; 2: Ramp; 3: Almost Ramp;
Filter type meaning (2)
11: Cosine; 12: Shepp-Logan; [100,200]: Generalized Hamming, alpha=(iFilter-100)/100
Undersampling factor=1
Threshold for defect pixel mask (%)=0
Beam Hardening Correction (%)=25
CS Static Rotation (deg)=0.00
Minimum for CS to Image Conversion=0.000000
Maximum for CS to Image Conversion=0.026002
HU Calibration=OFF
BMP LUT=0
Cone-beam Angle Horiz.(deg)=16.188761
Cone-beam Angle Vert.(deg)=8.524042

4 Thresholding statistics

Mean (total): 19.759

<u>Selection</u>

Begin: 21

End: 92

Number of voxels: 36547

Mean: 41.399

Standard deviation: 10.548

Standard error of mean: 0.055

95% confidence limits:-

Minimum: 41.289

Maximum: 41.509

5 Analysis

CT Analyser, Version: 1.16.1.0

Operator identity: sbhaduri

Computer name: ALOKE-GRAD03

Computation time 09:10:16

Dataset folder D:\Data\Data\CT Scans\Clogged\Sponge_clogged_Rec\

Pixel size 17.20874 µm

Lower grey threshold: 35

Upper grey threshold: 103

6 Summary (2D data)

Tissue volume, TV 3384000000.00000, pixel^3

Bone volume, BV 295582035.12500, pixel^3

Percent bone volume, BV/TV 8.73469, %

Tissue surface, TS 14767008.84935, pixel^2

Peripheral tissue surface, TS(per) 6767008.84935, pixel^2

Bone surface, BS 82171602.29635, pixel^2

Peripheral bone surface, BS(per) 57307991.29635, pixel^2

Bone surface / volume ratio, BS/BV 0.27800, 1/pixel

Mean total crossectional tissue area, T.Ar 4000000.00000, pixel^2

Mean total crossectional tissue perimeter, T.Pm 7998.82843, pixel

Mean total crossectional bone area, B.Ar 349387.74837, pixel^2

Mean total crossectional bone perimeter, B.Pm 67739.94243, pixel

Mean number of objects per slice, Obj.N 2214.81087, -

Average object area per slice, Av.Obj.Ar 170.42726, pixel^2

Average object area-equivalent circle diameter per slice, Av.Obj.ECDa 14.19053, pixel

Average moment of inertia (x), Av.MMI(x) 37303770416.61176, pixel^4

Average moment of inertia (y), Av.MMI(y) 40435298501.48386 pixel^4

Mean polar moment of inertia, MMI(polar) 77739068918.09547, pixel^4

Average principal moment of inertia (max), Av.MMI(max) 50061278675.04729, pixel^4

Average principal moment of inertia (min), Av.MMI(min) 27677790243.04837, pixel^4

Mean eccentricity, Ecc 0.69435, -

Crossectional thickness, Cs.Th 10.31556, pixel

Trabecular thickness (plate model), Tb.Th(pl) 7.19426, pixel

Trabecular separation (plate model), Tb.Sp(pl) 75.16996, pixel

Trabecular number (plate model), Tb.N(pl) 0.01214, 1/pixel

Trabecular diameter (rod model), Tb.Dm(rd) 14.38852, pixel
Trabecular separation (rod model), Tb.Sp(rd) 28.75716, pixel
Trabecular number (rod model), Tb.N(rd) 0.02318, 1/pixel
Mean trabecular pattern factor, Tb.Pf 0.07013, 1/pixel
Closed porosity (percent), Po(cl) 16.69089, %
Centroid (x), Crd.X 1074.98140, pixel
Centroid (y), Crd.Y 899.94113, pixel
Centroid (z), Crd.Z 338.15223, pixel
Mean fractal dimension, FD 1.48325, -
Total intersection surface, i.S 0.00000, pixel^2
Percent intersection surface, i.S/TS(per) 0.00000, %
Number of layers,,846
Lower vertical position, 5.000,pixel
Upper vertical position, 850.000,pixel
Pixel size, 17.20874,μm

7 Summary (3D data)

CT Analyzer

Version: 1.14.4.1

Lower grey threshold, 35
Upper grey threshold, 103
Degree of anisotropy, DA 1.93017 (0.48191)
Eigenvalue 1, 0.46132,
Eigenvalue 2, 0.76854,
Eigenvalue 3, 0.89044,

Date and time	15.03.2016 11:51		
Operator identity	skyscan		
Computer name	DOSCHAKCLUSTER0		
Computation time	10:02:05		
Dataset folder	X:\UofA Kumar - Sponge\Sponge_B_clogged\Sponge_clogged_Rec\VOI\		
Pixel size	17.20874	μm	
Lower grey threshold	29		
Upper grey threshold	255		
Total VOI volume	TV	7828.33863	mm^3
Object volume	Obj.V	1616.81819	mm^3
Percent object volume	Obj.V/TV	20.6534	%
Total VOI surface	TS	2338.15417	mm^2
Peripheral VOI surface	TS(per)	1262.72921	mm^2
Object surface	Obj.S	15310.15402	mm^2
Object surface / volume ratio	Obj.S/Obj.V	9.46931	1/mm
Mean total crossectional ROI area	T.Ar	537.71248	mm^2
Mean total crossectional ROI perimeter	T.Pm	86.73427	mm
Mean total crossectional object area	Obj.Ar	111.05592	mm^2
Mean total crossectional object perimeter	Obj.Pm	723.3792	mm
Mean number of objects per slice	Obj.N	507.76359	
Average object area per slice	Av.Obj.Ar	0.29648	mm^2
Average object area-equivalent circle diameter per slice	Av.Obj.ECDa	0.57575	mm
Average moment of inertia (x)	Av.MMI(x)	3407.50666	mm^4
Average moment of inertia (y)	Av.MMI(y)	3685.18746	mm^4
Mean polar moment of inertia	MMI(polar)	7092.69413	mm^4
Average principal moment of inertia (max)	Av.MMI(max)	4645.44981	mm^4
Average principal moment of inertia (min)	Av.MMI(min)	2447.24432	mm^4
Mean eccentricity	Ecc	0.70617	
Crossectional thickness	Cs.Th	0.30705	mm
Structure thickness (plate model)	St.Th(pl)	0.21121	mm
Structure separation (plate model)	St.Sp(pl)	0.81142	mm
Structure linear density (plate model)	St.Li.Dn(pl)	0.97787	1/mm
Structure diameter (rod model)	St.Dm(rd)	0.42242	mm
Structure separation (rod model)	St.Sp(rd)	0.40132	mm
Structure linear density (rod model)	St.Li.Dn(rd)	1.21397	1/mm
Mean surface convexity index	SCv.I	-15.64442	1/mm
Closed porosity (percent)	Po(cl)	22.99809	%
Centroid (x)	Crd.X	13.47657	mm
Centroid (y)	Crd.Y	12.69416	mm
Centroid (z)	Crd.Z	5.94048	mm

| Mean fractal dimension | FD | 1.49566 | |
| Total intersection surface | i.S | 0 | mm^2 |

8 Post-processing

CT Analyser	Version: 1.14.4.1	
Dataset name	G:\UofA Kumar - Sponge\Sponge_B_clogged\Sponge_clogged_Rec\VOI(1)\sponge_clogged_rec_voi_0182.bmp	
File postfix length	4	
File type	BMP	
Image size (W/H)	1271	1053
Total number of images	440	
Total Z-position range	182	621
Number of images inside VOI	440	
Z-position range of VOI	182	621
Z spacing	1	
Pixel size (µm)	17.208742	

Thresholding (3D space)

Mode	Automatic (Otsu method)
Background	Dark
Lower grey threshold	136
Upper grey threshold	255
Thresholding done	

Bitwise operations

\<Image\> = COPY \<Region of Interest\>

Bitwise operations done

Despeckle
Type: Remove
outer objects (3D
space)
Detected by: by
image borders
Apply to: Region
of Interest
Despeckle done

3D model
Model creation algorithm: Marching Cubes 33
Apply to: ROI
Model filename = G:\UofA Kumar -
Sponge\Sponge_B_clogged\Sponge_clogged_Rec\VOI(1)\sponge_clogged_rec_voi_.ctm

----

Thresholding (3D space) inside VOI

Mode	Multilevel (Otsu method)
Output color of class thresholding	Mean intensity in class
Number of threshold levels	2
Level 1	1
Level 2	1
Thresholding done	

2D analysis

Operator identity   sbhaduri
Computer name   DOSCHAKCLUSTER0
Computation time   10:00:35
Dataset folder   G:\UofA Kumar - Sponge\Sponge_B_clogged\Sponge_clogged_Rec\VOI(1)\
Pixel size   17.20874   μm

9 Histogram from ROI of file

Index (%), Area (pixel^2), Total (%), Selected (%)
0,0.0%,33013.000,40.360%,-
1,0.4%,1214.000,1.484%,-
2,0.8%,993.000,1.214%,-
3,1.2%,940.000,1.149%,-
4,1.6%,945.000,1.155%,-
5,2.0%,813.000,0.994%,-
6,2.4%,753.000,0.921%,-
7,2.7%,624.000,0.763%,-
8,3.1%,609.000,0.745%,-
9,3.5%,573.000,0.701%,-
10,3.9%,505.000,0.617%,-
11,4.3%,470.000,0.575%,-
12,4.7%,485.000,0.593%,-
13,5.1%,434.000,0.531%,-
14,5.5%,460.000,0.562%,-
15,5.9%,433.000,0.529%,-
16,6.3%,377.000,0.461%,-
17,6.7%,397.000,0.485%,-
18,7.1%,385.000,0.471%,-
19,7.5%,402.000,0.491%,-
20,7.8%,424.000,0.518%,-
21,8.2%,424.000,0.518%,1.160%
22,8.6%,484.000,0.592%,1.324%
23,9.0%,507.000,0.620%,1.387%
24,9.4%,477.000,0.583%,1.305%
25,9.8%,584.000,0.714%,1.598%
26,10.2%,590.000,0.721%,1.614%
27,10.6%,696.000,0.851%,1.904%
28,11.0%,732.000,0.895%,2.003%
29,11.4%,758.000,0.927%,2.074%
30,11.8%,809.000,0.989%,2.214%
31,12.2%,878.000,1.073%,2.402%
32,12.5%,919.000,1.124%,2.515%
33,12.9%,1034.000,1.264%,2.829%
34,13.3%,1043.000,1.275%,2.854%
35,13.7%,1177.000,1.439%,3.221%
36,14.1%,1135.000,1.388%,3.106%

37,14.5%,1222.000,1.494%,3.344%
38,14.9%,1231.000,1.505%,3.368%
39,15.3%,1288.000,1.575%,3.524%
40,15.7%,1306.000,1.597%,3.573%
41,16.1%,1292.000,1.580%,3.535%
42,16.5%,1350.000,1.650%,3.694%
43,16.9%,1314.000,1.606%,3.595%
44,17.3%,1321.000,1.615%,3.615%
45,17.6%,1343.000,1.642%,3.675%
46,18.0%,1248.000,1.526%,3.415%
47,18.4%,1177.000,1.439%,3.221%
48,18.8%,1116.000,1.364%,3.054%
49,19.2%,1065.000,1.302%,2.914%
50,19.6%,926.000,1.132%,2.534%
51,20.0%,981.000,1.199%,2.684%
52,20.4%,809.000,0.989%,2.214%
53,20.8%,736.000,0.900%,2.014%
54,21.2%,677.000,0.828%,1.852%
55,21.6%,569.000,0.696%,1.557%
56,22.0%,519.000,0.635%,1.420%
57,22.4%,444.000,0.543%,1.215%
58,22.7%,382.000,0.467%,1.045%
59,23.1%,346.000,0.423%,0.947%
60,23.5%,249.000,0.304%,0.681%
61,23.9%,219.000,0.268%,0.599%
62,24.3%,166.000,0.203%,0.454%
63,24.7%,154.000,0.188%,0.421%
64,25.1%,125.000,0.153%,0.342%
65,25.5%,124.000,0.152%,0.339%
66,25.9%,95.000,0.116%,0.260%
67,26.3%,74.000,0.090%,0.202%
68,26.7%,74.000,0.090%,0.202%
69,27.1%,59.000,0.072%,0.161%
70,27.5%,58.000,0.071%,0.159%
71,27.8%,47.000,0.057%,0.129%
72,28.2%,40.000,0.049%,0.109%
73,28.6%,35.000,0.043%,0.096%
74,29.0%,27.000,0.033%,0.074%
75,29.4%,19.000,0.023%,0.052%
76,29.8%,15.000,0.018%,0.041%
77,30.2%,18.000,0.022%,0.049%
78,30.6%,7.000,0.009%,0.019%
79,31.0%,10.000,0.012%,0.027%
80,31.4%,6.000,0.007%,0.016%
81,31.8%,3.000,0.004%,0.008%
82,32.2%,2.000,0.002%,0.005%
83,32.5%,2.000,0.002%,0.005%

84,32.9%,2.000,0.002%,0.005%
85,33.3%,2.000,0.002%,0.005%
86,33.7%,1.000,0.001%,0.003%
87,34.1%,1.000,0.001%,0.003%
88,34.5%,1.000,0.001%,0.003%
89,34.9%,2.000,0.002%,0.005%
90,35.3%,0.000,0.000%,0.000%
91,35.7%,0.000,0.000%,0.000%
92,36.1%,1.000,0.001%,0.003%
93,36.5%,0.000,0.000%,-
94,36.9%,0.000,0.000%,-
95,37.3%,0.000,0.000%,-
96,37.6%,0.000,0.000%,-
97,38.0%,0.000,0.000%,-
98,38.4%,0.000,0.000%,-
99,38.8%,0.000,0.000%,-
100,39.2%,0.000,0.000%,-
101,39.6%,0.000,0.000%,-
102,40.0%,0.000,0.000%,-
103,40.4%,0.000,0.000%,-
104,40.8%,0.000,0.000%,-
105,41.2%,0.000,0.000%,-
106,41.6%,0.000,0.000%,-
107,42.0%,0.000,0.000%,-
108,42.4%,0.000,0.000%,-
109,42.7%,0.000,0.000%,-
110,43.1%,0.000,0.000%,-
111,43.5%,0.000,0.000%,-
112,43.9%,0.000,0.000%,-
113,44.3%,0.000,0.000%,-
114,44.7%,0.000,0.000%,-
115,45.1%,0.000,0.000%,-
116,45.5%,0.000,0.000%,-
117,45.9%,0.000,0.000%,-
118,46.3%,0.000,0.000%,-
119,46.7%,0.000,0.000%,-
120,47.1%,0.000,0.000%,-
121,47.5%,0.000,0.000%,-
122,47.8%,0.000,0.000%,-
123,48.2%,0.000,0.000%,-
124,48.6%,0.000,0.000%,-
125,49.0%,0.000,0.000%,-
126,49.4%,0.000,0.000%,-
127,49.8%,0.000,0.000%,-
128,50.2%,0.000,0.000%,-
129,50.6%,0.000,0.000%,-
130,51.0%,0.000,0.000%,-

131,51.4%,0.000,0.000%,-
132,51.8%,0.000,0.000%,-
133,52.2%,0.000,0.000%,-
134,52.5%,0.000,0.000%,-
135,52.9%,0.000,0.000%,-
136,53.3%,0.000,0.000%,-
137,53.7%,0.000,0.000%,-
138,54.1%,0.000,0.000%,-
139,54.5%,0.000,0.000%,-
140,54.9%,0.000,0.000%,-
141,55.3%,0.000,0.000%,-
142,55.7%,0.000,0.000%,-
143,56.1%,0.000,0.000%,-
144,56.5%,0.000,0.000%,-
145,56.9%,0.000,0.000%,-
146,57.3%,0.000,0.000%,-
147,57.6%,0.000,0.000%,-
148,58.0%,0.000,0.000%,-
149,58.4%,0.000,0.000%,-
150,58.8%,0.000,0.000%,-
151,59.2%,0.000,0.000%,-
152,59.6%,0.000,0.000%,-
153,60.0%,0.000,0.000%,-
154,60.4%,0.000,0.000%,-
155,60.8%,0.000,0.000%,-
156,61.2%,0.000,0.000%,-
157,61.6%,0.000,0.000%,-
158,62.0%,0.000,0.000%,-
159,62.4%,0.000,0.000%,-
160,62.7%,0.000,0.000%,-
161,63.1%,0.000,0.000%,-
162,63.5%,0.000,0.000%,-
163,63.9%,0.000,0.000%,-
164,64.3%,0.000,0.000%,-
165,64.7%,0.000,0.000%,-
166,65.1%,0.000,0.000%,-
167,65.5%,0.000,0.000%,-
168,65.9%,0.000,0.000%,-
169,66.3%,0.000,0.000%,-
170,66.7%,0.000,0.000%,-
171,67.1%,0.000,0.000%,-
172,67.5%,0.000,0.000%,-
173,67.8%,0.000,0.000%,-
174,68.2%,0.000,0.000%,-
175,68.6%,0.000,0.000%,-
176,69.0%,0.000,0.000%,-
177,69.4%,0.000,0.000%,-

178,69.8%,0.000,0.000%,-
179,70.2%,0.000,0.000%,-
180,70.6%,0.000,0.000%,-
181,71.0%,0.000,0.000%,-
182,71.4%,0.000,0.000%,-
183,71.8%,0.000,0.000%,-
184,72.2%,0.000,0.000%,-
185,72.5%,0.000,0.000%,-
186,72.9%,0.000,0.000%,-
187,73.3%,0.000,0.000%,-
188,73.7%,0.000,0.000%,-
189,74.1%,0.000,0.000%,-
190,74.5%,0.000,0.000%,-
191,74.9%,0.000,0.000%,-
192,75.3%,0.000,0.000%,-
193,75.7%,0.000,0.000%,-
194,76.1%,0.000,0.000%,-
195,76.5%,0.000,0.000%,-
196,76.9%,0.000,0.000%,-
197,77.3%,0.000,0.000%,-
198,77.6%,0.000,0.000%,-
199,78.0%,0.000,0.000%,-
200,78.4%,0.000,0.000%,-
201,78.8%,0.000,0.000%,-
202,79.2%,0.000,0.000%,-
203,79.6%,0.000,0.000%,-
204,80.0%,0.000,0.000%,-
205,80.4%,0.000,0.000%,-
206,80.8%,0.000,0.000%,-
207,81.2%,0.000,0.000%,-
208,81.6%,0.000,0.000%,-
209,82.0%,0.000,0.000%,-
210,82.4%,0.000,0.000%,-
211,82.7%,0.000,0.000%,-
212,83.1%,0.000,0.000%,-
213,83.5%,0.000,0.000%,-
214,83.9%,0.000,0.000%,-
215,84.3%,0.000,0.000%,-
216,84.7%,0.000,0.000%,-
217,85.1%,0.000,0.000%,-
218,85.5%,0.000,0.000%,-
219,85.9%,0.000,0.000%,-
220,86.3%,0.000,0.000%,-
221,86.7%,0.000,0.000%,-
222,87.1%,0.000,0.000%,-
223,87.5%,0.000,0.000%,-
224,87.8%,0.000,0.000%,-

225,88.2%,0.000,0.000%,-
226,88.6%,0.000,0.000%,-
227,89.0%,0.000,0.000%,-
228,89.4%,0.000,0.000%,-
229,89.8%,0.000,0.000%,-
230,90.2%,0.000,0.000%,-
231,90.6%,0.000,0.000%,-
232,91.0%,0.000,0.000%,-
233,91.4%,0.000,0.000%,-
234,91.8%,0.000,0.000%,-
235,92.2%,0.000,0.000%,-
236,92.5%,0.000,0.000%,-
237,92.9%,0.000,0.000%,-
238,93.3%,0.000,0.000%,-
239,93.7%,0.000,0.000%,-
240,94.1%,0.000,0.000%,-
241,94.5%,0.000,0.000%,-
242,94.9%,0.000,0.000%,-
243,95.3%,0.000,0.000%,-
244,95.7%,0.000,0.000%,-
245,96.1%,0.000,0.000%,-
246,96.5%,0.000,0.000%,-
247,96.9%,0.000,0.000%,-
248,97.3%,0.000,0.000%,-
249,97.6%,0.000,0.000%,-
250,98.0%,0.000,0.000%,-
251,98.4%,0.000,0.000%,-
252,98.8%,0.000,0.000%,-
253,99.2%,0.000,0.000%,-
254,99.6%,0.000,0.000%,-
255,100.0%,0.000,0.000%,-

Appendix C

Single-cell motion tracking raw data for S. pasteurii transport in semi-solid agar medium

ND.T	Time [s]	x (um)	y(um)	n*MSDx	n*MSDy	delT	u (um/s)	v (um/s)	Speed (um/s)
1	0.15	32.57	21.56	34.086	84.3161				
2	0.25	32.64	21.64	33.3301	82.8424	0.1	0.651	0.806	1.036068048
3	0.36	32.65	21.67	33.187	82.3353	0.11	0.112727	0.253636	0.27755872
4	0.45	32.66	21.69	33.08	81.8858	0.09	0.103333	0.275556	0.294293462
5	0.55	32.67	21.72	32.9375	81.4376	0.1	0.124	0.248	0.277272429
6	0.65	32.68	21.74	32.8308	80.9349	0.1	0.093	0.279	0.294091822
7	0.76	32.7	21.77	32.6889	80.4892	0.11	0.112727	0.225455	0.252065845
8	0.85	32.71	21.8	32.5826	79.9894	0.09	0.103333	0.31	0.326768692
9	0.95	32.72	21.82	32.4412	79.5464	0.1	0.124	0.248	0.277272429
10	1.05	32.73	21.85	32.3354	79.1047	0.1	0.093	0.248	0.264864116
11	1.16	32.74	21.87	32.1945	78.6091	0.11	0.112727	0.253636	0.27755872
12	1.25	32.75	21.9	32.0891	78.17	0.09	0.103333	0.275556	0.294293462
13	1.35	32.76	21.93	31.9487	77.6774	0.1	0.124	0.279	0.305314592
14	1.45	32.77	21.95	31.8437	77.2409	0.1	0.093	0.248	0.264864116
15	1.56	32.78	21.98	31.7039	76.7513	0.11	0.112727	0.253636	0.27755872
16	1.65	32.79	22	31.5992	76.3173	0.09	0.103333	0.275556	0.294293462
17	1.75	32.8	22.03	31.46	75.8847	0.1	0.124	0.248	0.277272429
18	1.85	32.81	22.06	31.3557	75.3994	0.1	0.093	0.279	0.294091822
19	1.96	32.83	22.08	31.217	74.9156	0.11	0.112727	0.253636	0.27755872
20	2.05	32.84	22.11	31.1132	74.4869	0.09	0.103333	0.275556	0.294293462
21	2.15	32.85	22.13	30.975	74.0594	0.1	0.124	0.248	0.277272429
22	2.25	32.86	22.16	30.8716	73.58	0.1	0.093	0.279	0.294091822
23	2.36	32.87	22.19	30.7339	73.1552	0.11	0.112727	0.225455	0.252065845
24	2.45	32.88	22.21	30.6309	72.7316	0.09	0.103333	0.275556	0.294293462
25	2.55	32.89	22.24	30.4938	72.2565	0.1	0.124	0.279	0.305314592
26	2.65	32.9	22.26	30.3912	71.8355	0.1	0.093	0.248	0.264864116
27	2.76	32.91	22.29	30.2546	71.3633	0.11	0.112727	0.253636	0.27755872
28	2.85	32.92	22.32	30.1524	70.9449	0.09	0.103333	0.275556	0.294293462
29	2.95	32.93	22.34	30.0164	70.5277	0.1	0.124	0.248	0.277272429
30	3.05	32.94	22.37	29.9146	70.0599	0.1	0.093	0.279	0.294091822
31	3.16	32.96	22.4	29.7791	69.5936	0.11	0.112727	0.253636	0.27755872
32	3.25	32.97	22.42	29.6777	69.1805	0.09	0.103333	0.275556	0.294293462
33	3.35	32.98	22.45	29.5427	68.7685	0.1	0.124	0.248	0.277272429
34	3.45	32.99	22.48	29.4417	68.3066	0.1	0.093	0.279	0.294091822
35	3.56	33	22.5	29.3073	67.8973	0.11	0.112727	0.225455	0.252065845
36	3.65	33.01	22.52	29.2067	67.4892	0.09	0.103333	0.275556	0.294293462
37	3.75	33.02	22.55	29.0728	67.0316	0.1	0.124	0.279	0.305314592

38	3.85	33.03	22.58	28.9726	66.6261	0.1	0.093	0.248	0.264864116
39	3.96	33.04	22.61	28.8393	66.1714	0.11	0.112727	0.253636	0.27755872
40	4.05	33.05	22.63	28.7395	65.7685	0.09	0.103333	0.275556	0.294293462
41	4.15	33.06	22.66	28.6067	65.3168	0.1	0.124	0.279	0.305314592
42	4.25	33.07	22.68	28.5073	64.9165	0.1	0.093	0.248	0.264864116
43	4.36	33.09	22.71	28.375	64.4677	0.11	0.112727	0.253636	0.27755872
44	4.45	33.1	22.74	28.276	64.0701	0.09	0.103333	0.275556	0.294293462
45	4.55	33.05	22.7	28.7395	64.5673	0.1	-0.434	-0.31	0.533344167
46	4.65	33.11	22.8	28.1114	63.0814	0.1	0.589	0.93	1.100827416
47	4.76	33.12	22.83	28.0457	62.4919	0.11	0.056364	0.338182	0.342846615
48	4.85	33.12	22.87	27.9801	61.9539	0.09	0.068889	0.378889	0.385100596
49	5.04	33.13	22.94	27.8818	60.8849	0.19	0.048947	0.358947	0.362269317
50	5.19	33.14	22.99	27.8163	60.0653	0.15	0.041333	0.351333	0.353756351
51	5.37	33.12	23.05	28.0129	59.1081	0.18	-0.10333	0.344444	0.359610558
52	5.44	33.11	23.08	28.1114	58.6799	0.07	-0.13286	0.398571	0.420131175
53	5.63	33.09	23.15	28.375	57.6397	0.19	-0.13053	0.358947	0.381942839
54	5.79	33.07	23.2	28.5735	56.8423	0.16	-0.11625	0.329375	0.34928778
55	5.87	33.06	23.23	28.7062	56.3758	0.08	-0.155	0.3875	0.417350273
56	5.96	33.04	23.26	28.8393	55.9112	0.09	-0.13778	0.344444	0.37097802
57	6.02	33.04	23.28	28.9059	55.6334	0.06	-0.10333	0.31	0.326768692
58	6.14	33.02	23.32	29.0728	54.9879	0.12	-0.12917	0.361667	0.384040109
59	6.19	33.02	23.34	29.1397	54.7124	0.05	-0.124	0.372	0.39212243
60	6.24	33.01	23.36	29.2067	54.4833	0.05	-0.124	0.31	0.333880218
61	6.3	33	23.38	29.2737	54.2091	0.06	-0.10333	0.31	0.326768692
62	6.35	32.99	23.4	29.3744	53.9355	0.05	-0.186	0.372	0.415908644
63	6.41	32.99	23.42	29.4417	53.6172	0.06	-0.10333	0.361667	0.376139011
64	6.46	32.98	23.44	29.509	53.3452	0.05	-0.124	0.372	0.39212243
65	6.56	32.97	23.47	29.6777	52.8482	0.1	-0.155	0.341	0.374574425
66	6.68	32.96	23.51	29.7791	52.2191	0.12	-0.0775	0.361667	0.369877044
67	6.76	32.95	23.54	29.8468	51.8167	0.08	-0.0775	0.34875	0.357257348
68	6.85	32.94	23.58	29.9146	51.3269	0.09	-0.06889	0.378889	0.385100596
69	6.96	32.94	23.62	29.9824	50.7511	0.11	-0.05636	0.366364	0.370673945
70	7.07	32.93	23.65	30.0843	50.2225	0.11	-0.08455	0.338182	0.348589839
71	7.15	32.92	23.68	30.1524	49.784	0.08	-0.0775	0.3875	0.395174012
72	7.25	32.86	23.66	30.8371	50.0907	0.1	-0.62	-0.217	0.656878223
73	7.42	32.93	23.92	30.0164	46.5571	0.17	0.437647	1.495294	1.558024212
74	7.47	32.94	23.98	29.9485	45.7568	0.05	0.124	1.178	1.184508337
75	7.55	32.98	24.07	29.4753	44.4246	0.08	0.5425	1.24	1.353479313
76	7.66	33.05	24.2	28.806	42.787	0.11	0.563636	1.127273	1.260329224
77	7.77	33.1	24.31	28.1772	41.2996	0.11	0.535455	1.042727	1.172173936
78	7.86	33.16	24.42	27.5879	39.9169	0.09	0.62	1.205556	1.355641618
79	7.96	33.21	24.54	27.0371	38.4807	0.1	0.527	1.147	1.26227493

80	8.05	33.25	24.64	26.6516	37.1841	0.09	0.413333	1.171111	1.241912106
81	8.17	33.24	24.72	26.7157	36.2823	0.12	-0.05167	0.62	0.622149053
82	8.25	33.31	24.81	26.0786	35.1338	0.08	0.775	1.20125	1.429554673
83	8.36	33.32	24.87	25.9837	34.5119	0.11	0.084545	0.479091	0.486493611
84	8.45	33.33	24.91	25.889	34.04	0.09	0.103333	0.447778	0.459546207
85	8.57	33.33	24.96	25.7944	33.392	0.12	0.0775	0.465	0.471414096
86	8.66	33.34	25	25.7315	32.8923	0.09	0.068889	0.482222	0.487118005
87	8.76	33.35	25.05	25.6686	32.3611	0.1	0.062	0.465	0.469115124
88	8.86	33.34	25.1	25.7315	31.8342	0.1	-0.062	0.465	0.469115124
89	8.97	33.34	25.15	25.7629	31.277	0.11	-0.02818	0.450909	0.451788914
90	9.06	33.33	25.19	25.8259	30.7934	0.09	-0.06889	0.482222	0.487118005
91	9.16	33.33	25.24	25.8574	30.2454	0.1	-0.031	0.496	0.496967806
92	9.25	33.33	25.28	25.889	29.8037	0.09	-0.03444	0.447778	0.44910061
93	9.37	33.32	25.33	25.9521	29.2311	0.12	-0.05167	0.439167	0.442195438
94	9.45	33.32	25.37	25.9837	28.797	0.08	-0.03875	0.50375	0.505238186
95	9.56	33.31	25.43	26.0153	28.2341	0.11	-0.02818	0.479091	0.47991907
96	9.65	33.31	25.47	26.0786	27.7748	0.09	-0.06889	0.482222	0.487118005
97	9.77	33.3	25.52	26.1103	27.2221	0.12	-0.02583	0.439167	0.439925814
98	9.86	33.3	25.57	26.142	26.739	0.09	-0.03444	0.516667	0.517813542
99	10.05	33.3	25.66	26.142	25.8489	0.19	0	0.456842	0.456842105
100	10.32	33.3	25.78	26.142	24.5726	0.27	0	0.470741	0.470740741
101	10.36	33.3	25.8	26.142	24.358	0.04	0	0.5425	0.5425
102	10.41	33.24	25.77	26.7157	24.6957	0.05	-1.116	-0.682	1.307891433
103	10.47	33.3	25.84	26.1103	24.0225	0.06	0.981667	1.136667	1.501892325
104	10.52	33.31	25.85	26.0786	23.8708	0.05	0.062	0.31	0.31613921
105	10.58	33.31	25.87	26.0469	23.7498	0.06	0.051667	0.206667	0.213027124
106	10.65	33.31	25.89	26.0153	23.5689	0.07	0.044286	0.265714	0.269379483
107	10.76	33.32	25.91	25.9521	23.3287	0.11	0.056364	0.225455	0.232393226
108	10.85	33.33	25.93	25.889	23.1196	0.09	0.068889	0.241111	0.250759341
109	10.98	33.33	25.96	25.7944	22.8224	0.13	0.071538	0.238462	0.248961155
110	11.06	33.34	25.98	25.7629	22.6155	0.08	0.03875	0.27125	0.274003878
111	11.16	33.34	26.01	25.7	22.4096	0.1	0.062	0.217	0.225683407
112	11.25	33.35	26.03	25.6372	22.2046	0.09	0.068889	0.241111	0.250759341
113	11.37	33.36	26.06	25.5745	21.9425	0.12	0.051667	0.2325	0.238171565
114	11.46	33.37	26.08	25.4179	21.7397	0.09	0.172222	0.241111	0.296302315
115	11.56	33.39	26.1	25.2619	21.5378	0.1	0.155	0.217	0.266672083
116	11.65	33.4	26.12	25.1063	21.3655	0.09	0.172222	0.206667	0.269019711
117	11.77	33.42	26.14	24.9512	21.1368	0.12	0.129167	0.206667	0.243711179
118	11.85	33.43	26.16	24.7966	20.9661	0.08	0.19375	0.2325	0.302647175
119	11.97	33.45	26.19	24.6117	20.7396	0.12	0.155	0.206667	0.258333333
120	12.05	33.46	26.2	24.4888	20.5706	0.08	0.155	0.2325	0.279430224
121	12.17	33.48	26.23	24.3357	20.3462	0.12	0.129167	0.206667	0.243711179

122	12.26	33.5	26.25	24.183	20.1788	0.09	0.172222	0.206667	0.269019711
123	12.36	33.51	26.27	24.0308	19.9843	0.1	0.155	0.217	0.266672083
124	12.45	33.53	26.29	23.8791	19.8183	0.09	0.172222	0.206667	0.269019711
125	12.57	33.54	26.31	23.7278	19.5982	0.12	0.129167	0.206667	0.243711179
126	12.66	33.56	26.33	23.577	19.4065	0.09	0.172222	0.241111	0.296302315
127	12.76	33.57	26.36	23.4268	19.2158	0.1	0.155	0.217	0.266672083
128	12.85	33.59	26.37	23.277	19.0531	0.09	0.172222	0.206667	0.269019711
129	12.97	33.6	26.4	23.1276	18.8372	0.12	0.129167	0.206667	0.243711179
130	13.06	33.62	26.42	22.9788	18.6493	0.09	0.172222	0.241111	0.296302315
131	13.16	33.64	26.44	22.8304	18.4623	0.1	0.155	0.217	0.266672083
132	13.25	33.65	26.46	22.6825	18.3028	0.09	0.172222	0.206667	0.269019711
133	13.37	33.67	26.49	22.5351	18.0912	0.12	0.129167	0.206667	0.243711179
134	13.46	33.68	26.51	22.4176	17.9071	0.09	0.137778	0.241111	0.277699989
135	13.56	33.69	26.53	22.3003	17.7239	0.1	0.124	0.217	0.24992999
136	13.65	33.7	26.55	22.1833	17.5417	0.09	0.137778	0.241111	0.277699989
137	13.77	33.72	26.58	22.0667	17.3346	0.12	0.103333	0.206667	0.231060358
138	13.86	33.73	26.6	21.9503	17.1543	0.09	0.137778	0.241111	0.277699989
139	13.98	33.74	26.63	21.8054	16.924	0.12	0.129167	0.2325	0.265970445
140	14.05	33.75	26.64	21.7186	16.7967	0.07	0.132857	0.221429	0.25822787
141	14.17	33.77	26.67	21.6032	16.5941	0.12	0.103333	0.206667	0.231060358
142	14.26	33.72	26.63	22.0085	16.873	0.09	-0.48222	-0.37889	0.613265898
143	14.36	33.8	26.72	21.316	16.1426	0.1	0.744	0.899	1.166934874
144	14.45	33.81	26.75	21.1445	15.9191	0.09	0.206667	0.31	0.372573632
145	14.57	33.84	26.79	20.9455	15.6237	0.12	0.180833	0.31	0.358888136
146	14.66	33.86	26.82	20.7755	15.3796	0.09	0.206667	0.344444	0.401687797
147	14.76	33.87	26.85	20.6063	15.1374	0.1	0.186	0.31	0.361519017
148	14.85	33.89	26.88	20.4659	14.9211	0.09	0.172222	0.31	0.35462726
149	14.97	33.91	26.91	20.2421	14.6351	0.12	0.206667	0.31	0.372573632
150	15.06	33.93	26.95	20.0751	14.3988	0.09	0.206667	0.344444	0.401687797
151	15.16	33.95	26.98	19.9087	14.1645	0.1	0.186	0.31	0.361519017
152	15.25	33.97	27	19.7431	13.9553	0.09	0.206667	0.31	0.372573632
153	15.37	33.99	27.04	19.5233	13.6788	0.12	0.206667	0.31	0.372573632
154	15.46	34.01	27.07	19.3593	13.4504	0.09	0.206667	0.344444	0.401687797
155	15.56	34.03	27.1	19.1688	13.224	0.1	0.217	0.31	0.378403224
156	15.65	34.05	27.13	19.0063	13.0218	0.09	0.206667	0.31	0.372573632
157	15.77	34.08	27.17	18.8175	12.7548	0.12	0.180833	0.31	0.358888136
158	15.86	34.09	27.2	18.6565	12.5343	0.09	0.206667	0.344444	0.401687797
159	15.96	34.12	27.23	18.4695	12.3157	0.1	0.217	0.31	0.378403224
160	16.05	34.13	27.26	18.31	12.1207	0.09	0.206667	0.31	0.372573632
161	16.17	34.16	27.3	18.1248	11.8631	0.12	0.180833	0.31	0.358888136
162	16.26	34.17	27.32	17.9667	11.6717	0.09	0.206667	0.31	0.372573632
163	16.36	34.2	27.36	17.7833	11.4398	0.1	0.217	0.341	0.404190549

226

164	16.46	34.21	27.39	17.6267	11.2311	0.1	0.186	0.31	0.361519017
165	16.57	34.24	27.42	17.445	11.0037	0.11	0.197273	0.31	0.367445954
166	16.67	34.2	27.4	17.731	11.1481	0.1	-0.341	-0.217	0.404190549
167	16.76	34.28	27.51	17.0587	10.4153	0.09	0.895556	1.24	1.529581561
168	16.85	34.31	27.57	16.8545	10.0386	0.09	0.275556	0.654444	0.710090413
169	16.97	34.34	27.65	16.6009	9.57271	0.12	0.258333	0.62	0.671666667
170	17.06	34.36	27.71	16.3994	9.1929	0.09	0.275556	0.688889	0.74195604
171	17.16	34.38	27.77	16.2741	8.80238	0.1	0.155	0.651	0.669198027
172	17.25	34.39	27.83	16.1742	8.43833	0.09	0.137778	0.688889	0.702531577
173	17.37	34.41	27.91	16.0498	7.99408	0.12	0.129167	0.645833	0.658623354
174	17.47	34.42	27.98	15.9506	7.61307	0.1	0.124	0.682	0.693181073
175	17.56	34.43	28.04	15.8517	7.27478	0.09	0.137778	0.688889	0.702531577
176	17.65	34.44	28.1	15.7531	6.96052	0.09	0.137778	0.654444	0.668790137
177	17.77	34.46	28.18	15.6303	6.55759	0.12	0.129167	0.645833	0.658623354
178	17.87	34.48	28.25	15.508	6.19751	0.1	0.155	0.713	0.729653342
179	17.96	34.49	28.31	15.3862	5.90772	0.09	0.172222	0.654444	0.67672596
180	18.05	34.51	28.37	15.2648	5.61017	0.09	0.172222	0.688889	0.710090413
181	18.17	34.53	28.45	15.0957	5.26326	0.12	0.180833	0.62	0.645833333
182	18.26	34.49	28.45	15.3862	5.22068	0.09	-0.41333	0.103333	0.426054248
183	18.36	34.56	28.56	14.8558	4.76366	0.1	0.682	1.023	1.229492985
184	18.45	34.57	28.6	14.7603	4.57609	0.09	0.137778	0.482222	0.501518681
185	18.57	34.59	28.66	14.6178	4.34047	0.12	0.155	0.465	0.490153037
186	18.66	34.6	28.7	14.5231	4.14888	0.09	0.137778	0.516667	0.534721573
187	18.76	34.62	28.75	14.4052	3.94928	0.1	0.155	0.496	0.519654693
188	18.85	34.63	28.8	14.2878	3.77867	0.09	0.172222	0.482222	0.512053479
189	18.97	34.65	28.85	14.1475	3.57656	0.12	0.155	0.439167	0.46571704
190	19.07	34.67	28.9	14.008	3.38001	0.1	0.186	0.527	0.558860448
191	19.16	34.69	28.94	13.8922	3.23345	0.09	0.172222	0.447778	0.479755596
192	19.25	34.7	28.99	13.7769	3.07925	0.09	0.172222	0.482222	0.512053479
193	19.37	34.72	29.04	13.6391	2.88653	0.12	0.155	0.465	0.490153037
194	19.47	34.74	29.09	13.5021	2.72045	0.1	0.186	0.496	0.529728232
195	19.56	34.75	29.13	13.3884	2.57917	0.09	0.172222	0.482222	0.512053479
196	19.65	34.77	29.18	13.2978	2.44166	0.09	0.137778	0.482222	0.501518681
197	19.77	34.79	29.23	13.1625	2.27039	0.12	0.155	0.465	0.490153037
198	19.86	34.8	29.28	13.0503	2.13242	0.09	0.172222	0.516667	0.544614486
199	19.96	34.82	29.33	12.9386	1.99002	0.1	0.155	0.496	0.519654693
200	20.05	34.78	29.32	13.2301	2.02516	0.09	-0.44778	-0.13778	0.468495095
201	20.17	34.86	29.38	12.6282	1.85254	0.12	0.6975	0.516667	0.868015377
202	20.26	34.88	29.38	12.4745	1.8357	0.09	0.241111	0.068889	0.250759341
203	20.36	34.91	29.39	12.2999	1.81894	0.1	0.248	0.062	0.255632549
204	20.45	34.93	29.39	12.1482	1.81059	0.09	0.241111	0.034444	0.243559002
205	20.57	34.96	29.4	11.9544	1.78564	0.12	0.2325	0.0775	0.245076519

206	20.66	34.98	29.4	11.8049	1.79394	0.09	0.241111	-0.03444	0.243559002
207	20.76	35	29.39	11.6774	1.82731	0.1	0.186	-0.124	0.223544179
208	20.85	35.01	29.38	11.5717	1.86099	0.09	0.172222	-0.13778	0.220552057
209	20.97	35.03	29.36	11.4245	1.89497	0.12	0.180833	-0.10333	0.208274992
210	21.06	35.05	29.35	11.2991	1.92927	0.09	0.206667	-0.13778	0.248382421
211	21.16	35.07	29.34	11.1744	1.96387	0.1	0.186	-0.124	0.223544179
212	21.25	35.09	29.33	11.0711	1.99877	0.09	0.172222	-0.13778	0.220552057
213	21.37	35.11	29.31	10.9271	2.03399	0.12	0.180833	-0.10333	0.208274992
214	21.48	35.13	29.3	10.7841	2.07844	0.11	0.197273	-0.14091	0.242429167
215	21.56	35.14	29.29	10.6826	2.11435	0.08	0.19375	-0.155	0.248121064
216	21.65	35.16	29.27	10.6017	2.15056	0.09	0.137778	-0.13778	0.194847202
217	21.77	35.18	29.26	10.4809	2.19626	0.12	0.155	-0.12917	0.201764783
218	21.87	35.19	29.24	10.3608	2.24245	0.1	0.186	-0.155	0.24211774
219	21.96	35.21	29.23	10.2613	2.27974	0.09	0.172222	-0.13778	0.220552057
220	22.05	35.23	29.22	10.1622	2.31734	0.09	0.172222	-0.13778	0.220552057
221	22.17	35.24	29.2	10.044	2.37431	0.12	0.155	-0.155	0.219203102
222	22.27	35.26	29.18	9.94595	2.42232	0.1	0.155	-0.155	0.219203102
223	22.36	35.27	29.17	9.84842	2.46107	0.09	0.172222	-0.13778	0.220552057
224	22.45	35.29	29.16	9.75138	2.50013	0.09	0.172222	-0.13778	0.220552057
225	22.57	35.31	29.14	9.63556	2.54939	0.12	0.155	-0.12917	0.201764783
226	22.66	35.32	29.13	9.53957	2.59912	0.09	0.172222	-0.17222	0.243559002
227	22.76	35.34	29.12	9.44407	2.63926	0.1	0.155	-0.124	0.198496851
228	22.85	35.36	29.1	9.34904	2.6797	0.09	0.172222	-0.13778	0.220552057
229	22.97	35.37	29.08	9.23564	2.74095	0.12	0.155	-0.155	0.219203102
230	23.07	35.39	29.07	9.12294	2.78216	0.1	0.186	-0.124	0.223544179
231	23.16	35.41	29.06	9.04818	2.8341	0.09	0.137778	-0.17222	0.220552057
232	23.25	35.42	29.04	8.95518	2.87601	0.09	0.172222	-0.13778	0.220552057
233	23.37	35.44	29.03	8.8442	2.92882	0.12	0.155	-0.12917	0.201764783
234	23.46	35.45	29.01	8.75225	2.98211	0.09	0.172222	-0.17222	0.243559002
235	23.56	35.47	29	8.67903	3.03589	0.1	0.124	-0.155	0.198496851
236	23.65	35.48	28.99	8.60613	3.07925	0.09	0.137778	-0.13778	0.194847202
237	23.77	35.5	28.97	8.49734	3.14488	0.12	0.155	-0.155	0.219203102
238	23.86	35.51	28.95	8.4252	3.20009	0.09	0.137778	-0.17222	0.220552057
239	23.96	35.53	28.94	8.33546	3.25579	0.1	0.155	-0.155	0.219203102
240	24.05	35.54	28.92	8.26402	3.31196	0.09	0.137778	-0.17222	0.220552057
241	24.17	35.55	28.9	8.17514	3.36862	0.12	0.129167	-0.12917	0.182669252
242	24.26	35.57	28.89	8.10438	3.42576	0.09	0.137778	-0.17222	0.220552057
243	24.36	35.58	28.87	8.01637	3.48337	0.1	0.155	-0.155	0.219203102
244	24.46	35.6	28.86	7.91139	3.52981	0.1	0.186	-0.124	0.223544179
245	24.57	35.62	28.85	7.80711	3.5883	0.11	0.169091	-0.14091	0.220107036
246	24.67	35.64	28.83	7.70351	3.63543	0.1	0.186	-0.124	0.223544179
247	24.76	35.66	28.82	7.60061	3.68287	0.09	0.206667	-0.13778	0.248382421

248	24.85	35.67	28.81	7.51538	3.71865	0.09	0.172222	-0.10333	0.200843899
249	24.97	35.64	28.74	7.70351	3.99872	0.12	-0.28417	-0.59417	0.658623354
250	25.07	35.75	28.8	7.07996	3.7546	0.1	1.147	0.62	1.303843932
251	25.16	35.81	28.81	6.80229	3.73061	0.09	0.585556	0.068889	0.589593918
252	25.25	35.85	28.81	6.54602	3.71865	0.09	0.551111	0.034444	0.552186451
253	25.37	35.91	28.84	6.27913	3.62362	0.12	0.439167	0.206667	0.485364268
254	25.47	35.95	28.87	6.07879	3.50656	0.1	0.403	0.31	0.508437803
255	25.56	35.98	28.9	5.89674	3.40284	0.09	0.413333	0.31	0.516666667
256	25.65	36.02	28.92	5.71745	3.31196	0.09	0.413333	0.275556	0.496764842
257	25.77	36.07	28.95	5.49724	3.18901	0.12	0.3875	0.284167	0.480527777
258	25.87	36.11	28.99	5.32419	3.06838	0.1	0.372	0.341	0.504643438
259	25.98	36.15	29.02	5.13983	2.95008	0.11	0.366364	0.31	0.47991907
260	26.05	36.17	29.04	5.01411	2.87601	0.07	0.398571	0.31	0.504934831
261	26.17	36.21	29.08	4.83525	2.75122	0.12	0.335833	0.31	0.457038322
262	26.27	36.25	29.12	4.67303	2.63926	0.1	0.372	0.341	0.504643438
263	26.36	36.29	29.15	4.52677	2.5395	0.09	0.378889	0.344444	0.512053479
264	26.45	36.32	29.17	4.38283	2.45135	0.09	0.378889	0.31	0.489547536
265	26.57	36.36	29.21	4.21571	2.33625	0.12	0.335833	0.31	0.457038322
266	26.67	36.4	29.25	4.06434	2.23317	0.1	0.372	0.341	0.504643438
267	26.76	36.43	29.27	3.92801	2.15056	0.09	0.378889	0.31	0.489547536
268	26.85	36.46	29.3	3.80609	2.0606	0.09	0.344444	0.344444	0.487118005
269	26.97	36.5	29.34	3.66232	1.94653	0.12	0.31	0.335833	0.457038322
270	27.07	36.53	29.38	3.53297	1.85254	0.1	0.341	0.341	0.482246825
271	27.16	36.56	29.41	3.4174	1.76911	0.09	0.344444	0.344444	0.487118005
272	27.25	36.59	29.44	3.31502	1.68761	0.09	0.31	0.344444	0.463402606
273	27.37	36.63	29.48	3.1699	1.59234	0.12	0.335833	0.31	0.457038322
274	27.48	36.68	29.51	3.00648	1.50744	0.11	0.422727	0.31	0.52421212
275	27.56	36.71	29.54	2.89994	1.44716	0.08	0.3875	0.31	0.496242128
276	27.65	36.69	29.51	2.96363	1.51507	0.09	-0.20667	-0.31	0.372573632
277	27.77	36.77	29.59	2.69262	1.33029	0.12	0.671667	0.645833	0.931792255
278	27.87	36.79	29.61	2.62187	1.2807	0.1	0.217	0.217	0.306884343
279	27.98	36.82	29.63	2.54218	1.23206	0.11	0.225455	0.197273	0.299576837
280	28.05	36.83	29.65	2.49299	1.19789	0.07	0.221429	0.221429	0.313147289
281	28.17	36.86	29.67	2.41529	1.15086	0.12	0.206667	0.180833	0.2746121
282	28.27	36.88	29.69	2.34831	1.10477	0.1	0.217	0.217	0.306884343
283	28.36	36.9	29.71	2.29165	1.06601	0.09	0.206667	0.206667	0.292270803
284	28.45	36.92	29.73	2.22642	1.02795	0.09	0.241111	0.206667	0.317562087
285	28.56	36.94	29.75	2.16213	0.98442	0.11	0.197273	0.197273	0.278985766
286	28.67	36.97	29.77	2.08982	0.94183	0.11	0.225455	0.197273	0.299576837
287	28.76	36.99	29.79	2.03639	0.90018	0.09	0.206667	0.241111	0.317562087
288	28.85	37	29.81	2.00115	0.86523	0.09	0.137778	0.206667	0.248382421
289	28.97	37.02	29.84	1.94887	0.81411	0.12	0.155	0.2325	0.279430224

290	29.06	37.03	29.86	1.90584	0.77542	0.09	0.172222	0.241111	0.296302315
291	29.16	37.05	29.88	1.86328	0.73236	0.1	0.155	0.248	0.292453415
292	29.25	37.06	29.9	1.8212	0.70087	0.09	0.172222	0.206667	0.269019711
293	29.37	37.08	29.93	1.77135	0.65493	0.12	0.155	0.2325	0.279430224
294	29.47	37.1	29.96	1.73033	0.61541	0.1	0.155	0.248	0.292453415
295	29.56	37.11	29.97	1.68979	0.58657	0.09	0.172222	0.206667	0.269019711
296	29.65	37.13	30	1.65771	0.5538	0.09	0.137778	0.241111	0.277699989
297	29.77	37.14	30.02	1.61016	0.51306	0.12	0.155	0.2325	0.279430224
298	29.87	37.16	30.05	1.5633	0.48244	0.1	0.186	0.217	0.285805878
299	29.96	37.18	30.07	1.53245	0.45277	0.09	0.137778	0.241111	0.277699989
300	30.05	37.19	30.09	1.49431	0.42404	0.09	0.172222	0.241111	0.296302315
301	30.17	37.21	30.11	1.44918	0.39235	0.12	0.155	0.206667	0.258333333
302	30.27	37.22	30.14	1.4121	0.3619	0.1	0.155	0.248	0.292453415
303	30.36	37.24	30.16	1.37551	0.33626	0.09	0.172222	0.241111	0.296302315
304	30.45	37.25	30.18	1.34657	0.31156	0.09	0.137778	0.241111	0.277699989
305	30.57	37.27	30.21	1.30375	0.28449	0.12	0.155	0.206667	0.258333333
306	30.66	37.29	30.23	1.2686	0.26182	0.09	0.172222	0.241111	0.296302315
307	30.76	37.3	30.25	1.23392	0.23705	0.1	0.155	0.248	0.292453415
308	30.85	37.32	30.27	1.19973	0.21639	0.09	0.172222	0.241111	0.296302315
309	30.97	37.34	30.3	1.15933	0.19393	0.12	0.155	0.206667	0.258333333
310	31.07	37.36	30.32	1.11962	0.17529	0.1	0.186	0.217	0.285805878
311	31.16	37.37	30.34	1.08706	0.15759	0.09	0.172222	0.241111	0.296302315
312	31.25	37.39	30.36	1.04862	0.14317	0.09	0.206667	0.206667	0.292270803
313	31.37	37.41	30.39	1.01087	0.12284	0.12	0.155	0.2325	0.279430224
314	31.47	37.43	30.41	0.97381	0.1081	0.1	0.186	0.217	0.285805878
315	31.56	37.44	30.43	0.94346	0.0943	0.09	0.172222	0.241111	0.296302315
316	31.65	37.46	30.45	0.90768	0.08322	0.09	0.206667	0.206667	0.292270803
317	31.77	37.48	30.48	0.87258	0.06953	0.12	0.155	0.206667	0.258333333
318	31.87	37.5	30.5	0.83818	0.05706	0.1	0.186	0.248	0.31
319	31.96	37.46	30.47	0.90768	0.07452	0.09	-0.41333	-0.37889	0.560714932
320	32.05	37.55	30.53	0.74446	0.04451	0.09	0.998889	0.688889	1.21340303
321	32.17	37.59	30.54	0.67145	0.04067	0.12	0.361667	0.0775	0.369877044
322	32.27	37.63	30.55	0.60703	0.03701	0.1	0.403	0.093	0.413591586
323	32.36	37.65	30.53	0.57839	0.04583	0.09	0.206667	-0.24111	0.317562087
324	32.45	37.67	30.5	0.55505	0.05706	0.09	0.172222	-0.27556	0.324948239
325	32.57	37.69	30.47	0.52319	0.07117	0.12	0.180833	-0.2325	0.294545318
326	32.67	37.71	30.44	0.49227	0.08867	0.1	0.217	-0.31	0.378403224
327	32.76	37.73	30.42	0.47076	0.10207	0.09	0.172222	-0.24111	0.296302315
328	32.85	37.74	30.39	0.4539	0.12067	0.09	0.137778	-0.31	0.339238435
329	32.97	37.75	30.36	0.43325	0.14317	0.12	0.129167	-0.25833	0.288825447
330	33.07	37.77	30.33	0.41309	0.16759	0.1	0.155	-0.31	0.346590537
331	33.16	37.78	30.31	0.3973	0.18851	0.09	0.137778	-0.27556	0.308080477

332	33.25	37.8	30.28	0.38183	0.21066	0.09	0.137778	-0.27556	0.308080477
333	33.37	37.81	30.25	0.36291	0.24313	0.12	0.129167	-0.28417	0.312145354
334	33.47	37.83	30.22	0.34448	0.27142	0.1	0.155	-0.279	0.319164534
335	33.56	37.84	30.19	0.33007	0.30127	0.09	0.137778	-0.31	0.339238435
336	33.65	37.85	30.17	0.31598	0.32911	0.09	0.137778	-0.27556	0.308080477
337	33.77	37.87	30.14	0.29879	0.36564	0.12	0.129167	-0.25833	0.288825447
338	33.87	37.88	30.1	0.28539	0.40409	0.1	0.124	-0.31	0.333880218
339	33.96	37.89	30.08	0.27554	0.44034	0.09	0.103333	-0.31	0.326768692
340	34.05	37.89	30.05	0.26907	0.47387	0.09	0.068889	-0.27556	0.284036165
341	34.17	37.91	30.02	0.25636	0.52198	0.12	0.103333	-0.28417	0.302371414
342	34.27	37.92	29.99	0.24703	0.56773	0.1	0.093	-0.31	0.323649502
343	34.36	37.93	29.96	0.23787	0.61055	0.09	0.103333	-0.31	0.326768692
344	34.45	37.93	29.93	0.22889	0.64993	0.09	0.103333	-0.27556	0.294293462
345	34.57	37.96	29.9	0.20859	0.70087	0.12	0.180833	-0.25833	0.31533602
346	34.66	37.98	29.88	0.19195	0.74301	0.09	0.206667	-0.27556	0.344444444
347	34.76	37.94	29.79	0.22593	0.89431	0.1	-0.372	-0.837	0.915943776
348	34.85	37.99	29.86	0.18124	0.77542	0.09	0.551111	0.723333	0.909359427
349	34.97	37.98	29.87	0.18924	0.75913	0.12	-0.0775	0.0775	0.109601551
350	35.07	37.97	29.88	0.19742	0.74301	0.1	-0.093	0.093	0.131521861
351	35.16	37.96	29.89	0.20297	0.72706	0.09	-0.06889	0.103333	0.124191211
352	35.25	37.96	29.9	0.20859	0.71129	0.09	-0.06889	0.103333	0.124191211
353	35.37	37.95	29.91	0.21717	0.69569	0.12	-0.0775	0.0775	0.109601551
354	35.47	37.94	29.92	0.22593	0.68026	0.1	-0.093	0.093	0.131521861
355	35.56	37.93	29.92	0.23186	0.66501	0.09	-0.06889	0.103333	0.124191211
356	35.65	37.93	29.93	0.23787	0.65493	0.09	-0.06889	0.068889	0.097423601
357	35.77	37.92	29.94	0.24703	0.63502	0.12	-0.0775	0.103333	0.129166667
358	35.86	37.91	29.95	0.25323	0.62028	0.09	-0.06889	0.103333	0.124191211
359	35.96	37.9	29.96	0.26268	0.60572	0.1	-0.093	0.093	0.131521861
360	36.05	37.89	29.97	0.26907	0.59611	0.09	-0.06889	0.068889	0.097423601
361	36.17	37.89	29.98	0.27881	0.57711	0.12	-0.0775	0.103333	0.129166667
362	36.27	37.88	29.99	0.28539	0.56307	0.1	-0.062	0.093	0.11177209
363	36.36	37.87	30	0.29205	0.5538	0.09	-0.06889	0.068889	0.097423601
364	36.45	37.86	30	0.30219	0.54005	0.09	-0.10333	0.103333	0.146135401
365	36.57	37.86	30.02	0.30905	0.52198	0.12	-0.05167	0.103333	0.115530179
366	36.67	37.85	30.03	0.31947	0.50863	0.1	-0.093	0.093	0.131521861
367	36.76	37.84	30.03	0.32652	0.49982	0.09	-0.06889	0.068889	0.097423601
368	36.85	37.83	30.04	0.33724	0.48676	0.09	-0.10333	0.103333	0.146135401
369	36.97	37.83	30.05	0.34448	0.47387	0.12	-0.05167	0.0775	0.093143408
370	37.07	37.82	30.06	0.35548	0.45695	0.1	-0.093	0.124	0.155
371	37.16	37.81	30.07	0.36291	0.44861	0.09	-0.06889	0.068889	0.097423601
372	37.25	37.8	30.08	0.37042	0.43623	0.09	-0.06889	0.103333	0.124191211
373	37.37	37.8	30.09	0.38183	0.42404	0.12	-0.0775	0.0775	0.109601551

231

374	37.47	37.79	30.1	0.3934	0.41201	0.1	-0.093	0.093	0.131521861
375	37.56	37.78	30.11	0.40122	0.40016	0.09	-0.06889	0.103333	0.124191211
376	37.65	37.77	30.12	0.40911	0.38848	0.09	-0.06889	0.103333	0.124191211
377	37.77	37.76	30.13	0.4211	0.37697	0.12	-0.0775	0.0775	0.109601551
378	37.87	37.75	30.14	0.43325	0.36564	0.1	-0.093	0.093	0.131521861
379	37.96	37.75	30.14	0.44145	0.35448	0.09	-0.06889	0.103333	0.124191211
380	38.05	37.74	30.15	0.44973	0.34349	0.09	-0.06889	0.103333	0.124191211
381	38.17	37.73	30.16	0.46229	0.33268	0.12	-0.0775	0.0775	0.109601551
382	38.27	37.73	30.17	0.47076	0.32203	0.1	-0.062	0.093	0.11177209
383	38.36	37.72	30.18	0.47931	0.31156	0.09	-0.06889	0.103333	0.124191211
384	38.45	37.71	30.19	0.48793	0.30127	0.09	-0.06889	0.103333	0.124191211
385	38.57	37.71	30.2	0.50101	0.29115	0.12	-0.0775	0.0775	0.109601551
386	38.66	37.7	30.21	0.50982	0.2812	0.09	-0.06889	0.103333	0.124191211
387	38.76	37.69	30.22	0.51872	0.27142	0.1	-0.062	0.093	0.11177209
388	38.85	37.69	30.23	0.52769	0.26182	0.09	-0.06889	0.103333	0.124191211
389	38.97	37.68	30.24	0.54128	0.25239	0.12	-0.0775	0.0775	0.109601551
390	39.07	37.67	30.25	0.55045	0.24008	0.1	-0.062	0.124	0.138636215
391	39.16	37.67	30.26	0.55968	0.23404	0.09	-0.06889	0.068889	0.097423601
392	39.25	37.66	30.27	0.569	0.22513	0.09	-0.06889	0.103333	0.124191211
393	39.37	37.65	30.28	0.58312	0.21352	0.12	-0.0775	0.103333	0.129166667
394	39.47	37.64	30.29	0.59262	0.20501	0.1	-0.062	0.093	0.11177209
395	39.56	37.64	30.3	0.60221	0.19667	0.09	-0.06889	0.103333	0.124191211
396	39.65	37.63	30.3	0.61187	0.19121	0.09	-0.06889	0.068889	0.097423601
397	39.77	37.62	30.31	0.6265	0.18052	0.12	-0.0775	0.103333	0.129166667
398	39.87	37.62	30.32	0.63636	0.17271	0.1	-0.062	0.093	0.11177209
399	39.96	37.61	30.33	0.64629	0.16506	0.09	-0.06889	0.103333	0.124191211
400	40.05	37.6	30.34	0.65629	0.15759	0.09	-0.06889	0.103333	0.124191211
401	40.17	37.59	30.35	0.67145	0.1503	0.12	-0.0775	0.0775	0.109601551
402	40.27	37.59	30.36	0.68165	0.14317	0.1	-0.062	0.093	0.11177209
403	40.36	37.58	30.37	0.69192	0.13622	0.09	-0.06889	0.103333	0.124191211
404	40.45	37.58	30.38	0.70228	0.12944	0.09	-0.06889	0.103333	0.124191211
405	40.57	37.57	30.39	0.71795	0.12284	0.12	-0.0775	0.0775	0.109601551
406	40.67	37.56	30.4	0.7285	0.1164	0.1	-0.062	0.093	0.11177209
407	40.76	37.55	30.41	0.73912	0.11014	0.09	-0.06889	0.103333	0.124191211
408	40.85	37.55	30.42	0.74982	0.10406	0.09	-0.06889	0.103333	0.124191211
409	40.97	37.54	30.43	0.76601	0.09814	0.12	-0.0775	0.0775	0.109601551
410	41.07	37.53	30.44	0.7769	0.09053	0.1	-0.062	0.124	0.138636215
411	41.16	37.53	30.45	0.78787	0.08684	0.09	-0.06889	0.068889	0.097423601
412	41.25	37.52	30.45	0.79891	0.08144	0.09	-0.06889	0.103333	0.124191211
413	41.37	37.51	30.47	0.81563	0.07452	0.12	-0.0775	0.103333	0.129166667
414	41.47	37.5	30.48	0.82686	0.06953	0.1	-0.062	0.093	0.11177209
415	41.56	37.5	30.49	0.83818	0.06471	0.09	-0.06889	0.103333	0.124191211

416	41.65	37.49	30.49	0.84957	0.06159	0.09	-0.06889	0.068889	0.097423601
417	41.77	37.48	30.5	0.8668	0.05559	0.12	-0.0775	0.103333	0.129166667
418	41.87	37.48	30.51	0.87838	0.05129	0.1	-0.062	0.093	0.11177209
419	41.96	37.47	30.52	0.89004	0.04717	0.09	-0.06889	0.103333	0.124191211
420	42.05	37.46	30.53	0.90178	0.04321	0.09	-0.06889	0.103333	0.124191211
421	42.17	37.45	30.54	0.91953	0.03943	0.12	-0.0775	0.0775	0.109601551
422	42.27	37.45	30.55	0.93146	0.03583	0.1	-0.062	0.093	0.11177209
423	42.36	37.44	30.56	0.94346	0.03239	0.09	-0.06889	0.103333	0.124191211
424	42.45	37.44	30.57	0.95555	0.02913	0.09	-0.06889	0.103333	0.124191211
425	42.57	37.43	30.58	0.97381	0.02604	0.12	-0.0775	0.0775	0.109601551
426	42.67	37.42	30.59	0.98609	0.0222	0.1	-0.062	0.124	0.138636215
427	42.76	37.41	30.6	0.99844	0.02039	0.09	-0.06889	0.068889	0.097423601
428	42.85	37.41	30.61	1.01087	0.01782	0.09	-0.06889	0.103333	0.124191211
429	42.97	37.4	30.62	1.02966	0.01466	0.12	-0.0775	0.103333	0.129166667
430	43.07	37.39	30.63	1.04228	0.01249	0.1	-0.062	0.093	0.11177209
431	43.16	37.39	30.64	1.05498	0.0105	0.09	-0.06889	0.103333	0.124191211
432	43.25	37.38	30.64	1.06775	0.00927	0.09	-0.06889	0.068889	0.097423601
433	43.37	37.37	30.66	1.08706	0.00704	0.12	-0.0775	0.103333	0.129166667
434	43.47	37.36	30.67	1.10002	0.00556	0.1	-0.062	0.093	0.11177209
435	43.56	37.36	30.67	1.11307	0.00426	0.09	-0.06889	0.103333	0.124191211
436	43.65	37.35	30.68	1.12619	0.00313	0.09	-0.06889	0.103333	0.124191211
437	43.77	37.34	30.69	1.14601	0.00218	0.12	-0.0775	0.0775	0.109601551
438	43.87	37.34	30.7	1.15933	0.0014	0.1	-0.062	0.093	0.11177209
439	43.96	37.33	30.71	1.17272	0.00079	0.09	-0.06889	0.103333	0.124191211
440	44.05	37.32	30.72	1.18618	0.00035	0.09	-0.06889	0.103333	0.124191211
441	44.17	37.31	30.73	1.20653	9E-05	0.12	-0.0775	0.0775	0.109601551
442	44.27	37.31	30.74	1.22019	3.2E-08	0.1	-0.062	0.093	0.11177209
443	44.36	37.3	30.75	1.23392	8.3E-05	0.09	-0.06889	0.103333	0.124191211
444	44.45	37.29	30.76	1.25467	0.00034	0.09	-0.10333	0.103333	0.146135401
445	44.57	37.29	30.77	1.2686	0.00077	0.12	-0.05167	0.0775	0.093143408
446	44.67	37.28	30.78	1.2826	0.00161	0.1	-0.062	0.124	0.138636215
447	44.76	37.27	30.79	1.30375	0.00215	0.09	-0.10333	0.068889	0.124191211
448	44.85	37.27	30.8	1.31795	0.00309	0.09	-0.06889	0.103333	0.124191211
449	44.97	37.26	30.81	1.33222	0.00463	0.12	-0.05167	0.103333	0.115530179
450	45.06	37.25	30.81	1.34657	0.00551	0.09	-0.06889	0.068889	0.097423601
451	45.16	37.24	30.82	1.36824	0.00698	0.1	-0.093	0.093	0.131521861
452	45.25	37.24	30.83	1.38279	0.00862	0.09	-0.06889	0.103333	0.124191211
453	45.37	37.23	30.85	1.40475	0.01107	0.12	-0.0775	0.103333	0.129166667
454	45.47	37.22	30.85	1.41948	0.01311	0.1	-0.062	0.093	0.11177209
455	45.56	37.22	30.86	1.43429	0.01533	0.09	-0.06889	0.103333	0.124191211
456	45.65	37.21	30.87	1.44918	0.01691	0.09	-0.06889	0.068889	0.097423601
457	45.77	37.2	30.88	1.47166	0.02028	0.12	-0.0775	0.103333	0.129166667

458	45.87	37.19	30.89	1.48674	0.02302	0.1	-0.062	0.093	0.11177209
459	45.96	37.19	30.9	1.5019	0.02593	0.09	-0.06889	0.103333	0.124191211
460	46.05	37.18	30.91	1.52478	0.02796	0.09	-0.10333	0.068889	0.124191211
461	46.17	37.17	30.92	1.54013	0.03226	0.12	-0.05167	0.103333	0.115530179
462	46.27	37.16	30.93	1.5633	0.03569	0.1	-0.093	0.093	0.131521861
463	46.36	37.16	30.94	1.57884	0.03929	0.09	-0.06889	0.103333	0.124191211
464	46.45	37.15	30.95	1.59446	0.04306	0.09	-0.06889	0.103333	0.124191211
465	46.57	37.14	30.96	1.61016	0.04701	0.12	-0.05167	0.0775	0.093143408
466	46.67	37.13	30.97	1.63385	0.05113	0.1	-0.093	0.093	0.131521861
467	46.76	37.13	30.98	1.64973	0.05542	0.09	-0.06889	0.103333	0.124191211
468	46.85	37.12	30.98	1.6657	0.05989	0.09	-0.06889	0.103333	0.124191211
469	46.97	37.11	30.99	1.68979	0.06453	0.12	-0.0775	0.0775	0.109601551
470	47.07	37.11	31	1.70595	0.06934	0.1	-0.062	0.093	0.11177209
471	47.16	37.1	31.01	1.72218	0.07432	0.09	-0.06889	0.103333	0.124191211
472	47.25	37.09	31.02	1.73849	0.07948	0.09	-0.06889	0.103333	0.124191211
473	47.38	37.09	31.03	1.76311	0.08481	0.13	-0.07154	0.071538	0.101170663
474	47.47	37.08	31.04	1.78789	0.09031	0.09	-0.10333	0.103333	0.146135401
475	47.56	37.07	31.05	1.80451	0.09599	0.09	-0.06889	0.103333	0.124191211
476	47.65	37.06	31.06	1.8212	0.10184	0.09	-0.06889	0.103333	0.124191211
477	47.77	37.06	31.07	1.83798	0.10786	0.12	-0.05167	0.0775	0.093143408
478	47.87	37.05	31.08	1.86328	0.11405	0.1	-0.093	0.093	0.131521861
479	47.96	37.04	31.09	1.88024	0.12042	0.09	-0.06889	0.103333	0.124191211
480	48.05	36.98	31.04	2.05412	0.09031	0.09	-0.68889	-0.51667	0.861111111
481	48.17	37.03	31.12	1.90584	0.14763	0.12	0.439167	0.6975	0.824241234
482	48.27	37.03	31.15	1.9144	0.1673	0.1	-0.031	0.248	0.24992999
483	48.36	37.03	31.17	1.92299	0.18552	0.09	-0.03444	0.241111	0.243559002
484	48.45	37.02	31.19	1.9316	0.20189	0.09	-0.03444	0.206667	0.209517376
485	48.57	37.02	31.22	1.94023	0.22774	0.12	-0.02583	0.2325	0.233930783
486	48.67	37.03	31.24	1.90584	0.24892	0.1	0.124	0.217	0.24992999
487	48.76	37.05	31.26	1.86328	0.26783	0.09	0.172222	0.206667	0.269019711
488	48.85	37.06	31.28	1.8212	0.28742	0.09	0.172222	0.206667	0.269019711
489	48.97	37.08	31.3	1.77135	0.31463	0.12	0.155	0.206667	0.258333333
490	49.07	37.1	31.32	1.73033	0.33945	0.1	0.155	0.217	0.266672083
491	49.16	37.11	31.34	1.68979	0.36147	0.09	0.172222	0.206667	0.269019711
492	49.25	37.13	31.36	1.65771	0.38418	0.09	0.137778	0.206667	0.248382421
493	49.37	37.14	31.38	1.61016	0.41155	0.12	0.155	0.180833	0.238171565
494	49.47	37.17	31.4	1.55556	0.43986	0.1	0.217	0.217	0.306884343
495	49.56	37.18	31.42	1.51713	0.46488	0.09	0.172222	0.206667	0.269019711
496	49.65	37.2	31.44	1.47919	0.48626	0.09	0.172222	0.172222	0.243559002
497	49.77	37.22	31.46	1.42688	0.51699	0.12	0.180833	0.180833	0.255736953
498	49.87	37.24	31.48	1.37551	0.54867	0.1	0.217	0.217	0.306884343
499	49.96	37.26	31.5	1.33939	0.57657	0.09	0.172222	0.206667	0.269019711

500	50.05	37.27	31.51	1.30375	0.60035	0.09	0.172222	0.172222	0.243559002
501	50.17	37.29	31.54	1.25467	0.63444	0.12	0.180833	0.180833	0.255736953
502	50.27	37.31	31.56	1.20653	0.66948	0.1	0.217	0.217	0.306884343
503	50.36	37.33	31.58	1.17272	0.70027	0.09	0.172222	0.206667	0.269019711
504	50.45	37.35	31.59	1.13939	0.72645	0.09	0.172222	0.172222	0.243559002
505	50.57	37.37	31.61	1.09353	0.76391	0.12	0.180833	0.180833	0.255736953
506	50.67	37.39	31.64	1.05498	0.80231	0.1	0.186	0.217	0.285805878
507	50.76	37.4	31.65	1.01711	0.83598	0.09	0.206667	0.206667	0.292270803
508	50.85	37.42	31.67	0.98609	0.86457	0.09	0.172222	0.172222	0.243559002
509	50.97	37.44	31.69	0.94346	0.90539	0.12	0.180833	0.180833	0.255736953
510	51.07	37.46	31.71	0.90178	0.94716	0.1	0.217	0.217	0.306884343
511	51.16	37.48	31.73	0.8668	0.97757	0.09	0.206667	0.172222	0.269019711
512	51.25	37.5	31.74	0.83251	1.00846	0.09	0.206667	0.172222	0.269019711
513	51.37	37.53	31.77	0.78787	1.05251	0.12	0.206667	0.180833	0.2746121
514	51.47	37.55	31.78	0.74982	1.09102	0.1	0.217	0.186	0.285805878
515	51.56	37.57	31.8	0.71795	1.12364	0.09	0.206667	0.172222	0.269019711
516	51.65	37.58	31.82	0.68678	1.15674	0.09	0.206667	0.172222	0.269019711
517	51.77	37.61	31.84	0.65128	1.20389	0.12	0.180833	0.180833	0.255736953
518	51.87	37.63	31.86	0.61673	1.24505	0.1	0.217	0.186	0.285805878
519	51.96	37.64	31.87	0.59262	1.28691	0.09	0.172222	0.206667	0.269019711
520	52.05	37.66	31.89	0.57369	1.32946	0.09	0.137778	0.206667	0.248382421
521	52.16	37.67	31.92	0.54585	1.38726	0.11	0.169091	0.225455	0.281818182
522	52.27	37.69	31.94	0.51872	1.43885	0.11	0.169091	0.197273	0.259823526
523	52.36	37.65	31.9	0.58312	1.35099	0.09	-0.48222	-0.41333	0.635124174
524	52.45	37.72	31.97	0.47502	1.50656	0.09	0.826667	0.723333	1.098448401
525	52.56	37.75	31.98	0.44558	1.54485	0.11	0.197273	0.140909	0.242429167
526	52.67	37.77	32	0.41708	1.57583	0.11	0.197273	0.112727	0.227209082
527	52.76	37.79	32	0.3934	1.59926	0.09	0.206667	0.103333	0.231060358
528	52.85	37.8	32.02	0.37042	1.63078	0.09	0.206667	0.137778	0.248382421
529	52.97	37.83	32.03	0.34448	1.6626	0.12	0.180833	0.103333	0.208274992
530	53.07	37.85	32.04	0.31947	1.69474	0.1	0.217	0.124	0.24992999
531	53.16	37.87	32.05	0.29879	1.71904	0.09	0.206667	0.103333	0.231060358
532	53.25	37.89	32.06	0.27881	1.75171	0.09	0.206667	0.137778	0.248382421
533	53.37	37.91	32.07	0.25323	1.76816	0.12	0.206667	0.051667	0.213027124
534	53.47	37.93	32.07	0.22889	1.75992	0.1	0.248	-0.031	0.24992999
535	53.56	37.96	32.07	0.20577	1.75992	0.09	0.275556	0	0.275555556
536	53.65	37.98	32.06	0.18655	1.75171	0.09	0.241111	-0.03444	0.243559002
537	53.77	38.01	32.06	0.16323	1.74351	0.12	0.2325	-0.02583	0.233930783
538	53.87	38.04	32.06	0.14147	1.74351	0.1	0.279	0	0.279
539	53.96	38.06	32.06	0.12561	1.73533	0.09	0.241111	-0.03444	0.243559002
540	54.05	38.08	32.06	0.10865	1.73533	0.09	0.275556	0	0.275555556
541	54.16	38.11	32.05	0.09103	1.72717	0.11	0.253636	-0.02818	0.255197218

542	54.27	38.14	32.05	0.07498	1.71904	0.11	0.253636	-0.02818	0.255197218
543	54.36	38.16	32.05	0.06356	1.71904	0.09	0.241111	0	0.241111111
544	54.47	38.19	32.05	0.05027	1.71092	0.11	0.253636	-0.02818	0.255197218
545	54.57	38.21	32.04	0.04101	1.70282	0.1	0.217	-0.031	0.219203102
546	54.66	38.24	32.04	0.03158	1.70282	0.09	0.275556	0	0.275555556
547	54.76	38.26	32.04	0.02338	1.69474	0.1	0.248	-0.031	0.24992999
548	54.85	38.29	32.04	0.01641	1.69474	0.09	0.275556	0	0.275555556
549	54.99	38.32	32.04	0.00884	1.68667	0.14	0.243571	-0.02214	0.244575851
550	55.07	38.34	32.04	0.00523	1.67863	0.08	0.27125	-0.03875	0.274003878
551	55.16	38.36	32.04	0.00256	1.67863	0.09	0.241111	0	0.241111111
552	55.25	38.38	32.03	0.00084	1.67061	0.09	0.241111	-0.03444	0.243559002
553	55.37	38.42	32.03	4.3E-06	1.6626	0.12	0.258333	-0.02583	0.259621787
554	55.46	38.44	32.03	0.00057	1.67061	0.09	0.241111	0.034444	0.243559002
555	55.56	38.46	32.03	0.00236	1.67061	0.1	0.248	0	0.248
556	55.65	38.49	32.04	0.00538	1.67863	0.09	0.275556	0.034444	0.277699989
557	55.77	38.51	32.04	0.01026	1.68667	0.12	0.2325	0.025833	0.233930783
558	55.86	38.54	32.04	0.0159	1.69474	0.09	0.275556	0.034444	0.277699989
559	55.98	38.57	32.04	0.02467	1.70282	0.12	0.258333	0.025833	0.259621787
560	56.05	38.59	32.04	0.02978	1.70282	0.07	0.221429	0	0.221428571
561	56.16	38.61	32.05	0.04019	1.71092	0.11	0.253636	0.028182	0.255197218
562	56.26	38.64	32.05	0.05075	1.71904	0.1	0.248	0.031	0.24992999
563	56.36	38.61	32	0.03774	1.58362	0.1	-0.31	-0.527	0.611415571
564	56.46	38.68	32.08	0.07219	1.79297	0.1	0.744	0.806	1.096891973
565	56.56	38.7	32.11	0.08432	1.86847	0.1	0.217	0.279	0.353454382
566	56.66	38.72	32.13	0.09356	1.92827	0.1	0.155	0.217	0.266672083
567	56.76	38.74	32.16	0.10529	2.00653	0.1	0.186	0.279	0.335316269
568	56.85	38.76	32.18	0.1177	2.06848	0.09	0.206667	0.241111	0.317562087
569	56.96	38.78	32.21	0.13306	2.14951	0.11	0.197273	0.253636	0.321322165
570	57.06	38.79	32.23	0.14461	2.22284	0.1	0.155	0.248	0.292453415
571	57.16	38.81	32.26	0.15664	2.30681	0.1	0.155	0.279	0.319164534
572	57.25	38.82	32.28	0.16159	2.38276	0.09	0.068889	0.275556	0.284036165
573	57.36	38.82	32.32	0.16661	2.4892	0.11	0.056364	0.31	0.315082306
574	57.47	38.83	32.35	0.17171	2.57802	0.11	0.056364	0.253636	0.259823526
575	57.56	38.83	32.37	0.17689	2.66839	0.09	0.068889	0.31	0.317562087
576	57.65	38.84	32.4	0.18214	2.75003	0.09	0.068889	0.275556	0.284036165
577	57.77	38.85	32.43	0.18747	2.86429	0.12	0.051667	0.284167	0.288825447
578	57.86	38.85	32.46	0.19288	2.94884	0.09	0.068889	0.275556	0.284036165
579	57.96	38.86	32.49	0.19836	3.05627	0.1	0.062	0.31	0.31613921
580	58.05	38.86	32.51	0.20392	3.1436	0.09	0.068889	0.275556	0.284036165
581	58.16	38.87	32.54	0.20956	3.25449	0.11	0.056364	0.281818	0.287399282
582	58.27	38.88	32.57	0.21528	3.3673	0.11	0.056364	0.281818	0.287399282
583	58.36	38.88	32.6	0.22107	3.45893	0.09	0.068889	0.275556	0.284036165

584	58.47	38.89	32.63	0.22399	3.58693	0.11	0.028182	0.31	0.311278356
585	58.56	38.89	32.66	0.22694	3.68149	0.09	0.034444	0.275556	0.277699989
586	58.66	38.9	32.69	0.23288	3.78933	0.1	0.062	0.279	0.285805878
587	58.76	38.9	32.72	0.23589	3.91098	0.1	0.031	0.31	0.311546144
588	58.85	38.9	32.74	0.23891	4.00969	0.09	0.034444	0.275556	0.277699989
589	58.96	38.91	32.77	0.24501	4.1348	0.11	0.056364	0.281818	0.287399282
590	59.07	38.91	32.8	0.24808	4.26183	0.11	0.028182	0.281818	0.283223768
591	59.16	38.91	32.83	0.25118	4.3778	0.09	0.034444	0.31	0.31190771
592	59.25	38.92	32.86	0.25743	4.4822	0.09	0.068889	0.275556	0.284036165
593	59.37	38.92	32.89	0.26059	4.62775	0.12	0.025833	0.284167	0.285338493
594	59.47	38.93	32.92	0.26696	4.76208	0.1	0.062	0.31	0.31613921
595	59.57	38.93	32.95	0.27017	4.88463	0.1	0.031	0.279	0.280716939
596	59.65	38.94	32.97	0.2734	4.98102	0.08	0.03875	0.27125	0.274003878
597	59.76	38.94	33.01	0.27993	5.13439	0.11	0.056364	0.31	0.315082306
598	59.86	38.95	33.03	0.28322	5.26161	0.1	0.031	0.279	0.280716939
599	59.96	38.95	33.06	0.28652	5.39038	0.1	0.031	0.279	0.280716939
600	60.05	38.95	33.09	0.2932	5.50616	0.09	0.068889	0.275556	0.284036165
601	60.16	38.96	33.12	0.29657	5.66735	0.11	0.028182	0.31	0.311278356
602	60.27	38.96	33.15	0.30336	5.81591	0.11	0.056364	0.281818	0.287399282
603	60.36	38.97	33.18	0.30678	5.93614	0.09	0.034444	0.275556	0.277699989
604	60.45	38.97	33.2	0.31023	6.07287	0.09	0.034444	0.31	0.31190771
605	60.56	38.98	33.24	0.31717	6.22662	0.11	0.056364	0.281818	0.287399282
606	60.67	38.98	33.27	0.31717	6.38229	0.11	0	0.281818	0.281818182
607	60.76	38.98	33.29	0.32067	6.50821	0.09	0.034444	0.275556	0.277699989
608	60.85	38.98	33.32	0.32419	6.65134	0.09	0.034444	0.31	0.31190771
609	60.96	38.98	33.35	0.32419	6.8122	0.11	0	0.281818	0.281818182
610	61.06	38.99	33.38	0.32773	6.95862	0.1	0.031	0.279	0.280716939
611	61.16	38.99	33.41	0.33129	7.12313	0.1	0.031	0.31	0.311546144
612	61.25	38.99	33.43	0.33129	7.25613	0.09	0	0.275556	0.275555556
613	61.36	38.99	33.47	0.33487	7.441	0.11	0.028182	0.31	0.311278356
614	61.47	38.99	33.5	0.33847	7.61109	0.11	0.028182	0.281818	0.283223768
615	61.56	39	33.52	0.34208	7.74854	0.09	0.034444	0.275556	0.277699989
616	61.65	39	33.55	0.34208	7.88722	0.09	0	0.275556	0.275555556
617	61.76	39	33.58	0.34938	8.07992	0.11	0.056364	0.31	0.315082306
618	61.86	39.01	33.61	0.35674	8.23931	0.1	0.062	0.279	0.285805878
619	61.96	39.02	33.64	0.36419	8.40026	0.1	0.062	0.279	0.285805878
620	62.05	39.02	33.66	0.37171	8.54463	0.09	0.068889	0.275556	0.284036165
621	62.16	39.03	33.7	0.37931	8.74515	0.11	0.056364	0.31	0.315082306
622	62.27	39.04	33.73	0.38698	8.92946	0.11	0.056364	0.281818	0.287399282
623	62.36	39.04	33.75	0.39474	9.07829	0.09	0.068889	0.275556	0.284036165
624	62.45	38.99	33.72	0.33487	8.89244	0.09	-0.55111	-0.34444	0.649896478
625	62.56	39.06	33.79	0.41845	9.30384	0.11	0.62	0.62	0.876812409

626	62.67	39.07	33.8	0.43057	9.36066	0.11	0.084545	0.084545	0.119565328
627	62.76	39.08	33.81	0.44286	9.41766	0.09	0.103333	0.103333	0.146135401
628	62.85	39.09	33.82	0.45533	9.47482	0.09	0.103333	0.103333	0.146135401
629	62.96	39.1	33.83	0.46797	9.55131	0.11	0.084545	0.112727	0.140909091
630	63.07	39.11	33.84	0.48508	9.60888	0.11	0.112727	0.084545	0.140909091
631	63.16	39.12	33.85	0.49813	9.66663	0.09	0.103333	0.103333	0.146135401
632	63.25	39.13	33.86	0.51134	9.72454	0.09	0.103333	0.103333	0.146135401
633	63.36	39.14	33.87	0.52473	9.80203	0.11	0.084545	0.112727	0.140909091
634	63.47	39.15	33.88	0.54284	9.86035	0.11	0.112727	0.084545	0.140909091
635	63.56	39.17	33.88	0.56593	9.86035	0.09	0.172222	0	0.172222222
636	63.65	39.18	33.88	0.58949	9.86035	0.09	0.172222	0	0.172222222
637	63.76	39.2	33.88	0.61839	9.86035	0.11	0.169091	0	0.169090909
638	63.87	39.22	33.88	0.64301	9.86035	0.11	0.140909	0	0.140909091
639	63.96	39.23	33.88	0.66811	9.86035	0.09	0.172222	0	0.172222222
640	64.05	39.25	33.88	0.69369	9.86035	0.09	0.172222	0	0.172222222
641	64.16	39.26	33.88	0.72502	9.86035	0.11	0.169091	0	0.169090909
642	64.26	39.28	33.88	0.75165	9.86035	0.1	0.155	0	0.155
643	64.36	39.3	33.88	0.78425	9.86035	0.1	0.186	0	0.186
644	64.45	39.31	33.88	0.80637	9.86035	0.09	0.137778	0	0.137777778
645	64.56	39.33	33.88	0.84012	9.86035	0.11	0.169091	0	0.169090909
646	64.66	39.35	33.88	0.87456	9.86035	0.1	0.186	0	0.186
647	64.76	39.36	33.88	0.90379	9.86035	0.1	0.155	0	0.155
648	64.85	39.38	33.88	0.9335	9.86035	0.09	0.172222	0	0.172222222
649	64.96	39.4	33.88	0.96979	9.86035	0.11	0.169091	0	0.169090909
650	65.06	39.41	33.88	1.00056	9.84089	0.1	0.155	-0.031	0.158069605
651	65.17	39.43	33.88	1.03812	9.84089	0.11	0.169091	0	0.169090909
652	65.27	39.45	33.87	1.06994	9.82145	0.1	0.155	-0.031	0.158069605
653	65.36	39.46	33.87	1.10225	9.82145	0.09	0.172222	0	0.172222222
654	65.47	39.48	33.87	1.14165	9.80203	0.11	0.169091	-0.02818	0.171423308
655	65.57	39.5	33.87	1.17501	9.80203	0.1	0.155	0	0.155
656	65.72	39.52	33.87	1.22939	9.78263	0.15	0.165333	-0.02067	0.166619993
657	65.77	39.53	33.87	1.2501	9.78263	0.05	0.186	0	0.186
658	65.85	39.54	33.86	1.27799	9.76325	0.08	0.155	-0.03875	0.159770343
659	65.96	39.56	33.86	1.32038	9.76325	0.11	0.169091	0	0.169090909
660	66.05	39.58	33.86	1.35625	9.74389	0.09	0.172222	-0.03444	0.175632894
661	66.16	39.6	33.86	1.39991	9.74389	0.11	0.169091	0	0.169090909
662	66.26	39.61	33.86	1.43683	9.72454	0.1	0.155	-0.031	0.158069605
663	66.36	39.63	33.86	1.47423	9.72454	0.1	0.155	0	0.155
664	66.45	39.64	33.86	1.51211	9.70522	0.09	0.172222	-0.03444	0.175632894
665	66.58	39.66	33.86	1.56595	9.70522	0.13	0.166923	0	0.166923077
666	66.69	39.68	33.85	1.61285	9.68591	0.11	0.169091	-0.02818	0.171423308
667	66.8	39.7	33.85	1.65246	9.68591	0.11	0.140909	0	0.140909091

668	66.85	39.71	33.85	1.67646	9.66663	0.05	0.186	-0.062	0.196061215
669	66.95	39.72	33.85	1.71683	9.66663	0.1	0.155	0	0.155
670	67.06	39.74	33.85	1.76592	9.64736	0.11	0.169091	-0.02818	0.171423308
671	67.16	39.76	33.85	1.8157	9.64736	0.1	0.186	0	0.186
672	67.25	39.77	33.84	1.84927	9.62811	0.09	0.137778	-0.03444	0.142018083
673	67.36	39.79	33.84	1.90021	9.62811	0.11	0.169091	0	0.169090909
674	67.46	39.81	33.84	1.94318	9.60888	0.1	0.155	-0.031	0.158069605
675	67.56	39.83	33.84	1.99538	9.60888	0.1	0.186	0	0.186
676	67.65	39.84	33.84	2.03941	9.58967	0.09	0.172222	-0.03444	0.175632894
677	67.76	39.86	33.84	2.09288	9.58967	0.11	0.169091	0	0.169090909
678	67.86	39.88	33.83	2.13797	9.57048	0.1	0.155	-0.031	0.158069605
679	67.96	39.89	33.83	2.18354	9.57048	0.1	0.155	0	0.155
680	68.05	39.91	33.83	2.22959	9.55131	0.09	0.172222	-0.03444	0.175632894
681	68.16	39.92	33.83	2.28548	9.55131	0.11	0.169091	0	0.169090909
682	68.26	39.94	33.83	2.33258	9.53216	0.1	0.155	-0.031	0.158069605
683	68.36	39.96	33.82	2.38017	9.51303	0.1	0.155	-0.031	0.158069605
684	68.65	40	33.82	2.52581	9.47482	0.29	0.160345	-0.02138	0.161763836
685	68.7	40.01	33.81	2.55546	9.45575	0.05	0.186	-0.062	0.196061215
686	68.75	40.02	33.81	2.57532	9.45575	0.05	0.124	0	0.124
687	68.8	40.03	33.81	2.60525	9.43669	0.05	0.186	-0.062	0.196061215
688	68.86	40.04	33.81	2.63536	9.43669	0.06	0.155	0	0.155
689	68.95	40.05	33.81	2.68593	9.41766	0.09	0.172222	-0.03444	0.175632894
690	69.06	40.07	33.81	2.74724	9.39864	0.11	0.169091	-0.02818	0.171423308
691	69.15	40.08	33.8	2.7885	9.37964	0.09	0.137778	-0.03444	0.142018083
692	69.26	40.1	33.8	2.85096	9.36066	0.11	0.169091	-0.02818	0.171423308
693	69.36	40.12	33.8	2.90355	9.3417	0.1	0.155	-0.031	0.158069605
694	69.52	40.15	33.79	2.99941	9.32276	0.16	0.174375	-0.01937	0.175448087
695	69.59	40.15	33.79	3.03171	9.30384	0.07	0.132857	-0.04429	0.140043725
696	69.72	40.18	33.79	3.10775	9.28494	0.13	0.166923	-0.02385	0.168617771
697	69.78	40.19	33.78	3.14062	9.26606	0.06	0.155	-0.05167	0.163384346
698	69.85	40.2	33.78	3.18473	9.26606	0.07	0.177143	0	0.177142857
699	69.95	40.21	33.78	3.24029	9.24719	0.1	0.155	-0.031	0.158069605
700	70.08	40.23	33.78	3.31888	9.22835	0.13	0.166923	-0.02385	0.168617771
701	70.16	40.25	33.78	3.36422	9.22835	0.08	0.155	0	0.155
702	70.26	40.26	33.78	3.42132	9.22835	0.1	0.155	0	0.155
703	70.36	40.28	33.78	3.49047	9.22835	0.1	0.186	0	0.186
704	70.45	40.3	33.78	3.54863	9.22835	0.09	0.172222	0	0.172222222
705	70.56	40.32	33.78	3.61905	9.22835	0.11	0.169091	0	0.169090909
706	70.66	40.33	33.78	3.67826	9.22835	0.1	0.155	0	0.155
707	70.76	40.35	33.78	3.73796	9.22835	0.1	0.155	0	0.155
708	70.86	40.37	33.78	3.81023	9.22835	0.1	0.186	0	0.186
709	71.01	40.33	33.72	3.69016	8.89244	0.15	-0.20667	-0.372	0.425552712

239

710	71.06	40.4	33.77	3.94451	9.20953	0.05	1.302	1.054	1.675147755
711	71.16	40.42	33.77	4.03118	9.17193	0.1	0.217	-0.062	0.225683407
712	71.26	40.44	33.76	4.10622	9.13442	0.1	0.186	-0.062	0.196061215
713	71.36	40.46	33.76	4.19463	9.09698	0.1	0.217	-0.062	0.225683407
714	71.46	40.48	33.75	4.28399	9.05962	0.1	0.217	-0.062	0.225683407
715	71.56	40.5	33.74	4.36133	9.02233	0.1	0.186	-0.062	0.196061215
716	71.65	40.52	33.74	4.43936	8.98513	0.09	0.206667	-0.06889	0.217845794
717	71.76	40.54	33.73	4.54449	8.92946	0.11	0.225455	-0.08455	0.24078556
718	71.86	40.56	33.72	4.62413	8.89244	0.1	0.186	-0.062	0.196061215
719	71.96	40.59	33.72	4.71793	8.8555	0.1	0.217	-0.062	0.225683407
720	72.05	40.6	33.71	4.79908	8.81864	0.09	0.206667	-0.06889	0.217845794
721	72.16	40.63	33.7	4.89463	8.78186	0.11	0.197273	-0.05636	0.205166733
722	72.26	40.65	33.7	4.99111	8.74515	0.1	0.217	-0.062	0.225683407
723	72.36	40.66	33.69	5.06061	8.69023	0.1	0.155	-0.093	0.180759509
724	72.45	40.68	33.67	5.11655	8.59909	0.09	0.137778	-0.17222	0.220552057
725	72.56	40.68	33.66	5.15871	8.50842	0.11	0.084545	-0.14091	0.164326826
726	72.66	40.7	33.64	5.21519	8.41824	0.1	0.124	-0.155	0.198496851
727	72.76	40.71	33.63	5.25776	8.34644	0.1	0.093	-0.124	0.155
728	72.85	40.72	33.61	5.30049	8.25712	0.09	0.103333	-0.17222	0.200843899
729	72.96	40.73	33.6	5.35774	8.16828	0.11	0.112727	-0.14091	0.180451683
730	73.06	40.74	33.58	5.4153	8.07992	0.1	0.124	-0.155	0.198496851
731	73.16	40.75	33.57	5.45867	8.00958	0.1	0.093	-0.124	0.155
732	73.26	40.76	33.55	5.50221	7.92209	0.1	0.093	-0.155	0.180759509
733	73.36	40.77	33.54	5.56054	7.83507	0.1	0.124	-0.155	0.198496851
734	73.46	40.78	33.52	5.60449	7.74854	0.1	0.093	-0.155	0.180759509
735	73.56	40.79	33.51	5.66335	7.67966	0.1	0.124	-0.124	0.175362482
736	73.65	40.8	33.5	5.7077	7.59399	0.09	0.103333	-0.17222	0.200843899
737	73.76	40.81	33.48	5.76711	7.50881	0.11	0.112727	-0.14091	0.180451683
738	73.86	40.82	33.46	5.81186	7.4241	0.1	0.093	-0.155	0.180759509
739	73.96	40.84	33.45	5.8718	7.35668	0.1	0.124	-0.124	0.175362482
740	74.05	40.85	33.44	5.91696	7.27284	0.09	0.103333	-0.17222	0.200843899
741	74.16	40.86	33.42	5.97744	7.18948	0.11	0.112727	-0.14091	0.180451683
742	74.26	40.87	33.41	6.023	7.1066	0.1	0.093	-0.155	0.180759509
743	74.36	40.88	33.39	6.08402	7.04064	0.1	0.124	-0.124	0.175362482
744	74.45	40.89	33.38	6.12998	6.95862	0.09	0.103333	-0.17222	0.200843899
745	74.56	40.9	33.36	6.19154	6.87709	0.11	0.112727	-0.14091	0.180451683
746	74.66	40.91	33.35	6.23791	6.79603	0.1	0.093	-0.155	0.180759509
747	74.76	40.92	33.33	6.3	6.71546	0.1	0.124	-0.155	0.198496851
748	74.85	40.93	33.32	6.34677	6.65134	0.09	0.103333	-0.13778	0.172222222
749	74.96	40.94	33.3	6.39372	6.57163	0.11	0.084545	-0.14091	0.164326826
750	75.06	40.95	33.29	6.45658	6.49241	0.1	0.124	-0.155	0.198496851
751	75.16	40.97	33.28	6.51975	6.42937	0.1	0.124	-0.124	0.175362482

752	75.25	40.98	33.26	6.58323	6.36664	0.09	0.137778	-0.13778	0.194847202
753	75.36	40.99	33.25	6.66301	6.28866	0.11	0.140909	-0.14091	0.199275547
754	75.46	41.01	33.24	6.74327	6.22662	0.1	0.155	-0.124	0.198496851
755	75.55	41.02	33.22	6.80782	6.16489	0.09	0.137778	-0.13778	0.194847202
756	75.65	41.04	33.21	6.88895	6.10347	0.1	0.155	-0.124	0.198496851
757	75.76	41.05	33.2	6.97055	6.04235	0.11	0.140909	-0.11273	0.180451683
758	75.86	41.07	33.19	7.03618	5.98155	0.1	0.124	-0.124	0.175362482
759	75.97	41.08	33.17	7.1352	5.90597	0.11	0.169091	-0.14091	0.220107036
760	76.05	41.1	33.16	7.2016	5.86085	0.08	0.155	-0.11625	0.19375
761	76.16	41.11	33.15	7.28503	5.78605	0.11	0.140909	-0.14091	0.199275547
762	76.25	41.12	33.14	7.35212	5.74139	0.09	0.137778	-0.10333	0.172222222
763	76.36	41.14	33.12	7.43642	5.66735	0.11	0.140909	-0.14091	0.199275547
764	76.46	41.1	33.05	7.21825	5.34729	0.1	-0.403	-0.682	0.792169805
765	76.56	41.16	33.1	7.53821	5.57914	0.1	0.589	0.496	0.770024026
766	76.66	41.16	33.1	7.53821	5.54989	0.1	0	-0.062	0.062
767	76.76	41.16	33.09	7.55524	5.53529	0.1	0.031	-0.031	0.04384062
768	76.85	41.16	33.09	7.57229	5.50616	0.09	0.034444	-0.06889	0.077020119
769	76.98	41.16	33.08	7.57229	5.4771	0.13	0	-0.04769	0.047692308
770	77.06	41.17	33.08	7.58936	5.4626	0.08	0.03875	-0.03875	0.054800776
771	77.16	41.17	33.07	7.60645	5.43365	0.1	0.031	-0.062	0.069318107
772	77.25	41.17	33.06	7.60645	5.40479	0.09	0	-0.06889	0.068888889
773	77.36	41.17	33.06	7.62356	5.376	0.11	0.028182	-0.05636	0.063016461
774	77.47	41.18	33.05	7.64069	5.34729	0.11	0.028182	-0.05636	0.063016461
775	77.56	41.18	33.05	7.64069	5.33296	0.09	0	-0.03444	0.034444444
776	77.65	41.18	33.04	7.65784	5.30436	0.09	0.034444	-0.06889	0.077020119
777	77.77	41.18	33.04	7.67501	5.27584	0.12	0.025833	-0.05167	0.057765089
778	77.86	41.19	33.03	7.69219	5.26161	0.09	0.034444	-0.03444	0.0487118
779	77.96	41.19	33.03	7.69219	5.23321	0.1	0	-0.062	0.062
780	78.05	41.19	33.02	7.7094	5.20488	0.09	0.034444	-0.06889	0.077020119
781	78.16	41.19	33.02	7.72662	5.17663	0.11	0.028182	-0.05636	0.063016461
782	78.26	41.19	33.01	7.72662	5.16253	0.1	0	-0.031	0.031
783	78.36	41.2	33.01	7.74386	5.13439	0.1	0.031	-0.062	0.069318107
784	78.45	41.2	33	7.76113	5.10633	0.09	0.034444	-0.06889	0.077020119
785	78.56	41.2	32.99	7.76113	5.07835	0.11	0	-0.05636	0.056363636
786	78.66	41.2	32.99	7.77841	5.06439	0.1	0.031	-0.031	0.04384062
787	78.76	41.21	32.98	7.79571	5.03652	0.1	0.031	-0.062	0.069318107
788	78.85	41.21	32.98	7.79571	5.00873	0.09	0	-0.06889	0.068888889
789	78.96	41.21	32.97	7.81303	4.98102	0.11	0.028182	-0.05636	0.063016461
790	79.06	41.21	32.97	7.83037	4.96719	0.1	0.031	-0.031	0.04384062
791	79.16	41.21	32.96	7.84773	4.9396	0.1	0.031	-0.062	0.069318107
792	79.25	41.21	32.96	7.84773	4.91207	0.09	0	-0.06889	0.068888889
793	79.36	41.21	32.95	7.84773	4.88463	0.11	0	-0.05636	0.056363636

794	79.46	41.21	32.95	7.84773	4.87094	0.1	0	-0.031	0.031
795	79.56	41.21	32.94	7.84773	4.84361	0.1	0	-0.062	0.062
796	79.65	41.21	32.93	7.84773	4.81636	0.09	0	-0.06889	0.068888889
797	79.76	41.21	32.93	7.84773	4.78918	0.11	0	-0.05636	0.056363636
798	79.86	41.21	32.92	7.84773	4.76208	0.1	0	-0.062	0.062
799	79.96	41.21	32.92	7.84773	4.74856	0.1	0	-0.031	0.031
800	80.06	41.21	32.91	7.84773	4.72158	0.1	0	-0.062	0.062
801	80.16	41.21	32.91	7.84773	4.69468	0.1	0	-0.062	0.062
802	80.26	41.21	32.9	7.84773	4.66785	0.1	0	-0.062	0.062
803	80.36	41.21	32.89	7.84773	4.64109	0.1	0	-0.062	0.062
804	80.45	41.21	32.89	7.84773	4.62775	0.09	0	-0.03444	0.034444444
805	80.56	41.21	32.88	7.84773	4.60111	0.11	0	-0.05636	0.056363636
806	80.66	41.21	32.88	7.84773	4.57455	0.1	0	-0.062	0.062
807	80.76	41.21	32.87	7.84773	4.54807	0.1	0	-0.062	0.062
808	80.86	41.21	32.87	7.84773	4.52166	0.1	0	-0.062	0.062
809	80.98	41.21	32.86	7.84773	4.49533	0.12	0	-0.05167	0.051666667
810	81.06	41.21	32.86	7.84773	4.4822	0.08	0	-0.03875	0.03875
811	81.16	41.21	32.85	7.84773	4.45598	0.1	0	-0.062	0.062
812	81.25	41.21	32.84	7.84773	4.42985	0.09	0	-0.06889	0.068888889
813	81.36	41.21	32.84	7.84773	4.40379	0.11	0	-0.05636	0.056363636
814	81.47	41.21	32.83	7.84773	4.3778	0.11	0	-0.05636	0.056363636
815	81.56	41.21	32.83	7.84773	4.36484	0.09	0	-0.03444	0.034444444
816	81.66	41.21	32.82	7.84773	4.33897	0.1	0	-0.062	0.062
817	81.76	41.21	32.82	7.84773	4.31318	0.1	0	-0.062	0.062
818	81.86	41.21	32.81	7.84773	4.28747	0.1	0	-0.062	0.062
819	81.97	41.21	32.8	7.84773	4.26183	0.11	0	-0.05636	0.056363636
820	82.05	41.21	32.8	7.84773	4.24904	0.08	0	-0.03875	0.03875
821	82.16	41.21	32.79	7.84773	4.22352	0.11	0	-0.05636	0.056363636
822	82.26	41.21	32.79	7.84773	4.19807	0.1	0	-0.062	0.062
823	82.36	41.21	32.78	7.84773	4.1727	0.1	0	-0.062	0.062
824	82.45	41.21	32.78	7.84773	4.14741	0.09	0	-0.06889	0.068888889
825	82.56	41.21	32.77	7.84773	4.1222	0.11	0	-0.05636	0.056363636
826	82.66	41.21	32.77	7.84773	4.10962	0.1	0	-0.031	0.031
827	82.76	41.21	32.76	7.84773	4.08452	0.1	0	-0.062	0.062
828	82.85	41.21	32.75	7.84773	4.0595	0.09	0	-0.06889	0.068888889
829	82.97	41.21	32.75	7.84773	4.03455	0.12	0	-0.05167	0.051666667
830	83.06	41.21	32.74	7.84773	4.00969	0.09	0	-0.06889	0.068888889
831	83.16	41.21	32.74	7.84773	3.99728	0.1	0	-0.031	0.031
832	83.25	41.21	32.73	7.84773	3.97253	0.09	0	-0.06889	0.068888889
833	83.36	41.21	32.73	7.84773	3.94785	0.11	0	-0.05636	0.056363636
834	83.47	41.21	32.72	7.84773	3.92325	0.11	0	-0.05636	0.056363636
835	83.56	41.21	32.71	7.84773	3.89873	0.09	0	-0.06889	0.068888889

242

836	83.65	41.21	32.71	7.84773	3.8865	0.09	0	-0.03444	0.034444444
837	83.76	41.21	32.71	7.84773	3.86209	0.11	0	-0.05636	0.056363636
838	83.86	41.21	32.7	7.84773	3.83776	0.1	0	-0.062	0.062
839	83.96	41.21	32.69	7.83037	3.81351	0.1	-0.031	-0.062	0.069318107
840	84.05	41.21	32.69	7.83037	3.78933	0.09	0	-0.06889	0.068888889
841	84.16	41.21	32.68	7.83037	3.76523	0.11	0	-0.05636	0.056363636
842	84.26	41.21	32.68	7.83037	3.75321	0.1	0	-0.031	0.031
843	84.36	41.21	32.67	7.83037	3.72922	0.1	0	-0.062	0.062
844	84.45	41.21	32.66	7.83037	3.70532	0.09	0	-0.06889	0.068888889
845	84.56	41.21	32.66	7.83037	3.68149	0.11	0	-0.05636	0.056363636
846	84.66	41.21	32.65	7.83037	3.65773	0.1	0	-0.062	0.062
847	84.76	41.21	32.65	7.83037	3.64588	0.1	0	-0.031	0.031
848	84.85	41.21	32.64	7.81303	3.62225	0.09	-0.03444	-0.06889	0.077020119
849	84.96	41.21	32.64	7.81303	3.59868	0.11	0	-0.05636	0.056363636
850	85.06	41.21	32.63	7.81303	3.5752	0.1	0	-0.062	0.062
851	85.16	41.21	32.62	7.81303	3.55179	0.1	0	-0.062	0.062
852	85.26	41.21	32.62	7.81303	3.54012	0.1	0	-0.031	0.031
853	85.36	41.21	32.62	7.81303	3.51683	0.1	0	-0.062	0.062
854	85.46	41.21	32.61	7.81303	3.49361	0.1	0	-0.062	0.062
855	85.56	41.21	32.6	7.81303	3.47047	0.1	0	-0.062	0.062
856	85.65	41.21	32.6	7.79571	3.44741	0.09	-0.03444	-0.06889	0.077020119
857	85.76	41.21	32.59	7.79571	3.42442	0.11	0	-0.05636	0.056363636
858	85.86	41.21	32.59	7.79571	3.41296	0.1	0	-0.031	0.031
859	85.97	41.21	32.58	7.79571	3.39009	0.11	0	-0.05636	0.056363636
860	86.05	41.21	32.57	7.79571	3.3673	0.08	0	-0.0775	0.0775
861	86.16	41.21	32.57	7.79571	3.34458	0.11	0	-0.05636	0.056363636
862	86.26	41.21	32.56	7.79571	3.32194	0.1	0	-0.062	0.062
863	86.36	41.21	32.56	7.79571	3.31065	0.1	0	-0.031	0.031
864	86.46	41.21	32.55	7.79571	3.28813	0.1	0	-0.062	0.062
865	86.56	41.2	32.55	7.77841	3.26568	0.1	-0.031	-0.062	0.069318107
866	86.66	41.2	32.54	7.77841	3.24331	0.1	0	-0.062	0.062
867	86.76	41.2	32.53	7.77841	3.22102	0.1	0	-0.062	0.062
868	86.86	41.2	32.53	7.77841	3.1988	0.1	0	-0.062	0.062
869	86.96	41.2	32.53	7.77841	3.18772	0.1	0	-0.031	0.031
870	87.06	41.2	32.52	7.77841	3.16562	0.1	0	-0.062	0.062
871	87.16	41.2	32.51	7.77841	3.1436	0.1	0	-0.062	0.062
872	87.25	41.2	32.51	7.77841	3.12165	0.09	0	-0.06889	0.068888889
873	87.36	41.2	32.5	7.77841	3.09978	0.11	0	-0.05636	0.056363636
874	87.47	41.2	32.49	7.76113	3.07799	0.11	-0.02818	-0.05636	0.063016461
875	87.56	41.2	32.49	7.76113	3.06712	0.09	0	-0.03444	0.034444444
876	87.65	41.2	32.48	7.76113	3.04544	0.09	0	-0.06889	0.068888889
877	87.76	41.2	32.48	7.76113	3.02384	0.11	0	-0.05636	0.056363636

878	87.86	41.2	32.47	7.76113	3.00232	0.1	0	-0.062	0.062
879	87.98	41.2	32.47	7.76113	2.98087	0.12	0	-0.05167	0.051666667
880	88.05	41.2	32.46	7.76113	2.97018	0.07	0	-0.04429	0.044285714
881	88.16	41.2	32.46	7.76113	2.94884	0.11	0	-0.05636	0.056363636
882	88.26	41.2	32.45	7.74386	2.92759	0.1	-0.031	-0.062	0.069318107
883	88.36	41.2	32.44	7.74386	2.90641	0.1	0	-0.062	0.062
884	88.45	41.2	32.44	7.74386	2.89585	0.09	0	-0.03444	0.034444444
885	88.56	41.2	32.44	7.74386	2.87479	0.11	0	-0.05636	0.056363636
886	88.66	41.2	32.43	7.74386	2.8538	0.1	0	-0.062	0.062
887	88.76	41.2	32.42	7.74386	2.83289	0.1	0	-0.062	0.062
888	88.85	41.2	32.42	7.74386	2.81206	0.09	0	-0.06889	0.068888889
889	88.97	41.2	32.41	7.74386	2.79131	0.12	0	-0.05167	0.051666667
890	89.06	41.2	32.41	7.74386	2.78096	0.09	0	-0.03444	0.034444444
891	89.16	41.19	32.4	7.72662	2.76032	0.1	-0.031	-0.062	0.069318107
892	89.25	41.19	32.4	7.72662	2.73975	0.09	0	-0.06889	0.068888889
893	89.36	41.19	32.39	7.72662	2.71927	0.11	0	-0.05636	0.056363636
894	89.46	41.19	32.38	7.72662	2.69886	0.1	0	-0.062	0.062
895	89.56	41.19	32.38	7.72662	2.68868	0.1	0	-0.031	0.031
896	89.65	41.19	32.37	7.72662	2.66839	0.09	0	-0.06889	0.068888889
897	89.76	41.19	32.37	7.72662	2.64817	0.11	0	-0.05636	0.056363636
898	89.86	41.19	32.36	7.72662	2.62803	0.1	0	-0.062	0.062
899	89.96	41.19	32.35	7.72662	2.60797	0.1	0	-0.062	0.062
900	90.05	41.19	32.35	7.7094	2.59796	0.09	-0.03444	-0.03444	0.0487118
901	90.16	41.19	32.35	7.7094	2.57802	0.11	0	-0.05636	0.056363636
902	90.26	41.19	32.34	7.7094	2.55814	0.1	0	-0.062	0.062
903	90.36	41.19	32.33	7.7094	2.53835	0.1	0	-0.062	0.062
904	90.46	41.19	32.33	7.7094	2.51863	0.1	0	-0.062	0.062
905	90.57	41.19	32.32	7.7094	2.49899	0.11	0	-0.05636	0.056363636
906	90.66	41.19	32.32	7.7094	2.4892	0.09	0	-0.03444	0.034444444
907	90.76	41.19	32.31	7.7094	2.46968	0.1	0	-0.062	0.062
908	90.85	41.19	32.31	7.7094	2.45023	0.09	0	-0.06889	0.068888889
909	90.96	41.19	32.3	7.69219	2.43086	0.11	-0.02818	-0.05636	0.063016461
910	91.06	41.19	32.29	7.69219	2.41156	0.1	0	-0.062	0.062
911	91.16	41.19	32.29	7.69219	2.40194	0.1	0	-0.031	0.031
912	91.25	41.19	32.28	7.69219	2.38276	0.09	0	-0.06889	0.068888889
913	91.36	41.19	32.28	7.69219	2.36366	0.11	0	-0.05636	0.056363636
914	91.46	41.19	32.27	7.69219	2.34463	0.1	0	-0.062	0.062
915	91.56	41.19	32.26	7.69219	2.32569	0.1	0	-0.062	0.062
916	91.65	41.19	32.26	7.69219	2.31624	0.09	0	-0.03444	0.034444444
917	91.76	41.18	32.26	7.67501	2.29741	0.11	-0.02818	-0.05636	0.063016461
918	91.86	41.18	32.25	7.67501	2.27865	0.1	0	-0.062	0.062
919	91.97	41.18	32.24	7.67501	2.25997	0.11	0	-0.05636	0.056363636

244

920	92.06	41.18	32.24	7.67501	2.24137	0.09	0	-0.06889	0.068888889
921	92.16	41.18	32.23	7.67501	2.2321	0.1	0	-0.031	0.031
922	92.26	41.18	32.23	7.65784	2.21361	0.1	-0.031	-0.062	0.069318107
923	92.36	41.18	32.22	7.65784	2.1952	0.1	0	-0.062	0.062
924	92.46	41.18	32.22	7.65784	2.17686	0.1	0	-0.062	0.062
925	92.56	41.18	32.21	7.65784	2.15861	0.1	0	-0.062	0.062
926	92.66	41.18	32.2	7.64069	2.14043	0.1	-0.031	-0.062	0.069318107
927	92.76	41.18	32.2	7.64069	2.13137	0.1	0	-0.031	0.031
928	92.85	41.18	32.19	7.64069	2.1133	0.09	0	-0.06889	0.068888889
929	92.96	41.18	32.19	7.64069	2.09531	0.11	0	-0.05636	0.056363636
930	93.06	41.18	32.18	7.64069	2.0774	0.1	0	-0.062	0.062
931	93.16	41.17	32.17	7.62356	2.05957	0.1	-0.031	-0.062	0.069318107
932	93.25	41.17	32.17	7.62356	2.05068	0.09	0	-0.03444	0.034444444
933	93.37	41.17	32.17	7.62356	2.03296	0.12	0	-0.05167	0.051666667
934	93.46	41.17	32.16	7.62356	2.01532	0.09	0	-0.06889	0.068888889
935	93.56	41.17	32.15	7.60645	1.99776	0.1	-0.031	-0.062	0.069318107
936	93.65	41.17	32.15	7.60645	1.989	0.09	0	-0.03444	0.034444444
937	93.76	41.17	32.14	7.60645	1.97155	0.11	0	-0.05636	0.056363636
938	93.86	41.17	32.14	7.60645	1.95418	0.1	0	-0.062	0.062
939	93.96	41.17	32.13	7.58936	1.93688	0.1	-0.031	-0.062	0.069318107
940	94.05	41.17	32.13	7.58936	1.91967	0.09	0	-0.06889	0.068888889
941	94.16	41.17	32.12	7.58936	1.90252	0.11	0	-0.05636	0.056363636
942	94.26	41.17	32.12	7.58936	1.89398	0.1	0	-0.031	0.031
943	94.36	41.17	32.11	7.58936	1.87695	0.1	0	-0.062	0.062
944	94.45	41.16	32.1	7.57229	1.86	0.09	-0.03444	-0.06889	0.077020119
945	94.56	41.16	32.1	7.57229	1.84313	0.11	0	-0.05636	0.056363636
946	94.66	41.16	32.09	7.57229	1.82634	0.1	0	-0.062	0.062
947	94.76	41.16	32.09	7.57229	1.81797	0.1	0	-0.031	0.031
948	94.85	41.16	32.08	7.55524	1.80129	0.09	-0.03444	-0.06889	0.077020119
949	94.96	41.16	32.08	7.55524	1.78468	0.11	0	-0.05636	0.056363636
950	95.06	41.16	32.07	7.55524	1.76816	0.1	0	-0.062	0.062
951	95.16	41.16	32.06	7.55524	1.75171	0.1	0	-0.062	0.062
952	95.25	41.16	32.06	7.55524	1.74351	0.09	0	-0.03444	0.034444444
953	95.36	41.16	32.05	7.53821	1.72717	0.11	-0.02818	-0.05636	0.063016461
954	95.46	41.16	32.05	7.53821	1.71092	0.1	0	-0.062	0.062
955	95.56	41.16	32.04	7.53821	1.69474	0.1	0	-0.062	0.062
956	95.65	41.16	32.04	7.53821	1.67863	0.09	0	-0.06889	0.068888889
957	95.76	41.16	32.03	7.5212	1.67061	0.11	-0.02818	-0.02818	0.039855109
958	95.86	41.16	32.03	7.5212	1.65462	0.1	0	-0.062	0.062
959	95.96	41.16	32.02	7.5212	1.63871	0.1	0	-0.062	0.062
960	96.05	41.16	32.01	7.5212	1.62287	0.09	0	-0.06889	0.068888889
961	96.16	41.16	32.01	7.5212	1.60711	0.11	0	-0.05636	0.056363636

962	96.26	41.16	32	7.5212	1.59143	0.1	0	-0.062	0.062
963	96.36	41.16	32	7.5212	1.58362	0.1	0	-0.031	0.031
964	96.45	41.16	31.99	7.5212	1.56805	0.09	0	-0.06889	0.068888889
965	96.56	41.16	31.99	7.5212	1.55257	0.11	0	-0.05636	0.056363636
966	96.66	41.16	31.98	7.5212	1.53715	0.1	0	-0.062	0.062
967	96.76	41.16	31.97	7.5212	1.52182	0.1	0	-0.062	0.062
968	96.85	41.16	31.97	7.5212	1.51418	0.09	0	-0.03444	0.034444444
969	96.96	41.16	31.96	7.5212	1.49896	0.11	0	-0.05636	0.056363636
970	97.06	41.16	31.96	7.5212	1.48382	0.1	0	-0.062	0.062
971	97.16	41.16	31.95	7.5212	1.46875	0.1	0	-0.062	0.062
972	97.26	41.16	31.95	7.5212	1.45376	0.1	0	-0.062	0.062
973	97.36	41.16	31.94	7.5212	1.44629	0.1	0	-0.031	0.031
974	97.46	41.16	31.94	7.5212	1.43142	0.1	0	-0.062	0.062
975	97.56	41.16	31.93	7.5212	1.41662	0.1	0	-0.062	0.062
976	97.65	41.16	31.92	7.5212	1.4019	0.09	0	-0.06889	0.068888889
977	97.76	41.16	31.92	7.5212	1.38726	0.11	0	-0.05636	0.056363636
978	97.86	41.16	31.91	7.5212	1.37269	0.1	0	-0.062	0.062
979	97.96	41.16	31.91	7.5212	1.36544	0.1	0	-0.031	0.031
980	98.05	41.16	31.9	7.5212	1.35099	0.09	0	-0.06889	0.068888889
981	98.16	41.16	31.9	7.5212	1.33661	0.11	0	-0.05636	0.056363636
982	98.26	41.16	31.89	7.5212	1.32232	0.1	0	-0.062	0.062
983	98.36	41.16	31.88	7.5212	1.3081	0.1	0	-0.062	0.062
984	98.45	41.16	31.88	7.5212	1.30101	0.09	0	-0.03444	0.034444444
985	98.56	41.16	31.87	7.5212	1.28691	0.11	0	-0.05636	0.056363636
986	98.66	41.16	31.87	7.5212	1.27288	0.1	0	-0.062	0.062
987	98.76	41.1	31.81	7.21825	1.13683	0.1	-0.558	-0.62	0.834124691
988	98.85	41.16	31.83	7.53821	1.1971	0.09	0.654444	0.31	0.724152975
989	98.96	41.16	31.8	7.57229	1.13022	0.11	0.056364	-0.28182	0.287399282
990	99.06	41.17	31.77	7.60645	1.06527	0.1	0.062	-0.31	0.31613921
991	99.16	41.18	31.74	7.64069	1.00224	0.1	0.062	-0.31	0.31613921
992	99.25	41.18	31.71	7.65784	0.94716	0.09	0.034444	-0.31	0.31190771
993	99.36	41.19	31.68	7.69219	0.88778	0.11	0.056364	-0.28182	0.287399282
994	99.46	41.19	31.65	7.72662	0.83032	0.1	0.062	-0.31	0.31613921
995	99.56	41.2	31.62	7.74386	0.77479	0.1	0.031	-0.31	0.311546144
996	99.65	41.21	31.59	7.81303	0.72645	0.09	0.137778	-0.31	0.339238435
997	99.76	41.22	31.56	7.89992	0.67967	0.11	0.140909	-0.25364	0.290149577
998	99.86	41.24	31.53	7.98729	0.62952	0.1	0.155	-0.31	0.346590537
999	99.96	41.25	31.51	8.07515	0.58602	0.1	0.155	-0.279	0.319164534
1000	100.05	41.27	31.48	8.14577	0.54867	0.09	0.137778	-0.27556	0.308080477

Appendix D

Load – Displacement raw data for compression tests along <u>X</u> and <u>Y</u> axes

This section provides all the raw data sets corresponding to compression tests along x and y axes as discussed in Chapter 4 (Supplementary Material). It may be noted that all the conclusions drawn in this thesis have been based on results from compression tests performed along <u>**z-axes**</u>. These data are presented here for the sake of completeness and also to facilitate comparison with Appendix A where everything is along the *z-axes*.

 * All data points have been reported in N (load) and mm (displacement):

<u>Sample Control-X</u>

<u>N</u>	<u>mm</u>	-0.1	0.3	1.9	0.6	8.4	0.9	18.4	1.2	29.7	1.5
0.0	0.0	0.0	0.3	2.1	0.6	8.7	0.9	18.7	1.2	30.1	1.5
0.0	0.0	0.0	0.3	2.3	0.6	9.0	0.9	19.2	1.2	30.5	1.5
0.0	0.0	0.0	0.3	2.5	0.6	9.2	0.9	19.5	1.2	30.9	1.5
0.0	0.1	0.0	0.3	2.6	0.6	9.6	0.9	19.9	1.2	31.3	1.5
0.0	0.1	0.0	0.4	2.8	0.6	9.8	0.9	20.3	1.2	31.7	1.5
0.0	0.1	0.0	0.4	2.9	0.7	10.1	0.9	20.7	1.2	32.1	1.5
0.0	0.1	0.0	0.4	3.1	0.7	10.5	1.0	21.1	1.2	32.5	1.5
0.0	0.1	0.1	0.4	3.4	0.7	10.8	1.0	21.5	1.3	33.0	1.5
0.0	0.1	0.1	0.4	3.6	0.7	11.1	1.0	21.9	1.3	33.3	1.6
0.0	0.1	0.1	0.4	3.8	0.7	11.4	1.0	22.2	1.3	33.7	1.6
0.0	0.1	0.2	0.4	3.9	0.7	11.8	1.0	22.6	1.3	34.1	1.6
0.0	0.1	0.2	0.4	4.2	0.7	12.2	1.0	23.1	1.3	34.5	1.6
0.0	0.1	0.3	0.4	4.4	0.7	12.5	1.0	23.4	1.3	34.9	1.6
0.0	0.2	0.4	0.4	4.6	0.7	12.9	1.0	23.8	1.3	35.3	1.6
0.0	0.2	0.4	0.5	4.9	0.7	13.3	1.0	24.1	1.3	35.7	1.6
0.0	0.2	0.5	0.5	5.0	0.8	13.5	1.0	24.5	1.3	36.1	1.6
0.0	0.2	0.6	0.5	5.3	0.8	13.9	1.1	24.9	1.3	36.5	1.6
0.0	0.2	0.7	0.5	5.6	0.8	14.2	1.1	25.4	1.4	36.9	1.6
0.0	0.2	0.8	0.5	5.7	0.8	14.6	1.1	25.8	1.4	37.3	1.7
0.0	0.2	0.9	0.5	6.0	0.8	15.0	1.1	26.1	1.4	37.6	1.7
0.0	0.2	1.0	0.5	6.3	0.8	15.4	1.1	26.5	1.4	38.1	1.7
0.0	0.2	1.1	0.5	6.4	0.8	15.7	1.1	26.9	1.4	38.5	1.7
0.0	0.2	1.3	0.5	6.8	0.8	16.1	1.1	27.3	1.4	38.8	1.7
0.0	0.3	1.3	0.5	7.0	0.8	16.5	1.1	27.8	1.4	39.2	1.7
0.0	0.3	1.4	0.6	7.3	0.8	16.9	1.1	28.2	1.4	39.6	1.7
0.0	0.3	1.6	0.6	7.5	0.9	17.2	1.1	28.5	1.4	40.0	1.7
0.0	0.3	1.6	0.6	7.8	0.9	17.6	1.2	28.9	1.4	40.4	1.7
0.0	0.3	1.8	0.6	8.1	0.9	18.1	1.2	29.3	1.5	40.8	1.7

41.1	1.8	55.3	2.2	66.6	2.6	75.4	3.0	82.5	3.4	88.2	3.9
41.5	1.8	55.5	2.2	66.7	2.6	75.6	3.0	82.7	3.4	88.3	3.9
41.9	1.8	55.9	2.2	67.0	2.6	75.8	3.0	82.8	3.5	88.4	3.9
42.3	1.8	56.2	2.2	67.2	2.6	76.0	3.0	83.1	3.5	88.5	3.9
42.6	1.8	56.4	2.2	67.5	2.6	76.2	3.1	83.2	3.5	88.7	3.9
43.0	1.8	56.8	2.2	67.7	2.6	76.3	3.1	83.3	3.5	88.7	3.9
43.4	1.8	57.1	2.2	67.9	2.7	76.6	3.1	83.5	3.5	88.9	3.9
43.7	1.8	57.4	2.2	68.2	2.7	76.8	3.1	83.6	3.5	89.0	3.9
44.1	1.8	57.6	2.3	68.4	2.7	76.9	3.1	83.7	3.5	89.1	3.9
44.5	1.8	57.9	2.3	68.6	2.7	77.2	3.1	83.9	3.5	89.2	3.9
44.8	1.9	58.2	2.3	68.9	2.7	77.3	3.1	84.0	3.5	89.3	4.0
45.1	1.9	58.5	2.3	69.0	2.7	77.5	3.1	84.2	3.5	89.4	4.0
45.4	1.9	58.8	2.3	69.3	2.7	77.6	3.1	84.3	3.6	89.5	4.0
45.9	1.9	59.1	2.3	69.5	2.7	77.8	3.1	84.4	3.6	89.7	4.0
46.2	1.9	59.3	2.3	69.7	2.7	78.0	3.2	84.6	3.6	89.8	4.0
46.5	1.9	59.6	2.3	70.0	2.7	78.2	3.2	84.7	3.6	89.8	4.0
46.9	1.9	60.0	2.3	70.1	2.8	78.3	3.2	84.9	3.6	90.0	4.0
47.2	1.9	60.1	2.3	70.4	2.8	78.6	3.2	85.0	3.6	90.1	4.0
47.6	1.9	60.5	2.4	70.6	2.8	78.7	3.2	85.1	3.6	90.2	4.0
48.0	1.9	60.7	2.4	70.8	2.8	78.8	3.2	85.3	3.6	90.3	4.0
48.2	2.0	61.0	2.4	71.1	2.8	79.1	3.2	85.4	3.6	90.4	4.1
48.6	2.0	61.2	2.4	71.2	2.8	79.2	3.2	85.6	3.6	90.6	4.1
48.9	2.0	61.5	2.4	71.4	2.8	79.4	3.2	85.7	3.7	90.6	4.1
49.3	2.0	61.8	2.4	71.7	2.8	79.6	3.2	85.8	3.7	90.7	4.1
49.6	2.0	62.0	2.4	71.8	2.8	79.7	3.3	85.9	3.7	90.8	4.1
49.9	2.0	62.3	2.4	72.1	2.8	79.8	3.3	86.0	3.7	90.9	4.1
50.3	2.0	62.6	2.4	72.3	2.9	80.0	3.3	86.2	3.7	91.0	4.1
50.5	2.0	62.8	2.4	72.5	2.9	80.2	3.3	86.4	3.7	91.2	4.1
50.9	2.0	63.0	2.5	72.7	2.9	80.4	3.3	86.4	3.7	91.2	4.1
51.3	2.0	63.4	2.5	72.9	2.9	80.5	3.3	86.6	3.7	91.3	4.1
51.5	2.1	63.5	2.5	73.1	2.9	80.7	3.3	86.8	3.7	91.4	4.1
51.9	2.1	63.8	2.5	73.2	2.9	80.8	3.3	86.8	3.7	91.5	4.2
52.2	2.1	64.1	2.5	73.5	2.9	81.0	3.3	86.9	3.8	91.6	4.2
52.5	2.1	64.4	2.5	73.8	2.9	81.2	3.3	87.1	3.8	91.7	4.2
52.8	2.1	64.5	2.5	73.9	2.9	81.3	3.4	87.2	3.8	91.8	4.2
53.2	2.1	64.8	2.5	74.1	2.9	81.5	3.4	87.3	3.8	91.8	4.2
53.4	2.1	65.1	2.5	74.4	3.0	81.7	3.4	87.5	3.8	92.0	4.2
53.8	2.1	65.3	2.5	74.4	3.0	81.8	3.4	87.6	3.8	92.1	4.2
54.1	2.1	65.6	2.6	74.7	3.0	81.9	3.4	87.7	3.8	92.1	4.2
54.4	2.1	65.9	2.6	74.9	3.0	82.1	3.4	87.9	3.8	92.3	4.2
54.6	2.2	66.0	2.6	75.0	3.0	82.3	3.4	88.0	3.8	92.4	4.3
55.0	2.2	66.3	2.6	75.2	3.0	82.4	3.4	88.0	3.8	92.4	4.3

92.6	4.3	95.8	4.7	98.3	5.1	100.2	5.5	101.7	6.0	102.9	6.4
92.6	4.3	95.9	4.7	98.4	5.1	100.3	5.5	101.7	6.0	102.8	6.4
92.7	4.3	96.0	4.7	98.5	5.1	100.4	5.6	101.8	6.0	102.9	6.4
92.8	4.3	96.0	4.7	98.5	5.1	100.3	5.6	101.8	6.0	103.0	6.4
92.9	4.3	96.1	4.7	98.5	5.2	100.4	5.6	101.8	6.0	102.9	6.4
93.0	4.3	96.2	4.7	98.7	5.2	100.5	5.6	101.9	6.0	103.0	6.4
93.1	4.3	96.2	4.8	98.6	5.2	100.4	5.6	101.9	6.0	103.1	6.4
93.1	4.3	96.4	4.8	98.7	5.2	100.5	5.6	101.9	6.0	103.0	6.4
93.2	4.4	96.4	4.8	98.8	5.2	100.5	5.6	102.0	6.0	103.1	6.5
93.3	4.4	96.4	4.8	98.8	5.2	100.6	5.6	102.0	6.0	103.1	6.5
93.4	4.4	96.5	4.8	98.8	5.2	100.6	5.6	102.0	6.1	103.1	6.5
93.5	4.4	96.6	4.8	98.9	5.2	100.7	5.6	102.1	6.1	103.1	6.5
93.5	4.4	96.6	4.8	99.0	5.2	100.7	5.7	102.1	6.1	103.1	6.5
93.7	4.4	96.7	4.8	99.0	5.2	100.7	5.7	102.1	6.1	103.1	6.5
93.7	4.4	96.8	4.8	99.1	5.3	100.8	5.7	102.2	6.1	103.2	6.5
93.8	4.4	96.8	4.8	99.1	5.3	100.9	5.7	102.1	6.1	103.2	6.5
93.9	4.4	96.9	4.9	99.1	5.3	100.9	5.7	102.2	6.1	103.3	6.5
94.0	4.4	96.9	4.9	99.2	5.3	100.9	5.7	102.2	6.1	103.2	6.5
94.1	4.5	97.0	4.9	99.3	5.3	100.9	5.7	102.2	6.1	103.2	6.6
94.1	4.5	97.1	4.9	99.3	5.3	101.0	5.7	102.3	6.1	103.3	6.6
94.2	4.5	97.2	4.9	99.3	5.3	101.0	5.7	102.3	6.2	103.3	6.6
94.3	4.5	97.3	4.9	99.4	5.3	101.0	5.7	102.3	6.2	103.4	6.6
94.3	4.5	97.2	4.9	99.4	5.3	101.1	5.8	102.4	6.2	103.4	6.6
94.4	4.5	97.3	4.9	99.4	5.3	101.1	5.8	102.3	6.2	103.3	6.6
94.6	4.5	97.4	4.9	99.5	5.4	101.2	5.8	102.4	6.2	103.3	6.6
94.6	4.5	97.4	4.9	99.6	5.4	101.2	5.8	102.4	6.2	103.4	6.6
94.7	4.5	97.5	5.0	99.6	5.4	101.2	5.8	102.4	6.2	103.4	6.6
94.8	4.5	97.5	5.0	99.6	5.4	101.2	5.8	102.5	6.2	103.4	6.6
94.9	4.6	97.6	5.0	99.7	5.4	101.3	5.8	102.5	6.2	103.4	6.7
94.9	4.6	97.6	5.0	99.7	5.4	101.3	5.8	102.5	6.2	103.5	6.7
95.0	4.6	97.7	5.0	99.8	5.4	101.3	5.8	102.5	6.3	103.5	6.7
95.1	4.6	97.8	5.0	99.9	5.4	101.4	5.8	102.6	6.3	103.5	6.7
95.1	4.6	97.8	5.0	99.8	5.4	101.4	5.9	102.6	6.3	103.6	6.7
95.2	4.6	97.9	5.0	99.9	5.4	101.4	5.9	102.6	6.3	103.5	6.7
95.3	4.6	98.0	5.0	100.0	5.5	101.5	5.9	102.6	6.3	103.6	6.7
95.3	4.6	98.0	5.0	100.0	5.5	101.5	5.9	102.8	6.3	103.6	6.7
95.4	4.6	98.0	5.1	100.0	5.5	101.5	5.9	102.7	6.3	103.6	6.7
95.5	4.6	98.1	5.1	100.0	5.5	101.6	5.9	102.8	6.3	103.6	6.7
95.5	4.7	98.1	5.1	100.1	5.5	101.7	5.9	102.8	6.3	103.7	6.8
95.6	4.7	98.2	5.1	100.1	5.5	101.6	5.9	102.7	6.3	103.7	6.8
95.7	4.7	98.3	5.1	100.2	5.5	101.7	5.9	102.8	6.4	103.7	6.8
95.8	4.7	98.3	5.1	100.2	5.5	101.7	5.9	102.8	6.4	103.7	6.8

103.8	6.8	104.4	7.2	104.9	7.6	105.2	8.1	105.4	8.5	105.4	8.9
103.7	6.8	104.3	7.2	104.8	7.6	105.2	8.1	105.4	8.5	105.5	8.9
103.8	6.8	104.4	7.2	104.8	7.7	105.2	8.1	105.3	8.5	105.4	8.9
103.8	6.8	104.4	7.2	104.9	7.7	105.2	8.1	105.4	8.5	105.4	8.9
103.7	6.8	104.4	7.3	104.9	7.7	105.2	8.1	105.4	8.5	105.5	8.9
103.8	6.8	104.4	7.3	104.8	7.7	105.2	8.1	105.4	8.5	105.4	8.9
103.8	6.9	104.4	7.3	104.9	7.7	105.2	8.1	105.4	8.5	105.4	9.0
103.8	6.9	104.5	7.3	105.0	7.7	105.2	8.1	105.4	8.5	105.4	9.0
103.8	6.9	104.4	7.3	104.9	7.7	105.2	8.1	105.3	8.6	105.5	9.0
103.9	6.9	104.5	7.3	105.0	7.7	105.2	8.1	105.4	8.6	105.5	9.0
103.9	6.9	104.5	7.3	105.0	7.7	105.2	8.2	105.4	8.6	105.5	9.0
103.9	6.9	104.5	7.3	104.9	7.7	105.2	8.2	105.4	8.6	105.4	9.0
103.9	6.9	104.5	7.3	105.0	7.8	105.2	8.2	105.4	8.6	105.4	9.0
104.0	6.9	104.6	7.3	105.0	7.8	105.2	8.2	105.4	8.6	105.5	9.0
104.0	6.9	104.5	7.4	105.0	7.8	105.3	8.2	105.4	8.6	105.5	9.0
104.0	6.9	104.6	7.4	105.0	7.8	105.2	8.2	105.4	8.6	105.5	9.0
104.0	7.0	104.6	7.4	105.0	7.8	105.3	8.2	105.4	8.6	105.5	9.1
104.0	7.0	104.6	7.4	105.0	7.8	105.3	8.2	105.4	8.6	105.4	9.1
104.0	7.0	104.6	7.4	105.0	7.8	105.3	8.2	105.4	8.7	105.4	9.1
104.0	7.0	104.6	7.4	105.0	7.8	105.3	8.2	105.4	8.7	105.4	9.1
104.0	7.0	104.6	7.4	105.0	7.8	105.3	8.3	105.4	8.7	105.5	9.1
104.1	7.0	104.6	7.4	105.0	7.8	105.2	8.3	105.4	8.7	105.5	9.1
104.1	7.0	104.6	7.4	105.0	7.9	105.3	8.3	105.5	8.7	105.4	9.1
104.1	7.0	104.6	7.4	105.1	7.9	105.3	8.3	105.4	8.7	105.5	9.1
104.1	7.0	104.7	7.5	105.0	7.9	105.3	8.3	105.4	8.7	105.5	9.1
104.1	7.0	104.7	7.5	105.1	7.9	105.3	8.3	105.4	8.7	105.4	9.1
104.2	7.1	104.7	7.5	105.1	7.9	105.3	8.3	105.4	8.7	105.4	9.2
104.1	7.1	104.7	7.5	105.1	7.9	105.3	8.3	105.5	8.7	105.5	9.2
104.2	7.1	104.7	7.5	105.0	7.9	105.3	8.3	105.4	8.8	105.4	9.2
104.2	7.1	104.7	7.5	105.1	7.9	105.3	8.3	105.4	8.8	105.4	9.2
104.2	7.1	104.7	7.5	105.1	7.9	105.4	8.4	105.5	8.8	105.4	9.2
104.2	7.1	104.7	7.5	105.1	7.9	105.3	8.4	105.5	8.8	105.4	9.2
104.3	7.1	104.7	7.5	105.1	8.0	105.4	8.4	105.4	8.8	105.4	9.2
104.2	7.1	104.8	7.5	105.2	8.0	105.4	8.4	105.4	8.8	105.4	9.2
104.2	7.1	104.7	7.6	105.1	8.0	105.3	8.4	105.4	8.8	105.5	9.2
104.3	7.1	104.8	7.6	105.1	8.0	105.3	8.4	105.4	8.8	105.4	9.2
104.3	7.2	104.8	7.6	105.2	8.0	105.3	8.4	105.4	8.8	105.4	9.3
104.3	7.2	104.8	7.6	105.2	8.0	105.4	8.4	105.5	8.8	105.5	9.3
104.3	7.2	104.8	7.6	105.1	8.0	105.4	8.4	105.4	8.9	105.4	9.3
104.4	7.2	104.9	7.6	105.2	8.0	105.4	8.4	105.5	8.9	105.4	9.3
104.3	7.2	104.8	7.6	105.2	8.0	105.4	8.5	105.5	8.9	105.5	9.3
104.4	7.2	104.8	7.6	105.1	8.0	105.3	8.5	105.4	8.9	105.4	9.3

105.4	9.3	105.2	9.7	105.0	10.2	104.6	10.6	104.1	11.0	103.5	11.4
105.4	9.3	105.2	9.7	105.0	10.2	104.6	10.6	104.1	11.0	103.4	11.4
105.4	9.3	105.3	9.8	105.0	10.2	104.6	10.6	104.1	11.0	103.4	11.4
105.4	9.3	105.2	9.8	105.0	10.2	104.6	10.6	104.0	11.0	103.4	11.4
105.4	9.4	105.3	9.8	105.0	10.2	104.6	10.6	104.0	11.0	103.3	11.5
105.4	9.4	105.3	9.8	105.0	10.2	104.6	10.6	104.0	11.0	103.4	11.5
105.3	9.4	105.2	9.8	104.9	10.2	104.6	10.6	104.0	11.1	103.4	11.5
105.4	9.4	105.2	9.8	105.0	10.2	104.5	10.6	104.0	11.1	103.2	11.5
105.4	9.4	105.3	9.8	104.9	10.2	104.6	10.7	104.0	11.1	103.3	11.5
105.3	9.4	105.2	9.8	104.9	10.2	104.5	10.7	104.0	11.1	103.3	11.5
105.4	9.4	105.2	9.8	104.9	10.3	104.5	10.7	103.9	11.1	103.2	11.5
105.4	9.4	105.2	9.8	104.9	10.3	104.5	10.7	103.9	11.1	103.2	11.5
105.3	9.4	105.2	9.9	104.9	10.3	104.5	10.7	103.9	11.1	103.2	11.5
105.4	9.4	105.2	9.9	104.9	10.3	104.4	10.7	103.9	11.1	103.2	11.5
105.4	9.5	105.2	9.9	105.0	10.3	104.4	10.7	103.9	11.1	103.1	11.6
105.4	9.5	105.2	9.9	104.9	10.3	104.5	10.7	103.9	11.1	103.2	11.6
105.4	9.5	105.2	9.9	104.9	10.3	104.4	10.7	103.8	11.2	103.1	11.6
105.4	9.5	105.2	9.9	104.9	10.3	104.4	10.7	103.8	11.2	103.1	11.6
105.3	9.5	105.2	9.9	104.8	10.3	104.4	10.8	103.8	11.2	103.1	11.6
105.4	9.5	105.1	9.9	104.8	10.3	104.4	10.8	103.8	11.2	103.1	11.6
105.4	9.5	105.2	9.9	104.8	10.4	104.4	10.8	103.8	11.2	103.0	11.6
105.3	9.5	105.2	9.9	104.9	10.4	104.4	10.8	103.8	11.2	103.1	11.6
105.3	9.5	105.1	10.0	104.8	10.4	104.4	10.8	103.8	11.2	103.0	11.6
105.4	9.5	105.1	10.0	104.8	10.4	104.3	10.8	103.7	11.2	103.0	11.6
105.4	9.6	105.1	10.0	104.8	10.4	104.3	10.8	103.7	11.2	103.0	11.7
105.3	9.6	105.2	10.0	104.8	10.4	104.3	10.8	103.7	11.2	102.9	11.7
105.3	9.6	105.2	10.0	104.8	10.4	104.3	10.8	103.7	11.3	102.9	11.7
105.3	9.6	105.1	10.0	104.8	10.4	104.3	10.8	103.6	11.3	102.9	11.7
105.4	9.6	105.1	10.0	104.8	10.4	104.3	10.9	103.7	11.3	102.9	11.7
105.3	9.6	105.1	10.0	104.7	10.4	104.2	10.9	103.6	11.3	102.9	11.7
105.3	9.6	105.1	10.0	104.7	10.5	104.2	10.9	103.6	11.3	102.9	11.7
105.4	9.6	105.1	10.0	104.7	10.5	104.2	10.9	103.6	11.3	102.8	11.7
105.3	9.6	105.1	10.1	104.8	10.5	104.3	10.9	103.6	11.3	102.8	11.7
105.3	9.6	105.1	10.1	104.6	10.5	104.2	10.9	103.5	11.3	102.8	11.7
105.3	9.7	105.1	10.1	104.7	10.5	104.2	10.9	103.5	11.3	102.8	11.8
105.2	9.7	105.1	10.1	104.7	10.5	104.2	10.9	103.5	11.3	102.8	11.8
105.3	9.7	105.0	10.1	104.7	10.5	104.1	10.9	103.5	11.4	102.8	11.8
105.3	9.7	105.0	10.1	104.7	10.5	104.1	10.9	103.5	11.4	102.7	11.8
105.3	9.7	105.1	10.1	104.7	10.5	104.2	11.0	103.5	11.4	102.7	11.8
105.3	9.7	105.0	10.1	104.6	10.5	104.1	11.0	103.5	11.4	102.7	11.8
105.3	9.7	105.0	10.1	104.6	10.6	104.1	11.0	103.4	11.4	102.6	11.8
105.3	9.7	105.1	10.1	104.7	10.6	104.1	11.0	103.4	11.4	102.7	11.8

102.7	11.8	101.7	12.3	100.7	12.7	99.6	13.1	98.4	13.5	97.1	13.9
102.6	11.8	101.7	12.3	100.7	12.7	99.6	13.1	98.3	13.5	97.1	13.9
102.6	11.9	101.7	12.3	100.6	12.7	99.5	13.1	98.3	13.5	97.0	14.0
102.6	11.9	101.7	12.3	100.7	12.7	99.5	13.1	98.3	13.5	97.0	14.0
102.5	11.9	101.7	12.3	100.7	12.7	99.5	13.1	98.3	13.6	97.0	14.0
102.5	11.9	101.6	12.3	100.6	12.7	99.4	13.1	98.2	13.6	97.0	14.0
102.5	11.9	101.6	12.3	100.6	12.7	99.4	13.2	98.2	13.6	96.9	14.0
102.5	11.9	101.6	12.3	100.6	12.7	99.4	13.2	98.2	13.6	96.9	14.0
102.4	11.9	101.5	12.3	100.5	12.8	99.4	13.2	98.1	13.6	96.9	14.0
102.4	11.9	101.5	12.3	100.5	12.8	99.3	13.2	98.1	13.6	96.8	14.0
102.4	11.9	101.5	12.4	100.5	12.8	99.3	13.2	98.1	13.6	96.8	14.0
102.4	11.9	101.5	12.4	100.4	12.8	99.3	13.2	98.1	13.6	96.8	14.0
102.4	12.0	101.5	12.4	100.4	12.8	99.2	13.2	98.0	13.6	96.7	14.1
102.4	12.0	101.4	12.4	100.4	12.8	99.2	13.2	98.0	13.6	96.7	14.1
102.3	12.0	101.4	12.4	100.4	12.8	99.2	13.2	98.0	13.7	96.7	14.1
102.3	12.0	101.4	12.4	100.3	12.8	99.1	13.2	97.9	13.7	96.6	14.1
102.3	12.0	101.3	12.4	100.3	12.8	99.1	13.3	97.9	13.7	96.6	14.1
102.3	12.0	101.3	12.4	100.3	12.8	99.1	13.3	97.9	13.7	96.6	14.1
102.2	12.0	101.3	12.4	100.2	12.9	99.1	13.3	97.8	13.7	96.6	14.1
102.3	12.0	101.3	12.4	100.2	12.9	99.1	13.3	97.8	13.7	96.5	14.1
102.2	12.0	101.3	12.5	100.2	12.9	99.0	13.3	97.8	13.7	96.5	14.1
102.2	12.0	101.2	12.5	100.1	12.9	99.0	13.3	97.7	13.7	96.5	14.1
102.2	12.1	101.2	12.5	100.2	12.9	98.9	13.3	97.7	13.7	96.4	14.2
102.1	12.1	101.2	12.5	100.2	12.9	98.9	13.3	97.7	13.7	96.4	14.2
102.1	12.1	101.2	12.5	100.1	12.9	98.9	13.3	97.6	13.8	96.4	14.2
102.1	12.1	101.2	12.5	100.1	12.9	98.9	13.3	97.6	13.8	96.3	14.2
102.1	12.1	101.1	12.5	100.0	12.9	98.8	13.4	97.6	13.8	96.3	14.2
102.1	12.1	101.1	12.5	100.0	12.9	98.8	13.4	97.5	13.8	96.3	14.2
102.1	12.1	101.1	12.5	100.0	13.0	98.7	13.4	97.5	13.8	96.2	14.2
102.0	12.1	101.0	12.5	99.9	13.0	98.8	13.4	97.5	13.8	96.2	14.2
102.0	12.1	101.0	12.6	99.9	13.0	98.8	13.4	97.5	13.8	96.1	14.2
102.0	12.1	101.0	12.6	99.9	13.0	98.6	13.4	97.4	13.8	96.1	14.2
102.0	12.2	101.0	12.6	99.9	13.0	98.7	13.4	97.4	13.8	96.1	14.3
101.9	12.2	101.0	12.6	99.9	13.0	98.6	13.4	97.4	13.8	96.0	14.3
101.9	12.2	100.9	12.6	99.8	13.0	98.6	13.4	97.4	13.9	96.1	14.3
101.8	12.2	100.9	12.6	99.8	13.0	98.5	13.4	97.3	13.9	96.0	14.3
101.9	12.2	100.9	12.6	99.7	13.0	98.5	13.5	97.3	13.9	96.0	14.3
101.8	12.2	100.8	12.6	99.7	13.0	98.5	13.5	97.3	13.9	95.9	14.3
101.8	12.2	100.8	12.6	99.7	13.1	98.5	13.5	97.2	13.9	95.9	14.3
101.8	12.2	100.9	12.6	99.7	13.1	98.4	13.5	97.2	13.9	95.8	14.3
101.8	12.2	100.8	12.7	99.7	13.1	98.5	13.5	97.2	13.9	95.8	14.3
101.7	12.2	100.8	12.7	99.6	13.1	98.4	13.5	97.1	13.9	95.8	14.3

95.8	14.4	94.4	14.8	93.0	15.2	91.6	15.6	90.1	16.0	88.6	16.5
95.7	14.4	94.4	14.8	93.0	15.2	91.5	15.6	90.0	16.0	88.6	16.5
95.7	14.4	94.4	14.8	93.0	15.2	91.5	15.6	89.9	16.1	88.5	16.5
95.7	14.4	94.3	14.8	92.9	15.2	91.5	15.6	90.0	16.1	88.5	16.5
95.7	14.4	94.3	14.8	92.9	15.2	91.4	15.7	89.9	16.1	88.4	16.5
95.7	14.4	94.3	14.8	92.8	15.2	91.4	15.7	89.9	16.1	88.5	16.5
95.6	14.4	94.2	14.8	92.8	15.3	91.4	15.7	89.8	16.1	88.4	16.5
95.6	14.4	94.2	14.8	92.7	15.3	91.3	15.7	89.8	16.1	88.4	16.5
95.5	14.4	94.1	14.9	92.7	15.3	91.2	15.7	89.8	16.1	88.3	16.5
95.5	14.4	94.1	14.9	92.7	15.3	91.3	15.7	89.8	16.1	88.3	16.5
95.5	14.5	94.0	14.9	92.7	15.3	91.2	15.7	89.7	16.1	88.2	16.6
95.4	14.5	94.1	14.9	92.7	15.3	91.2	15.7	89.7	16.1	88.2	16.6
95.4	14.5	94.0	14.9	92.6	15.3	91.2	15.7	89.7	16.2	88.2	16.6
95.3	14.5	94.0	14.9	92.5	15.3	91.1	15.7	89.6	16.2	88.1	16.6
95.3	14.5	94.0	14.9	92.5	15.3	91.0	15.8	89.5	16.2	88.1	16.6
95.3	14.5	94.0	14.9	92.5	15.3	91.0	15.8	89.6	16.2	88.0	16.6
95.3	14.5	93.9	14.9	92.4	15.4	91.0	15.8	89.5	16.2	88.1	16.6
95.3	14.5	93.9	14.9	92.4	15.4	91.0	15.8	89.4	16.2	88.0	16.6
95.2	14.5	93.8	15.0	92.4	15.4	90.9	15.8	89.4	16.2	88.0	16.6
95.2	14.5	93.8	15.0	92.3	15.4	90.9	15.8	89.4	16.2	87.9	16.6
95.2	14.6	93.7	15.0	92.3	15.4	90.8	15.8	89.3	16.2	87.8	16.7
95.1	14.6	93.7	15.0	92.3	15.4	90.9	15.8	89.4	16.2	87.8	16.7
95.1	14.6	93.7	15.0	92.2	15.4	90.8	15.8	89.4	16.3	87.8	16.7
95.0	14.6	93.7	15.0	92.2	15.4	90.7	15.8	89.2	16.3	87.8	16.7
95.0	14.6	93.6	15.0	92.1	15.4	90.7	15.9	89.2	16.3	87.7	16.7
95.0	14.6	93.6	15.0	92.1	15.4	90.7	15.9	89.2	16.3	87.7	16.7
94.9	14.6	93.5	15.0	92.1	15.5	90.6	15.9	89.1	16.3	87.6	16.7
94.9	14.6	93.5	15.0	92.1	15.5	90.6	15.9	89.1	16.3	87.6	16.7
94.9	14.6	93.5	15.1	92.0	15.5	90.6	15.9	89.1	16.3	87.7	16.7
94.8	14.6	93.4	15.1	92.0	15.5	90.5	15.9	89.0	16.3	87.6	16.7
94.8	14.7	93.4	15.1	92.0	15.5	90.5	15.9	89.0	16.3	87.5	16.8
94.8	14.7	93.4	15.1	91.9	15.5	90.5	15.9	88.9	16.3	87.5	16.8
94.8	14.7	93.4	15.1	91.9	15.5	90.4	15.9	89.0	16.4	87.4	16.8
94.7	14.7	93.3	15.1	91.9	15.5	90.4	15.9	88.9	16.4	87.4	16.8
94.7	14.7	93.3	15.1	91.8	15.5	90.4	16.0	88.9	16.4	87.4	16.8
94.6	14.7	93.2	15.1	91.8	15.5	90.3	16.0	88.8	16.4	87.3	16.8
94.6	14.7	93.2	15.1	91.8	15.6	90.3	16.0	88.8	16.4	87.3	16.8
94.6	14.7	93.2	15.1	91.7	15.6	90.2	16.0	88.8	16.4	87.2	16.8
94.6	14.7	93.2	15.2	91.7	15.6	90.2	16.0	88.7	16.4	87.2	16.8
94.5	14.7	93.1	15.2	91.6	15.6	90.2	16.0	88.7	16.4	87.2	16.8
94.5	14.8	93.1	15.2	91.6	15.6	90.2	16.0	88.7	16.4	87.1	16.9
94.5	14.8	93.1	15.2	91.6	15.6	90.1	16.0	88.6	16.4	87.2	16.9

87.1	16.9	85.6	17.3	84.1	17.7	82.6	18.1	81.1	18.6	79.6	19.0
87.1	16.9	85.6	17.3	84.1	17.7	82.6	18.1	81.1	18.6	79.6	19.0
87.0	16.9	85.5	17.3	84.0	17.7	82.5	18.2	81.1	18.6	79.6	19.0
86.9	16.9	85.4	17.3	84.0	17.7	82.5	18.2	81.0	18.6	79.6	19.0
87.0	16.9	85.4	17.3	84.0	17.8	82.5	18.2	81.0	18.6	79.5	19.0
86.9	16.9	85.4	17.3	83.9	17.8	82.4	18.2	81.0	18.6	79.5	19.0
86.8	16.9	85.3	17.4	83.9	17.8	82.4	18.2	80.9	18.6	79.5	19.0
86.8	16.9	85.4	17.4	83.9	17.8	82.3	18.2	80.9	18.6	79.4	19.0
86.8	17.0	85.2	17.4	83.8	17.8	82.3	18.2	80.9	18.6	79.4	19.1
86.7	17.0	85.3	17.4	83.8	17.8	82.3	18.2	80.8	18.6	79.3	19.1
86.8	17.0	85.3	17.4	83.7	17.8	82.3	18.2	80.7	18.7	79.3	19.1
86.7	17.0	85.2	17.4	83.7	17.8	82.3	18.2	80.8	18.7	79.3	19.1
86.7	17.0	85.1	17.4	83.7	17.8	82.2	18.3	80.7	18.7	79.2	19.1
86.6	17.0	85.1	17.4	83.7	17.8	82.2	18.3	80.7	18.7	79.2	19.1
86.6	17.0	85.1	17.4	83.6	17.9	82.2	18.3	80.7	18.7	79.2	19.1
86.6	17.0	85.1	17.4	83.5	17.9	82.0	18.3	80.6	18.7	79.1	19.1
86.5	17.0	85.0	17.5	83.5	17.9	82.0	18.3	80.5	18.7	79.1	19.1
86.5	17.0	85.0	17.5	83.5	17.9	82.0	18.3	80.5	18.7	79.1	19.1
86.4	17.1	84.9	17.5	83.4	17.9	81.9	18.3	80.5	18.7	79.1	19.2
86.4	17.1	84.9	17.5	83.4	17.9	81.9	18.3	80.4	18.7	79.0	19.2
86.4	17.1	84.9	17.5	83.4	17.9	81.9	18.3	80.4	18.8	79.0	19.2
86.3	17.1	84.8	17.5	83.3	17.9	81.9	18.3	80.4	18.8	78.9	19.2
86.3	17.1	84.8	17.5	83.3	17.9	81.8	18.4	80.3	18.8	78.9	19.2
86.3	17.1	84.8	17.5	83.3	17.9	81.8	18.4	80.3	18.8	78.9	19.2
86.2	17.1	84.7	17.5	83.2	18.0	81.8	18.4	80.3	18.8	78.9	19.2
86.2	17.1	84.7	17.5	83.2	18.0	81.7	18.4	80.2	18.8	78.8	19.2
86.2	17.1	84.6	17.6	83.2	18.0	81.7	18.4	80.3	18.8	78.7	19.2
86.1	17.1	84.6	17.6	83.1	18.0	81.7	18.4	80.2	18.8	78.7	19.2
86.1	17.2	84.6	17.6	83.1	18.0	81.6	18.4	80.1	18.8	78.7	19.3
86.1	17.2	84.6	17.6	83.1	18.0	81.6	18.4	80.1	18.8	78.6	19.3
86.0	17.2	84.5	17.6	83.0	18.0	81.5	18.4	80.1	18.9	78.6	19.3
86.0	17.2	84.5	17.6	83.0	18.0	81.5	18.4	80.0	18.9	78.6	19.3
86.0	17.2	84.4	17.6	83.0	18.0	81.5	18.5	80.0	18.9	78.5	19.3
85.9	17.2	84.4	17.6	82.9	18.0	81.4	18.5	80.0	18.9	78.5	19.3
85.9	17.2	84.4	17.6	82.9	18.1	81.4	18.5	80.0	18.9	78.4	19.3
85.8	17.2	84.3	17.6	82.9	18.1	81.4	18.5	79.9	18.9	78.4	19.3
85.8	17.2	84.3	17.7	82.8	18.1	81.3	18.5	79.9	18.9	78.4	19.3
85.7	17.2	84.2	17.7	82.8	18.1	81.3	18.5	79.8	18.9	78.4	19.3
85.7	17.3	84.2	17.7	82.7	18.1	81.3	18.5	79.8	18.9	78.4	19.4
85.7	17.3	84.2	17.7	82.7	18.1	81.2	18.5	79.8	18.9	78.3	19.4
85.6	17.3	84.2	17.7	82.7	18.1	81.2	18.5	79.7	19.0	78.2	19.4
85.6	17.3	84.1	17.7	82.6	18.1	81.2	18.5	79.7	19.0	78.2	19.4

254

78.2	19.4	76.8	19.8	75.3	20.2	73.9	20.7	72.5	21.1	71.2	21.5
78.1	19.4	76.7	19.8	75.3	20.2	73.9	20.7	72.5	21.1	71.1	21.5
78.2	19.4	76.7	19.8	75.3	20.3	73.8	20.7	72.5	21.1	71.1	21.5
78.1	19.4	76.6	19.8	75.2	20.3	73.8	20.7	72.5	21.1	71.1	21.5
78.0	19.4	76.6	19.9	75.2	20.3	73.8	20.7	72.4	21.1	71.1	21.5
78.0	19.4	76.6	19.9	75.1	20.3	73.7	20.7	72.4	21.1	71.0	21.5
78.0	19.5	76.5	19.9	75.2	20.3	73.8	20.7	72.4	21.1	71.0	21.6
77.9	19.5	76.5	19.9	75.1	20.3	73.7	20.7	72.3	21.1	71.0	21.6
77.9	19.5	76.4	19.9	75.1	20.3	73.7	20.7	72.3	21.2	70.9	21.6
77.9	19.5	76.4	19.9	75.1	20.3	73.6	20.7	72.3	21.2	70.9	21.6
77.8	19.5	76.4	19.9	75.0	20.3	73.6	20.8	72.2	21.2	70.9	21.6
77.8	19.5	76.3	19.9	75.0	20.3	73.5	20.8	72.2	21.2	70.8	21.6
77.8	19.5	76.3	19.9	74.9	20.4	73.6	20.8	72.1	21.2	70.8	21.6
77.7	19.5	76.3	19.9	74.8	20.4	73.5	20.8	72.1	21.2	70.8	21.6
77.7	19.5	76.3	20.0	74.9	20.4	73.5	20.8	72.1	21.2	70.7	21.6
77.7	19.5	76.3	20.0	74.8	20.4	73.5	20.8	72.0	21.2	70.7	21.6
77.6	19.6	76.2	20.0	74.8	20.4	73.4	20.8	72.0	21.2	70.7	21.7
77.6	19.6	76.1	20.0	74.8	20.4	73.3	20.8	72.0	21.2	70.6	21.7
77.6	19.6	76.1	20.0	74.7	20.4	73.3	20.8	71.9	21.3	70.6	21.7
77.5	19.6	76.1	20.0	74.7	20.4	73.3	20.8	71.9	21.3	70.6	21.7
77.5	19.6	76.1	20.0	74.7	20.4	73.3	20.9	71.8	21.3	70.5	21.7
77.5	19.6	76.0	20.0	74.6	20.4	73.3	20.9	71.8	21.3	70.5	21.7
77.4	19.6	76.0	20.0	74.6	20.5	73.2	20.9	71.8	21.3	70.5	21.7
77.4	19.6	75.9	20.0	74.5	20.5	73.1	20.9	71.8	21.3	70.4	21.7
77.3	19.6	75.9	20.1	74.6	20.5	73.1	20.9	71.7	21.3	70.4	21.7
77.3	19.6	75.9	20.1	74.5	20.5	73.1	20.9	71.7	21.3	70.4	21.7
77.3	19.7	75.8	20.1	74.4	20.5	73.0	20.9	71.7	21.3	70.4	21.8
77.3	19.7	75.8	20.1	74.4	20.5	73.0	20.9	71.7	21.3	70.3	21.8
77.2	19.7	75.8	20.1	74.4	20.5	73.0	20.9	71.6	21.4	70.3	21.8
77.2	19.7	75.7	20.1	74.4	20.5	73.0	20.9	71.6	21.4	70.3	21.8
77.2	19.7	75.8	20.1	74.4	20.5	73.0	21.0	71.5	21.4	70.2	21.8
77.1	19.7	75.7	20.1	74.3	20.5	72.9	21.0	71.5	21.4	70.2	21.8
77.1	19.7	75.6	20.1	74.2	20.6	72.9	21.0	71.5	21.4	70.2	21.8
77.0	19.7	75.6	20.1	74.2	20.6	72.8	21.0	71.4	21.4	70.1	21.8
77.0	19.7	75.6	20.2	74.2	20.6	72.8	21.0	71.4	21.4	70.1	21.8
76.9	19.7	75.5	20.2	74.2	20.6	72.8	21.0	71.4	21.4	70.1	21.8
76.9	19.8	75.5	20.2	74.1	20.6	72.7	21.0	71.3	21.4	70.0	21.9
76.9	19.8	75.5	20.2	74.1	20.6	72.7	21.0	71.3	21.4	70.0	21.9
76.9	19.8	75.5	20.2	74.1	20.6	72.7	21.0	71.2	21.5	70.0	21.9
76.8	19.8	75.4	20.2	74.0	20.6	72.6	21.0	71.3	21.5	70.0	21.9
76.8	19.8	75.4	20.2	74.0	20.6	72.6	21.1	71.2	21.5	69.9	21.9
76.8	19.8	75.3	20.2	73.9	20.6	72.5	21.1	71.2	21.5	69.9	21.9

69.9	21.9	68.6	22.3	67.4	22.8	66.3	23.2	65.2	23.6	64.1	24.0
69.8	21.9	68.6	22.3	67.4	22.8	66.3	23.2	65.2	23.6	64.1	24.0
69.9	21.9	68.6	22.4	67.4	22.8	66.3	23.2	65.1	23.6	64.1	24.0
69.8	21.9	68.5	22.4	67.4	22.8	66.2	23.2	65.1	23.6	64.0	24.0
69.8	22.0	68.5	22.4	67.3	22.8	66.2	23.2	65.1	23.6	64.0	24.1
69.7	22.0	68.5	22.4	67.3	22.8	66.1	23.2	65.0	23.6	64.0	24.1
69.7	22.0	68.4	22.4	67.3	22.8	66.1	23.2	65.0	23.7	64.0	24.1
69.7	22.0	68.4	22.4	67.2	22.8	66.1	23.2	65.0	23.7	63.9	24.1
69.6	22.0	68.4	22.4	67.2	22.8	66.1	23.3	65.0	23.7	63.9	24.1
69.6	22.0	68.4	22.4	67.2	22.8	66.0	23.3	64.9	23.7	63.9	24.1
69.6	22.0	68.3	22.4	67.1	22.9	66.0	23.3	64.9	23.7	63.8	24.1
69.6	22.0	68.3	22.4	67.1	22.9	66.0	23.3	64.9	23.7	63.8	24.1
69.5	22.0	68.3	22.5	67.1	22.9	65.9	23.3	64.9	23.7	63.8	24.1
69.5	22.0	68.2	22.5	67.0	22.9	65.9	23.3	64.8	23.7	63.8	24.1
69.5	22.1	68.3	22.5	67.1	22.9	65.9	23.3	64.8	23.7	63.8	24.2
69.4	22.1	68.2	22.5	67.0	22.9	65.9	23.3	64.8	23.7	63.8	24.2
69.4	22.1	68.1	22.5	67.0	22.9	65.9	23.3	64.8	23.8	63.7	24.2
69.4	22.1	68.1	22.5	67.0	22.9	65.8	23.3	64.8	23.8	63.7	24.2
69.3	22.1	68.1	22.5	67.0	22.9	65.8	23.4	64.8	23.8	63.7	24.2
69.3	22.1	68.1	22.5	66.9	22.9	65.8	23.4	64.7	23.8	63.6	24.2
69.3	22.1	68.1	22.5	66.9	23.0	65.8	23.4	64.7	23.8	63.6	24.2
69.2	22.1	68.0	22.5	66.8	23.0	65.7	23.4	64.7	23.8	63.6	24.2
69.2	22.1	68.0	22.6	66.8	23.0	65.7	23.4	64.6	23.8	63.6	24.2
69.2	22.1	68.0	22.6	66.8	23.0	65.7	23.4	64.6	23.8	63.5	24.2
69.1	22.2	67.9	22.6	66.8	23.0	65.7	23.4	64.6	23.8	63.5	24.3
69.1	22.2	67.9	22.6	66.7	23.0	65.6	23.4	64.5	23.8	63.5	24.3
69.1	22.2	67.9	22.6	66.7	23.0	65.6	23.4	64.5	23.9	63.5	24.3
69.1	22.2	67.9	22.6	66.7	23.0	65.6	23.4	64.5	23.9	63.5	24.3
69.0	22.2	67.8	22.6	66.6	23.0	65.5	23.5	64.5	23.9	63.5	24.3
69.0	22.2	67.8	22.6	66.7	23.0	65.5	23.5	64.4	23.9	63.4	24.3
68.9	22.2	67.8	22.6	66.6	23.1	65.5	23.5	64.4	23.9	63.4	24.3
68.9	22.2	67.7	22.6	66.5	23.1	65.5	23.5	64.4	23.9	63.4	24.3
68.9	22.2	67.7	22.7	66.6	23.1	65.5	23.5	64.3	23.9	63.3	24.3
68.9	22.2	67.7	22.7	66.5	23.1	65.4	23.5	64.4	23.9	63.3	24.3
68.8	22.3	67.6	22.7	66.5	23.1	65.4	23.5	64.3	23.9	63.3	24.4
68.8	22.3	67.7	22.7	66.5	23.1	65.4	23.5	64.3	23.9	63.2	24.4
68.8	22.3	67.6	22.7	66.5	23.1	65.4	23.5	64.3	24.0	63.2	24.4
68.7	22.3	67.6	22.7	66.4	23.1	65.3	23.5	64.3	24.0	63.2	24.4
68.8	22.3	67.6	22.7	66.4	23.1	65.3	23.6	64.2	24.0	63.2	24.4
68.7	22.3	67.5	22.7	66.4	23.1	65.3	23.6	64.2	24.0	63.2	24.4
68.7	22.3	67.5	22.7	66.4	23.2	65.2	23.6	64.2	24.0	63.1	24.4
68.6	22.3	67.5	22.7	66.3	23.2	65.2	23.6	64.1	24.0	63.1	24.4

63.1	24.4	62.1	24.9	61.1	25.3	60.2	25.7	59.3	26.1	58.4	26.5
63.1	24.4	62.1	24.9	61.1	25.3	60.2	25.7	59.3	26.1	58.4	26.5
63.0	24.5	62.0	24.9	61.1	25.3	60.1	25.7	59.3	26.1	58.4	26.6
63.0	24.5	62.0	24.9	61.1	25.3	60.1	25.7	59.2	26.1	58.4	26.6
63.0	24.5	62.0	24.9	61.0	25.3	60.1	25.7	59.2	26.2	58.4	26.6
63.0	24.5	62.0	24.9	61.0	25.3	60.1	25.7	59.2	26.2	58.4	26.6
62.9	24.5	61.9	24.9	61.0	25.3	60.0	25.8	59.2	26.2	58.3	26.6
62.9	24.5	61.9	24.9	61.0	25.3	60.0	25.8	59.1	26.2	58.3	26.6
62.9	24.5	61.9	24.9	60.9	25.4	60.0	25.8	59.1	26.2	58.2	26.6
62.9	24.5	61.9	24.9	60.9	25.4	60.0	25.8	59.1	26.2	58.2	26.6
62.9	24.5	61.9	25.0	60.9	25.4	60.0	25.8	59.1	26.2	58.2	26.6
62.8	24.5	61.8	25.0	60.8	25.4	59.9	25.8	59.1	26.2	58.2	26.6
62.8	24.6	61.8	25.0	60.8	25.4	59.9	25.8	59.0	26.2	58.2	26.7
62.8	24.6	61.8	25.0	60.8	25.4	59.9	25.8	59.0	26.2	58.2	26.7
62.8	24.6	61.7	25.0	60.8	25.4	59.9	25.8	59.0	26.3	58.1	26.7
62.8	24.6	61.8	25.0	60.8	25.4	59.8	25.8	58.9	26.3	58.1	26.7
62.7	24.6	61.7	25.0	60.8	25.4	59.8	25.9	59.0	26.3	58.1	26.7
62.7	24.6	61.7	25.0	60.7	25.4	59.8	25.9	59.0	26.3	58.1	26.7
62.7	24.6	61.7	25.0	60.7	25.5	59.8	25.9	58.9	26.3	58.0	26.7
62.6	24.6	61.6	25.0	60.7	25.5	59.8	25.9	58.9	26.3	58.0	26.7
62.6	24.6	61.6	25.1	60.7	25.5	59.8	25.9	58.9	26.3	58.0	26.7
62.6	24.6	61.6	25.1	60.6	25.5	59.7	25.9	58.8	26.3	58.0	26.7
62.6	24.7	61.6	25.1	60.6	25.5	59.7	25.9	58.8	26.3	58.0	26.8
62.5	24.7	61.5	25.1	60.6	25.5	59.7	25.9	58.8	26.3	58.0	26.8
62.5	24.7	61.5	25.1	60.6	25.5	59.6	25.9	58.8	26.4	57.9	26.8
62.5	24.7	61.5	25.1	60.6	25.5	59.7	25.9	58.8	26.4	57.9	26.8
62.4	24.7	61.5	25.1	60.5	25.5	59.6	26.0	58.8	26.4	57.9	26.8
62.5	24.7	61.4	25.1	60.5	25.5	59.6	26.0	58.7	26.4	57.9	26.8
62.4	24.7	61.4	25.1	60.5	25.6	59.6	26.0	58.7	26.4	57.9	26.8
62.4	24.7	61.4	25.1	60.5	25.6	59.6	26.0	58.7	26.4	57.8	26.8
62.4	24.7	61.4	25.2	60.4	25.6	59.5	26.0	58.7	26.4	57.8	26.8
62.3	24.7	61.4	25.2	60.4	25.6	59.5	26.0	58.6	26.4	57.8	26.8
62.3	24.8	61.4	25.2	60.4	25.6	59.5	26.0	58.7	26.4	57.8	26.9
62.3	24.8	61.3	25.2	60.4	25.6	59.4	26.0	58.6	26.4	57.8	26.9
62.3	24.8	61.3	25.2	60.3	25.6	59.5	26.0	58.6	26.5	57.8	26.9
62.3	24.8	61.3	25.2	60.4	25.6	59.4	26.0	58.6	26.5	57.7	26.9
62.2	24.8	61.2	25.2	60.3	25.6	59.4	26.1	58.5	26.5	57.7	26.9
62.2	24.8	61.2	25.2	60.3	25.6	59.4	26.1	58.5	26.5	57.7	26.9
62.2	24.8	61.2	25.2	60.3	25.7	59.4	26.1	58.5	26.5	57.7	26.9
62.1	24.8	61.2	25.2	60.2	25.7	59.3	26.1	58.5	26.5	57.7	26.9
62.2	24.8	61.2	25.3	60.2	25.7	59.3	26.1	58.5	26.5	57.6	26.9
62.1	24.8	61.1	25.3	60.2	25.7	59.4	26.1	58.5	26.5	57.6	26.9

57.6	27.0	56.8	27.4	56.1	27.8	55.3	28.2	54.7	28.6	53.9	29.1
57.6	27.0	56.8	27.4	56.1	27.8	55.3	28.2	54.6	28.6	53.9	29.1
57.5	27.0	56.8	27.4	56.0	27.8	55.3	28.2	54.6	28.7	53.9	29.1
57.5	27.0	56.8	27.4	56.0	27.8	55.3	28.2	54.6	28.7	53.9	29.1
57.5	27.0	56.7	27.4	56.0	27.8	55.2	28.3	54.6	28.7	53.9	29.1
57.5	27.0	56.7	27.4	55.9	27.8	55.2	28.3	54.6	28.7	53.9	29.1
57.4	27.0	56.7	27.4	56.0	27.9	55.2	28.3	54.5	28.7	53.9	29.1
57.4	27.0	56.7	27.4	56.0	27.9	55.2	28.3	54.5	28.7	53.9	29.1
57.4	27.0	56.7	27.5	55.9	27.9	55.2	28.3	54.5	28.7	53.9	29.1
57.4	27.0	56.6	27.5	55.9	27.9	55.2	28.3	54.5	28.7	53.8	29.1
57.4	27.1	56.6	27.5	55.9	27.9	55.2	28.3	54.5	28.7	53.8	29.2
57.4	27.1	56.6	27.5	55.9	27.9	55.1	28.3	54.5	28.7	53.8	29.2
57.3	27.1	56.6	27.5	55.8	27.9	55.1	28.3	54.4	28.8	53.8	29.2
57.3	27.1	56.6	27.5	55.8	27.9	55.1	28.3	54.4	28.8	53.8	29.2
57.3	27.1	56.5	27.5	55.8	27.9	55.1	28.4	54.4	28.8	53.7	29.2
57.3	27.1	56.5	27.5	55.8	27.9	55.1	28.4	54.4	28.8	53.7	29.2
57.3	27.1	56.5	27.5	55.8	28.0	55.1	28.4	54.4	28.8	53.7	29.2
57.3	27.1	56.5	27.5	55.7	28.0	55.0	28.4	54.4	28.8	53.7	29.2
57.2	27.1	56.5	27.6	55.7	28.0	55.0	28.4	54.3	28.8	53.7	29.2
57.2	27.1	56.4	27.6	55.7	28.0	55.0	28.4	54.3	28.8	53.6	29.2
57.2	27.2	56.4	27.6	55.7	28.0	55.0	28.4	54.3	28.8	53.7	29.3
57.2	27.2	56.4	27.6	55.7	28.0	55.0	28.4	54.3	28.8	53.6	29.3
57.1	27.2	56.4	27.6	55.7	28.0	55.0	28.4	54.3	28.9	53.6	29.3
57.1	27.2	56.4	27.6	55.6	28.0	54.9	28.4	54.3	28.9	53.6	29.3
57.1	27.2	56.4	27.6	55.7	28.0	54.9	28.5	54.3	28.9	53.6	29.3
57.1	27.2	56.3	27.6	55.6	28.0	54.9	28.5	54.2	28.9	53.6	29.3
57.1	27.2	56.3	27.6	55.6	28.1	54.9	28.5	54.2	28.9	53.6	29.3
57.1	27.2	56.3	27.6	55.6	28.1	54.9	28.5	54.2	28.9	53.5	29.3
57.0	27.2	56.3	27.7	55.5	28.1	54.8	28.5	54.2	28.9	53.5	29.3
57.0	27.2	56.2	27.7	55.6	28.1	54.9	28.5	54.2	28.9	53.5	29.3
57.0	27.3	56.3	27.7	55.5	28.1	54.8	28.5	54.2	28.9	53.4	29.4
57.0	27.3	56.2	27.7	55.5	28.1	54.8	28.5	54.1	28.9	53.5	29.4
57.0	27.3	56.2	27.7	55.5	28.1	54.8	28.5	54.1	29.0	53.4	29.4
56.9	27.3	56.2	27.7	55.4	28.1	54.8	28.5	54.1	29.0	53.5	29.4
56.9	27.3	56.2	27.7	55.4	28.1	54.8	28.6	54.1	29.0	53.4	29.4
56.9	27.3	56.1	27.7	55.4	28.1	54.8	28.6	54.1	29.0	53.4	29.4
56.9	27.3	56.1	27.7	55.4	28.2	54.7	28.6	54.1	29.0	53.3	29.4
56.9	27.3	56.1	27.7	55.4	28.2	54.8	28.6	54.1	29.0	53.3	29.4
56.9	27.3	56.1	27.8	55.4	28.2	54.7	28.6	54.0	29.0	53.3	29.4
56.9	27.3	56.1	27.8	55.4	28.2	54.7	28.6	54.0	29.0	53.3	29.4
56.8	27.4	56.1	27.8	55.4	28.2	54.7	28.6	54.0	29.0	53.3	29.5
56.8	27.4	56.1	27.8	55.3	28.2	54.6	28.6	54.0	29.0	53.3	29.5

53.2	29.5	52.8	29.7	52.4	30.0
53.3	29.5	52.8	29.8		
53.3	29.5	52.8	29.8		
53.2	29.5	52.8	29.8		
53.2	29.5	52.8	29.8		
53.2	29.5	52.8	29.8		
53.2	29.5	52.8	29.8		
53.2	29.5	52.7	29.8		
53.1	29.6	52.7	29.8		
53.1	29.6	52.7	29.8		
53.1	29.6	52.7	29.8		
53.1	29.6	52.7	29.9		
53.1	29.6	52.7	29.9		
53.1	29.6	52.6	29.9		
53.0	29.6	52.6	29.9		
53.0	29.6	52.6	29.9		
53.0	29.6	52.6	29.9		
53.0	29.6	52.6	29.9		
53.0	29.7	52.6	29.9		
53.0	29.7	52.6	29.9		
53.0	29.7	52.5	29.9		
52.9	29.7	52.5	30.0		
52.9	29.7	52.5	30.0		
52.9	29.7	52.5	30.0		
52.9	29.7	52.5	30.0		
52.9	29.7	52.5	30.0		
52.9	29.7	52.4	30.0		

259

Sample Control-Y

N	mm	0.0	0.3	0.0	0.7	0.1	1.1	11.5	1.5	46.3	1.8
0.0	0.0	0.0	0.3	0.0	0.7	0.1	1.1	12.0	1.5	47.4	1.9
0.0	0.0	-0.1	0.3	0.0	0.7	0.1	1.1	12.8	1.5	48.4	1.9
0.0	0.0	0.0	0.4	0.0	0.7	0.1	1.1	13.6	1.5	49.5	1.9
0.0	0.0	0.0	0.4	0.0	0.7	0.2	1.1	14.2	1.5	50.6	1.9
0.0	0.0	0.0	0.4	0.0	0.8	0.2	1.1	15.0	1.5	51.5	1.9
0.0	0.0	0.0	0.4	0.0	0.8	0.3	1.1	15.7	1.5	52.6	1.9
0.0	0.0	0.0	0.4	0.0	0.8	0.4	1.2	16.4	1.5	53.7	1.9
0.0	0.0	0.0	0.4	0.0	0.8	0.5	1.2	17.2	1.5	54.8	1.9
0.0	0.0	0.0	0.4	0.0	0.8	0.7	1.2	17.9	1.6	55.8	1.9
0.0	0.0	0.0	0.4	0.0	0.8	0.9	1.2	18.8	1.6	56.8	1.9
0.0	0.1	0.0	0.4	0.0	0.8	1.1	1.2	19.5	1.6	57.9	2.0
0.0	0.1	0.0	0.4	0.0	0.8	1.2	1.2	20.4	1.6	58.8	2.0
0.0	0.1	0.0	0.5	0.0	0.8	1.4	1.2	21.4	1.6	60.0	2.0
0.0	0.1	0.0	0.5	0.0	0.9	1.6	1.2	22.1	1.6	61.1	2.0
0.0	0.1	0.0	0.5	0.0	0.9	1.8	1.2	23.1	1.6	61.9	2.0
0.0	0.1	0.0	0.5	0.0	0.9	2.0	1.2	24.0	1.6	63.0	2.0
0.0	0.1	0.0	0.5	0.0	0.9	2.3	1.3	24.9	1.6	64.0	2.0
0.0	0.1	0.0	0.5	0.0	0.9	2.6	1.3	25.8	1.6	64.9	2.0
0.0	0.1	0.0	0.5	0.0	0.9	2.8	1.3	26.8	1.7	65.9	2.0
0.0	0.1	0.0	0.5	0.0	0.9	3.1	1.3	27.8	1.7	66.8	2.0
0.0	0.2	0.0	0.5	0.0	0.9	3.4	1.3	28.7	1.7	67.9	2.1
0.0	0.2	-0.1	0.5	0.0	0.9	3.7	1.3	29.6	1.7	68.8	2.1
0.0	0.2	0.0	0.6	0.0	0.9	4.1	1.3	30.8	1.7	69.8	2.1
0.0	0.2	0.0	0.6	0.0	0.9	4.4	1.3	31.6	1.7	70.9	2.1
0.0	0.2	0.0	0.6	0.0	1.0	4.8	1.3	32.7	1.7	71.6	2.1
0.0	0.2	0.0	0.6	-0.1	1.0	5.1	1.3	33.8	1.7	72.8	2.1
0.0	0.2	0.0	0.6	0.0	1.0	5.6	1.4	34.6	1.7	73.7	2.1
0.0	0.2	0.0	0.6	0.0	1.0	6.0	1.4	35.8	1.7	74.5	2.1
0.0	0.2	0.0	0.6	0.0	1.0	6.4	1.4	36.8	1.8	75.5	2.1
0.0	0.2	0.0	0.6	0.0	1.0	6.9	1.4	37.7	1.8	76.5	2.1
0.0	0.3	0.0	0.6	0.0	1.0	7.3	1.4	38.8	1.8	77.3	2.2
0.0	0.3	0.0	0.6	0.0	1.0	7.8	1.4	39.9	1.8	78.2	2.2
0.0	0.3	0.0	0.7	0.0	1.0	8.3	1.4	41.0	1.8	79.1	2.2
0.0	0.3	0.0	0.7	0.0	1.0	8.9	1.4	42.0	1.8	80.1	2.2
0.0	0.3	0.0	0.7	0.0	1.1	9.5	1.4	43.1	1.8	80.8	2.2
0.0	0.3	0.0	0.7	0.0	1.1	10.1	1.4	44.3	1.8	81.8	2.2
0.0	0.3	0.0	0.7	0.0	1.1	10.8	1.5	45.2	1.8	82.8	2.2

83.4	2.2	114.4	2.6	136.9	3.1	151.7	3.5	161.0	3.9	167.1	4.3
84.4	2.2	115.1	2.7	137.3	3.1	151.8	3.5	161.0	3.9	167.1	4.3
85.4	2.2	115.8	2.7	137.7	3.1	152.2	3.5	161.3	3.9	167.2	4.3
86.0	2.3	116.3	2.7	138.2	3.1	152.6	3.5	161.5	3.9	167.3	4.4
86.9	2.3	116.9	2.7	138.5	3.1	152.6	3.5	161.5	3.9	167.6	4.4
87.8	2.3	117.5	2.7	139.0	3.1	153.0	3.5	161.7	4.0	167.6	4.4
88.6	2.3	118.2	2.7	139.5	3.1	153.3	3.5	161.9	4.0	167.7	4.4
89.4	2.3	118.7	2.7	139.8	3.1	153.4	3.6	162.1	4.0	167.9	4.4
90.2	2.3	119.3	2.7	140.3	3.1	153.7	3.6	162.3	4.0	167.9	4.4
91.1	2.3	120.0	2.7	140.8	3.2	154.0	3.6	162.4	4.0	168.0	4.4
91.8	2.3	120.4	2.7	141.0	3.2	154.2	3.6	162.7	4.0	168.3	4.4
92.6	2.3	121.1	2.8	141.5	3.2	154.4	3.6	162.7	4.0	168.3	4.4
93.5	2.4	121.7	2.8	141.9	3.2	154.6	3.6	162.9	4.0	168.4	4.4
94.1	2.4	122.1	2.8	142.3	3.2	155.0	3.6	163.1	4.0	168.6	4.5
95.0	2.4	122.8	2.8	142.6	3.2	155.1	3.6	163.1	4.0	168.5	4.5
95.9	2.4	123.4	2.8	143.0	3.2	155.4	3.6	163.4	4.1	168.7	4.5
96.4	2.4	123.9	2.8	143.4	3.2	155.7	3.6	163.6	4.1	168.8	4.5
97.3	2.4	124.4	2.8	143.7	3.2	155.8	3.7	163.6	4.1	168.9	4.5
98.1	2.4	124.9	2.8	144.1	3.2	156.1	3.7	163.8	4.1	169.0	4.5
98.8	2.4	125.6	2.8	144.5	3.3	156.4	3.7	163.9	4.1	169.1	4.5
99.5	2.4	126.0	2.8	144.7	3.3	156.5	3.7	164.1	4.1	169.2	4.5
100.2	2.4	126.6	2.9	145.2	3.3	156.7	3.7	164.2	4.1	169.3	4.5
101.1	2.4	127.3	2.9	145.6	3.3	157.0	3.7	164.3	4.1	169.5	4.5
101.7	2.5	127.6	2.9	145.8	3.3	157.2	3.7	164.6	4.1	169.6	4.6
102.5	2.5	128.2	2.9	146.2	3.3	157.4	3.7	164.6	4.1	169.6	4.6
103.3	2.5	128.8	2.9	146.5	3.3	157.5	3.7	164.8	4.2	169.8	4.6
103.8	2.5	129.2	2.9	146.8	3.3	157.9	3.8	165.0	4.2	169.9	4.6
104.6	2.5	129.7	2.9	147.1	3.3	157.9	3.8	165.0	4.2	169.9	4.6
105.3	2.5	130.3	2.9	147.5	3.3	158.2	3.8	165.3	4.2	170.0	4.6
105.8	2.5	130.7	2.9	147.8	3.4	158.5	3.8	165.4	4.2	170.1	4.6
106.6	2.5	131.2	2.9	148.1	3.4	158.6	3.8	165.4	4.2	170.2	4.6
107.4	2.5	131.7	3.0	148.4	3.4	158.9	3.8	165.6	4.2	170.2	4.6
108.0	2.5	132.3	3.0	148.8	3.4	159.1	3.8	165.8	4.2	170.4	4.6
108.6	2.6	132.6	3.0	149.0	3.4	159.2	3.8	165.9	4.2	170.5	4.7
109.2	2.6	133.2	3.0	149.4	3.4	159.4	3.8	166.0	4.2	170.5	4.7
110.0	2.6	133.7	3.0	149.8	3.4	159.6	3.8	166.1	4.3	170.7	4.7
110.6	2.6	134.1	3.0	149.9	3.4	159.8	3.8	166.4	4.3	170.8	4.7
111.3	2.6	134.6	3.0	150.2	3.4	160.0	3.9	166.4	4.3	170.8	4.7
112.0	2.6	135.2	3.0	150.5	3.4	160.1	3.9	166.6	4.3	170.9	4.7
112.5	2.6	135.5	3.0	150.8	3.5	160.4	3.9	166.7	4.3	171.1	4.7
113.3	2.6	136.0	3.0	151.0	3.5	160.5	3.9	166.7	4.3	171.1	4.7
113.9	2.6	136.4	3.1	151.3	3.5	160.8	3.9	166.9	4.3	171.2	4.7

171.2	4.7	174.2	5.2	176.3	5.6	177.7	6.0	178.7	6.4	179.3	6.8
171.4	4.8	174.3	5.2	176.4	5.6	177.8	6.0	178.7	6.4	179.4	6.9
171.4	4.8	174.3	5.2	176.3	5.6	177.8	6.0	178.8	6.4	179.4	6.9
171.5	4.8	174.4	5.2	176.4	5.6	177.8	6.0	178.7	6.5	179.3	6.9
171.6	4.8	174.5	5.2	176.5	5.6	177.8	6.0	178.8	6.5	179.4	6.9
171.6	4.8	174.5	5.2	176.5	5.6	177.9	6.1	178.9	6.5	179.4	6.9
171.8	4.8	174.6	5.2	176.5	5.6	177.9	6.1	178.8	6.5	179.4	6.9
171.9	4.8	174.6	5.2	176.5	5.7	178.0	6.1	178.9	6.5	179.4	6.9
171.9	4.8	174.7	5.2	176.7	5.7	178.0	6.1	179.0	6.5	179.5	6.9
172.0	4.8	174.7	5.3	176.6	5.7	178.0	6.1	178.8	6.5	179.5	6.9
172.1	4.8	174.8	5.3	176.7	5.7	178.1	6.1	178.9	6.5	179.4	6.9
172.1	4.9	174.9	5.3	176.8	5.7	178.1	6.1	178.9	6.5	179.4	7.0
172.2	4.9	174.8	5.3	176.7	5.7	178.1	6.1	178.9	6.5	179.5	7.0
172.3	4.9	174.9	5.3	176.9	5.7	178.1	6.1	178.9	6.6	179.4	7.0
172.4	4.9	175.1	5.3	176.9	5.7	178.2	6.1	178.9	6.6	179.5	7.0
172.4	4.9	175.0	5.3	176.9	5.7	178.1	6.2	179.0	6.6	179.6	7.0
172.5	4.9	175.1	5.3	176.9	5.7	178.1	6.2	178.9	6.6	179.4	7.0
172.6	4.9	175.2	5.3	177.0	5.8	178.1	6.2	179.0	6.6	179.5	7.0
172.6	4.9	175.1	5.3	177.0	5.8	178.3	6.2	179.1	6.6	179.6	7.0
172.7	4.9	175.3	5.4	177.0	5.8	178.2	6.2	179.0	6.6	179.5	7.0
172.9	5.0	175.4	5.4	177.0	5.8	178.3	6.2	179.0	6.6	179.5	7.0
172.8	5.0	175.3	5.4	177.2	5.8	178.3	6.2	179.1	6.6	179.5	7.1
173.0	5.0	175.4	5.4	177.1	5.8	178.3	6.2	179.0	6.6	179.6	7.1
173.0	5.0	175.4	5.4	177.2	5.8	178.4	6.2	179.1	6.7	179.5	7.1
173.1	5.0	175.5	5.4	177.3	5.8	178.5	6.3	179.1	6.7	179.6	7.1
173.1	5.0	175.6	5.4	177.2	5.8	178.3	6.3	179.1	6.7	179.6	7.1
173.2	5.0	175.6	5.4	177.3	5.8	178.4	6.3	179.1	6.7	179.6	7.1
173.3	5.0	175.7	5.4	177.4	5.9	178.4	6.3	179.1	6.7	179.6	7.1
173.3	5.0	175.6	5.4	177.3	5.9	178.5	6.3	179.2	6.7	179.7	7.1
173.4	5.0	175.8	5.5	177.4	5.9	178.5	6.3	179.2	6.7	179.5	7.1
173.5	5.0	175.9	5.5	177.4	5.9	178.5	6.3	179.2	6.7	179.7	7.1
173.5	5.1	175.8	5.5	177.4	5.9	178.5	6.3	179.2	6.7	179.7	7.2
173.6	5.1	175.9	5.5	177.4	5.9	178.5	6.3	179.2	6.7	179.6	7.2
173.8	5.1	176.0	5.5	177.4	5.9	178.6	6.3	179.3	6.8	179.6	7.2
173.7	5.1	176.0	5.5	177.6	5.9	178.7	6.3	179.3	6.8	179.7	7.2
173.8	5.1	176.0	5.5	177.6	5.9	178.5	6.4	179.2	6.8	179.6	7.2
173.9	5.1	176.0	5.5	177.6	5.9	178.6	6.4	179.3	6.8	179.7	7.2
173.9	5.1	176.1	5.5	177.7	6.0	178.7	6.4	179.3	6.8	179.7	7.2
174.0	5.1	176.1	5.5	177.6	6.0	178.6	6.4	179.3	6.8	179.7	7.2
174.0	5.1	176.2	5.6	177.7	6.0	178.7	6.4	179.3	6.8	179.6	7.2
174.1	5.1	176.3	5.6	177.8	6.0	178.7	6.4	179.4	6.8	179.7	7.2
174.2	5.2	176.2	5.6	177.7	6.0	178.8	6.4	179.3	6.8	179.8	7.3

179.6	7.3	179.9	7.7	179.9	8.1	179.9	8.5	179.6	8.9	179.1	9.4
179.7	7.3	179.9	7.7	179.9	8.1	179.7	8.5	179.4	9.0	179.1	9.4
179.7	7.3	179.9	7.7	179.9	8.1	179.8	8.5	179.5	9.0	179.0	9.4
179.7	7.3	179.9	7.7	179.9	8.1	179.8	8.6	179.5	9.0	178.9	9.4
179.7	7.3	179.9	7.7	179.9	8.1	179.7	8.6	179.5	9.0	179.1	9.4
179.8	7.3	179.9	7.7	179.9	8.2	179.8	8.6	179.5	9.0	179.0	9.4
179.7	7.3	180.0	7.7	179.9	8.2	179.8	8.6	179.4	9.0	179.0	9.4
179.8	7.3	179.9	7.8	179.9	8.2	179.7	8.6	179.5	9.0	179.0	9.4
179.7	7.3	179.9	7.8	179.9	8.2	179.8	8.6	179.4	9.0	178.9	9.4
179.8	7.4	180.0	7.8	179.9	8.2	179.7	8.6	179.4	9.0	179.0	9.5
179.7	7.4	179.9	7.8	179.9	8.2	179.7	8.6	179.5	9.1	179.0	9.5
179.8	7.4	179.9	7.8	179.8	8.2	179.7	8.6	179.3	9.1	178.9	9.5
179.8	7.4	180.0	7.8	179.9	8.2	179.7	8.6	179.5	9.1	178.9	9.5
179.7	7.4	179.9	7.8	179.9	8.2	179.8	8.7	179.4	9.1	178.9	9.5
179.8	7.4	179.9	7.8	179.8	8.2	179.7	8.7	179.3	9.1	178.9	9.5
179.8	7.4	179.9	7.8	179.9	8.3	179.7	8.7	179.3	9.1	178.9	9.5
179.7	7.4	179.9	7.8	180.0	8.3	179.7	8.7	179.4	9.1	178.9	9.5
179.8	7.4	179.9	7.9	179.8	8.3	179.6	8.7	179.3	9.1	178.9	9.5
179.8	7.4	179.9	7.9	179.9	8.3	179.7	8.7	179.3	9.1	178.8	9.5
179.8	7.5	179.9	7.9	180.0	8.3	179.7	8.7	179.3	9.1	178.8	9.6
179.8	7.5	179.8	7.9	179.8	8.3	179.6	8.7	179.3	9.1	178.9	9.6
179.8	7.5	179.9	7.9	179.9	8.3	179.6	8.7	179.3	9.2	178.8	9.6
179.8	7.5	179.9	7.9	179.9	8.3	179.6	8.7	179.3	9.2	178.8	9.6
179.8	7.5	179.8	7.9	179.8	8.3	179.7	8.8	179.4	9.2	178.9	9.6
179.9	7.5	179.9	7.9	179.8	8.3	179.6	8.8	179.3	9.2	178.7	9.6
179.9	7.5	180.0	7.9	179.9	8.4	179.6	8.8	179.3	9.2	178.7	9.6
179.8	7.5	179.9	7.9	179.9	8.4	179.7	8.8	179.3	9.2	178.8	9.6
179.8	7.5	179.9	8.0	179.8	8.4	179.6	8.8	179.2	9.2	178.8	9.6
179.9	7.5	179.8	8.0	179.8	8.4	179.6	8.8	179.2	9.2	178.7	9.6
179.8	7.6	179.9	8.0	179.9	8.4	179.6	8.8	179.2	9.2	178.7	9.7
179.8	7.6	179.9	8.0	179.8	8.4	179.6	8.8	179.2	9.2	178.7	9.7
179.8	7.6	179.9	8.0	179.8	8.4	179.6	8.8	179.2	9.3	178.6	9.7
179.9	7.6	179.9	8.0	180.0	8.4	179.6	8.8	179.1	9.3	178.7	9.7
179.8	7.6	179.9	8.0	179.8	8.4	179.6	8.9	179.2	9.3	178.7	9.7
179.8	7.6	179.9	8.0	179.8	8.4	179.5	8.9	179.1	9.3	178.6	9.7
179.9	7.6	180.0	8.0	179.8	8.5	179.5	8.9	179.2	9.3	178.7	9.7
179.8	7.6	179.9	8.0	179.8	8.5	179.6	8.9	179.2	9.3	178.7	9.7
179.9	7.6	179.9	8.1	179.8	8.5	179.5	8.9	179.1	9.3	178.5	9.7
180.0	7.7	179.9	8.1	179.8	8.5	179.5	8.9	179.2	9.3	178.6	9.7
179.8	7.7	179.8	8.1	179.8	8.5	179.6	8.9	179.2	9.3	178.6	9.8
179.9	7.7	179.9	8.1	179.8	8.5	179.5	8.9	179.1	9.3	178.6	9.8
179.9	7.7	179.9	8.1	179.8	8.5	179.6	8.9	179.1	9.4	178.5	9.8

178.5	9.8	177.9	10.2	177.2	10.6	176.5	11.0	175.7	11.5	175.0	11.9
178.5	9.8	178.0	10.2	177.2	10.6	176.5	11.1	175.7	11.5	175.0	11.9
178.4	9.8	177.8	10.2	177.2	10.6	176.5	11.1	175.8	11.5	175.0	11.9
178.5	9.8	177.9	10.2	177.2	10.7	176.4	11.1	175.7	11.5	175.0	11.9
178.5	9.8	177.9	10.2	177.1	10.7	176.4	11.1	175.7	11.5	175.0	11.9
178.4	9.8	177.8	10.3	177.1	10.7	176.5	11.1	175.7	11.5	175.0	11.9
178.5	9.8	177.8	10.3	177.1	10.7	176.4	11.1	175.6	11.5	174.9	11.9
178.5	9.9	177.8	10.3	177.0	10.7	176.4	11.1	175.7	11.5	174.9	12.0
178.4	9.9	177.8	10.3	177.1	10.7	176.4	11.1	175.7	11.5	174.9	12.0
178.4	9.9	177.7	10.3	177.0	10.7	176.3	11.1	175.6	11.6	174.9	12.0
178.3	9.9	177.7	10.3	177.0	10.7	176.3	11.1	175.6	11.6	174.9	12.0
178.4	9.9	177.7	10.3	177.1	10.7	176.3	11.2	175.6	11.6	174.8	12.0
178.3	9.9	177.6	10.3	177.0	10.7	176.3	11.2	175.6	11.6	174.9	12.0
178.3	9.9	177.7	10.3	177.0	10.8	176.3	11.2	175.5	11.6	174.8	12.0
178.3	9.9	177.7	10.4	177.0	10.8	176.2	11.2	175.5	11.6	174.8	12.0
178.3	9.9	177.6	10.4	176.9	10.8	176.2	11.2	175.5	11.6	174.8	12.0
178.3	9.9	177.7	10.4	176.9	10.8	176.2	11.2	175.4	11.6	174.7	12.0
178.3	10.0	177.7	10.4	176.9	10.8	176.2	11.2	175.5	11.6	174.7	12.1
178.2	10.0	177.5	10.4	176.9	10.8	176.2	11.2	175.5	11.6	174.7	12.1
178.3	10.0	177.5	10.4	176.9	10.8	176.2	11.2	175.4	11.7	174.7	12.1
178.3	10.0	177.6	10.4	176.8	10.8	176.2	11.2	175.4	11.7	174.6	12.1
178.2	10.0	177.5	10.4	176.9	10.8	176.2	11.3	175.4	11.7	174.7	12.1
178.2	10.0	177.5	10.4	176.8	10.8	176.1	11.3	175.4	11.7	174.7	12.1
178.1	10.0	177.5	10.4	176.9	10.9	176.1	11.3	175.4	11.7	174.6	12.1
178.1	10.0	177.5	10.4	176.9	10.9	176.1	11.3	175.3	11.7	174.6	12.1
178.1	10.0	177.4	10.5	176.7	10.9	176.0	11.3	175.4	11.7	174.7	12.1
178.1	10.0	177.4	10.5	176.8	10.9	176.0	11.3	175.3	11.7	174.5	12.1
178.1	10.1	177.5	10.5	176.8	10.9	176.0	11.3	175.3	11.7	174.6	12.2
178.1	10.1	177.4	10.5	176.7	10.9	176.1	11.3	175.3	11.7	174.6	12.2
178.1	10.1	177.4	10.5	176.7	10.9	176.0	11.3	175.3	11.8	174.5	12.2
178.1	10.1	177.4	10.5	176.7	10.9	176.0	11.3	175.3	11.8	174.5	12.2
178.0	10.1	177.4	10.5	176.7	10.9	176.0	11.4	175.3	11.8	174.5	12.2
178.0	10.1	177.3	10.5	176.6	10.9	175.9	11.4	175.2	11.8	174.5	12.2
178.0	10.1	177.3	10.5	176.6	11.0	176.0	11.4	175.2	11.8	174.4	12.2
177.9	10.1	177.3	10.5	176.7	11.0	176.0	11.4	175.2	11.8	174.5	12.2
178.0	10.1	177.3	10.6	176.6	11.0	175.9	11.4	175.1	11.8	174.4	12.2
178.0	10.1	177.3	10.6	176.6	11.0	175.9	11.4	175.1	11.8	174.4	12.2
178.0	10.2	177.3	10.6	176.6	11.0	175.9	11.4	175.1	11.8	174.4	12.3
177.9	10.2	177.2	10.6	176.5	11.0	175.9	11.4	175.1	11.8	174.4	12.3
177.9	10.2	177.3	10.6	176.5	11.0	175.8	11.4	175.1	11.9	174.3	12.3
177.9	10.2	177.3	10.6	176.6	11.0	175.8	11.4	175.1	11.9	174.4	12.3
177.9	10.2	177.2	10.6	176.5	11.0	175.8	11.5	175.1	11.9	174.4	12.3

174.3	12.3	173.5	12.7	172.7	13.1	171.8	13.6	170.8	14.0	169.8	14.4
174.3	12.3	173.5	12.7	172.7	13.2	171.7	13.6	170.8	14.0	169.8	14.4
174.3	12.3	173.5	12.7	172.6	13.2	171.8	13.6	170.7	14.0	169.7	14.4
174.2	12.3	173.6	12.8	172.7	13.2	171.7	13.6	170.7	14.0	169.7	14.4
174.2	12.3	173.4	12.8	172.5	13.2	171.6	13.6	170.7	14.0	169.8	14.5
174.2	12.4	173.4	12.8	172.6	13.2	171.7	13.6	170.7	14.0	169.6	14.5
174.2	12.4	173.4	12.8	172.6	13.2	171.6	13.6	170.6	14.0	169.6	14.5
174.1	12.4	173.3	12.8	172.5	13.2	171.6	13.6	170.7	14.1	169.7	14.5
174.2	12.4	173.4	12.8	172.5	13.2	171.6	13.6	170.6	14.1	169.5	14.5
174.2	12.4	173.4	12.8	172.5	13.2	171.6	13.7	170.6	14.1	169.6	14.5
174.1	12.4	173.3	12.8	172.5	13.2	171.5	13.7	170.6	14.1	169.6	14.5
174.1	12.4	173.3	12.8	172.4	13.3	171.5	13.7	170.5	14.1	169.5	14.5
174.1	12.4	173.3	12.8	172.4	13.3	171.5	13.7	170.5	14.1	169.5	14.5
174.0	12.4	173.3	12.9	172.4	13.3	171.5	13.7	170.5	14.1	169.5	14.5
174.0	12.4	173.2	12.9	172.4	13.3	171.4	13.7	170.4	14.1	169.4	14.5
174.0	12.5	173.2	12.9	172.3	13.3	171.5	13.7	170.4	14.1	169.4	14.6
174.0	12.5	173.2	12.9	172.4	13.3	171.4	13.7	170.4	14.1	169.4	14.6
174.0	12.5	173.1	12.9	172.3	13.3	171.4	13.7	170.5	14.2	169.5	14.6
173.9	12.5	173.2	12.9	172.3	13.3	171.3	13.7	170.4	14.2	169.3	14.6
173.9	12.5	173.2	12.9	172.3	13.3	171.3	13.8	170.3	14.2	169.3	14.6
173.9	12.5	173.1	12.9	172.2	13.3	171.3	13.8	170.4	14.2	169.3	14.6
173.9	12.5	173.1	12.9	172.2	13.4	171.3	13.8	170.2	14.2	169.2	14.6
173.9	12.5	173.1	12.9	172.2	13.4	171.3	13.8	170.3	14.2	169.2	14.6
173.8	12.5	173.0	13.0	172.2	13.4	171.3	13.8	170.3	14.2	169.3	14.6
173.9	12.5	173.0	13.0	172.1	13.4	171.2	13.8	170.2	14.2	169.2	14.6
173.9	12.6	173.0	13.0	172.1	13.4	171.2	13.8	170.2	14.2	169.1	14.7
173.8	12.6	173.0	13.0	172.1	13.4	171.2	13.8	170.2	14.2	169.1	14.7
173.8	12.6	173.0	13.0	172.1	13.4	171.1	13.8	170.1	14.3	169.1	14.7
173.8	12.6	172.9	13.0	172.1	13.4	171.1	13.8	170.1	14.3	169.0	14.7
173.8	12.6	172.9	13.0	172.1	13.4	171.1	13.9	170.1	14.3	169.1	14.7
173.7	12.6	172.9	13.0	172.0	13.4	171.0	13.9	170.1	14.3	169.1	14.7
173.7	12.6	172.9	13.0	172.0	13.5	171.0	13.9	170.1	14.3	169.0	14.7
173.8	12.6	172.9	13.0	172.0	13.5	171.0	13.9	170.0	14.3	169.0	14.7
173.7	12.6	172.8	13.1	171.9	13.5	171.0	13.9	170.0	14.3	169.0	14.7
173.7	12.6	172.9	13.1	171.9	13.5	170.9	13.9	169.9	14.3	168.9	14.7
173.7	12.7	172.9	13.1	171.9	13.5	171.0	13.9	170.0	14.3	168.9	14.8
173.6	12.7	172.8	13.1	171.9	13.5	171.0	13.9	169.9	14.3	168.9	14.8
173.6	12.7	172.8	13.1	171.9	13.5	170.9	13.9	169.9	14.4	168.8	14.8
173.7	12.7	172.7	13.1	171.8	13.5	170.9	13.9	169.9	14.4	168.8	14.8
173.6	12.7	172.7	13.1	171.8	13.5	170.9	14.0	169.9	14.4	168.8	14.8
173.5	12.7	172.7	13.1	171.8	13.5	170.8	14.0	169.8	14.4	168.8	14.8
173.5	12.7	172.7	13.1	171.8	13.6	170.8	14.0	169.8	14.4	168.7	14.8

168.8	14.8	167.6	15.2	166.7	15.7	165.6	16.1	164.6	16.5	163.7	16.9
168.7	14.8	167.7	15.3	166.6	15.7	165.6	16.1	164.6	16.5	163.7	16.9
168.6	14.8	167.6	15.3	166.6	15.7	165.6	16.1	164.6	16.5	163.7	16.9
168.7	14.9	167.6	15.3	166.6	15.7	165.5	16.1	164.5	16.5	163.6	17.0
168.7	14.9	167.6	15.3	166.6	15.7	165.5	16.1	164.5	16.5	163.6	17.0
168.6	14.9	167.6	15.3	166.6	15.7	165.5	16.1	164.6	16.6	163.6	17.0
168.6	14.9	167.5	15.3	166.5	15.7	165.4	16.1	164.4	16.6	163.5	17.0
168.6	14.9	167.5	15.3	166.5	15.7	165.5	16.2	164.4	16.6	163.5	17.0
168.5	14.9	167.5	15.3	166.5	15.7	165.5	16.2	164.5	16.6	163.5	17.0
168.5	14.9	167.4	15.3	166.4	15.8	165.4	16.2	164.4	16.6	163.5	17.0
168.5	14.9	167.4	15.3	166.4	15.8	165.4	16.2	164.4	16.6	163.5	17.0
168.4	14.9	167.5	15.4	166.4	15.8	165.3	16.2	164.4	16.6	163.5	17.0
168.4	14.9	167.3	15.4	166.4	15.8	165.3	16.2	164.4	16.6	163.5	17.0
168.4	15.0	167.4	15.4	166.3	15.8	165.3	16.2	164.3	16.6	163.4	17.1
168.4	15.0	167.4	15.4	166.3	15.8	165.2	16.2	164.3	16.6	163.4	17.1
168.3	15.0	167.3	15.4	166.3	15.8	165.3	16.2	164.3	16.7	163.4	17.1
168.4	15.0	167.3	15.4	166.2	15.8	165.2	16.2	164.2	16.7	163.3	17.1
168.3	15.0	167.3	15.4	166.2	15.8	165.2	16.3	164.3	16.7	163.3	17.1
168.3	15.0	167.2	15.4	166.2	15.8	165.2	16.3	164.3	16.7	163.3	17.1
168.2	15.0	167.2	15.4	166.2	15.9	165.1	16.3	164.2	16.7	163.3	17.1
168.3	15.0	167.2	15.4	166.2	15.9	165.2	16.3	164.2	16.7	163.3	17.1
168.2	15.0	167.2	15.5	166.2	15.9	165.1	16.3	164.1	16.7	163.3	17.1
168.2	15.0	167.1	15.5	166.1	15.9	165.1	16.3	164.2	16.7	163.3	17.1
168.1	15.1	167.1	15.5	166.1	15.9	165.0	16.3	164.1	16.7	163.2	17.2
168.1	15.1	167.1	15.5	166.1	15.9	165.0	16.3	164.1	16.7	163.2	17.2
168.1	15.1	167.0	15.5	166.0	15.9	165.0	16.3	164.1	16.8	163.3	17.2
168.1	15.1	167.1	15.5	166.0	15.9	165.0	16.3	164.0	16.8	163.1	17.2
168.1	15.1	167.1	15.5	166.0	15.9	164.9	16.4	164.0	16.8	163.2	17.2
168.0	15.1	166.9	15.5	166.0	15.9	165.0	16.4	164.1	16.8	163.1	17.2
168.0	15.1	167.0	15.5	165.9	16.0	164.9	16.4	164.0	16.8	163.0	17.2
168.0	15.1	166.9	15.5	165.9	16.0	164.9	16.4	164.0	16.8	163.0	17.2
167.9	15.1	166.9	15.6	165.9	16.0	164.9	16.4	164.0	16.8	163.1	17.2
167.9	15.1	166.9	15.6	165.8	16.0	164.8	16.4	163.9	16.8	163.0	17.2
167.9	15.2	166.9	15.6	165.9	16.0	164.8	16.4	163.9	16.8	163.0	17.3
167.9	15.2	166.8	15.6	165.9	16.0	164.8	16.4	163.9	16.8	162.9	17.3
167.8	15.2	166.8	15.6	165.7	16.0	164.7	16.4	163.9	16.9	163.0	17.3
167.8	15.2	166.8	15.6	165.8	16.0	164.7	16.4	163.8	16.9	162.9	17.3
167.8	15.2	166.8	15.6	165.8	16.0	164.7	16.5	163.8	16.9	162.9	17.3
167.8	15.2	166.7	15.6	165.7	16.0	164.7	16.5	163.8	16.9	162.9	17.3
167.8	15.2	166.8	15.6	165.7	16.1	164.7	16.5	163.8	16.9	162.8	17.3
167.8	15.2	166.7	15.6	165.7	16.1	164.6	16.5	163.8	16.9	162.8	17.3
167.7	15.2	166.7	15.7	165.6	16.1	164.7	16.5	163.8	16.9	162.8	17.3

162.8	17.3	161.8	17.8	160.8	18.2	159.8	18.6	158.6	19.0	157.5	19.4
162.8	17.4	161.7	17.8	160.7	18.2	159.6	18.6	158.6	19.0	157.5	19.5
162.7	17.4	161.7	17.8	160.7	18.2	159.7	18.6	158.5	19.0	157.4	19.5
162.7	17.4	161.7	17.8	160.7	18.2	159.6	18.6	158.5	19.1	157.4	19.5
162.7	17.4	161.6	17.8	160.7	18.2	159.6	18.6	158.5	19.1	157.4	19.5
162.6	17.4	161.7	17.8	160.6	18.2	159.6	18.7	158.5	19.1	157.4	19.5
162.6	17.4	161.7	17.8	160.6	18.2	159.6	18.7	158.5	19.1	157.4	19.5
162.6	17.4	161.6	17.8	160.6	18.3	159.5	18.7	158.5	19.1	157.3	19.5
162.6	17.4	161.6	17.8	160.6	18.3	159.5	18.7	158.3	19.1	157.3	19.5
162.6	17.4	161.6	17.9	160.5	18.3	159.5	18.7	158.4	19.1	157.3	19.5
162.5	17.4	161.5	17.9	160.6	18.3	159.5	18.7	158.4	19.1	157.2	19.5
162.5	17.5	161.5	17.9	160.5	18.3	159.4	18.7	158.3	19.1	157.2	19.6
162.5	17.5	161.5	17.9	160.4	18.3	159.4	18.7	158.3	19.1	157.2	19.6
162.5	17.5	161.5	17.9	160.4	18.3	159.4	18.7	158.3	19.2	157.1	19.6
162.4	17.5	161.4	17.9	160.4	18.3	159.3	18.7	158.2	19.2	157.2	19.6
162.4	17.5	161.4	17.9	160.4	18.3	159.3	18.8	158.2	19.2	157.1	19.6
162.4	17.5	161.4	17.9	160.4	18.3	159.3	18.8	158.2	19.2	157.1	19.6
162.4	17.5	161.3	17.9	160.3	18.4	159.3	18.8	158.2	19.2	157.1	19.6
162.3	17.5	161.4	17.9	160.3	18.4	159.2	18.8	158.1	19.2	157.0	19.6
162.4	17.5	161.3	18.0	160.3	18.4	159.2	18.8	158.1	19.2	157.0	19.6
162.3	17.5	161.3	18.0	160.3	18.4	159.2	18.8	158.1	19.2	157.0	19.6
162.3	17.6	161.3	18.0	160.2	18.4	159.2	18.8	158.0	19.2	156.9	19.7
162.3	17.6	161.3	18.0	160.2	18.4	159.1	18.8	158.1	19.2	156.9	19.7
162.2	17.6	161.2	18.0	160.2	18.4	159.1	18.8	158.0	19.3	156.9	19.7
162.2	17.6	161.2	18.0	160.1	18.4	159.1	18.8	158.0	19.3	156.8	19.7
162.2	17.6	161.2	18.0	160.1	18.4	159.0	18.9	157.9	19.3	156.9	19.7
162.2	17.6	161.1	18.0	160.1	18.4	159.1	18.9	157.9	19.3	156.8	19.7
162.1	17.6	161.1	18.0	160.0	18.5	159.0	18.9	157.9	19.3	156.8	19.7
162.1	17.6	161.1	18.0	160.1	18.5	159.0	18.9	157.9	19.3	156.7	19.7
162.1	17.6	161.1	18.1	160.1	18.5	158.9	18.9	157.8	19.3	156.8	19.7
162.1	17.6	161.0	18.1	160.0	18.5	158.9	18.9	157.8	19.3	156.7	19.7
162.0	17.7	161.0	18.1	160.0	18.5	158.9	18.9	157.8	19.3	156.6	19.8
162.1	17.7	161.0	18.1	160.0	18.5	158.9	18.9	157.8	19.3	156.7	19.8
162.0	17.7	160.9	18.1	159.9	18.5	158.9	18.9	157.8	19.4	156.6	19.8
162.0	17.7	161.0	18.1	159.9	18.5	158.8	18.9	157.7	19.4	156.6	19.8
162.0	17.7	160.9	18.1	159.9	18.5	158.8	19.0	157.7	19.4	156.6	19.8
161.9	17.7	160.9	18.1	159.9	18.5	158.8	19.0	157.7	19.4	156.5	19.8
161.9	17.7	160.9	18.1	159.8	18.6	158.7	19.0	157.6	19.4	156.5	19.8
161.9	17.7	160.8	18.1	159.8	18.6	158.7	19.0	157.6	19.4	156.4	19.8
161.8	17.7	160.8	18.2	159.8	18.6	158.7	19.0	157.6	19.4	156.4	19.8
161.8	17.7	160.8	18.2	159.7	18.6	158.6	19.0	157.6	19.4	156.5	19.8
161.8	17.8	160.8	18.2	159.8	18.6	158.6	19.0	157.5	19.4	156.4	19.9

156.4	19.9	155.3	20.3	154.1	20.7	153.1	21.1	152.0	21.5	151.0	22.0
156.4	19.9	155.3	20.3	154.1	20.7	153.1	21.1	152.0	21.6	151.0	22.0
156.3	19.9	155.2	20.3	154.1	20.7	153.0	21.1	152.0	21.6	150.9	22.0
156.3	19.9	155.2	20.3	154.1	20.7	153.0	21.2	151.9	21.6	150.9	22.0
156.4	19.9	155.2	20.3	154.1	20.7	153.0	21.2	151.9	21.6	150.9	22.0
156.2	19.9	155.2	20.3	154.1	20.8	152.9	21.2	151.9	21.6	150.9	22.0
156.2	19.9	155.1	20.3	154.0	20.8	152.9	21.2	151.8	21.6	150.9	22.0
156.2	19.9	155.1	20.4	154.0	20.8	152.9	21.2	151.8	21.6	150.8	22.0
156.2	19.9	155.1	20.4	154.0	20.8	152.9	21.2	151.8	21.6	150.8	22.0
156.1	20.0	155.0	20.4	153.9	20.8	152.8	21.2	151.8	21.6	150.8	22.1
156.1	20.0	155.0	20.4	153.9	20.8	152.8	21.2	151.7	21.6	150.8	22.1
156.1	20.0	155.0	20.4	153.9	20.8	152.8	21.2	151.7	21.7	150.7	22.1
156.1	20.0	154.9	20.4	153.9	20.8	152.7	21.2	151.8	21.7	150.8	22.1
156.1	20.0	154.9	20.4	153.8	20.8	152.7	21.3	151.7	21.7	150.7	22.1
156.0	20.0	154.9	20.4	153.8	20.8	152.7	21.3	151.7	21.7	150.7	22.1
155.9	20.0	154.8	20.4	153.8	20.9	152.7	21.3	151.7	21.7	150.7	22.1
155.9	20.0	154.8	20.4	153.7	20.9	152.6	21.3	151.6	21.7	150.7	22.1
156.0	20.0	154.8	20.5	153.7	20.9	152.7	21.3	151.6	21.7	150.6	22.1
155.9	20.0	154.8	20.5	153.7	20.9	152.6	21.3	151.6	21.7	150.6	22.1
155.9	20.1	154.7	20.5	153.6	20.9	152.5	21.3	151.5	21.7	150.6	22.2
155.8	20.1	154.7	20.5	153.7	20.9	152.6	21.3	151.5	21.7	150.5	22.2
155.8	20.1	154.7	20.5	153.7	20.9	152.6	21.3	151.5	21.8	150.6	22.2
155.8	20.1	154.7	20.5	153.5	20.9	152.5	21.3	151.5	21.8	150.6	22.2
155.7	20.1	154.7	20.5	153.6	20.9	152.4	21.4	151.4	21.8	150.4	22.2
155.8	20.1	154.7	20.5	153.6	20.9	152.4	21.4	151.4	21.8	150.5	22.2
155.7	20.1	154.6	20.5	153.5	21.0	152.5	21.4	151.4	21.8	150.5	22.2
155.7	20.1	154.6	20.5	153.5	21.0	152.3	21.4	151.3	21.8	150.4	22.2
155.7	20.1	154.6	20.6	153.4	21.0	152.3	21.4	151.4	21.8	150.4	22.2
155.6	20.1	154.5	20.6	153.4	21.0	152.4	21.4	151.4	21.8	150.4	22.2
155.6	20.2	154.5	20.6	153.4	21.0	152.3	21.4	151.3	21.8	150.4	22.3
155.6	20.2	154.5	20.6	153.4	21.0	152.3	21.4	151.3	21.8	150.3	22.3
155.5	20.2	154.5	20.6	153.4	21.0	152.3	21.4	151.2	21.9	150.3	22.3
155.5	20.2	154.4	20.6	153.3	21.0	152.2	21.4	151.3	21.9	150.3	22.3
155.5	20.2	154.4	20.6	153.3	21.0	152.2	21.5	151.2	21.9	150.3	22.3
155.5	20.2	154.4	20.6	153.3	21.0	152.2	21.5	151.2	21.9	150.3	22.3
155.4	20.2	154.3	20.6	153.2	21.1	152.1	21.5	151.2	21.9	150.3	22.3
155.4	20.2	154.3	20.6	153.2	21.1	152.1	21.5	151.1	21.9	150.2	22.3
155.5	20.2	154.3	20.7	153.2	21.1	152.1	21.5	151.2	21.9	150.2	22.3
155.3	20.2	154.3	20.7	153.2	21.1	152.1	21.5	151.1	21.9	150.2	22.3
155.3	20.3	154.2	20.7	153.1	21.1	152.1	21.5	151.0	21.9	150.1	22.4
155.3	20.3	154.2	20.7	153.1	21.1	152.1	21.5	151.1	21.9	150.2	22.4
155.2	20.3	154.2	20.7	153.1	21.1	152.1	21.5	151.1	22.0	150.1	22.4

150.1	22.4	149.2	22.8	148.3	23.2	147.3	23.6	146.3	24.1	145.3	24.5
150.1	22.4	149.1	22.8	148.2	23.2	147.3	23.7	146.3	24.1	145.4	24.5
150.0	22.4	149.1	22.8	148.2	23.2	147.3	23.7	146.2	24.1	145.3	24.5
150.0	22.4	149.1	22.8	148.2	23.3	147.2	23.7	146.2	24.1	145.3	24.5
150.0	22.4	149.1	22.8	148.1	23.3	147.2	23.7	146.2	24.1	145.3	24.5
150.0	22.4	149.1	22.9	148.1	23.3	147.2	23.7	146.2	24.1	145.2	24.5
150.0	22.4	149.1	22.9	148.1	23.3	147.2	23.7	146.2	24.1	145.2	24.5
149.9	22.5	149.0	22.9	148.1	23.3	147.1	23.7	146.2	24.1	145.2	24.6
149.9	22.5	149.0	22.9	148.0	23.3	147.1	23.7	146.1	24.1	145.2	24.6
149.9	22.5	149.0	22.9	148.0	23.3	147.1	23.7	146.1	24.2	145.1	24.6
149.8	22.5	148.9	22.9	148.1	23.3	147.1	23.8	146.1	24.2	145.1	24.6
149.8	22.5	148.9	22.9	147.9	23.3	147.0	23.8	146.1	24.2	145.1	24.6
149.8	22.5	148.9	22.9	148.0	23.3	147.0	23.8	146.0	24.2	145.0	24.6
149.8	22.5	148.9	22.9	148.0	23.4	147.0	23.8	146.0	24.2	145.0	24.6
149.7	22.5	148.8	22.9	147.9	23.4	147.0	23.8	146.0	24.2	145.0	24.6
149.7	22.5	148.8	23.0	147.9	23.4	146.9	23.8	146.0	24.2	144.9	24.6
149.8	22.5	148.8	23.0	148.0	23.4	146.9	23.8	145.9	24.2	144.9	24.6
149.7	22.6	148.7	23.0	147.9	23.4	146.9	23.8	146.0	24.2	145.0	24.7
149.7	22.6	148.8	23.0	147.8	23.4	146.9	23.8	145.9	24.2	144.9	24.7
149.7	22.6	148.8	23.0	147.8	23.4	146.8	23.8	145.9	24.3	144.9	24.7
149.6	22.6	148.7	23.0	147.8	23.4	146.8	23.8	145.9	24.3	144.9	24.7
149.6	22.6	148.7	23.0	147.8	23.4	146.8	23.9	145.8	24.3	144.9	24.7
149.6	22.6	148.6	23.0	147.7	23.4	146.8	23.9	145.9	24.3	144.8	24.7
149.5	22.6	148.6	23.0	147.7	23.5	146.8	23.9	145.8	24.3	144.8	24.7
149.5	22.6	148.6	23.0	147.6	23.5	146.7	23.9	145.7	24.3	144.8	24.7
149.5	22.6	148.6	23.1	147.7	23.5	146.7	23.9	145.7	24.3	144.7	24.7
149.5	22.6	148.6	23.1	147.7	23.5	146.7	23.9	145.7	24.3	144.7	24.7
149.5	22.7	148.6	23.1	147.6	23.5	146.7	23.9	145.7	24.3	144.8	24.8
149.4	22.7	148.5	23.1	147.6	23.5	146.6	23.9	145.7	24.3	144.7	24.8
149.4	22.7	148.5	23.1	147.7	23.5	146.6	23.9	145.7	24.4	144.7	24.8
149.4	22.7	148.4	23.1	147.5	23.5	146.6	23.9	145.7	24.4	144.7	24.8
149.4	22.7	148.5	23.1	147.6	23.5	146.5	24.0	145.6	24.4	144.6	24.8
149.4	22.7	148.4	23.1	147.5	23.5	146.6	24.0	145.6	24.4	144.6	24.8
149.3	22.7	148.4	23.1	147.5	23.6	146.6	24.0	145.6	24.4	144.6	24.8
149.3	22.7	148.4	23.1	147.5	23.6	146.5	24.0	145.5	24.4	144.5	24.8
149.4	22.7	148.4	23.2	147.5	23.6	146.6	24.0	145.5	24.4	144.5	24.8
149.3	22.7	148.4	23.2	147.5	23.6	146.6	24.0	145.5	24.4	144.5	24.8
149.3	22.8	148.3	23.2	147.4	23.6	146.4	24.0	145.4	24.4	144.5	24.9
149.3	22.8	148.3	23.2	147.4	23.6	146.4	24.0	145.4	24.4	144.4	24.9
149.2	22.8	148.3	23.2	147.4	23.6	146.4	24.0	145.4	24.5	144.4	24.9
149.2	22.8	148.3	23.2	147.3	23.6	146.4	24.0	145.4	24.5	144.4	24.9
149.2	22.8	148.3	23.2	147.4	23.6	146.3	24.1	145.3	24.5	144.3	24.9

144.4	24.9	143.3	25.3	142.4	25.7	141.4	26.2	140.5	26.6	139.7	27.0
144.3	24.9	143.3	25.3	142.3	25.8	141.4	26.2	140.5	26.6	139.7	27.0
144.3	24.9	143.3	25.3	142.3	25.8	141.4	26.2	140.6	26.6	139.7	27.0
144.3	24.9	143.2	25.4	142.3	25.8	141.3	26.2	140.5	26.6	139.7	27.0
144.3	24.9	143.2	25.4	142.2	25.8	141.4	26.2	140.4	26.6	139.7	27.0
144.2	25.0	143.3	25.4	142.3	25.8	141.3	26.2	140.4	26.6	139.6	27.1
144.2	25.0	143.1	25.4	142.2	25.8	141.3	26.2	140.4	26.6	139.6	27.1
144.2	25.0	143.2	25.4	142.2	25.8	141.3	26.2	140.4	26.7	139.6	27.1
144.2	25.0	143.2	25.4	142.2	25.8	141.3	26.2	140.4	26.7	139.6	27.1
144.1	25.0	143.1	25.4	142.1	25.8	141.2	26.3	140.4	26.7	139.6	27.1
144.1	25.0	143.1	25.4	142.2	25.8	141.2	26.3	140.3	26.7	139.5	27.1
144.1	25.0	143.2	25.4	142.1	25.9	141.1	26.3	140.4	26.7	139.5	27.1
144.1	25.0	143.1	25.4	142.1	25.9	141.2	26.3	140.4	26.7	139.5	27.1
144.1	25.0	143.1	25.5	142.0	25.9	141.1	26.3	140.3	26.7	139.5	27.1
144.0	25.0	143.0	25.5	142.0	25.9	141.1	26.3	140.3	26.7	139.5	27.1
144.0	25.1	143.0	25.5	142.0	25.9	141.1	26.3	140.3	26.7	139.4	27.2
143.9	25.1	142.9	25.5	142.0	25.9	141.1	26.3	140.2	26.7	139.4	27.2
144.0	25.1	142.9	25.5	142.0	25.9	141.1	26.3	140.2	26.8	139.4	27.2
143.9	25.1	142.9	25.5	142.0	25.9	141.1	26.3	140.2	26.8	139.4	27.2
143.9	25.1	142.9	25.5	141.9	25.9	141.0	26.4	140.2	26.8	139.4	27.2
143.8	25.1	142.9	25.5	141.9	25.9	141.0	26.4	140.1	26.8	139.4	27.2
143.8	25.1	142.9	25.5	141.9	26.0	141.0	26.4	140.2	26.8	139.3	27.2
143.8	25.1	142.8	25.5	141.8	26.0	140.9	26.4	140.2	26.8	139.3	27.2
143.8	25.1	142.8	25.6	141.9	26.0	140.9	26.4	140.1	26.8	139.3	27.2
143.8	25.1	142.8	25.6	141.9	26.0	140.9	26.4	140.1	26.8	139.3	27.2
143.7	25.2	142.7	25.6	141.8	26.0	141.0	26.4	140.1	26.8	139.3	27.3
143.8	25.2	142.7	25.6	141.7	26.0	140.9	26.4	140.0	26.8	139.2	27.3
143.7	25.2	142.7	25.6	141.8	26.0	140.8	26.4	140.0	26.9	139.2	27.3
143.7	25.2	142.7	25.6	141.8	26.0	140.9	26.4	140.0	26.9	139.2	27.3
143.6	25.2	142.6	25.6	141.7	26.0	140.8	26.5	140.0	26.9	139.2	27.3
143.6	25.2	142.6	25.6	141.7	26.0	140.8	26.5	140.0	26.9	139.1	27.3
143.6	25.2	142.6	25.6	141.7	26.1	140.8	26.5	139.9	26.9	139.1	27.3
143.5	25.2	142.6	25.6	141.6	26.1	140.7	26.5	139.9	26.9	139.2	27.3
143.6	25.2	142.5	25.7	141.6	26.1	140.7	26.5	139.9	26.9	139.1	27.3
143.5	25.2	142.6	25.7	141.6	26.1	140.7	26.5	139.9	26.9	139.1	27.3
143.5	25.3	142.5	25.7	141.5	26.1	140.7	26.5	139.9	26.9	139.1	27.4
143.5	25.3	142.5	25.7	141.5	26.1	140.6	26.5	139.8	26.9	139.1	27.4
143.5	25.3	142.5	25.7	141.5	26.1	140.7	26.5	139.8	27.0	139.1	27.4
143.4	25.3	142.5	25.7	141.5	26.1	140.7	26.5	139.8	27.0	139.1	27.4
143.4	25.3	142.4	25.7	141.5	26.1	140.6	26.6	139.8	27.0	139.0	27.4
143.4	25.3	142.4	25.7	141.5	26.1	140.6	26.6	139.8	27.0	139.0	27.4
143.3	25.3	142.4	25.7	141.5	26.2	140.6	26.6	139.8	27.0	139.0	27.4

138.9	27.4	138.2	27.9	137.5	28.3	136.7	28.7	136.0	29.1	135.3	29.5
138.9	27.4	138.2	27.9	137.4	28.3	136.7	28.7	136.0	29.1	135.3	29.5
138.9	27.4	138.2	27.9	137.4	28.3	136.7	28.7	136.0	29.1	135.2	29.5
138.9	27.5	138.2	27.9	137.4	28.3	136.6	28.7	135.9	29.1	135.2	29.6
138.8	27.5	138.1	27.9	137.4	28.3	136.6	28.7	136.0	29.1	135.2	29.6
138.9	27.5	138.1	27.9	137.3	28.3	136.7	28.7	135.9	29.2	135.2	29.6
138.9	27.5	138.1	27.9	137.3	28.3	136.7	28.7	135.9	29.2	135.1	29.6
138.8	27.5	138.0	27.9	137.3	28.3	136.6	28.8	135.9	29.2	135.2	29.6
138.8	27.5	138.0	27.9	137.3	28.3	136.6	28.8	135.9	29.2	135.1	29.6
138.8	27.5	138.0	27.9	137.3	28.4	136.6	28.8	135.9	29.2	135.1	29.6
138.7	27.5	138.0	27.9	137.3	28.4	136.6	28.8	135.8	29.2	135.1	29.6
138.7	27.5	138.0	28.0	137.2	28.4	136.5	28.8	135.8	29.2	135.1	29.6
138.7	27.5	138.0	28.0	137.3	28.4	136.5	28.8	135.8	29.2	135.0	29.6
138.7	27.6	138.0	28.0	137.3	28.4	136.5	28.8	135.8	29.2	135.0	29.7
138.7	27.6	137.9	28.0	137.2	28.4	136.5	28.8	135.8	29.2	135.1	29.7
138.6	27.6	138.0	28.0	137.2	28.4	136.5	28.8	135.7	29.3	135.0	29.7
138.7	27.6	137.9	28.0	137.2	28.4	136.5	28.8	135.7	29.3	135.0	29.7
138.6	27.6	137.9	28.0	137.2	28.4	136.5	28.9	135.7	29.3	135.0	29.7
138.6	27.6	137.9	28.0	137.2	28.4	136.4	28.9	135.7	29.3	134.9	29.7
138.7	27.6	137.9	28.0	137.1	28.5	136.4	28.9	135.7	29.3	134.9	29.7
138.6	27.6	137.8	28.0	137.1	28.5	136.4	28.9	135.7	29.3	134.9	29.7
138.6	27.6	137.8	28.1	137.0	28.5	136.4	28.9	135.6	29.3	134.9	29.7
138.5	27.6	137.8	28.1	137.1	28.5	136.4	28.9	135.6	29.3	134.9	29.7
138.6	27.7	137.8	28.1	137.1	28.5	136.4	28.9	135.6	29.3	134.8	29.8
138.5	27.7	137.7	28.1	137.0	28.5	136.3	28.9	135.5	29.3	134.9	29.8
138.5	27.7	137.7	28.1	137.0	28.5	136.3	28.9	135.6	29.4	134.8	29.8
138.5	27.7	137.8	28.1	137.0	28.5	136.2	28.9	135.6	29.4	134.8	29.8
138.4	27.7	137.7	28.1	137.0	28.5	136.3	29.0	135.5	29.4	134.8	29.8
138.4	27.7	137.7	28.1	137.0	28.5	136.2	29.0	135.5	29.4	134.7	29.8
138.5	27.7	137.7	28.1	137.0	28.6	136.2	29.0	135.5	29.4	134.8	29.8
138.4	27.7	137.6	28.1	136.9	28.6	136.2	29.0	135.5	29.4	134.8	29.8
138.4	27.7	137.6	28.2	136.9	28.6	136.2	29.0	135.4	29.4	134.7	29.8
138.4	27.7	137.6	28.2	136.9	28.6	136.2	29.0	135.5	29.4	134.7	29.8
138.3	27.8	137.6	28.2	136.9	28.6	136.2	29.0	135.4	29.4	134.7	29.9
138.3	27.8	137.6	28.2	136.8	28.6	136.1	29.0	135.4	29.4	134.7	29.9
138.3	27.8	137.6	28.2	136.9	28.6	136.1	29.0	135.4	29.5	134.6	29.9
138.3	27.8	137.6	28.2	136.9	28.6	136.1	29.0	135.4	29.5	134.6	29.9
138.3	27.8	137.5	28.2	136.8	28.6	136.0	29.1	135.4	29.5	134.6	29.9
138.3	27.8	137.5	28.2	136.8	28.6	136.1	29.1	135.3	29.5	134.6	29.9
138.3	27.8	137.5	28.2	136.8	28.7	136.0	29.1	135.3	29.5	134.6	29.9
138.2	27.8	137.5	28.2	136.7	28.7	136.0	29.1	135.3	29.5	134.6	29.9
138.2	27.8	137.5	28.3	136.7	28.7	136.0	29.1	135.3	29.5	134.5	29.9